



2019

## Modulating the Tumor Microenvironment to Induce Cross-Priming for Cancer Immunotherapy

Erica Fleming-Trujillo

Follow this and additional works at: [https://ecommons.luc.edu/luc\\_diss](https://ecommons.luc.edu/luc_diss)

 Part of the [Immunology of Infectious Disease Commons](#)

---

### Recommended Citation

Fleming-Trujillo, Erica, "Modulating the Tumor Microenvironment to Induce Cross-Priming for Cancer Immunotherapy" (2019). *Dissertations*. 3332.

[https://ecommons.luc.edu/luc\\_diss/3332](https://ecommons.luc.edu/luc_diss/3332)

This Dissertation is brought to you for free and open access by the Theses and Dissertations at Loyola eCommons. It has been accepted for inclusion in Dissertations by an authorized administrator of Loyola eCommons. For more information, please contact [ecommons@luc.edu](mailto:ecommons@luc.edu).



This work is licensed under a [Creative Commons Attribution-Noncommercial-No Derivative Works 3.0 License](#).  
Copyright © 2019 Erica Fleming-Trujillo

LOYOLA UNIVERSITY CHICAGO

MODULATING THE TUMOR MICROENVIRONMENT TO INDUCE  
CROSS-PRIMING FOR CANCER IMMUNOTHERAPY

A DISSERTATION SUBMITTED TO  
THE FACULTY OF THE GRADUATE SCHOOL  
IN CANDIDACY FOR THE DEGREE OF  
DOCTOR OF PHILOSOPHY

PROGRAM IN MICROBIOLOGY AND IMMUNOLOGY

BY

ERICA L. FLEMING-TRUJILLO

CHICAGO, IL

AUGUST 2019



## ACKNOWLEDGMENTS

Thank you to Mike Nishimura, for giving me the opportunity to travel and present my work and the freedom to become an independent scientist. Thank you to the Nishimura lab for your support, guidance, and friendship over the last four years. Thank you to Annika Dalheim and Natasha Lenhart for breeding and genotyping the mice used for these experiments. Thank you to Gina Scurti for your help and guidance. Thank you to Dr. Tamson Moore, who was always willing to discuss recent results or help plan experiments. Thank you to Sue Niccolai for your endless help and kindness, especially during the darkest of days. Your sense of humor and friendly smile has been a saving grace.

I would like to acknowledge my dissertation committee members, Drs. Phong Le, Jose Guevara, Makio Iwashima, Herb Mathews, and Lisa Butterfield, for their contributions to the success of my project and support through this process.

Thank you to Patricia Simms for your help (and friendly conversations) in the flow cytometry core. Thank you to Dr. Farshid and the Comparative Medicine Facility for providing guidance and assistance when performing mouse experiments.

I am grateful for the funding I have received through the National Cancer Institute, F31 CA206507. Thank you to Lynn Walter for providing her knowledge and assistance with my F31 grant.

I could not have survived grad school without my fellow classmates at Loyola. Thank you to Drs. Kendra Foley, Evann Hilt, Natalie Nidetz, and Doerte Lehmann for



always being down for a wine night to destress and vent about the perils of graduate school.

I would also like to acknowledge my very first research mentor, Dr. Stanley Perlman, and his research lab at the University of Iowa. Thank you for the opportunity to learn, grow, and fall in love with basic science research and immunology. Thank you for encouraging me to pursue a Ph.D. degree and helping me along the way. I will be forever grateful for the time spent in the Perlman lab and my first labmates, Craig Fett, Jonathan Trujillo, Rahul Vijay, and Rudra Channappanavar

To my parents, Linda and David: thank you for your unconditional love and support throughout my education. I am so fortunate that you invested so much time, money, and effort in my education. Thank you for raising me to be humble and kind. To my brother, Davey: thank you for always having a sense of humor. Your success has motivated me along the way. We did it!

To my emotional support baby, Dexter. Adopting you in 2013 was one of the most spontaneous and best decisions of my life. You have made the worst days disappear the moment I walk through the door and see your excited face.

To my loving husband, fur baby daddy, labmate and fellow immunologist, Jonathan Trujillo: thank you for sharing your passion for science, immunology, and life. You were my first labmate back in 2009 and I will cherish those years for life. Your unwavering support, encouragement and confidence has helped build the foundation of my career. I am more enamored by you each day. Together, the possibilities are endless.

## TABLE OF CONTENTS

ACKNOWLEDGMENTS	iii
LIST OF TABLES	ix
LIST OF FIGURES	x
LIST OF ABBREVIATIONS	xix
ABSTRACT	xxiv
CHAPTER ONE: REVIEW OF LITERATURE	
Introduction	1
T Cell-Mediated Immune Responses	3
T Cell Biology	3
T cell development	3
T cell receptor diversity	5
T cell signaling and activation	6
T Helper Cell Subsets and Function	9
T Cell Alloresponses	15
History	15
Pathways of allorecognition	16
Alloantigens	16
Effector response	17
Alloresponses in cancer	20
T Cell Cross-Priming	22
Historical Significance	22
Cell Biology of Antigen Cross-Presentation	23
Acquisition of antigen	24
Dendritic cell subsets and antigen cross-presentation	26
Factors Influencing Antigen Cross-Presentation	28
Means of antigen internalization	28
Types of antigens	29
Licensing of dendritic cells	31
T Cell Cross-Priming in Cancer Immunotherapy	33
Immunotherapies to Treat Cancer	37
Cytokines and Immune Adjuvants	37
Vaccine-Based Immunotherapy	40
Whole tumor cell vaccines	40
Dendritic cell vaccination	42
Anti-Tumor Monoclonal Antibodies	46
Immune Checkpoint Inhibitor Therapy	49
PD-1-targeted therapies	50
CTLA-4-targeted therapy	52
Immune-related adverse events	54

Oncolytic Virotherapy	55
Adoptive Cell Therapy	56
CAR T cell therapy	59
TCR gene-modified T cells	63
Predictive Biomarkers in Cancer Immunotherapy	68
Cellular analysis from the peripheral blood	68
Neoantigens and tumor mutation burden	69
Immune profiling the tumor microenvironment	70
Concluding Remarks	72
CHAPTER TWO: MATERIALS AND METHODS	
Cell Lines, Media, and Reagents	75
Mice	76
Transduction of Mouse T Cells	76
Tumor Challenges and Treatment	77
Tissue Preparation	79
Peptides	79
Intracellular Cytokine/Degranulation Bifunctional Assay	80
Antibody Staining and Flow Cytometry	80
Detection of IFN- $\gamma$ Secreting Cells by ELISPOT Assay	81
<i>In Vivo</i> Cytotoxicity Assay	82
Vector Construction	83
Statistical Analysis	84
CHAPTER THREE: INTRATUMORAL DELIVERY OF TIL 1383I TCR TRANSDUCED T CELLS EXTENDS SURVIVAL AND SUPPRESSES B16 A2/K <sup>b</sup> TUMOR GROWTH	
TIL 1383I TCR Transduced Mouse T Cells Recognize B16 A2/K <sup>b</sup> Tumors <i>In Vitro</i>	86
Intratumoral Treatment with TIL 1383I TCR Transduced Allogeneic T Cells Improves Survival and Suppresses B16 A2/K <sup>b</sup> Tumor Growth in Mice	93
Improved Anti-Tumor Responses Following TIL 1383I TCR Transduced Allogeneic T Cell Treatment Requires an Intact Recipient Immune System	104
Summary	112
CHAPTER FOUR: INTRATUMORAL DELIVERY OF TIL 1383I TCR TRANSDUCED ALLOGENEIC T CELLS STIMULATES DENDRITIC CELL RESPONSES	
Characterization of Dendritic Cells in the Tumor Microenvironment	115
Characterization of Dendritic Cells in the Tumor Draining Lymph Nodes	121
Summary	127

CHAPTER FIVE: INTRATUMORAL DELIVERY OF TIL 1383I TCR TRANSDUCED ALLOGENEIC T CELLS ENHANCES ACTIVATION OF T CELLS	
Characterization of T Cells in the Tumor Microenvironment	131
Characterization of T Cells in the Tumor and Tumor Draining Lymph Nodes Seven Days Post-T Cell Treatment	147
TIL 1383I TCR Transduced Allogeneic T Cell Treatment Generates Endogenous Tumor-Specific T Cells	153
Detection of Tumor-Specific Cells by IFN- $\gamma$ ELISPOT Assay	158
Detection of Cytolytic Activity by <i>In Vivo</i> CTL Assay	165
CHAPTER SIX: INTRATUMORAL TREATMENT WITH TIL 1383I TCR TRANSDUCED ALLOGENEIC T CELLS PREVENTS THE DEVELOPMENT OF DISTANT, UNTREATED B16 TUMORS	
Intratumoral Treatment of B16 A2/K <sup>b</sup> Tumors with TIL 1383I TCR Transduced Allogeneic T Cells Prevents Development of Untreated, Contralateral B16 Tumors	170
Adoptive Transfer of Splenocytes from Mice Treated with TIL 1383I TCR Transduced Allogeneic T Cells Suppresses Growth of Established B16 Tumors	179
CHAPTER SEVEN: COMBINATION IMMUNOTHERAPIES TO ENHANCE THE ANTI-TUMOR EFFICACY OF TIL 1383I TCR TRANSDUCED ALLOGENEIC T CELLS	
Rationale	185
Addition of the TLR3 Agonist, Poly I:C	185
Incorporation of the LIGHT Gene into the Retroviral Vector	197
Combination Therapy with Anti-PD-1 and Anti-CTLA-4 Monoclonal Antibodies	209
Summary	228
CHAPTER EIGHT: DISCUSSION	
Introduction	236
Intratumoral Delivery of TIL 1383I TCR Transduced T Cells Extends Survival and Suppresses B16 A2/K <sup>b</sup> Tumor Growth	237
The Recipient Immune Recognition of Foreign Allogeneic Donor Cells Enhances the Efficacy of Intratumoral Treatment with TIL 1383I TCR Transduced Allogeneic T Cells	239
TIL 1383I TCR Transduced Allogeneic T Cells Induce an Immune-Active Tumor Microenvironment	242
Induction of Immune Responses in the Tumor Draining Lymph Nodes Following TIL 1383I TCR Transduced Allogeneic T Cell Treatment	246
Intratumoral Treatment with TIL 1383I TCR Transduced Allogeneic T Cells Induces Cross-Priming of Endogenous, Tumor-Specific T Cells	249
Immunotherapy-Associated Adverse Events	251

Combination Immunotherapy to Enhance the Efficacy of TIL 1383I TCR Transduced Allogeneic T Cell Treatment	254
Concluding Remarks	259
APPENDIX	261
REFERENCE LIST	274
VITA	317

## LIST OF TABLES

Table 1.	Phenotype of TIL 1383I TCR Transduced T Cells	88
Table 2.	Log-Rank (Mantel-Cox) Test of Survival Following Combination Treatment with TIL 1383I TCR Transduced T Cells and Anti-PD-1 Monoclonal Antibody	213
Table 3.	Log-Rank (Mantel-Cox) Test of B16 Tumor-Free Mice Following Treatment with TIL 1383I TCR Transduced T Cells and Anti-PD-1 Monoclonal Antibody	215
Table 4.	Log-Rank (Mantel-Cox) Test of Survival Following Treatment with TIL 1383I TCR Transduced T Cells and Anti-PD-1/Anti-CTLA-4 Monoclonal Antibodies	219
Table 5.	Log-Rank (Mantel-Cox) Test of B16 Tumor-Free Mice Following Treatment with TIL 1383I TCR Transduced T Cells and Anti-PD-1/Anti-CTLA-4 Monoclonal Antibodies	222
Table 6.	Log-Rank (Mantel-Cox) Test of Survival Following Combination Treatment with TIL 1383I TCR Transduced T Cells and Anti-PD-1/Anti-CTLA-4 Monoclonal Antibodies	226
Table 7.	Statistical Analysis of the Slope of B16 A2/K <sup>b</sup> Tumors Following Treatment with TIL 1383I TCR Transduced T Cells and Anti-PD-1/Anti-CTLA-4 Monoclonal Antibodies	232
Table 8.	Log-Rank (Mantel-Cox) Test of B16 Tumor-Free Mice Following Treatment with TIL 1383I TCR Transduced T cells and Anti-PD-1/Anti-CTLA-4 Monoclonal Antibodies	234

## LIST OF FIGURES

Figure 1.	T Cell Development in the Thymus	4
Figure 2.	Effector Functions of CD4 <sup>+</sup> and CD8 <sup>+</sup> T Cells Following Activation by Antigen Presenting Cells	10
Figure 3.	Pathways of Antigen Cross-Presentation by Dendritic Cells	24
Figure 4.	Generations of CAR T Cells	60
Figure 5.	Schematic of Adoptive Transfer of TCR Gene-Modified T Cells	64
Figure 6.	Expression of the TIL 1383I TCR on Mouse T cells	87
Figure 7.	TIL 1383I TCR Transduced T Cells Recognize B16 A2/K <sup>b</sup> Tumors	91
Figure 8.	TIL 1383I TCR Transduced T Cells Recognize the Tyrosinase <sub>368-376</sub> Peptide	92
Figure 9.	Proposed Model to Enhance the Efficacy of Adoptive Transfer of TCR Gene-Modified T Cells for Cancer Immunotherapy	96
Figure 10.	Experimental Design to Determine if Intratumoral Treatment with TIL1383I TCR Transduced T Cells Induces Regression of B16 A2/K <sup>b</sup> Tumors	97
Figure 11.	TIL 1383I TCR Transduced Allogeneic T Cell Treatment Extends Survival of B16 A2/K <sup>b</sup> Tumor-Bearing Mice	100
Figure 12.	TIL 1383I TCR Transduced Allogeneic T Cell Treatment Suppresses B16 A2/K <sup>b</sup> Tumor Growth	101
Figure 13.	TIL 1383I TCR Transduced Allogeneic T cell Treatment Delays Progression of B16 A2/K <sup>b</sup> Tumors	102
Figure 14.	TIL 1383I TCR Transduced Allogeneic T Cell-Treated NSG A2 Mice Have Similar Survival Outcomes Compared to TIL 1383I TCR Transduced Syngeneic T Cell-Treated NSG A2 Mice	107

Figure 15.	TIL 1383I TCR Transduced Syngeneic and Allogeneic T Cells Have Equal Capacities to Suppress B16 A2/K <sup>b</sup> Tumors in NSG A2 Recipient Mice	108
Figure 16.	Linear Regression Analysis of B16 A2/K <sup>b</sup> Tumor Growth in NSG A2 Mice After TIL 1383I TCR Transduced T Cell Treatment	109
Figure 17.	TIL 1383I TCR Transduced T Cells are Undetectable in the Tumors From Immunocompetent HLA-A2 Transgenic Recipient Mice	110
Figure 18.	TIL 1383I TCR Transduced T Cells Persist in the Tumors From Immunodeficient NSG A2 Recipient Mice	111
Figure 19.	Representative Pictures of Treated B16 A2/K <sup>b</sup> Tumors Seven Days Post-T Cell Treatment	114
Figure 20.	CD11c <sup>+</sup> MHCII <sup>+</sup> Dendritic Cells in the Tumor Microenvironment Two Days Post-T Cell Treatment	116
Figure 21.	Expression of Co-Stimulatory Molecules on CD11c <sup>+</sup> MHCII <sup>+</sup> Dendritic Cells in the Tumor Two Days Post-T Cell Treatment	118
Figure 22.	Surface Expression of Co-Stimulatory Molecules on CD11c <sup>+</sup> MHCII <sup>+</sup> Dendritic Cells in the Tumor Two Days Post-T Cell Treatment	119
Figure 23.	TIL 1383I TCR Transduced Allogeneic T Cell Treatment Increases the Frequency of CD103 <sup>+</sup> Dendritic Cells in the Tumor Two Days Post-T Cell Treatment	120
Figure 24.	TIL 1383I TCR Transduced Allogeneic T Cell Treatment Increases the Frequency of CD205 <sup>+</sup> Dendritic Cells in the Tumor Two Days Post-T Cell Treatment	122
Figure 25.	TIL 1383I TCR Transduced Allogeneic T Cells Induce the Accumulation of CD11c <sup>+</sup> MHCII <sup>+</sup> Dendritic Cells in the Tumor Draining Lymph Nodes Two Days Post-T Cell Treatment	124
Figure 26.	TIL 1383I TCR Transduced Allogeneic T Cell Treatment Leads to an Increased Frequency and Number of CD80 <sup>+</sup> and CD86 <sup>+</sup> Dendritic Cells the Tumor Draining Lymph Nodes Two Days Post-T Cell Treatment	125
Figure 27.	TIL 1383I TCR Transduced Allogeneic T Cell Treatment Leads to Increased Surface Expression of CD80 on Dendritic Cells in the Tumor Draining Lymph Nodes Two Days Post-T Cell Treatment	126



Figure 28.	Treatment with TIL 1383I TCR Transduced Allogeneic T Cells Increases CD103 <sup>+</sup> Dendritic Cells in the Tumor Draining Lymph Nodes Two Days Post-T Cell Treatment	128
Figure 29.	TIL 1383I TCR Transduced Allogeneic T Cell Treatment Promotes the Accumulation of CD8 $\alpha$ <sup>+</sup> Dendritic Cells in the Tumor Draining Lymph Nodes Two Days Post-T Cell Treatment	129
Figure 30.	Treatment with TIL 1383I TCR Transduced Allogeneic T Cells Increases the Accumulation of CD205 <sup>+</sup> Dendritic Cells in the Tumor Draining Lymph Nodes Two Days Post-T Cell Treatment	130
Figure 31.	Frequency of CD3 <sup>+</sup> T Cells in the Tumor Microenvironment Two Days Post-T Cell Treatment	132
Figure 32.	Frequency of CD4 <sup>+</sup> and CD8 <sup>+</sup> T Cells in the Tumor Microenvironment Two Days Post-T Cell Treatment	133
Figure 33.	Frequency and Surface Expression of CD25 on CD4 <sup>+</sup> T Cells in the Tumor Microenvironment Two Days Post-T Cell Treatment	135
Figure 34.	Frequency and Surface Expression of CD44 on CD4 <sup>+</sup> T Cells in the Tumor Microenvironment Two Days Post-T Cell Treatment	136
Figure 35.	Frequency and Surface Expression of CD69 on CD4 <sup>+</sup> T cells in the Tumor Microenvironment Two Days Post-T Cell Treatment	137
Figure 36.	Frequency and Surface Expression of CD25 on CD8 <sup>+</sup> T Cells in the Tumor Microenvironment Two Days Post-T Cell Treatment	139
Figure 37.	Frequency and Surface Expression of CD44 on CD8 <sup>+</sup> T Cells in the Tumor Microenvironment Two Days Post-T Cell Treatment	140
Figure 38.	Frequency and Surface Expression of CD69 on CD8 <sup>+</sup> T Cells in the Tumor Microenvironment Two Days Post-T Cell Treatment	141
Figure 39.	Production of IL-2 by CD3 <sup>+</sup> T Cells in the Tumor Microenvironment Two Days Post-T Cell Treatment	143
Figure 40.	Intratumoral TIL 1383I TCR Transduced Allogeneic CD8 <sup>+</sup> T Cells Produce IFN- $\gamma$	144
Figure 41.	Intratumoral TIL 1383I TCR Transduced Allogeneic CD8 <sup>+</sup> T Cells Produce IFN- $\gamma$	145

Figure 42.	Intratumoral TIL 1383I TCR Transduced Allogeneic T Cells Produce TNF- $\alpha$	146
Figure 43.	Frequency of CD4 <sup>+</sup> and CD8 <sup>+</sup> T Cells in the Tumor Seven Days Post-T Cell Treatment	148
Figure 44.	Frequency of Activated CD4 <sup>+</sup> T Cells in the Tumor Seven Days Post-T Cell Treatment	149
Figure 45.	Frequency of Activated CD8 <sup>+</sup> T Cells in the Tumor Seven Days Post-T Cell Treatment	150
Figure 46.	Regulatory T Cells in the Tumor Microenvironment Seven Days Post-T Cell Treatment	151
Figure 47.	Frequency and Number of CD4 <sup>+</sup> and CD8 <sup>+</sup> T Cells in the Tumor Draining Lymph Nodes Seven Days Post-T Cell Treatment	154
Figure 48.	Activated CD4 <sup>+</sup> T Cells in the Tumor Draining Lymph Nodes Seven Days Post-T Cell Treatment	155
Figure 49.	Treatment with TIL 1383I TCR Transduced Allogeneic T Cells Increases the Frequency and Number of Activated CD8 <sup>+</sup> T Cells in the Tumor Draining Lymph Nodes Seven Days Post-T Cell Treatment	156
Figure 50.	Treatment with TIL 1383I TCR Transduced Allogeneic T Cells Leads to CXCR3 <sup>+</sup> T Cells in the Tumor Draining Lymph Nodes Seven Days Post-T Cell Treatment	157
Figure 51.	TIL 1383I TCR Transduced Allogeneic T Cell Treatment Induces Tumor-Specific IFN- $\gamma$ <sup>+</sup> Cells in the Tumor Draining Lymph Nodes	160
Figure 52.	TIL 1383I TCR Transduced Allogeneic T Cell Treatment Induces gp100-Specific IFN- $\gamma$ <sup>+</sup> Cells in the Tumor Draining Lymph Nodes	162
Figure 53.	Correlation between Final Tumor Size and the Frequency of Tumor-Specific IFN- $\gamma$ <sup>+</sup> Cells	163
Figure 54.	TIL 1383I TCR Transduced T Cells are Not Detectable in the Spleen or Tumor Draining Lymph Nodes	164
Figure 55.	<i>In Vivo</i> CTL Assay Experimental Design	168
Figure 56.	TIL 1383I TCR Transduced Allogeneic T Cells Induce TRP-2- and gp100-Specific CTL	169

Figure 57.	Experimental Design to Determine if Intratumoral Treatment with TIL 1383I TCR Transduced Allogeneic T Cells Induces Endogenous Tumor-Specific T Cells Capable of Preventing Development of Distant, Contralateral B16 Tumors	171
Figure 58.	TIL 1383I TCR Transduced Allogeneic T Cell Treatment of Primary B16 A2/K <sup>b</sup> Tumors Prevents Development of B16 Tumors Inoculated on the Contralateral Flank	173
Figure 59.	Development of Vitiligo in a Mouse with a TIL 1383I TCR Transduced Allogeneic T Cell-Treated Primary B16 A2/K <sup>b</sup> Tumor That Was Protected from B16 Tumor Development	174
Figure 60.	Treatment of Primary B16 A2/K <sup>b</sup> Tumors with TIL 1383I TCR Transduced T Cells Improves Survival Following Challenge with B16 on the Contralateral Flank	175
Figure 61.	TIL 1383I TCR Transduced T Cell Treatment of Primary B16 A2/K <sup>b</sup> Tumors Delays the Development of B16 Tumors Inoculated on the Contralateral Flank	177
Figure 62.	TIL 1383I TCR Transduced T Cell Treatment of Primary B16 A2/K <sup>b</sup> Tumors Improves Survival Following Challenge with B16 Tumors on the Contralateral Flank	178
Figure 63.	Experimental Design to Determine if the Transfer of Splenocytes From Mice Treated with TIL 1383I TCR Transduced T Cell-Treated Mice Can Reject Established B16 Tumors	180
Figure 64.	Adoptive Transfer of Splenocytes from TIL 1383I TCR Transduced Allogeneic T Cell-Treated Mice Suppresses Growth of B16 Tumors in Individual	182
Figure 65.	Delayed B16 Tumor Progression Following the Transfer of Splenocytes From TIL 1383I TCR Transduced Allogeneic T Cell-Treated Mice	183
Figure 66.	Tumor Reactivity of Donor Splenocytes from T Cell-Treated Mice Used for Adoptive Transfer	184
Figure 67.	Experimental Design to Determine if the Combination of TIL 1383I TCR Transduced Allogeneic T Cells and Poly I:C Improves Anti-Tumor Responses	187

Figure 68.	B16 A2/K <sup>b</sup> Tumor Growth in Individual Mice Following Intratumoral Treatment with TIL 1383I TCR Transduced Allogeneic T Cells and Poly I:C	188
Figure 69.	B16 A2/K <sup>b</sup> Tumor Growth Following Combination Treatment with T Cells and Poly I:C	189
Figure 70.	Experimental Design to Determine if T Cell Treatment-Induced Splenocytes Can Transfer Therapeutic or Prophylactic Immunity Against B16 Tumors in Naïve Mice	191
Figure 71.	B16 A2/K <sup>b</sup> Tumor Growth of Individual Mice Following Combination Therapy with T Cells and Poly I:C	192
Figure 72.	Average B16 A2/K <sup>b</sup> Tumor Growth of Individual Mice Following Combination Therapy with T Cells and Poly I:C	193
Figure 73.	B16 Tumor Growth in Individual Mice Following the Adoptive Transfer of Splenocytes from Mice with B16 A2/K <sup>b</sup> Tumors Treated with the Combination of TIL 1383I TCR Transduced Allogeneic T Cells and Poly I:C	195
Figure 74.	Average B16 Tumor Growth Group Averages Following the Adoptive Transfer of Splenocytes from Mice with B16 A2/K <sup>b</sup> Tumors Treated with the Combination of TIL 1383I TCR Transduced Allogeneic T Cells and Poly I:C	196
Figure 75.	Splenocytes from B16 A2/K <sup>b</sup> Tumor-Bearing Mice Treated with the Combination of TIL 1383I TCR Transduced Allogeneic T Cells and Poly I:C That Were Transferred into Naïve Mice Delay Progression of B16 Tumors	198
Figure 76.	Splenocytes from Mice Treated with the Combination of TIL 1383I TCR Transduced Allogeneic T Cells and Poly I:C Transfer Anti-Tumor Immunity to Naïve Mice	199
Figure 77.	Engineering T Cells to Express the TIL 1383I TCR and Extracellular LIGHT Domain	201
Figure 78.	B16 A2/K <sup>b</sup> Tumor Growth in Individual Mice Following Intratumoral Treatment with T Cells Transduced to Express the TIL 1383I TCR or Co-Express the TIL 1383I TCR + LIGHT Protein	203
Figure 79.	Linear Regression Analysis of B16 A2/K <sup>b</sup> Tumor Growth Following Treatment with T Cells Transduced to Co-Express the TIL 1383I TCR and LIGHT Protein	204

Figure 80.	Tumor-Specific IFN- $\gamma$ Production by Endogenous T Cells Following Intratumoral Treatment with T Cells That Co-Express the TIL 1383I TCR and LIGHT Protein	205
Figure 81.	B16 A2/K <sup>b</sup> Tumor Growth in Individual Mice Following Intratumoral Treatment with TIL 1383I TCR Transduced T Cells +/- Recombinant LIGHT Protein	207
Figure 82.	Linear Regression Analysis of B16 A2/K <sup>b</sup> Tumor Growth Following Treatment with TIL 1383I TCR Transduced T Cells and LIGHT Protein	208
Figure 83.	Expression of Immune Checkpoints on T Cells in the Tumor Microenvironment Following TIL 1383I TCR Transduced T Cell Treatment	210
Figure 84.	Experimental Design to Determine If the Combination of Anti-PD-1 Monoclonal Antibody and TIL 1383I TCR Transduced T Cell Treatment Enhances Anti-Tumor Responses	211
Figure 85.	Survival Following Treatment with TIL 1383I TCR Transduced T Cells and Anti-PD-1 Monoclonal Antibody	212
Figure 86.	Percentage of Mice Protected from Contralateral B16 Following Treatment of Primary B16 A2/K <sup>b</sup> Tumors with TIL 1383I TCR Transduced T Cells and Treatment with Anti-PD-1 Monoclonal Antibody	214
Figure 87.	Experimental Design to Determine if the Addition of Checkpoint Inhibitors Enhances the Efficacy of Intratumoral Treatment with TIL 1383I TCR Transduced Allogeneic T Cells	217
Figure 88.	The Combination of TIL 1383I TCR Transduced Allogeneic T Cells and Immune Checkpoint Inhibitors Improve Survival of B16 A2/K <sup>b</sup> Tumor-Bearing Mice	218
Figure 89.	Intratumoral Treatment with TIL 1383I TCR Transduced T Cells and Anti-PD-1/Anti-CTLA-4 Monoclonal Antibodies Suppresses B16 A2/K <sup>b</sup> Tumor Growth	221
Figure 90.	Experimental Design to Determine If the Combination of Anti-PD-1 and Anti-CTLA-4 Monoclonal Antibodies and TIL 1383I TCR Transduced T Cell Treatment Enhances Anti-Tumor Responses	223

Figure 91.	The Combination of TIL 1383I TCR Transduced Allogeneic T Cells and Anti-PD-1/Anti-CTLA-4 Monoclonal Antibodies Improves the Survival of B16 A2/K <sup>b</sup> Tumor-Bearing Mice	225
Figure 92.	The Combination of TIL 1383I TCR Transduced T Cells and Anti-PD-1/Anti-CTLA-4 Monoclonal Antibodies Suppresses B16 A2/K <sup>b</sup> Tumor Growth	230
Figure 93.	The Impact of Combination Therapy with TIL 1383I TCR Transduced T Cells and Anti-PD-1 and Anti-CTLA-4 Monoclonal Antibodies on the Slope of B16 A2/K <sup>b</sup> Progression Following Treatment	231
Figure 94.	The Combination of TIL 1383I TCR Transduced T Cells and Anti-PD-1/Anti-CTLA-4 Monoclonal Antibodies Mediates Complete Protection Against the Development of Contralateral B16 Tumors	233
Figure 95.	Increased Incidence of Vitiligo with the Combination of TIL 1383I TCR Transduced Allogeneic T Cells and Anti-PD-1/Anti-CTLA-4 Monoclonal Antibodies	235
Figure 96.	Intratumoral Treatment with TIL 1383I TCR Transduced C3H T Cells Promotes B16 A2/K <sup>b</sup> Tumor Suppression	262
Figure 97.	Intratumoral Treatment with TIL 1383I TCR Transduced C3H T Cells Promotes B16 A2/K <sup>b</sup> Tumor Regression	263
Figure 98.	Intratumoral Treatment with TIL 1383I TCR Transduced C3H T Cells Promotes Tumor-Specific IFN- $\gamma$ <sup>+</sup> Cells in the Tumor Draining Lymph Nodes	264
Figure 99.	Intratumoral Treatment with TIL 1383I TCR Transduced C3H T Cells Promotes Tumor Antigen-Specific IFN- $\gamma$ <sup>+</sup> Cells in the Tumor Draining Lymph Nodes	265
Figure 100.	CD11c <sup>+</sup> MHCII <sup>+</sup> Dendritic Cells in the Tumor Draining Lymph Nodes Three and Five Days Post-T Cell Treatment	266
Figure 101.	Expression of Co-Stimulatory Molecules on CD11c <sup>+</sup> MHCII <sup>+</sup> DCs in the Tumor Draining Lymph Nodes Three and Five Days Post-T Cell Treatment	267
Figure 102.	CD205 <sup>+</sup> Dendritic Cells in the Tumor Draining Lymph Nodes Three and Five Days Post-T Cell Treatment	268

Figure 103.	Tumor Antigen-Specific IFN- $\gamma$ <sup>+</sup> Cells in the Tumor Draining Lymph Nodes of Mice Treated with the Combination of Intratumoral TIL 1383I TCR Transduced Syngeneic T Cells and Poly I:C	269
Figure 104.	Tumor Antigen-Specific IFN- $\gamma$ <sup>+</sup> Cells in the Tumor Draining Lymph Nodes of Mice Treated with the Combination of Intratumoral TIL 1383I TCR Transduced Allogeneic T Cells and Poly I:C	270
Figure 105.	Average Growth of Contralateral B16 Tumors in Mice with B16 A2/K <sup>b</sup> Tumors Treated with TIL 1383I TCR Transduced Allogeneic T Cells	275
Figure 106.	Average Growth of Primary B16 A2/K <sup>b</sup> Tumors Following Intratumoral Treatment with TIL 1383I TCR Transduced Allogeneic T Cells	276
Figure 107.	Expression of HLA-A2 on B16 A2/K <sup>b</sup> Tumor Cells 10 Days Post-Intratumoral Treatment	277

## LIST OF ABBREVIATIONS

C	Degrees Celsius
μL	Microliter
μg	Microgram
μM	Micromolar
ACT	Adoptive cell transfer
AdV	Adenovirus
AF	Alexa Fluor
Ag(s)	Antigen(s)
AICD	Activation-induced cell death
ALL	Acute lymphoblastic leukemia
Allo	Allogeneic
APC	Antigen presenting cell
APC	Allophycocyanin
BM	Bone marrow
BSA	Bovine serum albumin
BV	Brilliant Violet
C	Constant
CAIX	Carbonic anhydrase IX
CAR	Chimeric antigen receptor
CD	Cluster of differentiation



CDR	Complementarity determining region
CEA	Carcinoembryonic antigen
CLL	Chronic lymphocytic leukemia
CLP	Common lymphoid progenitor
CMV	Cytomegalovirus
CTLA-4	Cytotoxic T-lymphocyte-associated protein-4
D	Diversity
DC	Dendritic cells
DMEM	Dulbecco's Modified Eagle's Medium
DMSO	Dimethyl sulfoxide
DN	Double negative
DNA	Deoxyribose nucleic acid
DP	Double Positive
EBV	Epstein-Barr virus
ELISA	Enzyme-linked immunosorbant assay
ELISPOT	Enzyme-linked ImmunoSpot
EMEM	Eagle's Minimum Essential Medium
ER	Endoplasmic reticulum
Fab	Antigen binding fragment
FACS	Fluorescence-activated cell sorting
FBS	Fetal bovine serum
FITC	Fluorescein isothiocyanate
G418	Geneticin

GFP	Green fluorescent protein
GM-CSF	Granulocyte-macrophage- colony stimulating factor
gp	Glycoprotein
GVHD	Graft versus host disease
HLA	Human leukocyte antigen
HPV	Human papilloma virus
hr	Hour
IFN- $\alpha$	Interferon- $\alpha$
IFN- $\gamma$	Interferon- $\gamma$
IL	Interleukin
ITAM	Immunoreceptor tyrosine-based activation motif
J	Joining
Kb	Kilobase, one thousand base pairs
LAK	Lymphokine activated killer cell
LB	Luria-Bertani
Lck	Lymphocyte-specific protein tyrosine kinase
LN	Lymph node
LTR	Long terminal repeats
M	Molar
mAb	Monoclonal antibody
MART-1	Melanoma antigen recognized by T cells-1
MDSC	Myeloid-derived suppressor cell
MHC	Major histocompatibility complex

min	Minute
mg	Milligram
mL	Milliliter
mM	Millimolar
Muritized	Of mouse origin
NF- $\kappa$ B	Nuclear factor- $\kappa$ B
ng	Nanogram
NHEJ	Nonhomologous end joining
NK	Natural killer
PBL	Peripheral blood lymphocyte
PBMC	Peripheral blood mononuclear cell
PBS	Phosphate buffered saline
PBSA	Phosphate buffered saline with bovine serum albumin
PCR	Polymerase chain reaction
PD-1	Programmed cell death 1
PE	Phycoerythrin
PerCP	Peridinin chlorophyll protein
pMHC	Peptide-major histocompatibility complex
RPMI	Roswell Park Memorial Institute
RS	Recombination signal
RT	Room temperature
SA	Splice acceptor
scFv	Single-chain variable fragment

SD	Splice donor
Syn	Syngeneic
TAP	Transporter associated with antigen processing
TCR	T cell receptor
Td	Transduced
TIL	Tumor infiltrating lymphocyte
TNF- $\alpha$	Tumor necrosis factor- alpha
Tyro	Tyrosinase
$\mu$ L	Microliter
UnTd	Untransduced
V	Variable
VSV	Vesicular stomatitis virus

## ABSTRACT

Adoptive cell therapy (ACT) using T cells engineered to express tumor-specific T cell receptors (TCR) holds great promise in treating patients with hematological malignancies and solid tumors. ACT involves the generation of large numbers of tumor-specific T cells *in vitro*, which later are administered to the patient, aiming to establish an *in vivo* response and effective tumor control. Our lab has identified a TCR (TIL 1383I TCR) specific to the melanoma antigen, tyrosinase, for ACT. In a phase I clinical trial, patients with metastatic melanoma were treated with a systemic infusion of autologous T cells transduced to express the TIL 1383I TCR. We observed clinical and biologic responses following ACT including tumor regression in one of seven patients and the development of vitiligo, indicative of T cell-mediated killing of melanocytes, in two of seven patients (one of which was the responder)<sup>1</sup>. Our findings demonstrate that the ACT of TCR gene-modified T cells has the potential to eliminate tumors, but the modest number of patients responding emphasizes the need for improvement.

Extensive investigation into resistance mechanisms has revealed key factors influencing outcomes to immunotherapy. Tumor cells can downregulate or lose the expression of the targeted antigen or the corresponding MHC alleles, which can lead to tumor escape variants that are no longer recognized by the transferred T cells. Additionally, the tumor microenvironment (TME) can be highly immunosuppressive and adept at impairing effector T cell responses. T cell-based immunotherapies should be designed to overcome resistance mechanisms to achieve durable responses.

A phase I clinical trial that our lab conducted in collaboration with Dr. Keld Kaltoft evaluated the feasibility and safety of a novel approach by which allogeneic TCR transduced T cells (C Cure 709) were delivered through direct injection into metastatic lesions of stage IV melanoma patients<sup>2</sup>. C Cure 709 is an allogeneic T cell line that was transduced to express a MART-1-specific TCR (TIL 5). Before intratumoral injection, C Cure 709 cells were irradiated with 60 Gy, which prevented *in vivo* proliferation but maintained effector function for 1-2 days. Significant regression of injected metastases was reported in four of fifteen patients. Two of fifteen patients had regression of non-injected lesions, and two patients developed vitiligo. One patient that developed vitiligo also had a local response. Biopsies from both injected and non-injected tumors from responding patients revealed that C Cure 709 cells were not detected within the tumors, suggesting the induction of systemic anti-tumor immunity and generation of additional tumor antigen-specific T cells, with specificities that differed from the original MART-1 target. These results indicated that intratumoral delivery of allogeneic TCR transduced T cells is safe, feasible, and capable of anti-tumor responses.

In the studies presented in this dissertation, we evaluated the intratumoral delivery of TIL 1383I TCR transduced T cells in a widely used B16 mouse melanoma model. To favorably modulate the TME and counteract immune suppression, we employed an alternative strategy and expressed the TIL 1383I TCR on allogeneic, as opposed to syngeneic, donor T cells. We rationalized that the allogeneic inflammatory response would combat the immunosuppressive tumor microenvironment. We demonstrated that intratumoral treatment with TIL 1383I TCR allogeneic T cells extended survival and suppressed tumor growth in mice more effectively than treatment

with TIL 1383I TCR syngeneic T cells. Tumors treated with TIL 1383I TCR allogeneic T cells exhibited more significant accumulation of mature dendritic cells and cross-presenting dendritic cell subsets, as well as increased T cell activation, in the tumor and tumor draining lymph nodes. TIL 1383I TCR allogeneic T cell treatment generated endogenous tumor-specific T cells that prevented the development of distant, untreated tumors. Furthermore, the addition of immune checkpoint inhibitors promoted tumor clearance and enhanced protection in mice treated with TIL 1383I TCR allogeneic T cells. Intratumoral delivery of allogeneic TCR gene-modified T cells can expand the available tumor antigen targets, without compromising safety, by avoiding systemic administration. Using allogeneic donor T cells as an “off-the-shelf” approach can contribute to the accessibility and efficacy of T cell-based immunotherapy.

## CHAPTER ONE: REVIEW OF LITERATURE

### **Introduction**

Not long ago, surgical resection of tumors and chemotherapy or radiotherapy were primary options available to treat patients with cancer. The concept of tumor immunity was established upon the identification of tumor-specific T cells within the tumors resected from cancer patients. Despite the existence of tumor-specific T cells, tumors from these patients escaped immune control and failed to regress. The ability to clone T cell receptor (TCR) genes from T cells reactive against tumor antigens into viral vectors and redirect the specificity of T cells through transduction, led to the use of TCR gene-modified T cells for cancer therapy. Adoptive cell transfer (ACT) of autologous TCR gene-modified T cells targeting tumor antigens is a promising therapeutic strategy currently in clinical trials to treat patients with advanced malignancies.

While immunotherapies can mediate acute anti-tumor responses that lead to remission in some patients, long-term and durable responses are rare, especially among solid cancer types. The immunosuppressive tumor microenvironment, heterogeneity of solid tumors, and evasion of immune cell detection are some of the factors that influence the outcome of immunotherapy. Understanding the mechanisms affecting the generation of anti-tumor responses are critical to enhancing the efficacy of T cell-based immunotherapies.



Personalized, rationally-designed combinations of immunotherapies based on tumor characteristics are likely necessary to overcome various immune resistance mechanisms and to achieve durable responses in a higher proportion of patients. To generate the most effective immunotherapies, there should be a tumor-specific component as well as an adjuvant, or immune-stimulating component. Intratumoral delivery of TCR gene-modified T cells is a potentially viable, safe, and effective alternative to the systemic infusion of genetically modified anti-tumor T cells. While this route eliminates the requirement of T cell trafficking into the tumor, the tumor microenvironment might still hinder the immune response. Therefore, it is critical to engineer TCR gene-modified T cells to endure or counteract immunosuppression following administration.

We have proposed an alternative strategy that utilizes allogeneic, rather than autologous, donor T cells that are then engineered to express a tumor-specific TCR that recognizes the melanoma antigen, tyrosinase, in the context of human MHC class I HLA-A2. As an alternative approach to systemic infusion of tumor antigen-specific T cells, we proposed to perform intratumoral delivery of TCR-transduced allogeneic T cells. We hypothesize that this approach will provide additional benefits: direct effector T cell-tumor interactions and, when combined with the allogeneic response, can induce local activation of immune cells within the suppressive tumor microenvironment, thus facilitating activation of antigen presenting cells and cross-priming of CD8<sup>+</sup> T cells and systemic anti-tumor immunity. The goal of this dissertation is to identify the immunological changes that occur following intratumoral delivery of allogeneic tumor-specific T cells that mediate improved anti-tumor immune responses.

## T Cell-Mediated Immune Responses

### T Cell Biology

T cells play a critical role in protecting us against pathogens, recognizing foreign components, and killing cancer cells. Several immunotherapies designed to treat cancer employ strategies that improve T cell function or induce tumor-specific T cell responses. Through a unique T Cell Receptor (TCR), T cells recognize determinant self- and non-self- proteins. The TCR is composed of alpha and beta chain ( $\alpha\beta$ TCR) or gamma and delta chain ( $\gamma\delta$ TCR) heterodimers that bind to antigens (Ags) presented in the context of Major Histocompatibility Complex (MHC) on the surface of a cell. The focus of this dissertation will be  $\alpha\beta$ TCR T cells.

**T cell development.** In the bone marrow (BM), the long-term hematopoietic stem cell (LT-HSC) gives rise to multipotent and lineage-committed hematopoietic progenitor cells, including common lymphoid progenitors (CLP), common myeloid progenitors (CMP), and granulocyte-macrophage progenitor (GMP).

T cells are generated in the thymus, which consists of the outer cortex and the inner medulla, in three major developmental steps: lineage commitment, TCR gene rearrangement, and selection (Fig 1). The earliest T lineage cell in the thymus is the early T-cell progenitor (ETP). The phenotype of the cells that seed the thymus remains controversial, but has been termed lineage negative. A fraction of the DN1 subset ( $CD44^+CD25^-$ ) then moves to the outer regions of the thymic cortex and transition to DN2 cells by gaining expression of  $CD25^{3,4}$ . Thymocytes are committed to T cell lineage during the DN2 to DN3 transition. DN3 ( $CD44^{lo}CD25^+CD117^{lo}$ ) thymocytes undergo  $\beta$  chain rearrangement and selection.

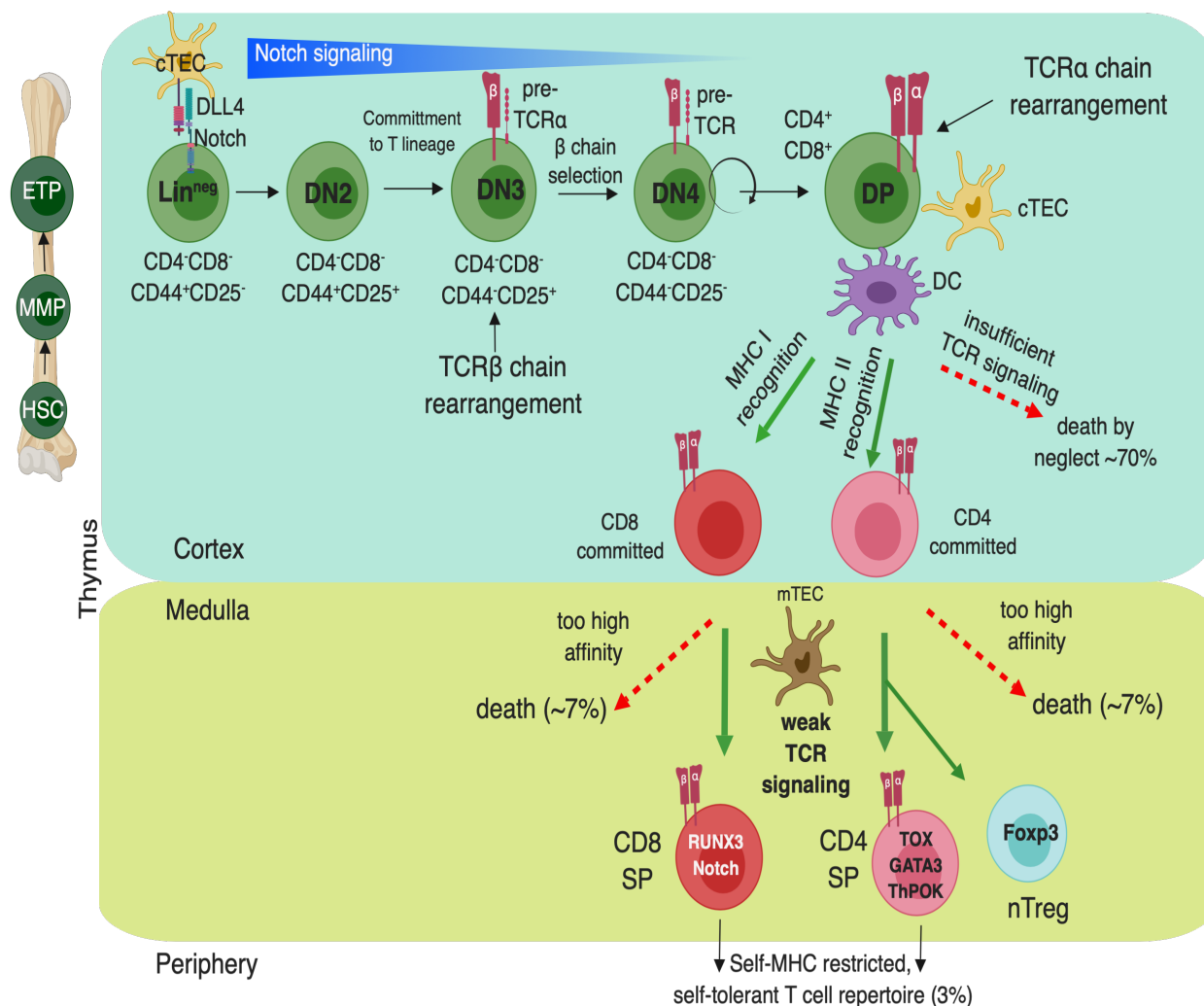


**Figure 1. T Cell Development in the Thymus.** The lineage negative ETP enters the thymus and becomes a DN2 thymocyte by acquiring expression of CD25. DN3 (CD44<sup>lo</sup>CD25<sup>+</sup>CD117<sup>lo</sup>) thymocytes undergo β chain rearrangement and selection. The TCRβ chain pairs with the pre-Tα chain, leading to RAG termination and allelic exclusion. If successful, DN3 become DN4 (CD44<sup>+</sup>CD25<sup>-</sup>CD117<sup>lo</sup>) thymocytes that proliferate and express CD4 and CD8. CD4<sup>+</sup>CD8<sup>+</sup> DP thymocytes rearrange TCRα chain alleles until a TCRαβ heterodimer engages with self-MHC and undergoes positive selection. Positively-selected CD4 or CD8 committed T cells encounter APCs and, based on affinity, become CD8<sup>+</sup> or CD4<sup>+</sup> (or nTreg cells) SP T cell that can enter the periphery. Red dashed arrows represent negative selection events and green arrows represent positive selection events. (HSC: hematopoietic stem cell; MMP: multipotent progenitors; CLP: common lymphoid progenitor; cTEC: cortical thymic epithelial cell; DN: double negative; DLL4: delta-like ligand 4; mTEC: medullary thymic epithelial cells; DC: dendritic cell; SP: single positive

TCR gene rearrangement requires transient expression of recombination-activating genes (RAG)<sup>5</sup>. Once the TCR $\beta$  chain pairs with the surrogate pre-T $\alpha$  chain and CD3 on the cell surface, RAG expression is downregulated and TCR  $\beta$  chain gene rearrangement is terminated, referred to as allelic exclusion<sup>6–8</sup>. If TCR $\beta$  chain gene rearrangement is successful, DN3 thymocytes become DN4 (CD44<sup>+</sup>CD25<sup>+</sup>CD117<sup>lo</sup>) thymocytes that undergo proliferation and express CD4 and CD8. Conversely, if  $\beta$  chain rearrangement on both alleles is unsuccessful, these thymocytes die by apoptosis. CD4<sup>+</sup>CD8<sup>+</sup> double positive (DP) thymocytes then relocate to the thymic cortex where rearrangement of TCR $\alpha$  chain alleles occurs. In contrast to  $\beta$  chain selection, both TCR  $\alpha$  chain alleles rearrange until a TCR $\alpha\beta$  heterodimer engages with self-MHC and undergoes positive selection. Positive selection occurs if a DP TCR $\alpha\beta$  thymocyte has the adequate affinity and reacts against self-peptide MHC presented by cortical thymic epithelial cells<sup>9</sup>. If the affinity is too low and antigen recognition does not occur, DP TCR $\alpha\beta$  thymocytes undergo death by neglect<sup>10</sup>. Positively selected DP T cells then encounter antigen presenting cells (APC) with high expression of self-peptide-MHC complexes. Initial TCR stimulation partially downregulates CD8 and upregulates the TCR. If DP T cells bind to thymic APCs with too high affinity, they undergo negative selection by apoptosis<sup>11</sup>. Lack of signaling results in MHC class I restriction and conversely, sustained signaling promotes MHC class II restriction<sup>12</sup>. Within a few days, mature, naïve T cells emigrate from the thymus and enter the periphery<sup>13</sup>.

**T cell receptor diversity.** TCR gene rearrangement, or somatic diversification, in the thymus generates TCRs with up to 100 million different specificities<sup>14</sup>. TCR genes are encoded from an extensive set of noncontiguous gene segments. The TCR $\alpha$  and

TCR $\beta$  chains each contain a variable (V) amino-terminal segment and a constant (C) segment. The TCR $\alpha$  locus contains V and joining (J) segments (V $\alpha$  and J $\alpha$ ). The TCR $\beta$  locus consists of V $\beta$  and J $\beta$  segments and additional diversity (D) gene segments. During TCR $\beta$  gene rearrangement in the thymus, one D $\beta$  segment and one J $\beta$  segment join, and then randomly combines with one of several V $\beta$  genes. During TCR $\alpha$  chain gene rearrangement, one of several V $\alpha$  genes combines with one of several J $\alpha$  genes. Recombination is mediated by heptamer and nonamer recombination signal sequences (RSS) that flank the gene segments. RSS are recognized by RAG enzymes, which create double-stranded breaks that are resolved by nonhomologous end joining. TCR diversification is further achieved through the addition and deletion of a random number of nucleotides at the V(D)J junction sites, referred to as N-region substitution<sup>15</sup>.

In addition to the already extensive diversity generated by V(D)J recombination and N-region substitution, three hypervariable loops that are called complementarity determining regions (CDR1-3) also contribute to further diversification and antigen binding<sup>16</sup>. CDR1 and 2 are found in the V region of the polypeptide chain and mediate TCR-peptide-MHC interactions. CDR3, which includes the N-region, some of the V, and the D and J regions, directly contacts the peptide<sup>17–19</sup>. CDR3, the most variable region, is used to determine T cell clonotypes<sup>20</sup>. Advanced technology, such as high-throughput sequencing, can efficiently permit in-depth measurements of TCR repertoire diversity from a single sample of blood, thus facilitating the study of TCR diversity in different contexts<sup>21</sup>. In summary, the extensive diversity of the TCR, generated by recombination, random insertions, deletions, and substitutions, is fundamental for adaptive immunity.

**T cell signaling and activation.** T cell function is controlled through TCR

activation and signaling. To generate fully functional T cells, three signals must usually be completed: 1) TCR engagement, 2) co-stimulation and 3) cytokine production.

First, the TCR must bind to cognate antigen presented by MHC proteins on the surface of an antigen presenting cell (APC). This initial interaction is insufficient for activation (most of the time) and requires additional help from the co-receptors, CD4 and CD8. CD4 or CD8 binds to MHC class II or MHC class I domains, respectively, to stabilize the protein complex<sup>22,23</sup>. Co-receptor-MHC interactions lead to conformational changes in CD3 (CD3 $\delta$ , CD3 $\epsilon$ , CD3 $\gamma$ ) proteins that are proximal to the TCR-peptide-MHC complexes. The CD3 and TCR $\zeta$  chain cytoplasmic domains contain immunoreceptor tyrosine-based activation motifs (ITAMs) composed of two tyrosines flanking a series of amino acids, including essential leucine and isoleucines with stereotypic spacing. ITAMs are phosphorylated by leukocyte-specific tyrosine kinase (Lck), which associates with the cytoplasmic tail of CD4 and CD8 co-receptors, allows docking of the SH2 domains of the  $\zeta$  chain-associated protein 70 (Zap70) kinase<sup>24</sup>. Zap70-mediated phosphorylation of adaptor proteins leads to activation of downstream signaling molecules<sup>25</sup>. The release of Ca<sup>2+</sup> from the endoplasmic reticulum (ER) into the cytosol activates calcineurin, which dephosphorylates NFAT (nuclear factors of activated T cells), allowing entry into the nucleus to induce gene transcription. Collectively, this first signal results in Ca<sup>2+</sup> release, cytoskeletal rearrangements, and the transcription of appropriate T cells genes<sup>26</sup>.

TCR signaling alone is usually insufficient for full T cell activation and requires the second signal, co-stimulation<sup>27</sup>. Co-stimulation can lower the threshold of signal 1 that is needed for activation by amplifying the signal<sup>28</sup>. Conversely, in the absence of

co-stimulation following signal 1, T cells can become anergic. For CD4<sup>+</sup> T helper cells, the co-stimulatory molecule CD28 binds to either CD80 (B7.1) or CD86 (B7.2) on the APC, which stimulates T cell proliferation and generates a clonal population of primed, antigen-specific T cells. Consequently, the binding of CD28 and CD4 also elicits a regulatory feedback mechanism to control T cell activation. CD28-CD80 ligation induces expression of CTLA-4 (CD152) on the T cell surface, which competes with CD28 for binding CD80, limiting T cell activation<sup>29,30</sup>. Cytotoxic T cells rely on a slightly different mechanism for signal 2. Less reliant on CD28, CD8<sup>+</sup> T cells require signals from other co-stimulatory molecules, such as CD70 and 4-1BB (CD137). With regards to tumor immunity, the absence of CD80/CD86 on cancer cells, required for signal 2 of T cell activation, can lead to tolerance, or subpar T cell responses<sup>28</sup>. Therefore, co-stimulation, the second signal, is important to amplify TCR stimulation, signal 1.

Naïve T cells require a third signal, along with antigen and co-stimulation, to achieve full activation and prevent death or induce tolerance<sup>31</sup>. The third signal comes in the form of cytokines that can dictate function. For example, activated CD8<sup>+</sup> T cells release cytotoxic granules, such as granzyme B and perforin, and produce immune-activating cytokines<sup>32</sup>. Naïve CD8<sup>+</sup> T cells that have received the first two signals required for activation, TCR-peptide+MHC engagement and co-stimulation, but had not received cytokine cues, failed to develop effector function<sup>33</sup>. Alternatively, CD4<sup>+</sup> T cells differentiate into T helper subsets according to the cytokines produced by antigen presenting cells encountered after activation (This will be further discussed in the following section). In conclusion, three signals, TCR-peptide-MHC binding, co-

stimulation, and cytokine exposure, are required to generate fully functional T cells with appropriate effector function (Fig 2).

### **T Helper Cell Subsets and Function**

A variety of factors influence the fate of T helper cells, including dose and type of antigen, APCs, and differential expression of cytokine genes and transcription factors. Upon activation of naïve CD4<sup>+</sup> T cells, extracellular cues initiate the process of phenotypic polarization of cells. Then, intracellular signaling cascades lead to signals in the nucleus to generate new gene expression profiles. The first specialized CD4<sup>+</sup> T cell subsets were identified in mice by Mosmann and Coffman in 1986 and classified as T helper (Th) 1 and Th2 subsets<sup>34</sup>.

Th1 cells are essential for immunity against intracellular pathogens. Polarization into Th1 cells occurs in the presence of IL-12, IL-2, and IFN- $\gamma$ , which then activate the transcription factors, STAT-1, T-bet, and STAT-4<sup>35</sup>. Transcription factor activation results in T cell production of IL-2, TNF- $\alpha$ , IFN- $\gamma$ , and GM-CSF that further elicit immune responses. For example, IFN- $\gamma$  production can activate macrophages and increase expression of MHC class I on APCs and some tumor cells. IFN- $\gamma$ -producing T cells have been shown to protect against the development of induced and spontaneous cancers in mouse models<sup>36</sup>. Th1 subsets can contribute to the induction of anti-tumor immune responses through the production of Th1 cytokines and chemokines, and the activation of antigen-specific cytotoxic CD8<sup>+</sup> T cells. Th1 cells also produce chemokines such as monocyte chemotactic protein-1 (MCP-1, also known as CCL2) and macrophage inflammatory protein-1 $\alpha$  (MIP-1 $\alpha$ , also known as CCL3), that can promote the recruitment of natural killer (NK) cells and M1 inflammatory macrophages to the tumor<sup>37</sup>.



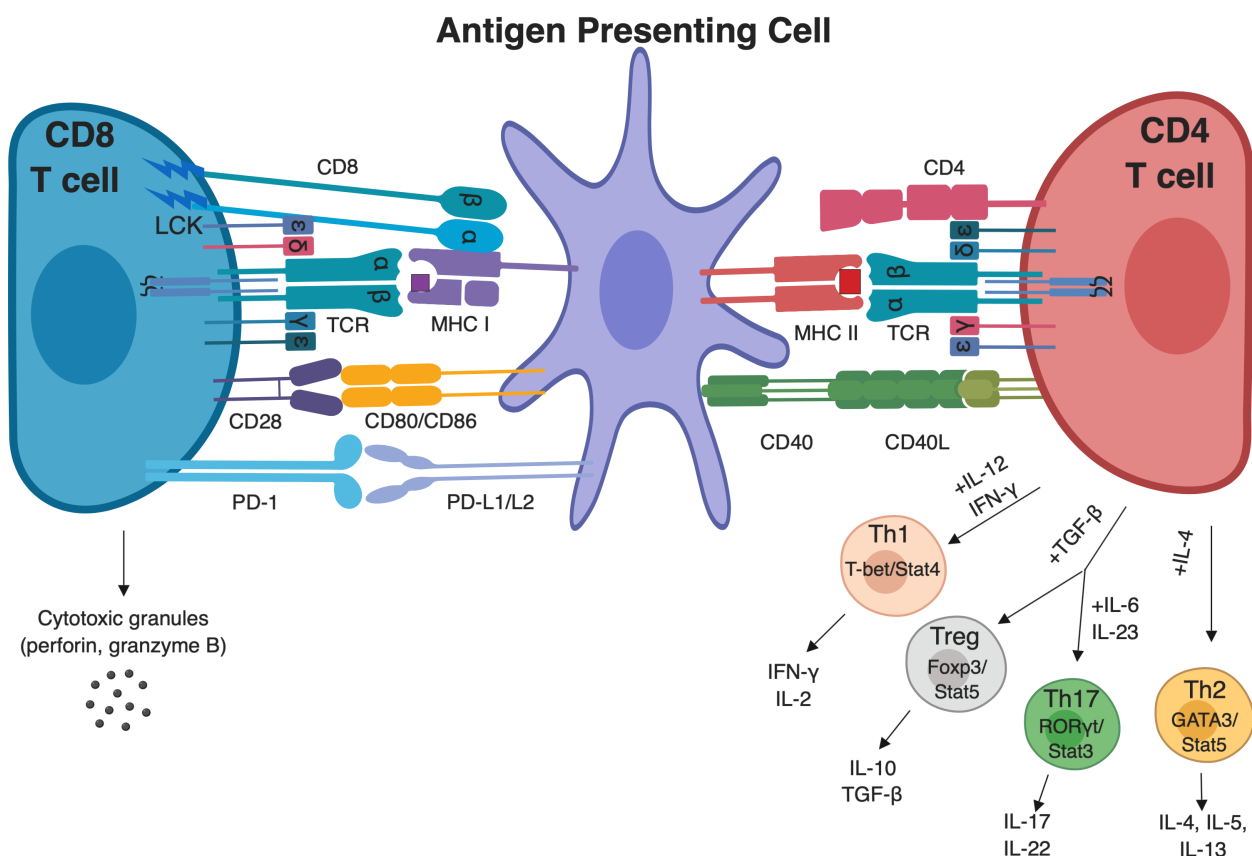


**Figure 2. Effector Functions of CD4<sup>+</sup> and CD8<sup>+</sup> T Cells Following Activation by Antigen Presenting Cells.** Dendritic cells present endogenous peptides on MHC class I molecules to CD8<sup>+</sup> T cells (left). CD8<sup>+</sup> T cells are stimulated to be cytotoxic T lymphocytes, which can directly kill targets through the release of cytotoxic granules, such as perforin and granzyme B, and production of cytokines TNF- $\alpha$  and IFN- $\gamma$ . Dendritic cells present exogenous antigens on MHC class II molecules to CD4<sup>+</sup> T cells. CD4<sup>+</sup> T cells are stimulated to become helper T cell subsets based on cytokine production by dendritic cells. In the presence of IL-12, Th1 subsets are promoted through induction of the transcription factors T-bet and Stat4. In the presence of IL-4, Th2 subsets are promoted through the induction of transcription factors GATA-3 and Stat5. In the presence of IL-6, Th17 subsets are promoted through induction of transcription factors ROR $\gamma$ t and Stat3. In the presence of TGF $\beta$ , T regulatory subsets are promoted through the induction of Foxp3 and Stat5.

Th1 cells also produce large quantities of IFN- $\gamma$ , which has a pleiotropic role in anti-tumor immunity<sup>38</sup>.

In tumor models, the adoptive co-transfer of *in vitro* polarized CD4<sup>+</sup> Th1 cells and CD8<sup>+</sup> CTL enhanced B16-OVA tumor regression, compared to CD8<sup>+</sup> CTL only, and resulted in the induction of endogenous immune responses to tumor epitopes other than OVA<sup>39</sup>. Additionally, the adoptive transfer of T-bet<sup>+</sup> Th1 *in vitro*-polarized cells into mice bearing B cell lymphoma resulted in the localization of transferred Th1 cells to the tumors and inhibition of tumor development and growth<sup>40</sup>. In summary, Th1 cells are good candidates to promote anti-tumor responses through the production of cytokines and chemokines that promote infiltration and activation of innate and adaptive immune cells.

Th2 subsets orchestrate humoral immunity and mediate responses against extracellular parasites as well as allergens. Th2 cells differentiate in the presence of IL-2 and IL-4, which leads to activation of the transcription factors GATA3 and STAT6. The effector function of Th2 cells includes production of IL-4, IL-5, IL-6, and IL-13 and activation of eosinophils and mast cells<sup>35</sup>. The production of these cytokines also supports B cell proliferation and differentiation<sup>41</sup>. The contribution of Th2 cells to anti-tumor immunity is still somewhat unclear and may be context-dependent. In one mouse study, B16 tumor cells engineered to express the cytokine IL-4 promoted anti-tumor responses through the recruitment of eosinophils and macrophages to the tumor<sup>42,43</sup>. Furthermore, adoptive transfer of *in vitro* polarized tumor-specific Th2 cells resulted in the regression of MHC class II negative mouse myelomas, which was mediated by type II inflammation and robust infiltration of inflammatory M2-type macrophages at the tumor site<sup>44</sup>. Conversely, in a mouse model of breast cancer, IL-4- and IL-13-producing Th2 CD4<sup>+</sup> T cells induced the polarization of M2 macrophages, which promoted relapse

of tumors following radiotherapy<sup>45</sup>. In summary, the role of Th2 cells in anti-tumor immune responses is most likely context- or tumor-dependent.

An additional T cell subset, Th9 cells differentiate in the presence of IL-2, IL-4, and TGF- $\beta$  and require the transcription factors STAT6, PU.1, IRF4 and GATA3 to produce IL-9<sup>46,47</sup>. Th9 cells have a role in the initiation of a broad range of inflammatory diseases such as allergic inflammation and autoimmune disorders. In tumor immunity, adoptive transfer of *in vitro* polarized Th9 cells were highly effective at suppressing B16 tumor growth, even in comparison to Th1 and Th17 cells<sup>48</sup>. Furthermore, anti-tumor benefits were abolished in the presence of an IL-9 neutralizing antibody. Additionally, in the B16 lung metastases model, IL-9-producing tumor-specific Th9 cells induced CCL20 expression in tumor cells, which promoted recruitment of DCs and activation of CD8<sup>+</sup> CTL in the tumor draining lymph nodes<sup>49</sup>. In contrast, a small frequency of IL-9 transgenic mice has been reported as susceptible to developing thymic T cell lymphomas, consistent with the role of IL-9 in mediating T cell proliferation and activation<sup>50</sup>. IL-9 has been shown to promote the survival and function of human melanoma tumor infiltrating CD4<sup>+</sup>CD8<sup>+</sup> double-positive T cells<sup>51</sup>. These findings suggest that IL-9-producing Th9 cells can promote anti-tumor immunity, but dysregulated IL-9 signaling might lead to T cell lymphomas through aberrant T cell stimulation.

Th17 cells are polarized in the presence of IL-6, IL-21, IL-23, and TGF- $\beta$  eliciting a signaling cascade that activates the transcription factors ROR $\gamma$ t and STAT3. Transcription factor activation results in the production of IL-17 and IL-22, which activate neutrophils and protect the host against extracellular pathogens, such as fungi. In cancer immunity, Th17 cells have been reported to both promote and inhibit anti-tumor

responses. The expression of IL-17 in the tumor microenvironment has been reported to induce angiogenesis and tumor progression through increased tumor-mediated production of pro-inflammatory cytokines. IL-17A also induces activation of STAT3 in tumor cells, which has been demonstrated to promote B16 tumor growth<sup>52</sup>. In a contrasting example, the adoptive transfer of tumor-specific Th17 cells, polarized *in vitro*, supported anti-tumor responses in the B16 mouse melanoma model by recruiting dendritic cells and priming CD8<sup>+</sup> T cells in an IFN- $\gamma$ -dependent manner. Interestingly, the anti-tumor responses following the adoptive transfer of Th17 cells were more effective than the adoptive transfer of Th1 cells in this model<sup>53</sup>. These findings indicate that Th17 cells have the potential to promote both anti- and pro-tumor responses.

Regulatory T cells (Tregs) are critical for regulating immune responses and maintaining immune tolerance. In the early 1970s, Gershon and Kondo performed experiments in which mice were immunized and challenged in the presence and absence of thymic-derived cells and established two different roles for thymic-derived cells: immune-activation and immune-dampening<sup>54</sup>. In 1995, Sakaguchi and colleagues facilitated the characterization of the immune-suppressing subset through the identification of CD25, the IL2R $\alpha$  chain, expressed on CD4<sup>+</sup> T cells<sup>55</sup>. A pivotal moment in Treg biology was the discovery of the transcription factor Foxp3 in 2001. Mutations in the FOXP3 gene were linked to severe spontaneous autoimmunity in Scurfy mice<sup>56</sup>. Foxp3 is now recognized as the main regulator of the development and function of natural Tregs (nTregs).

While natural Tregs develop in the thymus, inducible Tregs (iTregs) are generated when naïve T cells acquire Foxp3 expression and suppressive functions after

antigen stimulation in the presence of TGF- $\beta$  or after suboptimal chronic antigen stimulation<sup>57</sup>. Several preclinical and clinical studies have illustrated the ability of Tregs to suppress anti-tumor immunity. Tregs exert immunosuppressive effects through various mechanisms such as CTLA-4-mediated suppression of APCs, sequestering of IL-2, and production of immune inhibitory factors<sup>58</sup>. Tumors can promote the accumulation of Tregs, as supported by studies detecting intratumoral Treg frequencies as high as 20-30%, which is associated with a poor prognosis in various types of cancer<sup>59</sup>. In one mechanism, melanoma cells can secrete CCL22 that promotes infiltration of Foxp3<sup>+</sup> Tregs<sup>60</sup>. Additionally, tumor-derived suppressive factors can convert T effector subsets into Tregs through the induction of Foxp3<sup>61</sup>. Many Treg-focused therapies are under investigation but have been mostly ineffective clinically due to the difficulty in selectively targeting Tregs or the transient nature of the effects. Overall, T regulatory cells are critical regulators of immune responses that function to maintain homeostasis and prevent autoimmunity, but also are potent suppressors of anti-tumor immune responses. In summary, naïve CD4<sup>+</sup> T helper cells have the capacity to execute an extensive range of immune responses.

Although studies using mouse models have been invaluable to the advancement of scientific discoveries, they can have limitations. Some difficulties associated with using mouse models for human disease result from differences in metabolism, anatomy, and cellular characteristics<sup>519</sup>. Animals can be essential to transition from bench to bedside solutions, but it should be noted that animal models only represent part of the disease. Therefore, it is important to define a certain question to design and conduct an appropriate experiment using mouse models.

## T Cell Alloresponses

T cells, by way of their TCR, not only recognize antigens presented by self-MHC, but can also recognize non-self-peptide-MHC complexes as foreign in an allogeneic response. MHC mismatch is most commonly discussed in transplantation biology, where the recognition of allogeneic MHC molecules by recipient T cells (allorecognition) ignites a potent immune cascade ultimately resulting in the rapid elimination of the foreign donor cells and rejection of the graft. This section will discuss the foundation of allorecognition, the biology of the allogeneic response, and how allorecognition can be applied to tumor immunology and immunotherapies.

**History.** The allogeneic response is one of the oldest known immune reactions, dating back to 1944 when Medawar was studying allograft rejections<sup>62</sup>. In the early 1960s, alloreactive cells undergoing DNA synthesis were observed using radioactive labeling techniques after co-culturing blood samples from two individuals<sup>63</sup>. Soon after, human lymphocytes were identified as the alloreactive cells<sup>64</sup>. Advancements in understanding the genetic basis of alloreactivity were initiated when Bain and colleagues observed increased replication of alloreactive cells in co-cultures with blood samples from unrelated individuals compared to monozygotic twins<sup>65</sup>. The purpose of an immune reaction between two individuals of the same species was unclear, and therefore alloreactivity was initially thought of as biologically irrelevant. However, the study of alloreactivity paved the way for a series of important discoveries, such as evaluating the function of histocompatibility proteins<sup>65</sup>, identifying a central role for T cells<sup>66</sup>, the phenomenon of graft-versus-host disease (GVHD)<sup>67</sup>, and the function of cytotoxic T lymphocytes<sup>68</sup>.

**Pathways of allorecognition.** Despite undergoing an extensive selection process in the thymus, mature T cells exhibit a high frequency of cross-reactivity, or alloreactivity, against foreign peptide-MHC molecules to which they have not previously encountered. CD4<sup>+</sup> and CD8<sup>+</sup> T cells can respond to foreign donor determinants through two distinct mechanisms: direct or indirect alloreactivity. In the direct pathway, T cells recognize allo-MHC complexes present on the surface of APCs in the donor graft; alternatively, the indirect pathway occurs through recognition of self-restricted allopeptides, derived from allogeneic peptides or allogeneic MHC molecules, that have been processed and presented on APCs of the recipient<sup>69,70</sup>. Distinguishing features of the two pathways include the breadth of TCR repertoire, the timing of the responses, and the persistence of alloreactive T cells<sup>71</sup>.

During direct alloreactivity, T cells that were selected to bind non-self- peptide and self-MHC cross-react with non-self MHC and peptide complexes<sup>69</sup>. Direct allorecognition is the main contributor to cytotoxic T lymphocyte (CTL) responses that promote GVHD and early allograft rejection events<sup>72</sup>. Indirect alloreactivity occurs when donor T cells recognize minor histocompatibility antigens, which are peptides expressed by host polymorphic genes. Whereas direct allogeneic responses quickly diminish with the disappearance of donor cells, it is generally thought that the indirect pathway mediates chronic rejection<sup>73</sup>. T cells recognizing self-restricted allopeptides display limited TCR gene usage<sup>74</sup>. In acute GVHD, *in vivo* clonal expansion of T cells with selected TCR usage has been observed and can persist for up to one year<sup>75,76</sup>.

**Alloantigens.** Any antigen or group of antigens expressed on donor cells, but not expressed on cells of the recipient are considered allogeneic non-self<sup>77</sup>. Allogeneic

non-self-antigens are mostly MHC protein products, the MHC class I-related chain (MIC) system, minor histocompatibility proteins, and natural killer cell receptor ligands. The strongest alloantigens are major histocompatibility complex (MHC) proteins, due to their highly polymorphic nature, broad expression and capacity to generate expansive polyclonal T cell responses. These alloantigens can be recognized by T cells either directly or indirectly. Minor histocompatibility antigens (MiHA) are also highly polymorphic and expressed on the cell surface in association with MHC proteins. MiHA alloresponses are generally weaker; however, they are clinically significant especially in bone marrow transplant recipients. The rejection of grafts based on MHC mismatch occurs rapidly, whereas MiHAs slowly induce graft rejection.

MiHAs are short peptides with 9-12 amino acids that differ between individuals as a consequence of single- nucleotide polymorphisms (SNPs) in the coding regions of genes, gene deletions, frameshift mutations, or insertions<sup>78,79</sup>. Generation of MiHAs through the MHC class I antigen presentation pathway involves proteasomal processing followed by TAP-dependent transport to the ER for binding to MHC class I. Alternatively, MHC class II-associated MiHAs are non-self- proteins from phagocytosis or endocytosis. Because of the ubiquitous expression of MiHAs, graft rejection can occur despite identical MHC proteins<sup>80</sup>.

**Effector response.** The T cell-mediated allogeneic response is one of the most potent immune responses identified. The frequency of T cells that respond to allogeneic MHC molecules is  $\geq 1\%$ , which is 2-3 orders of magnitude higher than the frequency expected for a foreign non-MHC molecule<sup>81</sup>. The most well-studied alloresponse is graft-versus-host disease (GVHD). This section will discuss two alloresponses that are



currently being investigated. The first alloresponse will be graft-versus-host disease and the second alloresponse will be graft rejection.

**Graft-versus-host disease.** Immune cells and molecules mediate the pathology of GVHD. Acute GVHD is preceded by elevated CD4<sup>+</sup> and CD8<sup>+</sup> T cells while chronic GVHD is preceded by thymic damage, generation of aberrant B cells, and dysfunctional T cell responses<sup>82</sup>. Prior to transplantation, patients receive a conditioning regimen that damages host tissue and mucosa leading to microbial products that translocate from the intestinal lumen into circulation, which stimulate and activate DCs to secrete IL-1 and TNF- $\alpha$ <sup>83</sup>. Donor conventional DCs can take up antigens through the indirect pathway via MHC II to CD4<sup>+</sup> T cells<sup>84</sup>. Alternatively, recipient CCR7<sup>+</sup> DCs induced donor T cells to upregulate chemokine receptors allowing the migration of activated DCs from the tissue to the draining lymph nodes. Donor T cells first recognize host alloantigens, followed by production IFN- $\gamma$ , TNF- $\alpha$ , and IL-2, which collectively can mediate robust proliferation of allo-specific CD8<sup>+</sup> T cells and recruit macrophages and CD8<sup>+</sup> T cells to the graft<sup>85</sup>. Furthermore, CD4<sup>+</sup> T cells can stimulate B cells to produce highly specific alloreactive antibodies. The relationship between Th17 and Treg cells can play a role in GVHD<sup>86</sup>. Treg expansion can lessen the severity of GVHD. Conversely, a decrease in Tregs can result in the increased production of pro-inflammatory cytokines by Th17 and Th1 cells<sup>87</sup>. CD8<sup>+</sup> T cells also contribute to allogeneic responses by exerting cytolytic function against the donor cells within the graft.

TNF- $\alpha$  is a key cytokine that plays a role during all stages of GVHD. Blocking TNF- $\alpha$  diminished GVHD-related damage to the gastrointestinal tract in experimental allo-HSCT<sup>88</sup>. Additionally, elevated levels of Th17-related cytokines, such as IL-6, IL-1 $\beta$ ,

IL-17, IL-21, IL-23, and IL-23R, have been observed in patients with GVHD and associated with the differentiation and expansion of Th17 cells<sup>89</sup>. Conversely, regulatory cytokines can suppress GVHD. IL-10, for example, can be produced by both host and donor B cells. IL-10<sup>-/-</sup> mice had increased allogeneic T cell responses, enhanced activation of host DCs in lymphoid tissue, and accelerated GVHD<sup>90</sup>.

Co-stimulatory molecules, such as the CD80/86-CD28 family, the TNF receptor family, and adhesion molecules, can also have an important role in the development of GVHD<sup>91</sup>. Blocking CD80 and CD86 with monoclonal antibodies lowered the mortality rate in a mouse model of GVHD by preventing donor CD4 and CD8 T cell expansion<sup>92</sup>. Blocking CTLA-4 with a soluble fusion protein also reduced GVHD in mice, but the effects were not as strong as blocking CD28<sup>93</sup>. Inducible co-stimulatory (ICOS) is expressed on CD4 and CD8 T cells and facilitates P13K activation and intracellular calcium release. ICOS was upregulated on T cells isolated from dogs that were in the process of developing GVHD<sup>94</sup>. These studies highlight the therapeutic potential of modulating cytokines and blocking co-stimulatory molecules in treating GVHD.

Beilhack and colleagues performed an in-depth characterization of the events mediating GVHD following the transplantation of luciferase-labeled allogeneic splenocytes<sup>95</sup>. Using *in vivo* bioluminescence imaging, they first observed donor CD4<sup>+</sup> T cell proliferation, followed by CD8<sup>+</sup> T cell proliferation, in secondary lymphoid organs. Transplanted T cells then migrated to end-organs, including the intestines by day 5, and skin and liver acutely within 6 days of transplantation. Robust activation of CD4<sup>+</sup> and CD8<sup>+</sup> T cells, characterized by increased expression of CD69 and CD44 by immunofluorescence, also occurred acutely in secondary lymphoid organs. These

studies demonstrated the rapid kinetics and magnitude of immune activation generated during acute alloresponses.

**Graft rejection.** Acute allograft rejection prevents long-term graft survival, increases the risk for chronic rejection and decreases the half-life of the allograft by 34%<sup>96</sup>. The passenger leukocyte theory proposed that graft-derived cells had a role in the alloresponse<sup>97</sup>. Specifically, donor dendritic cells are largely responsible for promoting an acute anti-allograft response. Immature DCs in peripheral tissues can capture antigens and, upon receiving inflammatory signals- IL-1 $\beta$ , TNF- $\alpha$ , and CD40, mature and migrate to lymphoid tissue to stimulate naïve T cells<sup>98</sup>. The activated graft-specific T cells migrate back to the graft and eliminate alloantigen-expressing cells. Once the donor leukocytes have been eliminated from the graft, the response shifts to recipient DCs that have infiltrated into the graft and activate T cells via the indirect pathway<sup>99–101</sup>. T regulatory (Treg) cells can also influence graft rejection. Recipient and donor Treg cells have been detected within tolerized allografts<sup>102,103</sup>. Collectively, these studies demonstrate that graft rejection is a complex response influenced by both recipient and donor cells.

**Alloresponses in cancer.** Donor immune cell reactivity against host tissues and allograft rejection by the host can have severe consequences, but in some instances, the allogeneic response can have therapeutic benefits. The induction of mismatched donor immune cells into an allogeneic recipient with cancer can consist of three distinct allogeneic responses: 1) recipient T cell reactivity towards the graft (allograft rejection in immunocompetent hosts) 2) donor T cell reactivity towards normal host tissues (GVHD) or 3) donor T cell alloreactivity towards tumor (graft-versus-cancer). Allogeneic stem cell

transplantation has been adopted into a form of immunotherapy, harnessing the graft-versus-cancer effect for tumor control in patients with various hematologic malignancies<sup>104</sup>. For example, in cases of graft-versus-leukemia (GVL), the engrafting allogeneic hematopoietic stem cell transplant (HCT) graft includes cytotoxic T cells that recognize minor histocompatibility antigens (MiHA), polymorphic peptides presented in the context of (self)-HLA molecules as foreign antigens, thus rejecting and eliminating residual tumor cells<sup>105</sup>.

The efficacy and toxicity of allogeneic stem cell transplantation are dependent on the ability to control the immune reactivity between donor and host by selecting the degree of MHC incompatibility and the administration of immunosuppressive drugs. Several studies have demonstrated that the MiHAs that induce GVHD are potential candidates for a graft-versus-tumor response after allogeneic stem cell transplantation<sup>105–108</sup>. Because most MiHAs are a product of donor and recipient SNPs, it is possible to genotype patients and predict MiHA reactivity prior to transplant<sup>109</sup>. In one study, Marijt *et al.* used *in vitro*-selected and -expanded MiHA-specific T cells to treat patients with relapsed leukemia after allogeneic stem cell transplantation<sup>110</sup>. They concluded that this approach was feasible and capable of inducing GVL leading to complete remission in two of eight patients. In summary, therapeutic decisions should evaluate several MiHAs and select those anticipated to have the most impact on clinical outcomes.

Allogeneic DCs have also been tested as potential cancer therapeutics. Intratumoral delivery of allogeneic DCs that were matured in the presence of TLR ligands and IFN- $\gamma$  has been demonstrated as feasible and capable of inducing T cell-

mediated responses that might prolong survival of patients with metastatic renal cell carcinoma<sup>111</sup>. One possibility is that the allogeneic DCs promoted the production of immune-potentiating cytokines and activating factors that can activate immune cells independent of MHC restriction<sup>112</sup>. The Th1 alloresponse can also contribute to the generation of anti-tumor immunity<sup>113</sup>. Additionally, allogeneic DCs might serve as an “off-the-shelf” immunotherapy, focusing on local bystander immune cell activation and eliminating the need for personalization. In conclusion, the use of allogeneic immune cells for cancer immunotherapy is a promising strategy to stimulate recipient immune responses.

### **T Cell Cross-Priming**

#### **Historical Significance**

The presentation of exogenous antigen on MHC class I molecules is termed cross-presentation and is essential for APCs to induce CD8<sup>+</sup> T cell responses. Antigen cross-presentation was initially described in the context of CD8<sup>+</sup> T cell responses to grafts. In the 1970s, Bevan and colleagues demonstrated that engrafting H-2<sup>dx<sup>b</sup></sup> F1 mice with splenocytes from H-2<sup>b</sup> mice generated CD8<sup>+</sup> T cells restricted by host MHC class I H-2<sup>d</sup>. Evidence of recipient CD8<sup>+</sup> T cell activation suggested that the grafted cells contained minor histocompatibility antigens that were “cross-presented” by recipient antigen presenting cells that primed CD8<sup>+</sup> T cells<sup>114,115</sup>. This phenomenon was termed antigen cross-presentation, or T cell cross-priming.

Years later, dendritic cells (DC) were identified as the most potent inducers of cross-priming among antigen presenting cell subsets<sup>116</sup>. As professional APCs, DC are highly efficient at internalizing antigens that undergo further processing for presentation

on MHC class I or MHC class II complexes<sup>117,118</sup>. DCs generally reside as immature APCs within tissues until they capture antigen. Mature DCs upregulate MHC class II, CCR7 and additional co-stimulatory molecules and traffic to lymph nodes to stimulate antigen-specific CD4<sup>+</sup> and CD8<sup>+</sup> T cell responses. During the classical pathway of MHC class I antigen presentation, endogenously synthesized cellular proteins are ubiquitinated or trimmed by cytosolic peptidases followed by proteasomal degradation. Some of the resulting peptides are transported to the ER lumen or further trimmed by ER-associated proteases and loaded onto MHC class I complexes, which then enter the secretory pathway for cell surface expression and potential CD8<sup>+</sup> T cell engagement<sup>119</sup>. In contrast, the MHC class I cross-presentation pathway involves the uptake of exogenous antigens by DC, which are then processed and presented to CD8<sup>+</sup> T cells. The following sections will discuss the mechanisms of antigen cross-presentation, specialized DC subsets that excel at antigen cross-presentation, factors that influence antigen cross-presentation, and the importance of antigen cross-presentation in cancer immunotherapy.

### **Cell Biology of Antigen Cross-Presentation**

Dendritic cell-mediated MHC class I presentation of exogenous antigens can occur through two different pathways (Fig 3). The first, and most common, is the cytosolic pathway, which entails endosomal antigen uptake followed by translocation to the cytosol of the APC<sup>120,121</sup>. The second is the vacuolar pathway and involves the generation of peptides by lysosomal proteases within the phagosome and is less relevant *in vivo*<sup>122</sup>. The following sections will discuss the acquisition of antigen, intracellular pathways, and immunological outcomes in regards to T cell cross-priming.

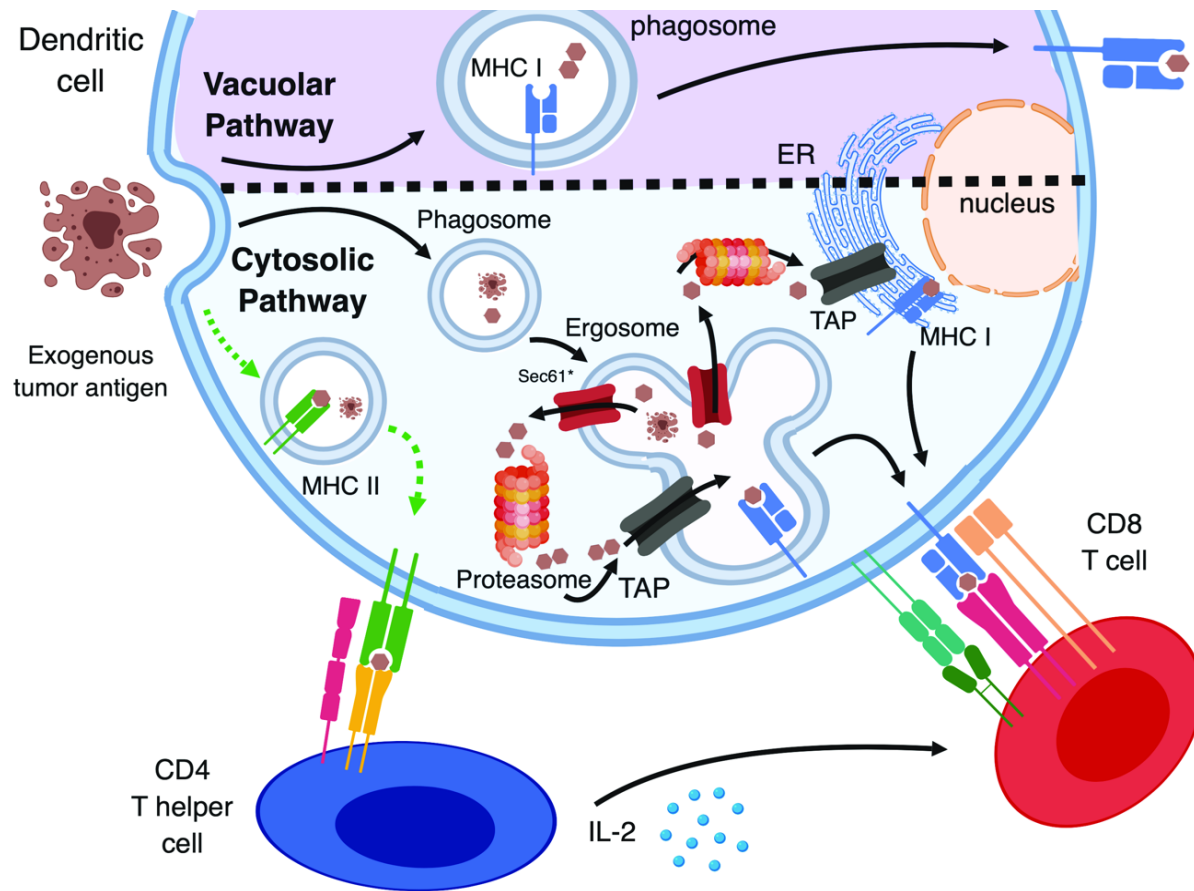


**Figure 3. Pathways of Antigen Cross-Presentation by Dendritic Cells.** The two known pathways for antigen cross-presentation are the vacuolar (top purple half) and cytosolic (blue lower half). In the vacuolar pathway, antigens are degraded by lysosomal proteases and peptides are loaded onto MHC class I in the phagosome. In the cytosolic pathway, internalized antigens are transported from the ergosome to the cytosol where they are degraded by the proteasome. TAP is required for transport into the ER or back into the ergosome for loading on to MHC class I. The black arrows indicate the pathways of MHC class I cross-presentation of exogenous antigens. The green arrows depict the classical MHC class II pathway for presentation of exogenous antigens, for reference.

**Acquisition of antigen.** The acquisition of antigen for MHC class I presentation is a highly complex process that has been extensively studied. The two principal sources of antigens for MHC class I presentation are derived from intracellular and extracellular environmental proteins. Intracellularly-derived cytosolic antigens, such as

viral proteins, are the most common source of peptides presented by MHC class I<sup>123</sup>. The classical MHC class I pathway is ubiquitous in cell types expressing MHC class I. Dendritic cells (DCs), however, have a remarkable ability to cross-present extracellular antigens for MHC class I presentation. To a lesser extent, B cells and macrophages are also capable of antigen cross-presentation. The canonical cytosolic pathway entails the transfer of antigens within the endosome to the cytosol of the DC followed by protein degradation and transport to the ER lumen<sup>120,121</sup>. In the ER lumen, MHC class I molecules are stabilized until a peptide is loaded into the peptide-binding groove of MHC class I complexes. Then, the peptide-MHC class I complex is transported to the cell surface. This process requires two components: the proteasome complex to degrade proteins in the cytosol and the transporter associated with antigen processing (TAP), which transports processed antigens to the ER<sup>121,124,125</sup>. The cytosolic pathway is most commonly used by DCs for antigen cross-presentation.

The second method to achieve antigen cross-presentation is through the vacuolar pathway. In the vacuolar pathway, endolysosomal proteases (or in some cases, proteasomes) degrade antigens, and the generated peptides are loaded onto MHC-I molecules that recycle from the cell membrane<sup>126,127</sup>. Cathepsin S, a lysosomal protease, has been reported to have a critical role in the vacuolar pathway<sup>122</sup>. In contrast to the cytosolic pathway, the vacuolar pathway is TAP-independent. This pathway is less common and not well-characterized; therefore, we will focus on the cytosolic pathway.

In the cytosolic pathway, the proteasome undergoes structural changes upon IFN- $\gamma$  stimulation or DC maturation that improves the quality and quantity of the



generated peptides<sup>128</sup>. It has been postulated that limited degradation of antigen is associated with more efficient cross-presentation, as rapid antigen degradation would destroy a vast number of epitopes before they could adequately be processed and loaded onto MHC class I molecules<sup>129</sup>. One might imagine that prolonged cross-presentation would be required to cross-prime CD8<sup>+</sup> T cells after migrating to the draining lymph nodes. In agreement with this hypothesis, the endosomes within DCs, compared to macrophages, have lower levels of proteases and higher pH levels, which restrict antigen degradation<sup>130</sup>. In both human and mouse DCs, phagosomes express NADPH oxidase (NOX)-2 at the phagosomal membrane that produces low levels of reactive oxygen species (ROS) to limit acidity<sup>131,132</sup>. The prevention of acidity in phagosomes and endosomes limits antigen degradation and facilitates cross-presentation. Overall, high pH and low levels of proteases are qualities of endosomal compartments within DCs that contribute to their superior ability to cross-present antigens.

**Dendritic cell subsets and antigen cross-presentation.** While all DC subsets have similar abilities to uptake soluble and particulate antigens, specific subsets are more effective at cross-presenting antigens to T cells<sup>75–77</sup>. Conventional (or myeloid) and plasmacytoid DCs are two broad subsets capable of antigen cross-presentation; however, cross-presentation by conventional DCs (cDCs) is more common and efficient. Human tissues, except for skin, contain low frequencies of cDCs. As a result of this limitation, most studies investigating cDC cross-presentation have been performed in mouse studies.

There are two subsets of mouse cDCs, cDC1 and cDC2, found in lymphoid and

non-lymphoid tissues, respectively. The cDC1 subset is generally the most effective at antigen cross-presentation *in vivo*. In mice, cDC1 DCs are composed of CD8 $\alpha$ <sup>-</sup> and CD8 $\alpha$ <sup>+</sup> cDC1s, which predominantly reside in lymphoid tissue, and migratory CD103<sup>+</sup> cDC1s<sup>133</sup>. In humans, these subsets correspond to CD1c<sup>+</sup> (also known as blood DC antigen (BDCA)1<sup>+</sup>) and CD141<sup>+</sup> (BDCA3<sup>+</sup>) DCs, respectively<sup>133</sup>. Both mice and humans share similar transcriptional programs and genetic requirements mediating the development of cDC1 subsets<sup>134</sup>. Human and mouse cDC1 can be characterized by the expression of XCR1, which is a chemokine receptor that promotes CD8<sup>+</sup> T cell chemotaxis<sup>135</sup>. Some of these factors include high levels of TLR3, Clec9A C-type lectin, interferon regulatory factor 8 (IRF8) and basic leucine zipper transcriptional factor ATF-like 2 (BATF3)<sup>136–138</sup>.

Cross-presentation is mostly mediated by the (mouse) CD8 $\alpha$ <sup>+</sup>/CD103<sup>+</sup> cDC1 subsets *in vivo*. CD8 $\alpha$ <sup>+</sup> cDC1 predominantly execute their functions within lymphoid organs. In contrast, CD103<sup>+</sup> cDC1 can acquire antigens in the non-lymphoid tissue sites. Early studies from the Bevan group observed antigen cross-presentation after analyzing peptide-MHC-I complexes on sorted populations of splenic DCs following the *in vivo* priming of mice with OVA peptide-loaded,  $\beta$ 2-microglobulin-deficient splenocytes. They further reported that CD8 $\alpha$ <sup>+</sup>CD11b<sup>-</sup> DCs were more efficient mediators of cross-presentation than CD8 $\alpha$ <sup>-</sup> CD11b<sup>+</sup> DCs by comparing their ability to endocytose fluorescent beads<sup>129</sup>. In contrast, migratory CD103<sup>+</sup> cDC1 can cross-present soluble and cell-associated antigens in the lung, intestine, and skin<sup>139–143</sup>. In summary, CD8 $\alpha$ <sup>+</sup>CD11c<sup>+</sup> MHC class II<sup>+</sup> DCs and CD103<sup>+</sup> CD11c<sup>+</sup> MHC class II<sup>+</sup> DCs are the most effective APC subset at cross-presenting tumor-derived antigens in the

lymphoid organs and non-lymphoid organs, respectively. The role of these cDC1 subsets in the context of cancer immunotherapy will be discussed further in a future section.

### **Factors Influencing Cross-Presentation**

As mentioned, specific DC subsets are more effective than other antigen presenting cells at antigen cross-presentation. Other factors that influence cross-presentation are means of antigen internalization, type of antigen, and status of DC maturation, which will be discussed in this section.

**Means of antigen internalization.** DCs can internalize antigen through three different cellular processes: receptor-mediated endocytosis, phagocytosis, and pinocytosis. However, even though the ability of DCs to phagocytose or pinocytose soluble antigen is essential, this does not correlate with efficient cross-presentation. One study reported that antigens internalized by fluid phase pinocytosis or scavenger receptor-mediated endocytosis were quickly targeted to lysosomes and degraded by lysosomal proteases, leading to poor cross-presentation<sup>144</sup>. In contrast, receptor-mediated endocytosis of the same antigen resulted in targeting to early endosomes where the antigen was protected from degradation and efficiently cross-presented<sup>144</sup>. These findings suggest that the most effective means of antigen internalization is receptor-mediated endocytosis.

DCs express a variety of receptors that facilitate the cross-presentation of antigens to T cells. Fc receptors cross-present immune complexes (IC), composed of immunoglobulin G (IgG) antibodies bound to cognate antigen, to both CD8<sup>+</sup> and CD8<sup>-</sup> DCs<sup>145,146</sup>. In one study, human BDCA1<sup>+</sup> DCs more efficiently cross-presented the NY-

ESO-1 antigen when delivered as an antigen-antibody IC compared to when the NY-ESO-1 antigen was administered as a soluble protein<sup>147</sup>. Additionally, members of the mannose receptor (MR) family, such as CD205 (DEC-205) and Dectin-1, also mediate endocytosis of extracellular complexes followed by transport to endosomal pathways for further processing and antigen presentation<sup>144,148</sup>. Although all of these receptors play a role in mediating endocytosis, CD205 is the most effective at directing endocytosed antigens into MHC class I and MHC class II presentation pathways.

CD205 is an endocytic receptor highly expressed on cortical thymic epithelial cells and peripheral DC subsets, including the specific cross-presenting CD8<sup>+</sup> splenic/lymph node DC subset mentioned above<sup>149,150</sup>. As a member of the MR family, CD205 is a type I C-type lectin-like molecule comprised of a single polypeptide chain. The extracellular region consists of an N-terminal cysteine-rich domain (CyR), a fibronectin type II domain (FnII) and ten structurally similar C-type lectin domains (CTLDs)<sup>149,151,152</sup>. Dendritic cells expressing CD205 (DEC-205) present antigens on MHC class I to CD8<sup>+</sup> lymphocytes and induce a Th1-like response<sup>153</sup>. This was demonstrated by Bonifaz and colleagues using anti-CD205 antibodies conjugated to OVA. They observed stronger CD8<sup>+</sup> T cell-mediated immunity when OVA was targeted to CD205 compared to other forms of antigen delivery<sup>148,154</sup>. These findings highlight the therapeutic potential of targeting antigens to CD205<sup>+</sup> DCs.

**Types of antigens.** Several types of antigens are capable of being cross-presented to T cells, including soluble proteins, immune complexes, and microbial components<sup>155,156</sup>. Antigens can also be conjugated to either antibodies that bind specific receptors on DCs or glycans that interact with C-type lectin receptors

(CLR)<sup>157,158</sup>. The properties of the cross-presented antigen, such as antigen dose, live or apoptotic cell-derived, modified self or mutated tumor antigen, and subcellular location within the tumor cell, can also influence DC cross-priming of T cells<sup>159–163</sup>.

Different types of antigens are more effectively cross-presented than others. Tumor antigens can be classified according to the pattern of expression of the parental gene. Mutated genes can give rise to a modified peptide that can bind HLA class I molecules, which can then be recognized by self<sup>155</sup>. Tumors express cancer germline genes, including those that encode for MAGE-type antigens, that are not expressed on normal tissue as a result of whole genome demethylation<sup>156</sup>. Genes that are expressed in specific tissue can encode for differentiation antigens, which can be expressed on both normal and tumor tissues. Antigens that are expressed more highly on tumor tissue compared to normal tissue usually occur due to the overexpression of these genes due to increased transcription or gene-amplification<sup>187</sup>. Cross-presentation *in vivo* favors cellular antigens that are highly expressed<sup>164</sup>. Differences in the cross-presentation of apoptotic- versus live cell-derived antigens have been described. Norbury *et al.* reported that proteins, instead of proteasomal-derived peptides, represent the source of cell-associated antigens entering the cross-presentation pathway<sup>165</sup>. Furthermore, when comparing cellular and soluble antigens, Li and colleagues demonstrated cellular OVA is cross-presented 50,000-fold more efficiently than soluble OVA<sup>166</sup>. Additionally, stable membrane proteins are more efficiently cross-presented than soluble, short-lived cytosolic proteins<sup>167</sup>. Targeting the melanoma antigen MART-1 to the CLR DC-SIGN using antibody- or glycan- conjugated liposomes resulted in enhanced antigen cross-presentation to MART-1-specific CD8<sup>+</sup> T cells<sup>168</sup>.

Anatomical location, such as the tissue from which tumor antigens are derived, can also influence antigen cross-presentation<sup>158</sup>. DC infiltration of solid tumors is well documented in both tumor animal models and human studies<sup>187</sup>. However, it is unknown what form of tumor antigens is captured by cross-presenting DCs. In one review, multiple potential mechanisms were described for the transfer of tumor antigens to DCs<sup>521</sup>. These mechanisms included phagocytosis of cell-associated tumor antigens, pinocytosis or endocytosis of soluble tumor antigens, HSP-bound soluble antigens, “nibbling” of tumor cell membranes, or “cross-dressing”. In summary, these studies provide evidence that cell-associated proteins, especially those derived from apoptotic cells, are the predominant source of antigens entering the cross-presentation pathway.

**Licensing of dendritic cells.** Two different outcomes are possible following DC-T cell interactions: T cell activation (priming) or T cell tolerance. The first half of this section will discuss factors that promote T cell activation. CD8<sup>+</sup> T cell activation is a tightly regulated process in order to limit destruction of normal tissues. As a result, initiation of T cell cross-priming depends on fully activated and mature DCs to provide all three signals required for T cell activation<sup>169</sup>. These appropriately activated DCs are referred to as “licensed” for T cell cross-priming<sup>170</sup>. DC licensing can occur through signals delivered via innate immune receptors and CD4<sup>+</sup> T helper cells (classical) or NKT (alternative) cells.

**Innate immune receptors.** Efficient T cell cross-priming requires stimulation through innate immune receptors called pattern recognition receptors (PRRs) on DCs. PRRs detect highly conserved pathogen-associated molecular patterns (PAMPs) on microorganisms<sup>171</sup>. PRRs can also sense damage-associated molecular patterns

(DAMPs), which are endogenous molecules released from damaged cells. The four subsets of PRRs identified thus far are Toll-like receptors (TLRs), C-type lectin receptors (CLRs), retinoic acid-inducible gene (RIG)-I-like receptors (RLRs) and NOD-like receptors (NLRs)<sup>172</sup>. Engagement of PRRs validates the type of antigen encountered and induces DC maturation and migration to lymphoid tissues to cross-prime T cells<sup>173</sup>.

Stimulation through PRRs generally induces expression of genes important for inflammatory processes, such as pro-inflammatory cytokines, type I interferons (IFNs), and chemokines<sup>171</sup>. Inflammatory cytokines critical to DC licensing include IL-1- $\beta$ , TNF- $\alpha$ , and IL-6. Additionally, cross-presenting DCs and cross-primed CD8<sup>+</sup> T cells can produce GM-CSF, which has been demonstrated to enhance antigen cross-presentation by DCs<sup>174</sup>. Zhan and colleagues observed that GM-CSF transgenic mice infected with *Listeria monocytogenes* exhibited an increase in antigen cross-presentation, which occurred by promoting the uptake of antigens by CD8<sup>+</sup> DCs and inducing expression of CD103. In a tumor model, vaccinating B16 tumor-bearing mice with irradiated, GM-CSF-producing B16 tumor cells elicited robust, specific, and durable anti-tumor responses<sup>175</sup>. Type I IFNs, especially IFN- $\alpha$ , are also potent inducers of antigen cross-presentation by DCs through several mechanisms. Type I IFNs promote the persistence of antigen by reducing the acidification rate within endosomes. Additionally, treating human DCs with IFN- $\alpha$  promotes the routing of antigens toward the MHC class I processing pathway<sup>176</sup>.

**Licensing by CD4<sup>+</sup> T helper cells.** CD4<sup>+</sup> T helper cells can also play a role in antigen cross-presentation through interacting with DCs. DCs can present the same

antigen on MHC class II to CD4<sup>+</sup> T cells and on MHC class I to CD8<sup>+</sup> T cells. CD4<sup>+</sup> T helper (Th) cells serve as a checkpoint to validate the appropriateness of the response (type of antigen and PRR stimulation). DC-CD4<sup>+</sup> Th cell interactions can upregulate the co-stimulatory marker CD40 on DCs. Upon binding to CD40L, CD40 induces downstream signals that lead to the production of IL-12 and increases expression of MHC class I and CD80/CD86 by DCs<sup>177</sup>. Licensed DCs can now engage the TCR and CD28 co-stimulatory molecules on CD8<sup>+</sup> T cells, thus culminating in efficient cross-priming of T cells<sup>178</sup>. The absence of CD4<sup>+</sup> T cell help during the priming phase results in CD8<sup>+</sup> T cells with defective effector functions and the inability to mount memory responses<sup>179</sup>.

**Cross-tolerance.** In contrast to cross-priming of CD8<sup>+</sup> T cells, “steady-state” DCs can render CD8<sup>+</sup> T cells functionally inactive<sup>180</sup>. This phenomenon termed “cross-tolerance” occurs in the absence of an inflammatory stimulus and in the presence of constitutive exposure to self-antigens<sup>181</sup>. For example, in the absence of an inflammatory stimulus, CD8<sup>+</sup> T cell tolerance was induced *in vivo* when CD205-targeted antigens were delivered to DCs in mice<sup>154,182</sup>. Cross-tolerance can also result in the deletion of self-reactive CTL<sup>182–185</sup>. Elimination of self-reactive CTL can occur when naïve CD8<sup>+</sup> T cells recognize peptide-MHC complexes, but do not engage or express co-stimulatory molecules<sup>182,183</sup>. While the induction of peripheral tolerance is critical to prevent over-stimulation of immune cells and autoimmunity, this can also negatively impact the ability to generate effective anti-tumor immune responses.

### **T Cell Cross-Priming in Cancer Immunotherapy**

In the 1990s, the Levitsky group provided early evidence that suggested that



antigen cross-presentation drove anti-tumor immunity<sup>186</sup>. They sought to determine the relative role of tumor- versus host-derived APCs to prime CD8<sup>+</sup> T cells. Mice were immunized with MHC class I-expressing or MHC class I-deficient B16 tumors and subsequently challenged with a lethal dose of live MHC class I<sup>+</sup> tumors. Strikingly, they observed that immunizing mice with MHC class I<sup>+</sup> or MHC class I<sup>-</sup> B16 tumors resulted in equal protection *in vivo*, indicating that host APC were capable of eliciting tumor-antigen-specific CTL in the absence of MHC class I on tumor cells<sup>186</sup>.

Generating an effective CD8<sup>+</sup> T cell response against cancer antigens, however, can be challenging to achieve. Cancer cells can engage T cells through TCR-pMHC interactions, thus inducing signal 1; however, cancer cells have developed mechanisms to inefficiently induce signal 2, which leads to tolerance. Therefore, T cells must be activated by mature APCs that have phagocytosed antigens from dying tumor cells. This has been confirmed through observations that CTL induction in secondary lymphoid tissues, while enhanced by CD28, was independent of CD80 on tumor cells<sup>187</sup>. Therefore, APC cross-priming of CD8<sup>+</sup> T cells elicits tumor-specific cytotoxic T lymphocytes that expand and migrate to the tumor where they can recognize and kill tumors cells<sup>188</sup>.

Intratumoral DCs have a critical role in anti-tumor immunity by coordinating T cell responses against tumor antigens<sup>189–193</sup>. Clinically, the frequency of tumor-infiltrating DCs has been reported to correlate with a favorable prognosis in melanoma patients<sup>194</sup>. In pre-clinical mouse models, there is mounting evidence that Batf3-lineage DCs are essential for effective anti-tumor T cell responses<sup>192</sup>. Murphy and colleagues demonstrated that mice deficient in Batf3 had reduced tumor-infiltrating CD8<sup>+</sup> T cells,

which produced inadequate tumor-specific CD8<sup>+</sup> T cell responses compared to wild type mice<sup>138</sup>. It was later demonstrated that Batf3<sup>+</sup> DCs within the tumor microenvironment produced the chemokines CXCL9 and CXCL10, which promote T cell infiltration.

It remains unclear if T cell cross-priming occurs in the tumor microenvironment or in the tumor-draining lymph nodes. CD103<sup>+</sup> cDCs can carry tumor-derived antigens from the tumor microenvironment to the tumor-draining lymph nodes, but the role of lymph node-resident DCs in tumor antigen cross-presentation is unknown. It has been proposed that CD103<sup>+</sup> DCs can transfer antigens to other lymph node DC populations<sup>195</sup>. There has been some evidence that cross-priming of T cells can occur in the tumor microenvironment, as *in situ* priming of naïve T cells has been observed in mice lacking spleens and lymph nodes<sup>196</sup>. Therefore, additional studies should be conducted to further elucidate if the tumor microenvironment is an effective site for T cell cross-priming.

Unfortunately, the tumor microenvironment can suppress the extent to which DCs can infiltrate tumors and elicit productive anti-tumor T cell responses. For example, induction of the tumor cell-intrinsic Wnt/ $\beta$ -catenin pathway inhibits recruitment of Batf3-dependent CD103<sup>+</sup> DCs into the tumor microenvironment and ultimately prevents CD8<sup>+</sup> T cell cross-priming<sup>192,197,198</sup>. The Gajewski group demonstrated that melanoma cell intrinsic  $\beta$ -catenin signaling contributed to the downregulation of CCL4 leading to a decrease in DC chemoattraction<sup>197,199</sup>. Furthermore, DCs that have infiltrated tumors often have functional deficiencies that result in impaired T cell cross-priming or even facilitate tolerance. DC-intrinsic  $\beta$ -catenin signaling also occurs in tumor-infiltrating DCs and results in defective cross-presentation and the induction of tolerance, which

generates Treg cells through TGF- $\beta$  production. Tumor-infiltrating DCs have low expression of co-stimulatory molecules and high levels of regulatory molecules<sup>200</sup>. This immunosuppressive DC phenotype can be induced by inhibitory factors secreted or expressed by tumors. For example, in a murine hepatoma model, tumor-derived factors such as TGF- $\beta$  and VEGF, converted CD11c<sup>+</sup>MHC II<sup>+</sup>CD205<sup>+</sup> DCs into tolerogenic cells that exhibited increased expression of PD-1 and impaired cross-presenting functions<sup>201</sup>. In combination with increased PD-L1/L2 expression on tumors, increased PD-1 expression on DCs can impair T cell and myeloid cell responses<sup>201</sup>. Fortunately, treatment with anti-PD-1 monoclonal antibodies has been observed to reverse this immunosuppression.

Tumor-induced suppression also affects infiltrating T cells. The conditions of the tumor microenvironment can affect the function of tumor-infiltrating immune cells. The hypoxic environment favors glycolytic metabolism<sup>202</sup>. A glycolytic shift is characteristic and a limiting factor of both T cell and DC activation and effector function<sup>203</sup>. Therefore, tumor cells and tumor-infiltrating immune cells compete for glucose within the tumor. The upregulation of T cell Ig and mucin domain 3 (TIM-3) on T cells also promotes the dampening of immune responses. Therefore, targeting these inhibitory ligands or receptors have the potential to rescue both DC and T cell effector functions in the tumor microenvironment. In conclusion, CD8 $\alpha$ <sup>+</sup>, CD103<sup>+</sup>, and CD205<sup>+</sup> DCs are critical subsets for antigen cross-presentation to CD8<sup>+</sup> T cells, a process required to generate anti-tumor immune responses. These cell types are critical targets when trying to overcome the tumor-induced immunosuppression that affects the generation of effective anti-tumor immune responses.

## **Immunotherapies to Treat Cancer**

Cancer is the second leading cause of death worldwide, with almost 10 million deaths in 2018<sup>169</sup>. In some cancer types, spontaneous regression of tumor burden has implicated the importance of host immunity. Host immune responses, such as T cell infiltration into tumors, can positively correlate with better outcomes<sup>147</sup>. Within the last decade, immunotherapies to treat various malignant cancers have shown promising results. A vast majority of these immunotherapies are designed to affect T cell responses. This section will discuss several immunotherapies that are in clinical trials or have already been FDA approved

### **Cytokines and Immune Adjuvants**

Cytokines act as messengers to induce signaling cascades that lead to rapid immune responses. Cytokines have broad anti-tumor potential such as activating numerous types of immune cells and stromal cells in the tumor microenvironment and facilitating CD8<sup>+</sup> T cell recognition of tumors. Because of their immune potentiating activity, cytokines have been tested in clinical trials for patients with metastatic disease, with two cytokines receiving FDA approval.

The first FDA-approved cytokine, IL-2, gained approval for the treatment of metastatic kidney cancer and metastatic melanoma in 1992 and 1998, respectively<sup>518</sup>. Out of 409 patients with metastatic melanoma and renal cell carcinoma receiving high dose IL-2 (720,000 U/kg, 3X/day), thirty-three (8.1%) achieved a complete response, and 37 (9%) achieved a partial response<sup>204</sup>. Durable responses observed after treatment with IL-2 provided evidence that modulating the immune system could induce anti-tumor responses.

The second FDA-approved cytokine was IFN- $\alpha$ , a type I IFN that has pleiotropic effects on multiple cell types, making it an attractive candidate for cancer immunotherapy<sup>520</sup>. IFN- $\alpha$  can induce DC maturation, stimulate cytotoxic NK and T cells responses, mediate tumor cell death and inhibit angiogenesis<sup>205</sup>. Early phase I-II clinical trials reported overall response rates of 15-17%, with one-third of patients maintaining long-term responses<sup>206–208</sup>. High-dose IFN- $\alpha$  (HDI) has also been tested in the adjuvant setting for patients with high-risk, resectable melanoma and improved relapse-free survival<sup>209,210</sup>. Furthermore, in the neoadjuvant setting, HDI treatment resulted in objective clinical responses in 55% of patients and complete pathologic responses in 15% of patients<sup>211</sup>. Currently, IFN- $\alpha$  has been approved to treat hairy cell leukemia<sup>212</sup>, follicular non-Hodgkin lymphoma<sup>213</sup>, melanoma<sup>214</sup>, and AIDS-related Kaposi sarcoma<sup>215</sup>. Some immunological events that have correlated with improved clinical responses following administration of IFN- $\alpha$  include: modulation of T cell and tumor cell signaling<sup>216,217</sup>, tumor infiltration of CD11c<sup>+</sup> and CD3<sup>+</sup> cells<sup>218</sup>, the polarization of M1 macrophages<sup>219</sup>, and acquisition of CD8<sup>+</sup> T cell effector phenotypes<sup>220</sup>.

IL-2 and IFN- $\alpha$  gained FDA approval because of their ability to induce durable responses, albeit in a small fraction of patients. Major limitations with these therapies included the low response rates and significant toxicity. In summary, IL-2 and IFN- $\alpha$  treatment can lead to clinical responses in a small subset of patients; however, there are several limitations that affect the efficacy of these immunotherapies.

Adjuvants, such as agonists of Toll-like receptors (TLRs) and stimulator of interferon genes (STING), have been utilized in cancer immunotherapy for their ability to enhance immune responses. Some adjuvants can induce the production of type I IFN

and IL-2 and consequently promote DC maturation and robust effector T cell responses. Activation of TLRs can elicit immune activation and directly lyse tumor cells<sup>221</sup>. TLR agonists can induce type I IFN production through the activation of nuclear factor- $\kappa$ B (NF- $\kappa$ B)<sup>222,223</sup>. The TLR2/4 agonist, Bacillus Calmette-Guerin (BCG), and TLR7 agonist, imiquimod, have been approved to treat patients with bladder cancer and breast cancer, respectively<sup>224,225</sup>. Additional TLR agonists under pre-clinical and clinical investigation include Ampligen<sup>226</sup> and poly I:C/poly-ICLC<sup>227–231</sup>, which target TLR3, or R848<sup>232–234</sup>, which targets TLR7/8, to treat various malignancies.

Adjuvants that target the STING pathway have also been utilized to promote robust anti-tumor immune responses and are under clinical development. The STING pathway is activated by DNA damage to induce anti-tumor immunity and inflammatory responses<sup>235</sup>. Induction of the STING pathway can lead to the production of type I IFNs, dendritic cell activation, T cell infiltration into the tumor microenvironment, and cross-presentation of tumor antigens to CD8<sup>+</sup> T cells<sup>236,237</sup>. Cytoplasmic dsDNA in cancer cells binds to and activates cGAS, an enzyme that induces production of cyclic GMP-AMP (cGAMP). cGAMP then binds to and stimulates STING<sup>238</sup>. Upon STING stimulation, conformational changes in STING recruit TANK binding kinase 1 (TBK1). TBK1 phosphorylates IRF3 and IRF3 translocates to the nucleus for induction of type I IFN production<sup>239</sup>.

Immunotherapies that stimulate innate and adaptive immune cells can promote robust and durable anti-tumor responses. In one study, the combination of two different immune modulatory drugs, IL-2/anti-IL-2 mAb complexes to target CD8<sup>+</sup> T cells and poly I:C to target innate immunity, resulted in complete tumor eradication in mice with

pancreatic tumors<sup>240</sup>. To further enhance the anti-tumor response, immune-potentiating adjuvants have been used in combination with tumor cell- or dendritic cell-based vaccines, which will be discussed in the next section.

### **Vaccine-Based Immunotherapy**

Vaccine-based immunotherapies can have both therapeutic and preventive benefits. The development of cancer vaccines entails a wide range of targets and vehicles for delivery. This section will discuss dendritic cell vaccines, tumor cell vaccines, and immune adjuvants and agonists.

**Whole tumor cell vaccines.** Vaccinations to treat or prevent cancer first utilized modified, irradiated whole tumor cells. The advantage of using whole tumor cell vaccines versus specific protein or peptide tumor antigen is the capacity to induce T cells with specificities to a broad range of antigens expressed by the tumor. This is critical especially considering that antigen loss is a prominent tumor escape mechanism. Furthermore, the immune response following vaccination can be utilized to identify novel tumor antigens or important immunological biomarkers associated with tumor control.

The use of irradiated syngeneic or allogeneic tumor cells to protect against cancer has been demonstrated in animal models and human clinical trials. Autologous tumor vaccination ensures that a patient is exposed to the same tumor antigens expressed on their tumor. Although biopsies are feasible, this would be difficult for inaccessible tumors and could become difficult to obtain sufficient numbers of tumor cells, especially if multiple rounds of vaccinations are required. Furthermore, maintaining a personalized tumor vaccine line *in vitro* would require extensive

resources<sup>241</sup>. To circumvent these issues, allogeneic tumor cell vaccines can be used. This eliminates the personalization barrier, as multiple tumor cell lines can be combined to increase the diversity and number of available antigenic targets. Although the development of anti-HLA responses can raise safety questions, some studies have demonstrated enhanced anti-tumor responses accompanied by the induction of cross-primed T cells following vaccination with allogeneic whole tumor cells<sup>242–244</sup>.

As emphasized in the above sections, combinatorial strategies have been promising to treat various cancer types. In the context of tumor cell vaccines, one way this has been demonstrated is by using allogeneic tumor cells modified to encode immune-stimulating elements, such as cytokines. A study encompassing both properties used an allogeneic tumor cell line that secreted GM-CSF to induce CD4<sup>+</sup> and CD8<sup>+</sup> T cells to prevent and treat B16-F10 melanoma<sup>245</sup>. A second study developed a whole cell B16 melanoma vaccine expressing 4-1BBL and CD80 co-stimulatory molecules that resulted in regression of live B16 tumors and induced protection against repeated challenge<sup>246</sup>. The pre-clinical results demonstrating the efficacy of these strategies have resulted in tumor vaccines entering Phase I and II trials.

One of the most successful vaccines, GVAX, consists of whole tumor cells genetically engineered to produce GM-CSF and then irradiated to inhibit cell division<sup>175</sup>. GVAX has been utilized in both autologous and allogeneic therapy. Patients with pancreatic adenocarcinoma that received vaccination with irradiated, allogeneic tumor cells expressing GM-CSF had prolonged survival accompanied by an expansion of tumor-specific CD8<sup>+</sup> T cells<sup>247</sup>. Unfortunately, even if engineered tumor vaccines stimulate robust priming of DCs, the immunosuppressive tumor microenvironment can



secrete factors, such as TGF- $\beta$ , that directly inhibit CD8<sup>+</sup> T cell responses and indirectly inhibit DC responses<sup>248</sup>. In summary, modified whole tumor vaccines, like GVAX, have shown promising clinical and biologic responses, but additional immune modulation should be considered to address tumor-induced suppression mechanisms.

**Dendritic cell vaccination.** Dendritic cell (DC)-based cancer vaccines have emerged as potential therapeutic and preventive immunotherapies to treat cancer patients. As described in detail above, DCs have superior abilities to stimulate T cell responses against self- and non-self- antigens<sup>249–251</sup>. The identification of optimal conditions that generate large scale DC cultures *in vitro* has contributed to the recent success and progress of DC vaccinations to treat cancer. DCs can be differentiated from blood monocyte precursors or CD34<sup>+</sup> progenitors in cord blood in the presence of recombinant cytokines such as FLT3-L, IL-4 and GM-CSF<sup>252</sup>. Early clinical trials testing the safety and efficacy of DC cancer vaccines entailed treating patients with tumor-loaded DCs matured with GM-CSF and IL-4. These studies concluded that DC cancer vaccines were relatively safe and capable of inducing tumor-specific T cells responses across multiple tumor types<sup>253–259</sup>. Achieving complete objective responses can be difficult, as patients enrolled in these trials already have progressive disease. Results from these early clinical trials have demonstrated that patients can be successfully vaccinated, and 5-10% of patients can experience tumor regression.

One consideration when rationally designing DC cancer vaccines is selecting target antigen(s) that will give optimal responses. The source of antigens has ranged from syngeneic or allogeneic tumor cells and lysates to MHC-restricted or synthetic peptides<sup>260–262</sup>. Some of the first genes encoding tumor antigens recognized by TIL

were identified within metastatic melanoma lesions resected from patients enrolled in clinical trials testing high-dose IL-2<sup>204</sup>. These antigens were mostly categorized as melanoma/melanocyte differentiation antigens (MDA), and to a lesser extent, mutated intracellular proteins.

A large portion of DC cancer vaccines utilizes synthetic peptides to generate tumor-specific CTL<sup>263–266</sup>. Peptide-based vaccine strategies generally achieve maximal tumor-specific CD8<sup>+</sup> T cell frequencies of between 0 and 0.3% (of all CD8 T cells)<sup>267</sup>. There are many strengths to utilizing synthetic peptide approaches for DC vaccination. First, synthetic peptides are generated through chemical synthesis that results in highly pure products with defined composition, which can eliminate the potential for biological contamination. Second, synthetic peptides are relatively stable and can be maintained in permissive storage conditions, which facilitates cost-effective large-scale production<sup>268</sup>. Additionally, synthetic peptides are highly customizable and can include post-translational modification.

Clinical success in patients receiving DC peptide vaccines has been observed. In metastatic melanoma patients receiving vaccinations with MAGE-3A1-pulsed DCs, significant frequencies of MAGE-3A1-specific CD8<sup>+</sup> T cells were detected in the peripheral blood and regressions of individual metastases were evident in about half of the eleven patients<sup>265</sup>. Another example illustrating the therapeutic potential of synthetic peptide DC vaccination was seen in a phase I trial that treated patients with autologous DCs pulsed with MART-1<sub>27–35</sub>, which is an immunodominant epitope derived from MART-1/Melan-A (MART-1) protein<sup>253,269</sup>. Examination of the peripheral blood post-vaccination demonstrated an increase in MART-1-reactive T cells measured by

ELISPOT assays and identified with tetramers. The expansion of MART-1-specific T cells did not coincide with clinical responses; however, one patient that achieved a complete response also had evidence of epitope spreading and generated both MHC class I restricted gp100- and tyrosinase-specific and MHC class II-restricted MART-1-specific CD8 and CD4 T cells, respectively<sup>253</sup>.

Although synthetic peptides are stable in storage, they can become unstable *in vivo*. Additional weakness to using synthetic peptides include the requirement of compatible MHC for identified epitopes and the variation in peptide affinity and kinetics<sup>218</sup>. Furthermore, synthetic peptides are generally weakly immunogenic and may require additional stimulation, such as adjuvants, to induce adequate T cell responses<sup>270</sup>. An alternative approach to using synthetic peptides is to express genes that encode full-length proteins in DCs through genetic modification. By processing full-length proteins, DCs can present both MHC class I- and MHC class II-restricted epitopes to elicit tumor-specific T cell responses that are polyclonal in nature<sup>271–275</sup>. Additionally, DCs expressing tumor proteins are capable of sustained antigen processing and presentation compared to DCs pulsed with synthetic peptides<sup>276</sup>. Genetic modification of DCs to express target antigens can be achieved using DNA delivery vehicles, such as viral vectors. This method has been demonstrated to stimulate tumor antigen-specific T cell responses<sup>277–279</sup>.

Promising biologic responses have been observed using Adenovirus (AdV) delivery vectors to express target proteins in DCs. AdV vectors are a useful tool due to durable transgene expression and minimal induction of neutralizing antibodies. DCs transduced with AdV have been characterized as more phenotypically mature and

capable of increased IL-12p70 production<sup>280–282</sup>. One study investigating T cell responses following vaccination with DCs transduced with adenovirus to express the full-length alpha fetoprotein (AFP), a well-characterized hepatocellular carcinoma antigen, reported increased generation and expansion of T cells with specificities to both immunodominant and subdominant epitopes compared to T cell responses following stimulation with AFP protein-stimulated DCs<sup>283</sup>. Adenovirus has also been used to deliver full-length MART-1 cDNA to autologous DC<sup>284</sup>. These findings demonstrate that AdV-mediated delivery of full-length proteins can be an effective strategy to induce tumor antigen-specific T cell responses.

Pre-clinical mouse models have been used to study the effect of DC vaccinations on tumor development. Vaccination with mature DCs loaded with tumor lysates has the capacity to induce protective T cell responses in mice. For example, using the weakly immunogenic B16 mouse melanoma model, murine DCs that were pulsed with apoptotic B16 tumor cells efficiently migrated to the draining lymph nodes and generated durable CD4<sup>+</sup> and CD8<sup>+</sup> T cell responses<sup>285</sup>. Assays commonly used to measure antigen-specific T cell responses include cytokine-production by ELISPOTs, identification by flow cytometry using tetramers or dextramers, and intracellular cytokine secretion. These studies have demonstrated the feasibility and efficacy of DC-based vaccinations.

DC vaccinations can also be improved by adding cytokines or agonists during *in vitro* maturation. By maturing autologous patient-derived DCs *in vitro* with tumor lysate, TLR3/7/8 agonists, and an IFN-containing cocktail of IFN- $\alpha$ , IFN- $\gamma$ , IL-1 $\beta$ , and CD40L, one study found significant production of IL-12-p70 and enhanced antigen-specific CD8<sup>+</sup>

T cells responses<sup>286</sup>. Therefore, licensing DCs prior to vaccination could further improve the induction of tumor antigen-specific T cells.

### **Anti-Tumor Monoclonal Antibodies**

Monoclonal antibodies (mAbs) have been successful in the treatment of various cancer types due to low toxicity and long half-life. Since the development of hybridoma technology, large quantities of mAbs can easily be produced<sup>287</sup>. A monoclonal antibody is composed of four polypeptides: two heavy chains and two light chains, which are further divided into two functionally different domains. The fragment of antigen binding (Fab) consists of the variable region and dictates antibody specificity. Similar to the TCR, the variable region harbors three hypervariable complementarity-determining regions (CDRs). Accordingly, the Fab is located at the antigen binding domains of the heavy and light chains. The constant domain (Fc) determines antibody function. Monoclonal antibodies have specificity to one epitope. Upon binding target binding, antibodies can interfere with signaling pathways within a tumor or directly induce cancer cell death through antibody-dependent cell-mediated cytotoxicity (ADCC) or complement-dependent cytotoxicity (CDC) pathways<sup>288</sup>. In this section, we will focus on antibodies that target tumor antigens.

The first mechanism by which mAbs exert anti-tumor responses is through the interruption of tumor-intrinsic signaling pathways. This can occur through targeting antigens that are growth factors involved in angiogenesis. A few examples of growth factor targets are CEA, EGFR, and Her-2/neu<sup>289–291</sup>. These antigens are generally cell surface receptors and are overexpressed in epithelial cancers. Activation through these growth receptors leads to robust proliferation and facilitates metastatic disease. MAb

can block these growth factor receptors to prevent downstream signaling. Through inhibiting cell cycle pathways in the tumor, these mAbs induce apoptosis.

Antibody-dependent cell-mediated cytotoxicity (ADCC) is another mechanism by which mAbs promote anti-tumor responses with the help of additional immune cells. Macrophages, NK cells, and neutrophils express Fc receptors (FcR) that bind to Fc regions of a mAb. Upon mAb binding the target tumor antigen, the available Fc domain interacts with the FcR on effector cells resulting in events that lead to tumor lysis<sup>292</sup>.

Complement-mediated toxicity is the third mechanism by which mAbs induce tumor cell killing. Complement is a highly complex network of plasma and membrane-bound serum proteins that mediate inflammatory and cytolytic immune responses<sup>293</sup>. Complement binds to the Fc region of the mAb and induces an extensive pathway that ends in the opsonization or lysis of the cancer cell. These three mechanisms by which mAbs mediate indirect or direct killing of tumor cells have resulted in promising clinical responses in patients.

The first mAb that was clinically tested was Orthoclone OKT (muromonab-CD3) to prevent kidney transplant rejection<sup>294</sup>. This mAb was mouse IgG2a and unfortunately was immunogenic, resulting in human anti-mouse responses in humans and weakly enabled effector T cell responses<sup>295</sup>. To circumvent these issues, chimeric and humanized antibodies were developed. Chimeric mAbs are generally composed of an antigen recognition domain from mouse genes and constant domains from human genes. Conversely, humanized mAbs are murine-derived antibodies that have been genetically engineered with protein sequences that resemble human antibodies. This eliminated immune responses against the antibodies and facilitated clinical use<sup>296</sup>.

Recently, novel approaches have led to the development of smaller antibody molecules, fusion proteins, and bispecific or conjugated mAbs. Conjugated monoclonal antibodies are attached to a chemotherapy drug, radioactive isotope or toxin<sup>297,298</sup>. Two FDA approved conjugated monoclonal antibodies are Trastuzumab emtansine for certain types of breast cancer and Brentuximab vedotin for refractory Hodgkin's lymphoma or large cell lymphoma<sup>299–302</sup>. Not only is the cytotoxic function advantageous, but targeted delivery can limit toxicities. Bispecific antibodies contain two different binding domains, one that targets the tumor antigen and one that binds to Fc receptors present on effector cells. Engaging these two targets induces tumor lysis<sup>303–305</sup>.

Rituximab, a monoclonal antibody that binds to CD20 on the surface of B cells, was the first to receive FDA approval to treat patients with non-Hodgkin's lymphoma in 1997<sup>306,307</sup>. Since then, more than a dozen humanized or chimeric mAbs, such as Alemtuzumab<sup>286</sup>, Bevacizumab<sup>308</sup>, Panitumumab<sup>309</sup> and Cetuximab<sup>310–312</sup>, have been approved by the FDA to treat patients with various cancer types. However, there are some disadvantages to using mAbs for cancer immunotherapy. Even though a majority of mAbs have minimal toxicities, there are some reports of adverse events, such as the case with gemtuzumab, which was associated with an increase in patient mortality following treatment<sup>313–315</sup>. The high cost of mAb administration has also contributed to the relative lack of commercial success seen with mAb immunotherapy<sup>316</sup>. Additionally, mAbs treatment alone is rarely curative for patients with cancer<sup>317</sup>. To summarize, although mAbs are relatively safe and can be effective, the high cost of treatment and a need for greater clinical efficacy can affect the commercial success of mAbs for cancer therapy.

## Immune Checkpoint Inhibitor Therapy

Activated T cells upregulate immune inhibitory molecules, or checkpoints, to prevent over-stimulation of T cells. Cancer cells hijack this immune regulatory process to induce immunosuppression. A huge milestone in the immune-oncology field has been the development of monoclonal antibodies (mAb) that block immune checkpoint pathways. The impressive clinical outcomes observed after treating cancer patients with checkpoint inhibitors have resulted in hundreds of clinical trials and recent FDA-approval of several immune checkpoint inhibitors. Two well-characterized immune checkpoint pathways, PD-1/PD-L1/2 and CTLA-4, will be discussed in this section.

**PD-1-targeted therapies.** Programmed death-1 (PD-1 or CD279) is a transmembrane protein in the CD28 superfamily that is expressed on myeloid cells and activated lymphocytes. PD-1 has two ligands: PD-L1 (B7-H1) is expressed on a broad range of tissue and primarily mediates peripheral tolerance. PD-L2 (B7-DC) is expressed on antigen presenting cells (APC) and controls T cell activation and tolerance<sup>318,319</sup>. PD-1 binding to PD-L1 or PD-L2 induces inhibitory signals that result in immune regulatory events that affect T cell activation, effector T cell responses, T cell tolerance and T cell exhaustion<sup>320–322</sup>.

The PD-1-PD-L1/PD-L2 pathway is particularly important in the context of anti-tumor immunity. PD-1 blockade can not only affect immune responses systemically, but also locally within the tumor microenvironment. Intratumoral lymphocytes, including tumor antigen-specific T cells, express high levels of PD-1<sup>323,324</sup>. As a result of chronic stimulation by tumor antigens, high levels of PD-1 on T cells coincides with T cell impaired effector function leading to exhaustion<sup>325–328</sup>. Additionally, a large frequency of



tumors expresses PD-L1<sup>329</sup>. Engagement of PD-L1 on tumors or APCs with PD-1 on T cells inhibits T cell proliferation, halts cytokine production, and diminishes cytotoxic activity<sup>319</sup>. These suppressive effects can be reversed using antibodies blocking PD-1-PD-L1 interactions<sup>5-7</sup>. The development of anti-PD-1 blocking antibodies has been instrumental in advancing the field of cancer immunotherapy. Clinically, anti-PD-1 therapy has been relatively successful in treating patients with various malignancies, including melanoma, non-small cell lung cancer, bladder cancer, renal cell carcinoma, lymphoma, and head and neck cancers<sup>330,331</sup>.

The promising clinical and biologic responses of patients treated with anti-PD-1 in early trials resulted in the FDA approval of pembrolizumab and nivolumab in 2014<sup>330,332</sup>. Pembrolizumab was first approved to treat patients with advanced or unresectable melanoma that had failed ipilimumab and a BRAF inhibitor<sup>333</sup>. Patients achieved an overall response rate (ORR) of 26% and upon follow-up, a progression-free survival (PFS) rate of 45% at 6 months<sup>334</sup>. Nivolumab received FDA approval in 2015 to treat patients with treatment-refractory clear-cell renal carcinoma (RCC). Patient OS was extended by 6 months with Nivolumab compared to oral everolimus<sup>335</sup>. In addition to solid tumors, Pembrolizumab and Nivolumab have also received FDA approval to treat relapsed or refractory classical Hodgkin Lymphoma with the latter reaching an ORR of 87% and 17% complete response<sup>336-338</sup>. Results from these clinical trials demonstrate that inhibiting PD-1 can be effective in treating a variety of tumor types.

Various pre-clinical and clinical studies have led to a better understanding of the mechanisms by which PD-1 inhibition promotes anti-tumor responses. Anti-PD-1 mAb treatment has been demonstrated to induce activation of CD4<sup>+</sup> and CD8<sup>+</sup> effector

memory T cells and central memory T cells and Th1 cells<sup>339</sup>. Inhibiting PD-1 can also impact on T cell metabolism. PD-1 activation induces metabolic reprogramming characterized by inhibiting glycolysis and increasing fatty acid oxidation<sup>340,341</sup>. Tumors have taken advantage of these metabolic changes and out-compete T cells for glucose intake resulting in dysfunctional effector T cells<sup>342–344</sup>. More studies are needed to better understand the modulatory effects of anti-PD-1 mAb therapy.

Inhibitors to PD-L1/L2 have also been tested in clinical trials and Atezolizumab received FDA approval in 2016 to treat non-small cell lung cancer (NSCLC)<sup>345,346</sup>. In these studies, overall survival was positively associated with increased PD-L1 expression on patient tumor cells and immune cells. A second PD-L1 inhibitor, durvalumab, received FDA approval in 2017 for patients with locally advanced or metastatic urothelial cancer that had failed chemotherapy<sup>347</sup>. Durvalumab was granted FDA breakthrough designation in 2018 as an adjuvant for locally advanced, unresectable NSCLC<sup>348,349</sup>. Clinical trials treating patients with anti-PD-L1/L2 mAb show great promise in treating patients with various cancer types.

Animal models are useful to investigate mechanisms by which the PD-1-PD-L1/PD-L2 interactions affect anti-tumor immunity. However, the outcome following PD-1 blockade differs with tumor type. For example, in the weakly immunogenic B16 mouse melanoma model, anti-PD-1 mAb alone was ineffective to improve survival or control tumor growth<sup>350</sup>. Although B16 tumor cells do in fact express PD-L1, Juneja, *et al.* reported that PD-L1 expression on tumors was not required to inhibit CD8 T cell cytotoxic responses. In contrast, PD-L1 expression on host cells was required to inhibit CD8 T cell responses<sup>351</sup>. Interestingly, data from the Allison lab have demonstrated that

significant responses against B16 tumors are only achieved when anti-PD-1 mAb is combined with GVAX (discussed in the previous section) or anti-CTLA-4 mAb (discussed in the following section)<sup>352</sup>.

**CTLA-4 targeted therapies.** CTLA-4 is rapidly and transiently expressed by activated T cells and suppresses immune responses by inhibiting IL-2 accumulation and reducing proliferation<sup>29</sup>. CTLA-4 engages with CD80/CD86 on antigen presenting cells (APCs), subsequently blocking the co-stimulatory molecule CD28<sup>30,353</sup>. Additionally, CTLA-4 is constitutively expressed on T regulatory cells (Treg)<sup>354</sup>. Monoclonal antibodies (mAb) blocking CTLA-4, such as ipilimumab, have recently demonstrated clinical success in treating various tumor types. In 2011, the FDA approved ipilimumab to treat metastatic melanoma patients<sup>355</sup>. In 2015, ipilimumab was granted FDA-approval after demonstrating improved relapse-free survival and overall survival in stage III melanoma patients<sup>355,356</sup>.

Inhibiting CTLA-4 is thought to promote anti-tumor responses through a variety of mechanisms. Anti-CTLA-4 mAb can disrupt inhibitory signals and stimulate systemic effector T cells. Additionally, anti-CTLA-4 mAbs can use their binding domain to engage CTLA-4 on Tregs and the Fc domains can bind to Fc receptors (FcR) on NK cells or macrophages leading to antibody-dependent cell cytotoxicity<sup>357</sup>. Treatment with anti-CTLA-4 mAb can result in increased CD8<sup>+</sup> T cell infiltration of tumors. Furthermore, some studies have reported an increase in TCR diversity and anti-tumor reactivity<sup>358,359</sup>. Anti-CTLA-4 mAb treatment can also mediate changes in peripheral and intratumoral T regulatory cells, myeloid-derived suppressor cells, and effector T cells<sup>330</sup>. In some studies, successful clinical responses following CTLA-4 blockade, as well as anti-PD-1,

correlated positively with patient tumors that harbored pre-existing CD8<sup>+</sup> T cells<sup>360,361</sup>.

Thus, therapeutic responses to immune checkpoint inhibitors might occur preferentially in patients with a pre-existing spontaneous anti-tumor T cell response. These studies demonstrate that, in some cancer settings, anti-CTLA-4 mAb therapy can significantly improve anti-tumor immune response both locally in the tumor microenvironment as well as systemically.

Pre-clinical mouse models have also demonstrated the therapeutic effects of CTLA-4 blockade against various tumors and have been useful to investigate immune mechanisms and combination strategies. Treatment of mice bearing colon carcinomas with anti-CTLA-4 mAb leads to tumor regression and protection from re-challenge with parental tumor lines<sup>362</sup>. In B16 melanoma, a notoriously aggressive and weakly immunogenic model, anti-CTLA-4 mAb, in combination with a GM-CSF-producing vaccine, was able to induce protective systemic anti-tumor T cell responses in a CD8<sup>+</sup> T cell- and NK cell-dependent manner<sup>347</sup>. In B16 melanoma, inhibiting PD-1 and CTLA-4 pathways significantly increased the ratios of CD8<sup>+</sup> T cell: Tregs and CD4<sup>+</sup> Teff:Tregs in the tumor microenvironment<sup>352</sup>. Dual blockade was also accompanied by an increase in IFN- $\gamma$ <sup>+</sup> and TNF $\alpha$ <sup>+</sup> CD8<sup>+</sup> T cells in the tumor and draining lymph nodes. Additionally, vaccination with a GM-CSF-expressing tumor cell line or anti-CTLA-4 mAb treatment individually resulted in poor responses against established B16-BL6 tumors; however, combination therapy led to B16 eradication in 80% of mice<sup>37</sup>. Dual treatment with anti-PD-1/PD-L1 and anti-CTLA-4 mAb mediated eradication of B16 in 50% of tumor-bearing mice, compared to 10-25% of mice treated with either anti-PD-1 or anti-CTLA-4 mAb monotherapy, respectively<sup>363</sup>. Collectively, these studies demonstrate that anti-

CTLA monotherapy can be successful in a small subset of cases, depending on the type of malignancies; however anti-CTLA-4 mAb in combination with other checkpoint inhibitors or vaccination therapies can significantly increase the number of responders.

**Immune-related adverse events.** Inhibitors to PD-1 and CTLA-4, or other checkpoint molecules, can cause immune-related adverse events (irAEs) that generally pertain to the gastrointestinal tract, endocrine glands, skin, liver, and to a lesser extent, central nervous system, cardiovascular, pulmonary, and hematologic systems<sup>364</sup>. As a consequence of mechanistic differences in how PD-1 and CTLA-4 impact T cell responses, adverse events are usually more frequent and more severe following CTLA-4 inhibition compared to PD-1-PD-L1 inhibition<sup>365</sup>. Severe autoimmunity has been reported following systemic administration of ipilimumab, particularly when combined with PD-1/PD-L1 inhibitors<sup>366</sup>. The first line of treatment for these severe irAEs is usually corticosteroids or additional immunosuppressive drugs if steroids are ineffective. It is unclear if the development of autoimmune responses is associated with clinical response to therapy, as conflicting data have been presented. Specific adverse events can sometimes indicate therapeutic efficacy. For example, vitiligo, a skin disorder involving the loss of pigmentation mediated by an immune response to melanocyte-derived antigens, is commonly observed in melanoma patients following checkpoint inhibitor therapy and indicative of T cell cross-reactivity against similar antigens shared by the tumor and normal melanocytes<sup>367</sup>. In summary, immune checkpoint inhibitor therapy can be remarkably effective in a proportion of patients with various cancers, but immune-mediated toxicities can limit their use and are important considerations that should be carefully assessed prior to and during therapy.

## **Oncolytic Virotherapy**

Oncolytic viruses (OVs) are a novel class of immunotherapy through which natural or modified viruses specifically infect and kill tumor cells, but not normal cells<sup>368</sup>. OVs can mediate anti-tumor responses utilizing two different mechanisms: directly killing tumor cells and inducing immune responses. The first takes advantage of the fact that during progression, tumor cells usually inactivate antiviral pathways, leaving them susceptible to infection and lysis by viruses. Lysis-induced release of viral particles propagates infection locally within the tumor microenvironment<sup>369,370</sup>. Consequently, the release of tumor antigens in combination with stimulation of innate immunity through the release of viral particles within the tumor microenvironment facilitates T cell cross-priming. The induction of a polyclonal T cell response serves as the second mechanism by which OVs enhance anti-tumor immunity.

The most well-characterized oncolytic virus is an attenuated herpes simplex virus, type I (HSV-1) that expresses human GM-CSF and is designated as tamlipogene laherparepvec (TVEC)<sup>285</sup>. In clinical trials, impressive durable responses were achieved in melanoma patients treated with TVEC. TVEC is administered directly into the tumor. Interestingly, regression of uninjected metastases has been observed after TVEC treatment, suggesting the induction of endogenous tumor-specific responses. These impressive outcomes resulted in FDA-approval of TVEC in 2015 for the treatment of unresectable melanoma. Since then, the efficacy of several other viruses is being evaluated in clinical trials to treat various types of cancer.

The addition of TVEC can improve the efficacy of other immunotherapies as well. In one study, patients with unresectable metastatic melanoma receiving TVEC and

ipilimumab had double the response rates (39%) compared to ipilimumab alone (18%)<sup>371</sup>. Improved clinical and biologic responses have also been observed in patients treated with the combination of TVEC and pembrolizumab<sup>372,373</sup>. Additionally, combination treatment facilitated a T cell-inflamed tumor phenotype. Interestingly, clinical responses did not correlate with pre-existing CD8 T cells in the tumors, generally seen with checkpoint inhibitors alone. These results demonstrate that combination treatment can generate anti-tumor responses without the requirement of pre-existing anti-tumor immunity.

### **Adoptive Cell Therapy**

Early experiments in the 1960s demonstrated that transferring cells from the draining lymph nodes, but not non-draining lymph nodes nor spleens, of tumor-bearing mice conferred immunity in secondary hosts<sup>374</sup>. Almost 20 years later, Berendt and North described the rejection of established tumors following intravenous adoptive transfer of T cells from tumor-immunized mice into thymectomized recipients, concluding that T cells harbored both effector and suppressor functions<sup>375</sup>. However, to achieve such robust responses, these experiments required large quantities of donor T cells from sensitized mice. Eberlein and colleagues addressed this problem by using the cytokine IL-2 to expand effector T cells *in vitro*<sup>376</sup>. Donor splenocytes that were sensitized with tumor cells and expanded with IL-2 *in vitro* could eliminate local tumors and disseminated metastases following intravenous adoptive transfer<sup>376</sup>. These therapeutic cells were termed lymphokine-activated killer (LAK) cells. LAK cells, in combination with recombinant IL-2, mediated the regression of established pulmonary sarcomas in mice<sup>377,378</sup>. These promising pre-clinical results in mouse models lead to

the first phase I clinical trial reported in 1985 in which 25 patients with metastatic cancer received intravenous infusion of LAK cells and high dose IL-2 leading to partial regression in almost half of the patients<sup>379,380</sup>. This process was extremely labor-intensive, requiring substantial quantities of LAK cells. Additionally, LAK cells were non-specifically activated and lacked the necessary tumor-specificity to mediate adequate responses. This study concluded that LAK cells had the potential to generate anti-tumor responses, but the laborious process and lack of antigen-specificity demonstrated the need for an improved strategy.

The problem of tumor-specificity was addressed through the identification of tumor-infiltrating lymphocytes (TIL), a subpopulation of lymphocytes found within resected patient tumors<sup>204</sup>. Following enzymatic digestion of tumors, single cell suspensions contained a range of 3%-74% lymphocytes that could undergo massive expansion when maintained in IL-2<sup>381</sup>. Expanded TIL exhibited reactivity against autologous tumors, measured by a chromium release assay, but spared normal cells<sup>382</sup>. Pre-clinical mouse studies reported that TIL were up to 100 times more effective than LAK cells, even in the absence of high dose IL-2, at mediating tumor regression in mice preconditioned with cyclophosphamide<sup>383</sup>. The first trial treating metastatic melanoma patients with TIL and IL-2 reported cancer regression in 9/15 patients that had not received prior treatment and 2/5 patients that had previously failed IL-2 therapy<sup>384</sup>. Proceeding trials with larger patient cohorts demonstrated a 31% overall response rate in patients receiving TIL plus IL-2 and a 35% overall response rate when patients were preconditioned with cyclophosphamide 36 hours before TIL and IL-2 treatment<sup>385</sup>. Importantly, patients that had previously failed on IL-2 were capable of achieving clinical



and biologic responses following treatment with TIL and IL-2, indicating the improved benefits when combined with TIL.

In follow-up studies, nonmyeloablative conditioning treatment prior to infusion of highly tumor-reactive TIL resulted in persistent clonal repopulation of T cells, with the infused cells dividing *in vivo* and trafficking to tumor sites<sup>386</sup>. They not only observed regression of metastatic melanoma lesions but also reported the development of autoimmune melanocyte destruction. We now know that TIL composition can be correlated with cancer prognosis in malignant melanoma, among other tumor types<sup>387</sup>. To date, adoptive cell transfer of TIL, in combination with high-dose IL-2 and non-myeloablative conditioning, has been clinically successful, resulting in a 40-50% objective response rate in metastatic melanoma patients<sup>388,389</sup>.

It is now appreciated that, although autoreactive T cells should be deleted following thymic selection, there is evidence of tumor-specific T cells that can be within the tumor microenvironment of cancer patients; however, these tumor infiltrating lymphocytes (TIL) are unable to effectively control tumor burden<sup>390,391</sup>. Upon further examination, these TIL are dysfunctional or exhausted due to the suppressive nature of the tumor microenvironment<sup>392</sup>. Albeit in low frequencies, these tumor-reactive T cells can be identified and used to generate large numbers of tumor-specific T cells for adoptive cellular therapy. The tumor-specific TCR $\alpha$  and  $\beta$  genes can be cloned into a viral vector. High-titer virus can then be produced upon the transfection of packaging and producer cell lines. The resulting viral supernatant can then be used to express the TCR on the surface of activated T cells through viral transduction<sup>393</sup>. Through this process, major forms of cellular therapy have risen: TCR gene-modified T cells and

Chimeric Antigen Receptor (CAR) T cells. Adoptive cell therapy serves as a personalized strategy to redirect the specificity of patient T cells to recognize and kill their tumor cells.

**CAR T cell therapy.** Chimeric antigen receptor (CAR) T cells have been a breakthrough tool in the field of immune-oncology and cellular therapy, particularly for hematological malignancies. CAR T cells are composed of an extracellular antigen recognition domain, a hinge linker, a transmembrane domain, and at least one cytoplasmic signaling domain (Fig 4). The first description of CARs dates back to 1989 when Eshhar and colleagues generated chimeric TCR genes, which were composed of the constant domain in order to maintain the intracellular signaling functions of the T cell, and were fused to the antibody's variable domains in order to direct specificity<sup>394</sup>. The antigen specificity was conferred by the immunoglobulin-derived extracellular single-chain variable fragment (scFv), which permitted recognition of native cell-surface antigens, including glycolipids, carbohydrates and proteins, without the need for antigen processing or MHC restriction. Transfection of the chimeric TCR into cytotoxic T cells induced antigen-specific killing and IL-2 release in a non-MHC- restricted manner<sup>394</sup>. In 1993, Eshhar designed what would be referred to as first-generation CAR T cells that consisted of antibody-derived scFv regions that recognized tumor antigens and were linked to the intracellular signaling domain of the TCR CD3 $\zeta$  chain (Fig 4)<sup>395</sup>. Unfortunately, these initial CARs failed to promote T cell proliferation and survival following constant exposure to antigen failed *in vivo* and were not clinically effective<sup>396</sup>.

A huge advance in CAR T cell therapy occurred after the addition of a co-stimulatory domain was found to improve T cell persistence and effector function.

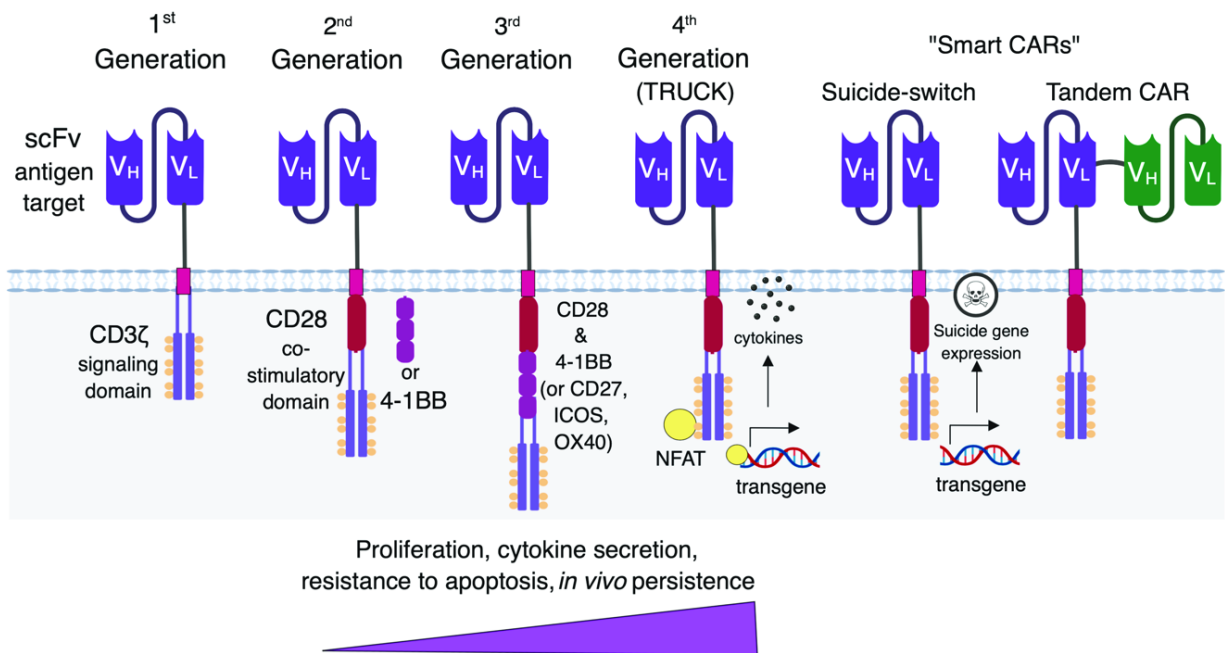


**Figure 4. Generations of CAR T Cells.** First-generation CAR T cells were composed of a single-chain variable fragment gene that directed antigen specificity linked to the cytoplasmic signaling domain of CD3ζ (represented as phosphorylated). Second-generation CAR T cells included one co-stimulatory domain such as CD28 or 4-1BB. Third-generation CAR T cells incorporated two co-stimulatory domains. Fourth-generation CAR T cells (or TRUCKs) added a transgene that encoded pro-inflammatory cytokines or a co-stimulatory molecule. Two examples of smart CARs are depicted: suicide switch CAR T cells contain an inducible transgene that can induce apoptotic events. Tandem CAR T cells link two scFv genes to target two different antigens. (V<sub>L</sub>: variable light chain; V<sub>H</sub>: variable heavy chain)

Second generation CARs were designed to include one co-stimulatory domain, such as CD28 or 4-1BB<sup>397</sup>. CD28-based signaling domains have been suggested to mediate constitutive activation and facilitate T cell exhaustion<sup>398</sup>. In contrast, 4-1BB- based signaling domains have been shown to reduce exhaustion and promote survival<sup>399</sup>. However, both signaling domains are required to achieve the best results. Compared to first-generation CARs, the addition of a co-stimulatory domain improved proliferation,

cytokine secretion, and resistance to apoptosis<sup>400</sup>. The feasibility of second-generation CAR T cells was confirmed in 2002 upon observation that prostate cancer antigen-specific CAR T cells survived, proliferated, and killed prostate cancer cells<sup>401</sup>. This led to pre-clinical mouse studies that demonstrated eradication of leukemia cells in immunodeficient mice treated with human CD19-specific CAR T cells<sup>402</sup>.

Early clinical studies treating leukemia patients with CD19 CAR T cells demonstrated promising results<sup>403</sup>. Seminal findings from these trials included the ability of CAR T cells to persist and mediate substantial tumor eradication and the observation that toxicity due to cytokine storm correlated with tumor burden<sup>404</sup>.<sup>405</sup> These promising clinical responses paved the way for FDA designation of CAR T cells as a breakthrough therapy in 2014. Three years later, the FDA finally approved CD19 CAR T cell treatment for children and young adults with relapsed, refractory ALL. Since then, CD19 CAR T cell therapy has gained approval in the treatment of certain large B cell lymphomas.

One strategy to enhance the efficacy of second-generation CAR T cells was the inclusion of two co-stimulatory domains. The so-called third-generation CARs in development demonstrated even better effector functions and *in vivo* persistence of transferred cells<sup>400</sup>. Additional improvements, resulting in fourth-generation CAR T cells, have included vector-incorporated transgenes that express pro-inflammatory cytokines or co-stimulatory molecules<sup>406</sup>. Furthermore, tandem CAR T cells, which encode two scFv domains recognizing two different antigens, are another promising strategy to improve the efficacy of CAR T cells.

CAR T cells can be clinically effective in treating various cancer types. However, severe toxicities have been reported in patients following treatment. One mediator of

toxicity can be on-target/off-tumor recognition by the introduced chimeric antigen receptor. The first report of on-target/off-tumor toxicity using receptor-modified T cells was reported in 2006 when patients with metastatic renal cell carcinoma received autologous CARs targeting carbonic anhydrase IX and developed liver toxicity. Two patients died as a result of low antigen expression in normal bile duct epithelial tissue<sup>407</sup>. Lethal on-target, off-tumor toxicity was reported in one patient treated with Her-2 CAR T cells. Upon further investigation, low levels of the target antigen were detected on normal lung epithelial cells<sup>408</sup>. The outcomes from these studies illustrate the need to carefully select antigen targets and assess expression on normal tissue to improve the safety of CAR T cell therapy.

The most common adverse event observed following CAR T cell treatment for hematologic malignancies is cytokine release syndrome (CRS), which is a multi-faceted toxicity that encompasses high fever and myalgias to unstable hypertension, multi-organ system toxicity, and respiratory failure<sup>409–413</sup>. Another primary toxicity encountered with CAR T cell therapy is neurotoxicity, which in rare cases can be severe and even fatal<sup>414</sup>. CRS is thought of as an off-target toxicity due to its antigen-independence<sup>415</sup>. Additionally, on-target toxicities have been observed following CAR T cell therapy. Tumor lysis syndrome is another on-target toxicity directly related to tumor cell destruction<sup>416</sup>. CAR T cell toxicities are managed with supportive care, corticosteroids, and tocilizumab, an anti-IL-6 therapy<sup>417</sup>. Another approach to limit CAR T cell toxicity is to incorporate suicide genes into the CAR vector<sup>418</sup>. One example is the inclusion of an inducible caspase-9 gene that can promote apoptosis of T cells<sup>419–421</sup>.

Robust responses in cancer patients receiving CAR T cells can be effective, however, the lack of regulatory mechanisms can lead to severe, and potentially fatal toxicities.

Another disadvantage to using CAR T cells to treat solid tumors is the limited breadth of antigen specificity. Under immune-selective pressure, tumor cell variants emerge that lost the target antigen through genetic mutation or reduced expression, leading to failed recognition by CAR T cells. The selection for pre-existing alternatively spliced CD19 isoforms with the compromised CAR T cell epitope is one mechanism by which tumors escape detection by CAR T cells<sup>422</sup>. In summary, CAR T cells can be extremely effective, particularly in hematologic malignancies; however, toxicities and immune resistance mechanisms are important limitations to their clinical use.

Additionally, CAR T cells are often less effective against solid tumors and can result in severe toxicities on-target, off-tumor toxicities. Some of these concerns can potentially be addressed by alternatively using TCR gene-modified T cells, described in the proceeding section.

**TCR gene-modified T cells.** Advances in the genetic engineering of T cells have facilitated the development of large scale, highly functional, tumor-reactive T cells that can be used to treat patients (Fig 5). In 1990, five patients with metastatic melanoma were treated with TIL transduced to express a neomycin-resistance gene, with the goal of monitoring the cells post-infusion<sup>393</sup>. To further address the issue of specificity, four years later, Shilyansky and colleagues identified T cell clonotypes with specificity to epitopes expressed on shared melanoma tumor-associated antigens<sup>423</sup>. The following year, Cole *et al.* identified and characterized a tumor-derived, antigen-specific TCR, which was HLA-A2- restricted and recognized the melanoma antigen, MART-1<sup>424</sup>.

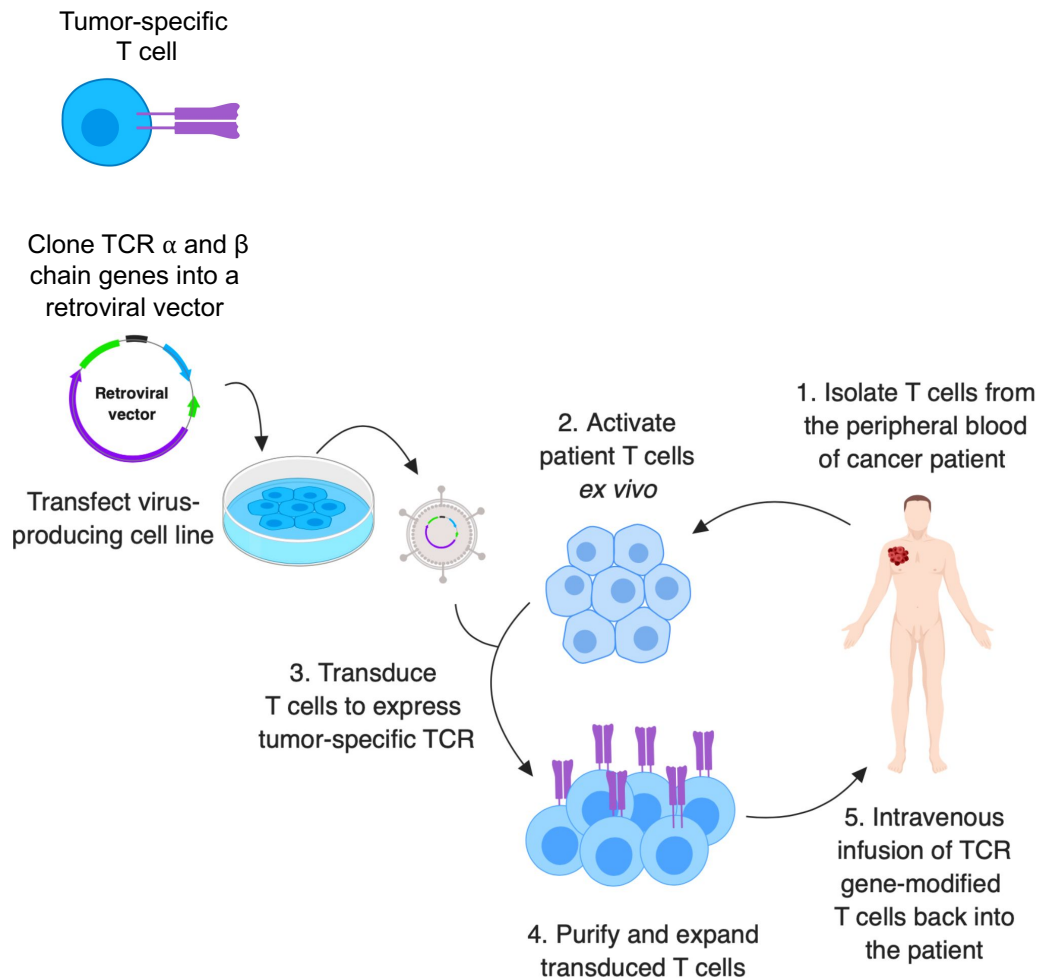


**Figure 5. Schematic of Adoptive Transfer of TCR Gene-Modified T Cells.** Upon identification of a tumor-specific T cell, the TCR  $\alpha$  and  $\beta$  chain genes are cloned into a retroviral vector. The retroviral vector is used to transfect a virus-producing cell line. Supernatant containing virus is added to activated T cells isolated from the peripheral blood of a cancer patient. T cells that express the tumor-specific TCR are purified and expanded to large quantities. TCR gene-modified T cells are then administered back to the patient through intravenous infusion.

Another strategy to identify tumor-reactive T cell receptors immunized mice transgenic for HLA-A2.1 or the chimeric molecule A2.1/K<sup>b</sup> with human p53 protein to generate A2-restricted TCRs with specificity to p53 peptides<sup>425</sup>. There have been tremendous advances using adoptive transfer of TCR gene-modified T cells. Upon

identification of a tumor-reactive TCR and cloning of the alpha and beta chain genes into a vector, activated patient T cells can be transduced to express the tumor-specific T cell receptor. TCR gene-modified T cells can be purified and expanded to large numbers and then infused back into the patient. In sum, the identifying functional tumor-specific TCRs has facilitated the development of new targets for a variety of cancers.

Our laboratory utilizes a TCR (referred to as the TIL 1383I TCR) isolated from a T cell clone within a population of TIL from a tumor that was resected from a melanoma patient<sup>426</sup>. The TIL 1383I TCR has specificity to the melanoma antigen, tyrosinase, and is restricted by human MHC class I HLA-A2. Our lab has also conducted a phase I clinical trial in which metastatic melanoma patients received an intravenous (i.v.) infusion of autologous T cells transduced to express the TIL 1383I TCR. Among three patients, one had a mixed response and developed vitiligo, and a second had a partial response by RECIST criteria and then progressed<sup>1</sup>. After receiving high dose IL-2, this patient developed vitiligo and entered complete remission. Immunological monitoring analysis revealed the persistence of transferred TIL 1383I TCR transduced T cells, which were detectable up to one year post-infusion in the responding patient<sup>1</sup>. This study demonstrated that the adoptive transfer of autologous TIL 1383I TCR transduced T cells can result in clinical and biologic activity without severe toxicity in metastatic melanoma patients.

Adoptive T cell therapy, while relatively safe compared to other immunotherapies, can have adverse events. Attempts to improve the function of tumor-specific TCR gene-modified T cells through affinity enhancement strategies have resulted in unintended toxicities. Such adverse events can occur if a TCR mediates on-



target/off-tumor or off-target/off-tumor effects. On-target/off-tumor reactivity occurs when a TCR reacts against the target antigen expressed on normal tissues. In a phase II clinical trial, patients with metastatic melanoma received infusions of autologous T cells transduced to express one of two high avidity TCRs recognizing the melanoma antigens MART-1 or gp100. Compared to a previous trial using a non-affinity enhanced MART-1-specific TCR, patients treated with the high-affinity TCRs developed on-target autoimmunity against normal melanocytes in the eye, inner ear, and skin<sup>427</sup>. In a second example, the functional avidity of a TCR recognizing the carcinoembryonic antigen (CEA) antigen was enhanced through a single amino acid substitution in the CDR3 region of the  $\alpha$  chain. Patients with metastatic colorectal cancer receiving autologous TCR transduced T cells developed severe inflammatory colitis due to low levels of CEA present in the colonic epithelium<sup>428</sup>. Additionally, off-target effects have been observed in patients receiving an affinity enhanced, MAGE-A3-specific TCR. Severe cardiac toxicity resulting in two deaths occurred due to TCR cross-reactivity with an unrelated protein expressed by contracting normal cardiac tissues<sup>429</sup>. These clinical trials demonstrate the need for improved methods to define the specificity of engineered T cells when performing autologous systemic infusion of gene-modified T cells.

Autologous TCR gene-modified T cells are most commonly infused back into the patient systemically, but intratumoral injections are also a feasible and effective route of delivery. The unintended toxicities mentioned in the previous paragraph might have been avoided if the affinity-enhanced TCR gene-modified T cells were delivered intratumorally, as opposed to systemically. Duval *et al.* demonstrated the feasibility, safety, and efficacy of intratumoral injections in a phase I dose-escalation trial using an

irradiated, MART-1-specific TCR-transduced allogeneic T cell line (C Cure 709) to treat metastatic melanoma lesions<sup>2</sup>. This method did not induce any treatment-related graft-versus-host disease, which is a well-characterized adverse event of allogeneic transplantation. Out of fifteen patients, one patient had a partial response, encompassing metastatic lesions that were injected with T cells and lesions that were uninjected. Additionally, two patients achieved local regression of injected metastatic lesions, and two patients developed vitiligo. The authors hypothesized that, in addition to the direct killing of MART-1<sup>+</sup> tumor cells within the injected lesion, intratumoral delivery of tumor-specific allogeneic T cells could induce epitope spreading through the combination of released antigens and cytokine production. In some cases, the authors observed acute symptoms of fever, chills, or injection site reactions that were often followed by local tumor regression. After observing the lack of symptoms in two patients after two cycles of treatment using the same lesion, they chose alternative lesions to inject, which subsequently resulted in the development of injection site reactions and tumor regression.

A follow-up study attempted to report on longitudinal immune monitoring of treated patients. They did not detect any of the C Cure 709 cells used for injection within the peripheral blood. They did not observe any treatment-induced increase in the frequency of antigen-specific T cells, but they noted a stable frequency of MART-1-specific T cells over the course of treatments (63-94% T<sub>EM</sub> or T<sub>EMRA</sub>) with new clonotypes emerging during treatment. Interestingly, although only a few clonotypes were recurrently detected in consecutive samples, one MART-1-specific T cell clone disappearing from peripheral blood was later discovered in a metastatic lesion, which

indicated the generation of tumor-specific T cells that could traffic to distant, uninjected lesions<sup>430</sup>. These findings demonstrated that intratumoral delivery of allogeneic, TCR gene-modified T cells is not only safe and feasible, but also effective, in a small subset of patients, at generating clinical and biologic responses.

### **Predictive Biomarkers in Cancer Immunotherapy.**

There is a great deal of interest in finding potential predictive biomarkers that help to identify patients that are likely to respond to a specific immunotherapy regimen. Increased accessibility to large patient data sets has significantly contributed to this rapidly evolving area of cancer immunotherapy. While there are several biomarkers among various tumor types, this section will focus on predictive biomarkers identified in the peripheral blood, in the immune signature within the tumor microenvironment and the tumor mutational load/identification of neoantigens.

**Cellular analysis from the peripheral blood.** The peripheral blood is a highly accessible source to obtain substantial numbers and subsets of immune cells, especially in circumstances where tumor lesions are inaccessible, making biopsies difficult. Therefore, the identification of predictive biomarkers extrapolated from the peripheral blood would be extremely beneficial. In leukemia and melanoma patients, some studies have reported biomarkers as general as an increased absolute number of lymphocytes in the peripheral blood. This increase in lymphocyte number positively correlated with immunological responses or outcomes to immunotherapy<sup>431,432</sup>. At the other end of the spectrum, advanced technologies such as CyTOF-based analysis has revealed large networks of predictive biomarkers identified from patients before and after treatment with PD-1 and CTLA-4 inhibitors<sup>433</sup>. One example was an increase in

CD4<sup>+</sup> and CD8<sup>+</sup> memory T cells, which were associated with improved responses to anti-CTLA-4 mAb. For anti-PD-1 mAb therapy, CD69<sup>+</sup> and MIP1 $\beta$ <sup>+</sup> NK cells in the peripheral blood was positively associated with a clinical response<sup>433</sup>. Obtaining peripheral blood samples is a relatively safe and easy method to identify potential biomarkers predictive of clinical or biologic responses.

Results from clinical trials investigating the efficacy of DC-based vaccinations have contributed to the identification of possible biomarkers predictive of clinical outcome. The diversity of TCR repertoires has recently been investigated as a biomarker to monitor immune responses in cancer patients<sup>434,435</sup>. Several studies have reported positive clinical outcomes in patients that had evidence of broad CD4<sup>+</sup> and CD8<sup>+</sup> T cell responses as a result of epitope spreading<sup>253,436,437</sup>. The induction of enhanced anti-tumor immune responses suggests that immunotherapies should be designed with the goal of inducing *in vivo* cross-presentation of tumor antigens and broadening the repertoire of TCRs specific to the tumor for more effective disease control. In support of this concept, TCR diversity and clonality can correlate with clinical outcome after various immunotherapy treatments, including adoptive transfer of TIL and administration of checkpoint inhibitors<sup>434,438–442</sup>. In summary, the analysis of TCR repertoires from peripheral blood samples can be a useful predictive biomarker to assess responses and treatment strategies.

**Neoantigens and tumor mutation burden.** Tumors with high mutation loads can often be associated with the increased presentation of tumor neoantigens<sup>443</sup>. Tumor-associated neoantigens can arise as a consequence of processed mutant cancer peptides or aberrant self-antigens, such as EGFR, resulting from oncogenic

protein overexpression<sup>444</sup>. Patients bearing tumors with high mutation loads often achieve better anti-tumor responses<sup>445</sup>. These improved outcomes have been proposed to be mediated by T cell responses against neoantigens<sup>361,446</sup>. Additionally, patients with tumors established as deficient in mismatch repair (dMMR) or microsatellite instability-high (MSI high) were more likely to respond to anti-PD-1 mAb treatment. The correlation between dMMR or MSI high tumors and patient response was validated across twelve different tumor types, resulting in objective radiographic responses in 53% of patients and complete responses in 21% of patients<sup>447,448</sup>. Therefore, tumor mutation load can be a useful predictor of outcome to immunotherapy using anti-PD-1 mAb blockade.

The relationship between neoantigen abundance, mutation load, and T cell diversity is still unclear. In one study that used whole exome sequencing, transcriptome profiling, and T cell repertoire analysis, the local tumor mutation burden correlated with neoantigens and TCR repertoire, but local CD8<sup>+</sup> T cell cytotoxicity did not correlate with neoantigen abundance<sup>449</sup>. These findings suggest that multiparameter analysis of T cell diversity, mutation load, neoantigen abundance, and T cell effector function might potentially be used to predict responses.

**Immune profiling the tumor microenvironment.** The immune composition of the tumor microenvironment prior to treatment can influence the response to immunotherapy. Gene expression analysis of tumors has been used to characterize the tumor microenvironment (TME). Through gene expression analysis, tumors can be segregated into: T cell-inflamed, T cell-excluded, and immune desert<sup>199,450,451</sup>. T cell-inflamed tumor signatures are identified by CD8<sup>+</sup> T cell infiltration, chemokines that promote infiltration of T cells, components involved in antigen presentation and

expression of type I IFN genes<sup>164,165</sup>. As a result of increased IFN pathway activation, these intratumoral CD8<sup>+</sup> T cells often exhibit a dysfunctional phenotype characterized by upregulation of immune inhibitory molecules including PD-1, CTLA-4, lymphocyte activation gene protein 3 (LAG-3), T cell immunoglobulin domain and mucin domain protein-3 (TIM-3)<sup>452,453</sup>. T cell-excluded (or non-T cell-inflamed) tumors are devoid of CD8<sup>+</sup> T cells and IFN gene expression. In contrast, immune desert tumors do not show any evidence of immune cells present<sup>454</sup>. Evaluation of 30 cancer types within The Cancer Genome Atlas (TCGA) database has confirmed the presence of these immune phenotypes, indicating that phenotypic characterization is broadly applicable across tumors<sup>455</sup>.

Further data support the utility of characterizing the tumor immune microenvironment as a means of predicting response to immunotherapy. Successful clinical responses to anti-PD-1 mAb therapy correlated with patient tumors that harbored pre-existing CD8<sup>+</sup> T cells, and expressed high level of interferon (IFN), IFN- $\gamma$ -inducible genes, chemokines, and immune checkpoints, including cytotoxic T lymphocyte antigen-4 (CTLA-4) and indoleamine 2,3-dioxygenase (IDO)<sup>456–459</sup>. Another group reported that increased overall survival (OS) correlated with increased CD4<sup>+</sup>, CD8<sup>+</sup> T cells, Foxp3<sup>+</sup> T cells, CD20<sup>+</sup> B cells, NKp46<sup>+</sup> cells and activated CD143<sup>+</sup> and CD137<sup>+</sup> cells in the tumor tissue<sup>460</sup>. Multiparameter flow cytometry of tumor samples from metastatic melanoma patients receiving anti-PD-1 mAb illustrated that high levels of PD-1 and CTLA-4 on CD8<sup>+</sup> T cells were associated with better clinical responses<sup>461</sup>.

Tumor PD-L1 expression has been one of the most predictive determinants that correlate with response to anti-PD-1 mAb therapy and is indicative of an active immune

response in the tumor microenvironment<sup>330</sup>. However, PD-L1 expression is highly variable and heterogeneous leading to some hesitation to rely on quantitative expression using immunohistochemistry as a reliable means of patient selection for therapy<sup>462</sup>. Additionally, the frequency of T regulatory cells, in relation to CD8<sup>+</sup> T cells, in the tumor can also serve as a biomarker. Patient tumors with high Foxp3<sup>+</sup>: CD8<sup>+</sup> T cell ratios have been demonstrated to correlate with better survival in multiple cancer types<sup>463–467</sup>. In summary, immunological changes in the peripheral blood, tumor microenvironment signatures, and tumor mutational burden can contribute to the identification and understanding of immune signatures to enhance the efficacy of immunotherapy.

### **Concluding Remarks**

Cancer immunotherapies have shown great promise in the treatment of various malignancies. A vast majority of immunotherapies aim to improve T cell function or induce anti-tumor T cell responses. The ACT of TCR gene-modified T cells has been a rapidly developing and promising strategy to treat various tumor types. Clinical and biologic responses have been observed following the ACT of autologous TCR gene-modified T cells, but there is still a need to improve the frequency and durability of responses. In patients receiving monospecific immunotherapy, poor response rates or high relapse rates are commonly observed. Contributing factors include immune-escape tumor variants that can arise through target antigen downregulation or MHC allele loss. Additionally, the tumor microenvironment is highly suppressive, and adept at excluding effector T cells or inhibiting effector functions. As a result, designing T cell-based immunotherapies that induce a broad T cell response (epitope spreading) or improve

the persistence and function of the transferred T cells within the suppressive microenvironment is critical to improving clinical and biologic responses in cancer patients.

The experiments described in this dissertation aim to improve the anti-tumor responses elicited by TCR gene-modified T cells used for immunotherapy. Generally, autologous patient T cells isolated from the peripheral blood are transduced to express a tumor antigen-specific TCR followed by enrichment and expansion and then infused intravenously back into the patient. To facilitate the interaction of transferred TCR gene-modified T cells with tumor cells, we proposed to administer transduced T cells directly into the tumor. We developed an animal model utilizing subcutaneous B16 A2/K<sup>b</sup> mouse melanoma tumors. B16 A2/K<sup>b</sup> tumor cells express the tyrosinase antigen in the context of HLA-A2 (A2), which permits recognition by T cells transduced to express the HLA-A2 (A2)-restricted TIL 1383I TCR.

We concluded that intratumoral delivery of TIL 1383I TCR transduced T cells prolonged survival and suppressed the growth of B16 A2/K<sup>b</sup> tumors. To favorably modulate the TME and counteract immune suppression, we employed an alternative strategy and expressed the TIL 1383I TCR on allogeneic, as opposed to syngeneic, donor T cells. We rationalized that the inflammatory allogeneic response would combat the immunosuppressive tumor microenvironment. We discovered that anti-tumor responses were further improved if TIL 1383I TCR T cells were derived from allogeneic, rather than autologous or syngeneic, donor mice. This mouse model also allowed us to assess the capacity of TIL 1383I TCR transduced T cell treatment to minimize the risk of immune escape, which was measured by the detection of B16-reactive endogenous



T cells. TIL 1383I TCR transduced allogeneic T cells were potent inducers of antigen cross-presentation that resulted in endogenous T cell-mediated protection against distant, untreated tumors. In conclusion, we demonstrate that the tumor-specific reactivity induced by the introduced TCR and alloreactivity mediated by anti-donor graft responses within the tumor microenvironment synergize to enhance the efficacy of T cell-based immunotherapy.

## CHAPTER TWO

### MATERIALS AND METHODS

#### **Cell Lines, Media, and Reagents**

T2, RMA/S, EL-4, EL-4 A2 and Phoenix Ecotropic (ECO) cell lines were obtained from the American Type Culture Collection (Rockford, MD). Human T2 cells are TAP deficient and therefore cannot load their own peptide onto MHC class I. These T2 cells were used as stimulator cells for T cell functional assays. The murine T2 equivalent is the RMA/S cell line. RMA/S cells were used as H-2<sup>b</sup>-restricted targets to assess cross priming. T2 and RMA/S cells were maintained in RPMI 1640 supplemented with 10% FBS (Atlanta Biologicals, Atlanta, GA). Phoenix E cells were maintained in Iscoves DMEM with 10% FBS.

B16 and B16 A2/K<sup>b</sup> melanoma cells were a kind gift from the lab of Dr. Jose Guevara-Patino at Loyola University of Chicago Health Science campus, Maywood, IL. EL-4, EL-4 A2, and B16 tumor cells were maintained in DMEM supplemented with 10% heat-inactivated fetal bovine serum (FBS) (Atlanta Biologicals, GA, USA), 100 U/mL penicillin, 100 µg/mL streptomycin (Invitrogen, Grand Island, NY). The same media was used for B16 A2/K<sup>b</sup> tumors with the addition of 1 mg/mL G418 (InvivoGen, San Diego, CA). One day prior to use in *in vitro* functional assays, 100 ng/mL mouse recombinant IFN-γ (PeproTech, NJ, USA) was added to B16 A2/K<sup>b</sup> cells. All medium components were obtained from Corning Life Sciences (Corning, NY), unless otherwise noted.

## **Mice**

HLA-A2 transgenic, BALB/c, C3H, and NSG A2 mice were obtained from The Jackson Laboratory and bred in house maintained under specific pathogen-free conditions. All animal experiments were performed in accordance with the National Institutes of Health Guidelines and approved by Loyola University Institutional Animal Care and Use Committee.

### **Transduction of Mouse T Cells**

Three days prior to transduction, Phoenix-E cells were seeded at  $4 \times 10^6$  in a 10 cm tissue culture dish (Falcon, Corning, NY) in 10 mL Iscoves DMEM with 10% FBS and incubated in a humidified chamber at 37°C with 5% CO<sub>2</sub>. The next day, Phoenix-E cells were transfected with 18 µg of vector DNA (Aldevron, Fargo, ND), Lipofectamine 2000 (Invitrogen, Grand Island, NY) and OPTI-MEM (Gibco, Waltham, MA) and incubated overnight. The day after transfection, the Phoenix-E media is replaced with Iscoves DMEM/10% FBS/ 4mM sodium butyrate and incubated in a humidified chamber at 37°C with 5% CO<sub>2</sub> overnight. Two days prior to transduction, spleens from HLA-A2 transgenic (syngeneic) and BALB/c (allogeneic) mice were harvested and mechanically disrupted over a 70 µm cell strainer (Falcon, Corning, NY) using the back of a 3 mL syringe (BD biosciences, San Jose, CA). The red blood cells were lysed with Ack lysis buffer (Lonza, Alpharetta, GA, USA). After washing and counting, mouse T cells were enriched using the Pan T Cell Isolation Kit II (Miltenyi Biotec) and activated with anti-CD3/anti-CD28 Dynabeads (Gibco). T cells were then seeded in 24 well tissue culture plates at  $1 \times 10^6$ /mL in 2 mL per well with IL-2 (20 IU/mL) and IL-15 (50 ng/mL) and incubated at 37°C with 5% CO<sub>2</sub> for 48 hours. On the day of transduction, virus was

collected and filtered with a 0.45  $\mu\text{m}$  PES syringe (Millipore, Ontario, Canada). T cells were collected and the anti-CD3/anti-CD28 magnetic activating beads were removed using a DynaMag. T cells were resuspended in viral supernatant containing 8  $\mu\text{g/mL}$  of hexadimethrine bromide (polybrene, Sigma) and seeded at  $1 \times 10^6/\text{mL}$  in 24 well tissue culture plates. Cells were spun at 1000 $\times g$  for 2 hours at 32°C. Following the spin, plates were removed and incubated in a humidified chamber for 2-4 hours at 37°C with 5%  $\text{CO}_2$ . Cells were collected and cultured in mouse media with IL-2 (20 IU/mL) and IL-15 (50 ng/mL) and incubated at 37°C with 5%  $\text{CO}_2$ . Media was refreshed every 2 days. Transduction efficiency was assessed 48-72 hours later by flow cytometry.

Mouse T cells were maintained in RPMI supplemented with 10% heat-inactivated fetal bovine serum (Atlanta Biologicals, GA, USA), 10 mM HEPES, 2 mM L-glutamine (Invitrogen, Grand Island, NY USA), 100 U/mL penicillin, 100  $\mu\text{g/mL}$  streptomycin (Invitrogen, Grand Island, NY USA), non-essential amino acids (Invitrogen, Grand Island, NY USA) and 50  $\mu\text{M}$  2-mercaptoethanol (Sigma), referred to as mouse media. For maintain mouse T cells in culture, mouse media was supplemented with 20 IU/mL IL-2 (Novartis Pharmaceuticals Corporation, East Hanover, NJ) and 50 ng/mL IL-15 (Biological Resources Branch, National Cancer Institute, Frederick, MD).

### **Tumor Challenges and Treatment**

B16 and B16 A2/K<sup>b</sup> tumor cells were cultured in T-175cm<sup>2</sup> flasks (Corning Life Sciences, Corning, NY) at 37°C with 5%  $\text{CO}_2$  to reach 80% confluency on the day of tumor injection. The hind flanks of the mice were shaved at least one day prior to injection. Mice subcutaneously received  $2.5 \times 10^5$  (B16 A2/K<sup>b</sup>) or  $1 \times 10^5$  (B16) cells in 100  $\mu\text{L}$  PBS in the right flank of 6-12 week old HLA-A2 transgenic mice. Tumor area was

measured 2-3 times weekly and calculated as the product of two opposing diameters. Tumor-bearing mice were sacrificed when the tumor area reached  $>150\text{mm}^2$  or  $>10\%$  body weight.

When tumors were clearly palpable, HLA-A2 transgenic mice were randomly divided into treatment groups ( $n=4-5/\text{group}$ ). Mice under inhalatory isoflurane anesthesia were intratumorally treated on day 10 post-tumor inoculation with TIL 1383I TCR transduced allogeneic, TIL 1383I TCR transduced syngeneic, or untransduced allogeneic T cells in  $50\ \mu\text{l}$  PBS. Intratumoral injections were performed using 31G ultrafine insulin needles. Transduction efficiency was assessed by  $V\beta 12$  and GFP expression. For TIL 1383I TCR transduced allogeneic and TIL 1383I TCR transduced syngeneic treatment, HLA-A2 transgenic mice received approximately  $8 \times 10^6$  total T cells, after adjusting for transduction efficiency. Untransduced allogeneic T cell treated-mice received the same number of total T cell as TIL 1383I TCR transduced allogeneic T cell-treated mice.

For experiments using checkpoint inhibitors, where indicated, tumor-bearing HLA-A2 transgenic mice received  $200\ \text{mg/kg}$  i.p of anti-PD-1 mAb (clone RPM1-14, BioCellX) or anti-CTLA-4 mAb (clone 9H10, BioCellX) or isotype control administered intraperitoneally on day 10 post-B16 A2/K<sup>b</sup> inoculation. Immune checkpoint inhibitor treatment continued throughout the experiment and were administered intraperitoneally every 3-4 days until the completion of the experiment. For experiments testing the TLR3 agonist, HLA-A2 transgenic mice received  $50\ \mu\text{g}$  polyinosinic:polycytidylic acid (Poly I:C) (InVivogen, San Diego, CA) in  $50\ \mu\text{l}$  PBS by intratumoral injection on day 11 post-B16 A2/K<sup>b</sup> inoculation .

## Tissue Preparation

Spleens, lymph nodes, and tumors were harvested and maintained in mouse media (described above). Single cell suspensions of tumors were obtained using the Miltenyi Biotec (Bergisch Gladbach, Germany) tumor dissociation kit II and collected in gentleMACS C tubes, then dissociated using gentleMACS Dissociator. Following dissociation, single cell suspensions of tumors were incubated in a humidified incubator at 37°C and 5% CO<sub>2</sub> for 30 minutes and then passed through a 70 µm cell strainer. For tumors harvested 2 days post- T cell treatment, cells were washed and stained immediately. For tumors harvested 7 days post-T cell treatment, cells were layered in a 40%/80% percoll (GE Healthcare) gradient and centrifuged for 25 minutes at 800 x g at 25°C with no brake. Cells at the interphase were collected, washed twice, and proceeded for staining. Spleens and lymph nodes were mechanically disrupted using the plunger of a 3 mL syringe over a 70 µm cell strainer. Red blood cells were lysed with ACK lysis buffer (Lonza, Alpharetta, GA, USA). Cells were then washed twice, counted and stained with antibodies for flow cytometric analysis, or used for functional assays.

## Peptides

Mouse melanoma peptides that were used for *in vitro* and *in vivo* functional assays were synthesized and high-performance liquid chromatography (HPLC) purified by GenScript (Piscataway, NJ, USA) at >95% purity. Mouse H-2<sup>b</sup> peptides (gp100<sub>25-33</sub> EGSRNQDWL and TRP-2<sub>180-188</sub> SVYDFFVWL) were dissolved in 100% dimethyl sulfoxide (DMSO, Sigma-Aldrich) and stored at a concentration of 5 µg/µL at 80°C. Peptides were used at a concentration of 10 µg/mL.

### **Intracellular Cytokine/Degranulation Bifunctional Assay**

To assess *in vitro* and *in vivo* cytokine production, we used intracellular cytokine or degranulation functional assays. CD107a expression was used as a surrogate marker for lytic function. Peptide-loaded T2 cells, B16, and B16-A2/K<sup>b</sup> cells were used as targets and TIL 1383I TCR transduced mouse T cells were used as effector cells. T2 cells were pulsed with 10 $\mu$ g/mL peptide for 2 hours at 37°C in a 5% CO<sub>2</sub> humidified incubator. After two washes with RPMI, 3 x 10<sup>5</sup> T cells were co-cultured with 3 x 10<sup>5</sup> target cells in 96 well U-bottom tissue culture plates at 37°C for 5 hours in the presence of 250 ng anti-CD107a mAb, 5 ng/mL brefeldin A (BioLegend), and 2 nM monensin (Biolegend). After 5 hours, the cells were stained with antibodies (described below) for 20 minutes at room temperature. Cells were fixed, permeabilized, and stained with anti-IFN- $\gamma$ , anti-GM-CSF, anti-TNF- $\alpha$ , and anti-IL-2 cytokine antibodies (described below) according to manufacturer's protocols (Biolegend). Flow cytometry was performed using a BD LSRII FACS Aria and analyzed using FlowJo software.

### **Antibody Staining and Flow Cytometry**

To characterize immune cell populations, we used antibody staining followed by flow cytometry. Antibodies were used at the concentrations recommended by the manufacturer. Antibodies were purchased from BioLegend, unless otherwise indicated: anti- CD3 $\epsilon$  (clone 145-2C11), CD4 (clone GK1.5), CD8 $\alpha$  (clone 53-6.7), CD11c (clone N418), CD11b (clone M1/70), CD205 (clone NLDC-145), CD80 (clone 16-10A1), CD86 (clone GL-1), CD103 (clone 2E7), I-A/I-E (clone M5/114.15.2), CD62L (clone MEL-14), CD44 (clone IM7), CD69 (clone H1.2F3), CD25 (clone 3C7), CD152 (clone UC10-4B9), FOXP3 (clone MF-14), PD-1 (clone 29F.1A12), TIM-3 (clone RMT3-23), PD-L1 (clone

10F.9G2), PD-L2 (clone TY25), CXCR3 (clone CXCR3-173), CD107a (clone 1D4B), IFN- $\gamma$  (clone XMG1.2), IL-2 (clone JES6-5H4), TNF- $\alpha$  (clone MP6-XT22), GM-CSF (clone MP1-22E9), TGF- $\beta$ /LAP (clone TW7-16B4), IL-10 (clone JES5-16E3), IL-17A (clone TC11-18H10.1), IL-22 (clone Poly5164), H-2D<sup>d</sup> (clone 34-2-12), H-2D<sup>b</sup> (clone KH95), human HLA-A2 (clone BB7.2), human TCR VB12 (Beckman Coulter, REF IM2291 clone). Intracellular IFN- $\gamma$  and IL-2 staining was performed using the cytofix/cytoperm kit (BD Biosciences) according to manufacturer's protocol. LIVE/DEAD Aqua fixable viability dye was purchased from Miltenyi Biotec (Auburn, CA, USA).

Tetramers were provided by the NIH Tetramer Core Facility, Atlanta, GA). CD8 alpha antibody clone KT15 was used when tetramer staining was performed. Cells were stained in PBS containing 2% bovine serum albumin for 20 minutes at room temperature. For intracellular markers, cells were fixed and permeabilized using eBioscience Foxp3/Transcription Factor Staining Buffer set according to manufacturer's protocol. Flow cytometry was performed using an LSRFortessa flow cytometer (BD Biosciences) and data were analyzed with FlowJoX software (Treestar, Ashland, OR).

### **Detection of IFN- $\gamma$ Secreting Cells by ELISPOT Assays**

IFN- $\gamma$  production by tumor-specific T cells isolated from the tumor draining lymph nodes and spleens of treated mice was measured by IFN- $\gamma$  ELISPOT assays (BD biosciences). ELISPOT plates (BD component No. 51-2447KC) were coated with 5  $\mu$ g/mL (final concentration) of purified anti-mouse IFN- $\gamma$  antibody and incubated overnight at 4°C. After washing the plates, 1-2x10<sup>5</sup> cells from the tumor draining lymph nodes or spleens were added and cocultured 1:1 with tumor targets (B16, B16 A2/K<sup>b</sup>, EL4, EL4 A2) or peptide (gp100<sub>25-33</sub>, TRP-2<sub>180-188</sub>; 10  $\mu$ g/mL)-pulsed RMA/S cells for 18



hours. After extensive washing, 2  $\mu\text{g/mL}$  (final concentration) of biotinylated anti-mouse IFN- $\gamma$  detection antibody was added for 2 hours. Streptavidin-HRP (1:100) was added for one hour and spots were developed with 2-Amino-9-ethylcarbazole (AEC) substrate solution (BD biosciences). Plates were dried in the dark overnight and spots were enumerated automatically using an ELISOPT plate reader (CTL cellular technology limited, Immunospot).

### ***In Vivo Cytotoxicity Assay***

Target cells were prepared from the spleens of C57Bl/6 mice, as described above. Splenocytes were pulsed 10  $\mu\text{g/mL}$  TRP-2<sub>180-188</sub> or gp100<sub>25-33</sub> peptides for 2 hours in a humidified chamber at 37°C with 10  $\mu\text{g/mL}$  TRP-2<sub>180-188</sub> or gp100<sub>25-33</sub>. Target splenocytes were washed twice with PBS, divided into 3 groups: no peptide, TRP2<sub>180-188</sub>, or gp100<sub>25-33</sub>, and labeled with 15  $\mu\text{M}$ , 5  $\mu\text{M}$ , or 0.5  $\mu\text{M}$  CellTrace™ CFSE dye (Thermofisher, Molecular Probes), respectively. After 10 minutes of incubation at 37°C, 30 mL of complete media was added to quench the CFSE and further incubated for 10 minutes. Cells were washed twice and counted.  $3 \times 10^6$  cells from each target group were combined 1:1:1, centrifuged at 1200 rpm for 5 minutes, and resuspended in 200  $\mu\text{L}$  of PBS. CFSE-labeled target cells were then retro-orbitally injected into recipient HLA-A2 transgenic mice 8 days post-intratumoral treatment when the induction of effector T cells had been observed. A group of naïve HLA-A2 transgenic mice (n=3, no tumor, no treatment) injected with CFSE-labeled target cells were used as a control. The following day, the spleens of recipient HLA-A2 transgenic mice were harvested and analyzed by flow cytometry. Cells were gated on the CFSE<sup>+</sup>HLA-A2<sup>-</sup> population and 50,000 events were collected. Specific lysis was calculated using the formula:

Percent specific lysis=  $[1 - (\text{naïve control ratio/experimental mice ratio})] \times 100$ . Results are presented as % Killing.

### Vector Construction

To co-express the TIL 1383I TCR and extracellular LIGHT domain, a DNA gene block with the sequence of the LIGHT extracellular domain was synthesized from Genscript (Piscataway, NJ) and ligated into the pCR2.1-TOPO TA vector with EcoRI (Thermo Scientific, Grand Island, NY), T4 DNA ligase and buffer (New England Biolabs, Ipswich, MA). Recombinant DNA was transformed into *E. coli* TOP10 competent cells (Invitrogen) and plated on LB ampicillin plates (25 g LB agar (Fisher, Hampton, NH) in 1 L deionized water supplemented with 100 µg/mL ampicillin (Sigma-Aldrich) and colonies were grown in superbroth (32 g Tryptone (Fisher), 20 g yeast extract (Fisher), and 5 g NaCl (Fisher) in 1 L deionized water) with 100 µg/mL ampicillin (Sigma-Aldrich)). Plasmid DNA from recombinant clones was extracted using a Miniprep Plasmid Isolation Kit (Qiagen, Hilden, Germany) according to manufacturer's protocol and then screened for LIGHT gene insertion by restriction enzyme digest using EcoRI (Thermo Scientific, Grand Island, NY).

After running the product on a 1% agarose gel, DNA bands corresponding to the LIGHT gene product were purified using a Gel purification kit (Qiagen) according to manufacturer's protocol. Next, LIGHT DNA was subcloned into the pMIG TIL 1383I TCR mCherry retroviral vector with compatible EcoRI restriction sites. DNA was ligated into the vector using T4 DNA ligase and buffer (New England Biolabs, Ipswich, MA), with vector DNA and insert DNA in a 1:5 ratio and was incubated at 16°C overnight. The next day, ligation products were transformed into TOP10 competent *E. coli* and DNA

was extracted (Qiagen). The DNA was then sequenced (Genewiz, South Plainfield, NJ) to confirm final product.

Sequence of the LIGHT extracellular domain:

CGAAGGTCTCACGAGGTCAACCCAGCAGCGCATCTCACAGGGGGCCAACTCCAGCT  
TGACCGGCAGCGGGGGGCGCTGTTATGGGAGACTCAGCTGGGCCTGGCCTTCC  
TGAGGGGGCCTCAGCTACCACGATGGGGGCCCTTGTGGTCACCAAAGCTGGCTACTA  
CTACATCTACTCCAAGGTGCAGCTGGGCGGTGTGGGCTGCCCCGCTGGGCCTGGC  
CAGCACCATCACCCACGGCCTCTACAAGCGCACACCCCGCTACCCCGAGGAGCT  
GGAGCTGTTGGTCAGCCAGCAGTCACCCTGCGGACGGGCCACCAGCAGCTCCCG  
GGTCTGGTGGGACAGCAGCTTCCTGGGTGGTGTGGTACACCTGGAGGCTGGGGA  
GAAGGTGGTCGTCCGTGTGCTGGATGAACGCCTGGTTCGACTGCGTGATGGTACC  
CGGTCTTACTTCGGGGCTTTCATGGTGTGA.

Purified LIGHT recombinant protein was purchased from Sino Biological (Wayne, Pennsylvania, USA). On day 10 post-B16 A2/K<sup>b</sup> tumor inoculation, HLA-A2 transgenic mice received intratumoral TIL 1383I TCR transduced T cells and recombinant LIGHT protein in PBS.

### **Statistical Analysis**

All results were analyzed with Prism (GraphPad software, Inc San Diego, CA). Statistical significance was determined with a regular one-way ANOVA with Tukey correction. Where indicated, statistical significance was determined using unpaired student's t test. Survival and B16 tumor-free graphs were presented using the Kaplan-Meier plots with significance determined by the log-rank (Mantel-Cox) test. Data represent means +/- SEM. P<0.05 was considered statistically significant. \*P<0.05,

\*\* $P < 0.01$ , \*\*\* $P < 0.001$ , \*\*\*\* $P < 0.0001$ . All experiments were performed at least twice to ensure consistency.

## CHAPTER THREE

### INTRATUMORAL DELIVERY OF TIL 1383I TCR TRANSDUCED T CELLS EXTENDS SURVIVAL AND SUPPRESSES B16 A2/K<sup>b</sup> TUMOR GROWTH

#### **TIL 1383I TCR Transduced Mouse T Cells Recognize**

##### **B16 A2/K<sup>b</sup> Tumors *In Vitro***

The TCR used in these studies was obtained from a tumor infiltrating lymphocyte (TIL) clone (1383I) that recognizes the tyrosinase<sub>368-376</sub> peptide in an HLA-A2-restricted manner, referred to as TIL 1383I TCR<sup>468</sup>. The retroviral vector contains the TIL 1383I TCR  $\alpha$  and  $\beta$  chain genes followed by a green fluorescent protein (GFP) gene, linked by self-cleaving 2A-like sequences (Fig 6A). Following retroviral transduction, TIL 1383I TCR<sup>+</sup> T cells can be identified through the expression of GFP and an antibody against the TCR  $\beta$  chain (anti-V $\beta$ 12) using flow cytometry (Fig 6B). Two days before transduction, T cells isolated from the spleens of mice were enriched for CD3 using magnetic labeling and activated with anti-CD3/anti-CD28 beads. This selection method resulted in  $\geq 95\%$  CD3<sup>+</sup> T cells (Table 1). We transduced cells by spinoculation and assessed for TCR expression after 3-4 days. We routinely achieved  $\geq 45\%$  CD4<sup>+</sup>GFP<sup>+</sup> V $\beta$ 12<sup>+</sup> and CD8<sup>+</sup>GFP<sup>+</sup> V $\beta$ 12<sup>+</sup> transduced T cells (Table 1). The final population of TIL 1383I TCR transduced T cells usually favored CD8<sup>+</sup> T cells ( $\sim 55\%$ ) over CD4<sup>+</sup> T cells ( $\sim 30\%$ ; Table 1). These experiments demonstrated that we could obtain relatively pure populations of mouse CD3<sup>+</sup> T cells, which were  $\geq 45\%$  GFP<sup>+</sup>V $\beta$ 12<sup>+</sup> TCR<sup>+</sup> cells.

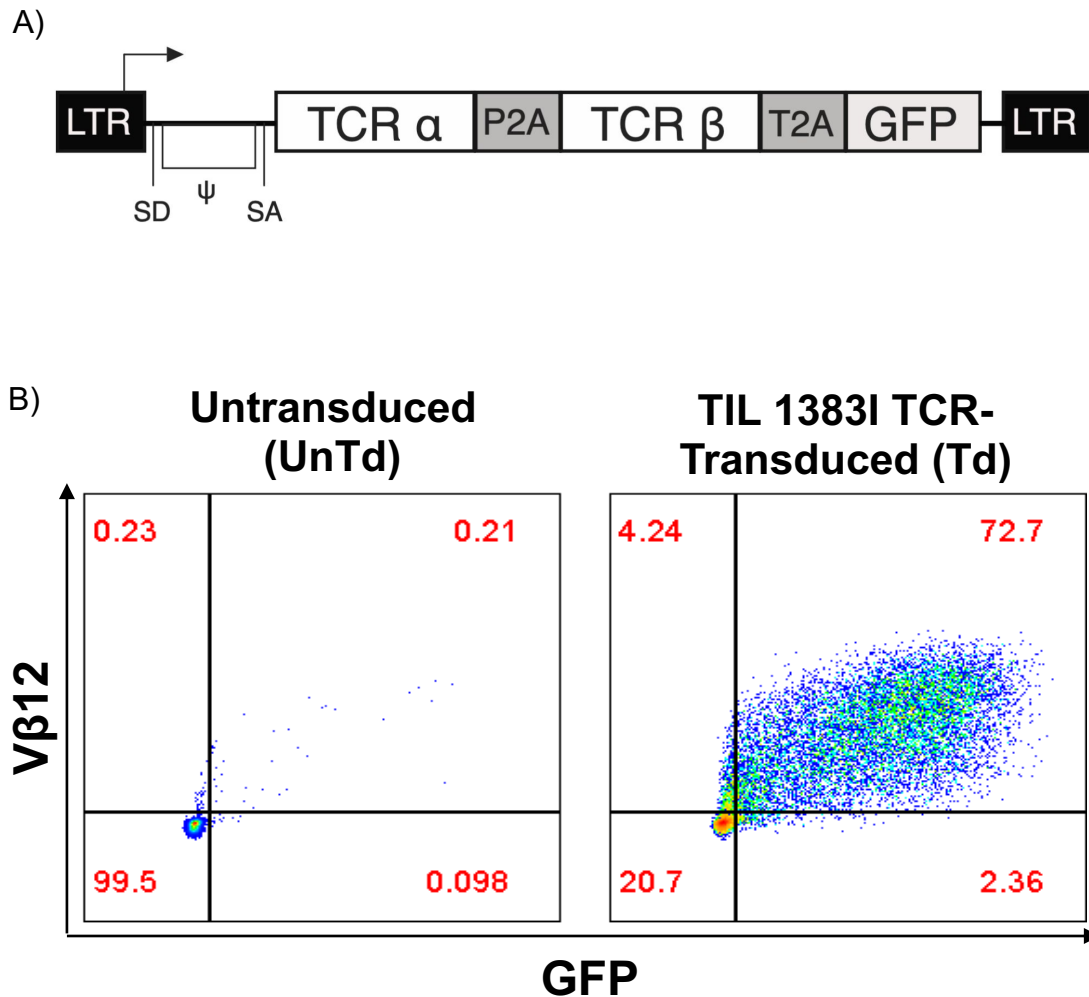


**Figure 6. Expression of the TIL 1383I TCR on Mouse T Cells.** A) The retroviral vector containing the TIL 1383I TCR  $\alpha$  and  $\beta$  genes linked by a P2A self-cleaving peptide segment followed by a T2A-linked GFP gene. B) Representative flow cytometry plots of GFP and V $\beta$ 12 expression on untransduced (UnTd, left panel) or TIL 1383I TCR transduced (Td, right panel) T cells. CD3-enriched splenocytes were activated with anti-CD3/anti-CD28 DynaBeads for 48 hours. Activated T cells were resuspended in supernatant containing the retrovirus with 8  $\mu$ g/mL polybrene. T cells were then transduced by spinoculation for 2 hours at 32°C. T cells were then resuspended in fresh mouse media with IL-2 (20 IU/mL) and IL-15 (50 ng/mL) and maintained in a humidified incubator at 37°C. Three to four days post-transduction, T cells were analyzed for expression of GFP and V $\beta$ 12 by flow cytometry. Gated on CD3<sup>+</sup> T cells. LTR: long terminal repeat;  $\psi$ : packaging signal; SD: splice donor; SA: splice acceptor; GFP: green fluorescent protein.

	Transduced Syngeneic	Transduced Allogeneic
%CD3 <sup>+</sup>	96 ± 0.96	96 ± 1.14
%CD4 <sup>+</sup>	31 ± 2.7	37 ± 3.2
%CD4 <sup>+</sup> Vβ12 <sup>+</sup> GFP <sup>+</sup>	64 ± 4.7	57 ± 4.07
%CD8 <sup>+</sup>	56 ± 2.92	54 ± 3.19
%CD8 <sup>+</sup> Vβ12 <sup>+</sup> GFP <sup>+</sup>	49 ± 4.25	50 ± 3.98

**Table 1. Phenotype of TIL 1383I TCR Transduced T Cells.** Enrichment of T cells isolated from the spleens by immunomagnetic separation resulted in ≥95% CD3<sup>+</sup> T cells. Three to four days after transduction, T cells were analyzed for expression of CD3, CD4, CD8, Vβ12, and GFP by flow cytometry. Generally, the population of TIL 1383I TCR transduced T cells was comprised of more CD8<sup>+</sup> T cells. Numerical values represent mean ± SEM (n=25). No statistical differences were observed between syngeneic and allogeneic T cells.

We first assessed the antigen-specific functional phenotypes of TIL 1383I TCR transduced T cells. T cells isolated from syngeneic HLA-A2 transgenic mice were transduced to express the TIL 1383I TCR. TIL 1383I TCR transduced syngeneic T cells were co-cultured with B16 or B16 A2/K<sup>b</sup> tumor targets for 5 hours and then analyzed by flow cytometry for expression of extracellular CD107a, a surrogate marker for cytotoxic degranulation, and intracellular cytokines: GM-CSF, IL-2, TNF-α, and IFN-γ. As expected, CD8<sup>+</sup> (gated on CD3<sup>+</sup>GFP<sup>+</sup>) TIL 1383I TCR transduced syngeneic T cells were highly reactive against B16 A2/K<sup>b</sup> tumor cells (Fig 7A, right panel, blue bars), but not the parental B16 line (Fig 7A, left panel, blue bars).

We observed a substantial frequency of TIL 1383I TCR transduced syngeneic T cells expressing the lytic marker, CD107a (44.55 ± 5.850%), as well as IFN-γ (32.833 ± 2.210%) and TNF-α (38.93 ± 8.392%) cytokines in response to B16 A2/K<sup>b</sup> tumors.

Additionally, TIL 1383I TCR transduced syngeneic T cells expressed IL-2 ( $12.12 \pm 3.471\%$ ) and GM-CSF ( $17.067 \pm 3.023\%$ ) when co-cultured with B16 A2/K<sup>b</sup> (Fig 7A, right panel, blue bars). TIL 1383I TCR transduced allogeneic T cells had similar frequencies of CD107a<sup>+</sup> cells (gated on CD3<sup>+</sup>GFP<sup>+</sup>CD8<sup>+</sup>) when stimulated with B16 A2/K<sup>b</sup> targets ( $50 \pm 1.2\%$ ;  $P=0.4578$ ) and similar frequencies of T cells expressing IFN- $\gamma$  ( $26.367 \pm 1.489\%$ ;  $P=0.0722$ ), TNF- $\alpha$  ( $45.033 \pm 7.841\%$ ;  $P=0.6234$ ), IL-2 ( $12.667 \pm 1.386\%$ ;  $P=0.8908$ ) and GM-CSF ( $14.667 \pm 1.592\%$ ;  $P=0.5212$ ) (Fig 7B, red bars). These results demonstrate that expression of the TIL 1383I TCR on CD8<sup>+</sup> T cells from syngeneic or allogeneic donors confers similar functional phenotypes against B16 A2/K<sup>b</sup> tumors and does not elicit tumor-specific responses or alloresponses against B16 *in vitro*.

The TIL 1383I TCR is CD8-independent; therefore, transduced CD4<sup>+</sup> T cells also have the capacity to recognize B16 A2/K<sup>b</sup> tumors. We examined the functional phenotype of CD3<sup>+</sup>CD4<sup>+</sup>GFP<sup>+</sup> T cells in response to tumor targets (Fig 7B, blue bars). TIL 1383I TCR transduced syngeneic CD4<sup>+</sup> T cells stimulated with B16 A2/K<sup>b</sup> cells (Fig 7B, right panel, blue bars) resulted in expression of CD107a ( $34.3\% \pm 11.9$ ), IFN- $\gamma$  ( $10.347\% \pm 3.713$ ), TNF- $\alpha$  ( $16.733\% \pm 4.191$ ), IL-2 ( $7.320\% \pm 2.209$ ), and GM-CSF ( $7.133\% \pm 2.313$ ). We also observed comparable functional phenotypes in CD4<sup>+</sup> TIL 1383I TCR transduced allogeneic T cells, which expressed CD107a ( $30.07 \pm 3.93\%$ ;  $P=0.7679$ ), IFN- $\gamma$  ( $6.613 \pm 3.387\%$ ;  $P=0.4988$ ), TNF- $\alpha$  ( $19.767 \pm 7.829\%$ ;  $P=0.7498$ ), IL-2<sup>+</sup> ( $7.967 \pm 3.353\%$ ;  $P=0.8799$ ), and GM-CSF ( $5.317 \pm 2.618\%$ ;  $P=0.6305$ ) cells (Fig 7D, red bars). As expected, TIL 1383I TCR transduced syngeneic CD4<sup>+</sup> T cells did not recognize B16 tumors, which lack HLA-A2 (Fig 7B, left panel, blue bars). These results

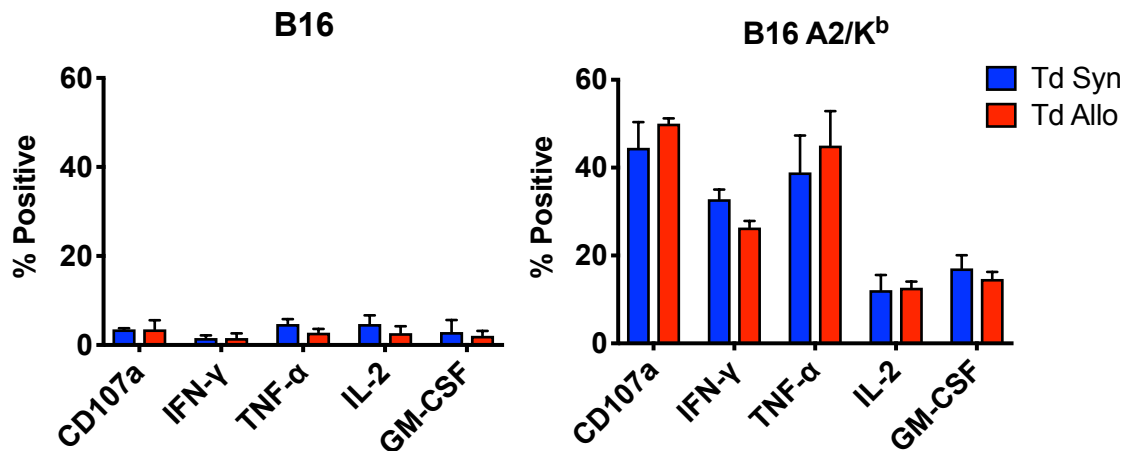


indicated that CD4<sup>+</sup> T cells expressing the TIL 1383I TCR are highly functional against B16 A2/K<sup>b</sup>, but not B16 tumors.

In addition to examining reactivity against whole B16 and B16 A2/K<sup>b</sup> tumor cells, we also tested the capacity of TIL 1383I TCR transduced syngeneic T cells and TIL 1383I TCR transduced allogeneic T cells to recognize the tyrosinase<sub>368-376</sub> peptide presented by T2 antigen presenting cells (APCs). We also tested recognition against an irrelevant negative control peptide, gp100<sub>209-217</sub>. As expected, significant frequencies of TIL 1383I TCR transduced syngeneic CD8<sup>+</sup> T cells expressed CD107a<sup>+</sup> (65.25% ± 0.650), IFN- $\gamma$  (49.2% ± 5.092), TNF- $\alpha$  (59.067% ± 5.843), IL-2 (25.067% ± 3.227), and GM-CSF (29.533% ± 7.835) after stimulation with tyrosinase<sub>368-376</sub>-pulsed T2 cells (Fig 8A, right panel, blue bars). In contrast, TIL 1383I TCR transduced syngeneic CD8<sup>+</sup> T cells did not recognize the negative control gp100<sub>209-217</sub> peptide (Fig 8A, left panel, blue bars), confirming antigen specificity.

We observed similar results when investigating the ability of TIL 1383I TCR transduced allogeneic T cells to recognize tyrosinase<sub>368-376</sub> peptide-pulsed T2 cells. CD8<sup>+</sup> TIL 1383I TCR transduced allogeneic T cells were also highly reactive against tyrosinase<sub>368-376</sub> peptide-pulsed T2 cells, and similar frequencies of CD107a<sup>+</sup> (75% ± 7.2), IFN- $\gamma$ <sup>+</sup> (41.4% ± 9.3), TNF- $\alpha$ <sup>+</sup> (62.3% ± 11.9), IL-2<sup>+</sup> (25% ± 6.1), and GM-CSF<sup>+</sup> (26.2% ± 11.2) cells were observed compared to TIL 1383I TCR transduced syngeneic T cells (Fig 8B, red bars). Additionally, TIL 1383I TCR transduced syngeneic CD4<sup>+</sup> T cells were highly reactive when co-cultured with tyrosinase<sub>368-376</sub> peptide-pulsed T2 APC cells, and expressed CD107a<sup>+</sup> (29.7 ± 17.2%), IFN- $\gamma$  (10.4 ± 3.01%), TNF- $\alpha$  (45.7 ± 5.0%), IL-2 (25.6 ± 8.4%), and GM-CSF (9.9 ± 4.8%) (Fig 8B, right panel, blue bars).

A) Gated on CD3<sup>+</sup>CD8<sup>+</sup>GFP<sup>+</sup> T cells



B) Gated on CD3<sup>+</sup>CD4<sup>+</sup>GFP<sup>+</sup> T cells

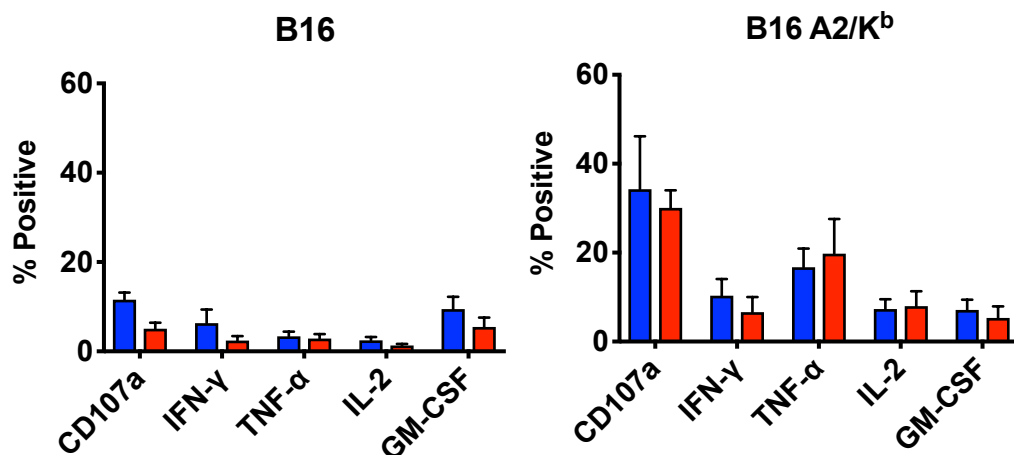
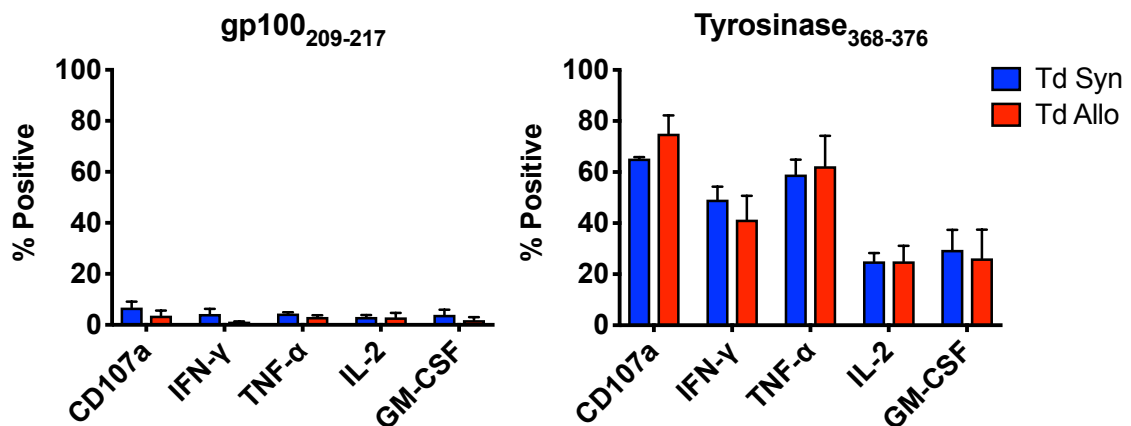


**Figure 7. TIL 1383I TCR Transduced T Cells Recognize B16 A2/K<sup>b</sup> Tumors.** B16 or B16 A2/K<sup>b</sup> tumors were co-cultured 1:1 with 300,000 TIL 1383I TCR transduced mouse T cells derived from the spleens of syngeneic HLA-A2 transgenic mice (blue bars) or allogeneic BALB/c mice (red bars) for 5 hours. Cells were collected and examined for expression of CD3, CD4, CD8, GFP, CD107a, IFN- $\gamma$ , TNF- $\alpha$ , IL-2, and GM-CSF by flow cytometry. 50,000 CD3<sup>+</sup> events were recorded. A) Reactivity of CD3<sup>+</sup>CD8<sup>+</sup>GFP<sup>+</sup> T cells in response to B16 (left panel) or B16 A2/K<sup>b</sup> (right panel) tumors. B) Reactivity of CD3<sup>+</sup>CD4<sup>+</sup>GFP<sup>+</sup> T cells in response to B16 (left panel) or B16 A2/K<sup>b</sup> (right panel) tumors. No statistically significant differences in functional markers were observed between syngeneic and allogeneic donor T cells using the student's t test.

A) Gated on CD3<sup>+</sup>CD8<sup>+</sup>GFP<sup>+</sup> T cells



B) Gated on CD3<sup>+</sup>CD4<sup>+</sup>GFP<sup>+</sup> T cells

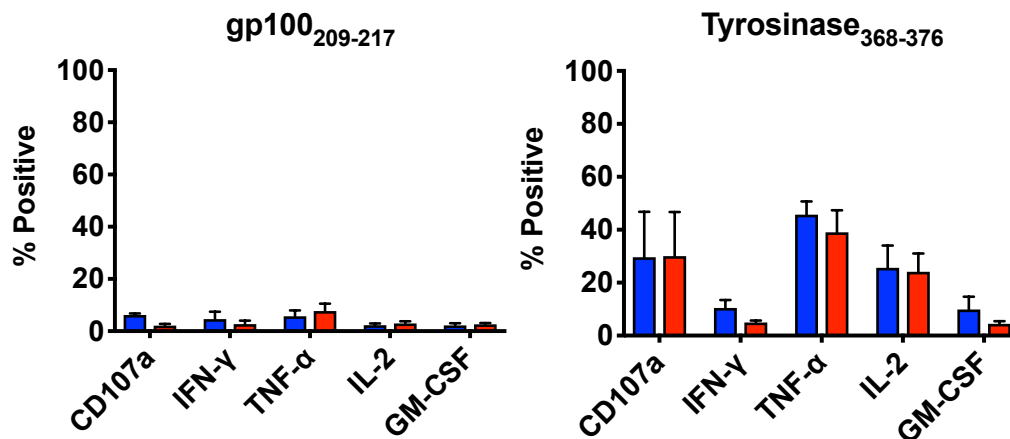


**Figure 8. TIL 1383I TCR Transduced T Cells Recognize Tyrosinase<sub>368-376</sub> Peptide.** T2 cells were pulsed with 10 ug/mL peptide for 2 hours in a humidified incubator at 37°C and then cocultured 1:1 with 300,000 TIL 1383I TCR transduced mouse T cells that were derived from the spleens of syngeneic HLA-A2 transgenic mice (blue bars) or allogeneic BALB/c mice (red bars). After 5 hours, co-cultures were analyzed for expression of CD3, CD4, CD8, GFP, CD107a, IFN-γ, TNF-α, IL-2, and GM-CSF by flow cytometry. 50,000 CD3<sup>+</sup> events were recorded. A) Reactivity of CD3<sup>+</sup>CD8<sup>+</sup>GFP<sup>+</sup> T cells in response to gp100<sub>209-217</sub>-pulsed (left panel) or tyrosinase<sub>368-376</sub>-pulsed (right panel) T2 cells. B) Reactivity of CD3<sup>+</sup> CD4<sup>+</sup> GFP<sup>+</sup> in response to gp100<sub>209-217</sub>-pulsed (left panel) or tyrosinase<sub>368-376</sub>-pulsed (right panel) T2 cells. No statistically significant differences in functional markers were observed between syngeneic and allogeneic T cells using the student's t test.

We confirmed antigen-specificity by the lack of reactivity of T cells isolated from the tumor draining lymph nodes of treated mice against the gp100<sub>209-217</sub> peptide (Fig 8B, left panel, blue bars). TIL 1383I TCR transduced allogeneic CD4<sup>+</sup> T cells were also highly reactive to the tyrosinase<sub>368-376</sub> peptide, but not statistically different from TIL 1383I TCR transduced syngeneic T cells. TIL 1383I TCR transduced allogeneic CD4<sup>+</sup> T cells expressed CD107a (30.05%  $\pm$  16.65), IFN- $\gamma$  (4.973%  $\pm$  0.713), TNF- $\alpha$  (39%  $\pm$  8.358), IL-2 (24.1%  $\pm$  6.974), and GM-CSF (4.417%  $\pm$  1.016) cells (Fig 8D, red bars). Neither TIL 1383I TCR transduced allogeneic nor syngeneic CD4<sup>+</sup> or CD8<sup>+</sup> T cells were reactive against gp100<sub>209-217</sub>-pulsed T2 cells (Fig 8A and C, red and blue bars). These *in vitro* results indicated that both TIL 1383I TCR transduced syngeneic and allogeneic T cells were equally polyfunctional against B16 A2/K<sup>b</sup> tumors *in vitro*. In general, stimulating TIL 1383I TCR transduced T cells with tyrosinase<sub>368-376</sub>-pulsed T2 cells resulted in a higher frequency of functional T cells compared to stimulation with B16 A2/K<sup>b</sup> tumors. The increased antigen-specific reactivity observed with T2 cells can likely be attributed to their TAP deficiency, which prevents the presentation of endogenously synthesized antigens and permits saturation with peptides loaded exogenously. Results from these *in vitro* experiments demonstrated that TIL 1383I TCR transduced syngeneic T cells were polyfunctional, producing IL-2, GM-CSF, IFN- $\gamma$ , and TNF- $\alpha$  and exhibiting cytolytic activity (CD107a<sup>+</sup>) when stimulated with B16 A2/K<sup>b</sup> tumors, but not B16 tumors.

### **Intratumoral Treatment with TIL 1383I TCR Transduced Allogeneic T Cells**

#### **Improves Survival and Suppresses B16 A2/K<sup>b</sup> Tumor Growth in Mice**

Previous pre-clinical mouse studies demonstrated that i.v. infusion of TIL 1383I TCR transduced HLA-A2 transgenic T cells, in combination with tyrosinase<sub>368-376</sub>

peptide-loaded dendritic cells (DCs) and high dose IL-2, prevented growth of established subcutaneous B16 A2/K<sup>b</sup> tumors in syngeneic HLA-A2 transgenic mice<sup>469</sup>. In patients with metastatic melanoma, i.v. infusion of TIL 1383I TCR transduced T cells has resulted in clinical and biological responses, exhibited by tumor regression and vitiligo, respectively; however, this route of delivery imposes additional barriers that could limit therapeutic efficacy<sup>470</sup>. Factors such as instability and inefficient trafficking *in vivo* can restrict the ability of transferred T cells to persist long enough to reach primary or metastatic lesions<sup>471–474</sup>. These are critical barriers, as the persistence of transferred tumor-specific T cells has been documented to correlate with clinical or biologic responses in some patients<sup>386,475</sup>. Furthermore, tumor cells exhibit a highly immunosuppressive microenvironment that can prevent the transferred T cells from accumulating effectively in the tumor and executing effector functions<sup>476–479</sup>. As a result, we aimed to directly modulate the tumor microenvironment in order to improve the chances of effector-tumor cell interactions.

We attempted to eliminate the requirement for transferred T cells to traffic to and infiltrate tumors utilizing an alternative strategy by which TIL 1383I TCR transduced T cells are delivered intratumorally, as opposed to systemically (Fig 9). This method not only bypasses the requirement of the transferred T cells to traffic to the tumor but also facilitates immediate and direct tumor cell interactions. TIL 1383I TCR transduced T cells exhibited cytolytic activity (CD107a<sup>+</sup>) and produced IFN- $\gamma$  and TNF- $\alpha$ ; therefore, we anticipated that TIL 1383I TCR transduced T cells would induce tumor-specific killing and cytokine production, leading to the regression of B16 A2/K<sup>b</sup> tumors *in vivo*. Furthermore, we hypothesized that if the TIL 1383I TCR were expressed on T cells

derived from MHC-mismatched allogeneic donors, as opposed to syngeneic donors, then the endogenous T cells present in the recipient would mount an alloresponse against the donor T cells and promote potent immune cell activation within the tumor, thus converting an immunosuppressive microenvironment into an immune-active microenvironment.

Substituting allogeneic donor T cells for syngeneic donor T cells can lead to two potential alloresponses within the tumor microenvironment. First, recipient endogenous T cells could recognize allogeneic MHC molecules expressed on the donor T cells and mount an anti-donor cell alloresponse locally in the injected tumor. Second, the endogenous TCR expressed on the transferred donor T cells could recognize recipient MHC molecules and mount an anti-recipient cell alloresponse within the tumor. In either scenario, the potent immune activation and cytokine production induced by alloreactivity between MHC-mismatched donor T cells and recipient cells could alter the tumor immune microenvironment. The human HLA-A2-restricted TIL 1383I TCR could potentially mediate a xenogeneic response against mouse H-2<sup>b</sup> MHC-expressing cells. We found this unlikely since xenoresponses are much weaker than alloresponses and are not mounted as rapidly<sup>480</sup>. We hypothesized that the cytokine profiles induced by the allogeneic response would promote the maturation and licensing of intratumoral dendritic cells (DCs). Concurrently, TIL 1383I TCR-mediated tumor-specific killing can induce the release of tumor antigens, and these exogenous tumor antigens can be phagocytosed by DCs that are present in the tumor (Fig 9). The mature, licensed DCs that have captured exogenous tumor antigens can then traffic to the tumor draining lymph node and, cross-present tumor-derived antigens and prime endogenous T cells.

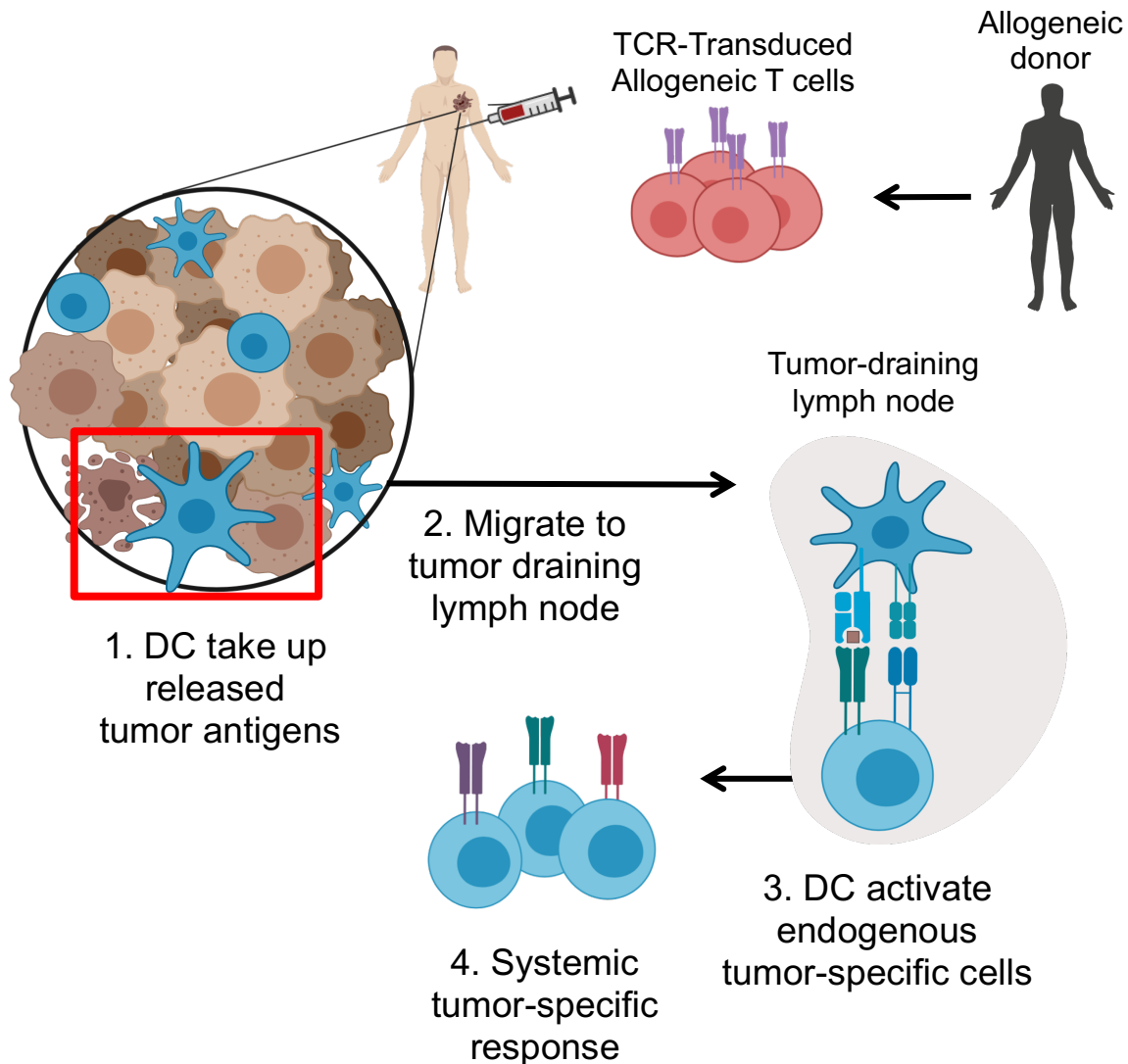


**Figure 9. Proposed Model to Enhance the Efficacy of Adoptive Transfer of TCR Gene-Modified T Cells for Cancer Immunotherapy.** Intratumoral delivery of allogeneic T cells transduced to express a tumor-specific TCR can lead to tumor killing and cytokine production, mediated by the tumor-specific TCR, and additional immune stimulation, mediated by alloreactivity. Within the tumor, cytokine-stimulated mature DCs can 1. internalize released tumor antigens, 2. traffic to tumor draining lymph nodes, and cross-present tumor antigens to endogenous T cells. 3. Systemic tumor-specific T cells with specificities to additional tumor antigens can induce further therapeutic or protective immune responses.

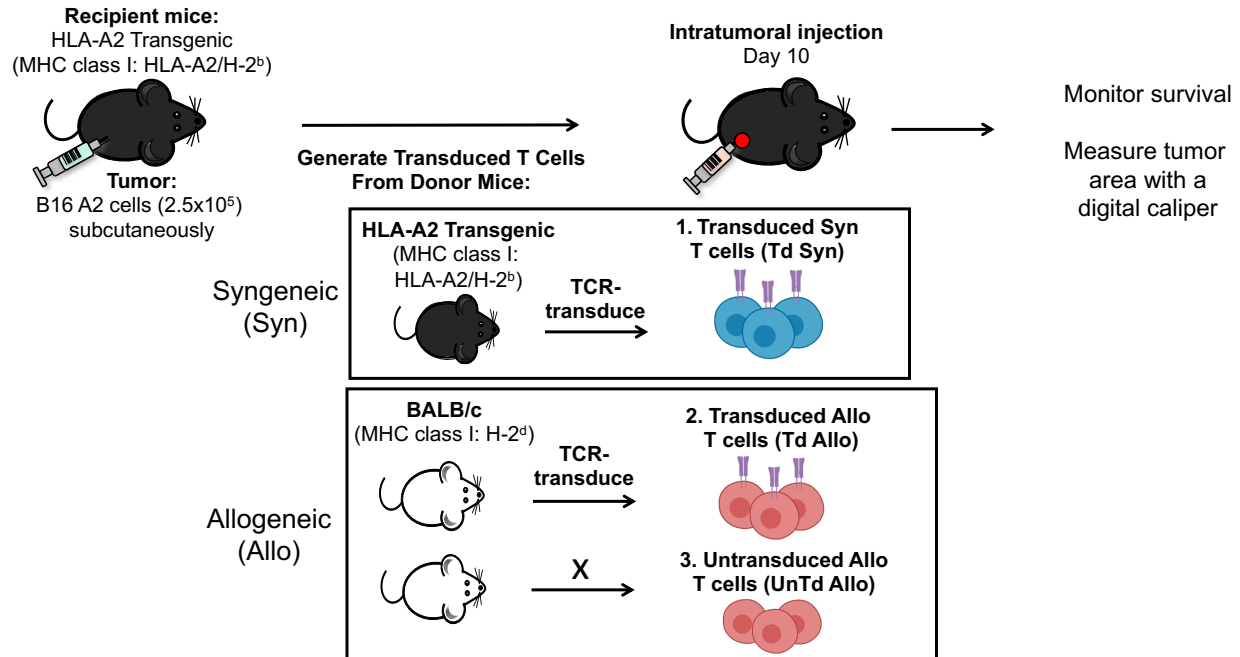


**Figure 10. Experimental Design to Determine If Intratumoral Treatment with TIL 1383I TCR Transduced T Cells Induces Regression of B16 A2/K<sup>b</sup> Tumors.** HLA-A2 transgenic recipient mice were subcutaneously inoculated with  $2.5 \times 10^5$  B16 A2/K<sup>b</sup> tumor cells. Ten days later, B16 A2/K<sup>b</sup> tumors were intratumorally injected with 1) TIL 1383I TCR transduced syngeneic T cells 2) TIL 1383I TCR transduced allogeneic T cells 3) untransduced allogeneic T cells or 4) PBS/untreated. Survival and tumor area were monitored. Mice were sacrificed when tumors reached  $>150 \text{ mm}^2$  or  $>10\%$  body weight.

T cell cross-priming, which is the generation of systemic, endogenous T cells with specificities to additional melanoma antigens (different than the initial target, tyrosinase and termed epitope spreading) could provide therapeutic responses against primary tumor lesions and protective responses against distant, untreated tumor lesions. In summary, the tumor-specificity and alloreactivity of TIL 1383I TCR



transduced allogeneic T cells can improve the efficacy of adoptive cell transfer using TCR gene-modified T cells for cancer immunotherapy.

We compared the effect of intratumoral delivery of TIL 1383I TCR transduced syngeneic T cells to TIL 1383I TCR transduced allogeneic T cells against B16 A2/K<sup>b</sup> tumors *in vivo* (Fig 10). HLA-A2 transgenic mice were used as recipients to receive  $2.5 \times 10^5$  B16 A2/K<sup>b</sup> tumor cells subcutaneous. After ten days, when tumors reached approximately 4 mm in one diameter, mice were intratumorally treated with a single dose of TIL 1383I TCR transduced syngeneic or allogeneic (GFP<sup>+</sup>VB12<sup>+</sup>) T cells, or untransduced (GFP<sup>-</sup>VB12<sup>-</sup>) allogeneic T cells or saline/PBS, as negative controls. We monitored the survival of mice and measured tumor growth every 2-3 days following intratumoral T cell treatment. B16 A2/K<sup>b</sup> tumor-bearing mice intratumorally injected with saline succumbed to tumor burden within three weeks post-treatment (Fig 11, black line; median survival: 13 days). Tumor-bearing mice treated with untransduced allogeneic T cells also succumbed to tumor burden within three weeks after T cell treatment (Fig 11, green line; median survival: 15 days), indicating that the allogeneic response alone did not improve survival compared to saline-treated mice (ns,  $P=0.1830$ ). In contrast, intratumoral injection of TIL1383I TCR transduced syngeneic T cells significantly extended survival compared to treatment with PBS ( $P<0.0001$ ) or untransduced allogeneic T cells ( $P=0.0005$ ; Fig 11, blue line; median survival: 21 days). Strikingly, mice intratumorally treated with TIL 1383I TCR transduced allogeneic T cells (red line) exhibited the best survival outcomes among treatment group (median survival: 28 days; Fig 11). TIL 1383I TCR transduced allogeneic T cells significantly extended survival compared to treatment with TIL 1383I TCR transduced syngeneic T cells ( $P=0.0005$ ),

untransduced allogeneic T cells ( $P < 0.0001$ ), and PBS ( $P < 0.0001$ ). These results demonstrated that the TIL 1383I TCR was required to prolong survival compared to PBS and untransduced allogeneic T cell treatment, and the allogeneic response synergized with the tumor-specific T cell response to improve the survival of mice treated with TIL 1383I TCR transduced allogeneic T cells compared to mice treated with TIL 1383I TCR transduced syngeneic T cells.

We also compared B16 A2/K<sup>b</sup> tumor progression in individual mice. B16 A2/K<sup>2</sup> tumors at the time of treatment are 15-20 mm<sup>2</sup>, however because B16 A2/K<sup>2</sup> is such an aggressive tumor model, we did not frequently observe complete regression. We therefore wanted to demonstrate the ability of intratumoral TIL 1383I TCR transduced T cells to control tumor burden. In order to visualize the ability to control tumor growth, we chose to draw a line at the tumor area measurement 50 mm<sup>2</sup>. We felt this was an intermediate-size tumor which could represent treatment-induced control of B16 A2/K<sup>b</sup> tumor growth, visualized by mice that maintained tumor areas below the dotted line. B16 A2/K<sup>b</sup> tumors treated with PBS or untransduced allogeneic T cells grew rapidly (Fig 12, black and green lines, respectively). Mice bearing B16 A2/K<sup>b</sup> tumors that were treated with TIL 1383I TCR transduced syngeneic (blue) T cells exhibited delayed tumor growth compared to tumors treated with PBS (black) or untransduced allogeneic T cells (green). The most effective control of B16 A2/K<sup>b</sup> tumor growth occurred after intratumoral treatment with TIL 1383I TCR transduced allogeneic T cells (red). We consistently observed improved survival and tumor control in mice treated with TIL 1383I TCR transduced allogeneic compared to syngeneic T cells over four independent experiments (Fig 12, solid, dashed, dotted, and dashed-dotted lines).

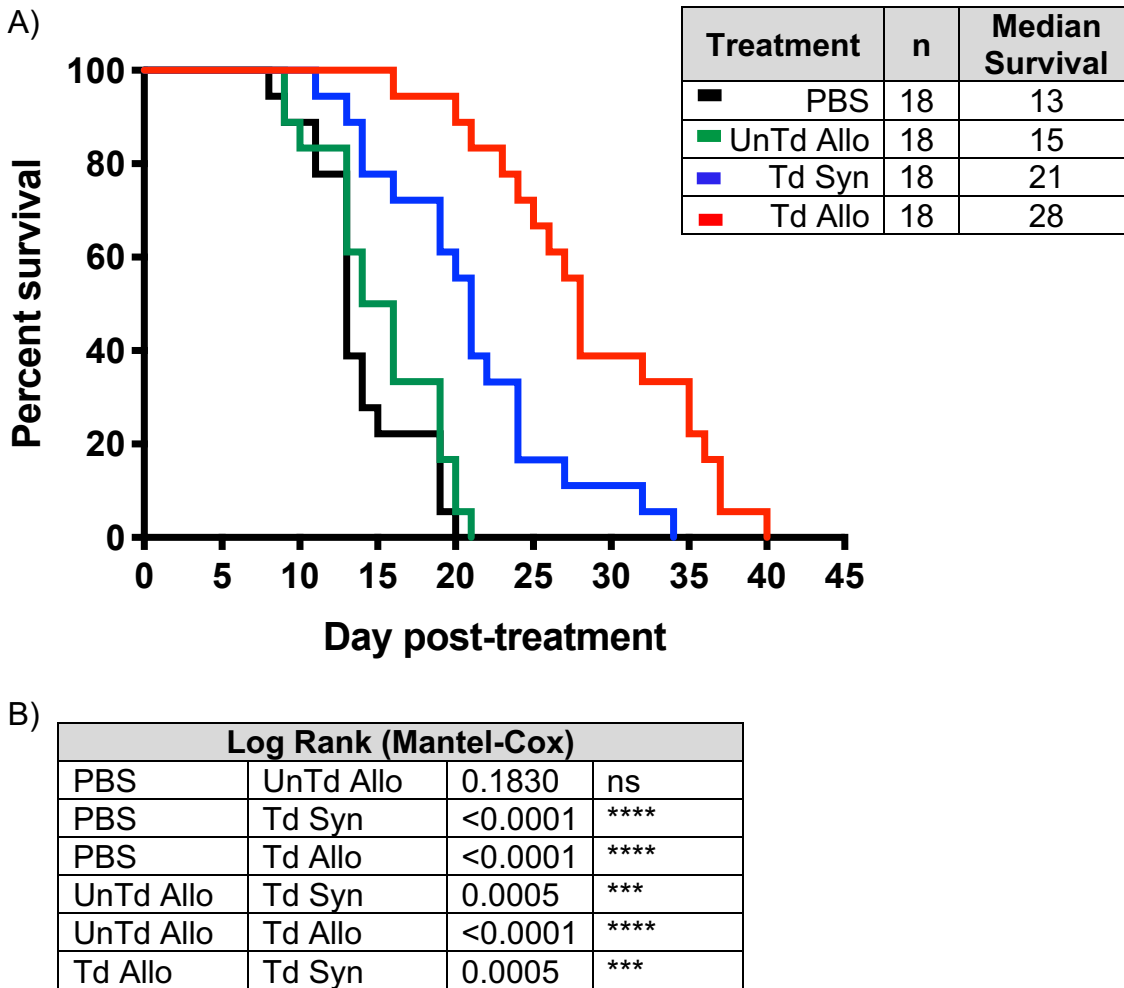


**Figure 11. TIL 1383I TCR Transduced Allogeneic T Cell Treatment Extends Survival of B16 A2/K<sup>b</sup> Tumor-Bearing Mice.** HLA-A2 transgenic mice received  $2.5 \times 10^5$  B16 A2/K<sup>b</sup> cells subcutaneously and 10 days later received an intratumoral injection with TIL 1383I TCR transduced syngeneic T cells (blue), TIL 1383I TCR transduced allogeneic T cells (red), untransduced allogeneic T cells (green) or saline (black). A) Survival of tumor-bearing mice following intratumoral treatment. Mice were sacrificed when tumors reached  $>150 \text{ mm}^2$  or  $>10\%$  body weight. Data represent a compilation of 4 independent experiments, 4-5 mice/group B) Statistical analysis was performed using the Log Rank (Mantel-Cox) test (\*\*\* $P < 0.001$ , \*\*\*\* $P < 0.0001$ ).

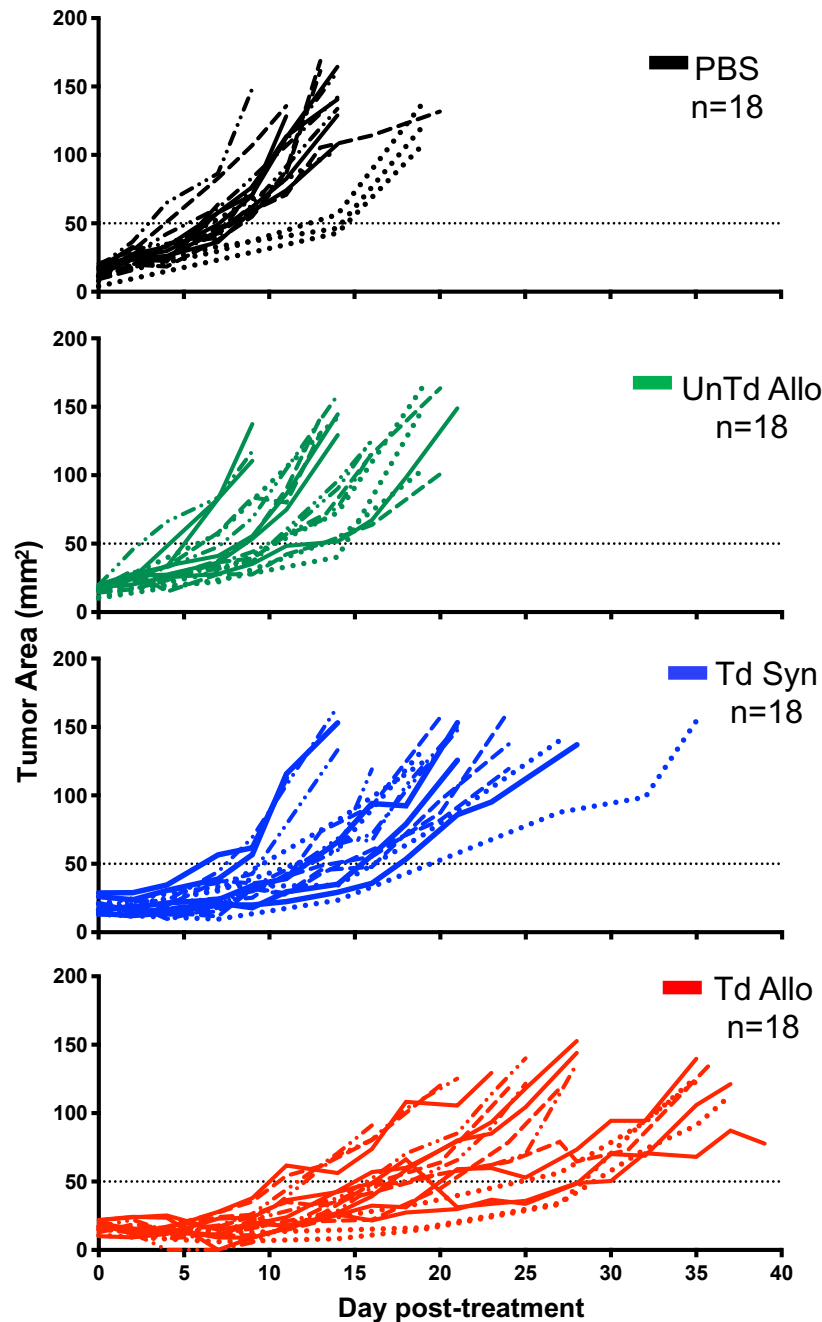


**Figure 12. TIL 1383I TCR Transduced Allogeneic T Cell Treatment Suppresses B16 A2/K<sup>b</sup> Tumor Growth.** B16 A2/K<sup>b</sup> tumor-bearing HLA-A2 transgenic mice were intratumorally treated on day 10 and tumor area was measured using a digital caliper 2-3 times weekly and calculated as the product of opposing diameters. Solid, dotted, dashed, and dash/dot lines represent individual mice from 4 independent experiments with 4-5 mice/group. Dotted line at 50 mm<sup>2</sup> serves as a reference for the capacity TIL 1383I TCR transduced T cells to control tumor burden. Mice were sacrificed when tumors reached >150 mm<sup>2</sup> or >10% body weight. Data represent a compilation of 4 independent experiments, 4-5 mice/group

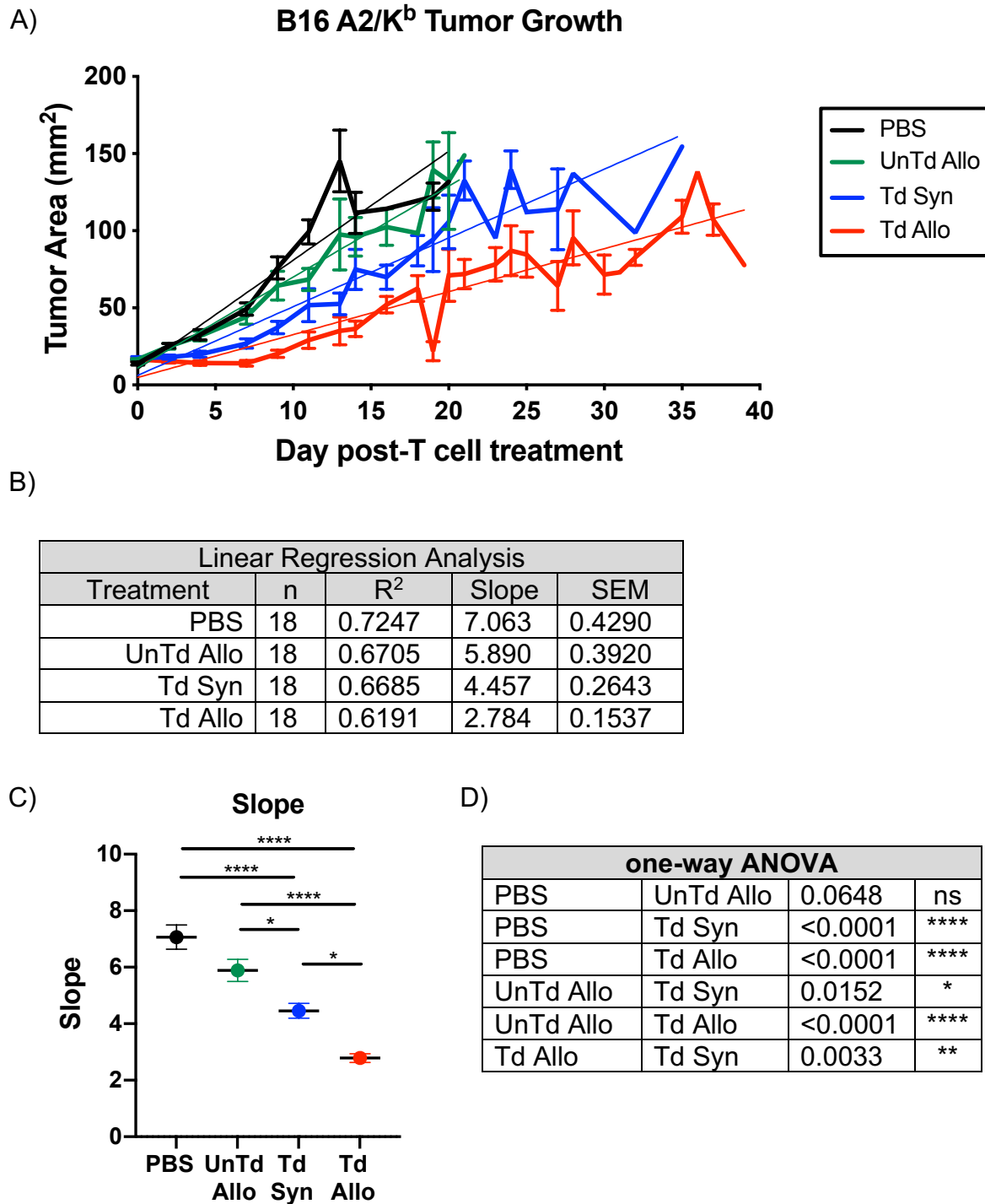


**Figure 13. TIL 1383I TCR Transduced Allogeneic T Cell Treatment Delays Progression of B16 A2/K<sup>b</sup> Tumors.** A) Average B16 A2/K<sup>b</sup> tumor growth obtained from individual mice shown in Figure 11. Data represent 4 independent experiments (4-5 mice/group) B) Linear regression analysis of data represented in A. C) Graphical analysis comparing the slope between treatment groups. Data points represent the mean slope  $\pm$  SEM D) Statistical analysis performed using one-way ANOVA with Tukey's correction [ $*P<0.05$ ,  $**P<0.01$ ,  $****P<0.0001$ ].

These results indicated that TIL1383I TCR transduced allogeneic T cells enhanced the anti-tumor responses in comparison to TIL 1383I TCR transduced syngeneic T cell treatment.

We wanted to use a second approach to re-evaluate the comparison of B16 A2/K<sup>b</sup> tumor growth curves more qualitatively to effectively illustrate the ability of TIL 1383I TCR transduced T cells to control tumor burden compared to the control treatment groups. For this approach, we averaged the B16 A2/K<sup>b</sup> tumor growth curves from the individual mice seen in Figure 12 and performed linear regression analysis. This method allowed us to obtain the slope of B16 A2/K<sup>b</sup> tumor growth following intratumoral T cell treatment (Fig 13A and B). We then compared the slopes of B16 A2/K<sup>b</sup> tumor growth among the different T cell treatment groups (Fig 13C and D). B16 A2/K<sup>b</sup> tumors from PBS-treated mice rapidly progressed over three weeks and, consequently, resulted in the highest slope ( $7.063 \pm 0.4290$ ). The slope of B16 A2/K<sup>b</sup> tumor growth following intratumoral treatment with untransduced allogeneic T cells was slightly, but not significantly, lower ( $5.890 \pm 0.3920$ ) than PBS treatment ( $P=0.0648$ ; Fig 13C and D). Treatment with TIL 1383I TCR transduced syngeneic T cells significantly delayed progression of B16 A2/K<sup>b</sup> tumors ( $4.457 \pm 0.2643$ ) compared to treatment with untransduced allogeneic T cells ( $P=0.0152$ ) and PBS ( $P<0.0001$ ). Injection with TIL 1383I TCR transduced allogeneic T cells resulted in the best inhibition of tumor growth, demonstrated by the lowest slope ( $2.784 \pm 0.1537$ ), in comparison to TIL 1383I TCR transduced syngeneic T cells ( $P=0.0033$ ), untransduced allogeneic T cells ( $P<0.0001$ ), and PBS ( $P<0.0001$ ). These results indicated that comparing the slope of B16 A2/K<sup>b</sup> tumor growth after intratumoral treatment represented an additional method to evaluate

the effects of T cell treatment on tumor progression. Furthermore, survival outcomes and tumor suppression were significantly enhanced with TIL 1383I TCR transduced allogeneic T cells compared to TIL 1383I TCR transduced syngeneic T cells.

### **Improved Anti-Tumor Responses Following TIL 1383I TCR Transduced Allogeneic T Cell Treatment Requires an Intact Recipient Immune System**

Intratumoral delivery of allogeneic TIL 1383I TCR modified T cells provided an improvement in anti-tumor immunity *in vivo*. One possibility is that TIL 1383I TCR transduced allogeneic T cells induced alloresponses against B16 A2/K<sup>b</sup> tumor cells, resulting in more robust cytokine production within the tumor. However, our *in vitro* functional assays argue against this hypothesis (Fig 7 and Fig 8). Syngeneic and allogeneic donor T cells expressing the TIL 1383I TCR displayed similar polyfunctional phenotypes when stimulated with B16 A2/K<sup>b</sup> tumor cells *in vitro*, but it is possible that there were differences in other cytokines not tested in the *in vitro* assay. However, TIL 1383I TCR transduced allogeneic T cells were more effective than TIL 1383I TCR transduced syngeneic T cells at suppressing the growth of B16 A2/K<sup>b</sup> tumors. In the *in vivo* tumor setting, there is the potential to mount two types of immune responses: the first can occur upon TIL 1383I TCR-mediated recognition of B16 A2/K<sup>b</sup> tumors, resulting in polyfunctional T cell responses. Second, allogeneic donor T cells can initiate a local inflammatory alloresponse. TIL 1383I TCR transduced syngeneic and allogeneic T cells share the same TCR and are capable of inducing tumor antigen-specific responses, but only the latter provides the additional host anti-donor alloresponse.

To determine if the synergy of alloresponses and tumor-specific responses contributed to the extended survival and delayed tumor growth observed in mice treated

with TIL 1383I TCR transduced allogeneic T cells, we eliminated the potential for host anti-donor alloresponses using immunodeficient recipient mice. The immunodeficient NSG A2 mouse strain is on an HLA-A2 and non-obese diabetic (NOD) background that results in defective macrophages, DCs, and natural killer (NK) cells<sup>481</sup>. Additionally, NSG A2 mice have impaired development of mature lymphocytes, as a result of a homozygous severe combined immunodeficiency (SCID) mutation, and impaired cytokine signaling and NK cell development due to the *IL2rg*<sup>null</sup> mutation<sup>482</sup>. Without functional lymphocytes and myeloid-lineage cells, NSG A2 recipients are incapable of mounting alloresponses.

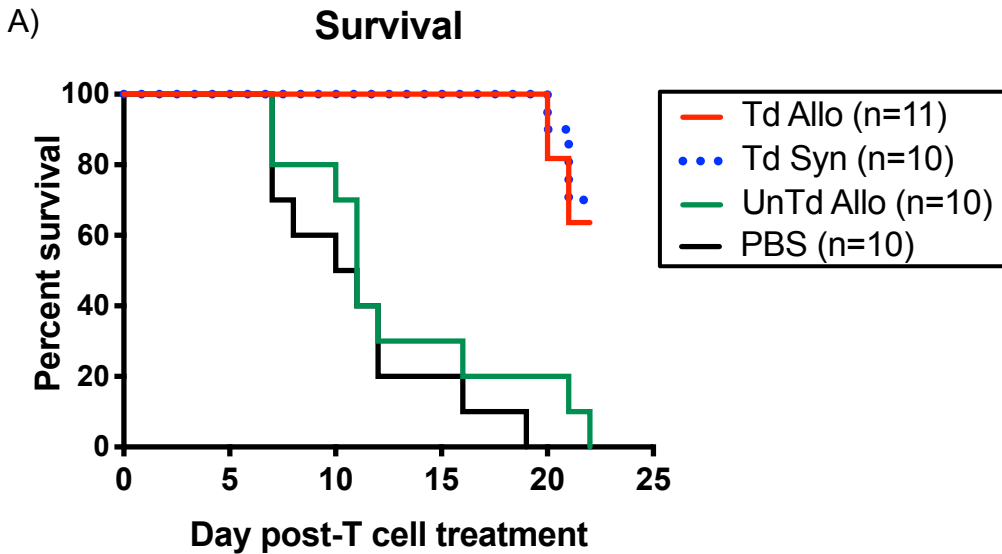
We compared survival of mice and B16 A2/K<sup>b</sup> tumor growth following treatment with TIL 1383I TCR transduced syngeneic and allogeneic T cells. Strikingly, we observed identical survival outcomes of NSG A2 mice treated with TIL 1383I TCR transduced allogeneic T cells (Fig 14, red line) compared to TIL 1383I TCR transduced syngeneic T cells (dotted blue line,  $P=0.7261$ ; Fig 14). Furthermore, both TIL 1383I TCR transduced syngeneic and TIL 1383I TCR transduced allogeneic T cell treatment significantly extended survival compared to untransduced allogeneic T cell treatment ( $P<0.0001$  and  $P=0.0001$ , respectively) and PBS ( $P<0.0001$ ). We also observed equal capacities of TIL 1383I TCR transduced syngeneic and allogeneic T cells to control B16 A2/K<sup>b</sup> tumor growth ( $P=0.9676$ ; Fig 15). These results suggest that in the absence of recipient immunity, treatment with TIL 1383I TCR transduced allogeneic T cells no longer provide an advantage over TIL 1383I TCR transduced syngeneic T cells.

The contribution of the alloresponse was further probed through linear regression analysis of B16 A2/K<sup>b</sup> tumor growth following intratumoral T cell treatment (Fig 16A). In



NSG A2 recipient mice, the slope of B16 A2/K<sup>b</sup> growth following intratumoral treatment with TIL 1383I TCR transduced allogeneic T cells (slope: 1.866) was no longer significantly lower than the slope of B16 A2/K<sup>b</sup> tumor growth following intratumoral treatment with TIL 1383I TCR transduced syngeneic T cells (slope: 2.205, P=0.2327; Fig 16B). These results suggest that the recipient-mediated alloresponse contributes to anti-tumor responses exhibited by prolonged survival and delayed tumor progression.

During an alloreactive response, host CD4<sup>+</sup> and CD8<sup>+</sup> T cells can initiate an inflammatory allogeneic immune response that ultimately leads to host T cell-mediated graft rejection<sup>77</sup>. Consistent with graft rejection, we were unable to detect TIL 1383I TCR transduced allogeneic T cells, which were identified by the expression of GFP using flow cytometry, in the tumors of intratumorally T cell-treated immunocompetent HLA-A2 transgenic recipient mice by seven days post-T cell treatment (Fig 17). Therefore, we predicted that the TIL 1383I TCR transduced allogeneic donor T cells would not be eliminated in the immunocompromised NSG A2 recipient mice, which do not have the capacity to mount effective alloresponses against introduced allogeneic donor T cells. We detected TIL 1383I TCR transduced syngeneic T cells and TIL 1383I TCR transduced allogeneic T cells in the tumors of NSG A2 recipient mice up to 22 days post-T cell treatment (Fig 18). Taken together, these data support our hypothesis that the recipient anti-donor T cell immune alloresponse, which could occur through recognition of foreign allogeneic donor T cells, improves upon the efficacy of intratumoral treatment with TIL 1383I TCR transduced allogeneic T cells compared to TIL 1383I TCR transduced syngeneic T cells.



B)

Log Rank (Mantel-Cox)			
PBS	UnTd Allo	0.3168	ns
PBS	Td Syn	<0.0001	****
PBS	Td Allo	<0.0001	****
UnTd Allo	Td Syn	<0.0001	****
UnTd Allo	Td Allo	0.0002	***
Td Allo	Td Syn	0.7047	ns

**Figure 14. TIL 1383I TCR Transduced Allogeneic T Cell-Treated NSG A2 Mice Have Similar Survival Outcomes Compared to TIL 1383I TCR Transduced Syngeneic Mice.** NSG A2 mice received  $2.5 \times 10^5$  B16 A2/K<sup>b</sup> cells subcutaneously and ten days later were treated with A) saline (black), untransduced allogeneic T cells (green), TIL 1383I TCR transduced syngeneic T cells (dotted blue), or TIL 1383I TCR transduced allogeneic T cells (red). Mice were sacrificed 22 days post-T cell treatment for further analysis or when tumors reached  $>150 \text{ mm}^2$  or  $>10\%$  of body weight. Graph represents 2 independent experiments with 5-6 mice per group. B) Statistical analysis performed using the Log Rank (Mantel-Cox) test (\*\*P<0.001, \*\*\*\*P<0.0001)

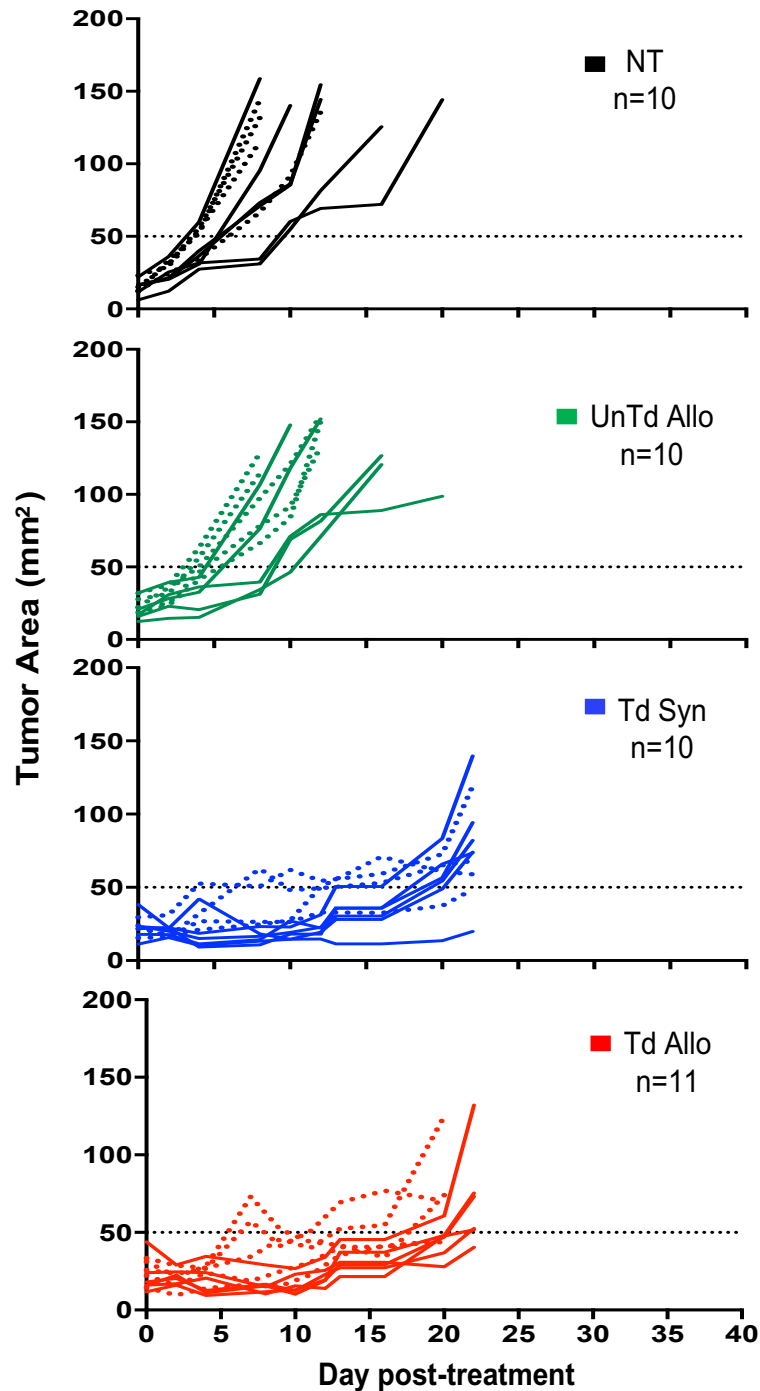


**Figure 15. TIL 1383I TCR Transduced Syngeneic and Allogeneic T Cells Have Equal Capacities to Suppress B16 A2/K<sup>b</sup> Tumors in NSG A2 Recipient Mice**

NSG A2 mice received  $2.5 \times 10^5$  B16 A2/K<sup>b</sup> cells subcutaneously and ten days later were treated with saline (black), untransduced allogeneic T cells (green), TIL 1383I TCR transduced syngeneic T cells (blue), TIL 1383I TCR transduced allogeneic T cells (red). Mice were sacrificed 22 days post-T cell treatment for further analysis or when tumors reached  $>150$  mm<sup>2</sup> or  $>10\%$  of body weight. Solid and dotted lines represent individual mice from 2 independent experiments with 5-6 mice/group.

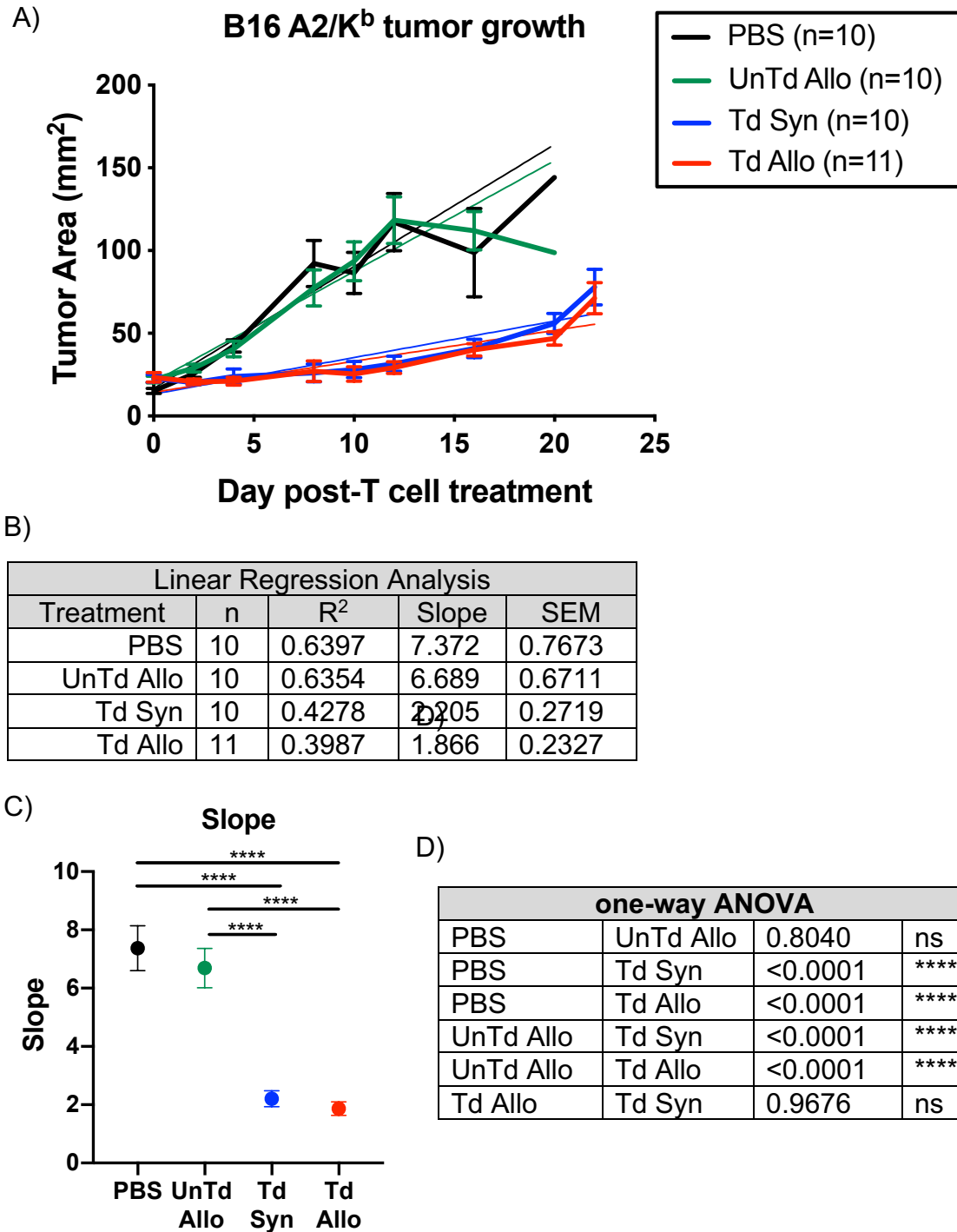


**Figure 16. Linear Regression Analysis of B16 A2/K<sup>b</sup> Tumor Growth in NSG A2 Mice After TIL 1383I TCR Transduced T Cell Treatment.** A-B) Linear regression analysis of B16 A2/K<sup>b</sup> tumor growth group averages from mice shown in Figure 15. C) Comparison of the slope among treatment groups. Graph represents two independent experiments with 5-6 mice/group. Data points represent the mean slope  $\pm$  SEM. D) Statistical analysis performed using one-way ANOVA with Tukey's correction [\*\*\*\*P<0.0001].

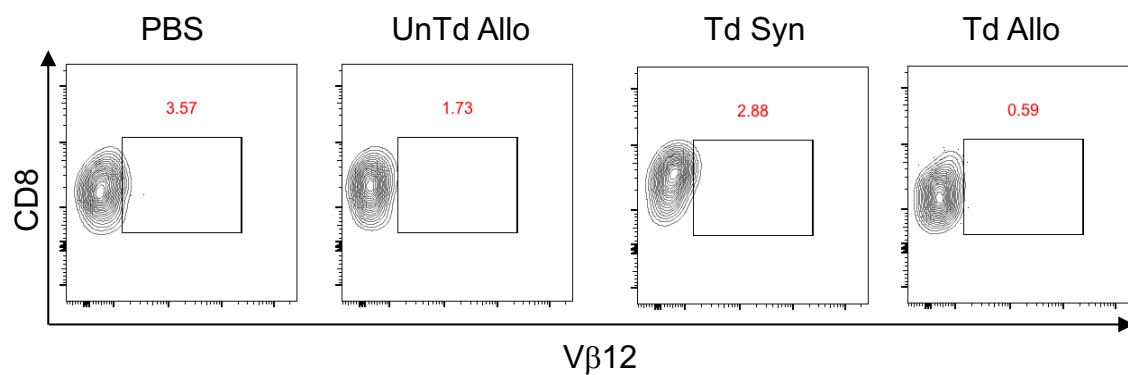
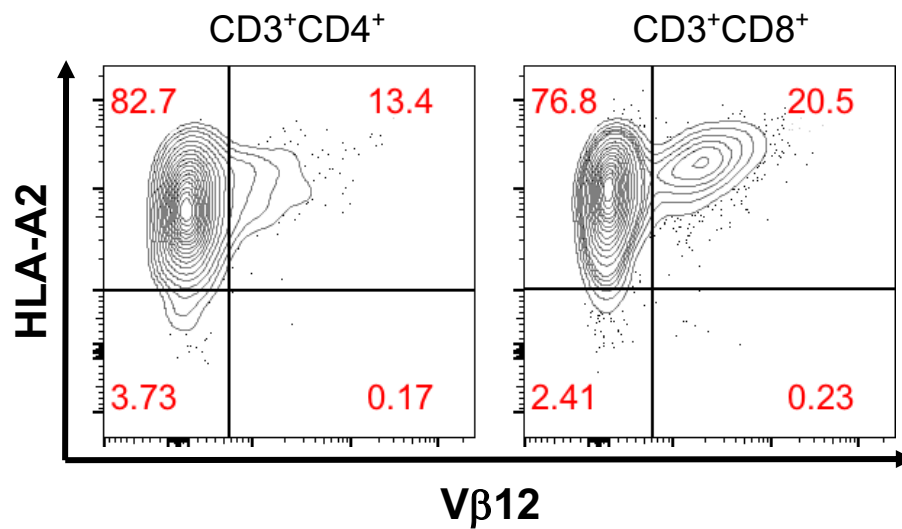


**Figure 17. TIL 1383I TCR Transduced T Cells are Undetectable in the Tumors from Immunocompetent HLA-A2 Transgenic Recipient Mice.** B16 A2/K<sup>b</sup> tumors were isolated seven days post-intratumoral T cell treatment and examined for the presence of cells expressing CD3, CD8, and V $\beta$ 12 by flow cytometry. Representative flow cytometry plots are shown. Cells are gated on live CD3<sup>+</sup> cells.

## A) Td Syn T cell-treated tumor



## B) Td Allo T cell-treated tumor

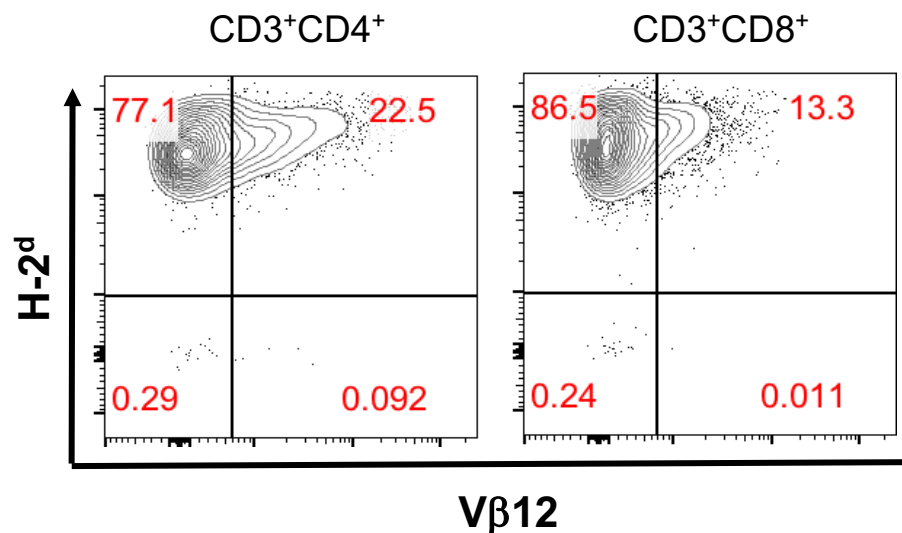


**Figure 18. TIL 1383I TCR Transduced T Cells Persist in the Tumors from Immunodeficient NSG A2 Recipient Mice.** NSG A2 recipient mice were inoculated with  $2.5 \times 10^5$  B16 A2/K<sup>b</sup> tumor cells and ten days later, received intratumoral treatment with A) TIL 1383I TCR transduced syngeneic T cells (left panel gated on CD3<sup>+</sup> CD4<sup>+</sup> cells, right panel gated on CD3<sup>+</sup> CD8<sup>+</sup> cells ) or B) TIL 1383I TCR transduced allogeneic T cells (left panel gated on CD3<sup>+</sup> CD4<sup>+</sup> cells, right panel gated on CD3<sup>+</sup> CD8<sup>+</sup> cells ). Twenty-two days post-T cell treatment, B16 A2/K<sup>b</sup> tumors were isolated and cells were examined for expression of CD3, CD4, CD8, H-2<sup>d</sup> and Vβ12 by flow cytometry. Representative flow cytometry plots are shown.

## Summary

The transplantable B16 melanoma model is one of the most commonly used mouse models in immuno-oncology and has greatly contributed to the identification and manipulation of actionable immune checkpoints that can be targeted therapeutically. Additionally, B16 has been used to evaluate the efficacy and mechanism of action of combination treatment strategies. B16 is a notoriously aggressive and weakly immunogenic tumor model, characterized by low MHC class I expression and minimal responsiveness to intravenous adoptive transfer of CTL for treatment of subcutaneously implanted tumors<sup>454</sup>. While these features are limitations in modeling human melanoma, B16 is a stringent test for the feasibility and efficacy of immunotherapeutic strategies. We observed a significant extension of survival in B16 A2/K<sup>b</sup> tumor-bearing mice treated with TIL 1383I TCR transduced syngeneic T cells by intratumoral delivery compared to untreated mice or untransduced allogeneic T cell-treated mice.

Survival was further improved after intratumoral delivery of TIL 1383I TCR transduced allogeneic T cells. B16 A2/K<sup>b</sup> tumors treated with TIL 1383I TCR transduced allogeneic T cells also displayed a significant reduction in growth compared to tumors treated with TIL 1383I TCR transduced syngeneic T cells. B16 A2/K<sup>b</sup> tumors treated with untransduced allogeneic T cells did not exhibit any delay in tumor progression compared to untreated tumors, indicating that the TIL 1383I tumor-specific TCR was required for B16 A2/K<sup>b</sup> tumor suppression and that the alloresponse alone was insufficient for tumor control. Furthermore, intact recipient immune systems were required to mediate the enhanced anti-tumor responses observed with TIL 1383I TCR transduced allogeneic T cells.

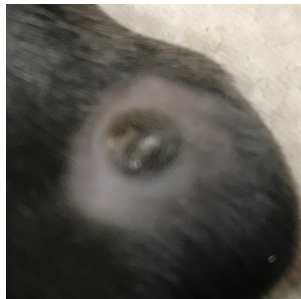
Following intratumoral delivery of TIL 1383I TCR transduced allogeneic T cells, B16 A2/K<sup>b</sup> tumors regressed within 1-3 days, sometimes accompanied by peri-tumor inflammation. We observed complete tumor regression in approximately 20% of mice treated with TIL 1383I TCR transduced allogeneic T cells compared to <10% of mice treated with TIL 1383I TCR transduced syngeneic T cells. After intratumoral treatment, individual B16 A2/K<sup>b</sup> tumors varied in size and morphology (Fig 19) as a result of either tumor regression or progression, as treatment resulted in tumor necrosis and ulceration. Therefore, we performed only one intratumoral injection for the purposes of reproducibility and consistency in measuring tumor development. In summary, intratumoral injection of TIL 1383I TCR transduced allogeneic T cells significantly extends survival and suppresses tumor growth in B16 A2/K<sup>b</sup> tumor-bearing mice.



A) PBS



B) UnTd Allo T cells



C) Td Syn T cells



D) Td Allo T cells



**Figure 19. Representative Pictures of Treated B16 A2/K<sup>b</sup> Tumors Seven Days Post-T Cell Treatment.** B16 A2/K<sup>b</sup> tumor-bearing mice were treated with A) PBS B) untransduced allogeneic T cells C) TIL 1383I TCR transduced syngeneic T cells or D) TIL 1383I TCR transduced allogeneic T cells. Pictures were taken at seven days post-T cell treatment.

## CHAPTER FOUR

### INTRATUMORAL DELIVERY OF TIL 1383I TCR TRANSDUCED ALLOGENEIC T CELLS STIMULATES DENDRITIC CELL RESPONSES

#### **Characterization of Dendritic Cells in the Tumor Microenvironment**

From the experiments performed in Chapter Three, we concluded that intratumoral treatment with TIL 1383I TCR transduced allogeneic T cell treatment extended survival and delayed tumor progression in B16 A2/K<sup>b</sup> tumor-bearing HLA-A2 transgenic immunocompetent mice. Based on the NSG A2 data, the improved anti-tumor responses induced by TIL 1383I TCR transduced allogeneic, compared to syngeneic, T cells required functional myeloid- and lymphoid-lineage cells in the treated recipient. Additionally, TIL 1383I TCR transduced T cell recognition of B16 A2/K<sup>b</sup> tumor targets *in vitro* resulted in robust cytokine production and surface expression of CD107a, indicative of cytolytic activity. The *in vitro* cytokine response was dominated by TNF- $\alpha$  and IFN- $\gamma$ , which are two cytokines reported to stimulate dendritic cells (DCs)<sup>483,484</sup>. Therefore, we next investigated whether intratumoral treatment with TIL 1383I TCR transduced T cells altered DC frequencies, co-stimulatory molecule expression, or DC subsets in the tumor. We observed similar frequencies of CD11c<sup>+</sup> MHCII<sup>+</sup> conventional DCs (cDCs) in the tumors isolated from untreated mice ( $9.48 \pm 1.01\%$ ) and mice treated with untransduced allogeneic T cells ( $10.27 \pm 1.09\%$ ), TIL 1383I TCR transduced syngeneic T cells ( $9.2 \pm 1.06\%$ ), and TIL 1383I TCR transduced allogeneic T cells ( $9.83 \pm 1.27\%$ ) two days post-intratumoral T cell treatment (Fig 20).

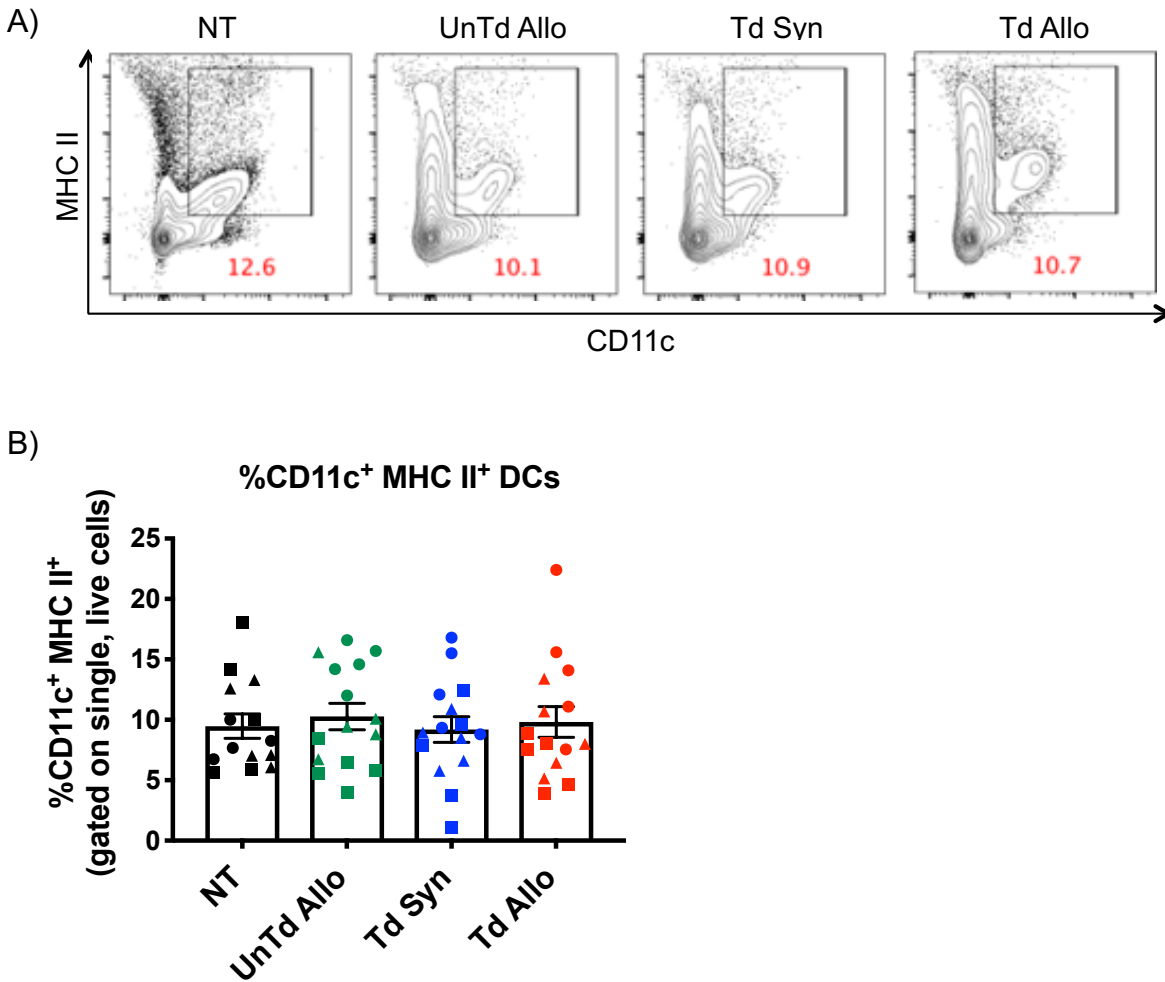


**Figure 20. CD11c<sup>+</sup>MHCII<sup>+</sup> Dendritic Cells in the Tumor Microenvironment Two Days Post-T Cell Treatment.** Two days following intratumoral T cell treatment, B16 A2/K<sup>b</sup> tumors were harvested and cells were analyzed for the presence of CD11c<sup>+</sup>MHCII<sup>+</sup> DCs by flow cytometry. A) Representative flow cytometry plots of CD11c<sup>+</sup> and MHCII<sup>+</sup> cells from B16 A2/K<sup>b</sup> tumors. Cells were gated on single, live cells. B) Percentage of CD11c<sup>+</sup>MHCII<sup>+</sup> dendritic cells in the tumor microenvironment. Symbols (Circles, squares, and triangles) represent individual mice from 3 independent experiments (n=4-5 mice/group). No statistical significance was detected by one-way ANOVA.

However, we observed a significant increase in the frequency of CD11c<sup>+</sup> MHC II<sup>+</sup> DCs expressing the co-stimulatory molecule, CD80, in B16 A2/K<sup>b</sup> tumors treated with TIL 1383I TCR transduced syngeneic T cells compared to tumors from untreated mice

( $P=0.0003$ ; Fig 21A and C). Interestingly, B16 A2/K<sup>b</sup> tumors from mice treated with untransduced allogeneic T cells and TIL 1383I TCR transduced allogeneic T cells had the highest increase in CD80<sup>+</sup> DCs ( $P<0.0001$ ) compared to tumors isolated from untreated mice. Additionally, the cell surface levels of CD80, as assessed by mean fluorescence intensity (MFI), were significantly higher on DCs isolated from tumors treated with TIL 1383I TCR transduced allogeneic T cells ( $P<0.0001$ ) and untransduced allogeneic T cells ( $P<0.00010$ ) compared to DCs from untreated tumors (Fig 22), supporting enhanced DC activation. DCs from TIL 1383I TCR transduced syngeneic T cell-treated tumors also had significantly higher surface expression of CD80 compared to untreated mice ( $P=0.0008$ ). Interestingly, we observed a large frequency of CD11c negative MHC class II positive in the T cell-treated tumors, which might indicate the presence of macrophages, but would have to be tested further. This suggested that both the tumor-specific response and the allogeneic response promoted the activation of intratumoral CD11c<sup>+</sup>MHC II<sup>+</sup> antigen presenting cells, while the tumor-specific TCR was required for the suppression of tumor growth.

We next wanted to determine if TIL 1383I TCR transduced allogeneic T cell treatment promoted the induction of specialized antigen cross-presenting DC subsets. CD103<sup>+</sup> DCs, or Batf3-lineage DCs, are critical for recruiting effector T cells to the tumor microenvironment as well as cross-presenting skin-derived antigens in the draining lymph node<sup>485</sup>. The frequency of CD103<sup>+</sup> DCs was significantly increased in the tumors that were intratumorally treated with TIL 1383I TCR transduced allogeneic T cells ( $9.43 \pm 1.37\%$ ) compared to the TIL 1383I TCR transduced syngeneic T cell-treated ( $4.9 \pm 0.66\%$ ,  $P=0.0152$ ) tumors or untreated tumors ( $5.14 \pm 1.03\%$ ;  $P=0.021$ ; Fig 23).

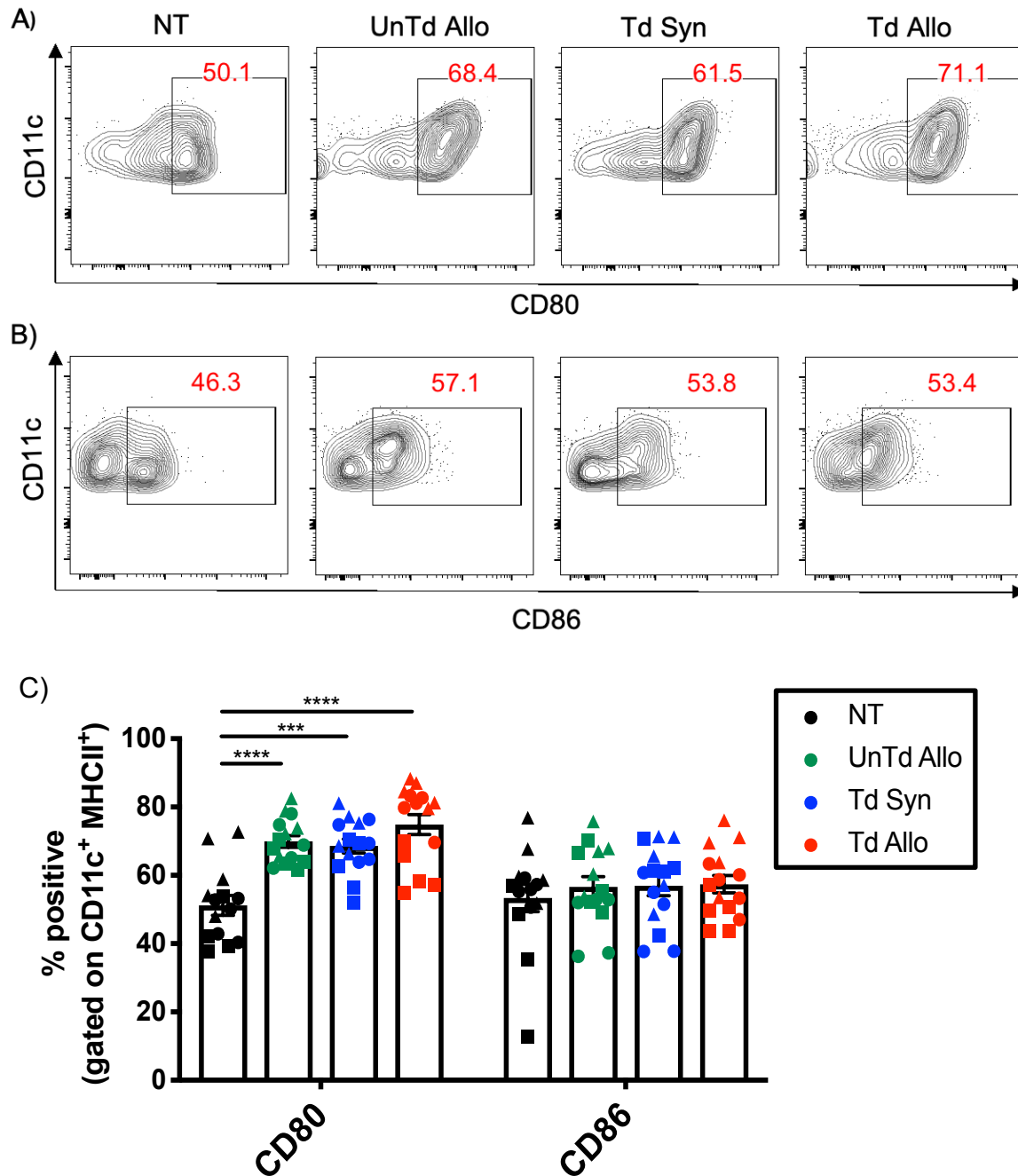


**Figure 21. Expression of Co-Stimulatory Molecules on CD11c<sup>+</sup> MHC II<sup>+</sup> Dendritic Cells in the Tumor Two Days Post-T Cell Treatment.** B16 A2/K<sup>b</sup> tumors were harvested two days post-T cell treatment and cells were analyzed for expression of CD11c, MHC class II, CD80 and CD86 by flow cytometry. Cells were gated on live, CD11c<sup>+</sup>MHCII<sup>+</sup> cells. Symbols (circles, squares, and triangles) represent individual mice from three independent experiments. Graph shows mean  $\pm$  SEM; statistical analysis by one-way ANOVA with Tukey's correction (\*\*\*P<0.001, \*\*\*\*P<0.0001)

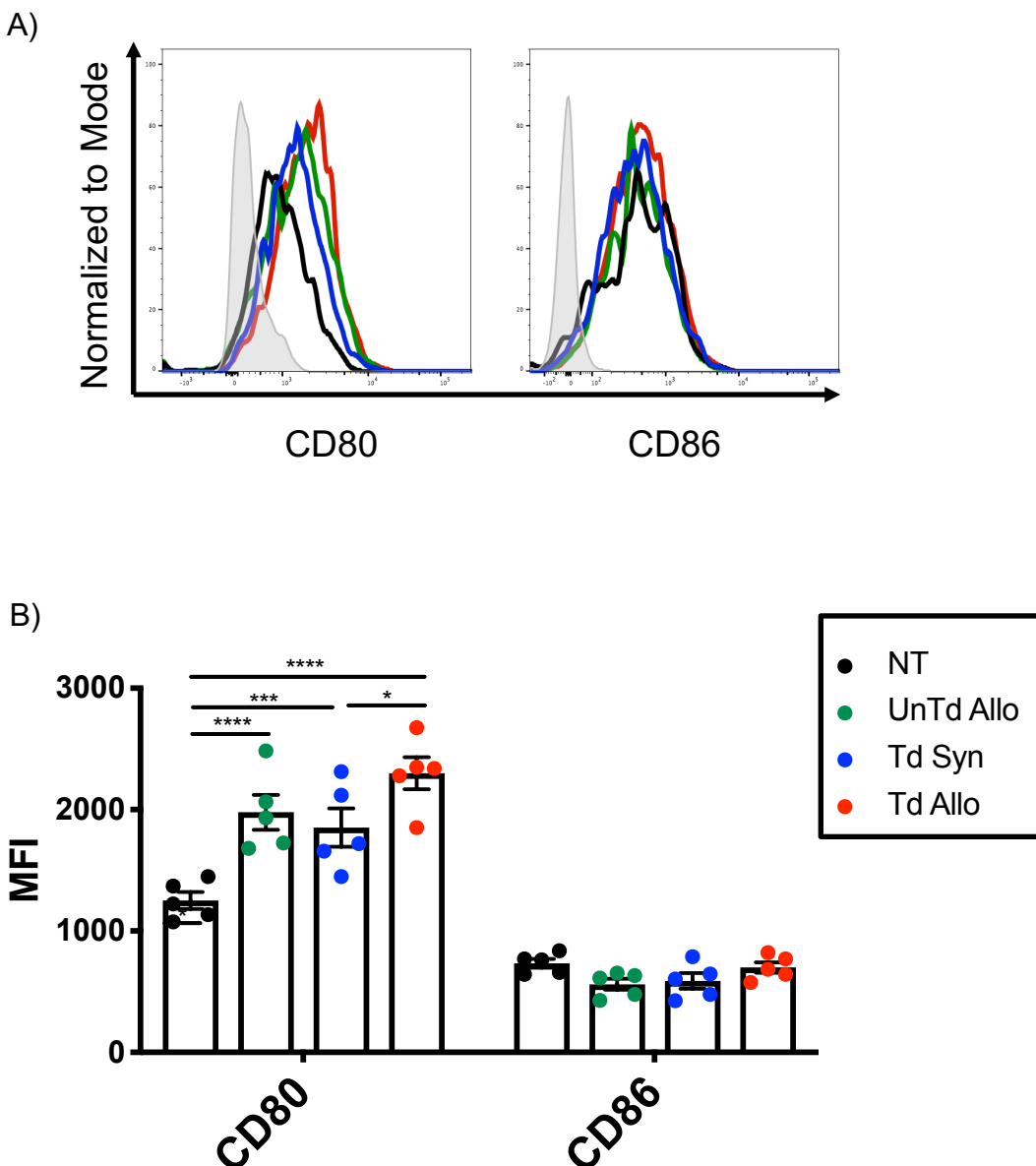


**Figure 22. Surface Expression of Co-Stimulatory Molecules on CD11c<sup>+</sup> MHC II<sup>+</sup> Dendritic Cells in the Tumor Two Days Post-T Cell Treatment.** B16 A2/K<sup>b</sup> tumors were harvested two days post-T cell treatment and cells were analyzed for expression of CD11c, MHC class II, CD80 and CD86 by flow cytometry. Cells were gated on live, CD11c<sup>+</sup>MHCII<sup>+</sup> cells. Results from one representative experiment are shown, out of three experiments with similar results. Graph shows mean  $\pm$  SEM; statistical analysis by 2way ANOVA with Tukey's correction (\* $P < 0.05$ , \*\*\* $P < 0.001$ , \*\*\*\* $P < 0.0001$ )

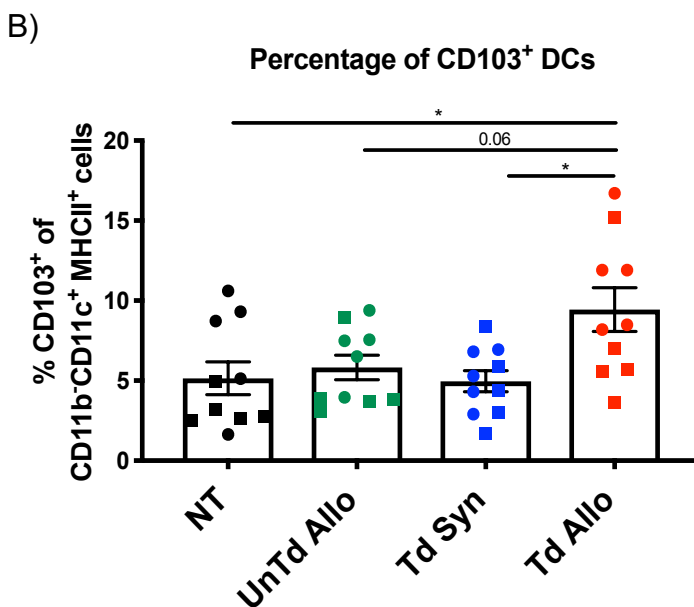
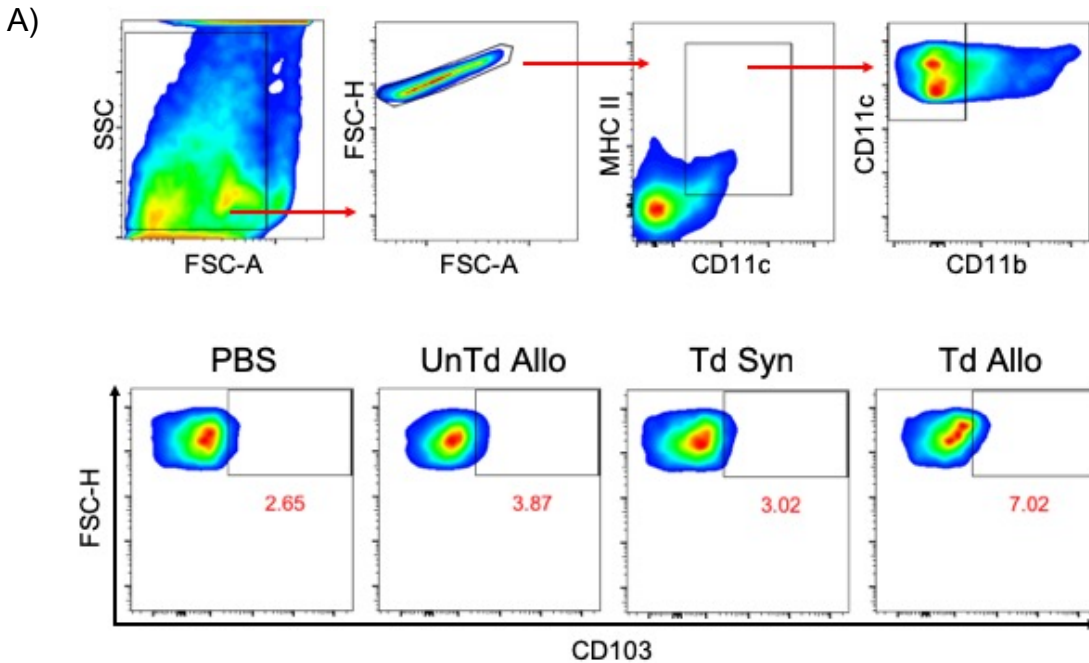


**Figure 23. TIL 1383I TCR Transduced Allogeneic T Cell Treatment Increases the Frequency of CD103<sup>+</sup>Dendritic Cells in the Tumor Two Days Post-T Cell Treatment.** B16 A2/K<sup>b</sup> tumors were harvested two days post-T cell treatment and cells were analyzed for expression of CD103 by flow cytometry. Cells were gated on live, CD11c<sup>+</sup>MHCII<sup>+</sup>CD11b<sup>-</sup>. Symbols (circles and squares) represent individual mice from two independent experiments. Graph shows mean  $\pm$  SEM; statistical analysis by one-way ANOVA with Tukey's correction (\*P<0.05)

These results suggested that intratumoral treatment with TIL 1383I TCR transduced allogeneic T cells promoted the accumulation of migratory CD103<sup>+</sup> DCs in the tumor microenvironment two days post-T cell treatment.

Within the tumor, we observed a large portion of CD11c<sup>+</sup>MHCII<sup>+</sup> DCs expressing the endocytic receptor, CD205, which facilitates antigen cross-presentation (Fig 24)<sup>150</sup>. We detected the highest frequency of CD205<sup>+</sup> CD11c<sup>+</sup>MHCII<sup>+</sup> DCs in tumors from mice treated with TIL 1383I TCR transduced allogeneic T cells ( $67.37 \pm 2.38\%$ ) in comparison to mice treated with untransduced allogeneic T cells ( $60.32 \pm 2.56\%$ ,  $P=0.1744$ ) and TIL 1383I TCR transduced syngeneic T cells ( $55.29 \pm 2.51\%$ ,  $P=0.0062$ ). Untreated tumors had significantly lower frequencies of CD205<sup>+</sup> CD11c<sup>+</sup>MHCII<sup>+</sup> DCs ( $42.73 \pm 3.21\%$ ) compared to untransduced allogeneic T cells ( $P=0.0001$ ), TIL 1383I TCR transduced syngeneic T cells ( $P=0.0085$ ), and TIL 1383I TCR transduced allogeneic T cells ( $P<0.0001$ ). These results indicated that intratumoral treatment with TIL 1383I TCR transduced allogeneic T cells increased the frequency of intratumoral CD205<sup>+</sup> DCs and CD103<sup>+</sup> DCs, two subsets that excel in antigen cross-presentation.

### **Characterization of Dendritic Cells in the Tumor Draining Lymph Nodes**

The induction of tumor antigen-specific T cell responses requires that DCs that have acquired tumor antigens then traffic to the tumor draining lymph nodes where they can present antigen in the context of MHC class I, engage co-stimulatory molecules, and cross-prime CD8<sup>+</sup> T cells. Therefore, we next examined the tumor draining lymph nodes two days post-intratumoral T cell treatment for the presence of activated DCs, as well as the specialized antigen cross-presenting DC subsets observed in the tumor.



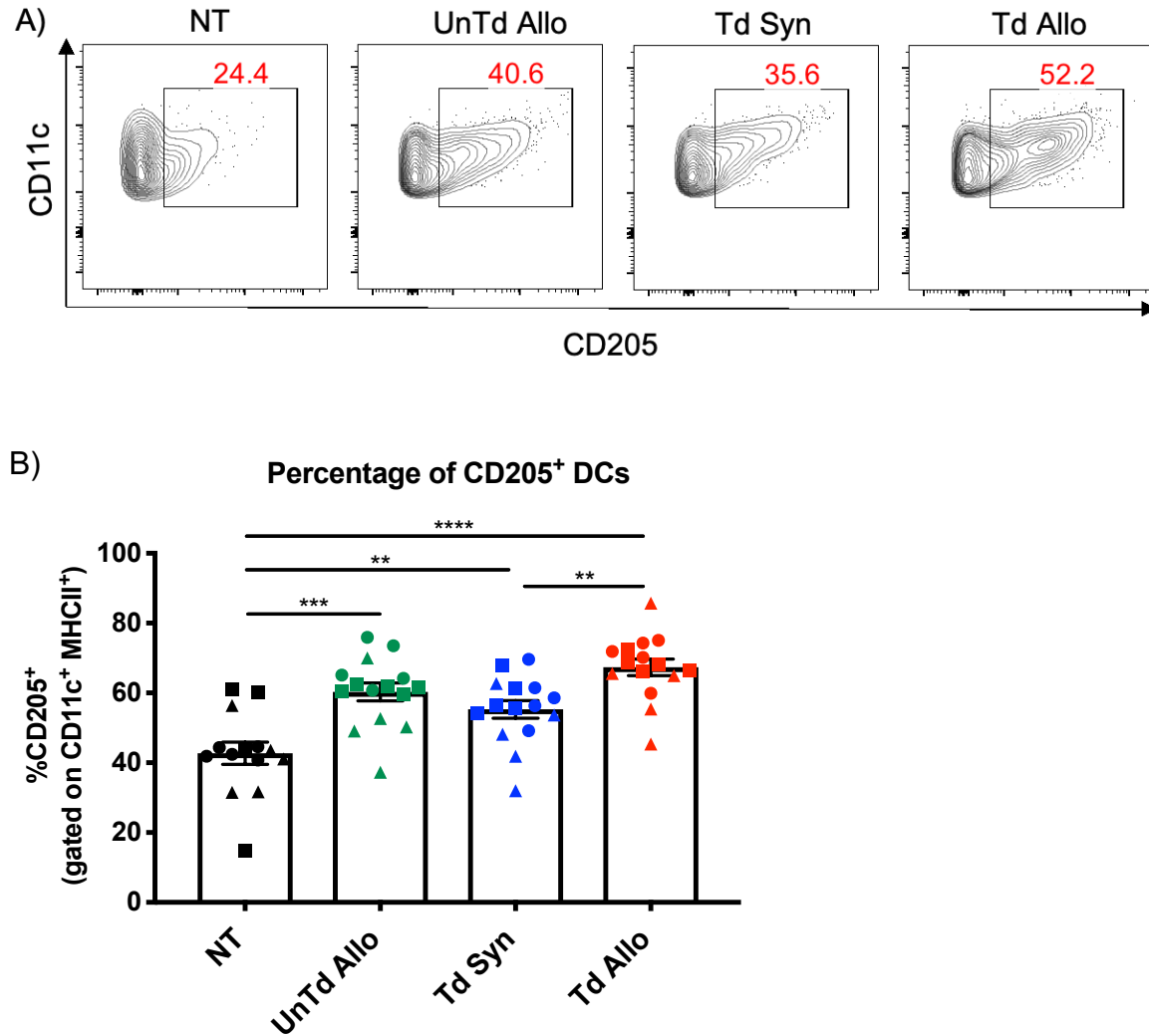


**Figure 24. TIL 1383I TCR Transduced Allogeneic T Cell Treatment Increases the Frequency of CD205<sup>+</sup> CD11c<sup>+</sup> MHC II<sup>+</sup> Dendritic Cells in the Tumor Two Days Post-T Cell Treatment.** B16 A2/K<sup>b</sup> tumors were harvested two days post-T cell treatment and cells were analyzed for expression of CD205. Cells were gated on live, CD11c<sup>+</sup>MHCII<sup>+</sup> cells. Symbols (circles, squares, and triangles) represent individual mice from three independent experiments. Graph shows mean  $\pm$  SEM; statistical analysis by one-way ANOVA with Tukey's correction (\*\*P<0.01, \*\*\*P<0.001, \*\*\*\*P<0.0001).

Two days following intratumoral T cell treatment, we isolated the tumor draining lymph to determine if intratumoral treatment with TIL 1383I TCR transduced T cell resulted in the migration of DCs from the tumor environment to the tumor draining lymph nodes.

Indeed, there was a significant increase in the frequency of CD11c<sup>+</sup> MHC II<sup>+</sup> conventional DCs (cDCs) in the tumor draining lymph nodes of TIL 1383I TCR transduced allogeneic T cell-treated mice compared to mice treated with TIL 1383I TCR transduced syngeneic T cells ( $P=0.005$ ) and untreated mice ( $P<0.0001$ ; Fig 25B-C). There was also a significant increase in the frequency of CD11c<sup>+</sup> MHC II<sup>+</sup> DCs in the tumor draining lymph nodes of mice treated with untransduced allogeneic T cells compared to untreated mice ( $P=0.0204$ ). These data suggested that both the anti-tumor and alloresponses promoted DC accumulation in the tumor draining lymph nodes early after T cell treatment.

We also observed an increased frequency of CD86-expressing CD11c<sup>+</sup> MHC II<sup>+</sup> DCs in the tumor draining lymph nodes of mice following intratumoral treatment with TIL 1383I TCR transduced allogeneic T cells compared to intratumoral treatment with TIL 1383I TCR transduced syngeneic T cells ( $P=0.0036$ ) and no treatment ( $P=0.0133$ ; Fig 26A). The number of cDCs expressing the co-stimulatory molecules CD80 or CD86 in the tumor draining lymph nodes were significantly greater in the TIL 1383I TCR transduced allogeneic T cell-treated mice compared to the tumor draining lymph nodes of mice that were treated with TIL 1383I TCR transduced syngeneic T cells ( $P<0.001$ ), untransduced allogeneic T cells ( $P=0.0001$ ), and untreated mice ( $P<0.0001$ ; Fig 26B). Moreover, the surface level of CD80 on CD11c<sup>+</sup> MHC II<sup>+</sup> DCs was generally highest in TIL 1383I TCR transduced allogeneic T cell treated mice (Fig 27). Collectively, these results indicated that intratumoral treatment with TIL 1383I TCR transduced allogeneic T cells promoted the accumulation of CD11c<sup>+</sup> MHC II<sup>+</sup> DCs expressing high levels of co-stimulatory molecules in the tumor draining lymph nodes.

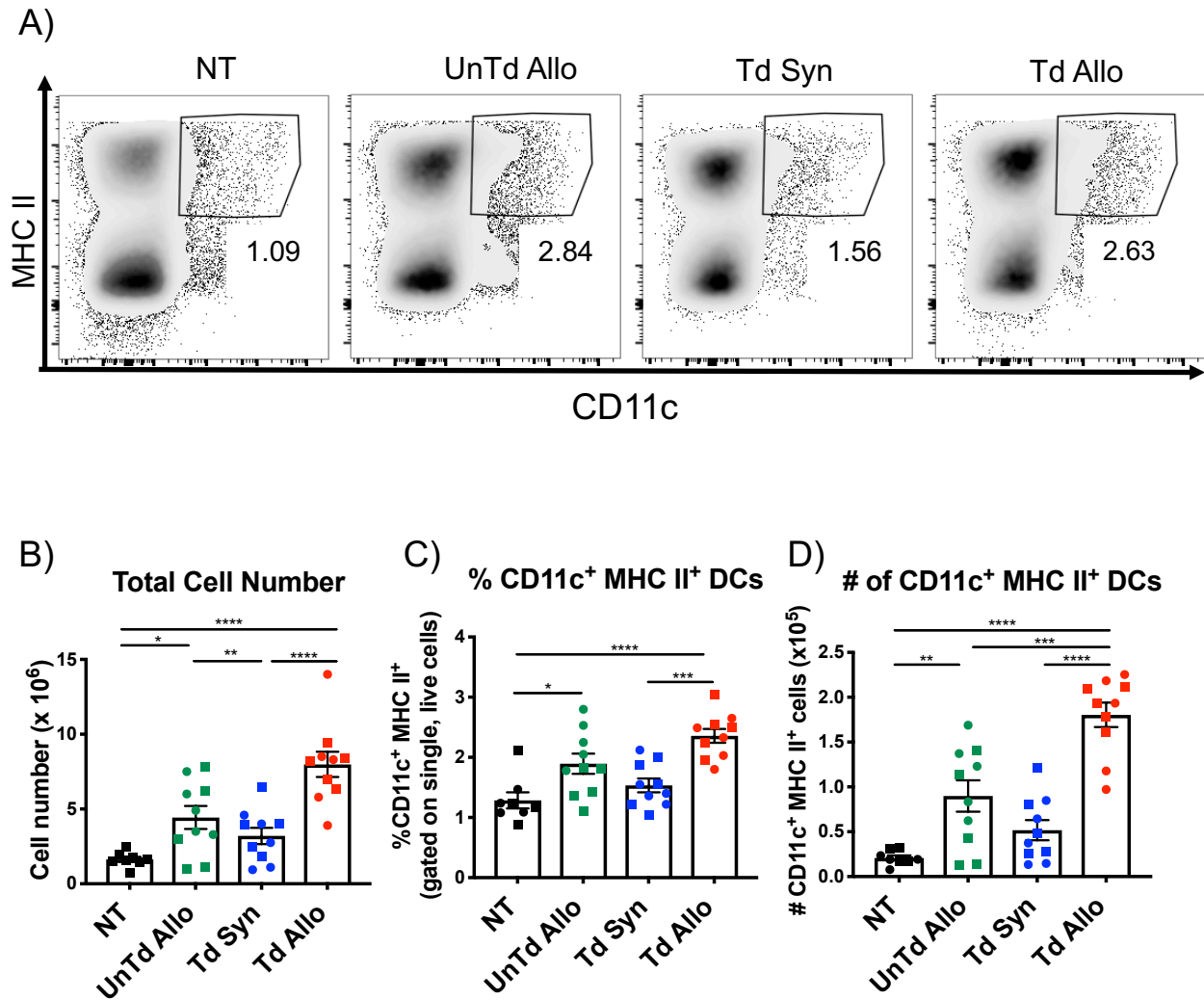


**Figure 25. TIL 1383I TCR Transduced Allogeneic T Cells Induce the Accumulation of CD11c<sup>+</sup> MHCII<sup>+</sup> Dendritic Cells in the Tumor Draining Lymph Nodes Two Days Post-T Cell Treatment.** Mice were intratumorally treated on day 10 and two days later the tumor draining lymph nodes were harvested and analyzed for expression of CD11c, MHC class II, CD80, and CD86 by flow cytometry. A) Representative flow cytometry plots of CD11c<sup>+</sup>MHCII<sup>+</sup> DCs. B) Absolute number of cells isolated from the tumor draining lymph node. C) Frequency and D) Absolute number of CD11c<sup>+</sup> MHC II<sup>+</sup> DCs. Cells were gated on live, singlet cells. Squares and circles represent individual mice from 2 independent experiments. Graph shows mean  $\pm$  SEM; statistical analysis by one-way ANOVA with Tukey's correction (\* $P < 0.05$ , \*\* $P < 0.01$ , \*\*\* $P < 0.001$ , \*\*\*\* $P < 0.0001$ )

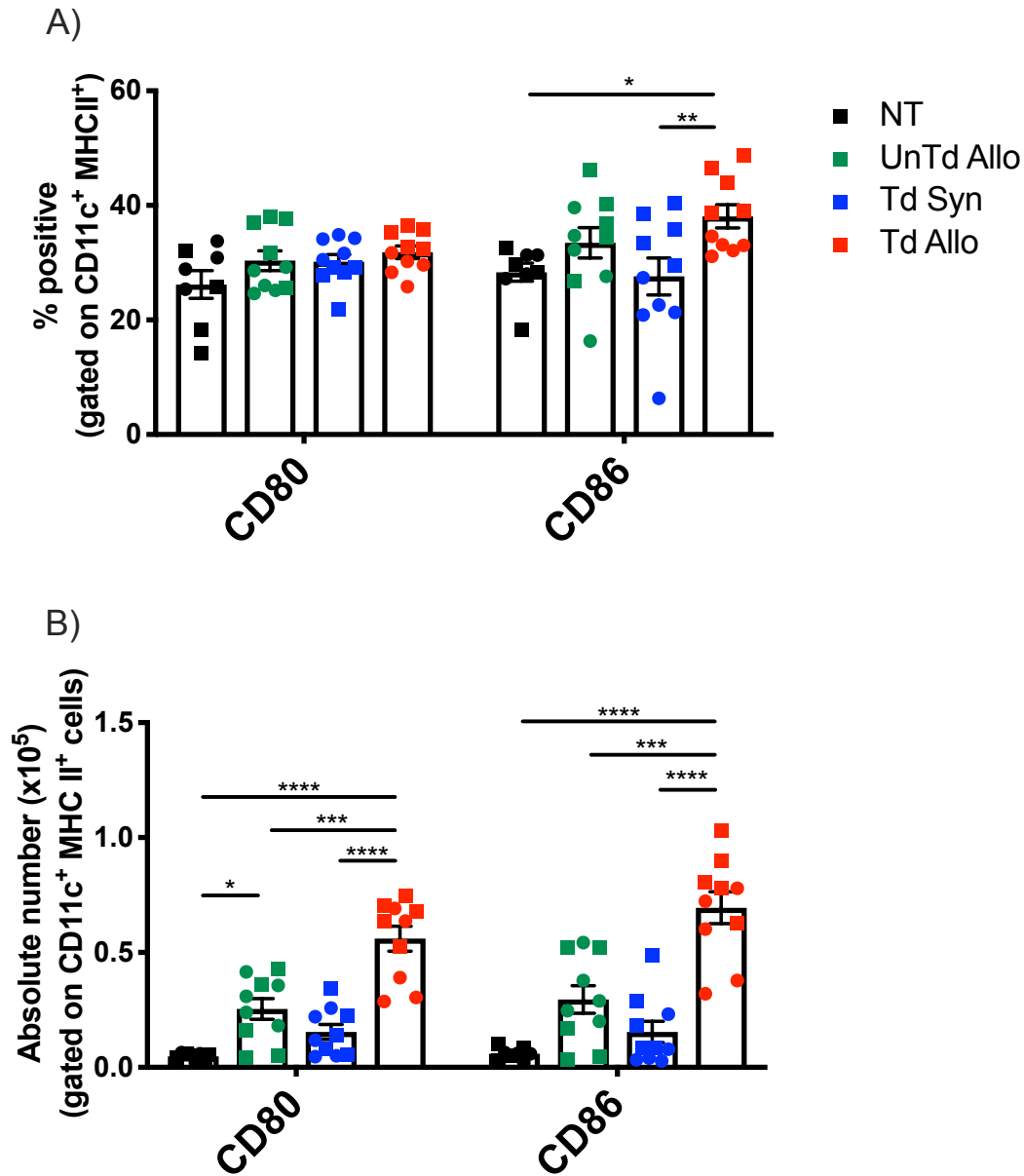


**Figure 26. TIL 1383I TCR Transduced Allogeneic T Cell Treatment Leads to an Increased Frequency and Total Number of CD80<sup>+</sup> and CD86<sup>+</sup> Dendritic Cells in the Tumor Draining Lymph Nodes Two Days Post-T Cell Treatment.** Tumor draining lymph nodes were isolated from B16 A2/K<sup>b</sup> tumor-bearing mice two days post-T cell treatment and cells were examined for expression of CD11c, MHC II, CD80 and CD86 by flow cytometry. A) Frequency and B) Total number of CD80 and CD86-expressing DCs. Cells were gated on live, CD11c<sup>+</sup>MHCII<sup>+</sup> cells. Symbols (circles and squares) represent individual mice from two independent experiments. Graph shows mean  $\pm$  SEM; statistical analysis performed using 2way ANOVA with Tukey's correction (\*P<0.05, \*\*P<0.01, \*\*\*P<0.001, \*\*\*\*P<0.0001)

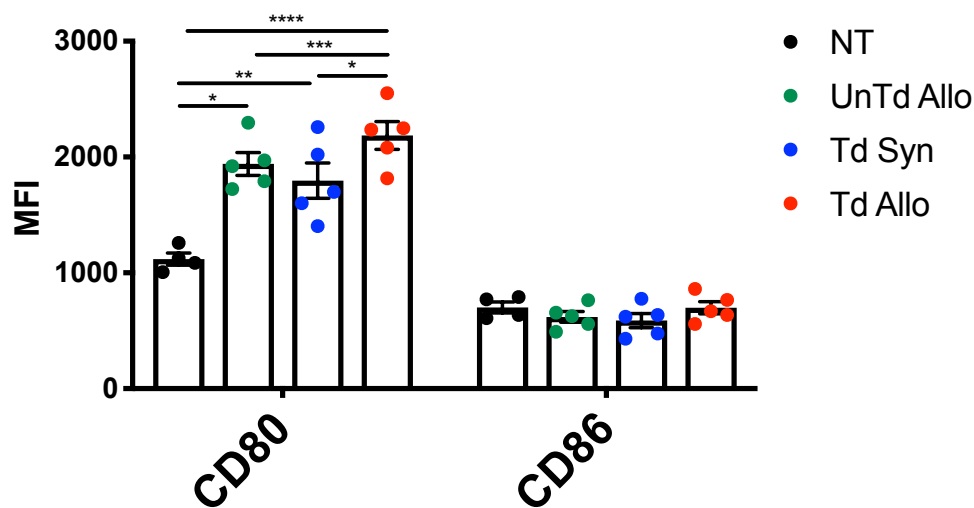


**Figure 27. TIL 1383I TCR Transduced Allogeneic T Cell Treatment Leads to Increased Surface Levels of the Co-Stimulatory Molecule CD80 on Dendritic Cells in the Tumor Draining Lymph Nodes Two Days Post-T Cell Treatment.**

Tumor draining lymph nodes were isolated from B16 A2/K<sup>b</sup> tumor-bearing mice two days post-T cell treatment and cells were analyzed for expression of CD11c, MHC II, CD80, and CD86. Cells were gated on live, CD11c<sup>+</sup>MHCII<sup>+</sup> cells. Symbols represent individual mice from one representative experiment with 4-5 mice/group. Graph shows mean  $\pm$  SEM; statistical analysis performed using 2way ANOVA with Tukey's correction (\* $P < 0.05$ , \*\* $P < 0.01$ , \*\*\* $P < 0.001$ , \*\*\*\* $P < 0.0001$ )

We further examined the tumor draining lymph nodes for evidence of cross-presenting DC subsets. The frequency and number of CD103<sup>+</sup> cDCs were significantly increased in the tumor draining lymph nodes isolated from mice treated with TIL 1383I TCR transduced allogeneic T cells compared to TIL 1383I TCR transduced syngeneic T cells ( $P = 0.0312$ ; Fig 28). Treatment with TIL 1383I TCR transduced allogeneic T cells also promoted an increase in the frequency and the number of lymphoid-resident CD8 $\alpha$  cDCs compared to TIL 1383I TCR transduced syngeneic T cell treatment ( $P = 0.0105$ ) and untreated mice ( $P = 0.0091$ ; Fig 29). Furthermore, the frequency and number of CD205-expressing cDCs were increased in the tumor draining lymph nodes following

intratumoral treatment with TIL 1383I TCR transduced allogeneic T cells compared to TIL 1383I TCR transduced syngeneic T cells ( $P=0.0220$ ) and no treatment ( $P=0.0003$ ; Fig 30). The differences in DC responses in the tumor draining lymph nodes were most pronounced at two days post-T cell treatment, whereas pilot experiments suggested a waning in response at day 3 and day 5 post-T cell treatment (Appendix Fig 100-102). Together, these results support our findings that intratumoral injection with TIL 1383I TCR transduced allogeneic T cells promotes the maturation of DCs and accumulation of cross-presenting DC subsets in the tumor draining lymph nodes two days post-T cell treatment.

### Summary

In this section, we examined the dendritic cell populations in the tumors and tumor draining lymph nodes of B16 A2/K<sup>b</sup> tumor-bearing mice treated with TIL 1383I TCR transduced T cells. In the tumor, the frequency of CD11c<sup>+</sup>MHC II<sup>+</sup> cDCs was similar among untreated and T cell-treated tumors; however, the CD11c<sup>+</sup> MHC II<sup>+</sup> DCs from tumors treated with allogeneic T cells exhibited increased surface levels of the co-stimulatory molecule CD80. We also observed an increased frequency of CD103<sup>+</sup> and CD205<sup>+</sup> DCs, two highly specialized subsets of cross-presenting DCs, in the tumors of mice treated with TIL 1383I TCR transduced allogeneic T cells. In accord with findings in the tumor, the tumor draining lymph nodes following T cell treatment showed a greater accumulation of CD11c<sup>+</sup>MHC II<sup>+</sup> DCs, particularly the cross-priming CD103<sup>+</sup> DC, CD8 $\alpha$ <sup>+</sup> DC, and CD205<sup>+</sup> DC subsets. The increased DC responses observed following TIL 1383I TCR transduced allogeneic T cell treatment led us to examine whether T cell activation was also enhanced in the tumor and tumor draining lymph nodes.

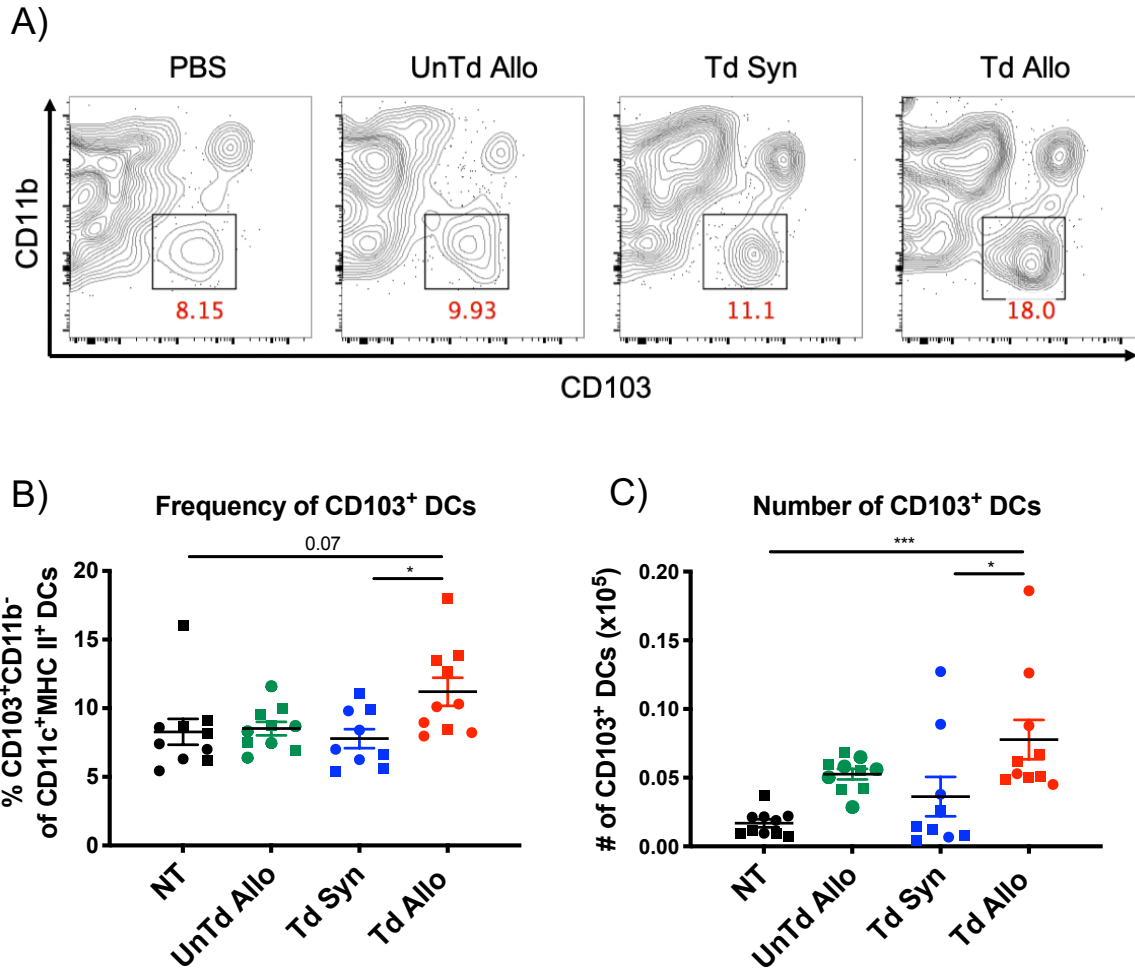


**Figure 28. Treatment with TIL 1383I TCR Transduced Allogeneic T Cells Increases CD103<sup>+</sup> Dendritic Cells in the Tumor Draining Lymph Nodes Two Days Post-T Cell Treatment.** Two days post-T cell treatment, the tumor draining lymph nodes of B16 A2/K<sup>b</sup> tumor-bearing mice were isolated and cells were examined for the expression of CD11c, CD11b, MHC II, and CD103 by flow cytometry. A) Representative flow cytometry plots of CD103<sup>+</sup>CD11b<sup>-</sup> DCs B) Percentage of CD103<sup>+</sup>CD11b<sup>-</sup> DCs (gated on live CD11c<sup>+</sup>MHCII<sup>+</sup> cells) C) Total number of CD103<sup>+</sup>CD11b<sup>-</sup> DCs. Symbols (circles and squares) represent individual mice from two independent experiments with 4-5 mice/group. Graph shows mean  $\pm$  SEM; statistical analysis by one-way ANOVA with Tukey's correction (\* $P < 0.05$ , \*\*\* $P < 0.001$ ).

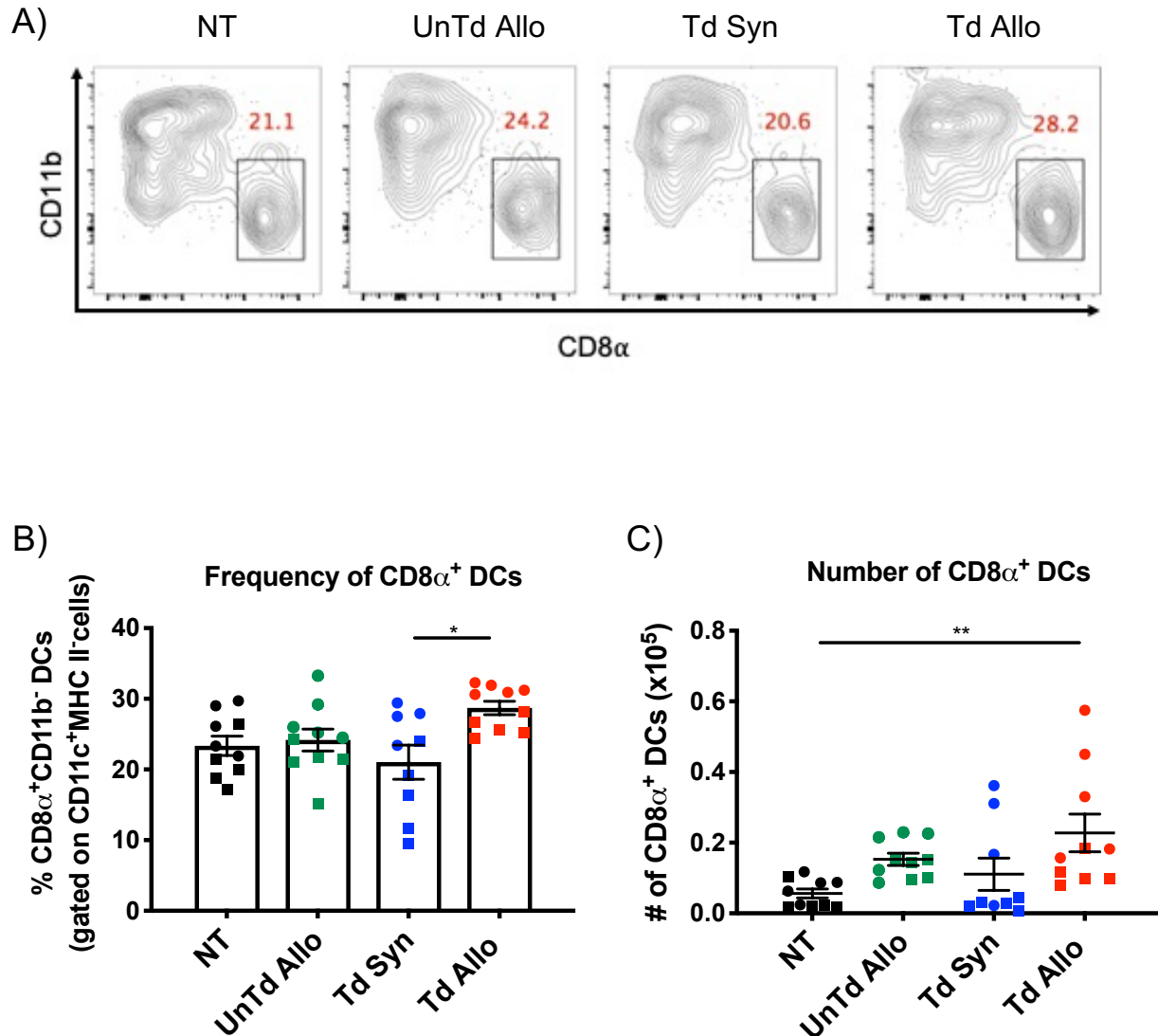


**Figure 29. TIL 1383I TCR Transduced Allogeneic T Cell Treatment Promotes the Accumulation of CD8α<sup>+</sup> Dendritic Cells in the Tumor Draining Lymph Nodes Two Days Post-T Cell Treatment.** Two days post-T cell treatment, the tumor draining lymph nodes of B16 A2/K<sup>b</sup> tumor-bearing mice were isolated and cells were examined for the presence of CD11c, CD11b, MHC II, and CD8α by flow cytometry A) Representative flow cytometry plots of CD8α<sup>+</sup>CD11b<sup>-</sup> DCs B) Percentage of CD8α<sup>+</sup> CD11b<sup>-</sup> DCs (gated on CD11c<sup>+</sup>MHCII<sup>+</sup> cells) C) Total number of CD8α<sup>+</sup>CD11b<sup>-</sup> DCs. Symbols (circles and squares) represent individual mice from two independent experiments with 4-5 mice/group. Graph shows mean ± SEM; statistical analysis performed using one-way ANOVA with Tukey's correction (\*P<0.05, \*\*P<0.01).



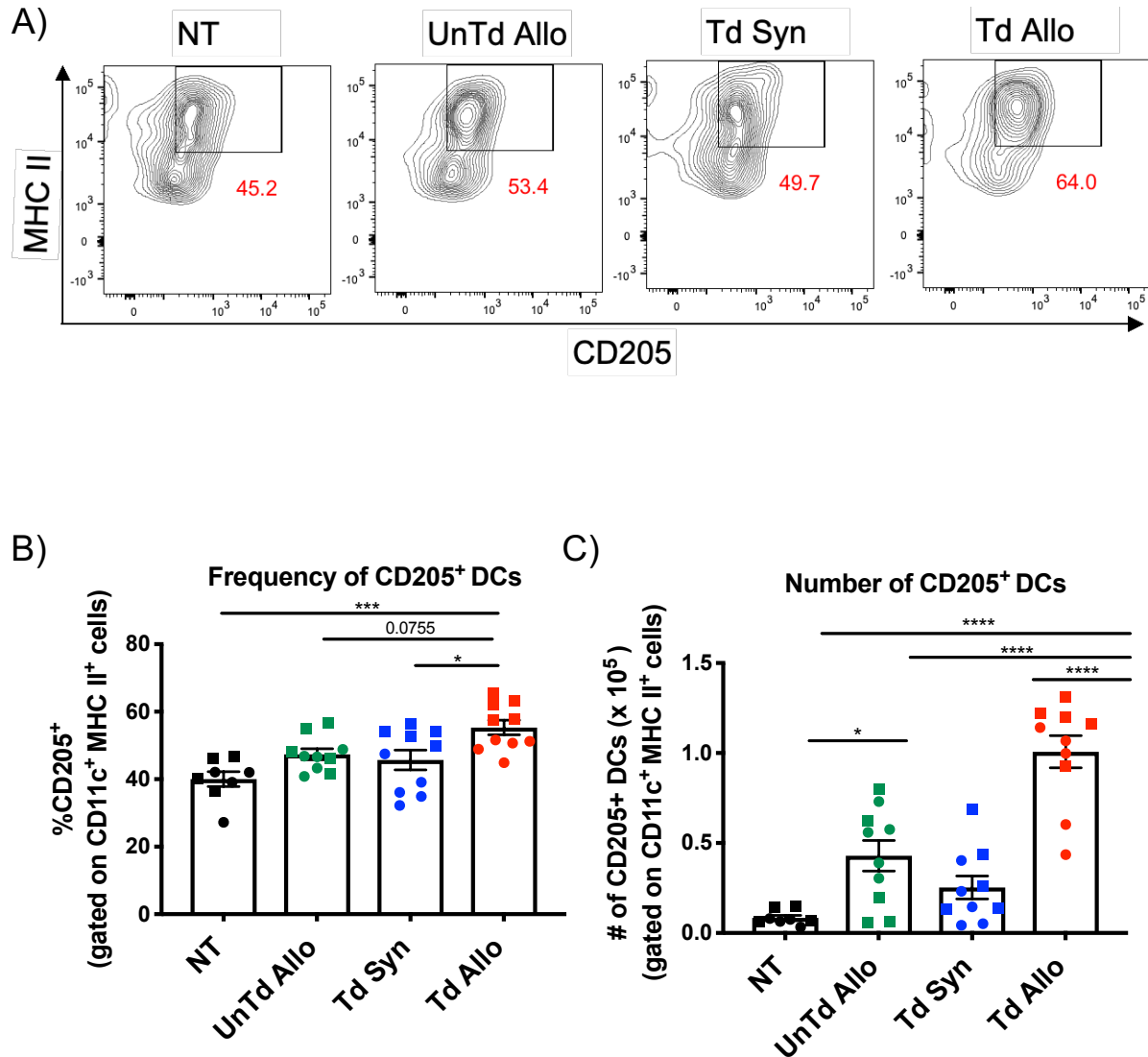


**Figure 30. Treatment with TIL 1383I TCR Transduced Allogeneic T Cells Increases CD205<sup>+</sup> Dendritic Cells in the Tumor Draining Lymph Nodes Two Days Post-T Cell Treatment.** Two days post-T cell treatment, the tumor draining lymph nodes of B16 A2/K<sup>b</sup> tumor-bearing mice were isolated and cells were examined for the expression of CD11c, CD11b, MHC II, and CD205 by flow cytometry A) Representative flow cytometry plots of CD205<sup>+</sup> DCs B) Percentage of CD205<sup>+</sup> MHCII<sup>+</sup> DCs (gated on CD11c<sup>+</sup>MHCII<sup>+</sup> cells) C) Total number of CD205<sup>+</sup> DCs. Circles and squares represent individual mice from two independent experiments with 4-5 mice/group. Graph shows mean  $\pm$  SEM; statistical analysis by one-way ANOVA with Tukey's correction (\*P<0.05, \*\*\*P<0.001, \*\*\*\*P<0.0001).

## CHAPTER FIVE

### TIL 1383I TCR TRANSDUCED ALLOGENEIC T CELL TREATMENT ENHANCES ACTIVATION OF T CELLS

#### **Characterization of T Cells in the Tumor Microenvironment**

Intratumoral treatment with TIL 1383I TCR transduced allogeneic T cells promoted dendritic cell (DC) responses in the tumor and tumor draining lymph nodes of B16 A2/K<sup>b</sup> tumor-bearing mice. We, therefore, examined the tumor microenvironment to determine if intratumoral treatment with TIL 1383I TCR transduced T cells impacted on the T cell response. Consistent with intratumoral delivery of T cells, all T cell treatment groups had a significant increase in the frequency of CD3<sup>+</sup> T cells compared to untreated tumors ( $P < 0.01$ , Fig 31) two days post-T cell treatment. The T cell infiltrates were predominantly CD8<sup>+</sup> T cells in the untransduced allogeneic T cell- and TIL 1383I TCR transduced syngeneic T cell- and TIL 1383I TCR transduced allogeneic T cell-treated tumors ( $P < 0.0001$ , Fig 32). Thus, as expected, the tumors of mice treated with untransduced allogeneic T cells and TIL 1383I TCR transduced syngeneic and TIL 1383I TCR transduced allogeneic T cells resulted in a greater accumulation of CD8<sup>+</sup> T cells in B16 A2/K<sup>b</sup> tumors.

We examined whether the combination of tumor-reactivity and alloreactivity promoted enhanced T cell activation compared to tumor-reactivity and alloreactivity alone. We examined B16 A2/K<sup>b</sup> tumors for the presence of CD4<sup>+</sup> and CD8<sup>+</sup> T cells within the tumor for the expression of the activation markers CD25, CD44, and CD69.

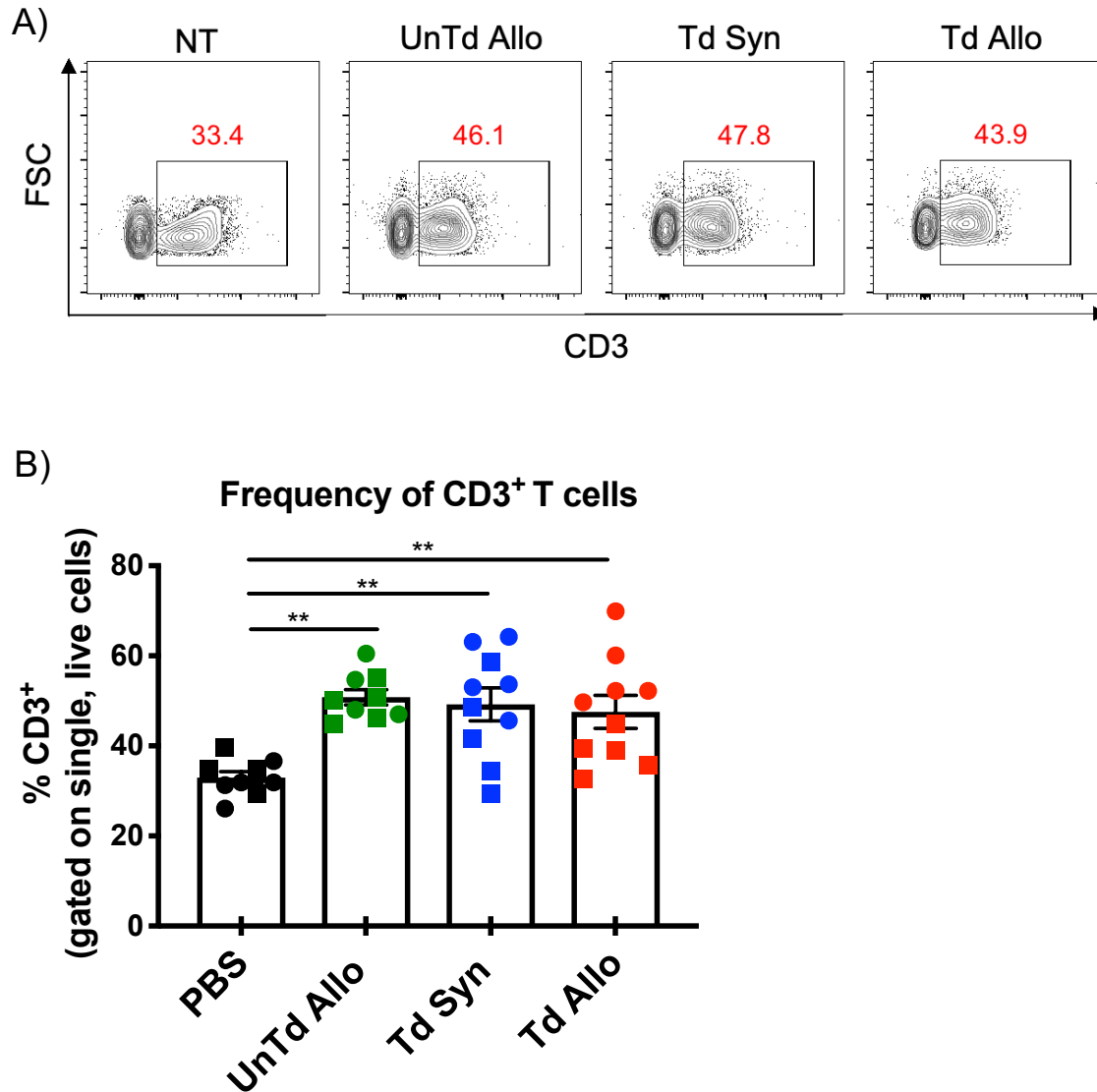


**Figure 31. Frequency of CD3<sup>+</sup> T Cells in the Tumor Microenvironment Two Days Post-T Cell Treatment.** Two days post-T cell treatment, tumors were isolated and cells were analyzed for expression of CD3 by flow cytometry. A) Representative flow cytometry plots of CD3<sup>+</sup> T cells B) Frequency of CD3<sup>+</sup> T cells. Gated on single, live cells. Circles and squares represent individual mice from two independent experiments with 4-5 mice per group. Graph shows mean  $\pm$  SEM; statistical analysis by one-way ANOVA with Tukey's correction (\*\*P<0.01).

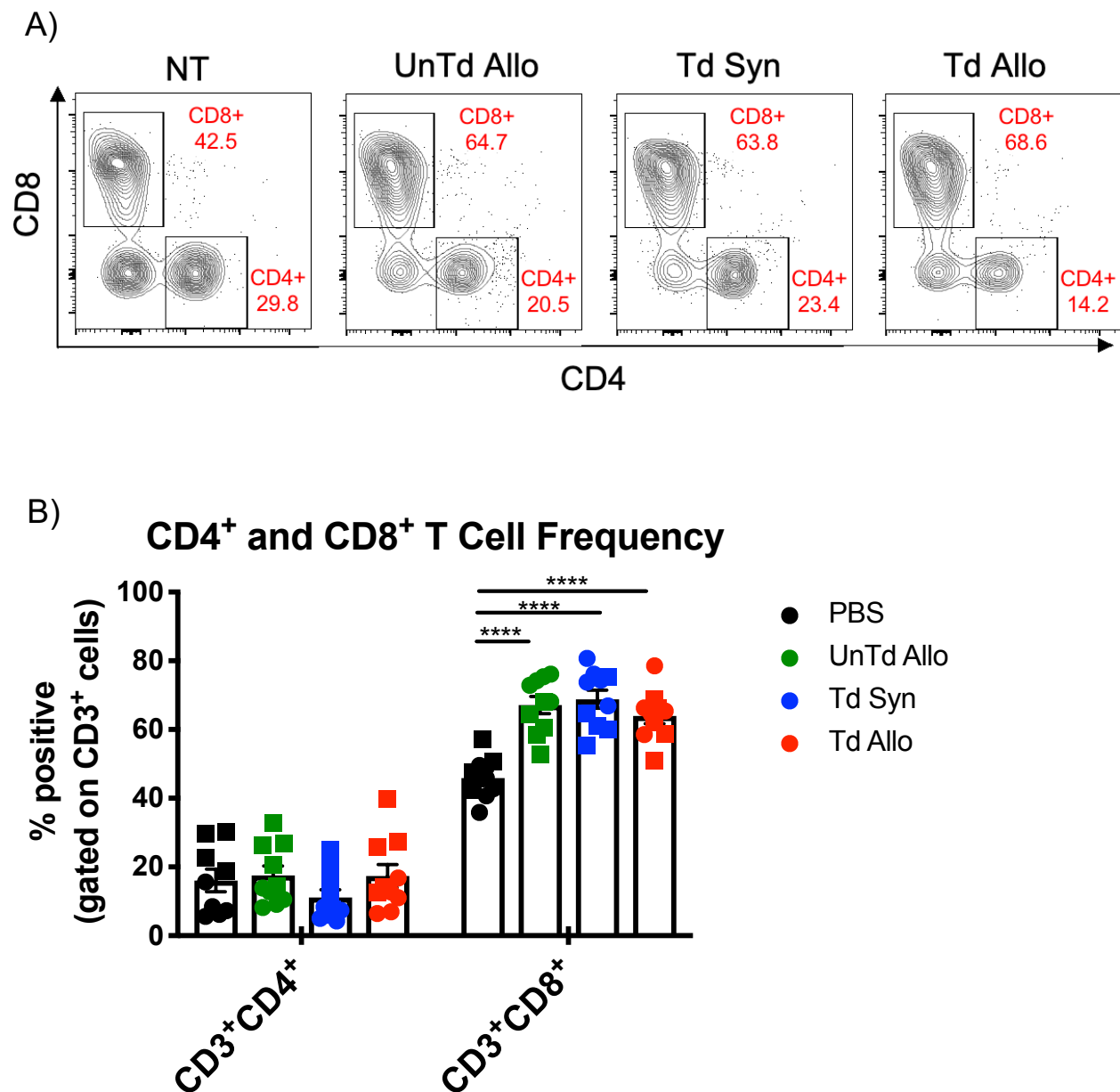


**Figure 32. Frequency of CD4<sup>+</sup> and CD8<sup>+</sup> T Cells in the Tumor Microenvironment Two Days Post-T Cell Treatment.** Two days post-T cell treatment, tumors were isolated and analyzed for expression of CD3, CD4, and CD8 by flow cytometry. A) Representative flow cytometry plots of CD4<sup>+</sup> and CD8<sup>+</sup> T cells B) Frequency of CD4<sup>+</sup> and CD8<sup>+</sup> T cells. Gated on live, CD3<sup>+</sup> T cells. Circles and squares represent individual mice from two independent experiments, with 4-5 mice per group. Graph shows mean  $\pm$  SEM; statistical analysis was performed using one-way ANOVA with Tukey's correction (\*\*\*\*P<0.0001).

Two days post-T cell treatment, the frequency of CD25<sup>+</sup> CD4<sup>+</sup> T cells in the tumors of TIL 1383I TCR transduced syngeneic T cells and untransduced allogeneic T cells were significantly increased compared to untreated tumors ( $P < 0.01$ , Fig 33A-B). TIL 1383I TCR transduced allogeneic T cell treatment resulted in the most significant increase of CD25<sup>+</sup>CD4<sup>+</sup> T cells compared to untreated mice ( $P < 0.001$ , Fig 33A-B). However, we did not notice any significant differences in the frequency of CD44<sup>+</sup> CD4<sup>+</sup> T cells between treatment groups (Fig 34). The proportion of CD69<sup>+</sup> CD4<sup>+</sup> T cells were increased in the untransduced allogeneic T cell-treated tumors compared to untreated mice ( $P = 0.0272$ ; Fig 35). The surface levels of CD25, CD44, and CD69 were equivalent between treatment groups (Fig 33-35). These results suggest that while the tumor-specific response mediated by intratumoral delivery of transduced T cells promotes moderate CD4<sup>+</sup> T cell activation, the allogeneic response seems to have more of an impact on CD4<sup>+</sup> T cell activation.

We also examined the activation status of CD8<sup>+</sup> T cells in the tumor microenvironment two days post-intratumoral T cell treatment. TIL 1383I TCR transduced syngeneic T cell treatment resulted in a significant increase in the frequency of CD25-expressing CD8<sup>+</sup> T cells compared to untreated mice ( $P < 0.0001$ ) or untransduced allogeneic T cell-treated mice. ( $P < 0.001$ , Fig 36A-B). TIL 1383I TCR transduced allogeneic T cell-treatment resulted in even higher frequencies of CD25<sup>+</sup> CD8<sup>+</sup> T cells compared to treatment with TIL 1383I TCR transduced syngeneic T cells, untransduced allogeneic T cells, and no treatment ( $P < 0.0001$ ). TIL 1383I TCR transduced allogeneic T cell treatment also promoted increased CD44-expressing CD8<sup>+</sup> T cells in the tumor compared to untransduced allogeneic T cells ( $P = 0.007$ ; Fig 37A-B).

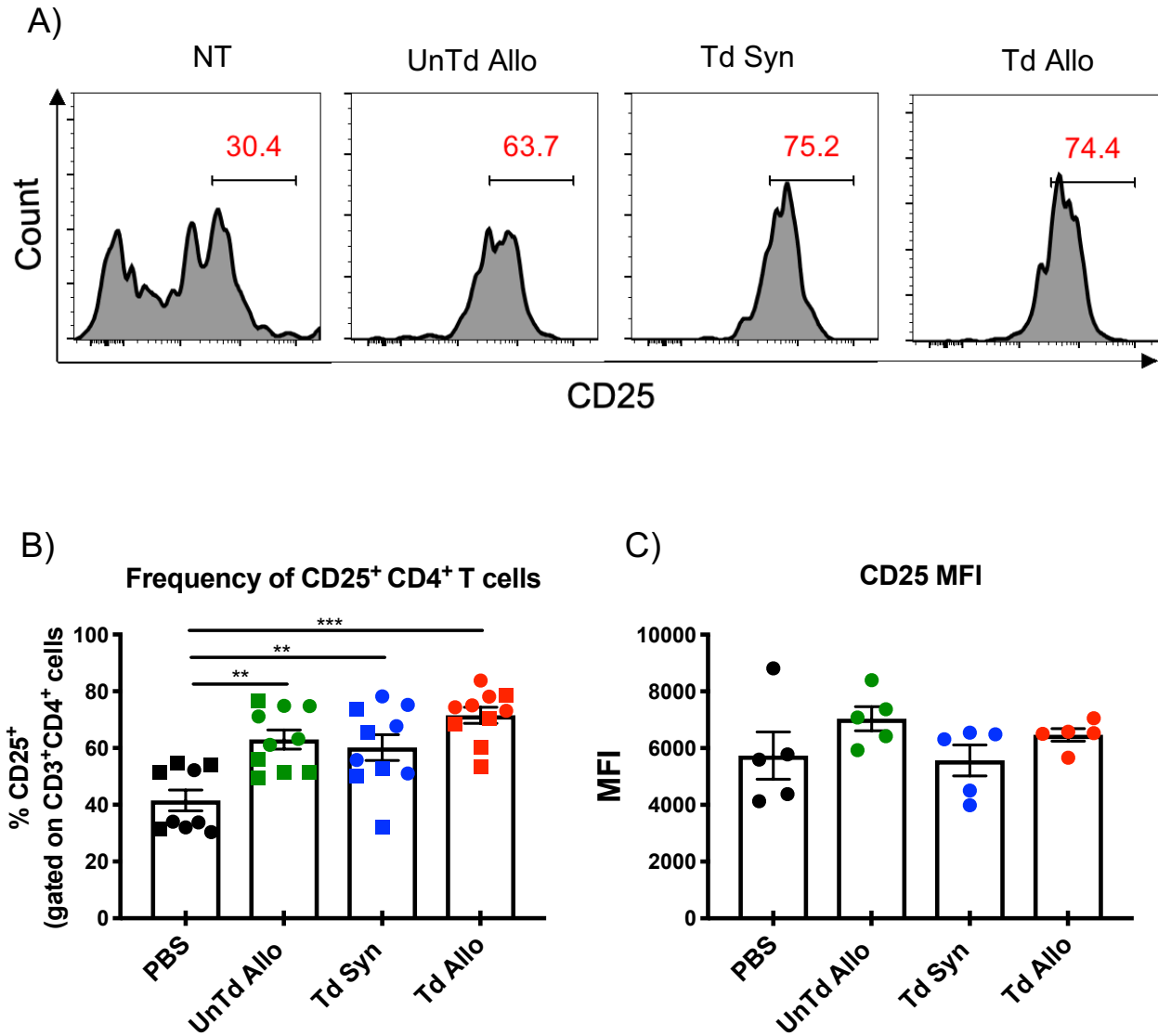


**Figure 33. Frequency and Surface Expression of CD25 on CD4<sup>+</sup> T Cells in the Tumor Microenvironment Two Days Post-T Cell Treatment.** Two days post-T cell treatment, B16 A2/K<sup>b</sup> tumors were isolated from mice and cells were analyzed for expression of CD3, CD4, and CD25 by flow cytometry. A) Representative histograms B) Frequency of CD25<sup>+</sup> T cells. Symbols (circles and squares) represent individual mice from two independent experiments C) CD25 MFI. Circles represent individual mice from one of two independent experiments. Cells were gated on live, CD3<sup>+</sup> CD4<sup>+</sup> T cells. Graph shows mean  $\pm$  SEM; statistical analysis by one-way ANOVA with Tukey's correction (\*\*P<0.01, \*\*\*P<0.001).

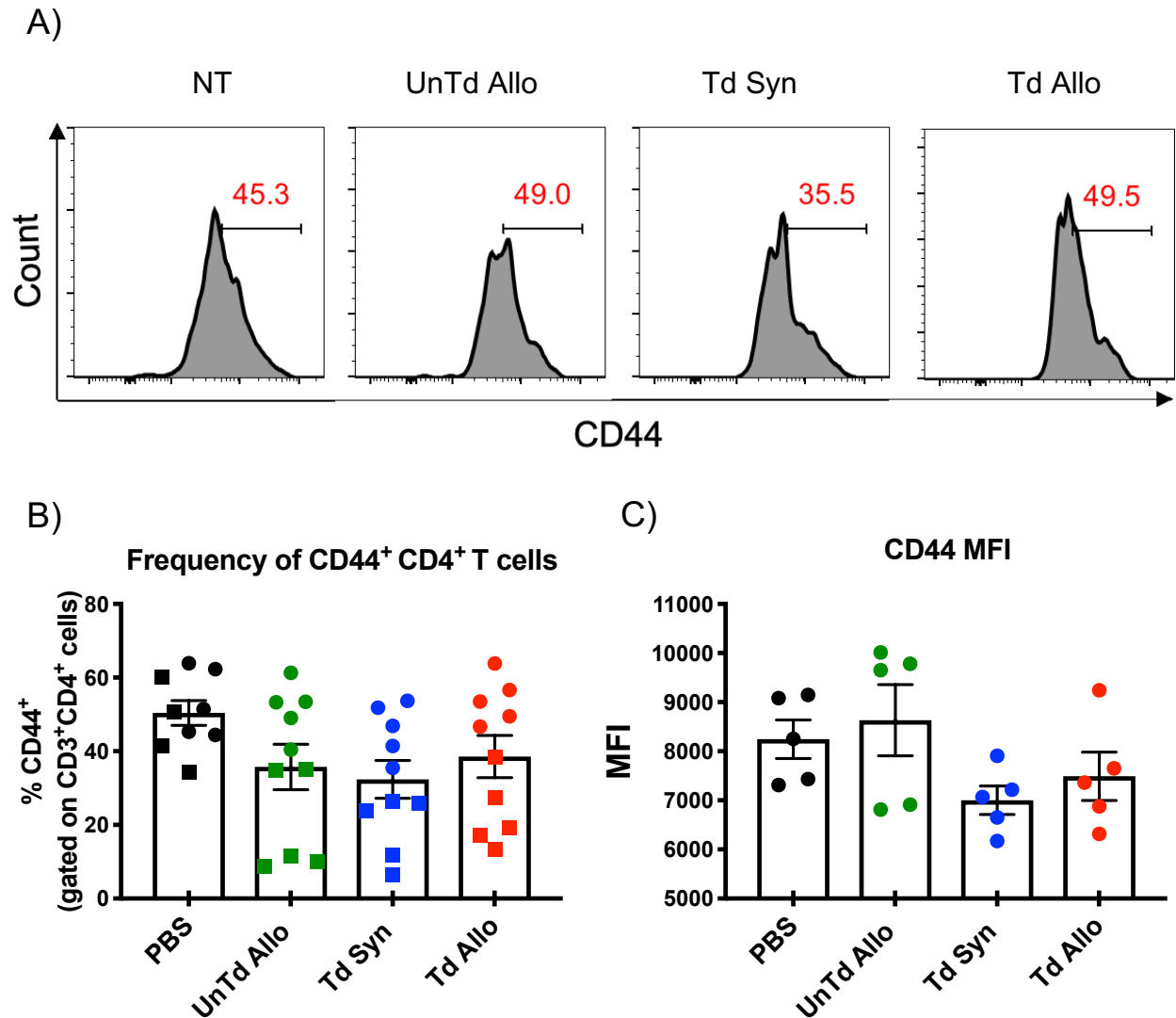


**Figure 34. Frequency and Surface Expression of CD44 on CD4<sup>+</sup> T Cells in the Tumor Microenvironment Two Days Post-T Cell Treatment.** Two days post-T cell treatment, B16 A2/K<sup>b</sup> tumors were isolated from mice and cells were analyzed for expression of CD3, CD4, and CD44 by flow cytometry. A) Representative histograms B) Frequency of CD44<sup>+</sup> T cells. Symbols (circles and squares) represent individual mice from two independent experiments. C) CD44 MFI. Circles represent individual mice from one of two independent experiments. Cells are gated on live, CD3<sup>+</sup> CD4<sup>+</sup> T cells. shows mean  $\pm$  SEM; No differences in statistical analysis were observed using one-way ANOVA with Tukey's correction.

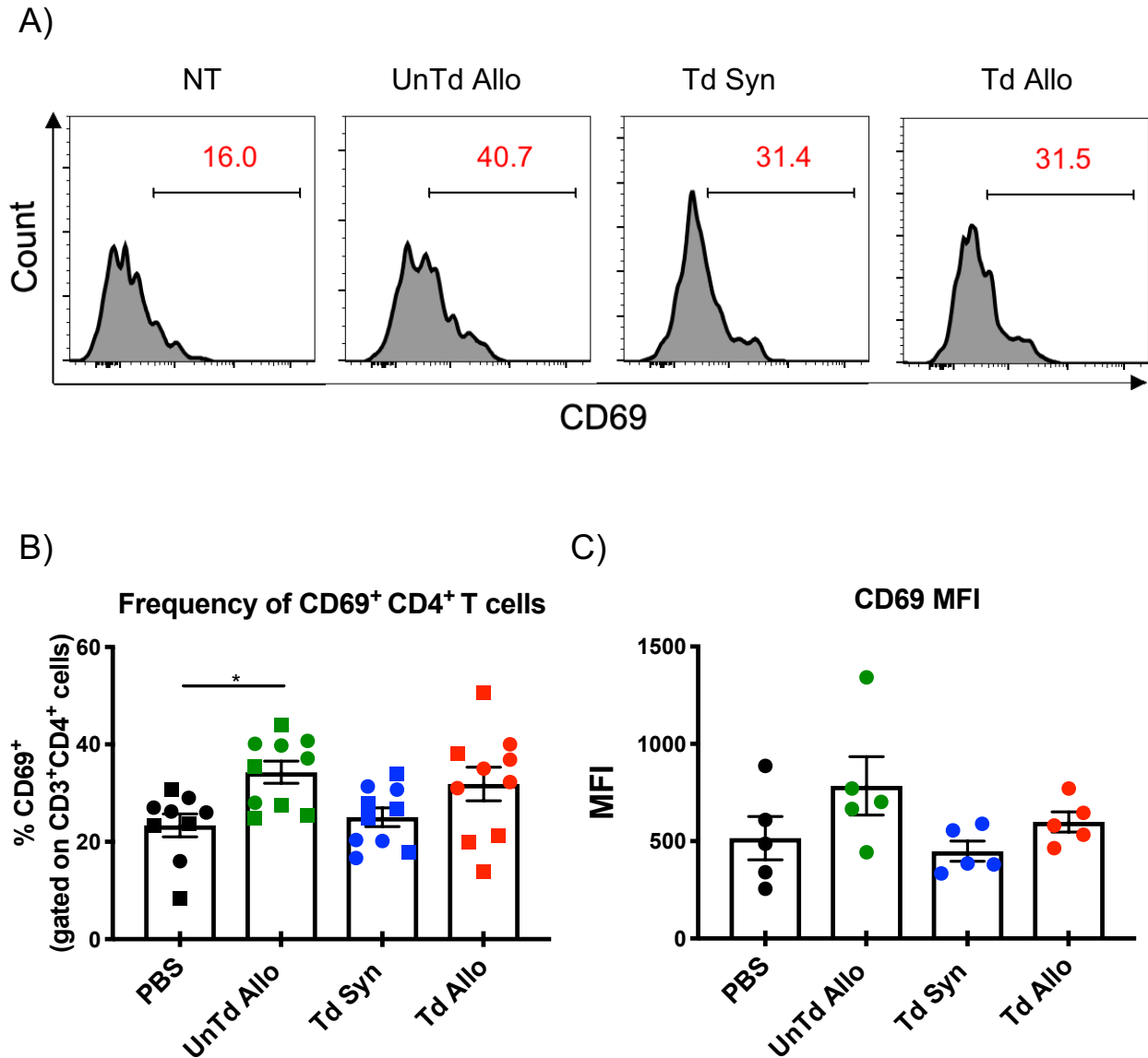


**Figure 35. Frequency and Surface Expression of CD69 on CD4<sup>+</sup> T Cells in the Tumor Microenvironment Two Days Post-T Cell Treatment.** Two days post-T cell treatment, B16 A2/K<sup>b</sup> tumors were isolated from mice and cells were analyzed for expression of CD3, CD4, and CD69 by flow cytometry. A) Representative histograms B) Frequency of CD69<sup>+</sup> T cells. Symbols (circles and squares) represent individual mice from two independent experiments C) CD69 MFI. Circles represent individual mice from one of two independent experiments. Cells were gated on live, CD3<sup>+</sup> CD4<sup>+</sup> T cells. Graph shows mean  $\pm$  SEM; statistical analysis by one-way ANOVA with Tukey's correction (\*P<0.05).



TIL 1383I TCR transduced syngeneic T cell promoted CD44<sup>+</sup>CD8<sup>+</sup> T cell accumulation compared to untransduced allogeneic T cell treatment ( $P=0.0069$ ; Fig 37A-B), suggesting that the accumulation of CD44<sup>+</sup>CD8<sup>+</sup> T cells is promoted by the tumor-specific response, rather than the alloresponse. The frequency of intratumoral CD69<sup>+</sup>CD8<sup>+</sup> T cell was also increased in all T cell-treated groups compared to untreated mice ( $P<0.0001$ , Fig 38A-B). In addition to the increased frequency of activated CD8<sup>+</sup> T cells present in the tumor of TIL 1383I TCR transduced T cell treatment, the cell surface expression of the activation markers tended to be higher as well (Fig 36C-38C). These results demonstrate that both the TIL 1383I TCR-directed response and the alloresponse can promote T cell activation within the tumor.

Allogeneic responses are mostly T cell-mediated, with indirect allorecognition characterized by IL-2-producing CD4<sup>+</sup> T cells and direct allorecognition characterized by TNF- $\alpha$ - and IFN- $\gamma$ -producing CD8<sup>+</sup> T cells<sup>77</sup>. In Chapter Four, we observed an increase in mature DCs in the tumor after treatment with TIL 1383I TCR transduced allogeneic T cells. We therefore performed one pilot experiment to examine the tumor for T cells producing cytokines that are involved in the allogeneic responses and that stimulate DC maturation. Two days post-T cell treatment, B16 A2/K<sup>b</sup> tumors were isolated from mice to assess CD4<sup>+</sup> and CD8<sup>+</sup> T cells for expression of IL-2, TNF- $\alpha$  or IFN- $\gamma$  to determine if TIL 1383I TCR transduced allogeneic T cell treatment altered the T cell cytokine response compared to TIL 1383I TCR transduced syngeneic T cell treatment. As expected, only the tumors that were treated with TIL 1383I TCR transduced T cells contained CD4<sup>+</sup>GFP<sup>+</sup> and CD8<sup>+</sup>GFP<sup>+</sup> T cells (Fig 39). We observed minimal production of IL-2 from CD4<sup>+</sup> and CD8<sup>+</sup> T cells within the tumors of T cell-treated mice (Fig 39).

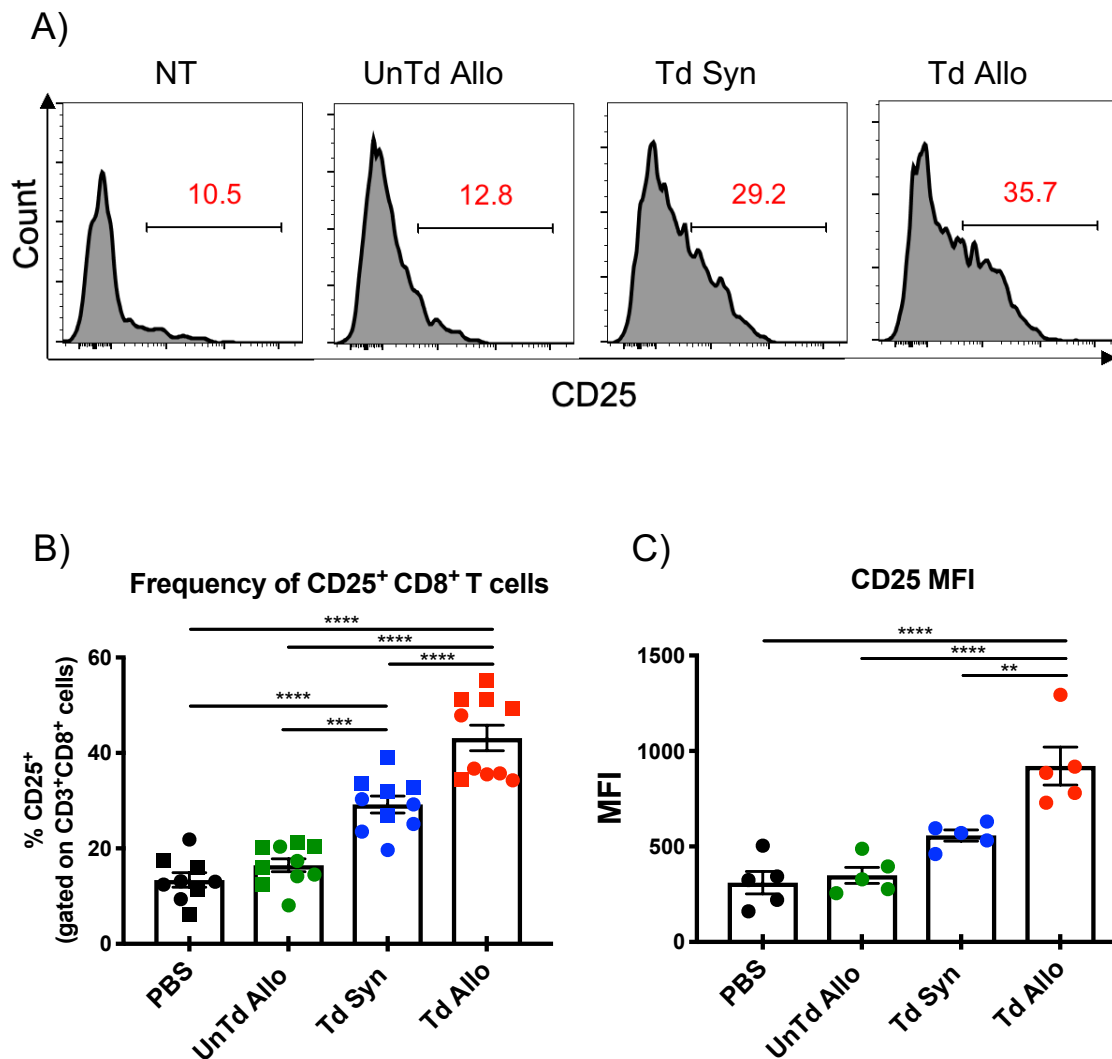


**Figure 36. Frequency and Surface Expression of CD25 on CD8<sup>+</sup> T Cells in the Tumor Microenvironment Two Days Post-T Cell Treatment.** Two days post-T cell treatment, B16 A2/K<sup>b</sup> tumors were isolated from mice and cells were analyzed for expression of CD3, CD8, and CD25 by flow cytometry. A) Representative histograms B) Frequency of CD25<sup>+</sup> T cells. Symbols (circles and squares) represent individual mice from two independent experiments. C) CD25 MFI. Circles represent individual mice from one of two independent experiments. Cells were gated on live, CD3<sup>+</sup> CD8<sup>+</sup> T cells. Graph shows mean  $\pm$  SEM; statistical analysis by one-way ANOVA with Tukey's correction (\*\* $P < 0.01$ , \*\*\* $P < 0.001$ , \*\*\*\* $P < 0.0001$ ).

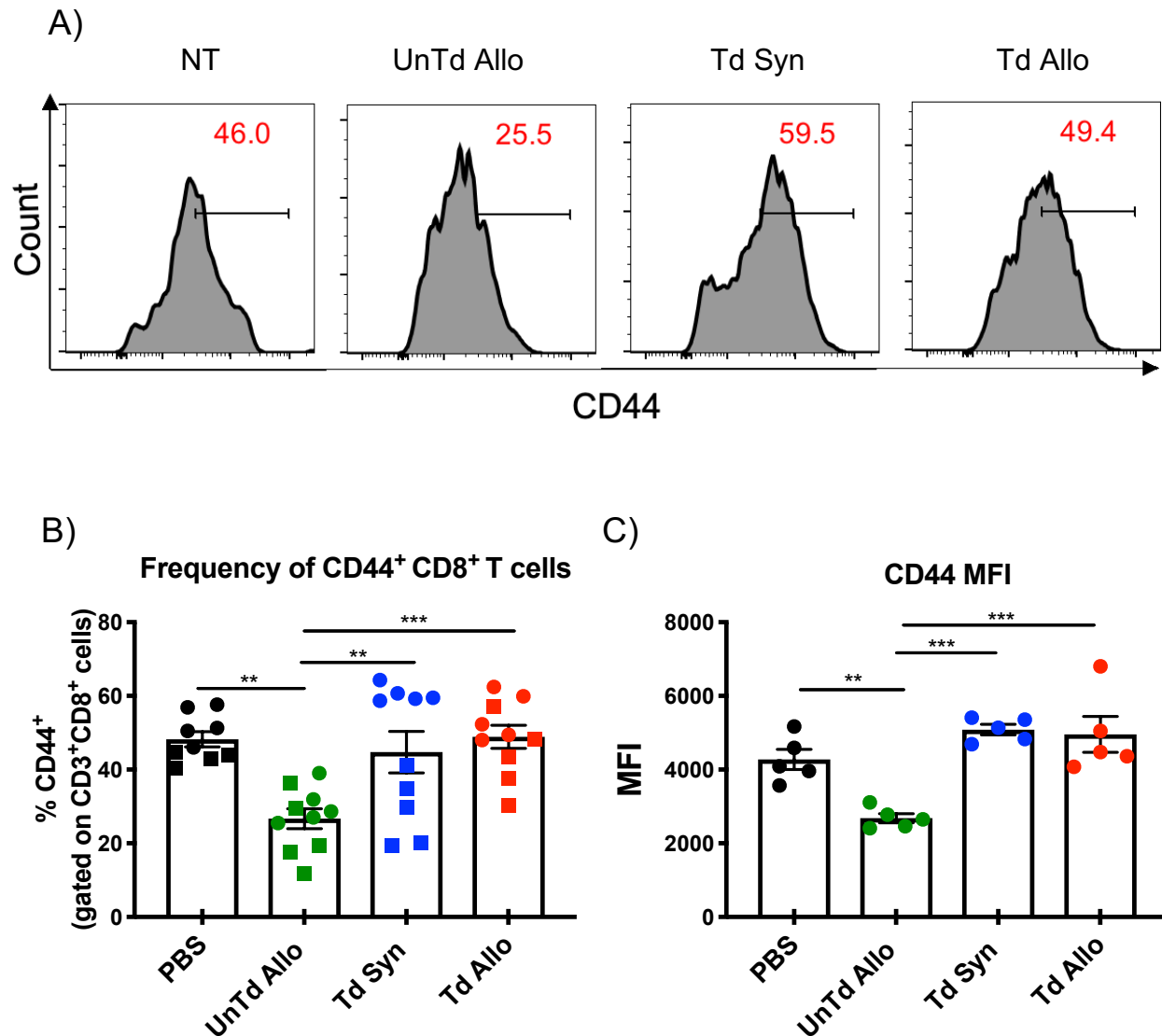


**Figure 37. Frequency and Surface Expression of CD44 on CD8<sup>+</sup> T Cells in the Tumor Microenvironment Two Days Post-T Cell Treatment.** Two days post-T cell treatment, B16 A2/K<sup>b</sup> tumors were isolated from mice and cells were analyzed for expression of CD3, CD8 and CD44 by flow cytometry. A) Representative histograms B) Frequency of CD44<sup>+</sup> T cells. Symbols (circles and squares) represent individual mice from two independent experiments. C) CD44 MFI. Circles represent individual mice from one of two independent experiments. Cells were gated on live, CD3<sup>+</sup> CD8<sup>+</sup> T cells. Graph shows mean  $\pm$  SEM; statistical analysis by one-way ANOVA with Tukey's correction (\*\*P<0.01, \*\*\*P<0.001).

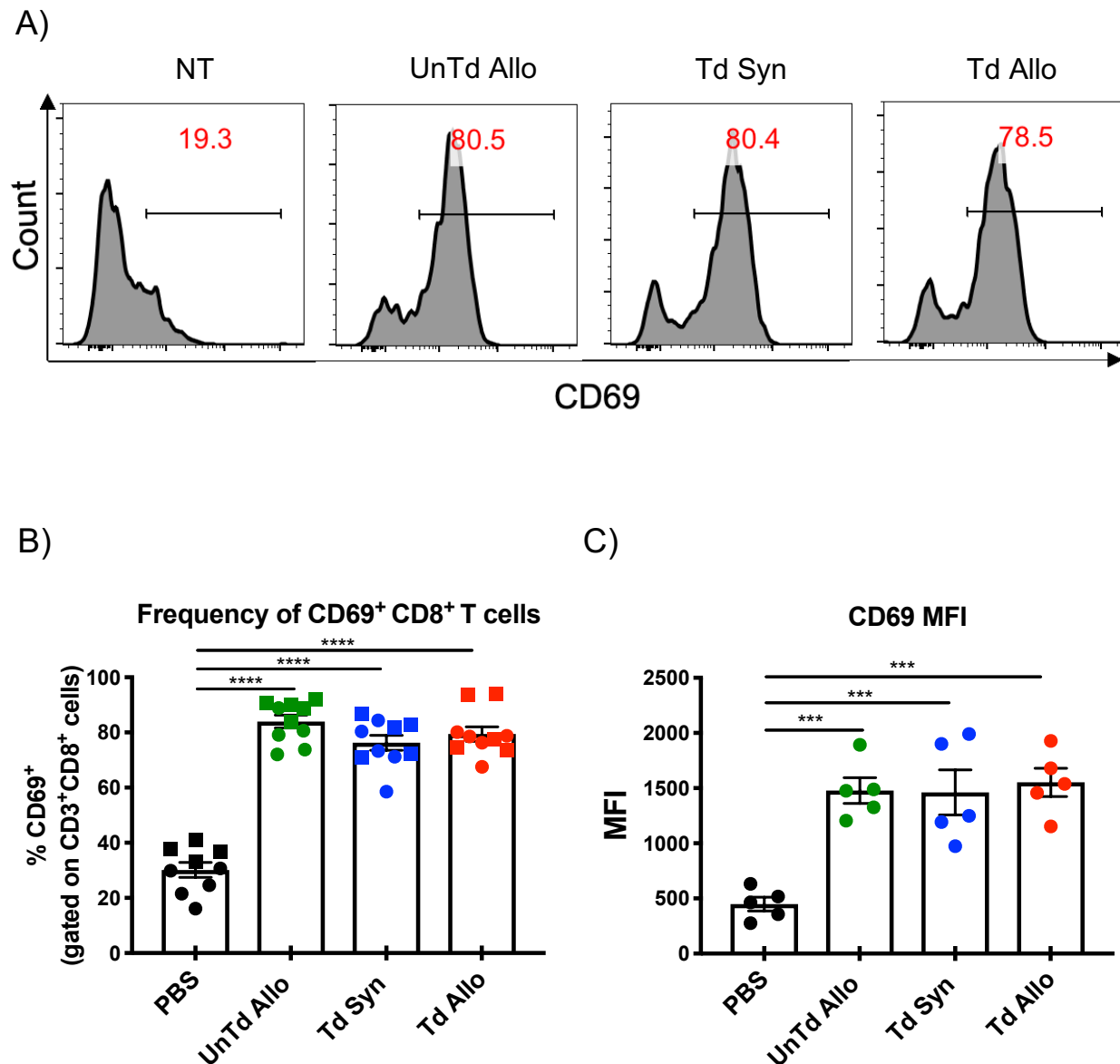


**Figure 38. Frequency and Surface Expression of CD69 on CD8<sup>+</sup> T Cells in the Tumor Microenvironment Two Days Post-T Cell Treatment.** Two days post-T cell treatment, B16 A2/K<sup>b</sup> tumors were isolated from mice and cells were analyzed for expression of CD3, CD8, and CD69 by flow cytometry. A) Representative histograms B) Frequency of CD69<sup>+</sup> T cells. Symbols (circles and squares) represent individual mice from two independent experiments. C) CD69 MFI. Circles represent individual mice from one of two independent experiments. Cells were gated on live, CD3<sup>+</sup> CD8<sup>+</sup> T cells. Graph shows mean  $\pm$  SEM; statistical analysis performed using one-way ANOVA with Tukey's correction (\*\*\*P<0.001, \*\*\*\*P<0.0001).

We did observe a small frequency of IFN- $\gamma$ <sup>+</sup>CD3<sup>+</sup>CD8<sup>+</sup> T cells (~3%) in the tumors treated with TIL 1383I TCR transduced allogeneic T cells. More than half of IFN- $\gamma$ <sup>+</sup> cells were detected in the TIL 1383I TCR transduced T cell population (from the GFP<sup>+</sup>; Fig 40). Interestingly, we only detected a small percentage of IFN- $\gamma$ <sup>+</sup>CD3<sup>+</sup>CD8<sup>+</sup> T cells within the GFP<sup>+</sup> population present in the TIL 1383I TCR transduced syngeneic T cell-treated tumors. GFP expression allows for the detection of TIL 1383I TCR transduced T cells, but the lack of GFP can include injected T cells that were untransduced or endogenous T cells.

In a small-scale follow-up experiment, we used a combination of PE-conjugated, anti-H-2<sup>d</sup> and anti-V $\beta$ 12 antibodies, which would further allow for the separation of the endogenous T cells from the total transferred allogeneic T cell population. We also examined TNF- $\alpha$  production from T cells within the tumors of treated mice. Overall, we observed more IFN- $\gamma$ <sup>+</sup> T cells in the tumors of all T cell-treated mice compared to the previous pilot experiment shown in Fig 41. Seven days post-intratumoral T cell treatment, CD4<sup>+</sup> and CD8<sup>+</sup> T cells from untransduced allogeneic and TIL 1383I TCR transduced syngeneic T cell-treated tumors had similar TNF- $\alpha$  expression, ranging from 4-8% of T cells (Fig 42). However, the tumors treated with TIL 1383I TCR transduced allogeneic T cells contained approximately 14.8% CD4<sup>+</sup> TNF- $\alpha$ <sup>+</sup> T cells and 12.5% CD8<sup>+</sup> TNF- $\alpha$ <sup>+</sup> T cells (Fig 42). These results suggested that treatment with untransduced allogeneic T cells and TIL 1383I TCR transduced syngeneic T cells induce low levels of cytokine production on their own, but TIL 1383I TCR transduced allogeneic T cells induce the most robust cytokine responses by CD8<sup>+</sup> T cells within the tumor microenvironment.

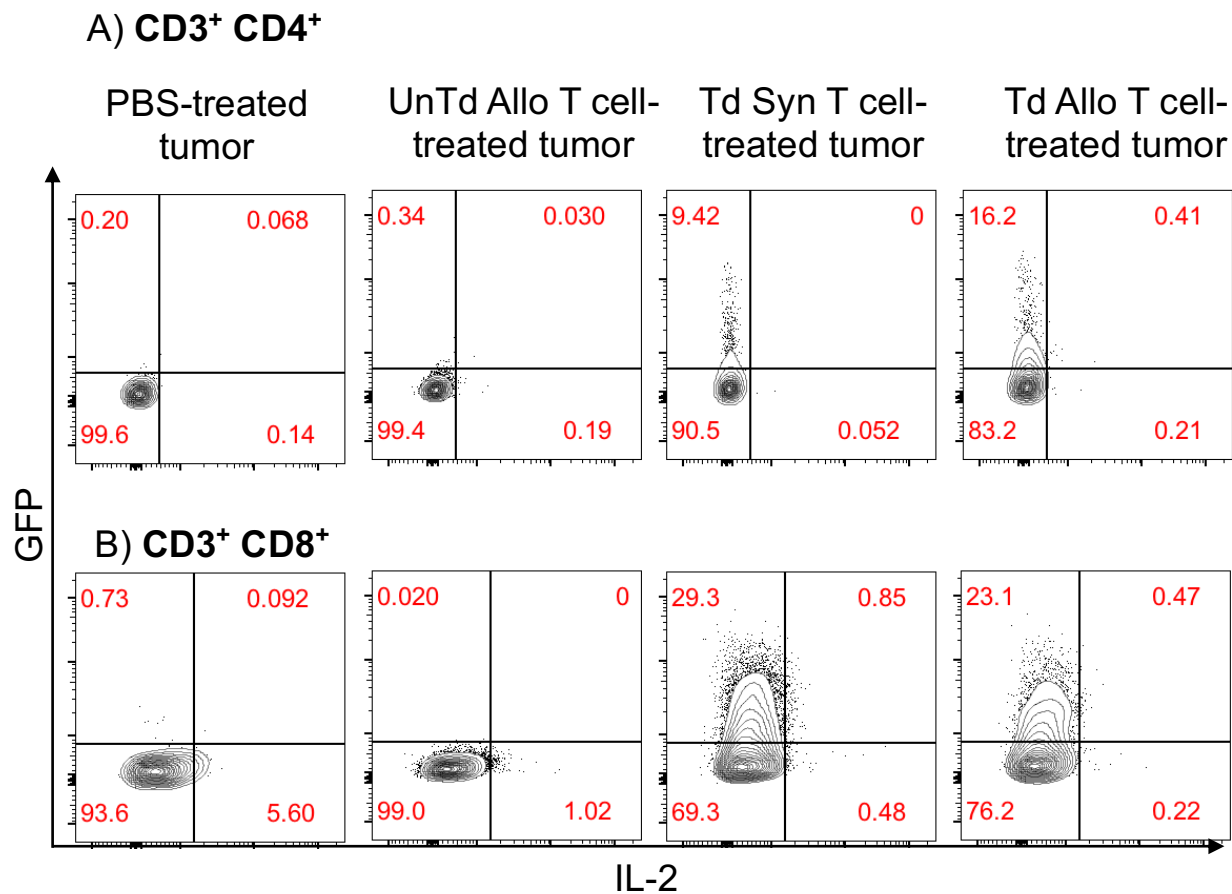


**Figure 39. Production of IL-2 from CD3<sup>+</sup> T Cells in the Tumor Microenvironment Two Days Post-T Cell Treatment.** Two days post-T cell treatment, B16 A2/K<sup>b</sup> tumors were isolated from mice and pooled. Cells were examined for expression of CD3, CD4, CD8, GFP, and IL-2 by flow cytometry. A) CD3<sup>+</sup>CD4<sup>+</sup> T cells B) CD3<sup>+</sup>CD8<sup>+</sup> T cells. Cells were gated on live, singlet, CD3<sup>+</sup> cells. Flow plots represent one pilot experiment with 5 mice/group.

### A) CD3<sup>+</sup> CD4<sup>+</sup>

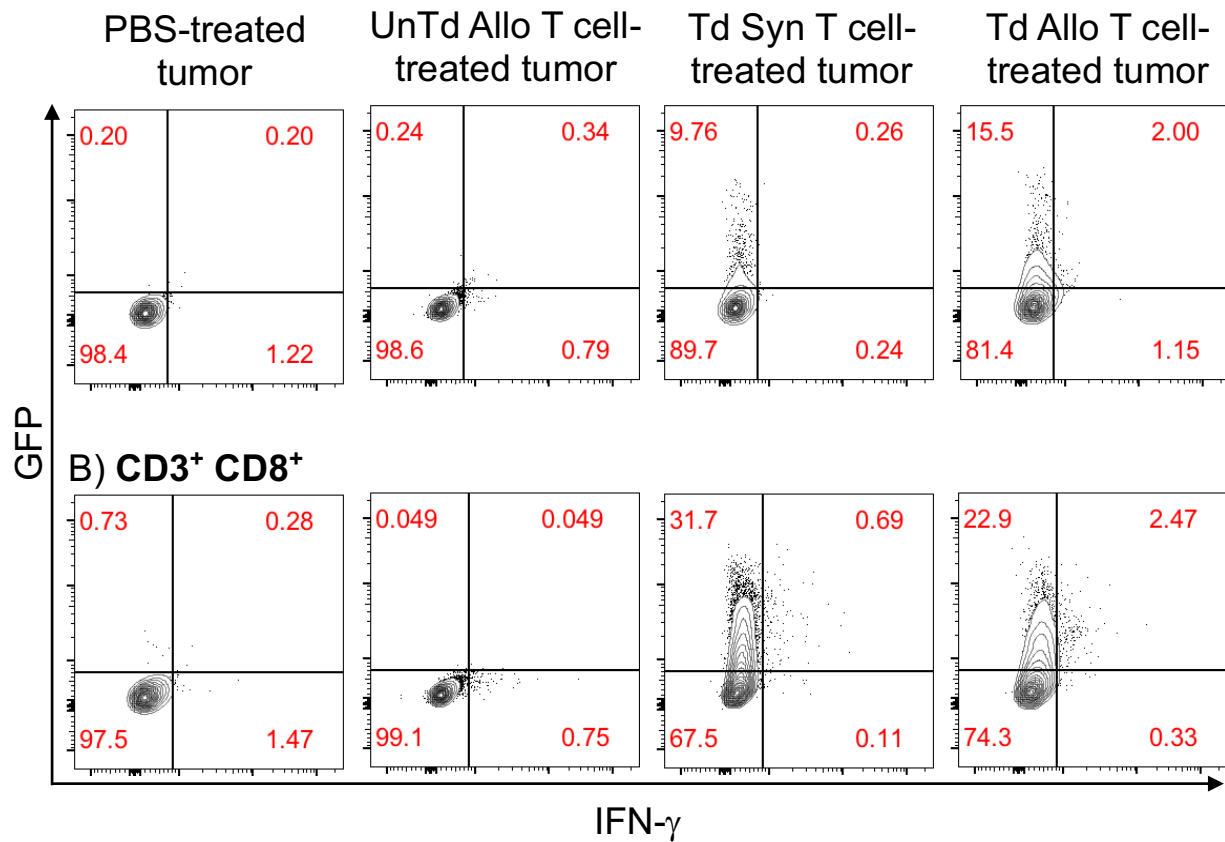


**Figure 40. Intratumoral TIL 1383I TCR Transduced Allogeneic T Cells Produce IFN- $\gamma$ .** Two days post-T cell treatment, B16 A2/K<sup>b</sup> tumors were isolated from mice and pooled. Cells were examined for expression of CD3, CD4, CD8, GFP and IFN- $\gamma$  by flow cytometry. A) CD3<sup>+</sup>CD4<sup>+</sup> T cells B) CD3<sup>+</sup>CD8<sup>+</sup> T cells. Cells were gated on live, singlet, CD3<sup>+</sup> cells. Flow plots represent one of two pilot experiment with 5 mice/group.

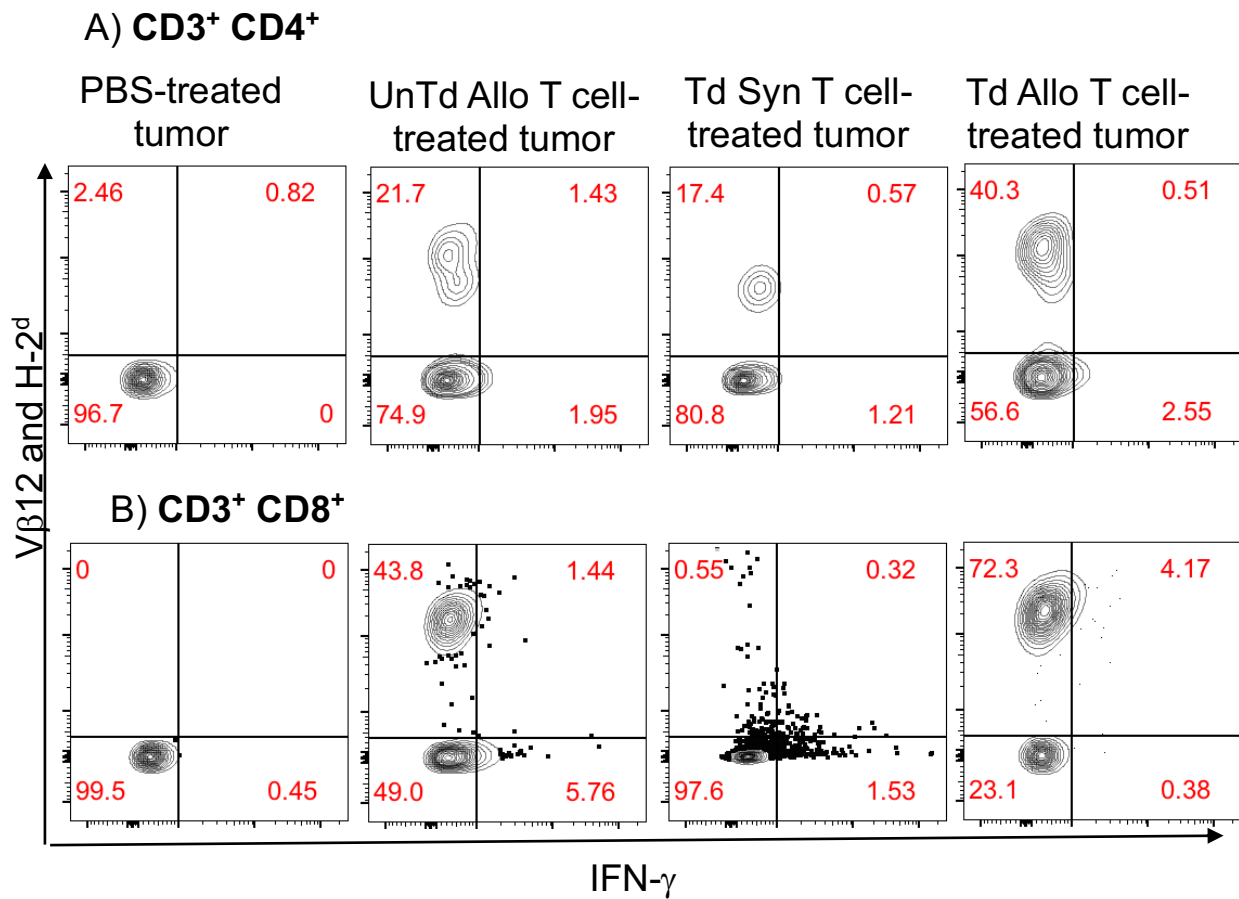


**Figure 41. Intratumoral TIL 1383I TCR Transduced Allogeneic T Cells Produce IFN-γ.** Two days post-T cell treatment, B16 A2/K<sup>b</sup> tumors were isolated from mice and pooled. Cells were examined for expression of CD3, CD4, CD8, Vβ12, H-2<sup>d</sup>, and IFN-γ by flow cytometry. A) CD3<sup>+</sup>CD4<sup>+</sup> T cells B) CD3<sup>+</sup>CD8<sup>+</sup> T cells. Cells were gated on live, singlet, CD3<sup>+</sup> cells. Flow plots represent one of two pilot experiment with 5 mice/group.



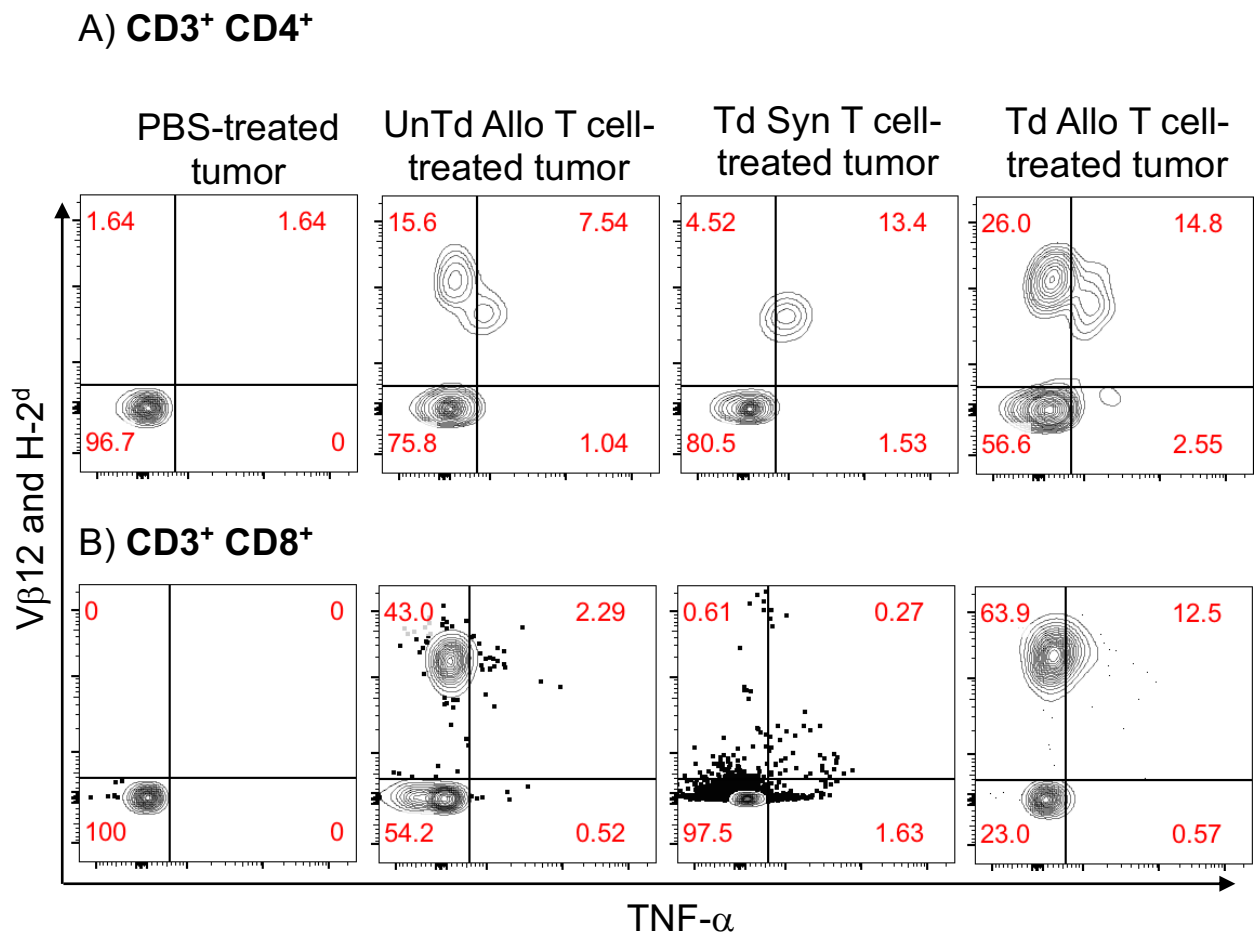


**Figure 42. Intratumoral TIL 1383I TCR Transduced Allogeneic T Cells Produce TNF-α.** Two days post-T cell treatment, B16 A2/K<sup>b</sup> tumors were isolated and pooled. Cells were examined for expression of CD3, CD4, CD8, Vβ12, H-2<sup>d</sup>, and TNF-α by flow cytometry. A) CD3<sup>+</sup>CD4<sup>+</sup> T cells B) CD3<sup>+</sup>CD8<sup>+</sup> T cells. Cells were gated on live, singlet, CD3<sup>+</sup> cells. Flow plots represent one pilot experiment with 5 mice/group.

The ability to comprehensively compare cytokine production from T cells among treatment groups and between endogenous and transferred T cells is limited by the ability to distinguish the untransduced transferred syngeneic T cells from the recipient HLA-A2 transgenic T cells. In spite of these limitations, results from these small-scale experiments suggested that the combined alloreactivity and tumor-specificity of TIL

1383I TCR transduced allogeneic T cells induce increased *in vivo* cytokine production within the tumors compared to the cytokine responses induced by alloreactivity (untransduced allogeneic T cells) or tumor-specificity (TIL 1383I TCR transduced syngeneic T cells) alone.

### **Characterization of T Cells in the Tumor and Tumor Draining Lymph Nodes Seven Days Post-T Cell Treatment**

Examining the phenotype of the T cell present in the tumor microenvironment two days post-T cell treatment had some limitations to distinguishing endogenous and transferred T cells. Therefore, we also looked at the tumor seven days post-T cell treatment when transferred T cells were undetectable and the endogenous T cells could be assessed. We did not observe differences in the frequency and activation of endogenous intratumoral CD4<sup>+</sup> T cells among treatment groups (Fig 43 and Fig 44). The tumors treated with untransduced allogeneic T cells and TIL 1383I TCR transduced allogeneic T cells had the greatest frequency of CD8<sup>+</sup> T cells (Fig 43). Interestingly, TIL 1383I transduced syngeneic T cell-treated tumors did not have an increase in CD8<sup>+</sup> T cell infiltration but did have increased frequencies of CD69<sup>+</sup> CD8<sup>+</sup> T cells (Fig 43 and Fig 45).

The increase in T cell activation led us to ask if there was also an increase in the frequency of regulatory T cells (Tregs) following treatment with TIL 1383I TCR transduced T cells. Surprisingly, seven days post-T cell treatment, the tumors from TIL 1383I TCR transduced syngeneic T cell-treated mice had the highest frequency of Foxp3<sup>+</sup>CD25<sup>+</sup> Tregs compared to tumors treated with TIL 1383I TCR transduced allogeneic T cells (P=0.0108) and untransduced allogeneic T cells (P=0.0302; Fig 46A)

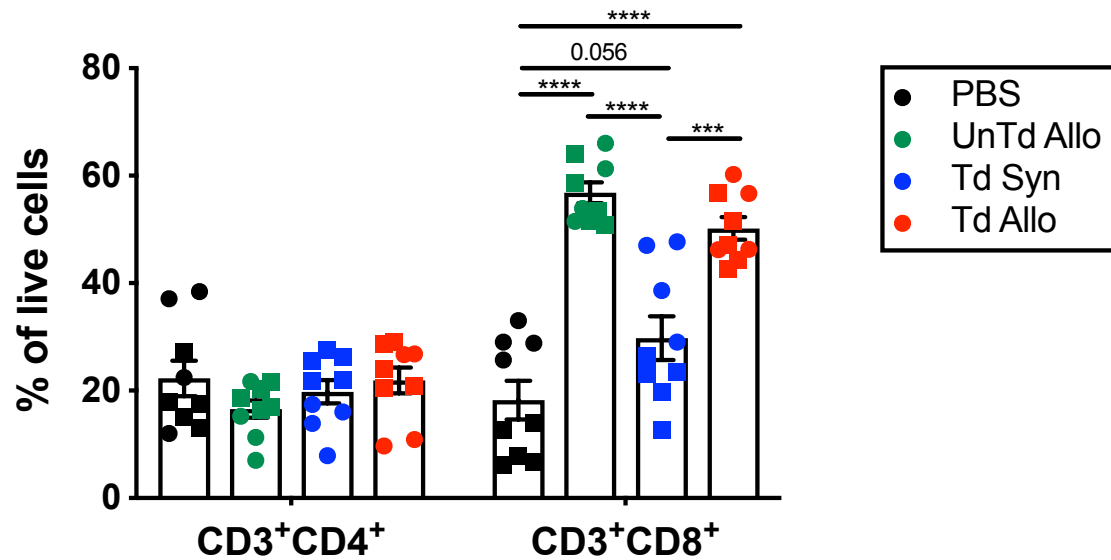


**Figure 43. Frequency of CD4<sup>+</sup> and CD8<sup>+</sup> T Cells in the Tumor Seven Days Post-T Cell Treatment.** Seven days post-T cell treatment, B16 A2/K<sup>b</sup> tumors were isolated from mice and cells were analyzed for expression of CD3, CD4 and CD8 by flow cytometry. Symbols (circles and squares) represent individual mice from two independent experiments. Cells were gated on live cells. Graph shows mean  $\pm$  SEM; statistical analysis performed using one-way ANOVA with Tukey's correction (\*\*\*P<0.001, \*\*\*\*P<0.0001).

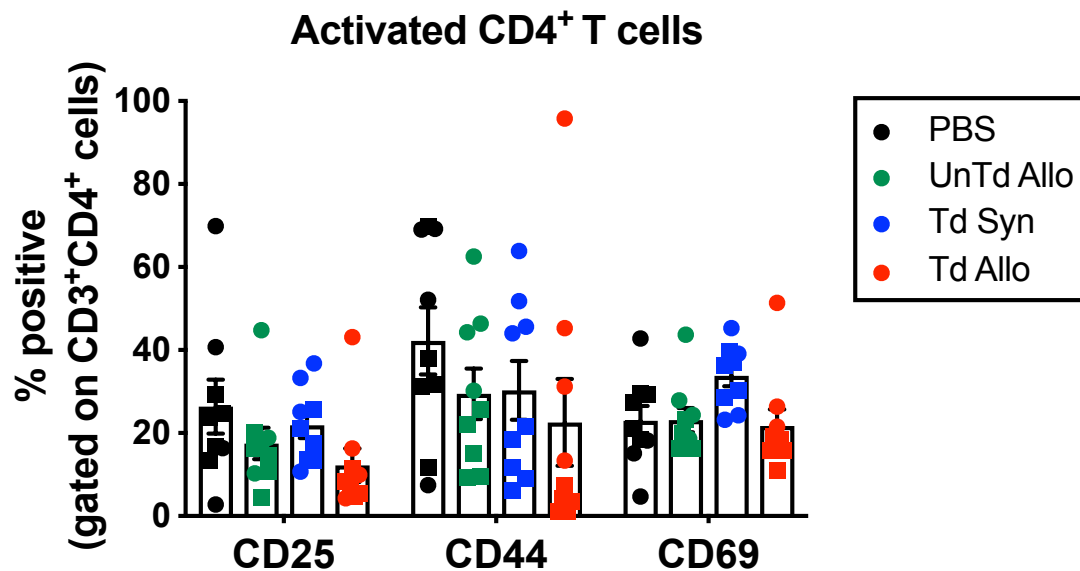


**Figure 44. Frequency of Activated CD4<sup>+</sup> T Cells in the Tumor Seven Days Post-T Cell Treatment.** Seven days post-T cell treatment, B16 A2/K<sup>b</sup> tumors were isolated from mice and cells were analyzed for expression of CD3, CD4, CD25, CD44, and CD69 by flow cytometry. Symbols (circles and squares) represent individual mice from two independent experiments. Cells were gated on live, CD3<sup>+</sup>CD4<sup>+</sup> T cells. Graph shows mean  $\pm$  SEM; statistical analysis performed using one-way ANOVA with Tukey's correction.

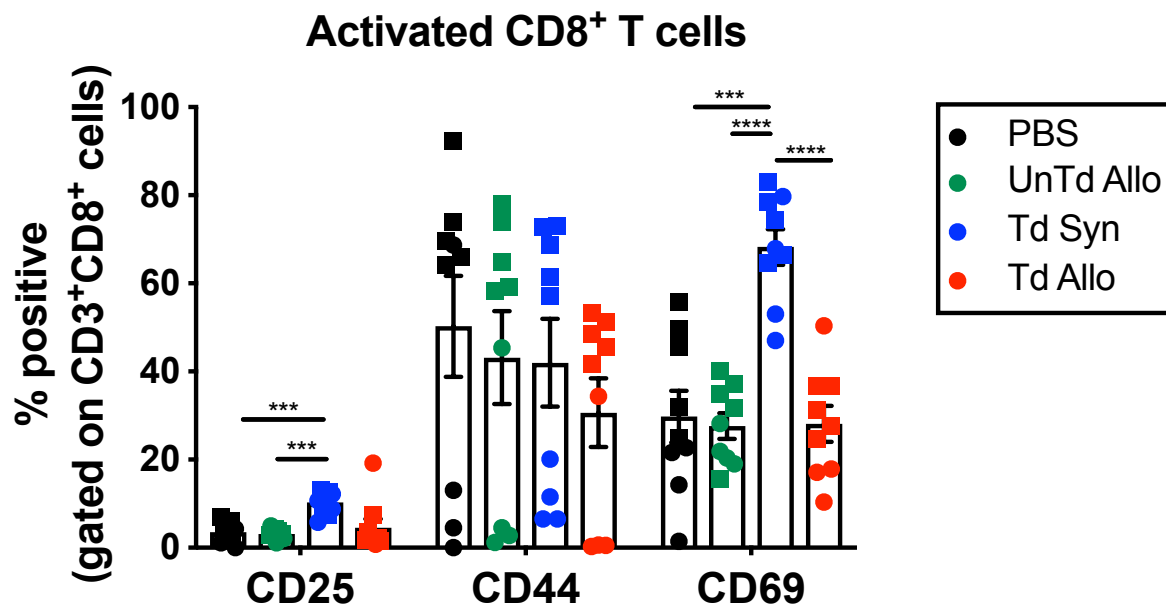


**Figure 45. Frequency of Activated CD8<sup>+</sup> T Cells in the Tumor Seven Days Post-T Cell Treatment.** Seven days post-T cell treatment, B16 A2/K<sup>b</sup> tumors were isolated from mice and cells were analyzed for expression of CD3, CD8, CD25, CD44, and CD69 by flow cytometry. Symbols (circles and squares) represent individual mice from two independent experiments. Cells were gated on live, CD3<sup>+</sup>CD8<sup>+</sup> T cells. Graph shows mean  $\pm$  SEM; statistical analysis performed using one-way ANOVA with Tukey's correction. [\*\*\*P<0.001, \*\*\*\*P<0.0001]

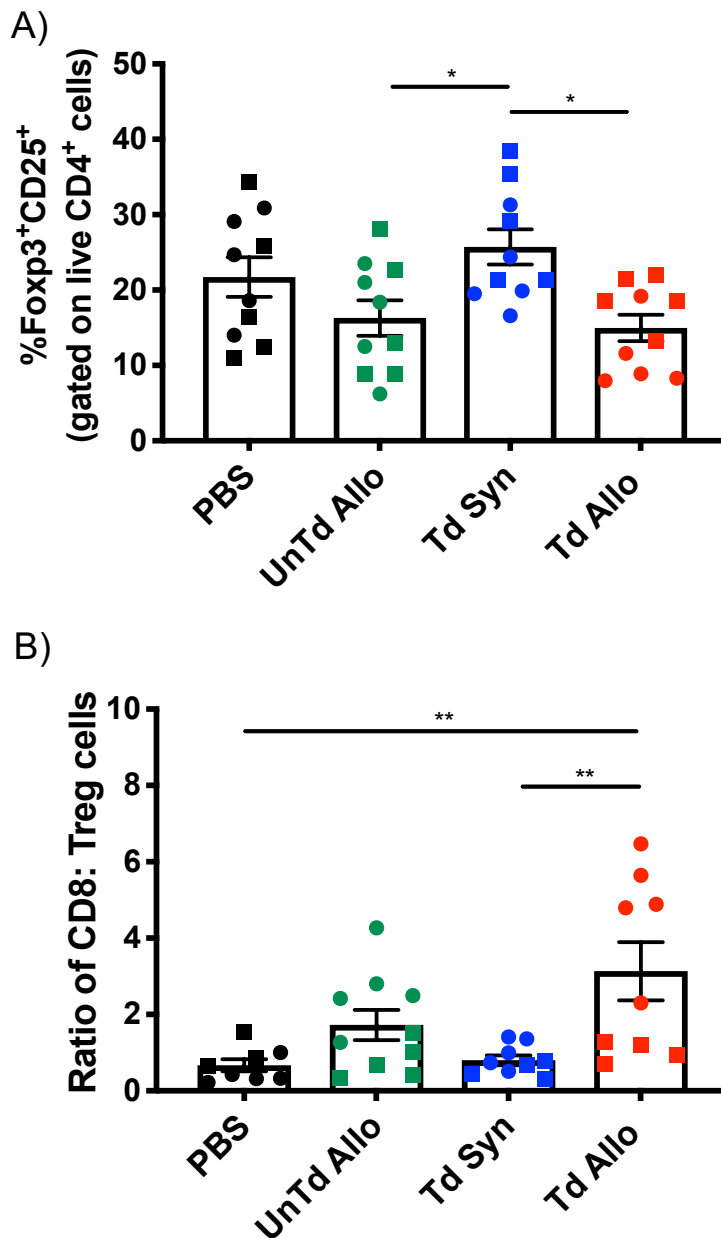


**Figure 46. Regulatory T cells in the Tumor Microenvironment Seven Days Post-T Cell Treatment.** Seven days post-T cell treatment, B16 A2/K<sup>b</sup> tumors were isolated from mice and cells were analyzed for expression of CD3, CD4, CD25, and Foxp3 by flow cytometry. A) Frequency of Foxp3<sup>+</sup>CD25<sup>+</sup> T cells, gated on CD3<sup>+</sup>CD4<sup>+</sup> cells B) Ratio of CD8<sup>+</sup> T cells: Tregs. Symbols (circles and squares) represent individual mice from two independent experiments. Cells were gated on live, CD3<sup>+</sup> CD8<sup>+</sup> T cells. Graph shows mean  $\pm$  SEM; statistical analysis performed using one-way ANOVA with Tukey's correction (\*\*P<0.01, \*\*\*P<0.001, \*\*\*\*P<0.0001).

Furthermore, the tumors treated with TIL 1383I TCR transduced allogeneic T cells had the highest CD8<sup>+</sup> T cells: Treg ratio compared to tumors treated with TIL 1383I TCR transduced syngeneic T cells ( $P=0.0048$ ) and PBS ( $P=0.0038$ ), suggesting enhanced cytotoxic T cell infiltration (Fig 46B). The robust activation of dendritic cells in the tumor and the tumor draining lymph nodes after treatment with TIL 1383I TCR transduced allogeneic T cells (Fig 21-30) suggested the potential to induce anti-tumor T cell immune responses. We next examined the T cells present in the tumor draining lymph nodes seven days following intratumoral T cell treatment, usually when peak T cell responses occur. We did not detect differences in frequency or number of CD4<sup>+</sup> and CD8<sup>+</sup> T cells in the tumor draining lymph nodes in any of the treatment groups (Fig 47).

We further investigated the presence of CD4<sup>+</sup> and CD8<sup>+</sup> T cells in the tumor draining lymph nodes seven days post-T cell treatment and assessed expression of the T cell activation molecules, CD44 and CD69. We did not observe a significant difference in the frequency or number of CD44<sup>+</sup> or CD69<sup>+</sup> CD4<sup>+</sup> T cells among T cell treatment groups (Fig 48). However, the frequency of CD44<sup>+</sup> CD8<sup>+</sup> T cells was significantly higher in the tumor draining lymph nodes isolated from TIL 1383I TCR transduced allogeneic T cell-treated mice compared to the tumor draining lymph nodes isolated from mice treated with PBS ( $P<0.0001$ ) and untransduced allogeneic T cells ( $P=0.0469$ ; Fig 49A). Furthermore, the tumor draining lymph nodes isolated from TIL 1383I TCR transduced syngeneic T cell-treated mice also had significantly increased CD44<sup>+</sup>CD8<sup>+</sup> T cells compared to PBS treatment ( $P=0.0045$ ; Fig 49A). The tumor draining lymph nodes of untransduced allogeneic T cell-treated mice also had increased frequencies of CD44<sup>+</sup>CD8<sup>+</sup> T cells compared to PBS-treated mice ( $P=0.042$ ). We

additionally assessed CD69 expression on T cells isolated from the tumor draining lymph nodes of mice seven days post-intratumoral T cell treatment. We observed an increased frequency of CD69<sup>+</sup> CD8<sup>+</sup> T cells following treatment with TIL 1383I TCR transduced allogeneic T cell treatment compared to PBS (P=0.002) and TIL 1383I TCR transduced syngeneic T cell treatment (P=0.0178; Fig 46B). Untransduced allogeneic T cell treatment promoted CD69<sup>+</sup> CD8<sup>+</sup> T cells compared to PBS treatment (P=0.0171). These results indicated that intratumoral treatment with TIL 1383I TCR transduced allogeneic T cells promoted the activation of endogenous CD8<sup>+</sup> T cells in the tumor draining lymph nodes.

CXCR3 is highly expressed on activated and memory T cells<sup>486</sup>. We observed increased CXCR3<sup>+</sup>CD4<sup>+</sup> T cells in the tumor draining lymph nodes from mice treated with TIL 1383I TCR transduced allogeneic T cells compared to the other T cell treatment groups (Fig 50). Additionally, CXCR3<sup>+</sup>CD8<sup>+</sup> T cells were present at an increased frequency in the tumor draining lymph nodes of TIL 1383I TCR transduced allogeneic T cell-treated mice compared to the tumor draining lymph nodes of PBS-treated mice. These results suggested that TIL 1383I TCR transduced allogeneic T cell intratumoral treatment promotes the activation of endogenous CD8<sup>+</sup> T cells in the tumor draining lymph nodes of tumor-bearing mice seven days post-T cell treatment.

### **TIL 1383I TCR Transduced Allogeneic T Cell Treatment Generates Endogenous Tumor-Specific T Cells**

Intratumoral delivery of TIL 1383I TCR transduced allogeneic T cells promoted the expression of DC maturation markers CD80 and CD86 and T cell activation molecules in the tumor microenvironment two days post-intratumoral T cell treatment.



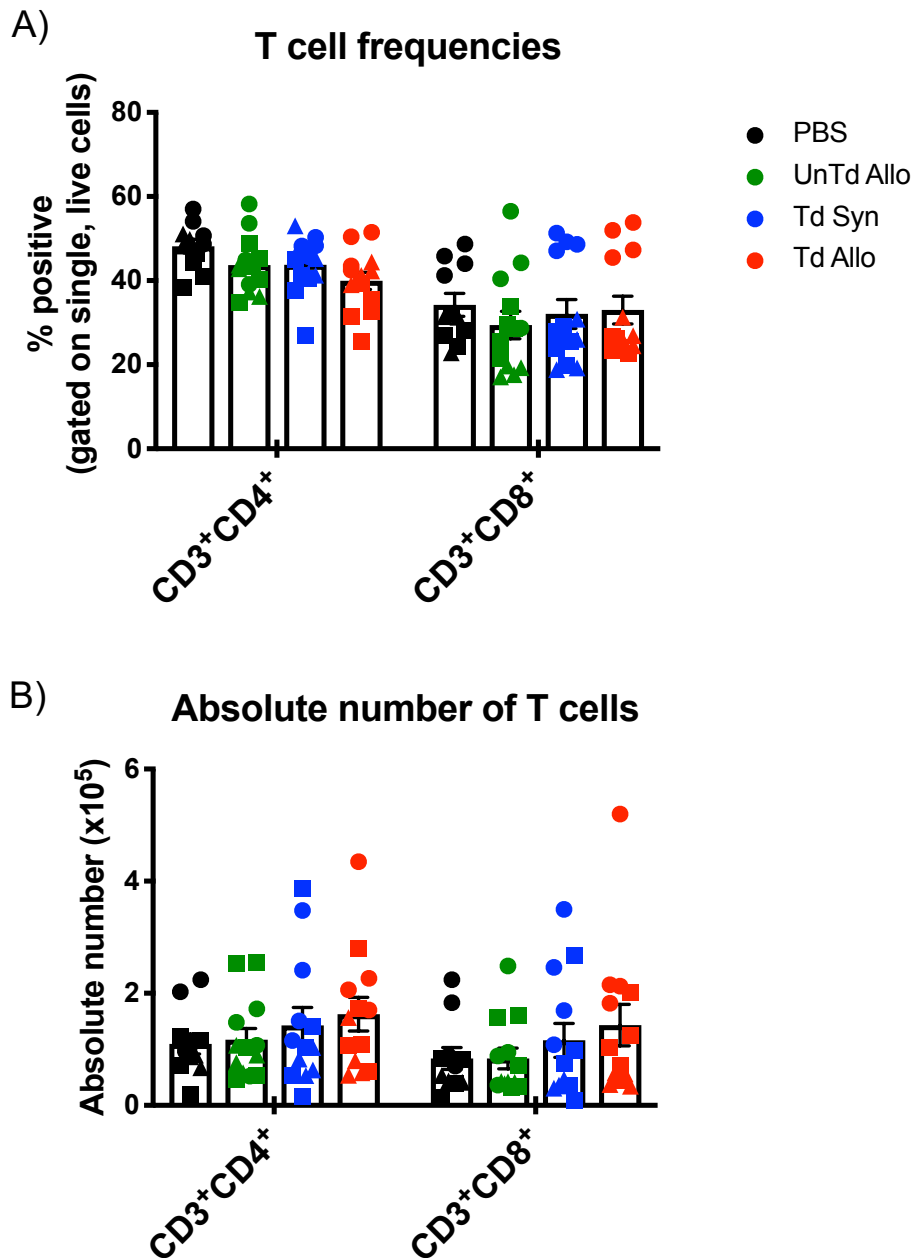


**Figure 47. Frequency and Number of CD4<sup>+</sup> and CD8<sup>+</sup> T Cells in the Tumor Draining Lymph Nodes Seven Days Post-T Cell Treatment.** Seven days post-T cell treatment, tumor draining lymph nodes from B16 A2/K<sup>b</sup> tumor-bearing mice were isolated and cells were examined for expression of CD3, CD4, and CD8 by flow cytometry. A) Frequency and B) Total number of CD4<sup>+</sup> and CD8<sup>+</sup> T cells. Cells were gated on live, single, CD3<sup>+</sup> T cells. Symbols (circles and squares) represent individual mice from two independent experiments. Graph shows mean  $\pm$  SEM; No statistically significant differences were observed using one-way ANOVA with Tukey's correction.

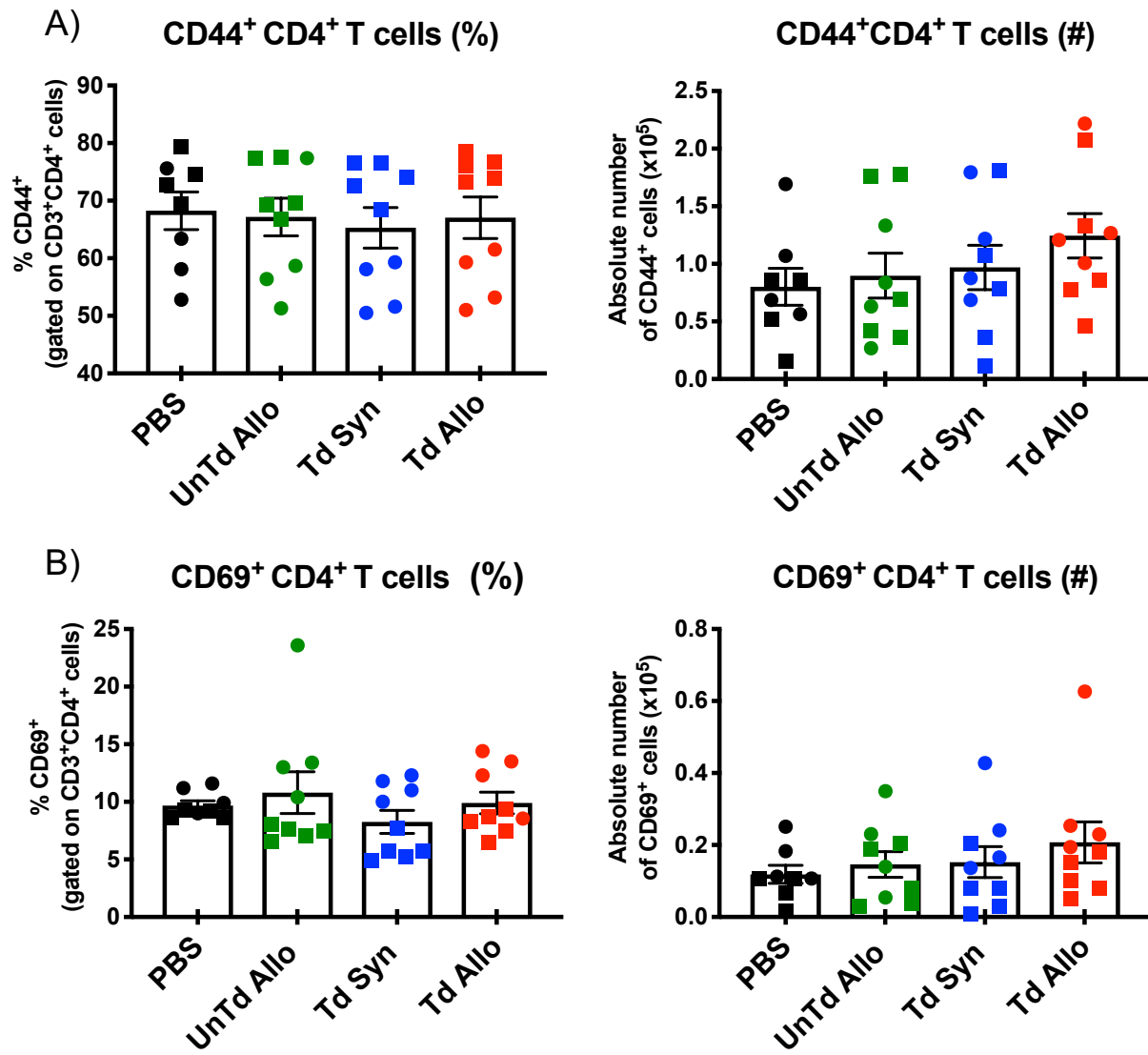


**Figure 48. Activated CD4<sup>+</sup> T Cells in the Tumor Draining Lymph Nodes Seven Days Post-T Cell Treatment.** Seven days post-T cell treatment, tumor draining lymph nodes were isolated from B16 A2/K<sup>b</sup> tumor-bearing mice and cells were examined for expression of CD3, CD4, CD44, and CD69 by flow cytometry. A) Frequency (left panel) and number (right panel) of CD44<sup>+</sup>CD4<sup>+</sup> T cells. B) Frequency (left panel) and number (right panel) of CD69<sup>+</sup>CD4<sup>+</sup> T cells. Cells were gated on single, live, CD3<sup>+</sup> T cells. Symbols (circles and squares) represent individual mice from two independent experiments with 4-5 mice/group. Graph shows mean  $\pm$  SEM; No statistically significant differences were observed using one-way ANOVA with Tukey's correction.

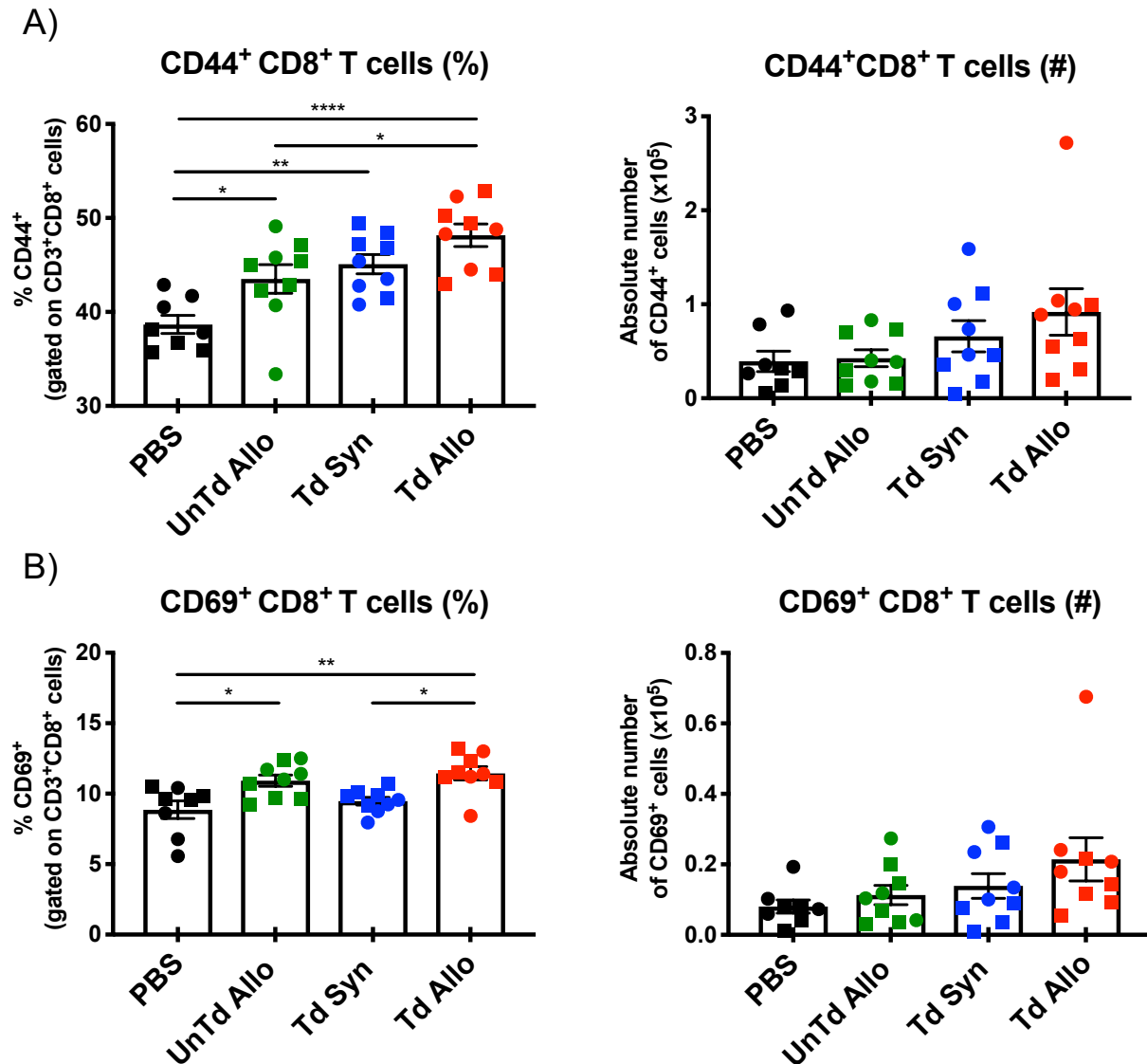


**Figure 49. Treatment with TIL 1383I TCR Transduced Allogeneic T Cells Increases the Frequency and Number of Activated CD8<sup>+</sup> T Cells in the Tumor Draining Lymph Nodes Seven Days Post-T Cell Treatment.** Seven days post-T cell treatment, tumor draining lymph nodes were isolated from B16 A2/K<sup>b</sup> tumor-bearing mice and cells were examined for expression of CD3, CD4, CD8, CD44, and CD69 by flow cytometry. A) Frequency (left panel) and number (right panel) of CD44<sup>+</sup>CD8<sup>+</sup> T cells. B) Frequency (left panel) and number (right panel) of CD69<sup>+</sup>CD8<sup>+</sup> T cells. Cells were gated on single, live, CD3<sup>+</sup> T cells. Symbols (circles and squares) represent individual mice from two independent experiments with 4-5 mice/group. Graph shows mean  $\pm$  SEM; statistical analysis using one-way ANOVA with Tukey's correction (\* $P < 0.05$ , \*\* $P < 0.01$ , \*\*\*\* $P < 0.0001$ ).

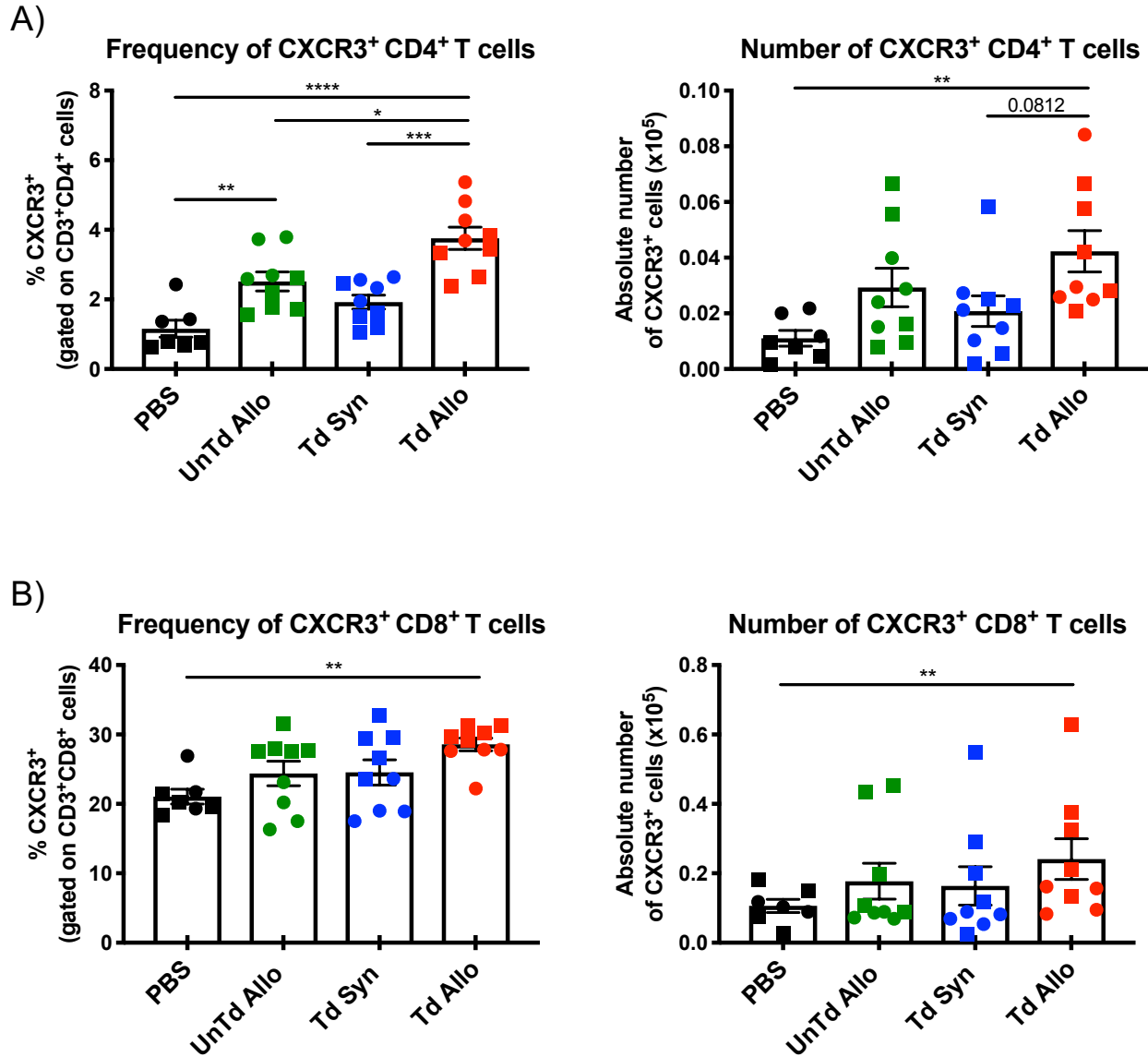


**Figure 50. Treatment with TIL 1383I TCR Transduced Allogeneic T Cells Leads to CXCR3<sup>+</sup> T Cells in the Tumor Draining Lymph Nodes Seven Days Post-T Cell Treatment.** Seven days post-T cell treatment, tumor draining lymph nodes were isolated from B16 A2/K<sup>b</sup> tumor-bearing mice and cells were examined for expression of CD3, CD4, CD8 and CXCR3 by flow cytometry. A) Frequency (left panel) and number (right panel) of CXCR3<sup>+</sup>CD4<sup>+</sup> T cells. B) Frequency (left panel) and number (right panel) of CXCR3<sup>+</sup>CD8<sup>+</sup> T cells. Cells were gated on single, live, CD3<sup>+</sup> T cells. Symbols (circles and squares) represent individual mice from two independent experiments with 4-5 mice/group. Graph shows mean  $\pm$  SEM; statistical analysis by one-way ANOVA with Tukey's correction (\*P<0.05, \*\*P<0.01, \*\*\*P<0.001, \*\*\*\*P<0.0001).

We also observed increased frequencies of CD205<sup>+</sup> and CD103<sup>+</sup> cross-presenting DC subsets in the tumors treated with TIL 1383I TCR transduced T cells (Fig 23-24).

Furthermore, we detected CD8 $\alpha$ <sup>+</sup> DC, CD205<sup>+</sup> DC, and CD103<sup>+</sup> DC cross-presenting subsets at an increased frequency and number in the tumor draining lymph nodes of mice treated with TIL 1383I TCR transduced allogeneic T cells (Fig 28-30). The accumulation of cross-presenting DCs and activated T cells in the tumor draining lymph nodes suggested that TIL 1383I TCR transduced allogeneic T cell treatment could promote antigen cross-presentation by DCs to induce endogenous tumor-specific T cell responses. We used two established methods to detect antigen-specific T cell responses *in vitro* and *in vivo*. We first performed *in vitro* IFN- $\gamma$  ELISPOT assays to determine if we could identify B16-reactive cells in treated mice. The second method, an *in vivo* CTL assay, determined if antigen-specific T cells were capable of lysing appropriate targets.

### **Detection of Tumor-Specific Cells by IFN- $\gamma$ ELISPOT Assay**

Ten days after intratumoral T cell treatment, we harvested the tumor draining lymph nodes from B16 A2/K<sup>b</sup> tumor-bearing mice and co-cultured cells with B16 and B16 A2/K<sup>b</sup> tumor targets for 18 hours. HLA-A2 transgenic mice can mount MHC class I HLA-A2- or H-2<sup>b</sup>- restricted T cell responses. Because TIL 1383I TCR transduced T cells used for treatment are HLA A2-restricted, we tested T cell reactivity against B16 and B16 A2/K<sup>b</sup> tumor targets, as the presence of H-2<sup>b</sup>-restricted, B16-reactive cells would provide evidence that T cell cross-priming has occurred. The tumor draining lymph nodes from mice treated with TIL 1383I TCR transduced allogeneic T cells had significantly higher frequencies of B16-reactive, IFN- $\gamma$ -producing cells (mean number of

spots:  $105 \pm 29.8$ ) compared to tumor draining lymph nodes isolated from TIL 1383I TCR transduced syngeneic T cell ( $27.62 \pm 9.53$ ;  $P=0.0013$ )- and untransduced allogeneic T cell ( $39.87 \pm 20.7$ ;  $P=0.0099$ )- treated mice (Fig 51). The tumor draining lymph nodes from mice treated with TIL 1383I TCR transduced allogeneic T cells also had a significant frequency of B16 A2/K<sup>b</sup>-reactive, IFN- $\gamma$ -producing cells compared to TIL 1383I TCR transduced syngeneic T cells ( $P=0.0308$ ) and untransduced allogeneic T cells ( $P=0.0099$ ).

To confirm that the observed reactivity of the endogenous immune response was melanoma antigen-specific, we also compared IFN- $\gamma$ -production from host cells co-cultured with the melanoma antigen-negative targets, EL4 and EL4 A2/K<sup>b</sup>. The tumor draining lymph nodes isolated from TIL 1383I TCR transduced allogeneic T cell treated mice had a substantial increase in cells reactive against B16 tumor targets compared to EL4 ( $P<0.0001$ ) and against B16 A2/K<sup>b</sup> compared to EL4 A2/K<sup>b</sup> ( $P<0.0001$ ; Fig 51). In contrast, the tumor draining lymph nodes from TIL 1383I TCR transduced syngeneic T cell- or untransduced allogeneic T cell-treated mice failed to exhibit B16 or B16 A2/K<sup>b</sup> responses above the levels of EL4 and EL4 A2/K<sup>b</sup>. These results indicated that intratumoral treatment with TIL 1383I TCR transduced allogeneic T cells induced endogenous tumor-specific H-2<sup>b</sup>- and human HLA-A2-restricted cells.

We also measured reactivity of cells from the tumor draining lymph nodes against H-2K<sup>b</sup>-restricted TRP-2<sub>180-188</sub> and H-2D<sup>b</sup>-restricted gp100<sub>25-33</sub>- peptide-pulsed RMA/S cells (H-2<sup>b</sup>). We chose TRP-2<sub>180-188</sub> and gp100<sub>25-33</sub> peptides because they are two melanocyte antigens restricted by H-2<sup>b</sup>, which would suggest the induction of cross-primed T cells. Additionally, TRP-2 and gp100 are highly expressed on B16 tumors.

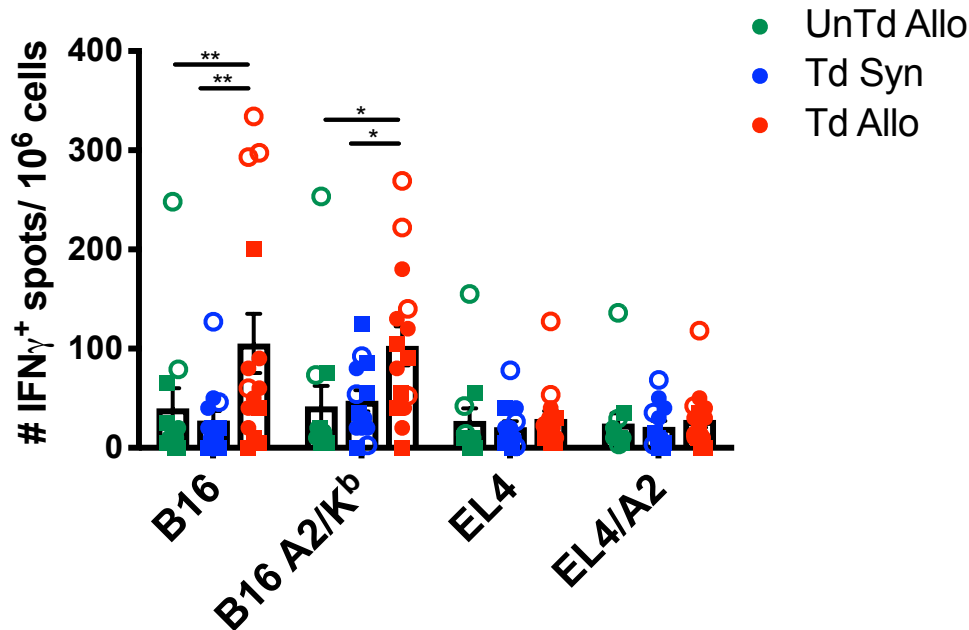


**Figure 51. TIL 1383I TCR Transduced Allogeneic T Cell Treatment Induces Tumor-Specific IFN-γ<sup>+</sup> Cells in the Tumor Draining Lymph Nodes.** Ten days post-T cell treatment, tumor draining lymph nodes were isolated from mice. 100,000 effector cells and 100,000 target cells were co-cultured for 18 hours. Spots were automatically enumerated using an ELISPOT plate reader. Data represent the average of duplicates from individual mice. Symbols (squares and closed and open circles) represent the individual mice from 3 independent experiments. Graph shows mean ± SEM; Statistical analysis using one-way ANOVA with Tukey correction [\* P<0.05, \*\*P<0.01]

To determine if we could detect peptide-specific responses, we co-cultured cells isolated from the tumor draining lymph nodes of treated mice with gp100<sub>25-33</sub>- and TRP-2<sub>180-188</sub>-pulsed RMA/S antigen presenting cells (H-2<sup>b</sup>). We detected a significant frequency of gp100<sub>25-33</sub>-reactive cells from the tumor draining lymph nodes of mice intratumorally treated with TIL 1383I TCR transduced allogeneic T cells (mean number of spots: 144.167 ± 31.5) compared to treatment with TIL 1383I TCR transduced syngeneic T cells (48.93 ± 16.56; P = 0.0034) and compared to treatment with untransduced allogeneic T cells (36.7 ± 21.45; P=0.0011, Fig 52). We also observed a

trending increase in TRP-2<sub>180-188</sub>-specific cells in the tumor draining lymph nodes of TIL 1383I TCR transduced allogeneic T cell treated-mice (mean number of spots:  $82 \pm 23.6$ ) compared to TIL 1383I TCR transduced syngeneic T cell- ( $39.654 \pm 17.34$ ; ns,  $P=0.3052$ ) or untransduced allogeneic T cell- ( $39.71 \pm 22.12$ ; ns,  $P=0.3217$ ) treated mice (Fig 52). These results indicated that treatment with TIL 1383I TCR transduced allogeneic T cells induced H-2<sup>b</sup> and HLA-A2-restricted tumor antigen-specific responses.

We further increased the ability to detect IFN- $\gamma$ - producing cells by re-stimulating splenocytes from mice intratumorally treated with TIL 1383I TCR transduced T cells with irradiated B16 A2/K<sup>b</sup> tumors for five days prior to ELISPOT co-cultures. Re-stimulation of splenocytes yielded higher frequencies of B16 and B16 A2/K<sup>b</sup> tumor-reactive cells, but we generally observed higher non-specific background reactivity as well (Supplemental Fig 102 and 103) These results demonstrated that IFN- $\gamma$ - producing cells can be detected in the tumor draining lymph nodes of mice treated with TIL 1383I TCR transduced allogeneic T cells, both with and without re-stimulation.

We wanted to determine if T cell cross-priming correlated with control B16 A2/K<sup>b</sup> tumor progression. We retrospectively compared the final B16 A2/K<sup>b</sup> tumor area (at day 10 post-T cell treatment when tumor-bearing mice were sacrificed) to the number of IFN- $\gamma$  spots produced in response to B16 and B16 A2/K<sup>b</sup> tumors and TRP-2 and gp100-loaded RMA/S (Fig 53). There appeared to be a trend between the IFN- $\gamma$ - producing cells in the tumor draining lymph nodes and the tumor area at the time of analysis, suggesting that the induction of T cell cross priming might correlate with regression of B16 A2/K<sup>b</sup> tumors



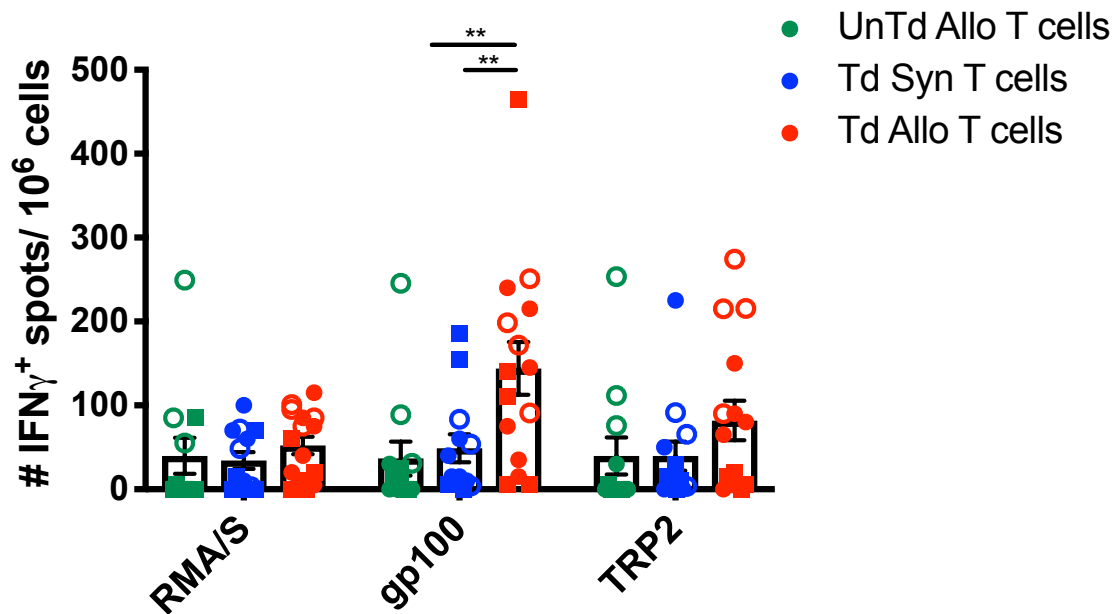


**Figure 52. TIL 1383I TCR Transduced Allogeneic T Cell Treatment Induces gp100-Specific IFN- $\gamma$ <sup>+</sup> Cells in the Tumor Draining Lymph Nodes.** Ten days post-T cell treatment, tumor draining lymph nodes were isolated from mice. RMA/S cells were pulsed with 10  $\mu$ g/mL peptide for 2 hours. 100,000 effector cells and 100,000 target cells were co-cultured for 18 hours. Spots were automatically enumerated using an ELISPOT plate reader. Squares and open and closed circles represent individual mice from 3 independent experiments. Graph shows mean  $\pm$  SEM; Statistical analysis using one- way ANOVA with Tukey correction [\*\*P<0.01]

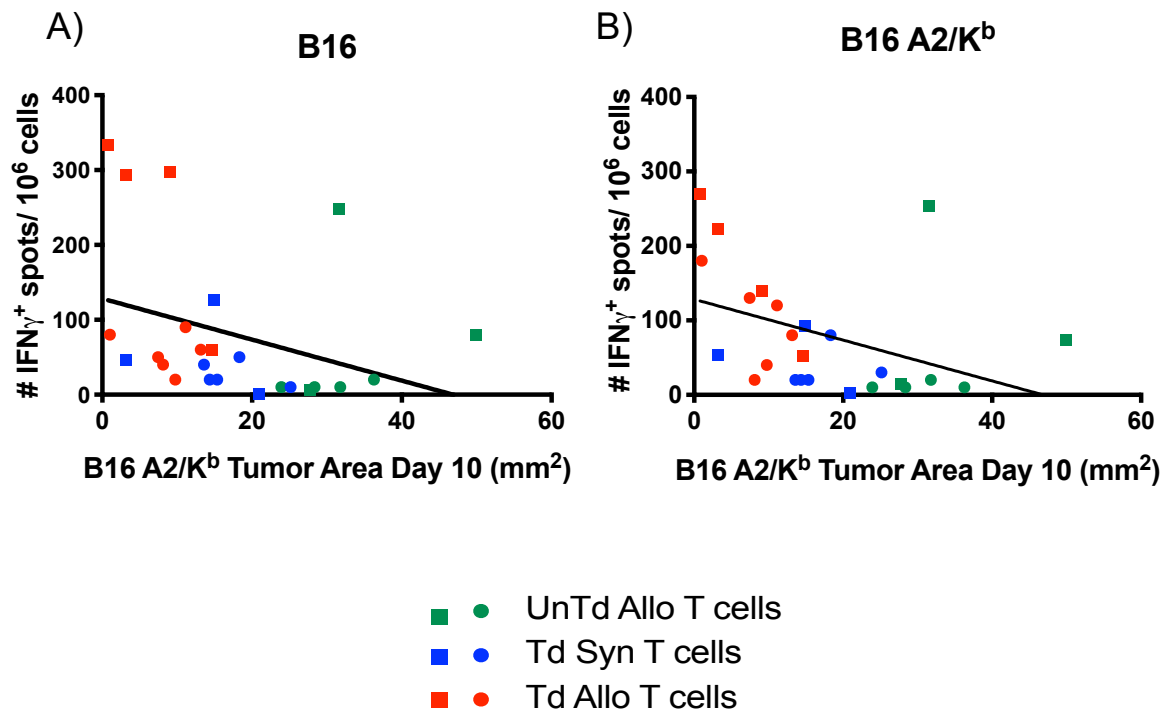


**Figure 53. Correlation Between Final B16 A2/K<sup>b</sup> Tumor Size and Frequency of IFN- $\gamma^+$  Tumor-Specific Cells.** The number of IFN- $\gamma^+$  spots after co-culturing recipient cells with A) B16 and B) B16 A2/K<sup>b</sup> tumors by ELISPOT assays were plotted against the area of B16 A2/K<sup>b</sup> tumors on day 10, when mice were sacrificed for ELISPOT assays. Symbols (Circles and squares) represent individual mice from 2 independent experiments.

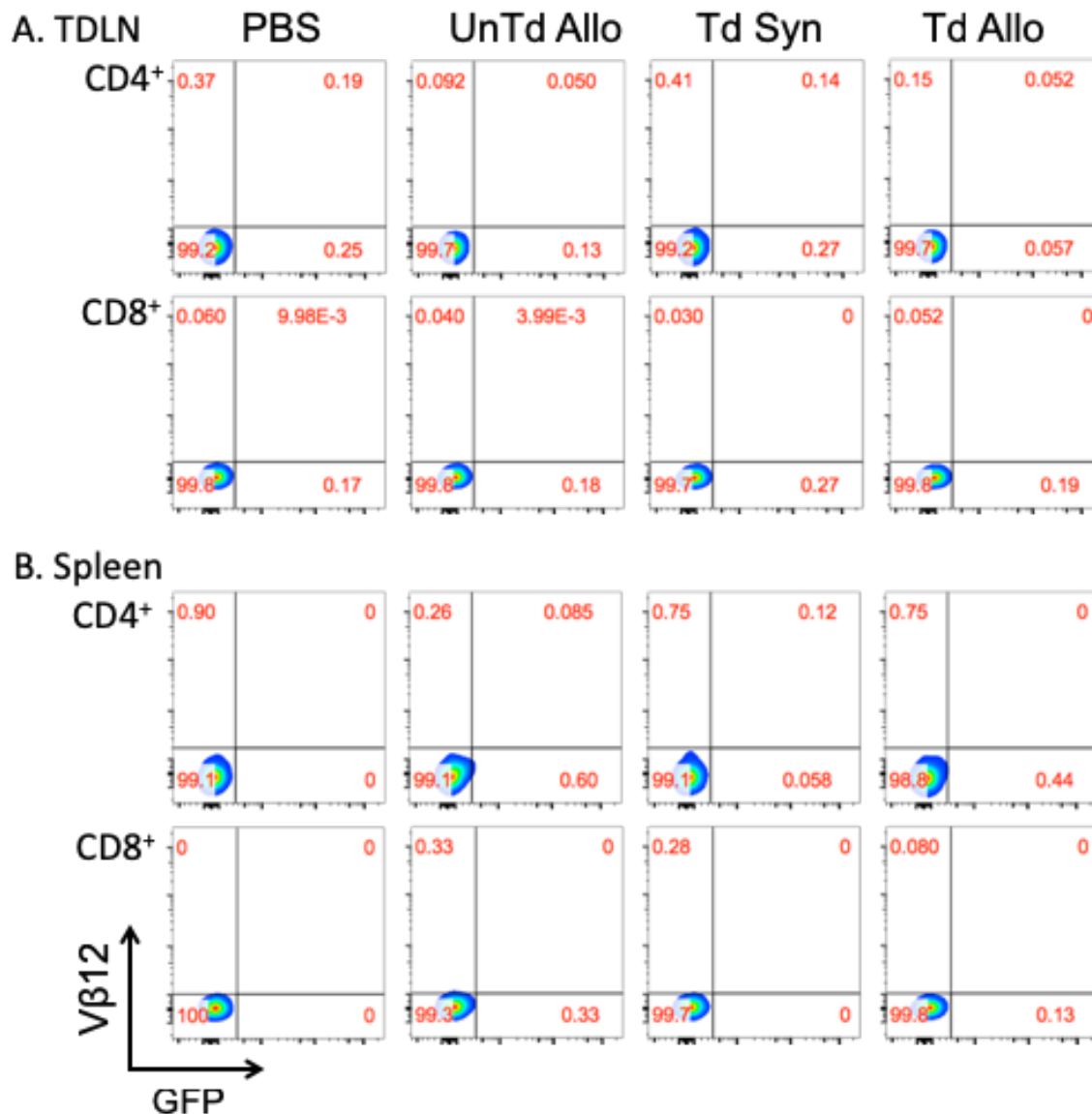


**Figure 54. TIL 1383I TCR Transduced T Cells Are Not Detectable in the Spleens or Tumor Draining Lymph Nodes.** Mice were inoculated with  $2.5 \times 10^5$  B16 A2/K<sup>b</sup> tumor cells and nine days post-T cell treatment, A) tumor draining lymph nodes and B) spleens were isolated and cells were examined for the presence of CD3, CD4, CD8, Vβ12, and GFP by flow cytometry.

We simultaneously examined the spleens and tumor draining lymph nodes of T cell-treated mice for GFP<sup>+</sup> or Vβ12<sup>+</sup> T cells by flow cytometry to confirm that the tumor

specific response was truly recipient-mediated. We were unable to detect any GFP<sup>+</sup> or VB12<sup>+</sup> expression above the background of mice treated with untransduced allogeneic T cells or PBS (Fig 54). This demonstrated that intratumoral treatment with TIL 1383I TCR transduced allogeneic T cells induced cross-priming of recipient cells that produced IFN- $\gamma$  in response to B16 and B16 A2/K<sup>b</sup> tumors, and gp100<sub>25-33</sub>- and TRP-2<sub>180-188</sub>- pulsed RMA/S cells.

### **Detection of Cytolytic Activity by *In Vivo* CTL Assay**

Results from the ELISPOT assays suggested that tumor antigen-specific cells were functional *in vitro*; however, it was still unknown if treatment-induced, endogenous cells were functionally capable of inducing tumor antigen-specific killing *in vivo*. To determine if endogenous cells generated after intratumoral treatment with TIL 1383I TCR transduced T cells could effectively eliminate TRP-2<sub>180-188</sub> and gp100<sub>25-33</sub> peptide-loaded target cells, we utilized a well-established *in vivo* cytotoxicity assay (Fig 55). C57Bl/6 (H-2<sup>b</sup>) splenocytes were used as antigen presenting cells and were pulsed with TRP-2<sub>180-188</sub> and gp100<sub>25-33</sub> peptides and labeled with 5  $\mu$ M (CFSE<sup>mid</sup>) and 10  $\mu$ M (CFSE<sup>hi</sup>) CFSE, respectively. We labeled a group of unpulsed splenocytes with 0.5 $\mu$ M (CFSE<sup>low</sup>) CFSE as a negative control. We retro-orbitally transferred an equal ratio of CFSE-labeled splenocytes into recipient mice that had been treated with TIL 1383I TCR transduced syngeneic T cells, TIL 1383I TCR transduced allogeneic T cells or untransduced allogeneic T cells eight days prior. The following day, we harvested the spleens and assessed the ratios of HLA-2<sup>+</sup>CFSE<sup>+</sup> cells by flow cytometry (Fig 55).

We detected relatively similar ratios of gp100-pulsed CFSE<sup>hi</sup> cells, TRP-2-pulsed CFSE<sup>mid</sup> cells, and unpulsed CFSE<sup>low</sup> cells in untreated mice and untransduced

allogeneic T cell-treated mice, indicating that neither group generated functional, tumor-specific T cells (Fig 56B and C). TIL 1383I TCR transduced syngeneic T cell treatment resulted in a moderate induction of cytotoxic gp100<sub>25-33</sub>-specific T cells (Fig 56C). Interestingly, we did not detect TRP-2<sub>180-188</sub>-specific killing above background (Fig 56B). In contrast, TIL 1383I TCR transduced allogeneic T cell treatment promoted the induction of cytotoxic T cells specific to both gp100<sub>25-33</sub> and TRP2<sub>180-188</sub>-peptides (Fig 56B and C). Intratumoral TIL 1383I TCR transduced allogeneic T cell treatment induced a significant frequency of TRP2<sub>180-188</sub>-specific CTL compared to untreated mice (P=0.0059) and TIL 1383I TCR transduced syngeneic T cell-treated mice (P= 0.0390; Fig 56B).

Treatment with TIL 1383I TCR transduced allogeneic T cell mediated significant gp100<sub>25-33</sub>-specific lysis compared to untransduced allogeneic T cell treatment (P=0.0045) and untreated mice (P=0.0047; Fig 56C). These results were consistent with ELISPOT data demonstrating the ability of TIL 1383I TCR transduced allogeneic T cells to induce gp100<sub>25-33</sub> and TRP-2<sub>180-188</sub>- specific responses, with a more dominant response against gp100<sub>25-33</sub>. It is possible that differences in antigen composition could affect the ability to be cross-presented by DCs. We will explore this idea further in the discussion. Overall, these data confirm our findings that TIL 1383I TCR transduced allogeneic T cell treatment is inducing endogenous tumor-specific cells capable of producing cytokines and killing tumor antigen-loaded targets *in vitro* and *in vivo*.

We observed a small percentage of untreated or untransduced allogeneic T cell-treated mice that generated cytolytic T cells against gp100<sub>25-33</sub>-or TRP-2<sub>180-188</sub>-pulsed

target cells. We postulate that these responses result from acute inflammation induced by the implantable B16 melanoma. The tumor inoculation itself results in a low percentage of dying B16 cells which could stimulate endogenous tumor-specific T cells. These results provided evidence that cross-primed tumor antigen-specific T cells generated after treatment with TIL 1383I TCR transduced allogeneic T cells eliminated gp100<sub>25-33</sub> and TRP-2<sub>180-188</sub> peptide-pulsed cells.

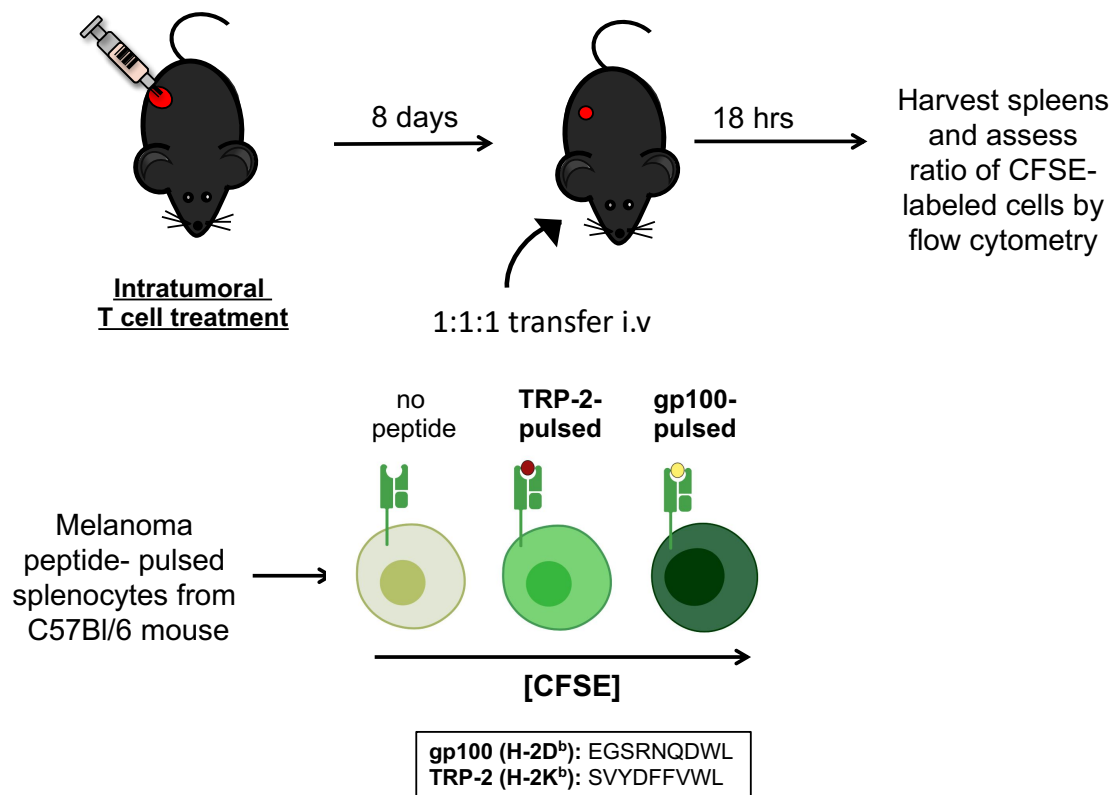


**Figure 55. *In Vivo* CTL Assay Experimental Design.** Eight days post-T cell treatment, mice received transfers of  $3 \times 10^6$  gp100 [ $10 \mu\text{M}$ ],  $3 \times 10^6$  TRP-2 [ $5 \mu\text{M}$ ], and  $3 \times 10^6$  unpulsed [ $0.5 \mu\text{M}$ ] CFSE-labeled C57Bl/6 splenocytes. The following day, spleens were collected and 100,000 total HLA-A2-CFSE<sup>+</sup> cells were collected using flow cytometry.

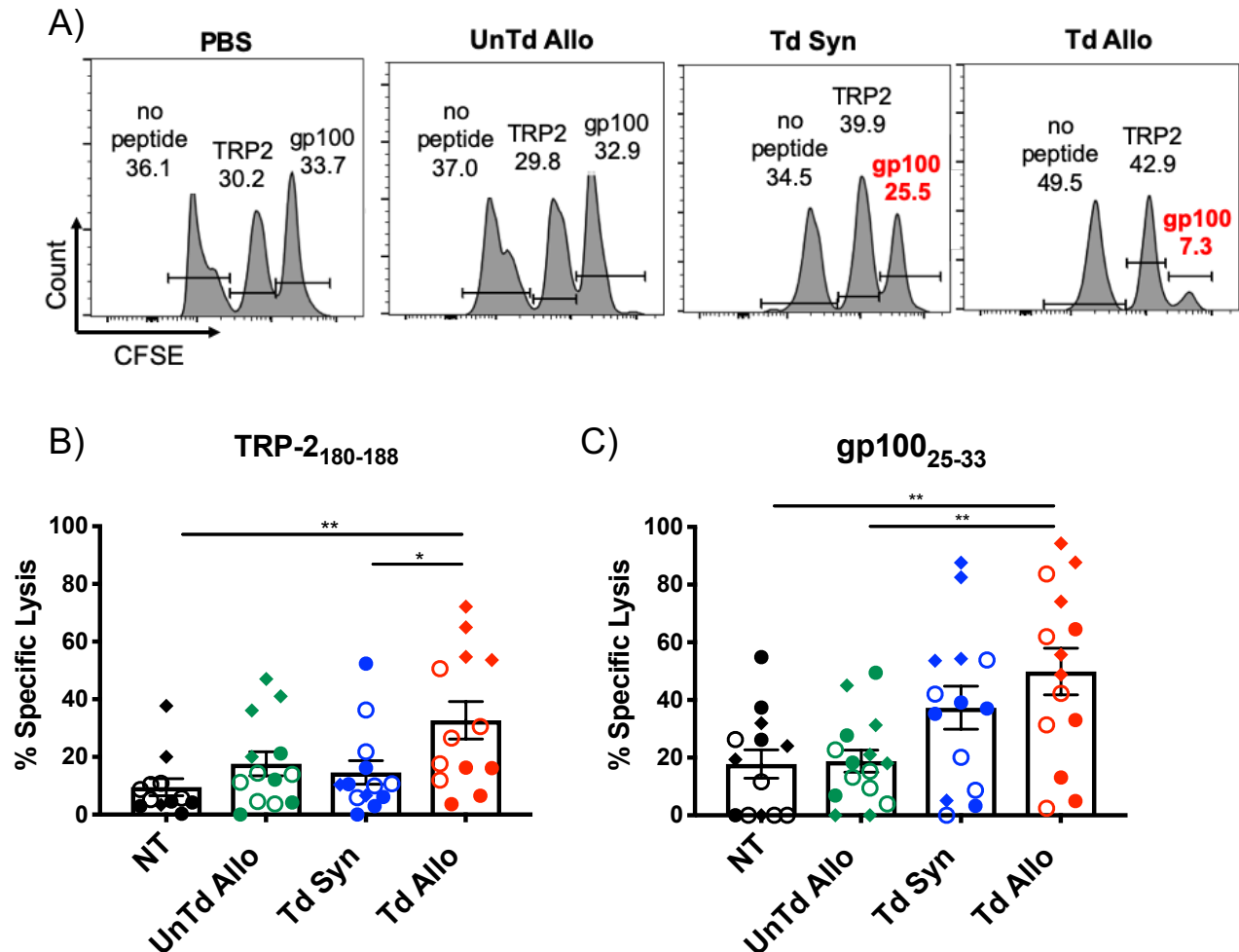


**Figure 56. TIL 1383I TCR Transduced Allogeneic T Cells Induce TRP-2- and gp100- Specific CTL.** Eight days post-T cell treatment, B16 A2/K<sup>b</sup> tumor-bearing mice received  $3 \times 10^6$  gp100 [ $10 \mu\text{M}$ ],  $3 \times 10^6$  TRP-2 [ $5 \mu\text{M}$ ], and  $3 \times 10^6$  unpulsed [ $0.5 \mu\text{M}$ ] CFSE-labeled C57Bl/6 splenocytes i.v. The following day, spleens were isolated from T cell-treated, tumor-bearing HLA-A2 transgenic mice and 100,000 total HLA-A2<sup>-</sup> CFSE<sup>+</sup> cells were collected. A) Representative histograms of collected CFSE labeled cells. B) Specific killing of TRP2-pulsed splenocytes C) Specific killing of gp100-pulsed splenocytes. Symbols (Open and closed circles and diamonds) represents individual mice from 3 independent experiments. Graph shows mean  $\pm$  SEM; Statistical analysis performed using one-way ANOVA with Tukey correction [ $*P < 0.05$ ,  $**P < 0.01$ ]



CHAPTER SIX

INTRATUMORAL TREATMENT WITH TIL 1383I TCR TRANSDUCED  
ALLOGENEIC T CELLS PREVENTS DEVELOPMENT OF  
DISTANT, UNTREATED B16 TUMORS

**Intratumoral Treatment with TIL 1383I TCR Transduced Allogeneic T Cells  
Prevents Development of Untreated, Contralateral B16 Tumors**

The previous experiments demonstrated that intratumoral treatment with TIL 1383I TCR transduced allogeneic T cells induced cross priming of endogenous tumor antigen-specific T cells. Cross-primed T cells produced IFN- $\gamma$  and eliminated tumor antigen-loaded targets *in vitro* and *in vivo*. Generally, cytotoxic T cells are more reactive against peptide-pulsed targets compared to tumors, most likely due to peptide-saturating conditions that result in the supraphysiologic expression of antigen compared to the expression of antigens normal presented on tumor cells. Therefore, we determined if intratumoral treatment with TIL 1383I TCR transduced T cells induced host cells capable of recognizing and eliminating B16 tumor targets. If TIL 1383I TCR transduced allogeneic T cell treatment induced systemic cross-primed T cells capable of recognizing B16 tumor cells, then we would expect these endogenous T cells to prevent the development of B16 tumors that were inoculated on the contralateral flank of mice with pre-existing treated B16 A2/K<sup>b</sup> tumors. To test this hypothesis, we first treated B16 A2/K<sup>b</sup> tumor-bearing mice with TIL 1383I TCR transduced T cells and seven days later inoculated the same mice on the contralateral flank with  $1 \times 10^5$  B16 tumor cells (Fig 57).

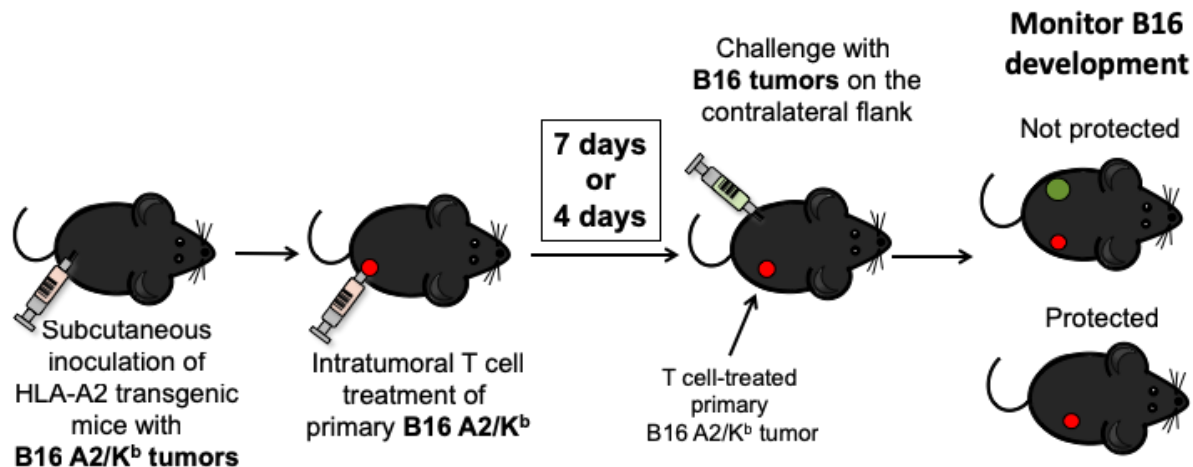


**Figure 57. Experimental Design to Determine if Intratumoral Treatment with TIL 1383I TCR Transduced Allogeneic T Cells Induces Endogenous T Cells Capable of Preventing Development of Distant, Contralateral B16 Tumors.** Primary B16 A2/K<sup>b</sup> tumors, implanted on the right flank of mice, were treated with TIL 1383I TCR transduced T cells. Seven or four days later, mice were inoculated with  $1 \times 10^5$  B16 tumor cells on the left, contralateral flank. Mice were monitored for survival and development of B16 tumors.

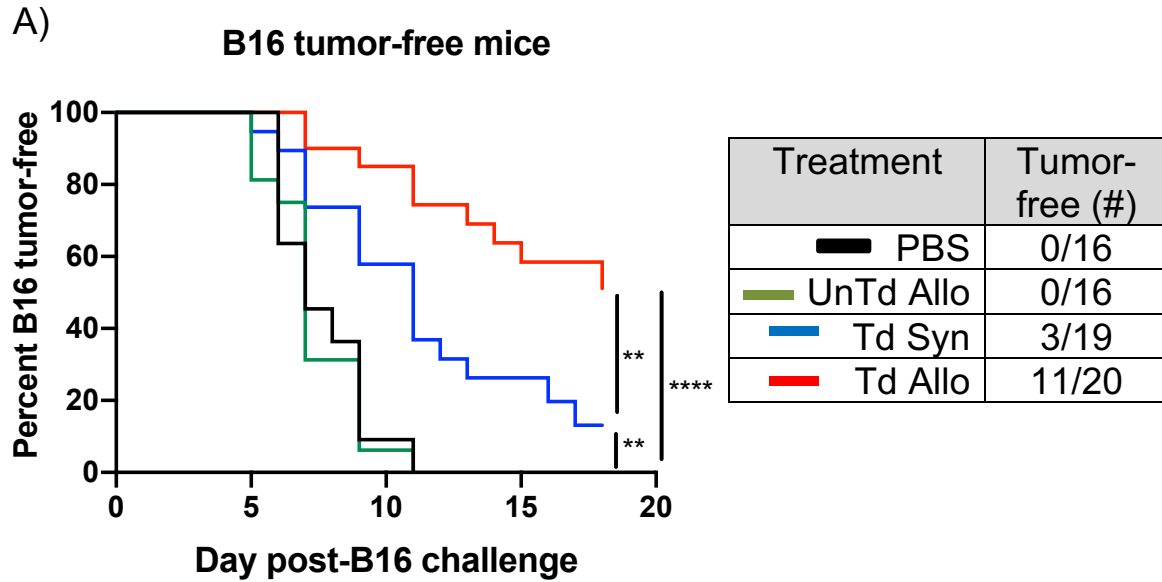
Mice were monitored for the development of contralateral B16 tumors and survival.

B16-inoculated mice without primary B16 A2/K<sup>b</sup> tumors all developed B16 tumors within seven days of challenge (Fig 58, purple line). Treating B16 A2/K<sup>b</sup> primary tumors with saline (black line) or untransduced allogeneic T cells (green line) failed to induce protection and all mice developed B16 tumors within 7-11 days following B16 inoculation ( $P=0.8037$ , Fig 58). TIL 1383I TCR transduced syngeneic T cell treatment (blue line) prevented the development of B16 in approximately 20% of mice ( $P=0.0027$  vs. PBS;  $P=0.0021$  vs untransduced allogeneic T cells, Fig 58). However, treating primary B16 A2/K<sup>b</sup> tumors with TIL 1383I TCR transduced allogeneic T cells (red line) resulted in protection against B16 tumor development in approximately 50% of TIL 1383I TCR transduced allogeneic T cell-treated mice ( $P=0.0049$  vs. TIL 1383I TCR

transduced syngeneic T cells and  $P < 0.0001$  vs. PBS and untransduced allogeneic T cell-treated mice). This supported our previous findings that TIL 1383I TCR transduced allogeneic T cell treatment promoted the induction of T cell cross-priming to promote systemic, anti-tumor T cell responses to protect against distant, untreated tumors.

Interestingly, we also observed the development of vitiligo in one mouse that received intratumoral treatment of the primary B16 A2/K<sup>b</sup> tumor with TIL 1383I TCR transduced allogeneic T cells and was protected from developing the B16 tumor on the contralateral flank (Fig 59). The vitiligo developed at the site of the primary tumor. In some melanoma patients receiving immunotherapy, the development of vitiligo can indicate an active T cell response directed against melanoma differentiation antigens and can occasionally correlate positively with the induction of a clinical responses<sup>1</sup>. For example, in our phase I clinical trial treating metastatic melanoma patients with autologous TIL 1383I TCR transduced T cells, one of the patients achieving a complete response also developed widespread vitiligo. Together, these observations supported our hypothesis that intratumoral treatment of primary B16 A2/K<sup>b</sup> tumors with TIL 1383I TCR transduced allogeneic T cells induces systemic endogenous, tumor-specific T cells with the capacity to prevent the development of B16 tumors inoculated on the contralateral flank.

Intratumoral treatment of B16 A2/K<sup>b</sup> tumor-bearing mice with TIL 1383I TCR transduced allogeneic T cells considerably extended survival (median survival: 26 days) compared to intratumoral treatment with TIL 1383I TCR transduced syngeneic T cells (median survival: 21 days;  $P = 0.001$ ), untransduced allogeneic T cells (median survival: 15.5 days;  $P < 0.0001$ ) and PBS (median survival: 14 days;  $P < 0.0001$ , Fig 60).



B)

Log Rank (Mantel-Cox)			
PBS	UnTd Allo	0.8037	ns
PBS	Td Syn	0.0027	**
PBS	Td Allo	<0.0001	****
UnTd Allo	Td Syn	0.0021	**
UnTd Allo	Td Allo	<0.0001	****
Td Allo	Td Syn	0.0049	**

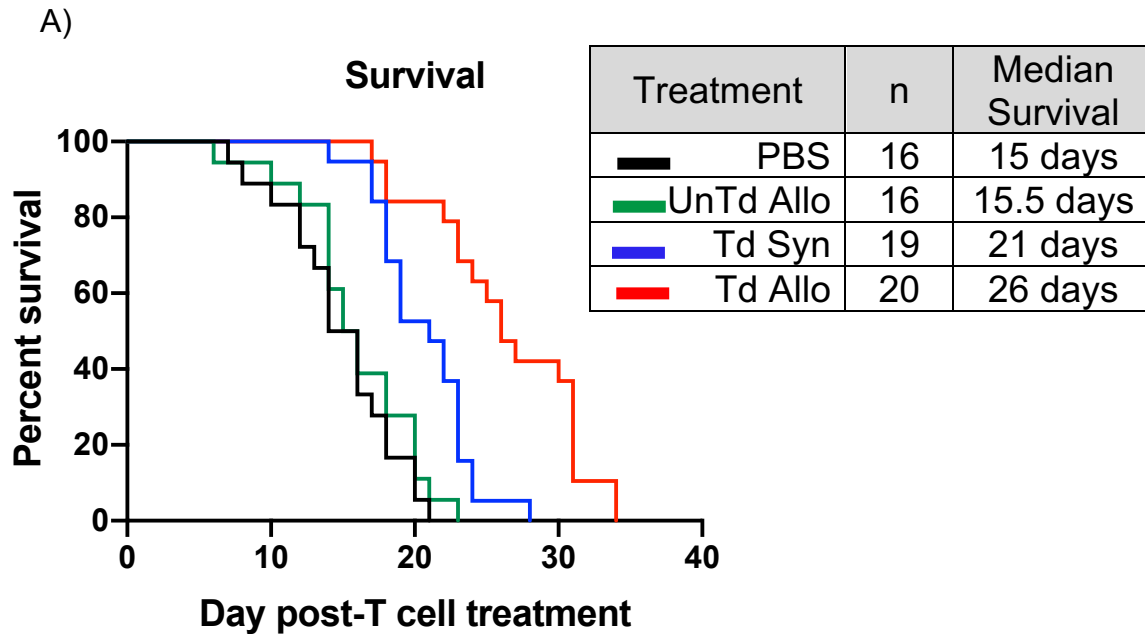
**Figure 58. TIL 1383I TCR Transduced Allogeneic T Cell Treatment of Primary B16 A2/K<sup>b</sup> Primary Tumors Prevents Development of B16 Tumors Inoculated on the Contralateral Flank.** Primary B16 A2/K<sup>b</sup> tumors, implanted on the right flank of mice, were treated with TIL 1383I TCR transduced T cells. Seven days later, mice were inoculated with  $1.0 \times 10^5$  B16 tumor cells on the left, contralateral flank. Mice were monitored for the development of B16 tumors. A) Percentage of B16 tumor-free mice. B) Statistical analysis using the Log Rank test (\* $P < 0.05$ , \*\*\* $P < 0.001$ ) Data compiled from four independent experiments with 4-5 mice/group.



**Vitiligo near the primary  
B16 A2/K<sup>b</sup>  
tumor treated with  
Td Allo T cells**

**Figure 59. Development of Vitiligo in a Mouse with a TIL 1383I TCR Transduced Allogeneic T Cell-Treated Primary B16 A2/K<sup>b</sup> Tumor That Was Protected from B16 Tumor Development.** Primary B16 A2/K<sup>b</sup> tumors, implanted on the right flank of mice, were treated with TIL 1383I TCR transduced T cells. Seven days later mice were inoculated with  $1 \times 10^5$  B16 tumor cells on the left, contralateral flank. Mice were monitored for development of B16 tumors

Generally, mice succumbed to B16 A2/K<sup>b</sup> tumor burden, and not secondary B16 tumors. In some cases, B16 A2/K<sup>b</sup> tumor-bearing mice treated with PBS or untransduced allogeneic T cells succumbed to primary B16 A2/K<sup>b</sup> tumors before we could visualize B16 development. To attempt to address this issue, we performed a small-scale pilot experiment and shortened the time frame between B16 A2/K<sup>b</sup> intratumoral treatment and B16 tumor challenge. Instead of challenging with B16 seven days after intratumoral treatment, we challenged with B16 four days after intratumoral treatment with the anticipation that untreated and untransduced allogeneic T cell-treated mice would survive long enough post-B16 A2/K<sup>b</sup> inoculation to detect the development of B16 tumors (Fig 57).



B)

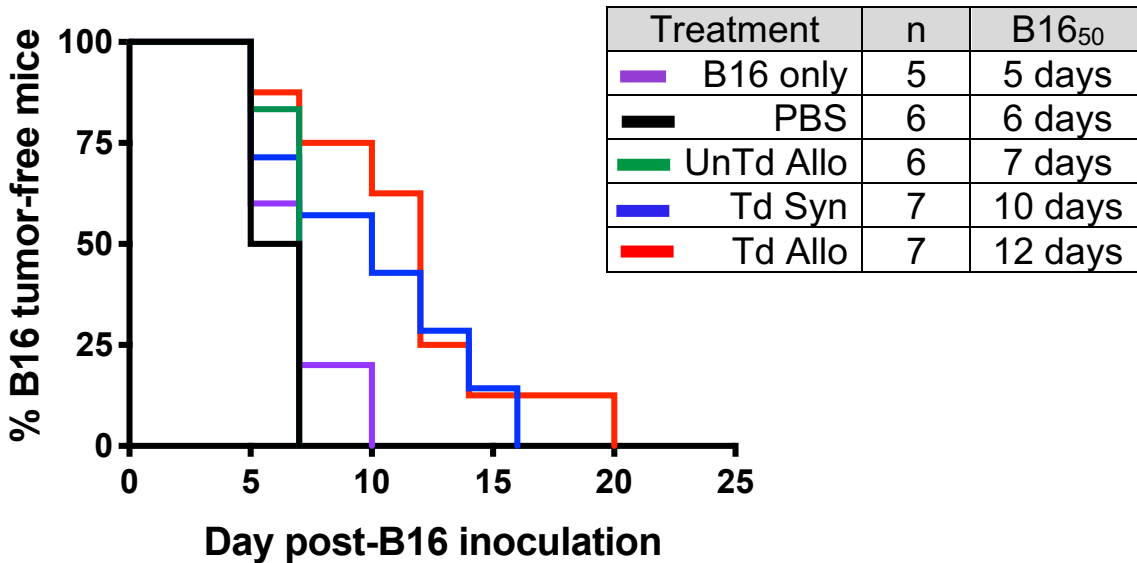
Log Rank (Mantel-Cox)			
PBS	UnTd Allo	0.3470	ns
PBS	Td Syn	0.001	***
PBS	Td Allo	<0.0001	****
UnTd Allo	Td Syn	0.001	***
UnTd Allo	Td Allo	<*0.0001	****
Td Allo	Td Syn	0.0001	***

**Figure 60. Treatment of Primary B16 A2/K<sup>b</sup> Tumors with TIL 1383I TCR Transduced T Cells Improves Survival Following Challenge with B16 on the Contralateral Flank.** Primary B16 A2/K<sup>b</sup> tumors, implanted on the right flank of mice, were treated with TIL 1383I TCR transduced T cells. Seven days later mice were inoculated with  $1.0 \times 10^5$  B16 tumor cells on the left, contralateral flank. Mice were monitored for survival and sacrificed when one tumor or the sum of both tumors reached  $>150 \text{ mm}^2$  or  $>10\%$  body weight. Data compiled from four independent experiments with 4-5 mice/group. Statistical analysis using the Log Rank test (\*\*P<0.001, \*\*\*\*P<0.0001)

We still observed differences among T cell treatment groups in the ability to generate anti-B16 responses; however, we did not see complete protection in mice treated with TIL 1383I TCR transduced syngeneic or allogeneic T cells (Fig 61). Because all mice developed B16 tumors, we could not compare the percentage of B16 tumor-free mice; therefore, we compared the median time for B16 tumors to develop. The median time for B16 tumors to develop in 50% of mice ( $B16_{50}$ ) was 10 days for TIL 1383I TCR transduced syngeneic T cell-treated mice and 12 days for TIL 1383I TCR transduced allogeneic T cell-treated mice ( $P=0.5509$ ). The  $B16_{50}$  for TIL 1383I TCR transduced syngeneic T cell-treated mice was not significantly different from untransduced allogeneic T cell-treated mice ( $B16_{50}$ : 7 days,  $P=0.1546$ ) or untreated mice ( $B16_{50}$ : 5 days,  $P=0.0605$ ; Fig 61). However, the  $B16_{50}$  for TIL 1383I TCR transduced allogeneic T cell-treated mice was significantly shorter compared to untransduced allogeneic T cell-treated mice ( $P=0.018$ ) and untreated mice ( $P=0.0071$ ). The results from this pilot experiment suggested that endogenous T cells induced by TIL 1383I TCR transduced allogeneic T cell treatment might delay the progression of four-day-old B16 tumors, but this experiment would need to be repeated.

One possible explanation for the lack of complete protection against the development of B16 tumors on the contralateral flank is that the absence of cross-primed T cells at the time of B16 challenge permitted three days of B16 tumor formation before the induction of cross-primed T cells observed seven days post-T cell treatment. These results indicated that treatment with TIL 1383I TCR transduced allogeneic T cells is more effective than TIL 1383I TCR transduced T cells in the induction of systemic, endogenous tumor-specific T cells capable of preventing B16 tumor development.

A) **% B16 tumor-free mice**



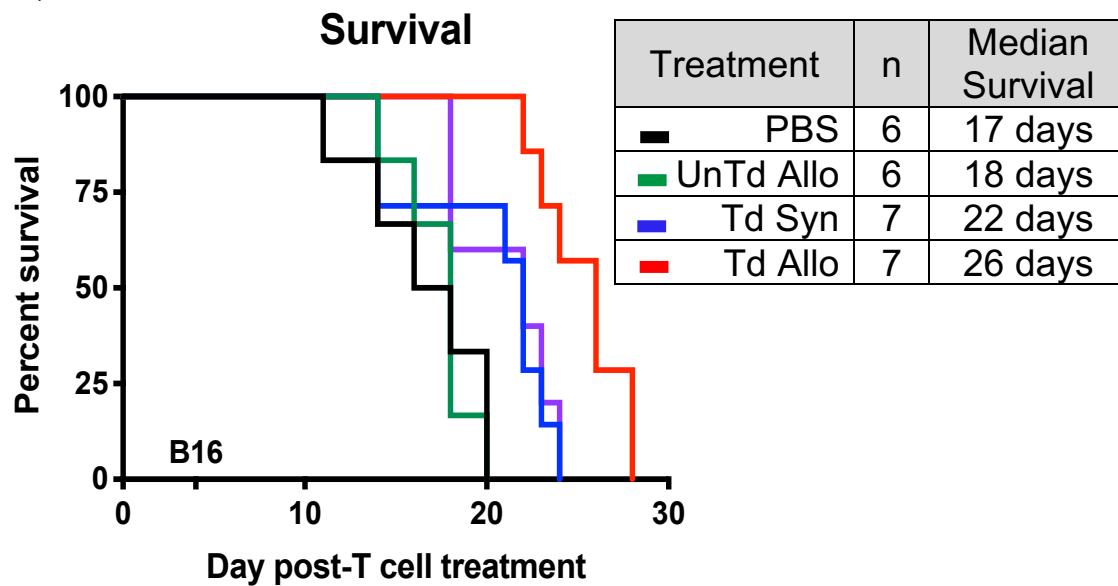
B)

Log Rank (Mantel-Cox)			
PBS	UnTd Allo	0.2410	ns
PBS	Td Syn	0.0605	ns
PBS	Td Allo	0.0071	**
UnTd Allo	Td Syn	0.1546	ns
UnTd Allo	Td Allo	0.0180	*
Td Allo	Td Syn	0.5509	ns

**Figure 61. TIL 1383I TCR Transduced T Cell Treatment of Primary B16 A2/K<sup>b</sup> Tumors Delays the Development of B16 Tumors Inoculated on the Contralateral Flank.** Primary B16 A2/K<sup>b</sup> tumors, implanted on the right flank of mice, were treated with TIL 1383I TCR transduced T cells and four days later were inoculated with  $1.0 \times 10^5$  B16 tumor cells on the left, contralateral flank. Mice were monitored for the development of B16 tumors. Mice were sacrificed when one tumor or the sum of two tumors reached  $>150 \text{ mm}^2$  or  $>10\%$  body weight. B) Statistical analysis performed using the Log Rank test (\* $P < 0.05$ , \*\* $P < 0.01$ ). Data represent one pilot experiment with 5-7 mice/group



A)



B)

Log Rank (Mantel-Cox)			
PBS	UnTd Allo	0.9923	ns
PBS	Td Syn	0.0248	*
PBS	Td Allo	0.0071	**
UnTd Allo	Td Syn	0.0366	*
UnTd Allo	Td Allo	0.0003	***
Td Allo	Td Syn	0.0064	**

**Figure 62. TIL 1383I TCR Transduced T Cell Treatment of Primary B16 A2/K<sup>b</sup> Tumors Improves Survival Following Challenge with B16 Tumors on the Contralateral Flank.** Primary B16 A2/K<sup>b</sup> tumors, implanted on the right flank of mice, were treated with TIL 1383I TCR transduced T cells and four days later were inoculated with  $1.0 \times 10^5$  B16 tumor cells on the left, contralateral flank. Mice were monitored for survival. Mice were sacrificed when one tumor or the sum of both tumors reached  $>150 \text{ mm}^2$  or  $>10\%$  body weight. Data represent one pilot experiment with 5-7 mice/group. Statistical analysis using the Log Rank test (\* $P < 0.05$ , \*\* $P < 0.01$ , \*\*\* $P < 0.001$ )

Intratumoral treatment with TIL 1383I TCR transduced T cells improved the survival of mice despite B16 challenge prior to induction of T cell cross-priming (Fig 62). TIL 1383I TCR transduced syngeneic T cells (median survival: 22 days) significantly prolonged survival compared to untransduced allogeneic T cell-treated mice (median survival: 18 days,  $P=0.0366$ ) and untreated mice (median survival: 17 days,  $P=0.0248$ ). Furthermore, TIL 1383I TCR transduced allogeneic T cell-treated mice had the best overall survival (median survival: 26 days) in comparison to mice treated with TIL 1383I TCR transduced syngeneic ( $P=0.0064$ ) and untransduced allogeneic ( $P=0.0003$ ) T cells, or untreated mice ( $P=0.0003$ ). Together these data indicated that TIL 1383I TCR transduced T cell treatment can induce endogenous T cell cross-priming that can prevent or delay the development of B16 tumors inoculated on the contralateral flank, depending on when cross-priming occurs. Additionally, expressing the tumor-specific TCR on allogeneic donor T cells is more effective than expressing the tumor-specific TCR on syngeneic donor T cells.

### **Adoptive Transfer of Splenocytes from Mice Treated with TIL 1383I TCR Transduced Allogeneic T Cells Suppresses Growth of Established B16 Tumors**

We next tested if adoptively transferring splenocytes from TIL 1383I TCR transduced mice into a second group of untreated mice bearing established B16 tumors could impact on tumor progression (Fig 63). B16 A2/K<sup>b</sup> tumor-bearing mice were first treated with TIL 1383I TCR transduced T cells or controls. Seven days later, spleens were harvested and adoptively transferred into a second group of mice with 7 day old established, palpable B16 tumors. B16 tumors grew rapidly in mice that did not receive T cells or mice treated with untransduced allogeneic T cells (Fig 64A and B).

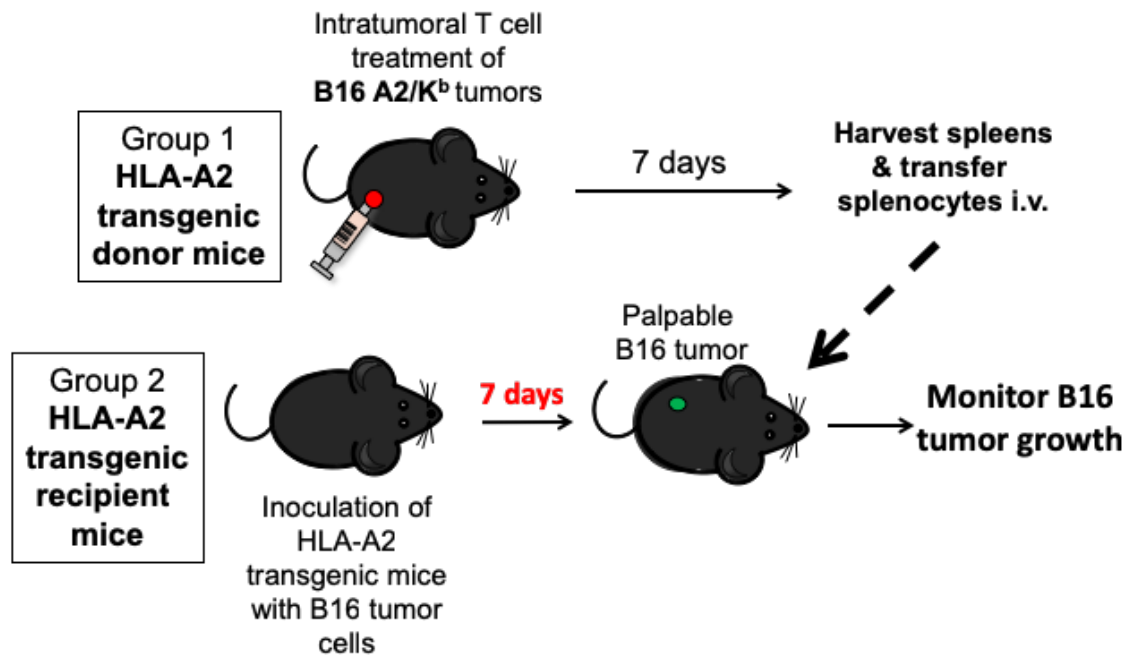


**Figure 63. Experimental Design to Determine If the Transfer of T Cells from TIL 1383I TCR Transduced Allogeneic T Cell-Treated Mice Can Reject Established B16 Tumors.** Seven days after treatment of B16 A2/K<sup>b</sup> tumors with TIL 1383I TCR transduced T cells, spleens were isolated and  $1 \times 10^6$  splenocytes were adoptively transferred i.v. into mice bearing established 7- day old B16 tumors. Mice were monitored for survival and B16 tumor growth.

Unexpectedly, splenocytes transferred from mice treated with TIL 1383I TCR transduced syngeneic T cells did not have a therapeutic effect on B16 tumors (Fig 64C). In contrast, we observed substantial attenuation of B16 tumor growth in mice that received splenocytes isolated from mice bearing B16 A2/K<sup>b</sup> tumors that were treated with TIL 1383I TCR transduced allogeneic T cells (Fig 64D). Linear regression analysis of B16 tumor growth demonstrated that adoptive transfer of TIL1383I TCR transduced allogeneic T cells significantly impaired B16 tumor progression compared to TIL1383I TCR transduced syngeneic T cells ( $P=0.0028$ , Fig 65). In a follow-up experiment, the transfer of splenocytes from mice treated from TIL 1383I TCR transduced allogeneic T

cells also similarly delayed the progression of established B16 tumors (Fig 73-74).

These results suggested that TIL 1383I TCR transduced allogeneic T cells could induce cross-primed T cells capable of transferring anti-tumor immunity to naïve mice with established B16 tumors.

B16 tumor-bearing mice that received splenocytes isolated from mice treated with TIL 1383I TCR transduced syngeneic T cells-treated unexpectedly exhibited rapid B16 growth. This contrasted with previous experiments where the therapeutic efficacy of TIL 1383I TCR transduced syngeneic T cells was usually better than untransduced allogeneic T cells. In parallel to splenocyte transfers, we also tested the B16 and B16 A2/K<sup>b</sup> tumor reactivity of donor splenocytes used for adoptive transfer by IFN- $\gamma$  ELISPOT assay. In support of the results from the adoptive transfer pilot experiment, the splenocytes from TIL 1383I TCR transduced allogeneic T cell-treated mice had a significant frequency of IFN- $\gamma$ <sup>+</sup> cells when co-cultured with B16 tumors *in vitro* compared to splenocytes transferred from untreated mice (P=0.0412), untransduced allogeneic T cell-treated mice (P=0.0035) and TIL 1383I TCR transduced syngeneic T cell-treated mice (P=0.0047; Fig 66). Furthermore, we detected an increased frequency of B16 A2/K<sup>b</sup>-reactive splenocytes following TIL 1383I TCR transduced allogeneic T cell treatment compared to PBS (P=0.0931), untransduced allogeneic T cells (P=0.0773), and TIL 1383I TCR transduced syngeneic T cells (P=0.0171). Splenocytes from mice treated with TIL 1383I TCR transduced allogeneic T cells were significantly more reactive against B16 and B16 A2/K<sup>b</sup> cells compared to EL4 and EL4 A2 cells (P=0.0135 and P= 0.0056, respectively; Fig 66), confirming the tumor antigen-specificity of treatment-induced endogenous T cells found in the tumor draining lymph nodes of mice.

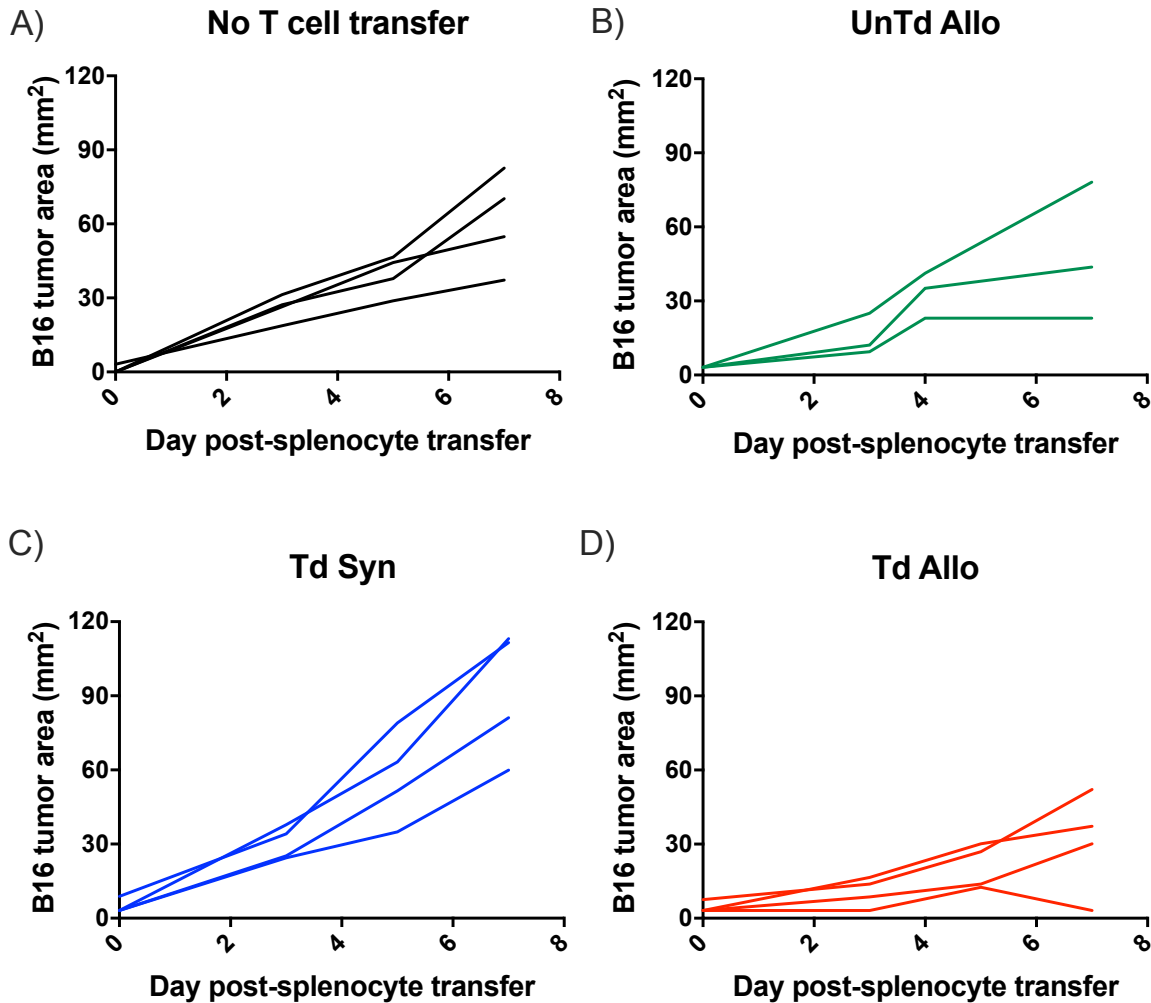


**Figure 64. Adoptive Transfer of Splenocytes from TIL 1383I TCR Transduced Allogeneic T Cell-Treated Mice Suppresses Growth of B16 Tumors in Individual Mice.** B16 tumor cells were inoculated into recipient mice, and seven days later, recipient mice received  $1 \times 10^6$  splenocytes i.v. from donor mice bearing B16 A2/K<sup>b</sup> tumors A) untreated or treated with B) untransduced allogeneic T cells C) TIL 1383I TCR transduced syngeneic T cells D) TIL 1383I TCR transduced allogeneic T cells. B16 tumors were measure 2-3 times per week. Mice were sacrificed when tumors reached  $>150 \text{ mm}^2$  or  $>10\%$  body weight. Data represent one pilot experiment with 3-5 mice/group.

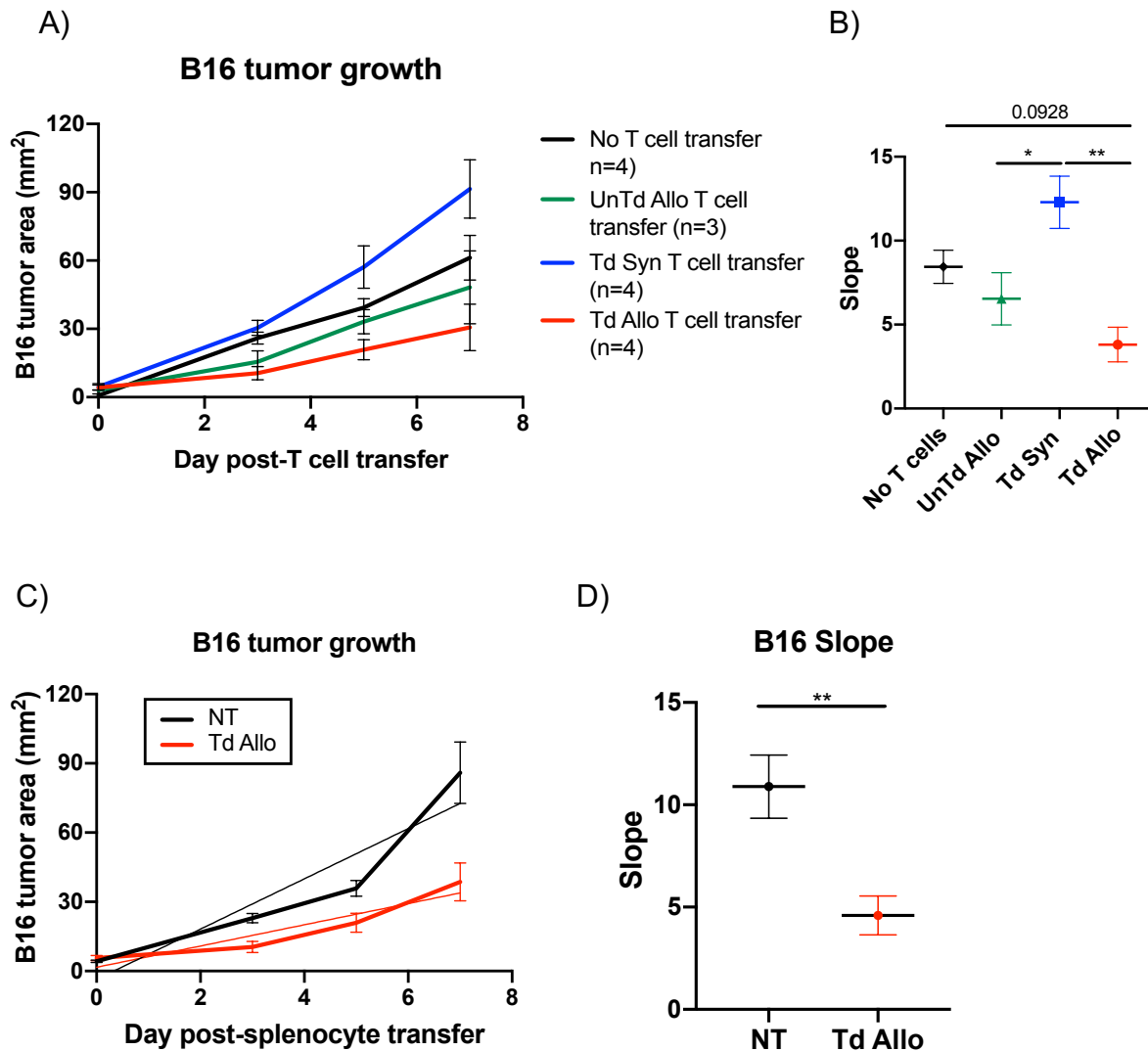


**Figure 65. Delayed B16 Tumor Progression Following Transfer of T Cells from TIL 1383I TCR Transduced Allogeneic T Cell-Treated Mice.** B16 tumor cells were inoculated into recipient mice, and seven days later, recipient mice received  $1 \times 10^6$  splenocytes i.v. from donor mice bearing B16 A2/K<sup>b</sup> tumors treated with untransduced allogeneic T cells, TIL 1383I TCR transduced syngeneic T cells, or TIL 1383I TCR transduced allogeneic T cells. Recipient mice were monitored for survival and B16 tumor growth. Mice were sacrificed when tumors reached  $>150 \text{ mm}^2$  or  $>10\%$  body weight. A) Average B16 tumor growth curves B) Slope determined by linear regression analysis of group averages of B16 tumor growth. Data from A-B represents one pilot experiment with 3-4 mice/group. C) B16 tumor growth after receiving splenocytes from B16 A2/K<sup>b</sup> tumor-bearing mice treated with TIL 1383I TCR transduced allogeneic T cells or untreated mice. D) B16 slope. Data from C-D represents two independent experiments with 7 (NT)- 8 (Td Allo) mice. Graph shows mean  $\pm$  SEM; Statistical analysis using one- way ANOVA with Tukey correction [ $*P<0.05$ ,  $**P<0.01$ ]

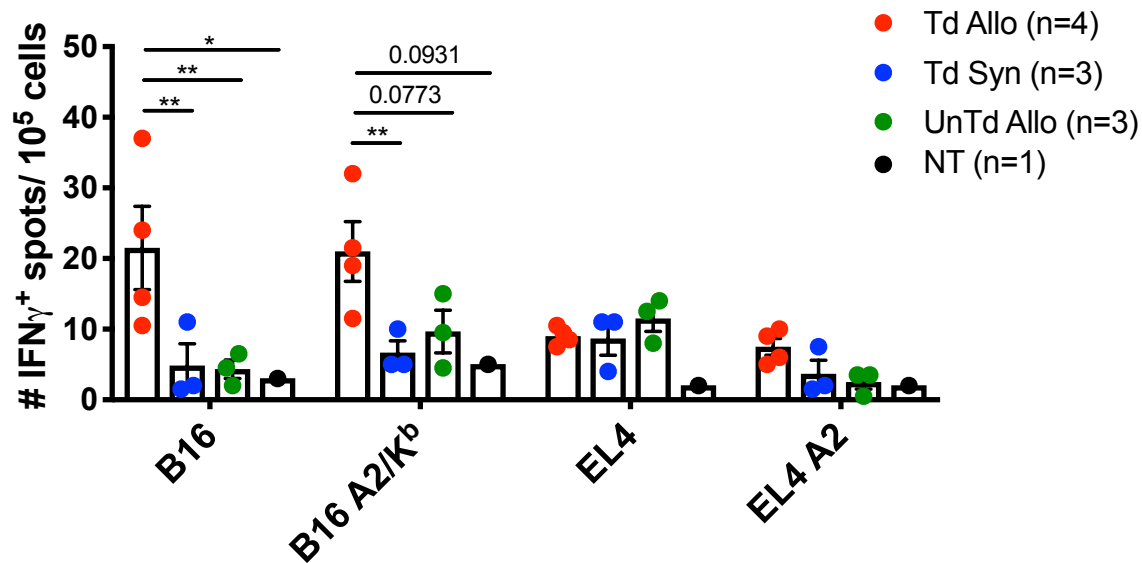


**Figure 66. Tumor Reactivity of Donor Splenocytes Isolated from T Cell-Treated Mice Used for Adoptive Transfer.** Seven days after treating B16 A2/K<sup>b</sup> tumors-bearing donor mice with TIL 1383I TCR transduced T cells, spleens were isolated and 100,000 splenocytes were co-cultured with 100,000 B16, B16 A2/K<sup>b</sup>, EL4, or EL4 A2 tumor targets in an IFN- $\gamma$  ELISPOT assay. Data represent one pilot experiment. Graph shows mean  $\pm$  SEM; Statistical analysis using 2way ANOVA with Tukey correction [\*P<0.05, \*\*P<0.01]

These data further support our hypothesis that intratumoral treatment with TIL 1383I TCR transduced allogeneic T cells induces cross-primed T cells that can transfer anti-tumor immunity to treat establish B16 tumors in naïve mice.

CHAPTER SEVEN

COMBINATION IMMUNOTHERAPIES TO ENHANCE THE EFFICACY OF  
INTRATUMORAL TREATMENT WITH TIL 1383I TCR TRANSDUCED ALLOGENEIC  
T CELLS

**Rationale**

Intratumoral treatment with TIL 1383I TCR transduced allogeneic T cells improved anti-tumor outcomes compared to TIL 1383I TCR transduced syngeneic T cells. Although we observed protection against B16 tumors in approximately 50% of mice treated with TIL 1383I TCR transduced allogeneic T cells, there remained room for improvement. We next sought to improve upon anti-tumor responses using additional immunomodulatory agents. In our studies, we explored three different approaches that have been reported to modulate the tumor microenvironment and enhance T cell responses: 1) Stimulating innate immune responses with the addition of the TLR3 agonist, poly I:C 2) Adding an immune-stimulating gene, LIGHT, to the retroviral vector 3) Activating T cell responses with the addition of checkpoint inhibitors, anti-PD-1 mAb and anti-CTLA-4 mAb.

**Addition of the TLR3 Agonist Poly I:C**

Previous experiments demonstrated that intratumoral treatment with TIL 1383I TCR transduced allogeneic T cells resulted in the induction of specialized antigen cross-presenting DC subsets and the promotion of T cell activation, which culminated in the cross-priming of functional, endogenous tumor antigen-specific T cells that mediated



protective and therapeutic effects. TLR stimulation has been demonstrated to induce DC maturation, antigen presentation, and tumor-specific CTL<sup>487,488,157</sup>. For example, administration of the TLR3 agonist, poly I:C, has been effective at inducing anti-tumor responses in pre-clinical mouse studies and one pilot trial with two cancer patients<sup>130,137,142</sup>. There have been additional reports demonstrating that poly I:C can be effective at inducing immune responses against B16 tumors<sup>489</sup>. Therefore, we first performed a series of small-scale pilot experiments to test if combination therapy with poly I:C and TIL 1383I TCR transduced T cells could further suppress B16 A2/K<sup>b</sup> tumor growth and enhance cross-priming of T cells.

We intratumorally treated B16 A2/K<sup>b</sup> tumors with TIL 1383I TCR transduced syngeneic T cells, TIL 1383I TCR transduced allogeneic T cells or untransduced allogeneic T cells and the following day, mice received 40 µg of poly I:C or saline intratumorally (Fig 67). We measured B16 A2/K<sup>b</sup> tumors every 2-3 days and sacrificed mice seven days after intratumoral treatment with poly I:C (or PBS) to assess cross-priming by IFN-γ ELISPOT assays. The addition of poly I:C did not appear to improve upon B16 A2/K<sup>b</sup> tumor suppression compared to intratumoral treatment with only untransduced T cells, TIL 1383I TCR transduced syngeneic T cells, or TIL 1383I TCR transduced allogeneic T cells (Fig 68 and Fig 69). When cells from the tumor draining lymph nodes of treated mice were re-stimulated with irradiated B16 A2/K<sup>b</sup> tumors *ex vivo* for 5 days and then co-cultured with B16 and B16 A2/K<sup>b</sup> tumors in an IFN-γ ELISPOT assay, we observed extremely robust reactivity accompanied with high background and unfortunately could not interpret the results (Appendix Fig 103 and Fig 104).

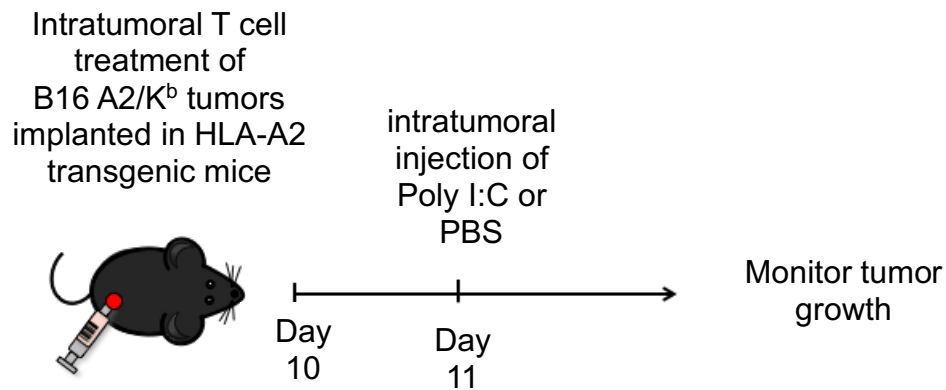


**Figure 67. Experimental Design to Determine If the Combination of TIL 1383I TCR Transduced Allogeneic T Cells and Poly I:C Improves Anti-Tumor Responses.** B16 A2/K<sup>b</sup> tumor-bearing mice were intratumorally treated on day 10 post-tumor inoculation with TIL 1383I TCR transduced allogeneic T cells or untransduced allogeneic T cells and one day later received an intratumoral injection of 40  $\mu$ g poly I:C or PBS. Tumor area was measured with a digital caliper 2-3x/week and presented as the product of two opposing diameters. Mice were sacrificed 11 days after poly I:C treatment for further analysis.

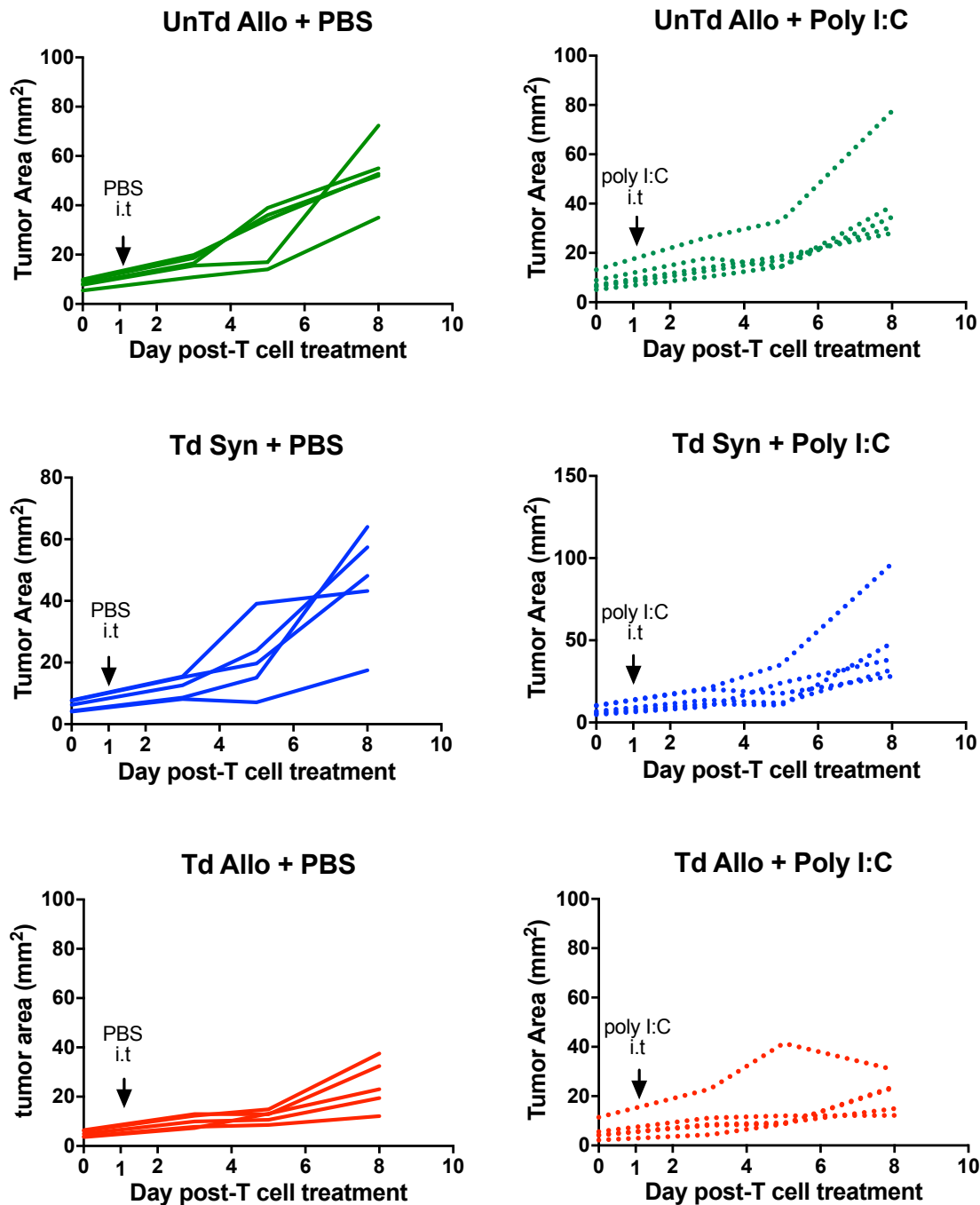


**Figure 68. B16 A2/K<sup>b</sup> Tumor Growth of Individual Mice Following Combination Treatment with T Cells and Poly I:C.** B16 A2/K<sup>b</sup> tumor-bearing mice were intratumorally treated on day 10 with A) PBS B) untransduced allogeneic T cells C-D) TIL 1383I TCR transduced allogeneic T cells and one day later received an intratumoral injection of B and D) poly I:C or C) PBS. Mice were sacrificed eleven days later to examine T cell cross-priming by IFN- $\gamma$  ELISPOT assay. (i.t.= intratumoral). Graphs represent one pilot experiment.

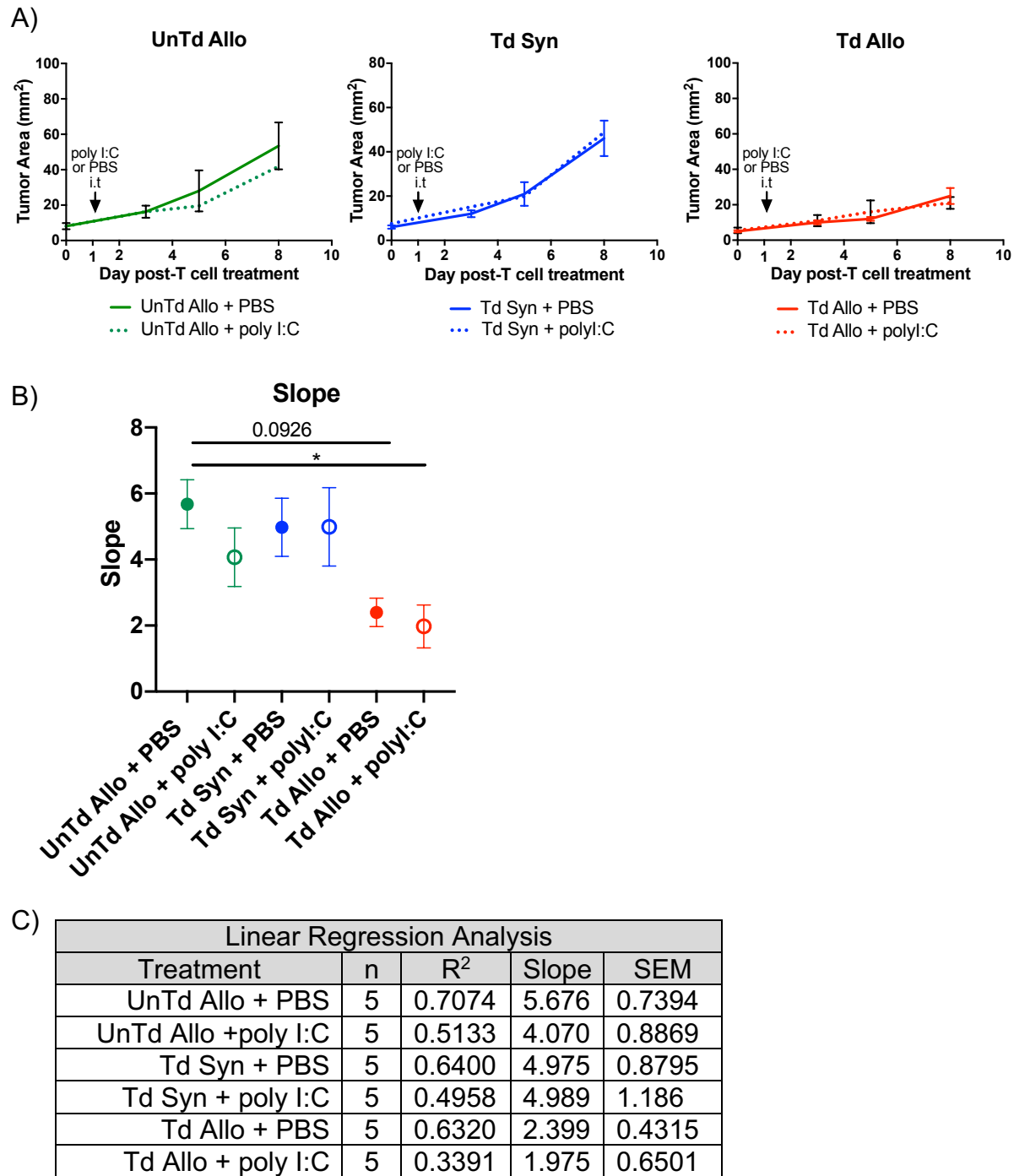


**Figure 69. B16 A2/K<sup>b</sup> Tumor Growth Following Combination Treatment with T Cells and Poly I:C.** B16 A2/K<sup>b</sup> tumor-bearing mice were intratumorally treated on day 10 with untransduced allogeneic T cells, TIL 1383I TCR transduced syngeneic T cells, or TIL 1383I TCR transduced allogeneic T cells. The next day, mice were intratumorally injected with PBS (solid line) or 40  $\mu$ g poly I:C (dotted line) and sacrificed one week later. A) Average B16 A2/K<sup>b</sup> tumor growth. B) Slope derived from linear regression analysis. C) Linear regression analysis. Graphs represent one pilot experiment with 5 mice per group. Statistical analysis was performed using one-way ANOVA (\*P<0.05).

We then performed a second pilot experiment using an adoptive transfer experimental approach to determine if T cell cross-priming could be enhanced (Fig 70). Ten days after intratumoral poly I:C treatment, we harvested the spleens of treated B16 A2/K<sup>b</sup> tumor-bearing mice (donors, Group 1) to determine if treatment-induced T cells could treat established B16 tumors (therapy, Group 2, Fig 70) or could prevent tumor formation following challenge with B16 (protection, Group 3, Fig 70). We first examined the effect of combination therapy on B16 A2/K<sup>b</sup> tumors implanted in mice from Group 1 (Fig 71 and 72). The combination of poly I:C and untransduced allogeneic T cell treatment slightly delayed the growth of B16 A2/K<sup>b</sup> tumors compared to the combination of no T cells and PBS ( $P=0.0473$ ; Fig 71 and 72). When mice were treated with the combination of TIL 1383I TCR transduced allogeneic T cell and poly I:C, we were unable to detect a significant difference in the ability to suppress B16 A2/K<sup>b</sup> tumor growth compared to the combination of TIL 1383I TCR transduced T cells and PBS ( $P=0.7023$ ), consistent with the previous pilot experiment (Fig 68 and 69).

We adoptively transferred splenocytes from mice bearing B16 A2/K<sup>b</sup> tumors that had been treated with T cells (Group 1; Fig 70-72) into mice bearing seven-day-old subcutaneous B16 tumors (Group 2) to test the therapeutic efficacy of the combination of TIL 1383I TCR transduced allogeneic T cells and poly I:C. In this small-scale pilot experiment, B16 tumor-bearing mice receiving splenocytes from mice treated with the combination of TIL 1383I TCR transduced allogeneic T cells and PBS (Group 1) had evidence of B16 tumor regression compared to B16 tumor-bearing mice receiving splenocytes isolated from mice treated with the combination of untransduced allogeneic T cells and poly I:C ( $P=0.0016$ ), or no T cells and PBS ( $P<0.0001$ ; Fig 73 and 74).

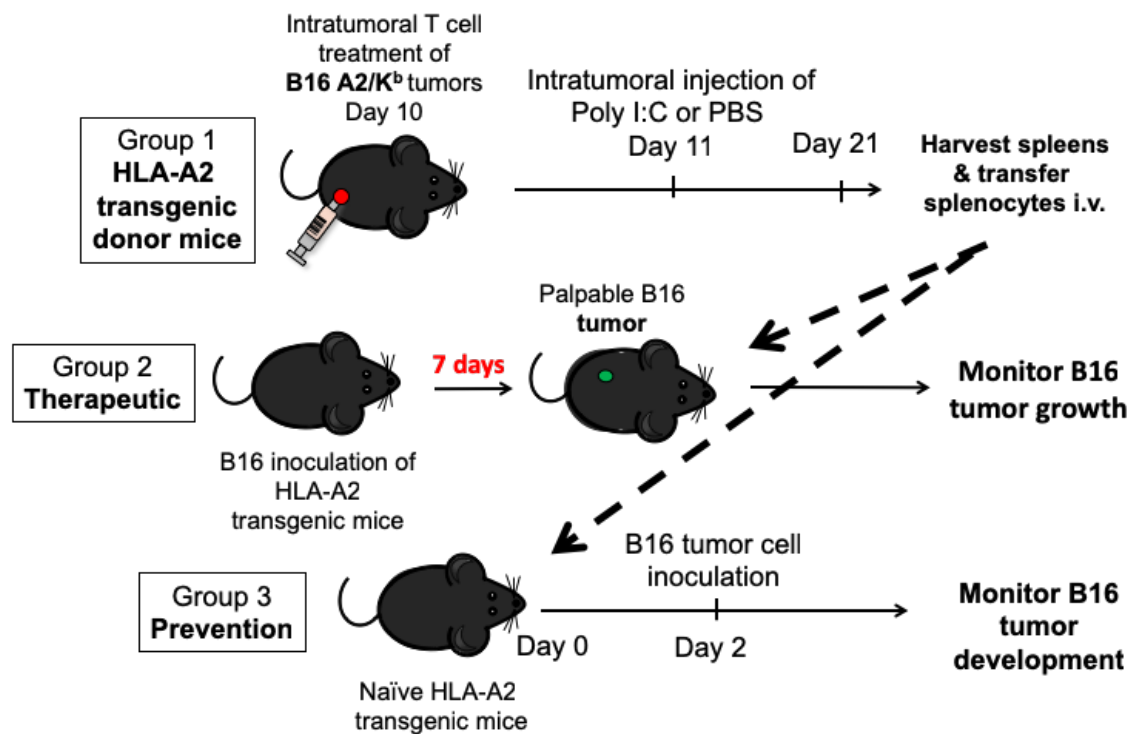


**Figure 70. Experimental Design to Determine if T Cell-Induced Splenocytes Can Transfer Therapeutic or Prophylactic Immunity Against B16 Tumors in Naïve Mice.** B16 A2/K<sup>b</sup> tumor-bearing mice were treated with TIL 1383I TCR transduced allogeneic T cells or untransduced allogeneic T cells and the following day received an intratumoral injection of poly I:C or PBS (Group 1). Ten days later, splenocytes were isolated and transferred into a) Mice bearing 7-day-old B16 tumors (Group 2) or b) Naïve mice that were then challenged with B16 two days post-T cell transfer (Group 3). Mice were monitored for development of B16 tumors.

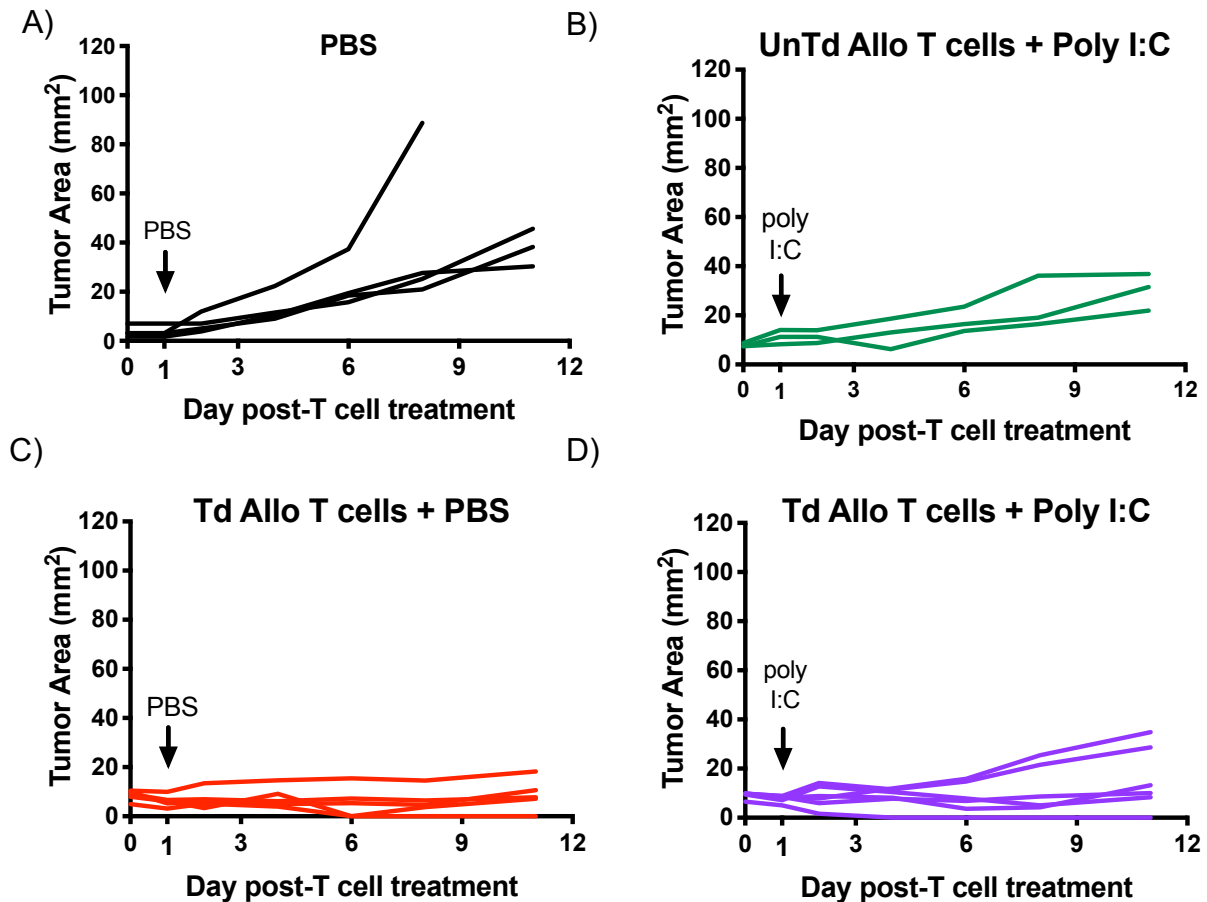
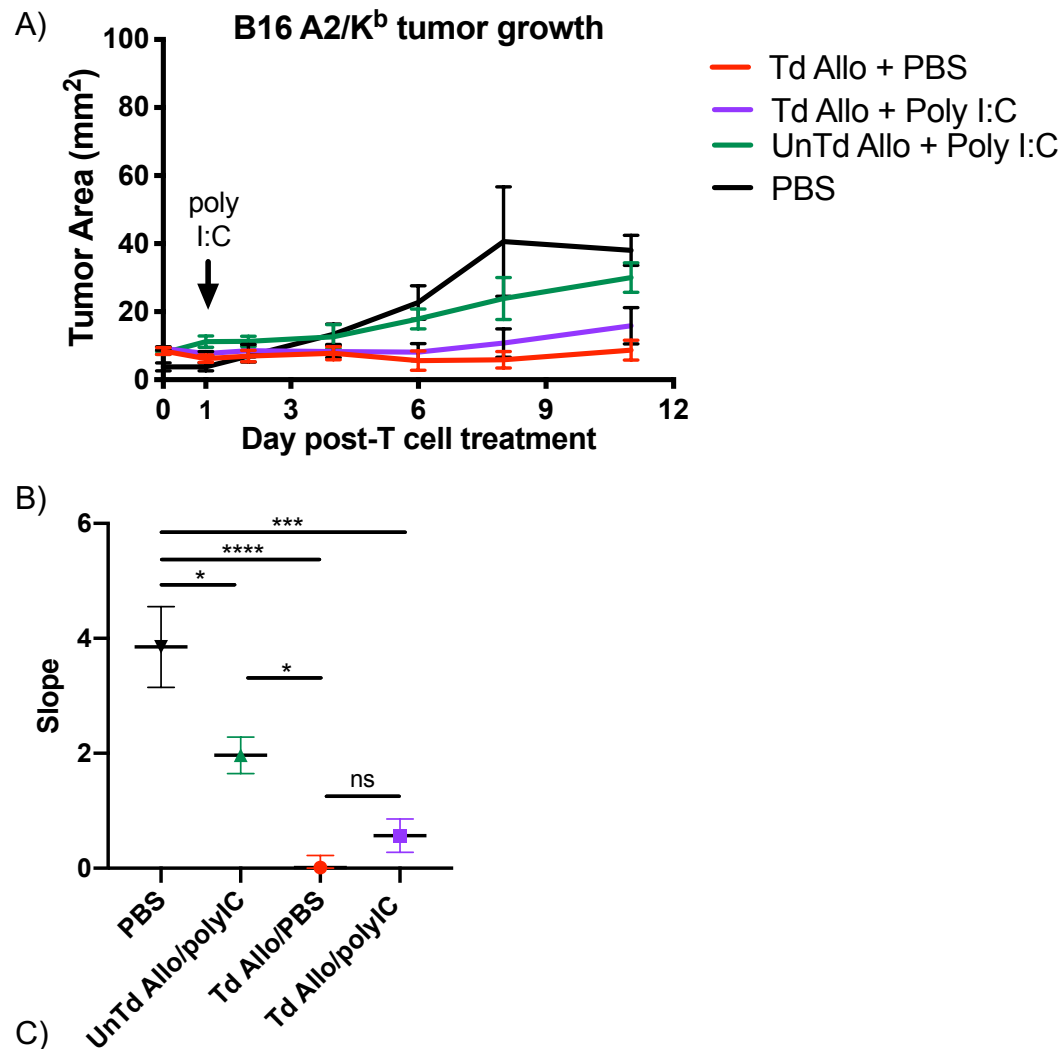


**Figure 71. B16 A2/K<sup>b</sup> Tumor Growth of Individual Mice Following Combination Treatment with T Cells and Poly I:C.** Group 1 B16 A2/K<sup>b</sup> tumor-bearing mice were intratumorally treated on day 10 with A) PBS B) untransduced allogeneic T cells C-D) TIL 1383I TCR transduced allogeneic T cells and one day later received an intratumoral injection of D) poly I:C or C) PBS. Mice were sacrificed eleven days later to examine T cell cross-priming by IFN- $\gamma$  ELISPOT assay. (i.t.= intratumoral). Graphs represent one pilot experiment with 3-6 mice per group.



Linear Regression Analysis				
Treatment	n	R <sup>2</sup>	Slope	SEM
No T cells + PBS	4	0.5462	3.852	0.7022
UnTd Allo +PolyI:C	3	0.6695	1.967	0.3171
Td Allo + PBS	5	0.0001	0.014	0.2073
Td Allo + Poly I:C	6	0.0877	0.587	0.2892

**Figure 72. Average B16 A2/K<sup>b</sup> Tumor Growth Following Intratumoral Combination Therapy with T Cells and Poly I:C.** B16 A2/K<sup>b</sup> tumor-bearing mice were intratumorally treated on day 10 post-B16 A2/K<sup>b</sup> with PBS, untransduced allogeneic T cells or TIL 1383I TCR transduced allogeneic T cells and one day later received an intratumoral injection of poly I:C or PBS. A) Average B16 A2/K<sup>b</sup> growth following intratumoral treatment. B) Slope of B16 A2/K<sup>b</sup> growth from group averages. Data represent one pilot experiment with 3-6 mice per group. Graph shows mean  $\pm$  SEM; Statistical analysis performed using one-way ANOVA with Tukey correction [ $*P < 0.05$ ,  $***P < 0.001$ ,  $****P < 0.0001$ ]



Splenocytes transferred from mice intratumorally treated with the combination of TIL 1383I TCR transduced allogeneic T cells and poly I:C also significantly improved anti-B16 tumor responses following adoptive transfer into B16 tumor-bearing mice compared to the adoptive transfer of splenocytes isolated from mice intratumorally treated with untransduced allogeneic T cells and poly I:C ( $P=0.0013$ ), or PBS ( $P<0.0001$ ; Fig 73 and 74). The therapeutic effect observed following intratumoral treatment with TIL 1383I TCR transduced allogeneic T cells was independent of the addition of TLR3 stimulation (ns,  $P=0.9981$ ). However, the addition of poly I:C to untransduced allogeneic T cell-treated mice induced moderate therapeutic anti-B16 responses compared to PBS-treated mice ( $P=0.0152$ ). These preliminary data suggest that the addition of poly I:C might improve the therapeutic efficacy of T cell responses, as demonstrated by the slight improvement when added to untransduced allogeneic T cells treatment alone or in comparison to PBS (Fig 69 and Fig 72) but the lack of improvement when combined with transduced T cell treatment indicated that these experiments should be repeated in order to reach conclusive findings.

The transfer of anti-tumor immunity to treat established B16 tumors is generally more difficult than prevention experiments. Therefore, we performed a small-scale pilot experiment to determine if splenocytes from mice with B16 A2/K<sup>b</sup> tumors treated with the combination of TIL 1383I TCR transduced allogeneic T cells and poly I:C (Group 1) could transfer protection and prevent the development of B16 tumors in naïve mice (Group 3; Fig 70). We adoptively transferred splenocytes from the T cell-treated mice in Group 1 into naïve mice, allowed engraftment for two days, and then subcutaneously inoculated mice with B16 tumor cells. The transfer of splenocytes from mice treated with

### B16 tumor growth (Therapeutic effect)

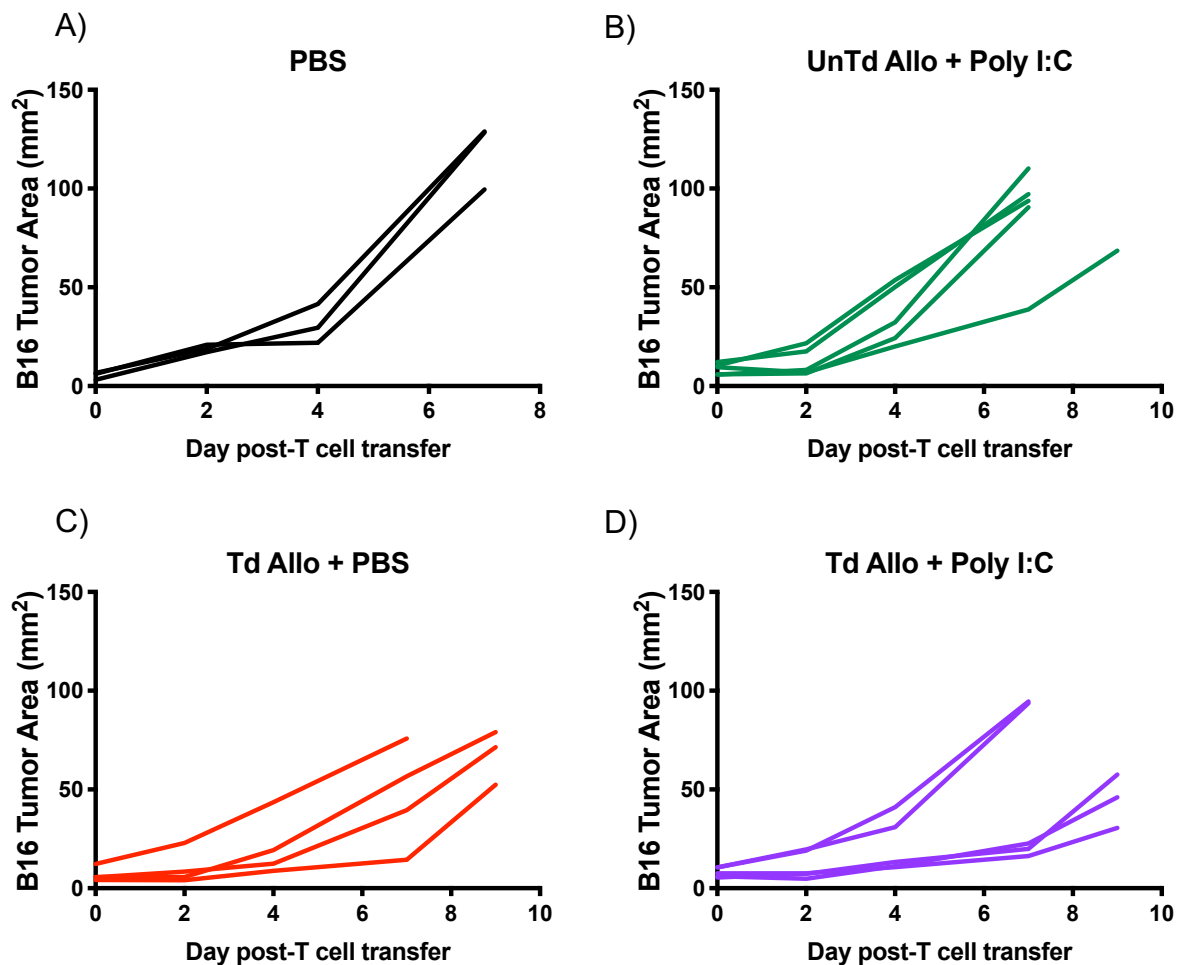


**Figure 73. B16 Tumor Growth in Individual Mice Following the Adoptive Transfer of Splenocytes From Mice Treated with the Combination of TIL 1383I TCR Transduced T Cells and Poly I:C.** Mice were inoculated with  $1.5 \times 10^5$  B16 tumor cells and seven days later received adoptive transfer of splenocytes from B16 A2/K<sup>b</sup> tumor-bearing HLA-A2 transgenic mice treated with A) PBS B) untransduced allogeneic T cells and poly I:C C) TIL 1383I TCR transduced allogeneic T cells and PBS, or D) TIL 1383I TCR transduced allogeneic T cells and poly I:C. Graphs represent one pilot experiment with 3-5 mice per group.

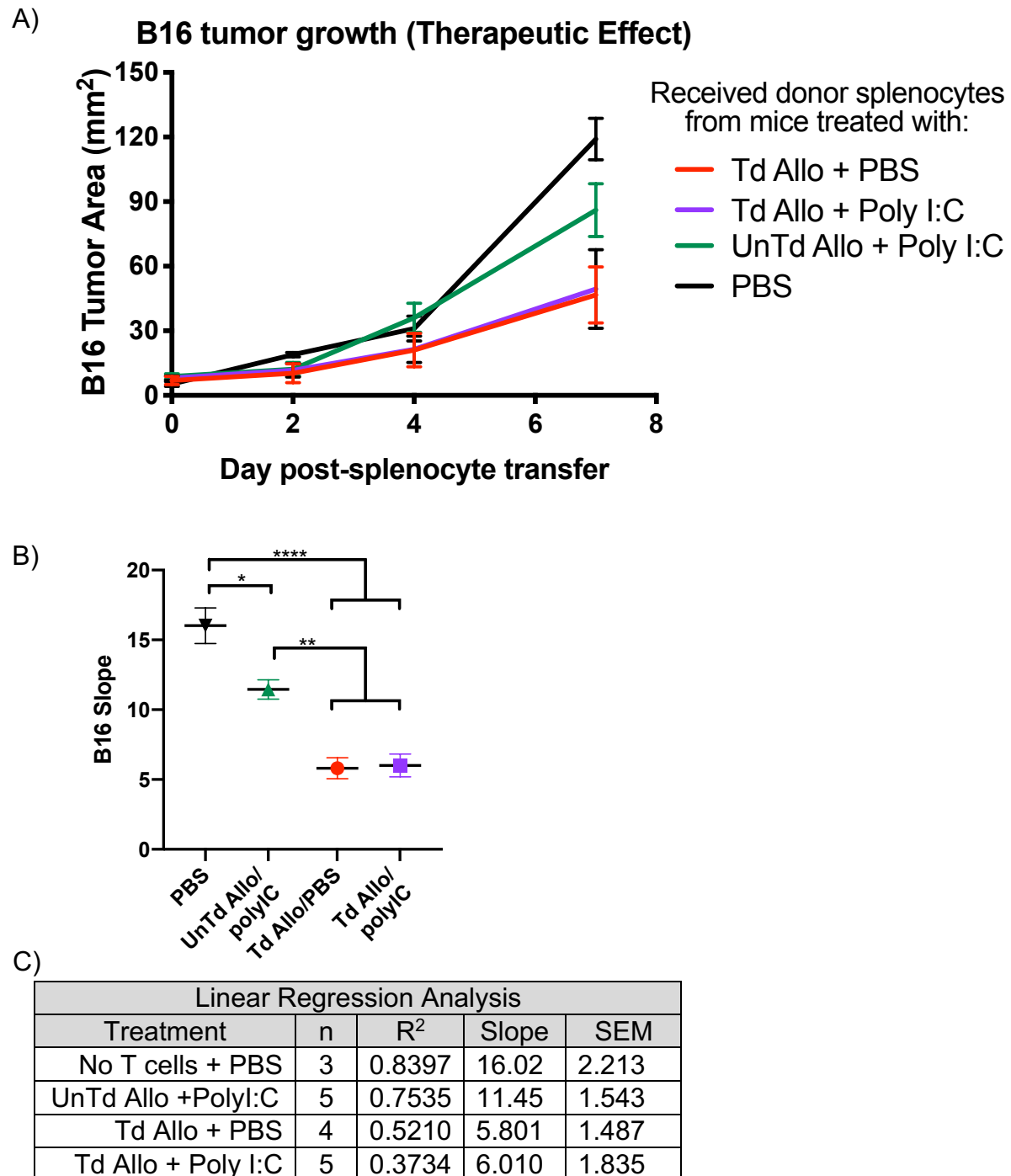


**Figure 74. Average B16 Tumor Growth Following the Adoptive Transfer of Splenocytes from Mice Treated with the Combination of TIL 1383I TCR Transduced Allogeneic T cells and Poly I:C.** Mice were inoculated with  $1.5 \times 10^5$  B16 tumor cells and 7 days later received adoptive transfer of splenocytes from T cell-treated, B16 A2/K<sup>b</sup> tumor-bearing mice (Group 1). A) Average B16 tumor growth following T cell transfer B) Slope of B16 tumor progression from group averages. Data represent one pilot experiment. Graph shows mean  $\pm$  SEM; C) Statistical analysis using one-way ANOVA with Tukey correction [ $*P < 0.05$ ,  $**P < 0.01$ ,  $****P < 0.0001$ ]

TIL 1383I TCR transduced allogeneic T cells, regardless of poly I:C addition, did not prevent the development of B16 tumors following transfer into recipient mice (Fig 75). When we compared the slope of B16 tumor progression among treatment groups, we observed a modest suppression of B16 tumor growth in mice that received splenocytes isolated from B16 A2/K<sup>b</sup> tumor-bearing mice that had been intratumorally treated with the combination of TIL 1383I TCR transduced allogeneic T cells and poly I:C (slope: 2.450) compared to B16 tumor-bearing mice that had received splenocytes from B16 A2/K<sup>b</sup> tumor-bearing mice treated with TIL 1383I TCR transduced allogeneic T cells and PBS (slope: 3.092,  $P=0.0396$ ), untransduced allogeneic T cells and poly I:C (slope: 3.384,  $P=0.0021$ ) and no T cells and PBS (slope: 3.838,  $P<0.0001$ , Fig 76). The results from these pilot experiments suggest that, in our model of using intratumoral delivery of TCR gene-modified T cells, the combination of TIL 1383I TCR transduced allogeneic T cells and subsequent poly I:C might possibly improve the suppression of primary B16 A2/K<sup>b</sup> tumor growth or transfer anti-tumor immunity to mice bearing established B16 tumors. However, in these small scale experiments, we cannot draw a reliable conclusion from the limited number of mice and limited treatment strategies. Therefore, the addition of poly I:C to TIL 1383I TCR transduced allogeneic T cell treatment might enhance the induction of cross-primed T cells, which would have to be further verified in replicate experiments.

### **Incorporation of the LIGHT Gene into the Retroviral Vector**

The addition of a TLR agonist, such as poly I:C, to stimulate an innate immune response is only one potential approach that one could use to modulate the tumor microenvironment (TME) in order to facilitate DC activation and T cell cross-priming.

### B16 tumor growth (Preventive effect)

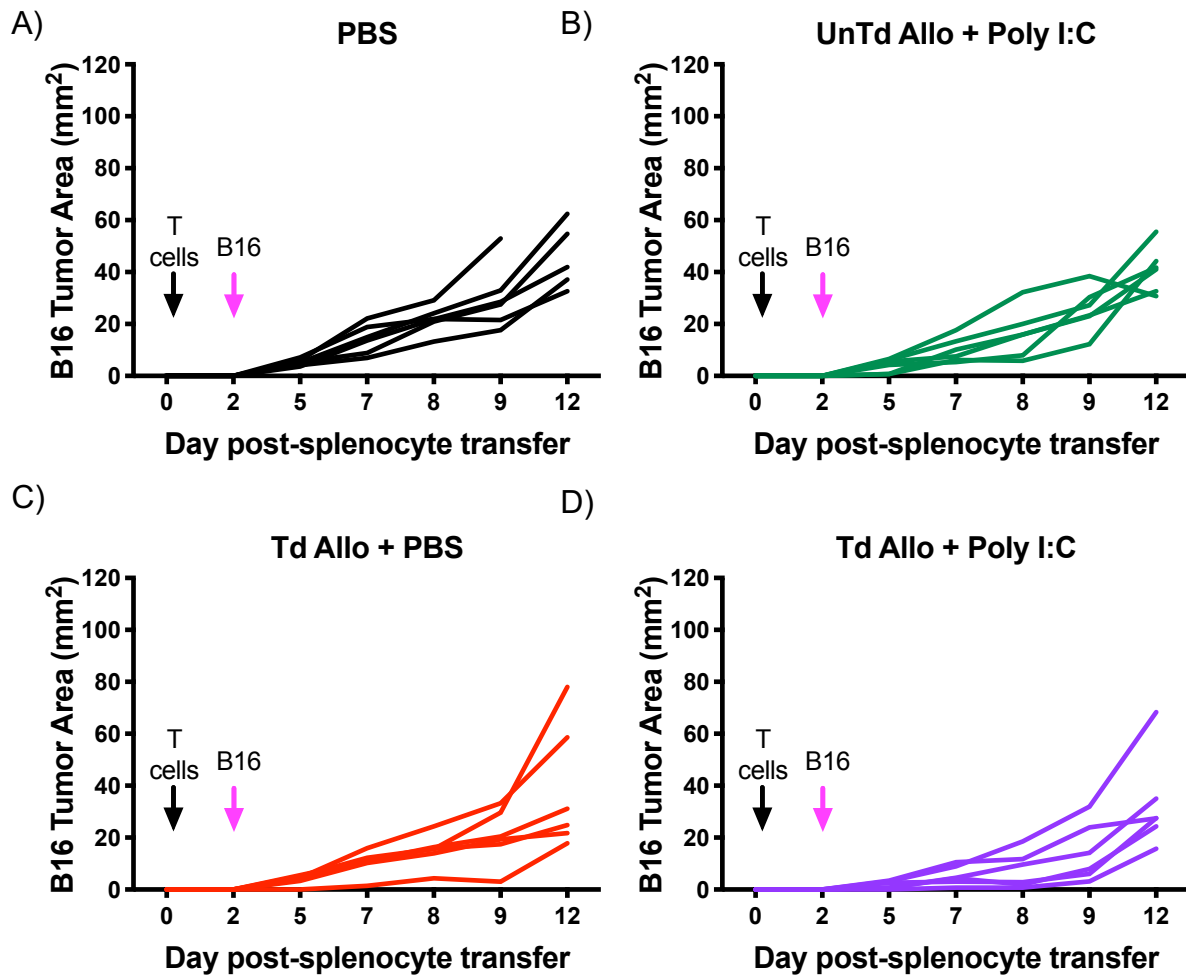
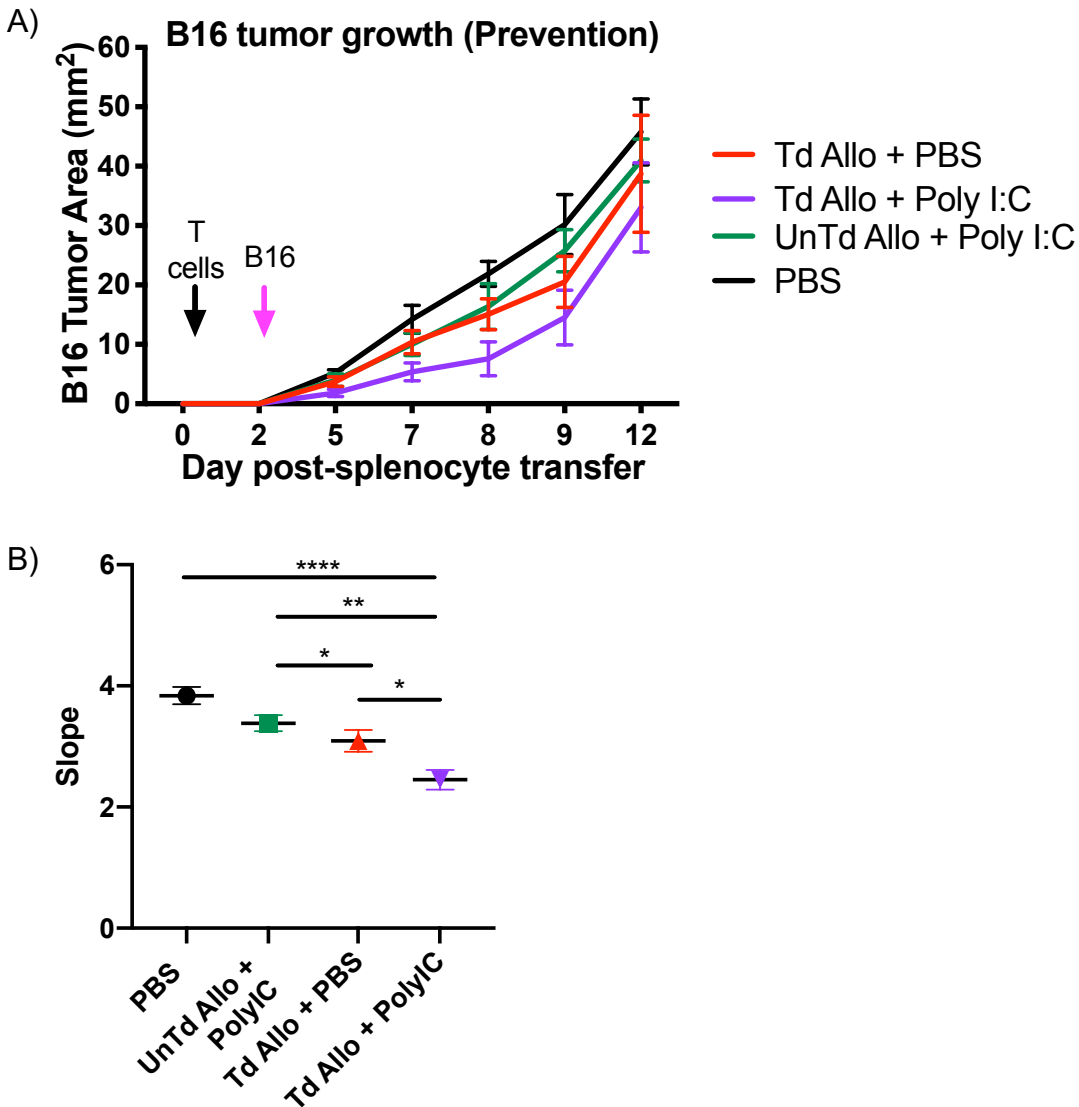


**Figure 75. Splenocytes from B16 A2/K<sup>b</sup> Tumor-Bearing Mice Treated with the Combination of TIL 1383I TCR Transduced Allogeneic T Cells and Poly I:C Transferred into Naïve Mice Delay Progression of B16 Tumors.** Naïve mice received  $1.0 \times 10^6$  splenocytes (black arrow) from B16 A2/K<sup>b</sup> tumor-bearing mice (Group 1) intratumorally treated with A) PBS, B) untransduced allogeneic T cells and poly I:C, C) TIL 1383I TCR transduced allogeneic T cells and PBS, or D) TIL 1383I TCR transduced allogeneic T cells and poly I:C. Two days later, mice were subcutaneously inoculated with  $1.0 \times 10^5$  B16 tumor cells (pink arrow) and monitored for the development of B16 tumors. Graphs represent one pilot experiment with 6 mice per group.



Linear Regression Analysis				
Treatment	n	R <sup>2</sup>	Slope	SEM
No T cells + PBS	6	0.7563	3.838	0.3488
UnTd Allo + Poly I:C	6	0.7327	3.384	0.3232
Td Allo + PBS	6	0.5493	3.092	0.4428
Td Allo + Poly I:C	6	0.4821	2.450	0.4014

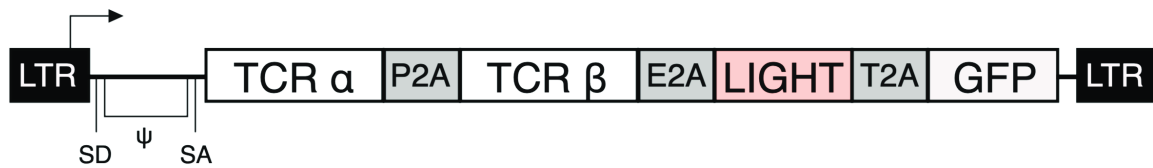
**Figure 76. Splenocytes From Mice Treated with the Combination of TIL 1383I TCR Transduced Allogeneic T Cells and Poly I:C Transfer Anti-Tumor Immunity to naïve mice.** Naïve mice received  $1 \times 10^6$  splenocytes from T cell-treated donor mice (Group 1) and two days later were inoculated with  $1 \times 10^5$  B16 tumor cells subcutaneously. A) Average B16 tumor growth following the transfer of T cells. B) Slope of B16 tumor progression from group averages. Data represent one pilot experiment with 6 mice per group. Graph shows mean  $\pm$  SEM C) Statistical analysis using one-way ANOVA with Tukey correction [\*  $P < 0.05$ , \*\* $P < 0.01$ , \*\*\*\* $P < 0.0001$ ]

Another approach is to modify the retroviral vector used to express the TCR genes to incorporate additional genes that encode for proteins that alter the TME and stimulate immune responses. One candidate gene, LIGHT [TNFSF14 (homologous to Lymphotoxins, shows Inducible expression, and competes with herpes simplex virus Glycoprotein D for Herpesvirus entry mediator, a receptor expressed by T lymphocytes)], is a TNF superfamily member and ligand for the lymphotoxin beta receptor (LT $\beta$ R)<sup>490</sup>. The LIGHT protein is expressed on activated T cells and dendritic cells (DCs). Upon interaction with LT $\beta$ R on stromal cells, LIGHT recruits and activates T cells and DCs to form lymphoid-like tissue structures inside the tumor microenvironment, which can result in the maturation of DCs and the induction of T cell cross-priming, ultimately leading to an effective anti-tumor response<sup>491,492,493</sup>.

Because our ultimate goal is to induce T cell cross-priming, we hypothesized that engineering the TIL 1383I TCR-encoding retroviral vector to express the LIGHT gene could further improve tumor antigen cross-presentation by DCs and anti-tumor T cell responses. We cloned the extracellular domain of the LIGHT protein into the vector containing the TIL 1383I TCR  $\alpha$  and  $\beta$  chain genes (Fig 77A). We were able to detect low surface levels of LIGHT expression following transduction and were able to identify intracellular LIGHT protein after permeabilizing T cells and staining with anti-LIGHT antibody (Fig 77B). These data confirmed the feasibility of generating TIL 1383I TCR transduced T cells that co-express the LIGHT extracellular domain.

In a pilot study, we tested the efficacy of TIL 1383I TCR<sup>+</sup>LIGHT<sup>+</sup> transduced T cells *in vivo*. We transduced syngeneic and allogeneic T cells with a vector encoding the TIL 1383I TCR only or a vector co-expressing the TIL 1383I TCR and LIGHT genes.

A)



B)

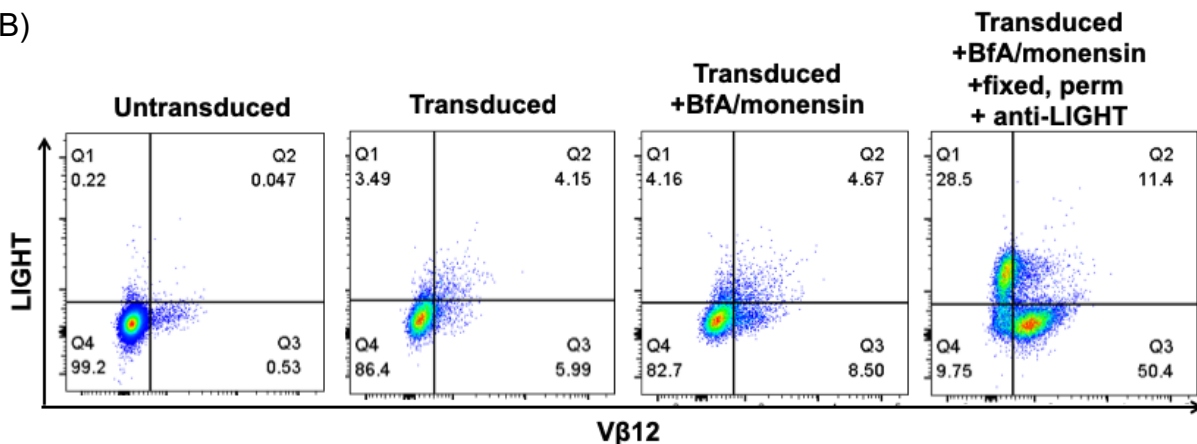


**Figure 77. Engineering T Cells to Express the TIL 1383I TCR and Extracellular LIGHT Domain.** Mouse T cells were activated for 48 hours with Dynabeads and then transduced with retrovirus. Three days post-transduced, T cells were examined for expression of CD3, CD4, CD8, Vβ12 and LIGHT. A) Schematic of the retroviral vector containing the TIL 1383I TCR α and β chain genes and extracellular LIGHT gene. B) Expression of the TIL 1383I TCR and LIGHT protein following retroviral transduction. Prior to flow cytometry, T cells were treated with brefeldin A (BfA) and monensin with and without permeabilization.

On day 10 post-B16 A2/K<sup>b</sup> injection, mice were intratumorally treated with TIL 1383I TCR transduced syngeneic or allogeneic T cells with or without LIGHT. Surprisingly, treatment with TIL 1383I TCR<sup>+</sup>LIGHT<sup>+</sup> transduced allogeneic T cells (slope:  $0.4847 \pm 0.7920$ ) was slightly less effective at suppressing B16 A2/K<sup>b</sup> tumor growth than TIL



1383I TCR transduced allogeneic T cells alone (slope:  $-0.6423 \pm 0.3486$ ,  $P=0.7469$ ; Fig 78 and 79). TIL 1383I TCR transduced syngeneic T cells co-expressing LIGHT (slope:  $1.498 \pm 0.5305$ ) were equally effective at suppressing B16 A2/K<sup>b</sup> tumor growth as TIL 1383I TCR transduced syngeneic T cells alone (slope:  $1.666 \pm 0.6916$ ,  $P=0.9999$ ). From these pilot experiments, the co-expression of LIGHT and TIL 1383I TCR did not appear to have an impact on anti-tumor responses. These results suggested that further replicate experiments should be performed in order to determine if the addition of LIGHT enhances the efficacy of TIL 1383I TCR transduced T cell treatment.

We entertained the possibility that LIGHT-expressing TIL 1383I TCR transduced T cells might enhance T cell cross-priming without having a noticeable effect on the size of primary B16 A2/K<sup>b</sup> tumors. We, therefore, examined the tumor draining lymph nodes after intratumoral treatment with TIL 1383I TCR<sup>+</sup> LIGHT<sup>+</sup> transduced T cells for evidence of T cell cross-priming by IFN- $\gamma$  ELISPOT assays (Fig 80). The tumor draining lymph nodes isolated from mice treated with TIL 1383I TCR transduced allogeneic T cells contained a significant frequency of IFN- $\gamma$ <sup>+</sup> cells in response to B16 tumors (spots:  $178.75 \pm 39.76$ ) compared to the tumor draining lymph nodes of mice treated with TIL 1383I TCR transduced syngeneic T cells ( $31.667 \pm 17.407$ ,  $P<0.01$ ), TIL 1383I TCR<sup>+</sup>LIGHT<sup>+</sup> transduced syngeneic T cells ( $15.0 \pm 3.536$ ,  $P<0.001$ ), untreated mice ( $13.33 \pm 6.667$ ,  $P<0.001$ ) and naïve mice ( $13.33 \pm 13.33$ ,  $P<0.001$ ; Fig 80A). However, we were unable to detect a significant frequency of B16-reactive T cells from the lymph nodes of mice treated with TIL 1383I TCR<sup>+</sup>LIGHT<sup>+</sup> transduced allogeneic T cells (spots:  $91.250 \pm 57.387$ ) compared to TIL 1383I TCR<sup>+</sup> transduced allogeneic T cells only.

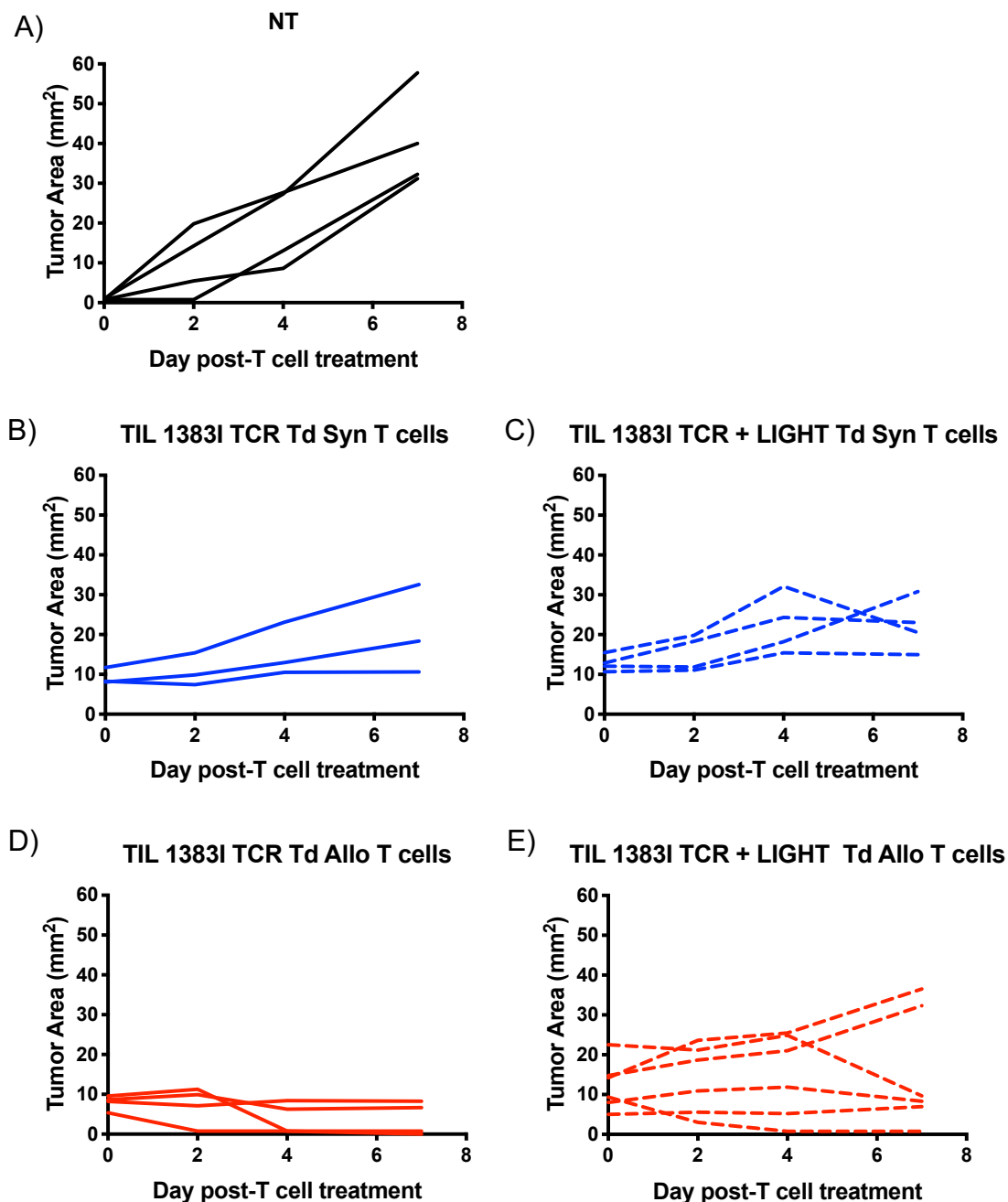
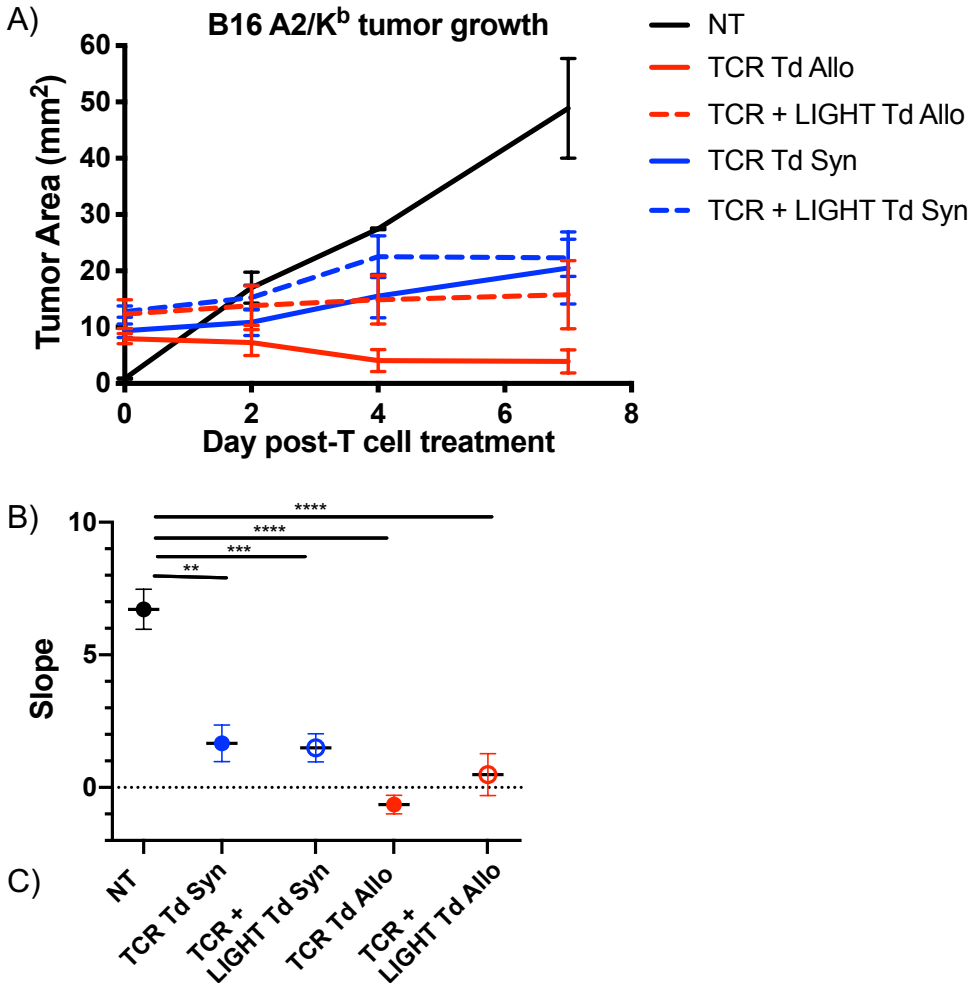


**Figure 78. B16 A2/K<sup>b</sup> Tumor Growth in Individual Mice Following Intratumoral Treatment with T Cells Transduced to Express the TIL 1383I TCR or Co-Express the TIL 1383I TCR + LIGHT Protein.** Syngeneic or allogeneic T cells were transduced with retroviral vectors encoding the TIL 1383I TCR or TIL 1383I TCR + LIGHT. On day 10 post-B16 A2/K<sup>b</sup> tumor inoculation, mice were A) left untreated or treated with B) TIL 1383I TCR Td Syn T cells C) TIL 1383I TCR + LIGHT Td Syn T cells D) TIL 1383I TCR Td Allo T cells E) TIL 1383I TCR + LIGHT Td Allo T cells. Tumors were measured 2-3 times/week and mice were sacrificed on day 7 post-T cell treatment for ELISPOT assays. Graphs represent one pilot experiment with 3-6 mice per group.



Linear Regression Analysis				
Treatment	n	R <sup>2</sup>	Slope	SEM
No Treatment	4	0.9292	6.720	0.7574
TCR Td Syn	3	0.3672	1.666	0.6916
TCR Td Syn + LIGHT	4	0.3627	1.498	0.5305
TCR Td Allo	4	0.1951	-0.6423	0.3486
TCR Td Allo + LIGHT	6	0.0167	0.4847	0.7920

**Figure 79. Linear Regression Analysis of B16 A2/K<sup>b</sup> Tumor Growth Following Treatment with T Cells Transduced to Co-Express the TIL 1383I TCR and LIGHT Protein.** Syngeneic or allogeneic T cells were transduced with retroviral vectors encoding the TIL 1383I TCR or TIL 1383I TCR and LIGHT. On day 10 post-B16 A2/K<sup>b</sup> tumor inoculation, mice were left untreated or treated with TIL 1383I TCR Td Syn T cells, TIL 1383I TCR + LIGHT Td Syn T cells, TIL 1383I TCR Td Allo T cells or TIL 1383I TCR + LIGHT Td Allo T cells. Tumors were measured 2-3 times/week and mice were sacrificed on day 7 post-T cell treatment for ELISPOT assays. A) Average B16 A2/K<sup>b</sup> tumor growth following T cell treatment B) Slope of B16 A2/K<sup>b</sup> growth derived from C) linear regression analysis of group averages. Data represent one pilot experiment with 3-6 mice per group. Graph shows mean  $\pm$  SEM; Statistical analysis using one-way ANOVA with Tukey correction [ $**P < 0.01$ ,  $***P < 0.001$ ,  $****P < 0.0001$ ]

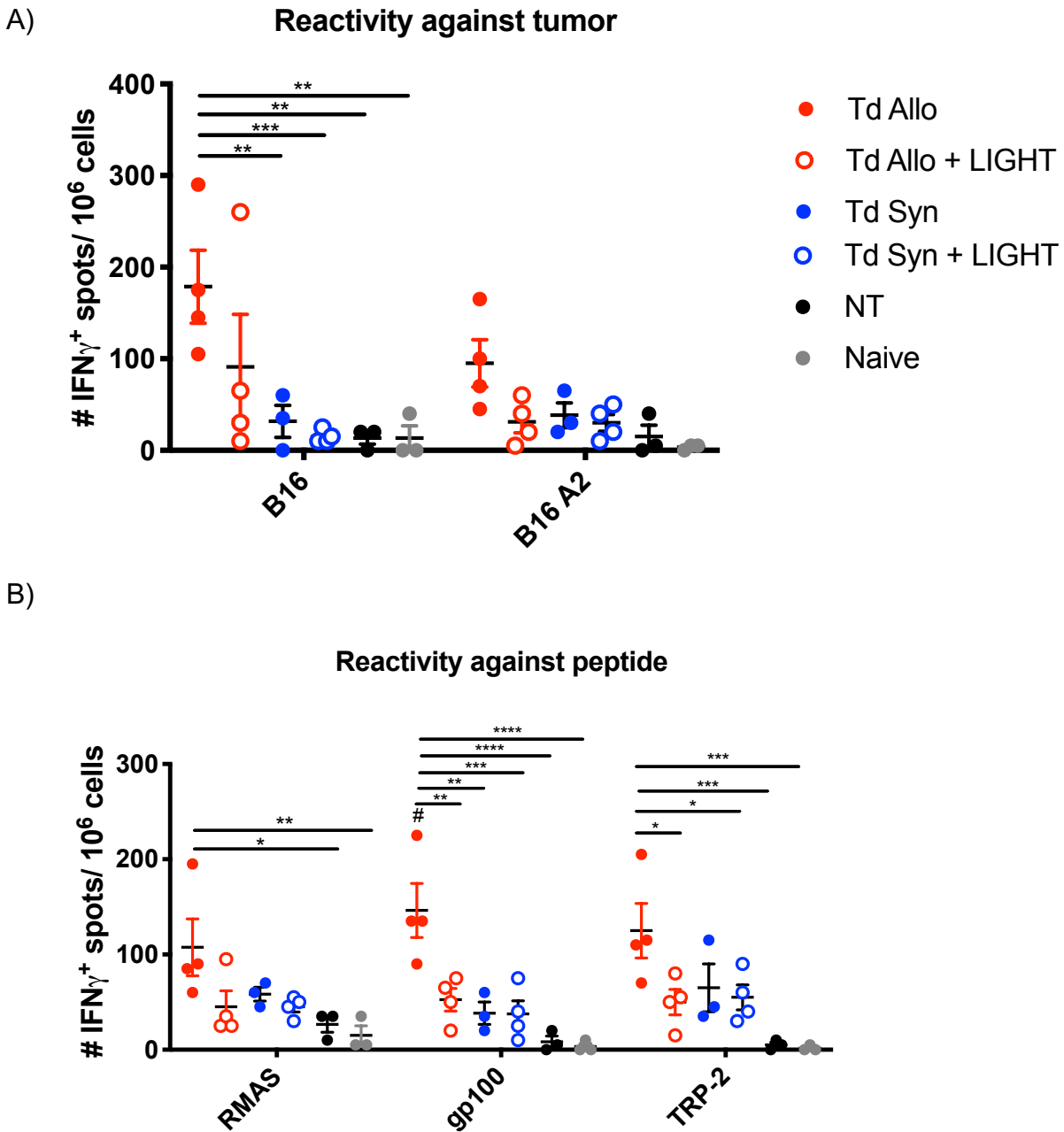


**Figure 80. Tumor-Specific IFN- $\gamma$  Production by Endogenous T Cells Following Intratumoral Treatment with T Cells that Co-Express the TIL 1383I TCR and LIGHT Protein.** Seven days post-intratumoral T cell treatment, cells from the tumor draining lymph nodes were isolated and co-cultured with A) Tumor targets or B) gp100- or TRP-2-loaded RMA/S cells for 18 hours. Data represent one pilot experiment with 3-6 mice per group. Graph shows mean  $\pm$  SEM; Statistical analysis using 2way ANOVA with Tukey correction [\* P<0.05, \*\*P<0.01, \*\*\*P<0.001, \*\*\*\*P<0.0001; #P<0.05 RMAS vs gp100]

We observed a significant frequency of gp100-reactive T cells the tumor draining lymph nodes of mice treated with TIL 1383I TCR transduced allogeneic T cells compared to unpulsed RMA/S cells ( $P=0.0229$ ; Fig 80B). None of the cells isolated from the tumor draining lymph nodes of treated mice were reactive against gp100- or TRP-2-loaded RMA/S cells (Fig 80B). The results from this pilot experiment suggested that co-expressing LIGHT with the TIL 1383I TCR may or may not enhance cross-primed T cells reactive against B16 or B16 A2/K<sup>b</sup> tumors, and further replicate experiments should be performed.

It was possible that co-expressing the TIL 1383I TCR and LIGHT intrinsically diminished the function of TIL 1383I TCR transduced T cells. We decided to perform another pilot experiment to test whether the administration of recombinant LIGHT protein could improve the anti-tumor efficacy following treatment with TIL 1383I TCR transduced T cells. Interestingly, intratumoral administration of recombinant LIGHT protein concurrent with TIL 1383I TCR transduced allogeneic T cells (slope: 2.125) did not delay B16 A2/K<sup>b</sup> tumor growth compared to TIL 1383I TCR transduced allogeneic T cells alone (slope: 2.871,  $P=0.9993$ ; Fig 81 and 82). Similarly, TIL 1383I TCR transduced syngeneic T cells with recombinant LIGHT (slope: 4.684) did not improve tumor suppression compared to TIL 1383I TCR transduced syngeneic T cells alone (slope: 4.589,  $P>0.9999$ ). The lack of improved anti-tumor responses following intratumoral treatment with the recombinant LIGHT protein was not limited to mice treated with TIL 1383I TCR transduced T cell treatment, as we did not observe a significant anti-tumor response in mice treated with recombinant LIGHT alone (slope: 6.615) compared to mice treated with PBS (slope: 8.053,  $P=0.9854$ ; Fig 81 and 82).

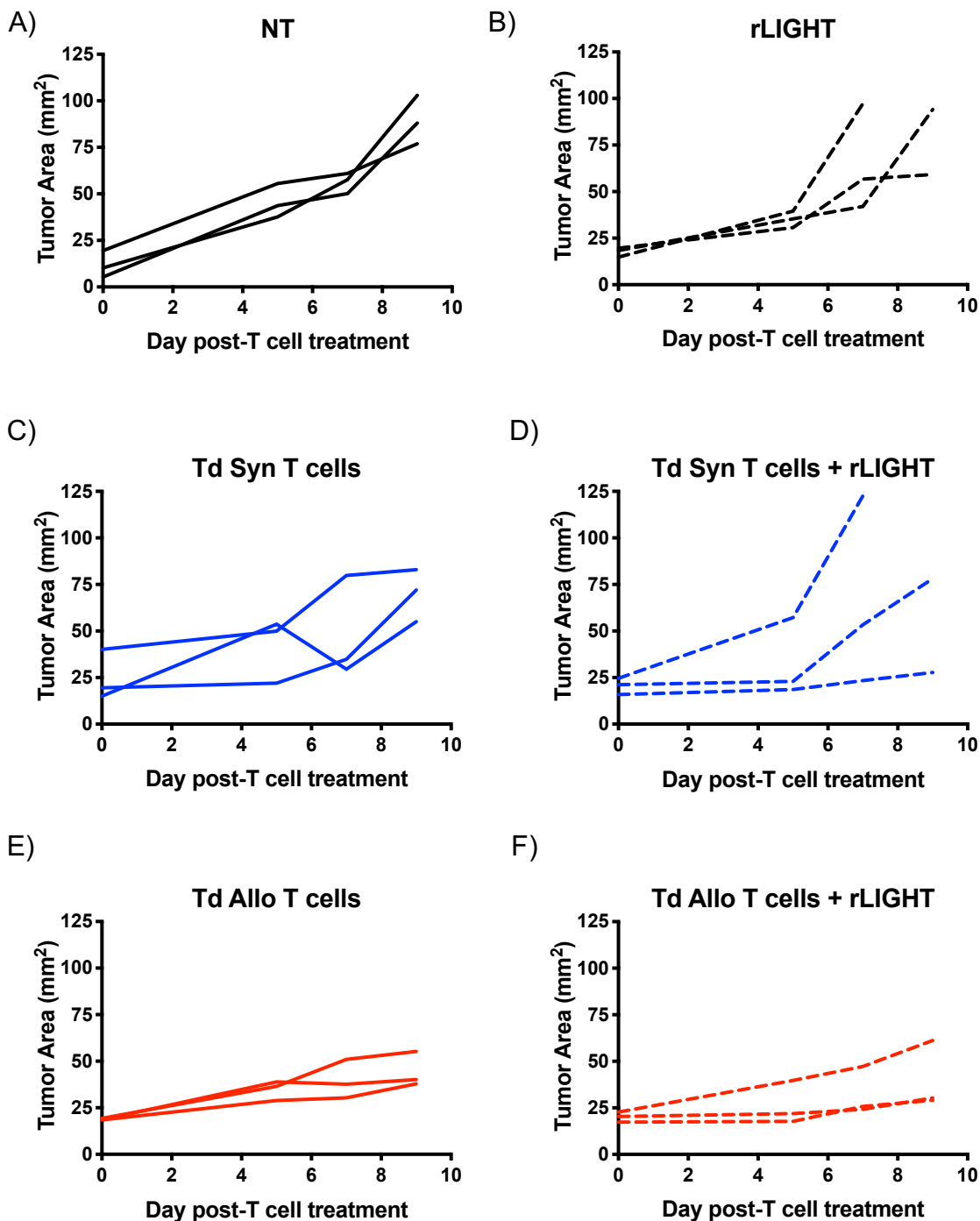


**Figure 81. B16 A2/K<sup>b</sup> Tumor Growth in Individual Mice Following Intratumoral Treatment with TIL 1383I TCR Transduced T Cells +/- Recombinant LIGHT Protein.** B16 A2/K<sup>b</sup> tumor-bearing mice were A) left untreated or B) treated with rLIGHT C) TIL 1383I TCR transduced syngeneic T cells D) TIL 1383I TCR transduced syngeneic T cells + rLIGHT E) TIL 1383I TCR transduced allogeneic T cells F) TIL 1383I TCR transduced allogeneic T cells + LIGHT. Tumors were measured 2-3 times per week. Graphs represent one pilot experiment with 3 mice per group.

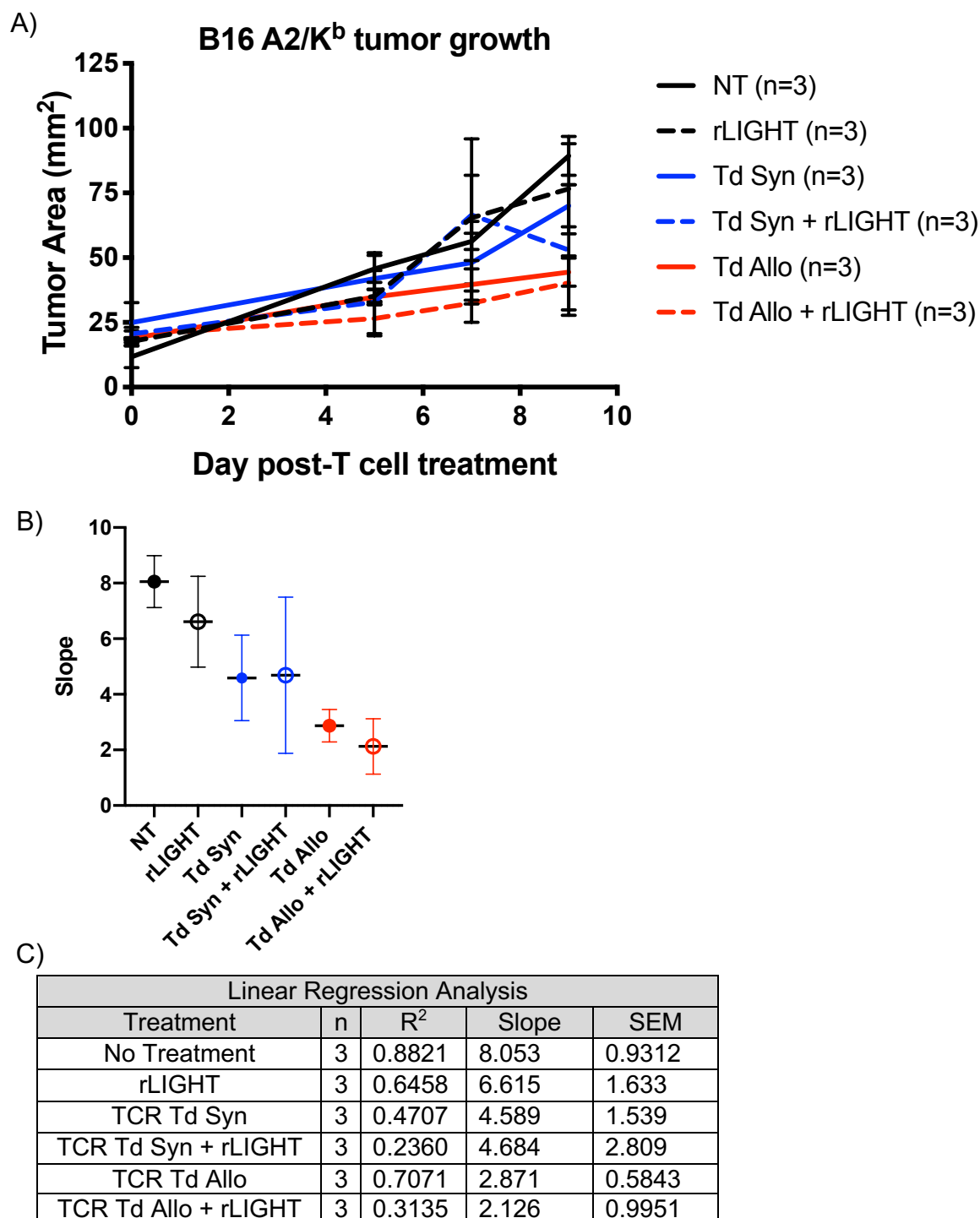


**Figure 82. Linear Regression Analysis of B16 A2/K<sup>b</sup> Tumor Growth Following Treatment with TIL 1383I TCR Transduced T Cells and Recombinant LIGHT Protein.** A) Group averages of B16 A2/K<sup>b</sup> tumors following intratumoral treatment. B) Slope of B16 A2/K<sup>b</sup> growth from group averages. Graph shows mean  $\pm$  SEM; No statistical significance was observed using one-way ANOVA with Tukey correction. Graph represent one pilot experiment with 3 mice per group.

From these pilot studies, we concluded that co-expressing LIGHT with the TIL 1383I TCR on transduced T cells may improve responses against B16 A2/K<sup>b</sup> primary tumors and enhance T cell cross-priming. Furthermore, the addition of intratumoral recombinant LIGHT protein to TIL 1383I TCR transduced T cells might mediate improved anti-tumor responses compared to TIL 1383I TCR transduced T cell treatment. Future replicate experiments should be performed to address these treatments.

### **Combination Therapy with Anti-PD-1 and Anti-CTLA-4 Monoclonal Antibodies**

There has been rising success in the use of checkpoint inhibitors to treat various malignancies. We wanted to determine if the addition of checkpoint inhibitors could enhance the therapeutic efficacy of TIL 1383I TCR transduced allogeneic T cells. We observed an increase in PD-1 expression on CD8<sup>+</sup> T cells in the tumor microenvironment following treatment with TIL 1383I TCR transduced allogeneic T cells compared to treatment with TIL 1383I TCR transduced syngeneic T cells ( $P < 0.0001$ ) and PBS ( $P = 0.0006$ ; Fig 83). We first investigated whether the addition of anti-PD-1 monoclonal antibodies (mAb) could improve anti-tumor responses in a pilot study. Mice were intratumorally treated with TIL 1383I TCR transduced T cells and intraperitoneally injected with 200  $\mu$ g of anti-PD-1 mAb. Seven days post-treatment, mice were challenged with B16 on the contralateral flank (Fig 84). We monitored survival and the development of B16 tumors. For overall survival, the addition of anti-PD-1 mAb did not significantly increase median survival post-treatment (Fig 85, Table 2). Additionally, when mice were monitored for B16 tumor development, we observed a delay in B16 tumors in mice treated with TIL 1383I TCR transduced allogeneic T cells. However, the addition of anti-PD-1 mAb did not improve anti-tumor responses (Fig 86, Table 3).



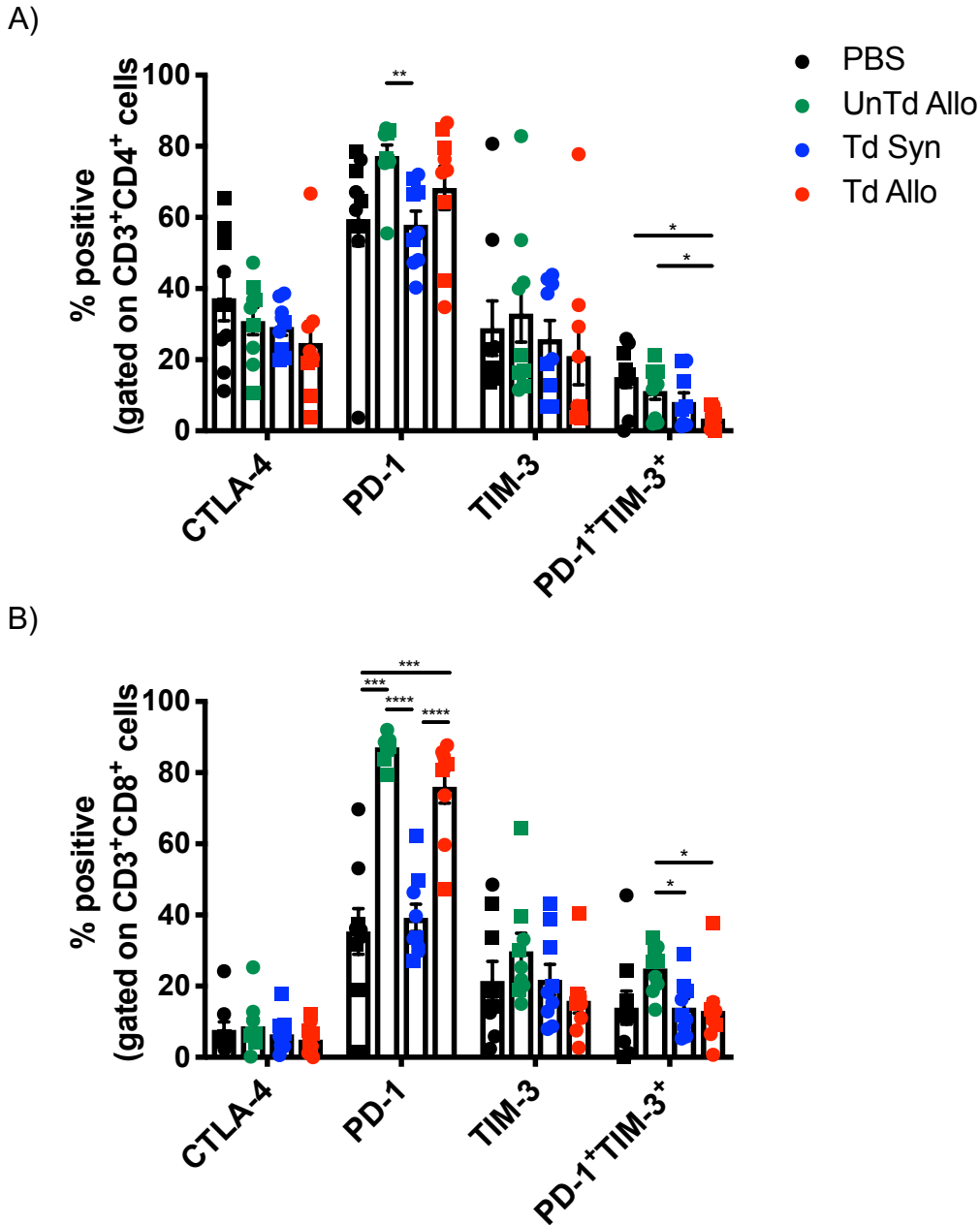


**Figure 83. Expression of Immune Checkpoints on T Cells in the Tumor Microenvironment Following TIL 1383I TCR Transduced T Cell Treatment.**

Seven days after intratumoral treatment with TIL 1383I TCR syngeneic T cells, TIL 1383I TCR transduced allogeneic T cells, untransduced allogeneic T cells, or PBS, B16 A2/K<sup>b</sup> tumors were harvested and cells were analyzed for expression of CD3, CD4, CD8, CTLA-4, PD-1, and TIM-3 by flow cytometry. A) CD3<sup>+</sup>CD4<sup>+</sup> T cells B) CD3<sup>+</sup>CD8<sup>+</sup> T cells. Symbols (circles and squares) represent two independent experiments with 4-5 mice/group. Cells were gating on live, single cells. Graph shows mean  $\pm$  SEM; Statistical analysis using one-way ANOVA with Tukey correction [\* P<0.05, \*\*\*P<0.001, \*\*\*\*P<0.0001]

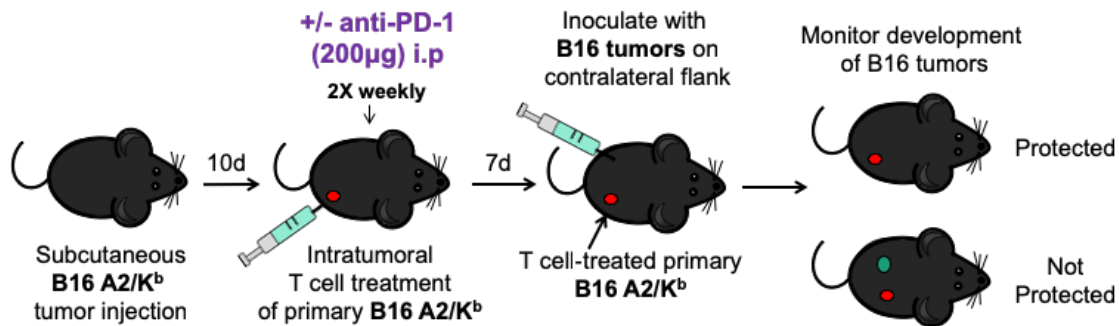
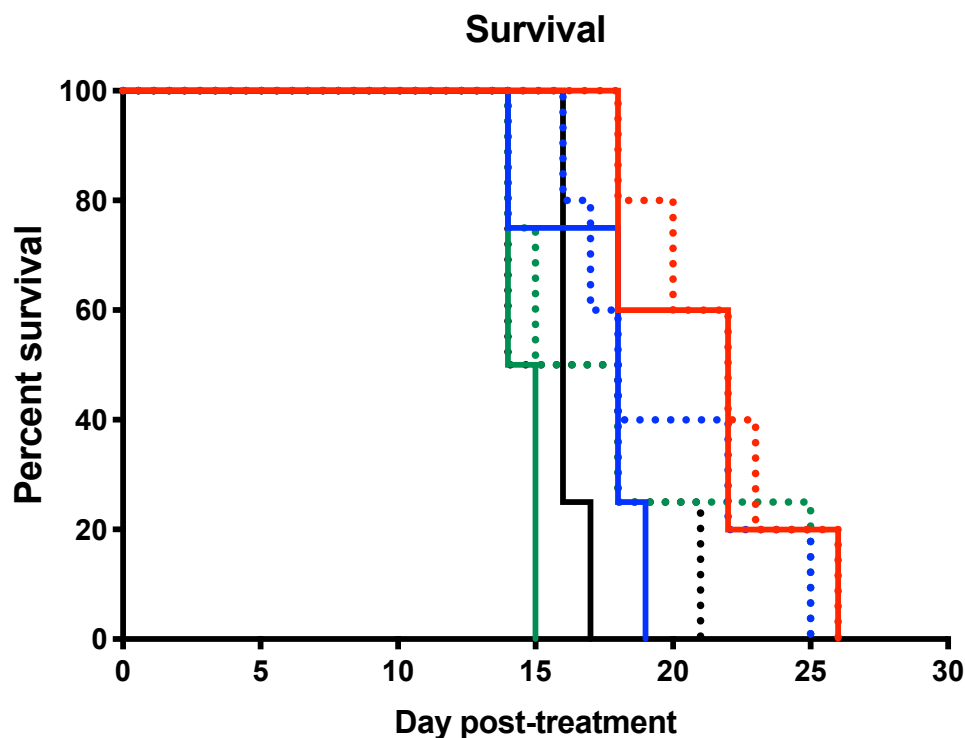


**Figure 84. Experimental Design to Determine if the Combination of Anti-PD-1 Monoclonal Antibody and TIL 1383I TCR Transduced T Cell Treatment Enhances Anti-Tumor Responses.**

Mice were subcutaneously inoculated with  $2.5 \times 10^5$  B16 A2/K<sup>b</sup> tumor cells and ten days later, were treated i.p. with anti-PD-1 mAb or control mAb and intratumoral injections of TIL 1383I TCR transduced allogeneic T cells, TIL 1383I TCR transduced syngeneic T cells, untransduced allogeneic T cells, or PBS. Administration of anti-PD-1 mAb continued 2x/week. Seven days post-T cell treatment, mice were challenged with  $1.0 \times 10^5$  B16 tumor cells on the left contralateral flank. Mice were monitored for survival and the appearance of B16 tumors. Mice were sacrificed when one tumor or the sum of both tumors exceeded  $>150 \text{ mm}^2$  or  $>10\%$  body weight.



Treatment	n	Median Survival (days)
— PBS	4	16
... PBS/ anti-PD-1	4	16
— UnTd Allo	4	14.5
... UnTd Allo/ anti-PD-1	4	16.5
— Td Syn	4	18
... Td Syn + anti-PD-1	5	18
— Td Allo	5	22
... Td Allo/ anti-PD-1	5	22

**Figure 85. Survival of B16 A2/K<sup>b</sup> Tumor Bearing Mice Following Treatment with TIL 1383I TCR Transduced T cells and Anti-PD-1 Monoclonal Antibody.** B16 A2/K<sup>b</sup> tumor-bearing mice were intratumorally treated with TIL 1383I TCR transduced syngeneic T cells, TCR transduced allogeneic T cells, untransduced allogeneic T cells or PBS and treated i.p with anti-PD-1 mAb (solid lines) or isotype (dotted lines). Mice were sacrificed when tumors reached >150 mm<sup>2</sup> or >10% body weight. Data represent one pilot experiment with 4-5 mice/group. Statistics performed using the Log Rank (Mantel-Cox) test. [\* P<0.05, \*\*P<0.01]

T cells + anti-PD-1 mAb			
NT	UnTd Allo	0.6068	ns
NT	Td Syn	0.2576	ns
NT	Td Allo	0.0483	*
UnTd Allo	Td Syn	0.7297	ns
UnTd Allo	Td Allo	0.3007	ns
Td Syn	Td Allo	0.9178	ns

T cells			
NT	UnTd Allo	0.0084	**
NT	Td Syn	0.1108	ns
NT	Td Allo	0.0027	**
UnTd Allo	Td Syn	0.0725	ns
UnTd Allo	Td Allo	0.0039	**
Td Syn	Td Allo	0.015	*

NT			
T cells only	anti-PD-1 mAb	0.5156	ns
UnTd Allo			
T cells only	anti-PD-1 mAb	0.1696	ns
Td Syn			
T cells only	anti-PD-1 mAb	0.4373	ns
Td Allo			
T cells only	anti-PD-1 mAb	0.92	ns

**Table 2. Log Rank (Mantel-Cox) Test of Survival Following Combination Treatment with TIL 1383I TCR Transduced T Cells and Anti-PD-1 Monoclonal Antibody.** Mice were intratumorally treated with PBS, untransduced allogeneic T cells, TIL 1383I TCR transduced syngeneic T cells, or TIL 1383I TCR transduced allogeneic T cells alone or in combination with 200 µg of anti-PD-1 and anti-CTLA-4 in 100 µl volume intraperitoneally. Tumors were measured with a digital caliper 2-3 times per week. Mice were sacrificed when tumors reached >150 mm<sup>2</sup> or >10% body weight. Data represent one pilot experiment with 4-5 mice/group. Statistics performed using the Log Rank (Mantel-Cox) test. [\* p<0.05, \*\*p<0.01]

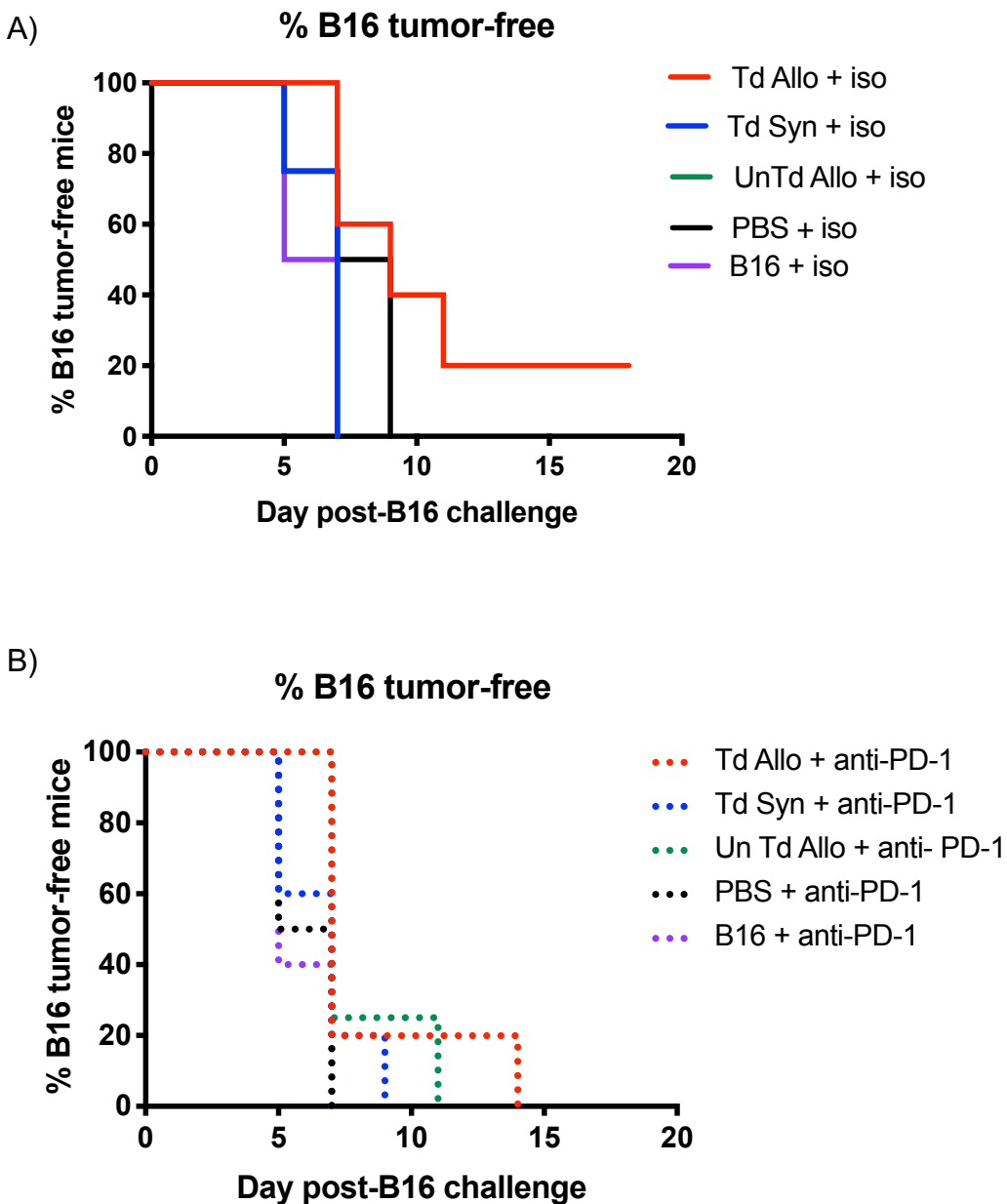


**Figure 86. Percentage of Mice Protected from Contralateral B16 Following Treatment of Primary B16 A2/K<sup>b</sup> Tumors with TIL 1383I TCR Transduced T Cells and Treatment with Anti-PD-1 Monoclonal Antibody.** B16 A2/K<sup>b</sup> tumor-bearing mice were intratumorally treated with TIL 1383I TCR transduced syngeneic T cells, TCR transduced allogeneic T cells, untransduced allogeneic T cells or PBS and treated i.p with A) control mAb or B) anti-PD-1 mAb. Mice were sacrificed when one tumor or the sum of both tumors reached >150 mm<sup>2</sup> or >10% body weight. Data represent one pilot experiment with 4-5 mice/group.

T cells + anti-PD-1			
NT	UnTd Allo	0.0984	ns
NT	Td Syn	0.5016	ns
NT	Td Allo	0.0799	ns
UnTd Allo	Td Syn	0.2327	ns
UnTd Allo	Td Allo	0.6377	ns
Td Syn	Td Allo	0.2325	ns

T cells			
NT	UnTd Allo	0.2719	ns
NT	Td Syn	0.2719	ns
NT	Td Allo	0.2426	ns
UnTd Allo	Td Syn	>0.999	ns
UnTd Allo	Td Allo	0.0522	ns
Td Syn	Td Allo	0.0522	ns

NT			
T cells only	anti-PD-1	0.1696	ns
UnTd Allo			
T cells only	anti-PD-1	0.1869	ns
Td Syn			
T cells only	anti-PD-1	0.8527	ns
Td Allo			
T cells only	anti-PD-1	0.4261	ns

**Table 3. Log-Rank (Mantel-Cox) Test of B16 Tumor-Free Mice Following Treatment with TIL 1383I TCR Transduced T Cells and Anti-PD-1 Monoclonal Antibody.** Mice were intratumorally treated with PBS, untransduced allogeneic T cells, TIL 1383I TCR transduced syngeneic T cells, or TIL 1383I TCR transduced allogeneic T cells alone or in combination with 200 µg of anti-PD-1 and anti-CTLA-4 in 100 µl volume intraperitoneally. Tumors were measured with a digital caliper 2-3 times per week. Mice were sacrificed when tumors reached >150 mm<sup>2</sup> or >10% body weight. Data represent one pilot experiment with 4-5 mice/group. Statistics performed using the Log Rank (Mantel-Cox) test.

These data are consistent with previous reports examining the therapeutic effects and anti-tumor effects of systemic administration of anti-PD-1 mAb in the B16 mouse model of melanoma<sup>352</sup>. These results indicate that anti-PD-1 mAb alone does not improve anti-tumor responses following intratumoral treatment with TIL 1383I TCR transduced allogeneic T cells.

The addition of anti-CTLA-4 mAb to anti-PD-1 mAb treatment has been demonstrated to improve responses in pre-clinical and clinical studies<sup>360,494–496</sup>. Seven days post-T cell treatment, we observed similar expression of CTLA-4 on T cells isolated from the tumor draining lymph nodes of mice from all treatment groups, with about 25-35% CTLA-4<sup>+</sup>CD4<sup>+</sup> T cells and 4-8% CTLA-4<sup>+</sup> CD8<sup>+</sup> T cells in the tumor microenvironment (Fig 83). We then tested whether anti-CTLA-4 mAb, in combination with anti-PD-1 mAb, could enhance the efficacy of intratumoral treatment with TIL 1383I TCR transduced allogeneic T cells (Fig 87). Mice were inoculated with B16 A2/K<sup>b</sup> tumor cells on the right flank and ten days later were intratumorally injected with TIL 1383I TCR transduced T cells only or in combination with i.p anti-PD-1 mAb (200 µg) and anti-CTLA-4 mAb (200 µg). We continued administering the checkpoint inhibitors twice weekly. The addition of dual anti-PD-1 mAb/anti-CTLA-4 mAb significantly extended the median survival of mice treated with TIL 1383I TCR transduced allogeneic T cells (median survival: 39 days post-treatment vs 27 days post-treatment,  $P < 0.001$ ; Fig 88, Table 4). The addition of anti-CTLA-4 mAb and anti-PD-1 mAb also significantly extended survival compared to PBS alone (median survival: 29 vs. 13 days,  $P = 0.01$ ). These results demonstrated that the combination of anti-PD-1 mAb and anti-CTLA-4 mAb with TIL 1383I TCR transduced allogeneic T cell treatment can improve survival.

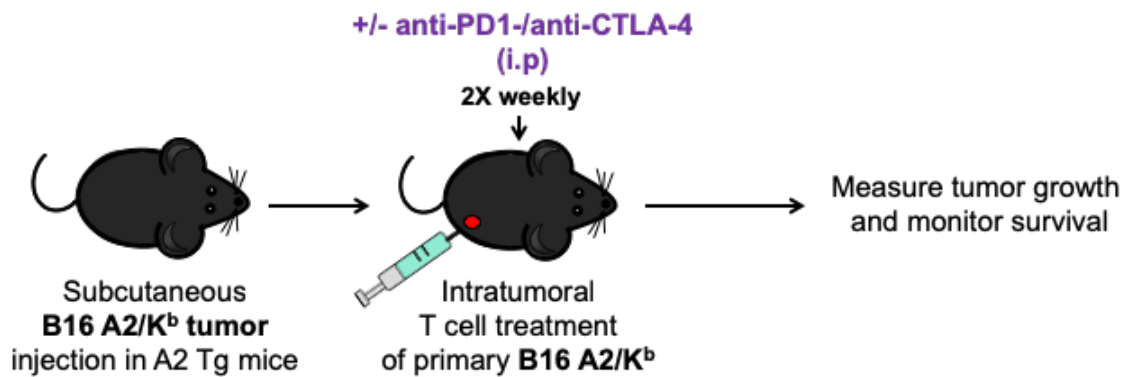


**Figure 87. Experimental Design to Determine If the Addition of Checkpoint Inhibitors Enhances the Efficacy of Intratumoral Treatment with TIL 1383I TCR Transduced Allogeneic T Cells.** B16 A2/K<sup>b</sup> tumor-bearing mice were intratumorally treated with PBS, untransduced allogeneic T cells, TIL 1383I TCR transduced syngeneic T cells, or TIL 1383I TCR transduced allogeneic T cells. On the same day, mice were given 200  $\mu$ g of anti-PD-1 and anti-CTLA-4 in 100  $\mu$ l volume intraperitoneally and twice weekly thereafter. Tumors were measured with a digital caliper 2-3 time per week. Mice were sacrificed when tumors reached >150 mm<sup>2</sup> or >10% body weight.



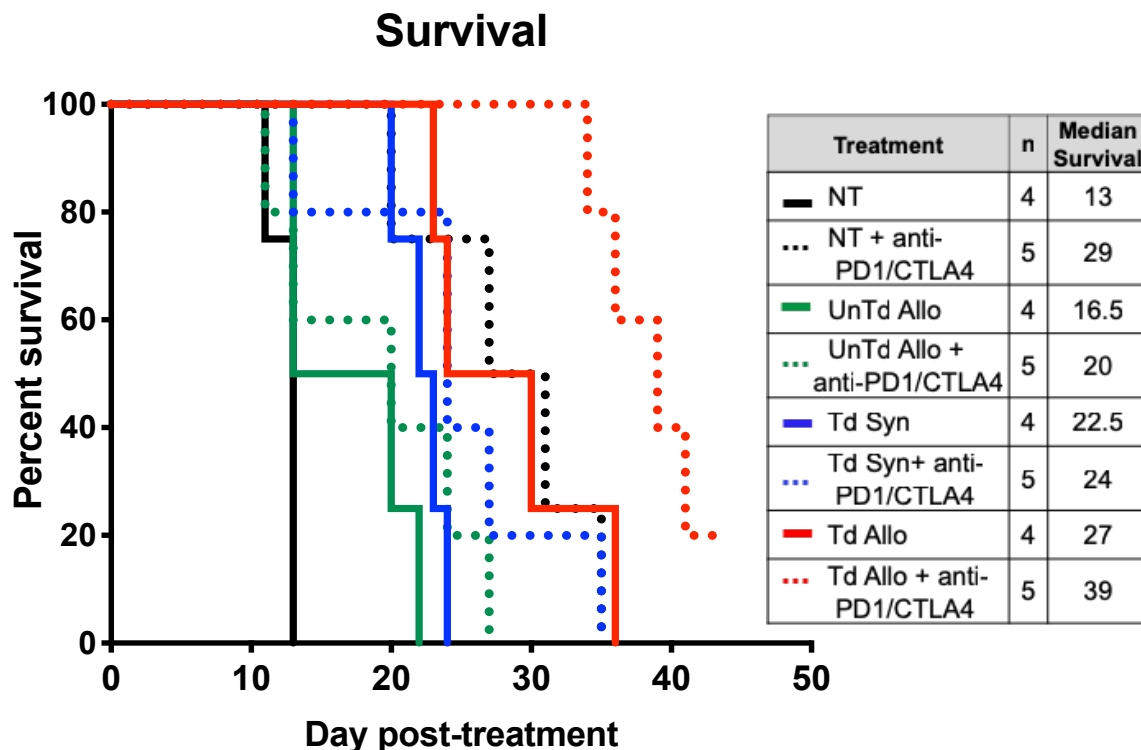


**Figure 88. The Combination of TIL 1383I TCR Transduced Allogeneic T Cells and Checkpoint Inhibitors Improves Survival of B16 A2/K<sup>b</sup> Tumor-Bearing Mice.** Mice were intratumorally treated with A) PBS, untransduced allogeneic T cells, TIL 1383I TCR transduced syngeneic T cells, or TIL 1383I TCR transduced allogeneic T cells alone (solid lines) or in combination with 200  $\mu$ g of anti-PD-1 and anti-CTLA-4 in 100  $\mu$ l volume intraperitoneally (dotted lines). Tumors were measured with a digital caliper 2-3 time per week. Mice were sacrificed when tumors reached  $>150$  mm<sup>2</sup> or  $>10\%$  body weight. Data represent one independent experiment with 4-5 mice/group.

A)

T cells + anti-PD-1 mAb/anti-CTLA-4 mAb			
NT	UnTd Allo	0.064	ns
NT	Td Syn	0.5837	ns
NT	Td Allo	0.0108	*
UnTd Allo	Td Syn	0.2233	ns
UnTd Allo	Td Allo	0.0018	**
Td Syn	Td Allo	0.0066	**

T cells			
NT	UnTd Allo	0.0944	ns
NT	Td Syn	0.02	*
NT	Td Allo	0.01	*
UnTd Allo	Td Syn	0.0714	ns
UnTd Allo	Td Allo	0.0062	**
Td Syn	Td Allo	0.0694	ns

B)

NT			
T cells only	anti-PD-1 mAb/anti-CTLA-4 mAb	0.01	*
UnTd Allo			
T cells only	anti-PD-1 mAb/anti-CTLA-4 mAb	0.4299	ns
Td Syn			
T cells only	anti-PD-1 mAb/anti-CTLA-4 mAb	0.1227	ns
Td Allo			
T cells only	anti-PD-1 mAb/anti-CTLA-4 mAb	0.024	*

**Table 4 Log Rank (Mantel-Cox) Test of Survival Following Treatment with TIL 1383I TCR Transduced T Cells and Anti-PD-1/Anti-CTLA-4 Monoclonal Antibodies.** On day 10 post- B16 A2/K<sup>b</sup> tumor inoculation, mice were treated with intratumoral T cells only intratumoral T cells and i.p anti-anti-PD-1, intratumoral T cells and i.p anti-CTLA-4, intratumoral T cells and i.p anti-PD-1/anti-CTLA-4. A) Comparison of checkpoint inhibitor treatment groups B) Comparison of T cell treatment groups. Data represent one experiment with 4-5 mice/group. Statistics performed using the Log Rank (Mantel-Cox) test. [\* P<0.05, \*\*P<0.01]

In these experiments, we only examined survival and protection against B16 tumors, but it would be interesting to determine if combination therapy with checkpoint inhibitors and TIL 1383I TCR transduced allogeneic T cells also resulted in enhanced CD80 and CD86 expression on intratumoral or lymph node-resident DCs.

Linear regression analysis of B16 A2/K<sup>b</sup> tumors indicated that the addition of anti-PD-1 mAb and anti-CTLA-4 mAb also affected tumor progression (Fig 89 and Table 5). Comparing the slopes of B16 A2/K<sup>b</sup> tumor growth curves, we did not observe a significant difference between B16 A2/K<sup>b</sup> tumor growth after the combination of anti-PD-1 mAb and anti-CTLA-4 mAb with TIL 1383I TCR transduced allogeneic T cells; however, the addition of anti-PD-1 mAb and anti-CTLA-4 mAb to PBS treated mice significantly suppressed B16 A2/K<sup>b</sup> tumor growth ( $P=0.0001$ ; Fig 89, Table 5). There was a moderate difference in B16 A2/K<sup>b</sup> tumor suppression with TIL 1383I TCR transduced syngeneic T cells and anti-PD-1 mAb and anti-CTLA-4 mAb ( $P=0.0603$ ). These results suggested that the addition of anti-CTLA-4 mAb was improving anti-tumor responses following intratumoral T cell treatment.

To confirm that the addition of anti-CTLA-4 mAb was responsible for mediating the observed enhanced anti-tumor responses, we intratumorally treated mice with PBS, untransduced allogeneic T cells, TIL 1383I TCR transduced syngeneic T cells, and TIL 1383I TCR transduced allogeneic T cells alone or in combination with intraperitoneal administration of 1) anti-PD-1 mAb monotherapy, 2) anti-CTLA-4 mAb monotherapy, or 3) anti-PD-1 mAb/anti-CTLA-4 mAb dual therapy (Fig 90). We continued to administer checkpoint inhibitors twice weekly. We additionally wanted to determine if the combination of checkpoint inhibitors further improved systemic anti-tumor responses.

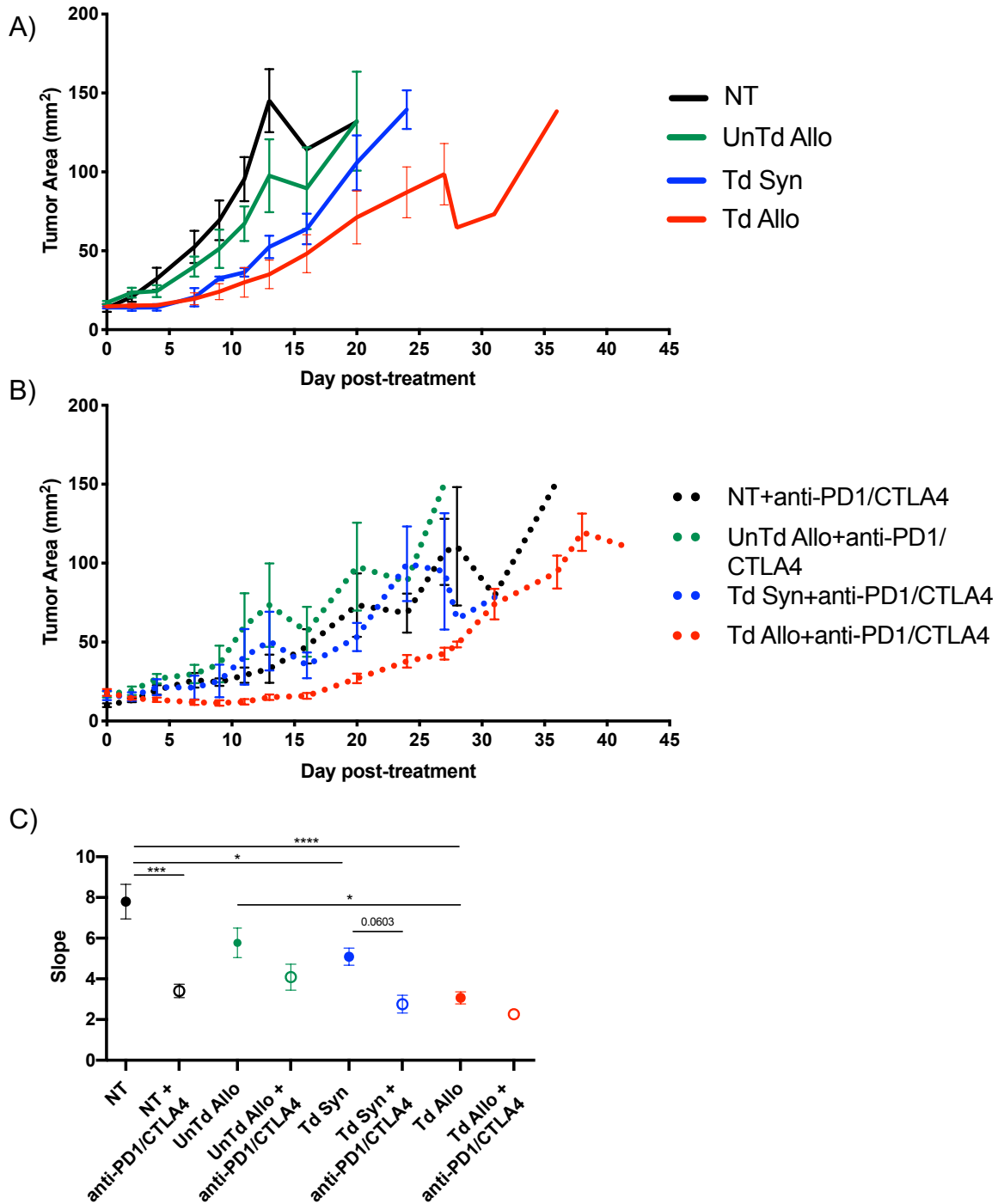


**Figure 89. Intratumoral Treatment with TIL 1383I TCR Transduced T Cells and Anti-PD-1/Anti-CTLA-4 Monoclonal Antibodies Suppresses B16 A2/K<sup>b</sup> Tumor Growth.** B16 A2/K<sup>b</sup> tumor-bearing mice were treated with A) intratumoral T cells only or B) intratumoral T cells and intraperitoneal anti-PD-1 mAb (200 µg) and anti-CTLA-4 mAb (200 µg) in 100 µl volume. C) Slope obtained through linear regression analysis of B16 A2/K<sup>b</sup> tumor growth averaged from one experiment with 4-5 mice/group. Graph shows mean ± SEM; Statistical analysis performed using one-way ANOVA with Tukey correction [\*P<0.05, \*\*\*P<0.001, \*\*\*\*P<0.0001]

A)

T cells + anti-PD-1 mAb/anti-CTLA-4 mAb			
NT	UnTd Allo	0.9805	ns
NT	Td Syn	0.9845	ns
NT	Td Allo	0.7621	ns
UnTd Allo	Td Syn	0.5453	ns
UnTd Allo	Td Allo	0.1817	ns
Td Syn	Td Allo	0.9955	ns

T cells			
NT	UnTd Allo	0.1912	ns
NT	Td Syn	0.0297	*
NT	Td Allo	<0.0001	****
UnTd Allo	Td Syn	0.9849	ns
UnTd Allo	Td Allo	0.0292	*
Td Syn	Td Allo	0.189	ns

B)

NT			
T cells only	anti-PD-1 mAb/anti-CTLA-4 mAb	0.0001	***
UnTd Allo			
T cells only	anti-PD-1 mAb/anti-CTLA-4 mAb	0.3238	ns
Td Syn			
T cells only	anti-PD-1 mAb/anti-CTLA-4 mAb	0.0603	ns
Td Allo			
T cells only	anti-PD-1 mAb/anti-CTLA-4 mAb	0.9501	ns

**Table 5. Log-Rank (Mantel-Cox) Test of B16 Tumor-Free Mice Following Treatment with TIL 1383I TCR Transduced T Cells and Anti-PD-1/Anti-CTLA-4 Monoclonal Antibodies.** On day 10 post- B16 A2/K<sup>b</sup> tumor inoculation, mice were treated with intratumoral T cells and i.p anti-CTLA-4/anti-PD-1 monoclonal antibodies. A) Comparison of checkpoint inhibitor treatment groups B) Comparison of T cell treatment groups. Data represent one experiment with 4-5 mice/group. Statistics performed using the Log Rank (Mantel-Cox) test. [\*P<0.05, \*\*\*P<0.001, \*\*\*\*P<0.0001]

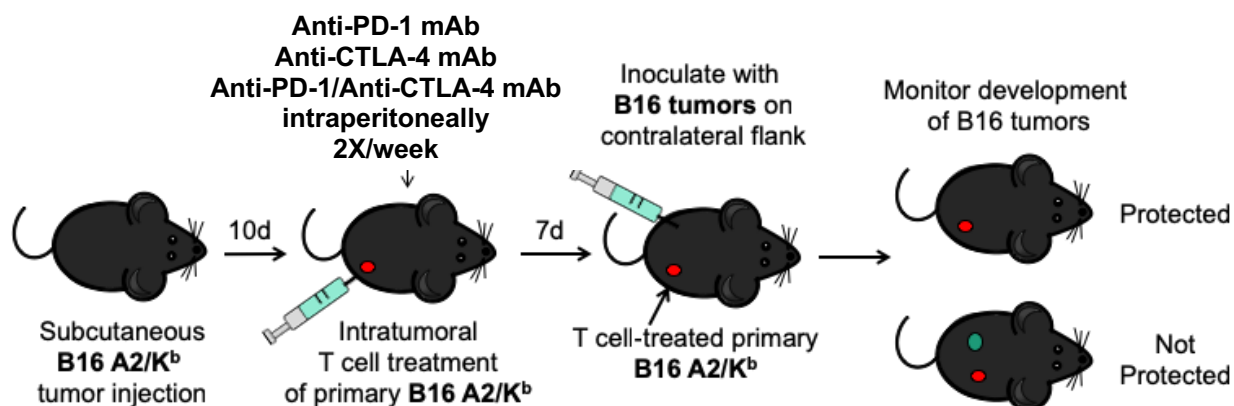


**Figure 90. Experimental Design to Determine If the Combination of Anti-PD-1 and Anti-CTLA-4 Monoclonal Antibodies and TIL 1383I TCR Transduced T Cell Treatment Enhances Anti-Tumor Responses.** Mice were subcutaneously inoculated with  $2.5 \times 10^5$  B16 A2/K<sup>b</sup> tumor cells and ten days later, were treated i.p with PBS, anti-PD-1 mAb, anti-CTLA-4 mAb, or dual anti-PD-1 mAb/anti-CTLA-4 mAb, and intratumoral injections of TIL 1383I TCR transduced allogeneic T cells, TIL 1383I TCR transduced syngeneic T cells, untransduced allogeneic T cells, or PBS. Administration of anti-PD-1 mAb and anti-CTLA-4 mAb continued 2x/week. Seven days post-T cell treatment, mice were challenged with  $1.0 \times 10^5$  B16 tumor cells on the left contralateral flank. Mice were monitored for survival and the appearance of B16 tumors. Mice were sacrificed when one tumor or the sum of both tumors exceeded  $150 \text{ mm}^2$  or  $>10\%$  of body weight.

Therefore, seven days after intratumoral treatment, mice were challenged with B16 on the contralateral flank and monitored for survival and development of B16. The addition of anti-PD-1 mAb and anti-CTLA-4 mAb to all intratumoral treatment groups significantly improved the survival of B16 A2/K<sup>b</sup> tumor-bearing mice (Fig 91, Table 6). Additionally, the median survival of mice treated with the combination of systemic anti-PD-1 mAb/anti-CTLA-4 mAb and intratumoral TIL 1383I TCR transduced T cells was 55 days post-T cell treatment compared to a median survival of 30 days following intratumoral treatment with TIL 1383I TCR transduced allogeneic T cells only ( $P=0.0002$ ). The

addition of anti-CTLA-4 mAb monotherapy significantly improved the survival of tumor-bearing mice compared to the addition of anti-PD-1 mAb monotherapy ( $P=0.0003$ ; Fig 91, Table 6), indicating that anti-CTLA-4 mAb was predominantly mediating the improved survival in the dual therapy-treated mice. Even with the addition of anti-CTLA-4 mAb and anti-PD-1 mAb, treatment with TIL 1383I TCR transduced allogeneic T cells significantly improved survival compared to TIL 1383I TCR transduced syngeneic T cells (median survival: 55 vs. 42.5 days;  $P=0.0266$ ). These results supported our hypothesis that anti-CTLA-4 mAb monotherapy or anti-CTLA-4 mAb/anti-PD-1 mAb dual therapy significantly prolonged survival of B16 A2/K<sup>b</sup> tumor-bearing mice.

The addition of anti-CTLA-4 mAb monotherapy or anti-PD-1 mAb and anti-CTLA-4 mAb dual therapy induced significant regression of B16 A2/K<sup>b</sup> tumors compared to intratumoral T cells only or in combination with anti-PD-1 monotherapy (Fig 92 and 93, Table 7). The combination of intratumoral TIL 1383I TCR transduced allogeneic T cells and dual checkpoint therapy often resulted in complete regression of B16 A2/K<sup>b</sup> primary tumors ( $P<0.0001$  compared to TIL 1383I TCR transduced allogeneic T cells only). Dual anti-PD-1 mAb/ anti-CTLA-4 mAb or anti-CTLA-4 mAb monotherapy significantly attenuated B16 A2/K<sup>b</sup> tumor progression compared to intratumoral treatment with PBS ( $P=0.0002$ ), untransduced allogeneic T cells ( $P<0.0001$ ), and TIL 1383I TCR transduced allogeneic T cells only ( $P<0.0001$ ). These results demonstrated that anti-CTLA-4 mAb or anti-PD-1 mAb/anti-CTLA-4 mAb dual therapy can promote complete regression of B16 A2/K<sup>b</sup> tumors following treatment with TIL 1383I TCR transduced allogeneic T cells.

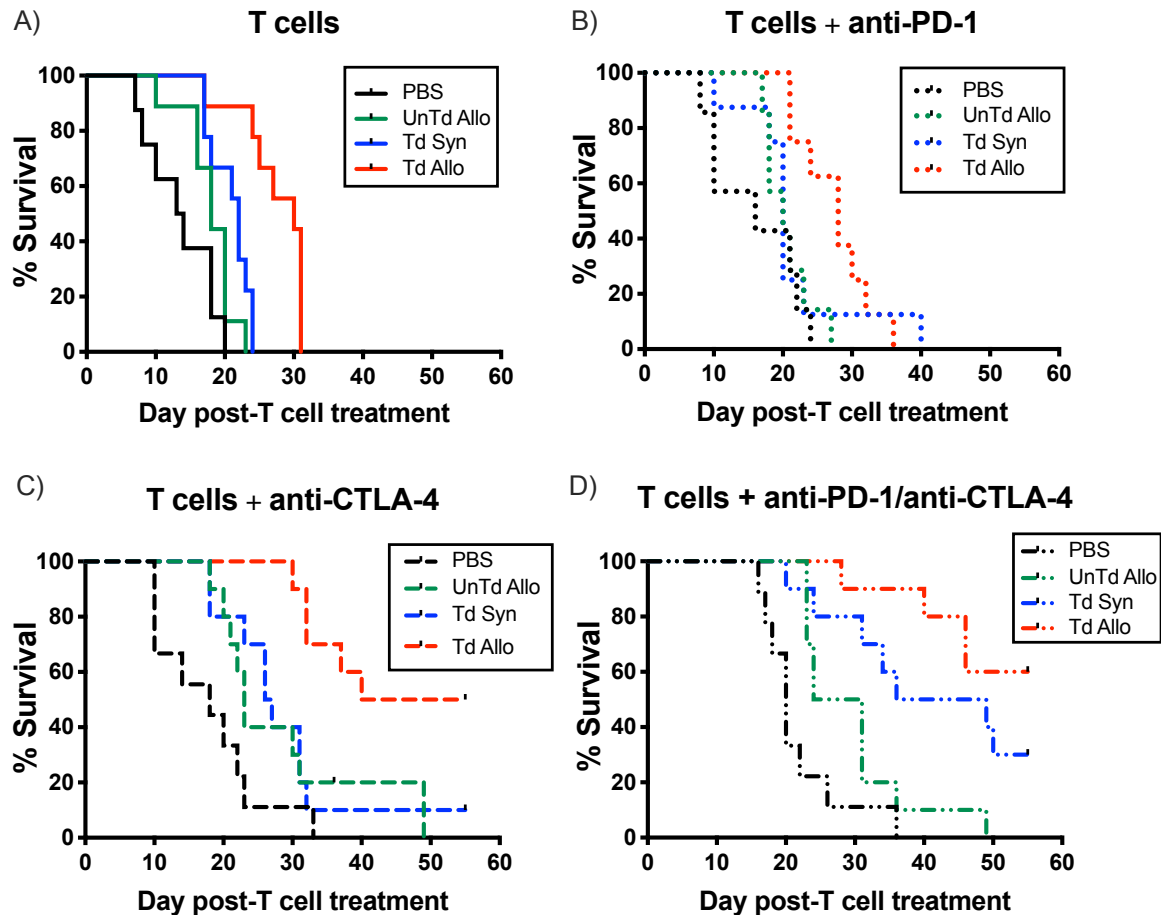


**Figure 91. The Combination of TIL 1383I TCR Transduced Allogeneic T Cells and Anti-PD-1/Anti-CTLA-4 Improves Survival of B16 A2/K<sup>b</sup> Tumor-Bearing Mice.** On day 10 post-B16 A2/K<sup>b</sup> tumor inoculation, mice were treated with (A) intratumoral T cells only (B) intratumoral T cells and i.p anti-PD-1 mAb (C) intratumoral T cells and i.p anti-CTLA-4 mAb (D) intratumoral T cells and i.p anti-PD-1/anti-CTLA-4 mAbs. Tumors were measured with a digital caliper 2-3 times per week. Mice were sacrificed when tumor reached >150 mm<sup>2</sup> or >10% body weight. Data represent two independent experiments with 4-5 mice/group.



A)

T cells				T cells + anti-PD-1			
PBS	UnTd Allo	0.0656	ns	PBS	UnTd Allo	0.7593	ns
PBS	Td Syn	0.0021	**	PBS	Td Syn	0.6132	ns
PBS	Td Allo	0.0001	***	PBS	Td Allo	0.0029	**
UnTd Allo	Td Syn	0.0621	ns	UnTd Allo	Td Syn	0.1154	ns
UnTd Allo	Td Allo	0.0003	***	UnTd Allo	Td Allo	0.0035	**
Td Syn	Td Allo	0.0007	***	Td Syn	Td Allo	0.0151	*
T cells + anti-CTLA-4				T cells + anti-PD-1/anti-CTLA-4			
PBS	UnTd Allo	0.051	ns	PBS	UnTd Allo	0.0202	*
PBS	Td Syn	0.0478	*	PBS	Td Syn	0.0012	**
PBS	Td Allo	<0.0001	****	PBS	Td Allo	<0.0001	****
UnTd Allo	Td Syn	0.1468	ns	UnTd Allo	Td Syn	0.0201	*
UnTd Allo	Td Allo	0.0031	**	UnTd Allo	Td Allo	0.0003	***
Td Syn	Td Allo	0.0035	**	Td Syn	Td Allo	0.0266	*

B)

PBS				UnTd Allo			
T cells only	anti-PD-1	0.1705	ns	T cells only	anti-PD-1	0.2223	ns
T cells only	anti-CTLA-4	0.0967	ns	T cells only	anti-CTLA-4	0.003	**
T cells only	anti-PD-1/anti-CTLA-4	0.0078	**	T cells only	anti-PD-1/anti-CTLA-4	<0.0001	****
anti-PD-1	anti-CTLA-4	0.6599	ns	anti-PD-1	anti-CTLA-4	0.0405	*
anti-PD-1	anti-PD-1/anti-CTLA-4	0.248	ns	anti-PD-1	anti-PD-1/anti-CTLA-4	0.0015	**
anti-CTLA-4	anti-PD-1/anti-CTLA-4	0.3397	ns	anti-CTLA-4	anti-PD-1/anti-CTLA-4	0.3828	ns
Td Syn				Td Allo			
T cells only	anti-PD-1	0.8327	ns	T cells only	anti-PD-1	0.8675	ns
T cells only	anti-CTLA-4	0.0031	**	T cells only	anti-CTLA-4	0.0001	***
T cells only	anti-PD-1/anti-CTLA-4	0.0003	***	T cells only	anti-PD-1/anti-CTLA-4	0.0002	***
anti-PD-1	anti-CTLA-4	0.1373	ns	anti-PD-1	anti-CTLA-4	0.0003	***
anti-PD-1	anti-PD-1/anti-CTLA-4	0.002	**	anti-PD-1	anti-PD-1/anti-CTLA-4	<0.0001	****
anti-CTLA-4	anti-PD-1/anti-CTLA-4	0.0509	ns	anti-CTLA-4	anti-PD-1/anti-CTLA-4	0.7604	ns

**Table 6. Log-Rank (Mantel-Cox) Test of Survival Following Combination Treatment with TIL 1383I TCR Transduced T Cells and Anti-PD-1/Anti-CTLA-4 Monoclonal Antibodies.** A) Comparing the efficacy of PBS, untransduced allogeneic T cells, TIL 1383I TCR transduced syngeneic T cells and TIL 1383I TCR transduced allogeneic T cells within checkpoint inhibitor treatment groups B) Comparing the efficacy of anti-PD-1, anti-CTLA-4, and anti-PD-1/CTLA-4 within T cell treatment groups. Results represent two independent experiments with 4-5 mice/group. Statistical analysis using the Log Rank (Mantel-Cox) test. [\* P<0.05, \*\*P<0.01, \*\*\*P<0.001, \*\*\*\*P<0.0001]

Intratumoral treatment with TIL 1383I TCR transduced allogeneic T cells in combination with systemic anti-PD-1 mAb/anti-CTLA-4 mAb dual therapy resulted in nearly 100% protection from developing B16 tumors in comparison to TIL 1383I TCR transduced allogeneic T cells alone ( $P=0.0051$ ; Fig 94 and Table 8). Intratumoral treatment with TIL 1383I TCR transduced allogeneic T cells in combination with anti-CTLA-4 mAb monotherapy resulted in B16 protection in approximately 80% of mice ( $P=0.0056$  compared to TIL 1383I TCR transduced allogeneic T cells only). Consistent with previous experiments, intratumoral treatment with TIL 1383I TCR transduced allogeneic T cells alone or in combination with anti-PD-1 mAb monotherapy protected approximately 30-40% of mice from B16 development.

In mice that were intratumorally treated with TIL 1383I TCR transduced syngeneic T cells, the addition of anti-PD-1 mAb /anti-CTLA-4 mAb dual therapy resulted in approximately 80% protection from developing B16 tumors ( $P= 0.0003$  compared to TIL 1383I TCR transduced syngeneic T cells only) and the addition of anti-CTLA-4 mAb monotherapy resulted in approximately 40% of mice that were B16 tumor-free ( $P=0.5445$  compared to TIL 1383I TCR transduced syngeneic T cells only). The addition of anti-CTLA-4 monotherapy or anti-PD-1 mAb/anti-CTLA-4 mAb dual therapy to PBS- or untransduced allogeneic T cell- treated mice resulted in the protection of 5% and 10% of mice, respectively, from developing B16 tumors. In some cases, there were mice that were protected from developing B16 tumors but succumbed to B16 A2/K<sup>b</sup> tumor burden. These mice are reflected in Fig 94 as a black mark on the curve. The final number of B16 tumor-free mice is indicated at the end of each line. Furthermore, we observed a substantially higher number of mice developing vitiligo after treatment

with TIL 1383I TCR transduced allogeneic T cells and dual anti-PD-1 mAb/anti-CTLA-4 mAb or mono-anti-CTLA-4 mAb checkpoint inhibitor therapy (Fig 95). Interestingly, vitiligo was present at the primary B16 A2/K<sup>b</sup> tumor site or at the contralateral flank where B16 was inoculated. One mouse developed evidence of vitiligo under the belly. These data provide evidence that the combination of intratumoral treatment with TIL 1383I TCR transduced allogeneic T cells and anti-PD-1 mAb/anti-CTLA-4 mAb dual therapy can mediate complete regression of primary B16 A2/K<sup>b</sup> tumors and provide durable immunity to prevent the development of distant, untreated B16 tumors on the contralateral flank.

### Summary

In this section, we investigated whether combination therapies might augment the efficacy of intratumoral delivery of TIL 1383I TCR transduced T cells. We targeted the innate immune components by stimulating TLR3 with poly I:C in combination with intratumoral T cells. However, we were unable to observe a substantial difference in primary B16 A2/K<sup>b</sup> tumor growth and T cells cross-priming when intratumoral poly I:C was given the day after T cell treatment. In the second method, we engineered the retroviral vector used to express the TIL 1383I TCR to include the extracellular domain of the LIGHT protein. Treatment with T cells co-expressing the TIL 1383I TCR and LIGHT protein resulted in equal or worse anti-tumor responses compared to TIL 1383I TCR transduced T cells alone. We observed similar results when recombinant LIGHT protein was administered with TIL 1383I TCR transduced T cell treatment. The best anti-tumor responses were observed in mice following the combination of TIL 1383I TCR transduced allogeneic T cells and anti-CTLA-4 mAb monotherapy or anti-CTLA-

4/anti-PD-1 dual therapy, which resulted in protection from developing contralateral B16 tumors in nearly all treated mice.

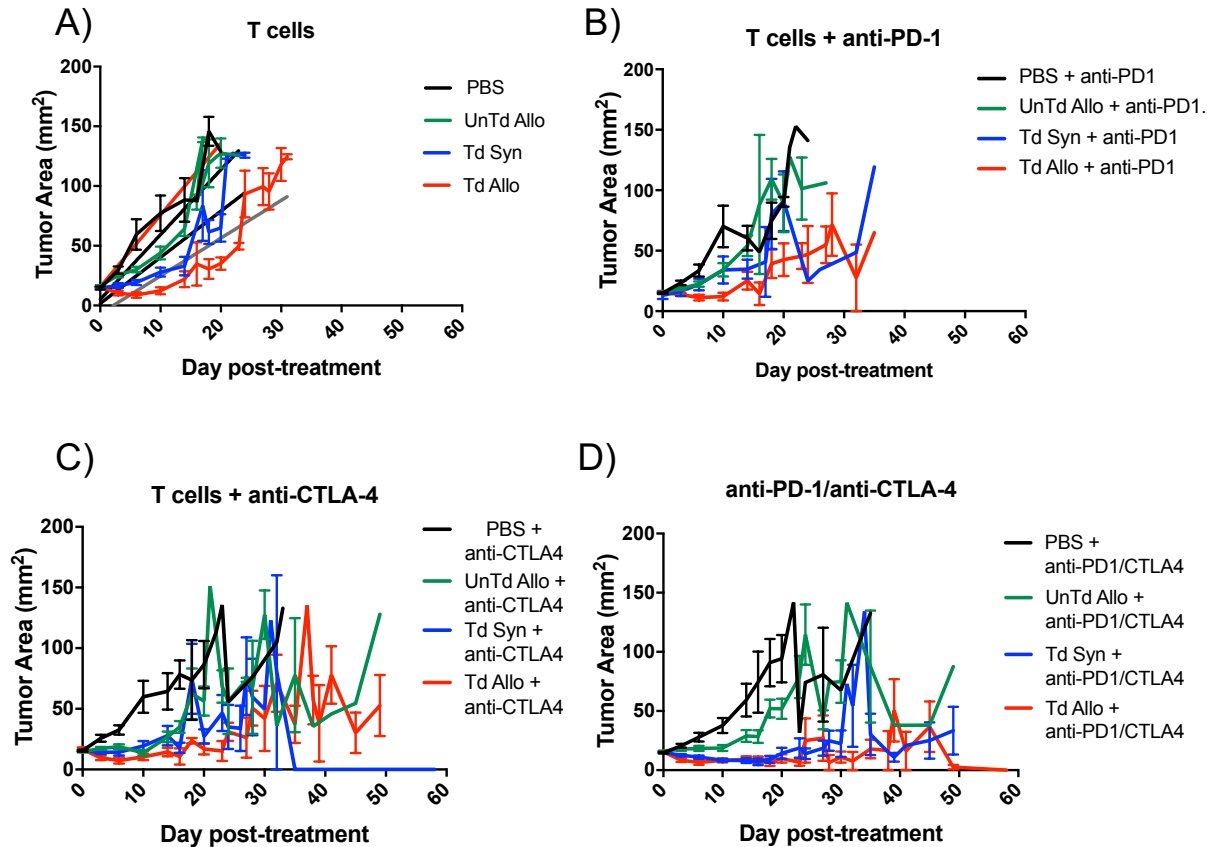


**Figure 92. The Combination of TIL 1383I TCR Transduced T Cells and Anti-PD-1/Anti-CTLA-4 Suppresses B16 A2/K<sup>b</sup> Tumor Growth.** On day 10 post-B16 A2/K<sup>b</sup> tumor inoculation, mice were treated with (A) intratumoral T cells only (B) intratumoral T cells and i.p anti-PD-1 mAb (C) intratumoral T cells and i.p anti-CTLA-4 mAb (D) intratumoral T cells and i.p anti-PD-1/anti-CTLA-4 mAbs. Tumors were measured with a digital caliper 2-3 times per week. Mice were sacrificed when one tumor or the sum of both tumors reached >150 mm<sup>2</sup> or >10% body weight. Data represent two independent experiments with 4-5 mice/group. [i.p: intraperitoneal]

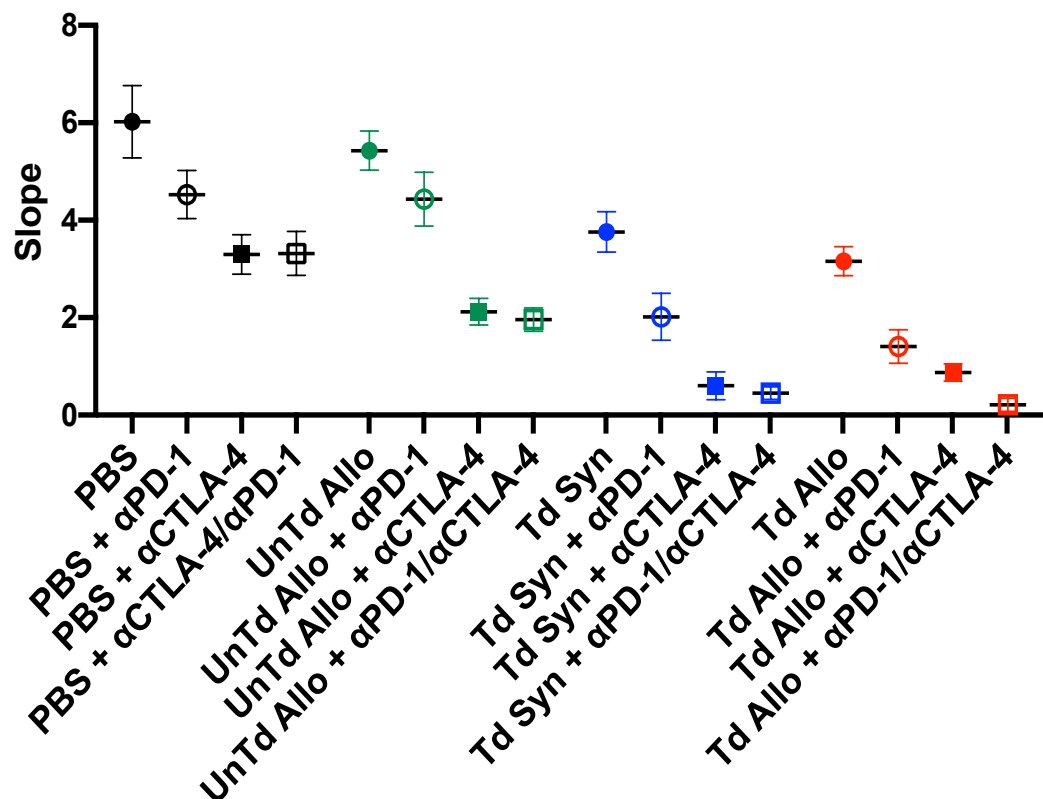


**Figure 93. The Impact of Combination Therapy with TIL 1383I TCR Transduced T Cells and Anti-PD-1/Anti-CTLA-4 on the Slope of B16 A2/K<sup>b</sup> Progression Following Treatment.** On day 10 post-B16 A2/K<sup>b</sup> tumor inoculation, mice were treated with intratumoral T cells only; intratumoral T cells and i.p anti-PD-1; intratumoral T cells and i.p anti-CTLA-4; intratumoral T cells and i.p anti-PD-1/anti-CTLA-4. Tumors were measured with a digital caliper 2-3 time per week. Mice were sacrificed when one tumor or the sum of both tumors reached >150 mm<sup>2</sup> or >10% body weight. Slopes were obtained through linear regression analysis of B16 A2/K<sup>b</sup> tumor growth from group averages shown in Fig 88. Data represent two independent experiments with 4-5 mice/group.

A)

T cells				T cells + anti-PD-1			
PBS	UnTd Allo	0.9993	ns	PBS	UnTd Allo	>0.9999	ns
PBS	Td Syn	0.0048	**	PBS	Td Syn	0.0025	**
PBS	Td Allo	<0.0001	****	PBS	Td Allo	<0.0001	****
UnTd Allo	Td Syn	0.1125	ns	UnTd Allo	Td Syn	0.0048	**
UnTd Allo	Td Allo	0.0027	**	UnTd Allo	Td Allo	<0.0001	****
Td Syn	Td Allo	0.9987	ns	Td Syn	Td Allo	0.9992	ns
T cells + anti-CTLA-4				T cells + anti-PD-1/anti-CTLA-4			
PBS	UnTd Allo	0.6123	ns	PBS	UnTd Allo	0.356	ns
PBS	Td Syn	<0.0001	****	PBS	Td Syn	<0.0001	****
PBS	Td Allo	0.0005	***	PBS	Td Allo	<0.0001	****
UnTd Allo	Td Syn	0.1583	ns	UnTd Allo	Td Syn	0.165	ns
UnTd Allo	Td Allo	0.4645	ns	UnTd Allo	Td Allo	0.0452	*
Td Syn	Td Allo	>0.9999	ns	Td Syn	Td Allo	>0.9999	ns

B)

PBS				UnTd Allo			
T cells only	anti-PD-1	0.3998	ns	T cells only	anti-PD-1	0.9158	ns
T cells only	anti-CTLA-4	0.0002	***	T cells only	anti-CTLA-4	<0.0001	****
T cells only	anti-PD-1/ar	0.0002	***	T cells only	anti-PD-1/ar	<0.0001	****
anti-PD-1	anti-CTLA-4	0.6941	ns	anti-PD-1	anti-CTLA-4	0.0042	**
anti-PD-1	anti-PD-1/ar	0.7198	ns	anti-PD-1	anti-PD-1/ar	0.0013	**
anti-CTLA-4	anti-PD-1/ar	>0.9999	ns	anti-CTLA-4	anti-PD-1/ar	>0.9999	ns
Td Syn				Td Allo			
T cells only	anti-PD-1	0.1014	ns	T cells only	anti-PD-1	0.0961	ns
T cells only	anti-CTLA-4	<0.0001	****	T cells only	anti-CTLA-4	0.0016	**
T cells only	anti-PD-1/ar	<0.0001	****	T cells only	anti-PD-1/ar	<0.0001	****
anti-PD-1	anti-CTLA-4	0.3437	ns	anti-PD-1	anti-CTLA-4	0.9997	ns
anti-PD-1	anti-PD-1/ar	0.1896	ns	anti-PD-1	anti-PD-1/ar	0.642	ns
anti-CTLA-4	anti-PD-1/ar	>0.9999	ns	anti-CTLA-4	anti-PD-1/ar	0.9935	ns

**Table 7. Statistical Analysis of the Slope of B16 A2/K<sup>b</sup> Tumors Following Treatment with TIL 1383I TCR Transduced T Cells and Anti-PD-1/Anti-CTLA-4 Monoclonal Antibodies.** A) Comparing the efficacy of PBS, untransduced allogeneic T cells, TIL 1383I TCR transduced syngeneic T cells and TIL 1383I TCR transduced allogeneic T cells within checkpoint inhibitor treatment groups B) Comparing the efficacy of anti-PD-1 mAb, anti-CTLA-4 mAb, and anti-PD-1/CTLA-4 mAbs within T cell treatment groups. Results represent two independent experiments with 4-5 mice/group. Statistical analysis using the Log Rank (Mantel-Cox) test. [\* P<0.05, \*\*P<0.01, \*\*\*P<0.001, \*\*\*\*P<0.0001]

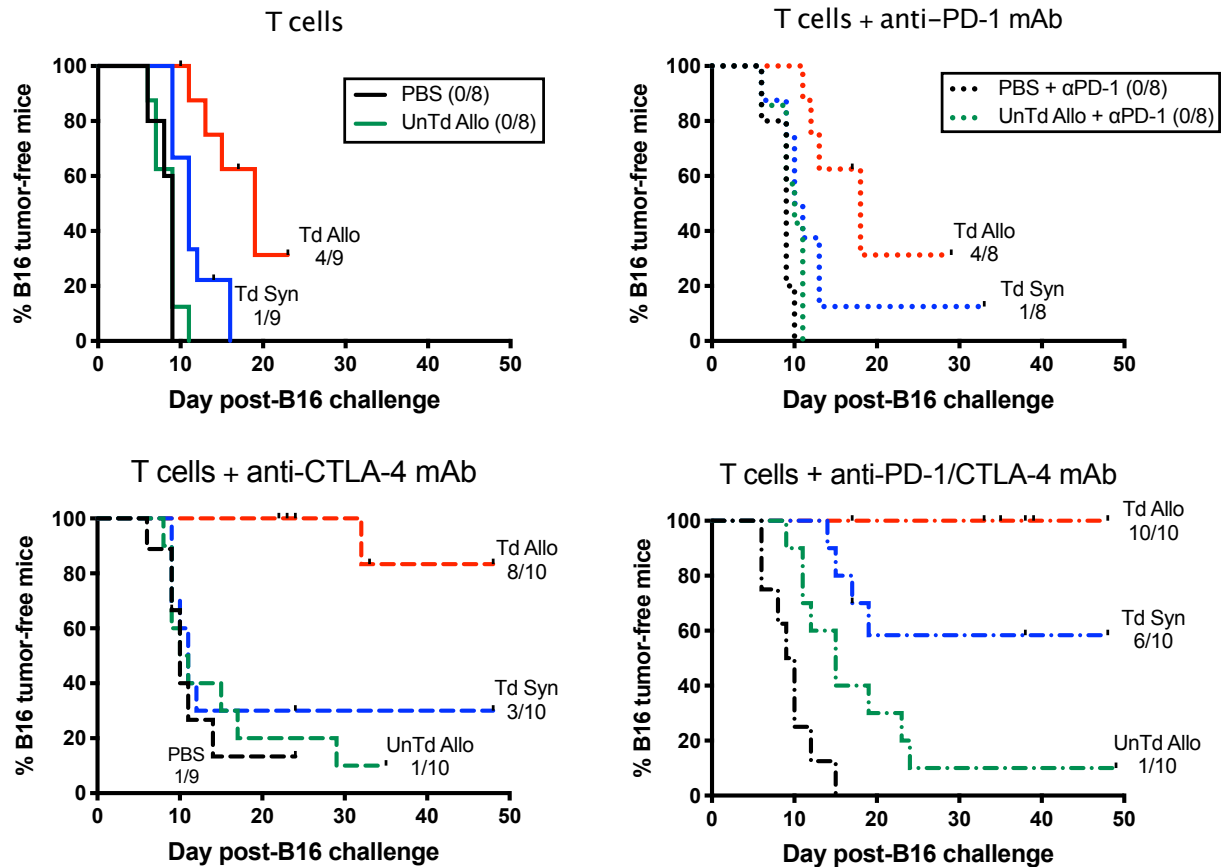


**Figure 94. The Combination of TIL 1383I TCR Transduced T Cells and Anti-PD-1/Anti-CTLA-4 Monoclonal Antibodies Mediates Complete Protection Against the Development of Contralateral B16 Tumors.** On day 10 post-B16 A2/K<sup>b</sup> tumor inoculation, mice were treated with (A) intratumoral T cells only (B) intratumoral T cells and i.p anti-anti-PD-1 (C) intratumoral T cells and i.p anti-CTLA-4 (D) intratumoral T cells and i.p anti-PD-1/anti-CTLA-4. Tumors were measured with a digital caliper 2-3 times per week. Mice were sacrificed when tumor reached >150 mm<sup>2</sup> or >10% body weight. Data represent two independent experiments with 4-5 mice/group. Number of B16 tumor-free mice shown at the end of each line.



A)

T cells				T cells + anti-PD-1			
PBS	UnTd Allo	0.7068	ns	PBS	UnTd Allo	0.1282	ns
PBS	Td Syn	0.0058	**	PBS	Td Syn	0.0415	*
PBS	Td Allo	0.0002	***	PBS	Td Allo	0.0002	***
UnTd Allo	Td Syn	0.0079	**	UnTd Allo	Td Syn	0.2262	ns
UnTd Allo	Td Allo	<0.0001	****	UnTd Allo	Td Allo	0.0005	***
Td Syn	Td Allo	0.0059	**	Td Syn	Td Allo	0.0572	ns
T cells + anti-CTLA-4				T cells + anti-PD-1/anti-CTLA-4			
PBS	UnTd Allo	0.6308	ns	PBS	UnTd Allo	0.0056	**
PBS	Td Syn	0.426	ns	PBS	Td Syn	<0.0001	****
PBS	Td Allo	0.0001	***	PBS	Td Allo	<0.0001	****
UnTd Allo	Td Syn	0.5718	ns	UnTd Allo	Td Syn	0.0268	*
UnTd Allo	Td Allo	0.0001	***	UnTd Allo	Td Allo	<0.0001	****
Td Syn	Td Allo	0.0025	**	Td Syn	Td Allo	0.028	*

B)

PBS				UnTd Allo			
T cells only	anti-PD-1	0.338	ns	T cells only	anti-PD-1	0.1529	ns
T cells only	anti-CTLA-4	0.0201	*	T cells only	anti-CTLA-4	0.0191	*
T cells only	anti-PD-1/anti-CTL	0.2149	ns	T cells only	anti-PD-1/anti-CTLA-4	0.0003	***
anti-PD-1	anti-CTLA-4	0.0713	ns	anti-PD-1	anti-CTLA-4	0.2067	ns
anti-PD-1	anti-PD-1/anti-CTL	0.411	ns	anti-PD-1	anti-PD-1/anti-CTLA-4	0.0024	**
anti-CTLA-4	anti-PD-1/anti-CTL	0.3936	ns	anti-CTLA-4	anti-PD-1/anti-CTLA-4	0.5282	ns
Td Syn				Td Allo			
T cells only	anti-PD-1	0.9905	ns	T cells only	anti-PD-1	0.8336	ns
T cells only	anti-CTLA-4	0.5445	ns	T cells only	anti-CTLA-4	0.0051	**
T cells only	anti-PD-1/anti-CTL	0.0003	***	T cells only	anti-PD-1/anti-CTLA-4	0.0056	**
anti-PD-1	anti-CTLA-4	0.5965	ns	anti-PD-1	anti-CTLA-4	0.0051	**
anti-PD-1	anti-PD-1/anti-CTL	0.002	**	anti-PD-1	anti-PD-1/anti-CTLA-4	0.0056	**
anti-CTLA-4	anti-PD-1/anti-CTL	0.0382	*	anti-CTLA-4	anti-PD-1/anti-CTLA-4	0.2207	ns

**Table 8. Log-Rank (Mantel-Cox) Test of B16 Tumor-Free Mice Following Treatment with TIL 1383I TCR Transduced T Cells and Anti-PD-1/Anti-CTLA-4 Monoclonal Antibodies.** A) Comparing the efficacy of PBS, untransduced allogeneic T cells, TIL 1383I TCR transduced syngeneic T cells and TIL 1383I TCR transduced allogeneic T cells within checkpoint inhibitor treatment groups B) Comparing the efficacy of anti-PD-1, anti-CTLA-4, and anti-PD-1/CTLA-4 within T cell treatment groups. Results represent two independent experiments with 4-5 mice/group. Statistical analysis using the Log Rank (Mantel-Cox) test. [\* P<0.05, \*\*P<0.01, \*\*\*P<0.001]

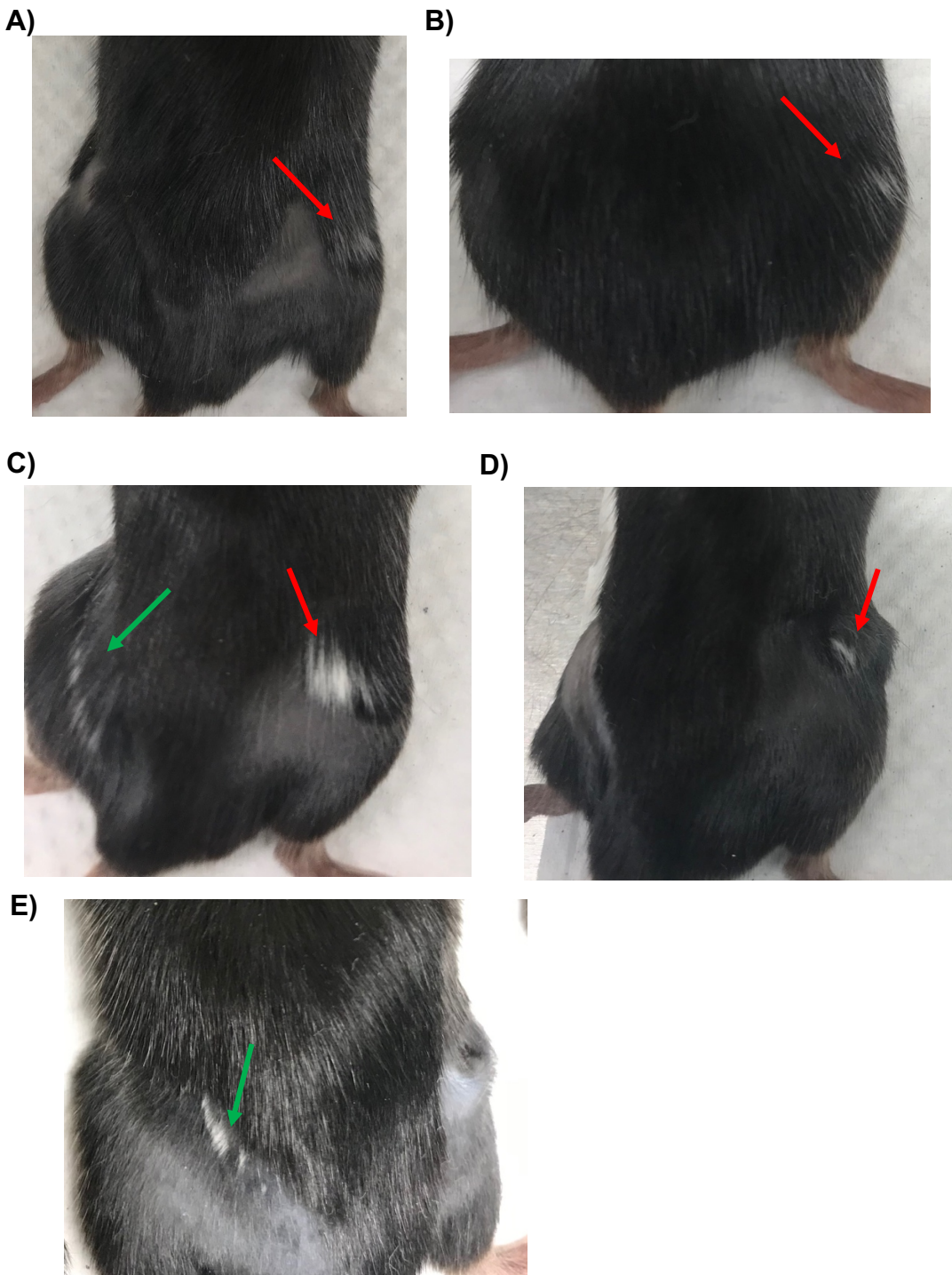


**Figure 95. Increased Incidence of Vitiligo with the Combination of TIL 1383I TCR Transduced Allogeneic T Cells and Anti-PD-1/Anti-CTLA-4 Monoclonal Antibodies.** Development of vitiligo following intratumoral treatment with TIL 1383I TCR transduced allogeneic T cells in combination with A-B) anti-CTLA mAb or C-E) anti-PD-1 mAb/anti-CTLA-4 mAb. Red arrow indicates site of B16 A2/K<sup>b</sup> primary tumor and green arrow indicates site of B16 inoculation.

## CHAPTER EIGHT

### DISCUSSION

#### **Introduction**

Adoptive cell transfer (ACT) of autologous TCR gene-modified T cells targeting tumor antigens is a promising therapeutic strategy currently in clinical trials for patients with advanced malignancies. We have seen clinical and biologic responses treating patients with autologous TIL 1383I TCR transduced T cells administered intravenously, as well as treating patients with allogeneic MART-1- specific TCR transduced T cells administered intratumorally<sup>1,2</sup>. However, only a small subset of patients achieved long-term and durable responses. Some of the factors that influence the outcome of immunotherapy are the immunosuppressive tumor microenvironment (TME), heterogeneity of solid tumors, and evasion of immune cell detection. Patients presenting with cold tumors, which are characterized by a lack of CD8<sup>+</sup> T cells and interferon-stimulatory genes, often have poor prognoses. Conversely, patients presenting with hot, or T cell-inflamed, tumors are more likely to respond to immunotherapies. Therefore, it would be advantageous to engineer TCR gene-modified T cells capable of converting cold tumors into hot tumors to counteract the immunosuppressive TME.

The goal of this dissertation was to utilize intratumoral injections of TCR gene-modified allogeneic T cells to mediate direct interactions for tumor-specific killing and induce local inflammatory immune responses. We developed an animal model utilizing subcutaneous B16 A2/K<sup>b</sup> mouse melanoma tumors that express the tyrosinase antigen

in the context of HLA-A2, which permits recognition by TIL 1383I TCR transduced T cells. This mouse model also allowed us to assess the capacity of TIL 1383I TCR transduced T cell treatment to generate B16-reactive endogenous T cells, thus broadening the anti-tumor T cell response beyond the TCR specificity conferred by the adoptively transferred cells. We conclude that the tumor-specific response, characterized by TIL 1383I TCR-mediated tumor destruction leading to the release of tumor antigens, and the allogeneic response, mediated by the host recognition of foreign donor T cells, synergize to improve responses against injected B16 A2/K<sup>b</sup> tumors and to promote systemic, endogenous tumor-specific T cell responses that can protect against distant, uninjected B16 tumors.

### **Intratumoral Delivery of TIL 1383I TCR Transduced T Cells Extends Survival and Suppresses B16 A2/K<sup>b</sup> Tumor Growth**

Mouse T cells transduced to express the TIL 1383I TCR recognize B16 A2/K<sup>b</sup> tumor cells, but not B16 tumor cells, in a CD8-independent manner. We observed a significant frequency of TIL 1383I TCR transduced T cells expressing CD107a, IFN- $\gamma$  and TNF- $\alpha$  in response to B16 A2/K<sup>b</sup> tumors *in vitro*, indicating the potential for therapeutic efficacy *in vivo*<sup>497</sup>. Intratumoral treatment of B16 A2/K<sup>b</sup> tumors with TIL 1383I TCR transduced allogeneic T cells improved survival and suppressed B16 A2/K<sup>b</sup> tumor growth compared to intratumoral treatment of B16 A2/K<sup>b</sup> tumors with TIL 1383I TCR transduced syngeneic T cells or untransduced allogeneic T cells. After one intratumoral injection, we observed differences in B16 A2/K<sup>b</sup> progression between TIL 1383I TCR transduced syngeneic and TIL 1383I TCR transduced allogeneic T cell-treated mice that remained consistent among independent experiments. Translationally,

current clinical trials testing intratumoral delivery of TCR gene-modified T cells have demonstrated the feasibility of multiple injections into metastatic lesions<sup>2,111,498</sup>.

Therefore, while our studies performed one intratumoral injection for the purposes of reproducibility and consistency in measuring tumor development, we expect that multiple intratumoral injections would likely lead to more effective regression of injected lesions in patients with cancer.

We observed additional factors that influenced the robustness and breadth of the anti-tumor response following T cell treatment. One factor that affected anti-tumor responses was the transduction efficiency of transferred TIL 1383I TCR transduced T cells. The transduction efficiency, measured by expression of GFP and V $\beta$ 12, averaged  $51.2 \pm 3.5\%$  GFP<sup>+</sup>V $\beta$ 12<sup>+</sup> T cells for syngeneic HLA-A2 transgenic mice and  $49.5 \pm 3.5\%$  GFP<sup>+</sup>V $\beta$ 12<sup>+</sup> T cells for allogeneic BALB/c mice. In earlier experiments, we obtained 30-40% TIL1383I TCR transduced T cells, with later experiments reaching  $\geq 60$ -70% GFP<sup>+</sup>V $\beta$ 12<sup>+</sup> T cells. Experiments performed with T cells that were transduced at efficiencies  $\geq 60\%$  tended to result in better regression of B16 A2/K<sup>b</sup> tumors and more robust anti-tumor immunity upon characterization of the tumor and tumor draining lymph nodes. These findings suggest that the maximum frequency of TCR gene-modified T cells within the infused T cell product should be used.

Our lab has developed a novel approach to enrich for T cells expressing the tumor-specific TCR following transduction. The retroviral vector includes a truncated CD34 molecule (CD34t) to serve as a transgene selection marker. Using a CliniMacs, TIL 1383I TCR transduced T cells are purified through CD34t selection and expanded to large quantities. We would anticipate that intratumoral injection with a high dose of pure

TIL 1383I TCR transduced allogeneic T cells would lead to more efficient killing of primary, injected tumors leading to either complete regression of injected lesions or to prolonged progression-free survival.

The second factor that influenced the outcome of treatment with TIL 1383I TCR transduced T cells was the size of the primary tumor at the time of treatment. As expected, larger tumors ( $>30\text{mm}^2$ ) were typically more difficult to control following intratumoral T cell treatment compared to smaller tumors. Generally, this problem mostly affects mouse studies, as patient tumors are often much smaller in relative size to their body. Additionally, the final size of T cell-treated B16 A2/K<sup>b</sup> tumors correlated with the extent of T cell cross-priming. Therefore, smaller tumors at the time of T cell injection, which correlated with tumor regression, might also increase systemic anti-tumor T cell responses. Taken together, the frequency of tumor-specific transduced T cells and size of the tumor lesion used for injection can influence the anti-tumor responses following intratumoral T cell treatment.

### **The Recipient Immune Recognition of Foreign Allogeneic Donor Cells Enhances the Efficacy of Intratumoral Treatment with TIL 1383I TCR Transduced Allogeneic T Cell Treatment**

Syngeneic and allogeneic donor T cells transduced to express the TIL 1383I TCR exhibited similar polyfunctional phenotypes against B16 A2/K<sup>b</sup> tumors cells *in vitro*. TIL 1383I TCR transduced allogeneic T cells were more effective than TIL 1383I TCR transduced syngeneic T cells at suppressing the growth of B16 A2/K<sup>b</sup> tumors. Using recipient NSG A2 mice, which are defective in myeloid and lymphoid lineage-derived cells, we observed that the injection of B16 A2/K<sup>b</sup> tumors with TIL 1383I TCR

transduced allogeneic T cells resulted in strikingly similar survival outcomes and ability to suppress tumor growth compared to TIL 1383I TCR transduced syngeneic T cell-treated mice. We also detected TIL 1383I TCR transduced T cells in the tumors of NSG A2 recipient mice up to twenty days post-T cell treatment. In comparison, TIL 1383I TCR transduced T cells were undetectable in the tumors implanted in immunocompetent HLA-A2 transgenic mice by day 7 post-T cell treatment. Although not directly tested, we speculated that the host T cells eliminated the donor T cells, which is why they were undetectable in the tumor by day 7 post-T cell treatment in the immunocompetent recipient mice.

The differences in T cell persistence raises the question of whether the persisting TIL1383I TCR transduced T cells within the tumors of NSG A2 mice continued to mediate tumor killing and cytokine production. If so, the prolonged presence of TIL 1383I TCR transduced T cells could further improve upon the suppression of primary B16 A2/K<sup>b</sup> tumors. However, the persistence of intratumoral tumor-specific T cells required an immunodeficient recipient, which would prevent the induction of DC activation and cross-priming of endogenous T cells. Although the lack of systemic T cell responses would fail to prevent escape of tumor immune variants, the persistence of functional TIL 1383I TCR transduced T cells in the tumors of immunodeficient recipients could potentially induce complete regression of primary tumors. It is unknown whether an immunodeficient recipient, with T cell persistence, would be more advantageous than an immunocompetent recipient, with cross-primed T cells but the transient presence of TIL 1383I TCR transduced T cells.

We retrospectively compared the slopes of B16 A2/K<sup>b</sup> growth following TIL 1383I TCR transduced T cell treatment of HLA-A2 transgenic mice compared to NSG A2 mice. The slope of B16 A2/K<sup>b</sup> growth in NSG A2 mice treated with TIL 1383I TCR transduced syngeneic and TIL 1383I TCR transduced allogeneic T cells was 2.205 and 1.866, respectively. In immunocompetent HLA-A2 transgenic recipient mice, the slope of B16 A2/K<sup>b</sup> tumor progression (within the same time frame as NSG A2 mice) was 3.447 and 1.364 following treatment with TIL 1383I TCR transduced syngeneic T cells and TIL 1383I TCR transduced allogeneic T cells, respectively. This retrospective analysis suggests that the induction of endogenous host T cell cross-priming, which resulted in the induction of epitope spreading (Fig 52 and 56), is more advantageous than the persistence of TIL 1383I TCR transduced allogeneic T cells in the tumor. Interestingly, we observed the opposite findings during treatment with TIL 1383I TCR transduced syngeneic T cells. We observed a lower slope, indicating better tumor suppression, in NSG A2 mice (2.205) compared to slope in HLA-A2 transgenic mice (3.447). This would suggest that in the absence of adequate host T cell cross-priming, as observed in the mice treated with TIL 1383I TCR transduced syngeneic T cells, the persistence of tumor-specific T cells in the tumor might provide additional benefits. NSG A2 mice are defective in both innate and adaptive immunity and it is most likely that the best anti-tumor responses require both components. In our studies, we have demonstrated that the host immune system can contribute to altering the TME to drive the process of T cell cross-priming, which results epitope spreading (the induction of T cells specific to gp100 and TRP-2, Fig 52 and 56), ultimately leading to effective, durable anti-tumor immunity.



## **TIL 1383I TCR Transduced Allogeneic T Cells Induce an Immune-Active Tumor Microenvironment**

Our results indicated that the recipient immune system had the capacity to alter the tumor microenvironment and contribute to the anti-tumor response. Additionally, TIL 1383I TCR transduced T cells produced IFN- $\gamma$  and TNF- $\alpha$  and mediated lytic responses (CD107a<sup>+</sup>) against B16 A2/K<sup>b</sup> tumor targets within 24 hours *in vitro*. This prompted us to investigate the immune components within the tumor. The cytokines IFN- $\gamma$  and TNF- $\alpha$  can promote maturation of dendritic cells. At two days post-T cell treatment, the frequency of CD11c<sup>+</sup>MHCII<sup>+</sup> DCs was 10% of total cells in the tumors of all treatment groups. This is consistent with previous literature indicating that the syngeneic implantable B16 tumor model, in the absence of treatment, contains variable percentages of tumor-infiltrating DCs depending on the size of the tumor<sup>517</sup>. Two days post-T cell treatment, the size of tumors from mice treated with T cells are still relatively similar to the size of tumors from untreated mice, supporting the similar percentages of DCs observed. We observed an increased frequency of CD11c<sup>+</sup>MHCII<sup>+</sup> DCs expressing the co-stimulatory molecule CD80 in the tumors treated with TIL 1383I TCR transduced allogeneic T cells.

Consistent with previous reports, untreated B16 A2/K<sup>b</sup> tumors contained a small subset of CD103<sup>+</sup> and CD205<sup>+</sup>CD11c<sup>+</sup>MHCII<sup>+</sup> DCs<sup>499</sup>. We detected an increase in CD205<sup>+</sup>CD11c<sup>+</sup>MHCII<sup>+</sup>, but not CD103<sup>+</sup>, DCs in tumors from untransduced allogeneic or TIL 1383I TCR transduced syngeneic mice. However, intratumoral treatment with TIL 1383I TCR transduced allogeneic T cells resulted in a significant increase in CD8 $\alpha$ <sup>+</sup> DC, CD103<sup>+</sup> DC, and CD205<sup>+</sup> cross-presenting DC subsets in the tumor two days post-T cell

treatment. There are two possible explanations: 1) the enhanced pro-inflammatory response, due to the allogeneic T cells, was capable of recruiting additional cross-presenting DC subsets to the tumor; however, without the release of tumor antigens, which requires the TIL 1383I TCR, these cross-presenting DC subsets don't acquire tumor antigen and therefore don't migrate to a tumor draining lymph node. 2) in the presence of only antigen release but without the additional inflammatory response, as in the case of TIL 1383I TCR transduced syngeneic T cells, the cross-presenting DCs are not recruited to the tumor and therefore, these mice are unable to generate tumor draining lymph node-activated cross-primed T cells. These results suggested that the allogeneic response, through producing inflammatory cytokines, and tumor-specific responses, through production of inflammatory cytokines, alone can promote the accumulation of DCs expressing CD205 in the tumor; however, the synergy of the two responses, enhanced cytokine production with antigen release, manifested in TCR gene-modified allogeneic T cells, can further promote the accumulation of additional cross-presenting DC subsets.

We also observed increased frequencies of T cells expressing activation markers CD25, CD44, and CD69, and increased frequencies of IFN- $\gamma$ <sup>+</sup> or TNF $\alpha$ <sup>+</sup> CD8<sup>+</sup> T cells in the tumor microenvironment of mice treated with TIL 1383I TCR transduced allogeneic T cells. In support of these findings, we also observed an increase in PD-L1 expression, which has been demonstrated to occur in response to IFN- $\gamma$ , on CD11b<sup>+</sup>CD11c<sup>+</sup> cells. The impact of IFN- $\gamma$ <sup>+</sup> T cells within the tumor microenvironment remains controversial. While IFN- $\gamma$ <sup>+</sup> CD8<sup>+</sup> T cells in the tumor microenvironment can correlate with positive outcomes, IFN- $\gamma$  production also induces PD-L1 expression on tumors which can inhibit

T cell responses and promote angiogenesis. We did not look at the production of IL-12 by DCs, but it is possible that IL-12 could play a role in stimulating T cell responses.

Tumors treated with TIL 1383I TCR transduced syngeneic T cells unexpectedly had the highest frequency of T regulatory (Treg) cells, whereas tumors treated with TIL 1383I TCR transduced allogeneic T cells had the lowest frequency of Tregs. We examined tumors for the presence of Treg seven days post-intratumoral T cells treatment. At this time, we were unable to detect any T cells expressing GFP or H-2<sup>d</sup>, suggesting that the observed Tregs were derived from the host and not the donor T cells. Interestingly, in a small scale experiments, the tumors from NSG A2 recipient mice, where donor T cells had been detected for up to 3 weeks post-T cell treatment, we observed an increased ratio of CD4:CD8 transduced T cells in the tumors of mice treated with TIL 1383I TCR transduced allogeneic T cells. This contrasted to the initial population of transduced T cells that were used for treatment, which was predominantly CD8<sup>+</sup> transduced T cells. Although we did not pursue the observation of increased CD4:CD8 transduced T cells, i.e. whether there was an expansion of CD4<sup>+</sup> Tregs or if the CD8<sup>+</sup> transduced T cells underwent apoptosis, this would be a feasible and interesting future direction.

The Tregs present in the tumors of treated mice could have been induced (iTregs) in the microenvironment or, alternatively, thymic-derived Tregs (nTregs) can be recruited to tumors or expand in tumors<sup>522</sup>. In these experiments, Tregs could have a role in two different ongoing immune responses, anti-tumor and allogeneic, adding another level of complexity. One study demonstrated that 15-40% of CD4<sup>+</sup> T cells in B16 tumors express Foxp3 and indirectly argued in favor of a preferential accumulation

of intratumoral nTregs<sup>524</sup>. One future direction could examine the treated tumors for differences in CCR4, CCL22, or CXCR4, which promote nTreg migration to the tumors<sup>523</sup>, or TGF- $\beta$  which can promote proliferation of Treg *in vivo*<sup>524</sup>.

Tregs are induced in the presence of antigen and TGF- $\beta$  and in the absence of inflammatory stimuli<sup>500</sup>. It is possible that the absence of the potent alloresponse in the tumors treated with TIL 1383I TCR transduced syngeneic T cells promoted the induction of Treg. cells Alloantigen-specific Treg preferentially reside in the spleen, less in the lymph nodes, and not in the thymus or bone marrow<sup>501</sup>. In the context of transplantation tolerance, studies have demonstrated that Treg cells use mainly the indirect antigen recognition pathway to control alloreactive responses<sup>502</sup>. Results from our experiments suggest that direct alloreactive responses are contributing to enhanced anti-tumor immunity. Therefore, Treg cells might not be induced in response to allogeneic T cells within the time frame of the B16 melanoma mouse model. For these experiments, we only examined the tumors for the presence of Tregs, and therefore we cannot determine if there were any treatment related changes in the frequency of Tregs in the spleens or tumor draining lymph nodes of mice.

Tumor-specific and allogeneic responses occur quite rapidly, and therefore it is difficult to determine if the secretion of cytokines by TIL 1383I TCR transduced T cells precedes maturation of DCs. Alternatively, mature, cytokine-producing DCs could be promoting sustained cytokine production by T cells. It is most likely that these immune responses overlap, and the combination of alloreactivity and tumor reactivity extend that activation window leading to more effective DC responses. Collectively, we have demonstrated that intratumoral treatment with TIL 1383I TCR transduced allogeneic T

cells induces DC maturation and T cell activation and cytokine production in the tumor two days post-T cell treatment.

### **Induction of Immune Responses in the Tumor Draining Lymph Nodes**

#### **Following TIL 1383I TCR Transduced Allogeneic T Cell Treatment**

Intratumoral treatment with TIL 1383I TCR transduced allogeneic T cells promoted higher numbers and frequencies of CD11c<sup>+</sup> MHC II<sup>+</sup> conventional DCs in the tumor draining lymph nodes. In contrast to the tumor, we observed more CD86<sup>+</sup> DCs in the tumor draining lymph nodes of T cell-treated mice.

Studies have demonstrated that CD86 is rapidly and abundantly expressed, while CD80 is slowly expressed but has a higher affinity to CD28 and CTLA-4 and, thus, the more potent ligand<sup>503, 504</sup>. Expression of CD80 and CD86 is upregulated in response to the cytokines IFN- $\alpha$ , IFN- $\gamma$ , and GM-CSF<sup>505</sup>. It is possible that the stronger stimulation from the combination of tumor antigen-specific reactivity and alloresponse promoted the increased CD80 expression in the tumor. CD80/CD86 and CD28/CTLA-4 interactions also play a role in the induction and function of T regulatory (Treg) cells. Zheng *et al.* demonstrated that allogeneic mature DCs expressing high levels of CD86 were resistant to Treg suppression<sup>506</sup>. The increased expression of CD80 and CD86 on DCs from the tumors treated with TIL 1383I TCR allogeneic T cells could also prevent Treg suppression. Furthermore, during alloresponses, tolerogenic DCs can promote the induction of Treg cells<sup>507</sup>. The allogeneic response is characterized by the production of inflammatory cytokines, which might overcome the microenvironment-induced tumor suppression. It is possible that the tumor-specific response alone is not enough to overcome tumor resistance mechanisms. The untransduced allogeneic T cell-treated

tumors have the contribution of the alloresponse, which resulted in the activation of DCs and T cells, however without the released tumor antigens from lysed tumors cells mediated by the transduced TCR, these mice are unable to mount a tumor antigen-specific response. Our data suggest that TIL 1383I TCR transduced allogeneic T cell treatment induced mature, conventional DCs that would not promote the induction of Treg cells.

We also observed an accumulation of CD205<sup>+</sup> DCs in the tumor draining lymph nodes of mice treated with TIL 1383I TCR transduced allogeneic T cells. The tumor draining lymph nodes of mice treated with TIL 1383I TCR transduced allogeneic T cells also contained significantly higher frequencies and absolute numbers of mature CD8 $\alpha$ <sup>+</sup> and CD205<sup>+</sup>CD11c<sup>+</sup>MHCII<sup>+</sup> DCs. We also observed an increase in the migratory CD103<sup>+</sup> DCs in the mice treated with TIL 1383I TCR transduced allogeneic T cells. Interestingly, the mice treated with untransduced allogeneic T cells failed to promote these cross-presenting DC subsets. It is possible that the lack of tumor antigens in the microenvironment resulted in the inability to induce cross-presenting DC subsets. These data suggest that the combination of tumor-specificity and alloreactivity can promote cross-presenting DC subsets compared to either response alone.

Previous studies have demonstrated that targeting tumor antigens to CD205<sup>+</sup> DCs enhances tumor-specific CTL responses. Wu and colleagues observed the priming of autologous tumor-specific T cells upon stimulation with allogeneic CD205<sup>+</sup> DCs engineered to express hTERT antigen<sup>508</sup>. Additionally, CD205 expression increases as DC maturation occurs, with peak upregulation occurring at 48 hours<sup>509</sup>. CD11c<sup>+</sup>MHCII<sup>+</sup> DCs extracted from the tumors of TIL 1383I TCR transduced allogeneic T cell-treated

mice expressed the highest levels of CD205, measured by mean fluorescence intensity (MFI), confirming the induction of mature cross-presenting DC subsets in the tumor draining lymph nodes. In support of previous reports, we also observed the most significant differences in mature CD205<sup>+</sup> DCs two days post-intratumoral T cell treatment.

The tumor draining lymph nodes isolated from B16 A2/K<sup>b</sup> tumor-bearing mice seven days after treatment with TIL 1383I TCR transduced allogeneic T cells exhibited increased frequencies of activated CD4<sup>+</sup> and CD8<sup>+</sup> T cells. As demonstrated by ELISPOT assays, these endogenous cells produced IFN- $\gamma$  in response to B16 and B16 A2/K<sup>b</sup> tumor targets, as well as in response to gp100<sub>25-33</sub> - and TRP-2<sub>181-188</sub> peptide-pulsed RMA/S cells. TRP-2 and gp100 are melanocyte differentiation antigens (MDAs), the most common group of antigens, compared to mutated antigens and cancer/testis antigens, recognized by CTL in human melanomas. We chose the TRP-2 peptide because the literature has reported that naïve mice have relatively high numbers of TRP-2-specific CTL precursors and therefore, this self-antigen is relatively easy to generate low-affinity CD8<sup>+</sup> T cells<sup>510</sup>. Additionally, it has been demonstrated that T cells specific to the TRP-2 antigen predominate in mice vaccinated with irradiated B16 tumors<sup>511</sup>.

Endogenous T cells induced after treatment with TIL 1383I TCR transduced allogeneic T cells were also capable of mediating tumor antigen-specific killing, as demonstrated by the *in vivo* CTL assay. As mentioned in the literature review, different types of antigens are more efficiently cross-presented than other types of antigens<sup>159-164</sup>. This may explain why we more frequently observed the induction of gp100-specific

reactivity and killing in comparison to TRP-2-specific reactivity and killing. Even though we observed increased gp100-specific T cells compared to TRP-2-specific T cells, mice treated with TIL 1383I TCR transduced allogeneic T cells commonly generated T cell responses against both B16-associated tumor antigens. In a previous report, the immunization of mice with plasmids that encoded either gp100 or TRP-2 proteins resulted in only partial protection against B16 melanoma challenge. In contrast, when mice were immunized with both antigens, they observed complete protection in 100% of the mice<sup>512</sup>. It would be interesting to retrospectively compare anti-tumor responses in mice that generated endogenous T cell responses against gp100 or TRP-2 only versus responses against both antigens. These results suggest that treatment with TIL 1383I TCR transduced allogeneic T cells promoted more robust tumor antigen-specific T cell responses and increased epitope spreading compared to TIL 1383I TCR transduced syngeneic T cells.

### **Intratumoral treatment with TIL 1383I TCR Transduced Allogeneic T Cells**

#### **Induces Cross-Priming of Endogenous, Tumor-Specific T Cells**

We tested if the endogenous recipient T cells induced after treatment with TIL 1383I TCR transduced allogeneic T cells protected against B16 development on the contralateral flank. Following intratumoral treatment of primary B16 A2/K<sup>b</sup> tumors with TIL 1383I TCR transduced allogeneic T cells, approximately half of the mice were protected from B16 following inoculation on the contralateral flank. In contrast, approximately 20% of mice with primary B16 A2/K<sup>b</sup> tumors treated with TIL 1383I TCR transduced syngeneic T cells were protected from developing B16. These results were consistent with the increased DC and T cell activation in the tumor and tumor draining



lymph nodes. Although intratumoral treatment with TIL 1383I TCR transduced syngeneic T cells prevented the development of contralateral B16 tumors in a small fraction of mice, it is clear that TIL 1383I TCR transduced allogeneic T cells provided an enhanced protective benefit.

While the observation that treatment with TIL 1383I TCR transduced allogeneic T cells had impressive protective effects, we wanted to determine if intratumoral T cell treatment could also provide therapeutic benefits. Transferring the splenocytes from tumor-bearing mice intratumorally treated with TIL 1383I TCR transduced allogeneic T cells into mice with established B16 tumors can suppress tumor growth. In these experiments we only transferred  $1 \times 10^6$  splenocytes and therefore it is possible that transferring more cells or selecting for T cells could provide an enhanced therapeutic response. It is notoriously more difficult to achieve *in vivo* responses when utilizing transfer experiments and therefore the impact of TIL 1383I TCR transduced allogeneic T cell treatment against B16 tumors is very impressive.

Treatment with TIL 1383I TCR transduced allogeneic T cells induced significant epitope spreading compared to the other treatments. The extent of cross-priming in these experiments may be underestimated due to two factors. We initially began interrogating the ability of TIL 1383I TCR transduced T cell treatment to generate T cells specific to MHC class I-restricted melanoma antigens, which are better characterized and more commonly generated *in vivo* compared to MHC class II-restricted tumor-specific T cells. It is possible that TIL 1383I TCR transduced T cells induced tumor-specific CD4<sup>+</sup> T cells with specificities to mouse H-2 I-A<sup>b</sup> I-E<sup>b</sup>- restricted peptides. Recent mapping of non-synonymous mutations in B16 tumors by next-generation

sequencing and subsequent vaccination with synthetic peptides harboring the mutated epitope lead to the observation that responses against neo-epitopes were nearly all CD4<sup>+</sup> T cell-mediated. Therefore, it would be highly beneficial for future experiments to investigate the contribution of MHC class II-restricted tumor antigen-specific CD4 T cells to anti-tumor immunity following intratumoral treatment with TIL 1383I TCR transduced allogeneic T cells.

### **Immunotherapy-Associated Adverse Events**

One must take into consideration the possibility of immunotherapy-associated adverse events that can occur using TCR gene-modified T cells. TCR mispairing between the introduced and endogenous TCR chains could result in the generation of self-reactive T cells (off-target). The cross-reactivity against antigens expressed on normal tissue can limit the efficacy and impact safety. We did not anticipate this to be a problem, as the targeting of melanoma/melanocyte shared antigens is relatively safe and the TIL 1383I TCR used in these experiments has already been tested pre-clinically in mice and used to treat patients. Both human and mouse studies have demonstrated the safety of the TIL 1383I TCR with minimal toxicity. In patients, these have included lymphopenia, neutropenia, thrombocytopenia, and rash, which can be a consequence of non-myeloablative lymphodepletion. Toxicity related to the administration of melanoma/melanocyte-specific T cells seen in our clinical trial included vitiligo, but others have observed uveitis or hearing loss<sup>2,470</sup>.

We have demonstrated that intratumoral injections of TCR gene-modified allogeneic T cells is an effective and safe approach to mediate tumor regression. However, adverse events have been reported in other studies using intravenous (i.v)

infusions of TCRs that turned out to be dangerous or cross-reactive. Severe inflammatory colitis was observed in patients with colorectal cancer that received i.v infusions of T cells transduced to express an affinity-enhanced TCR specific to the carcinoembryonic antigen (CEA). Later, they discovered that low levels of CEA were present in the colonic epithelium<sup>428</sup>. On-target toxicity events have also been reported with CAR T cell therapy. In one study using CAR T cells that targeted the carbonic anhydrase IX (CAIX) antigen, lethal liver toxicity was reported in two patients with metastatic renal cell carcinoma. Upon further examination, they detected low expression of the CAIX antigen on normal bile duct epithelial tissue<sup>407</sup>. Our strategy using intratumoral delivery of TCR gene-modified T cells can potentially prevent the systemic on-target effects against normal tissue. We have demonstrated that intratumorally-injected allogeneic TCR gene-modified T cells do not migrate out of the tumor and are eliminated within seven days after injection.

In our experiments, we observed only one case of vitiligo when mice were treated with TIL 1383I TCR transduced allogeneic T cells only. In contrast, we observed the development of vitiligo in 6/20 mice following treatment with TIL 1383I TCR transduced allogeneic T cells and anti-CTLA-4 mAb monotherapy or anti-CTLA-4 mAb/anti-PD-1 mAb dual therapy. Therefore, caution should be used when attempting to achieve epitope spreading depending on the expression of target antigen on normal tissue. The advantage to our approach is the ability to confine robust immune responses to the microenvironment by intratumoral delivery of the TIL 1383I TCR gene-modified T cells. An additional safety measure that could be taken is irradiating the TIL 1383I TCR transduced allogeneic T cells before delivery. We chose not to irradiate the

TIL 1383I TCR transduced allogeneic T cells in our experiments, but the clinical trial testing MART-1-specific TCR transduced allogeneic T cells irradiated the cells prior to intratumoral delivery. They noted that the irradiated T cells maintained lytic function and produced cytokines in response to tumor targets for up to 48 hours after radiation. We concluded that intratumoral delivery of TIL 1383I TCR transduced allogeneic T cells was safe, with vitiligo as the only TCR-specific toxicity to our knowledge.

We were also aware of the possible induction of graft-versus-host disease (GVHD) mediated by complete MHC-mismatched allogeneic T cells. GVHD can be acute or chronic and can be life-threatening in patients receiving a hematopoietic stem cell transplant<sup>513</sup>. In mouse models, GVHD can induce severe disease; however, in our model using intratumoral delivery of allogeneic T cells, we did not observe severe or lethal GVHD following intratumoral injection of TIL 1383I TCR transduced allogeneic T cells or untransduced allogeneic T cells. We demonstrated that TIL 1383I TCR transduced allogeneic T cells and untransduced allogeneic T cells do not egress from the tumor microenvironment, as they were undetected in the spleens or tumor draining lymph nodes and are eliminated by seven days post-intratumoral injection. This is one hypothesis explaining the lack of severe GVHD.

A second potential explanation for the lack of severe GVHD could be the phenotype of the TIL 1383I TCR transduced T cells used for treatment. Beilhack and colleagues performed an extensive characterization of the events mediating GVHD<sup>95</sup>. Through *in vivo* bioluminescence imaging, they observed the proliferation of donor CD4<sup>+</sup> T cells, followed by CD8<sup>+</sup> T cells, that initiated GVHD in secondary lymphoid organs when transplants contained pure naïve donor T cells. In contrast, grafts containing CD4<sup>+</sup>

effector memory T cells did not proliferate *in vivo*, despite their alloreactivity *in vitro*. In our experiments, T cells used for therapy are activated with anti-CD3/anti-CD28 beads prior to transduction, and presumably more closely resemble effector memory T cells when delivered intratumorally. The effector memory phenotype of TIL 1383I TCR transduced allogeneic T cells or untransduced allogeneic T cells could limit the extent of alloreactivity induced. Future experiments purifying different T cell subsets either before or after transduction could further elucidate the impact of T cell phenotypes on the alloreactive response and anti-tumor immunity.

### **Combination Immunotherapy to Enhance the Efficacy of TIL 1383I TCR Transduced T Cell Treatment**

We observed significant improvements in anti-tumor responses in B16 A2/K<sup>b</sup> tumor-bearing mice treated with TIL 1383I TCR transduced allogeneic T cells compared to TIL 1383I TCR transduced syngeneic T cells or untransduced allogeneic T cells. We sought to further improve T cell cross-priming and systemic anti-tumor immunity using additional immunotherapies that have been reported to modulate anti-tumor immune responses. In a series of pilot experiments, we investigated three different approaches that varied in therapeutic targets and route of delivery. We targeted innate immunity, the tumor microenvironment, or adaptive T cell responses through intratumoral delivery, modification of transduced T cells, and systemic infusion, respectively.

The first pilot experiments we performed tested if the combination of intratumoral treatment with TIL 1383I TCR transduced T cells and TLR3 stimulation using poly I:C could improve suppression of B16 A2/K<sup>b</sup> tumor progression or T cell cross-priming. The timing of poly I:C delivery to the tumor microenvironment could also affect the outcome

of therapy. It would have been interesting to test if intratumoral delivery of poly I:C and TIL 1383I TCR transduced T cells on the same day affected B16 A2/K<sup>b</sup> tumor growth or cross-priming. However, technical difficulties prevented us from addressing this question. First, two separate intratumoral injections on the same day is not feasible because the therapeutic agent in the second injection would leak out of the injection site from the first therapeutic agent. The alternative option would require pre-mixing the T cells and poly I:C prior to intratumoral injection. However, TLR3 is expressed on CD4 and CD8 T cells from C57Bl/6 and BALB/c mice and the magnitude of TLR3 expression is strain-dependent. Therefore, it would be almost impossible to control for the effect of poly I:C on TIL 1383I TCR transduced T cells isolated from HLA-A2 transgenic mice, which are on a C57Bl/6 background, compared to BALB/c mice.

We were unable to achieve better anti-tumor responses, using the retroviral vector as delivery method, upon co-expression of the TIL 1383I TCR and the LIGHT protein to the tumor in a single exploratory experiment. Additionally, injecting tumors with the combination of TIL 1383I TCR transduced allogeneic T cells and poly I:C were inconclusive. There remains the question, can too much immune stimulation within the tumor microenvironment, in the context of cancer immunotherapy, cause harm? In two of the three combination strategies employed, the addition of poly I:C and incorporation of the LIGHT gene into the vector, the anti-tumor responses were either equal to or worse than intratumoral treatment with TIL 1383I TCR transduced allogeneic T cells. In some reports, TLR-mediated chronic inflammation induced tumorigenesis<sup>58,514</sup>. In contrast, when intratumoral treatment with TIL 1383I TCR transduced allogeneic T cells was combined with systemic administration of immune checkpoint inhibitors anti-CTLA-

4 mAb or anti-CTLA4/anti-PD-1 mAb, we observed a substantial improvement in anti-tumor responses. The route of delivery is one difference that distinguishes the former strategies from the latter approach. It is possible that administering poly I:C or expressing the LIGHT protein in the tumor microenvironment, in which immune cells were already stimulated via alloreactivity and the tumor-specific TCR, resulted in activation-induced death or quiescence.

Intratumoral treatment with TIL 1383I TCR transduced allogeneic T cells in combination with systemic administration of anti-PD-1 mAb and anti-CTLA-4 mAb further enhanced anti-tumor responses, protecting nearly 100% of mice from the development of B16 tumors when challenged on the contralateral flank. We also observed increased incidences of the development of vitiligo in mice intratumorally treated with TIL 1383I TCR transduced allogeneic T cells and anti-CTLA-4 mAb monotherapy or anti-CTLA-4 mAb/anti-PD-1 mAb dual therapy. The addition of anti-CTLA-4 mAb presumably induced robust autoreactive T cell responses that would otherwise be maintained through peripheral tolerance. The mechanisms governing tumor immunity versus autoimmunity have yet to be clearly defined. In one study, CD8<sup>+</sup> T cells required perforin to mediate the induction of autoimmunity whereas perforin was dispensable for tumor immunity<sup>515</sup>. Because TIL 1383I TCR transduced syngeneic T cell-treated mice did not develop vitiligo, it is possible that TIL 1383I TCR transduced allogeneic T cell treatment with anti-CTLA-4 mAb induces a more potent cytotoxic CD8<sup>+</sup> T cell response. This hypothesis is further supported by previous reports demonstrating that CD4<sup>+</sup> T cells were not required for vitiligo development following whole tumor cell vaccination with anti-CTLA-4 mAb<sup>37</sup>.

A moderate number of mice treated with TIL 1383I TCR transduced allogeneic T cells and anti-CTLA-4 mAb developed vitiligo at the site of the primary B16 A2/K<sup>b</sup> tumor and, in some cases, the contralateral B16 tumor. These findings are further evidence that TIL 1383I TCR transduced allogeneic T cells in combination with anti-CTLA-4 mAb induced systemic cross-primed T cells.

The addition of the allogeneic component to TIL 1383I TCR transduced T cells can also be considered a combination therapy. The contribution of allogeneic response clearly improved outcomes; however, one factor that has yet to be explicitly tested is the level or threshold of alloreactivity that is sufficient to promote superior anti-tumor immunity. The frequency of alloreactive T cells in mice varies 30-fold ( $0.71 \pm 0.31\%$  to  $21.05 \pm 3.62\%$ ), which could influence immune activation. Presumably, TCR transduced T cells that generate the highest frequency of alloreactive T cells would be preferable over transduced T cells that minimally induce alloreactivity.

About one-third of minor histocompatibility antigens are generated from the Y chromosome<sup>516</sup>. Does this make a difference in the impact of alloreactivity to enhance anti-tumor responses? We did not observe notably different outcomes that correlated with the sex of the donor T cells or recipient mice. We used a mixture of female and male mice as recipients for B16 A2/K<sup>b</sup> throughout every experiment. For the donor T cells, we used the same sex (male or female) of HLA-A2 transgenic and BALB/c mice for donor T cells within each experiment, but among independent experiments, we used both male and female mice. In this manner, we can conclude that major histocompatibility protein mismatch is sufficient to engage the recipient immune



response to contribute to enhanced anti-tumor responses, but the extent to which minor histocompatibility proteins can contribute to these responses remains to be elucidated.

The allogeneic response is primarily T cell-mediated and is characterized by the production of IL-2, IFN- $\gamma$ , and TNF- $\alpha$ . As described in the literature review, these cytokines are also critical components in generating anti-tumor immunity. TNF- $\alpha$  was initially defined as the mediator of hemorrhagic necrosis of tumors and contributing to tumor regression<sup>497</sup>. Clinical and biologic responses have been observed in patients following the administration of high-dose IL-2. The presence of interferon-stimulating genes and IFN-producing T cells can correlate with positive anti-tumor responses. Supplementing immunotherapies with adjuvants, agonists, and vaccines aim for the induction of these cytokines. Direct or indirect administration of IL-2, IFN- $\gamma$ , and TNF- $\alpha$  induce potent immune responses, but the critical missing component is tumor antigen-specificity. With our strategy, intratumoral delivery of TIL 1383I TCR transduced allogeneic T cells elicited the robust immune responses described above but provided tumor antigen-specific killing directly in the tumor microenvironment.

The experiments described in this dissertation have centered around a unique tumor-specific TCR in the setting of a mouse melanoma model. While MHC-restriction and lack of suitable tumor-specific TCR limit the experimental scope of this dissertation, the overall conclusions that, in the setting of tumor immunology, an allogeneic donor cell can provide additional advantageous qualities, such as combating the immunosuppressive tumor microenvironment. The underlying principles of allogeneic immune responses remain constant among species and in between individuals. Additionally, expression and function of antigen cross-presenting CD205 DC and

CD103 DC subsets are maintained across humans and mice. Therefore, we believe that our approach of utilizing intratumoral delivery of allogeneic TCR gene-modified T cells is feasible and more effective immunotherapeutic strategy that can induce protective, therapeutic systemic anti-tumor immunity.

### **Concluding Remarks**

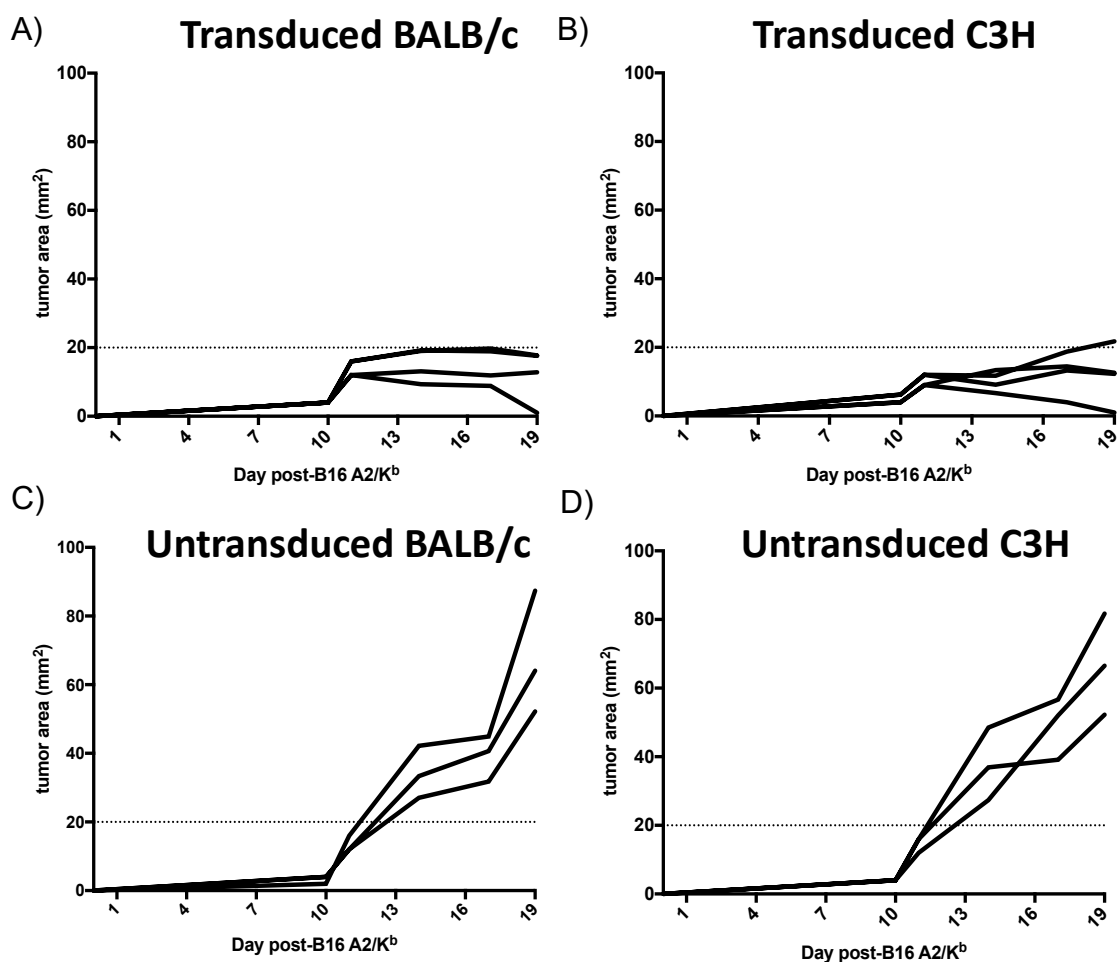
Cancer immunotherapies have shown great promise in the treatment of various malignancies. A vast majority of immunotherapies aim to improve T cell function or induce anti-tumor T cell responses. The ACT of TCR gene-modified T cells has been a rapidly developing and promising strategy to treat various tumor types. Clinical and biologic responses have been observed following the ACT of autologous TCR gene-modified T cells, but there is still a need to improve the frequency and durability of responses. In patients receiving monospecific immunotherapy, poor response rates or high relapse rates are commonly observed. Contributing factors include immune-escape tumor variants that can arise through target antigen downregulation or MHC allele loss. Additionally, the tumor microenvironment is highly suppressive, and adept at excluding effector T cells or inhibiting effector functions. As a result, designing T cell-based immunotherapies that induce a broad T cell response (epitope spreading) or improve the persistence and function of the transferred T cells within the suppressive microenvironment is critical to improving clinical and biologic responses in cancer patients.

In this dissertation, we explored the mechanisms underlying the improved anti-tumor responses mediated by TIL 1383I TCR-transduced allogeneic T cells. We report that intratumoral treatment with TIL 1383I TCR-transduced allogeneic T cells resulted in

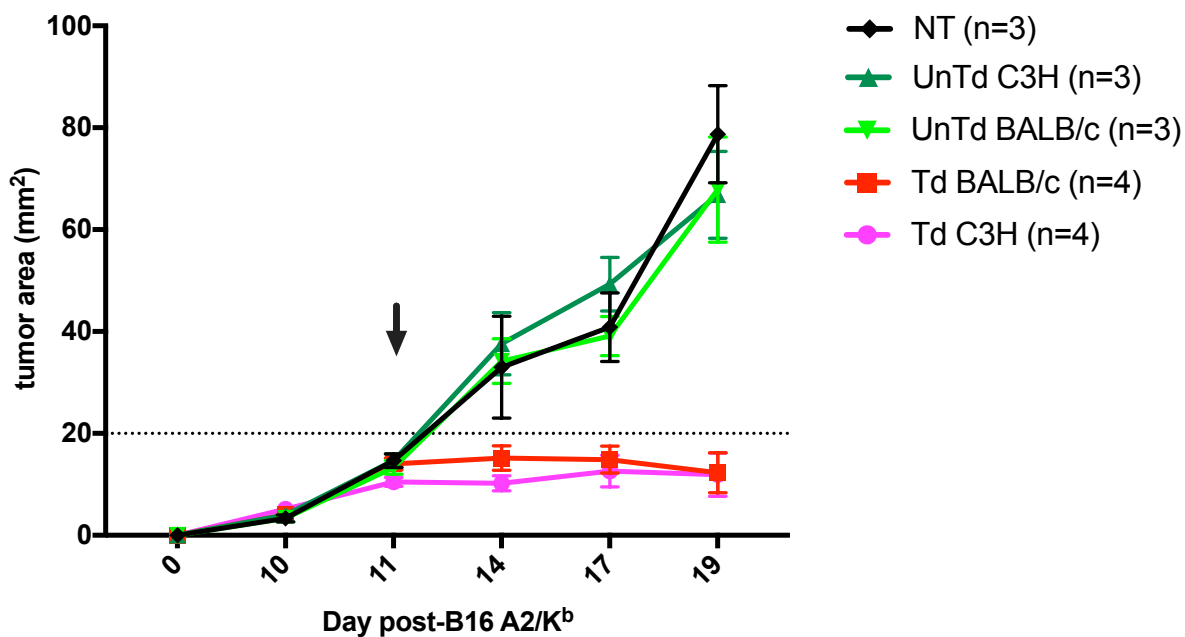
enhanced T cell activation and dendritic cell maturation-locally within the tumor microenvironment and in the tumor draining lymph nodes. Furthermore, TIL 1383I TCR transduced allogeneic T cells generated protective and therapeutic endogenous tumor-specific T cells through dendritic cell cross-presentation. The effective tumor control by intratumoral delivery of allogeneic TIL 1383I TCR-transduced T cell was further improved upon with the addition of anti-PD-1 mAb and anti-CTLA-4 mAb immune checkpoint inhibitors. We concluded that tumor specificity via the transduced TCR and alloreactivity synergized to enhance anti-tumor immune responses. By understanding mechanisms that enhance T cell function in the tumor microenvironment and generate systemic anti-tumor immunity, we can improve upon the therapeutic efficacy and safety of T cell-based immunotherapies.

## APPENDIX

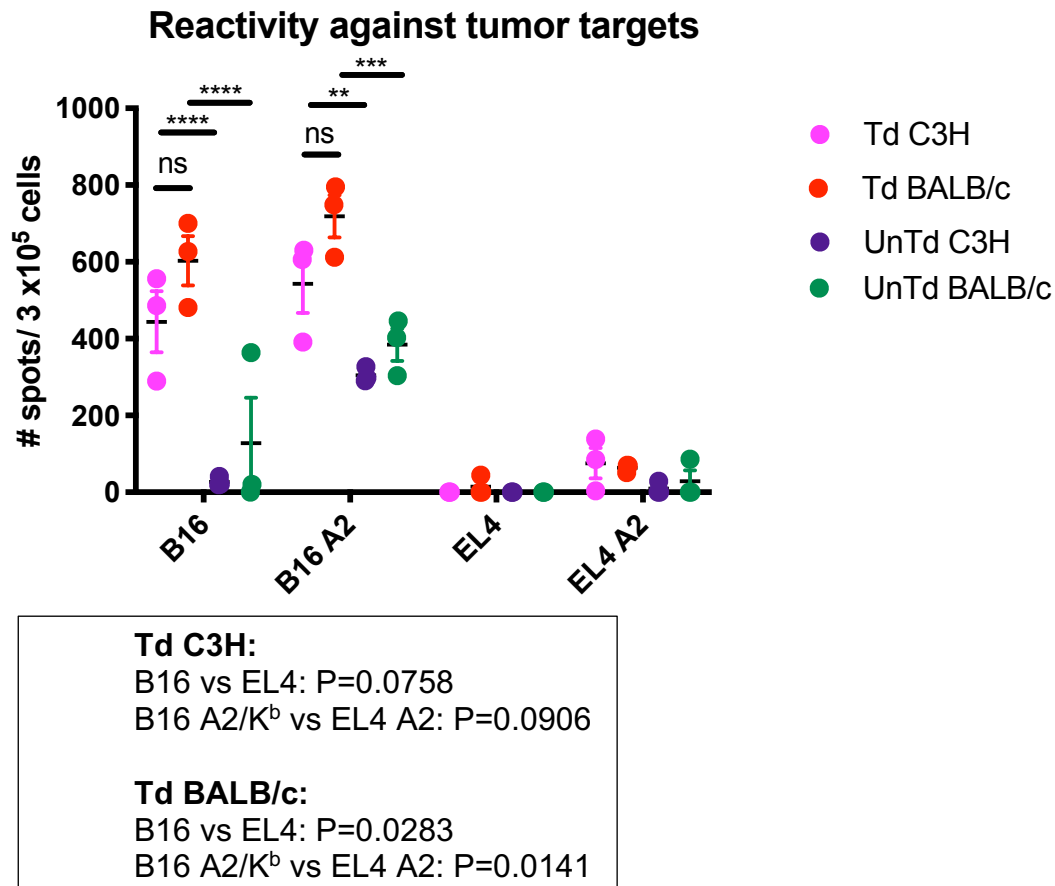
### ADDITIONAL FIGURES



**Figure 96. Intratumoral Treatment with TIL 1383I TCR Transduced C3H T Cells Promotes B16 A2/K<sup>b</sup> Tumor Suppression.** B16 A2/K<sup>b</sup> tumors were intratumorally treated on day 10 with A) untransduced BALB/c T cells B) untransduced C3H T cells C) TIL 1383I TCR transduced BALB/c T cells and D) TIL 1383I TCR transduced C3H T cells. Two opposing diameters were measured with a digital caliper every 2-3 days per week. Mice were sacrificed when tumors reached >150 mm<sup>2</sup> or >10% of body weight. Data represent one pilot experiment with 3-4 mice per group.

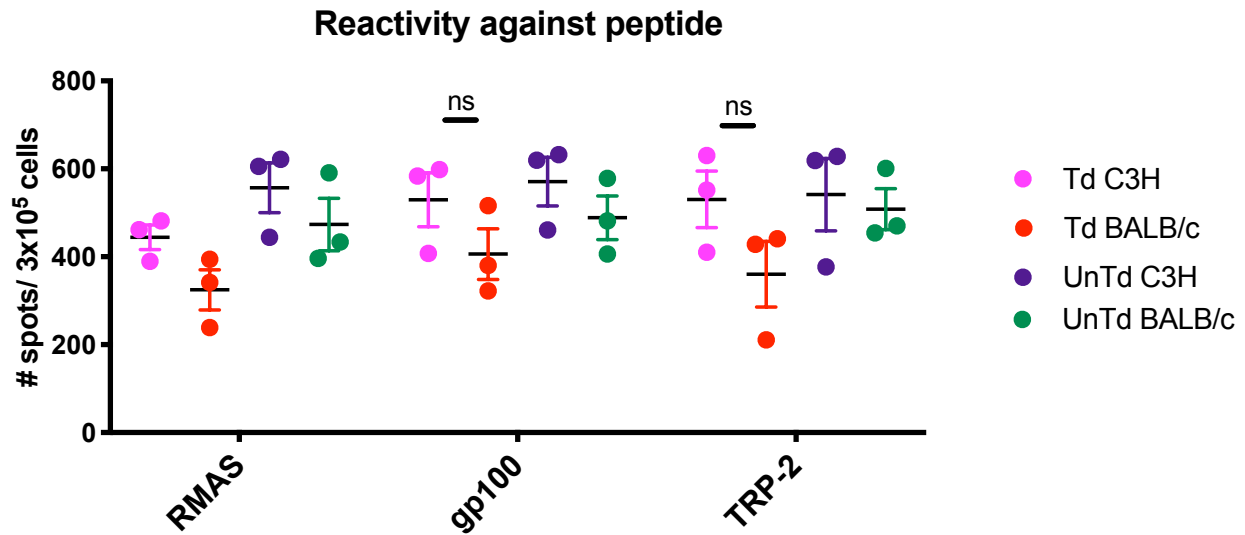


**Figure 97. Intratumoral Treatment with TIL 1383I TCR Transduced C3H T cells Promotes B16 A2/K<sup>b</sup> Tumor Regression.** B16 A2/K<sup>b</sup> tumors were intratumorally treated on day 10 with A) untransduced BALB/c T cells B) untransduced C3H T cells C) TIL 1383I TCR transduced BALB/c T cells and D) TIL 1383I TCR transduced C3H T cells. Two opposing diameters were measured with a digital caliper every 2-3 days per week. Mice were sacrificed when tumors reached >150 mm<sup>2</sup> or >10% of body weight. Data represent one pilot experiment with 3-4 mice per group.



**Figure 98. Intratumoral Treatment with TIL 1383I TCR Transduced C3H T Cells Promotes Tumor-Specific IFN- $\gamma$ <sup>+</sup> Cells in the Tumor Draining Lymph Nodes.**

Eight days post-T cell treatment, tumor draining lymph nodes were isolated and re-stimulated with irradiated B16 tumor cells for 5 days. 100,000 effector cells and 100,000 target cells were co-cultured for 18 hours. Spots were automatically enumerated using an ELISPOT plate reader. Data represent the average of duplicates from individual mice, with 3 mice per group from one pilot experiment. Statistical analysis performed using 2way ANOVA with Tukey's correction. [ $**P<0.01$ ,  $***P<0.001$ ,  $****P<0.0001$ ]

**Td C3H:**

RMA/S vs gp100: P=0.0724

RMA/S vs TRP-2: P=0.0693

**Td BALB/c:**

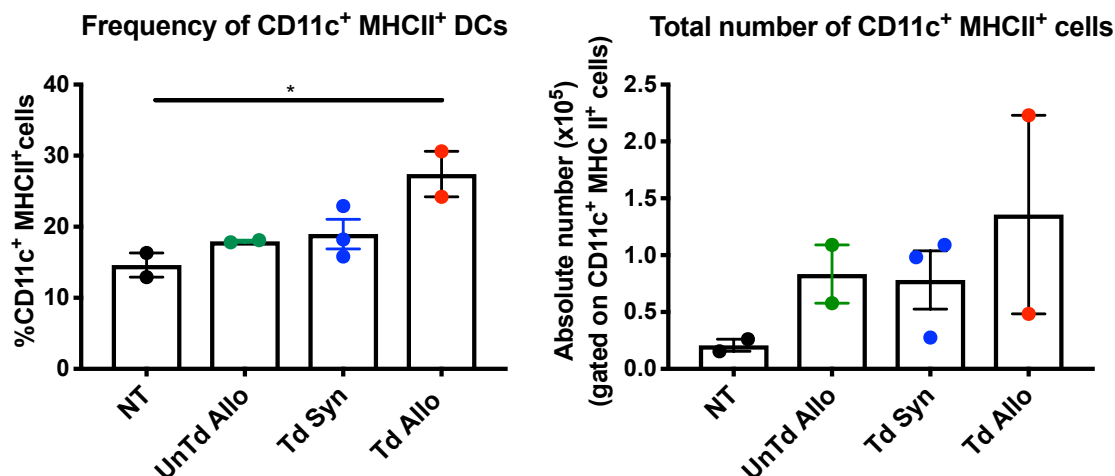
RMA/S vs gp100: P=0.0905

RMA/S vs TRP-2: P=0.5960

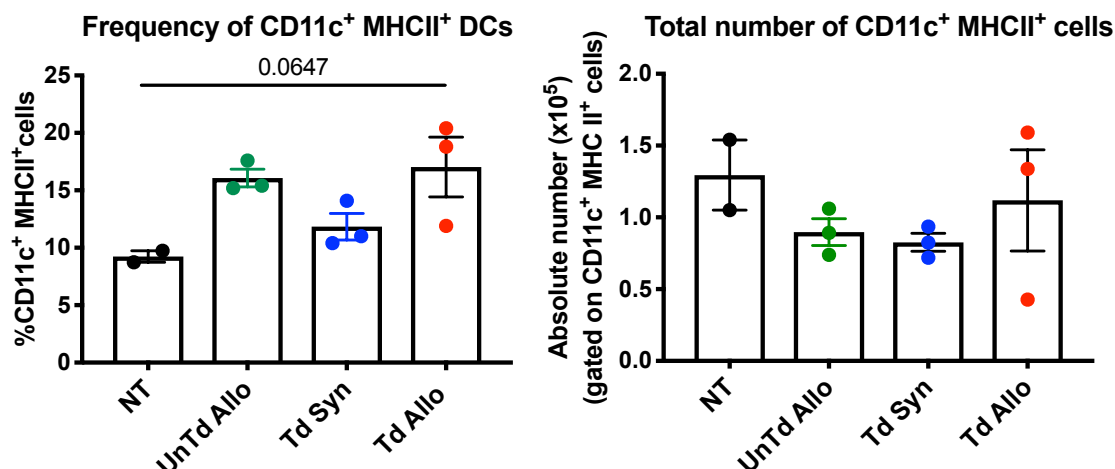
**Figure 99. Intratumoral Treatment with TIL 1383I TCR Transduced C3H T Cells Promotes Tumor Antigen-Specific IFN- $\gamma$ <sup>+</sup> Cells in the Tumor Draining Lymph Nodes** Eight days post-T cell treatment, tumor draining lymph nodes were isolated and re-stimulated with irradiated B16 tumor cells for 5 days. 100,000 effector cells and 100,000 target cells were co-cultured for 18 hours. Spots were automatically enumerated using an ELISPOT plate reader. Data represent the average of duplicates from individual mice, 3 mice per group, from one pilot experiment. No statistically significant differences were observed using 2way ANOVA with Tukey's correction.



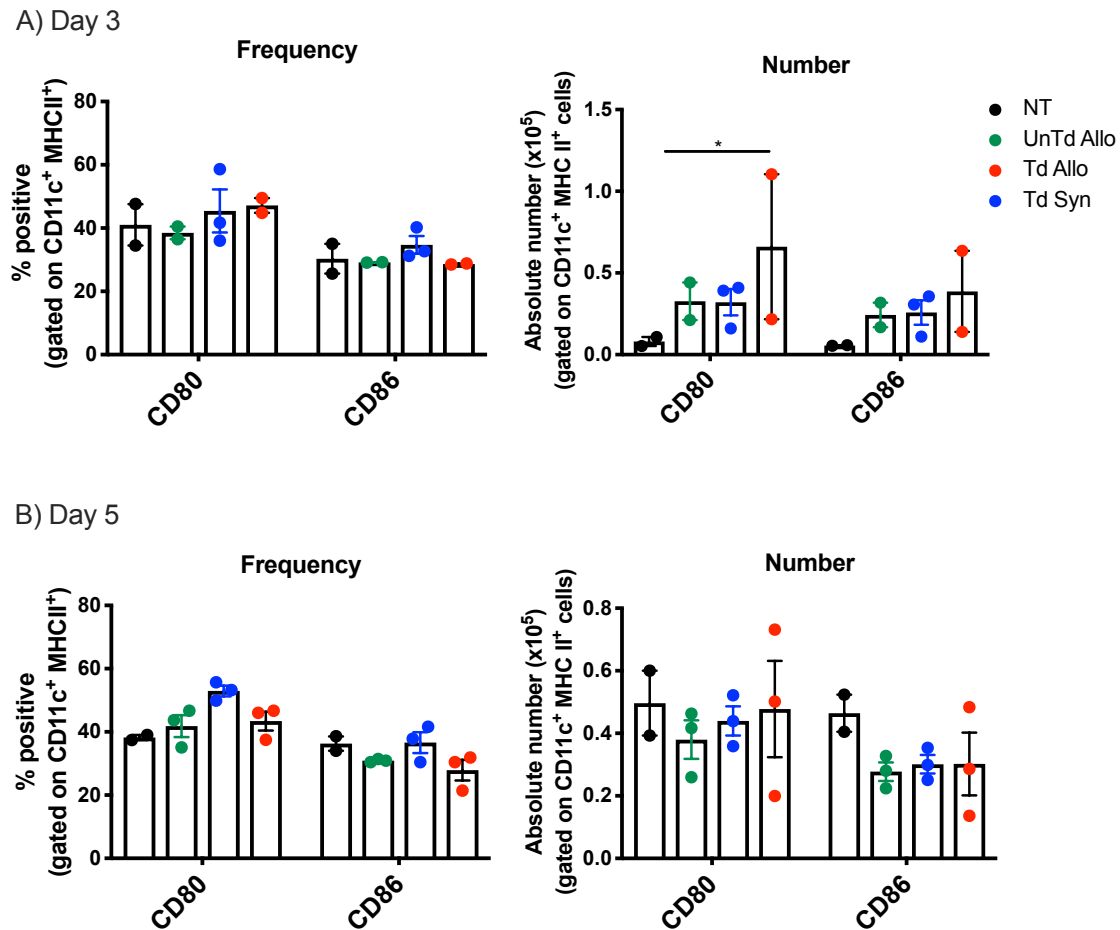
## A) Day 3 post-T cell treatment



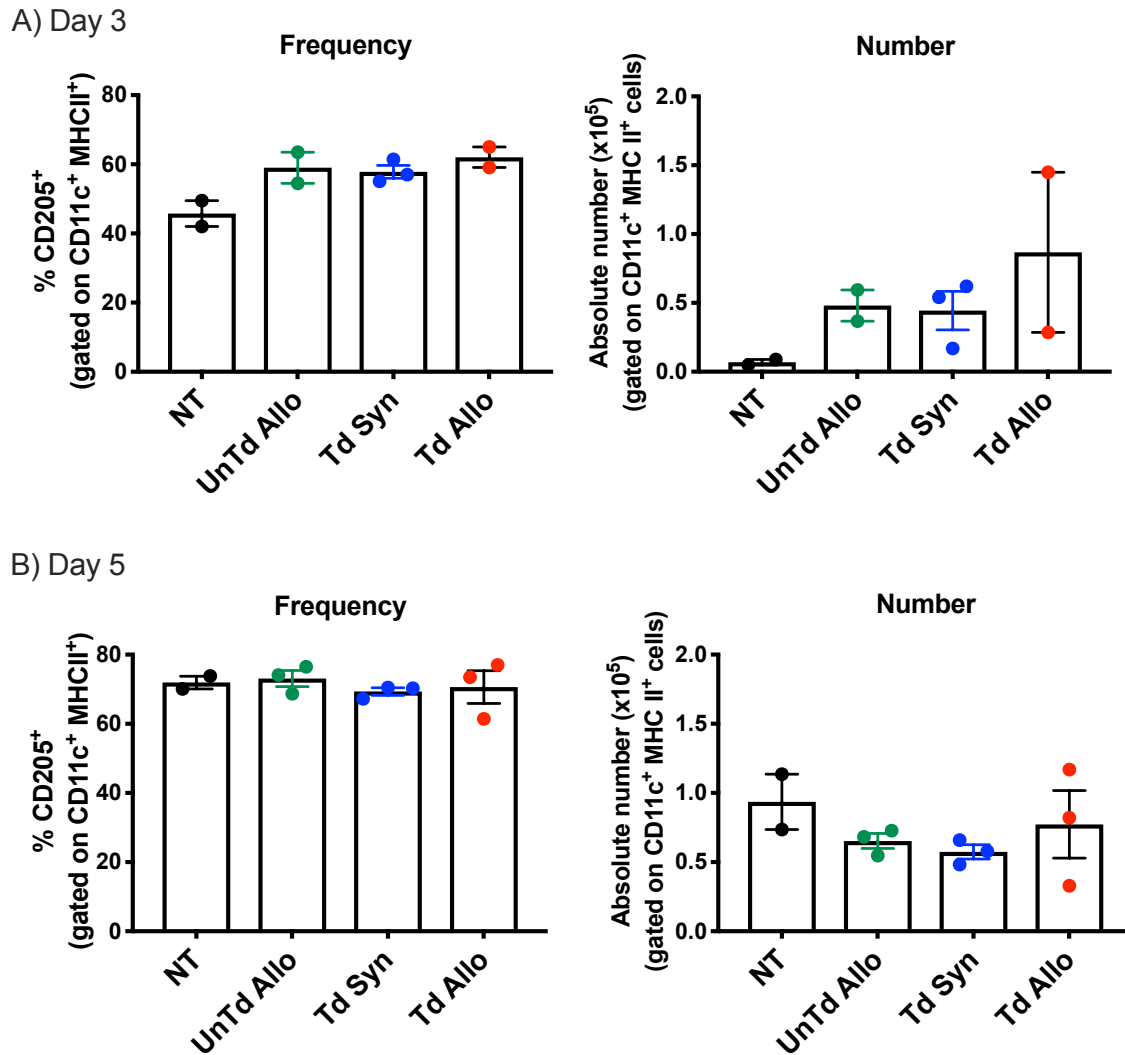
## B) Day 5 post-T cell treatment



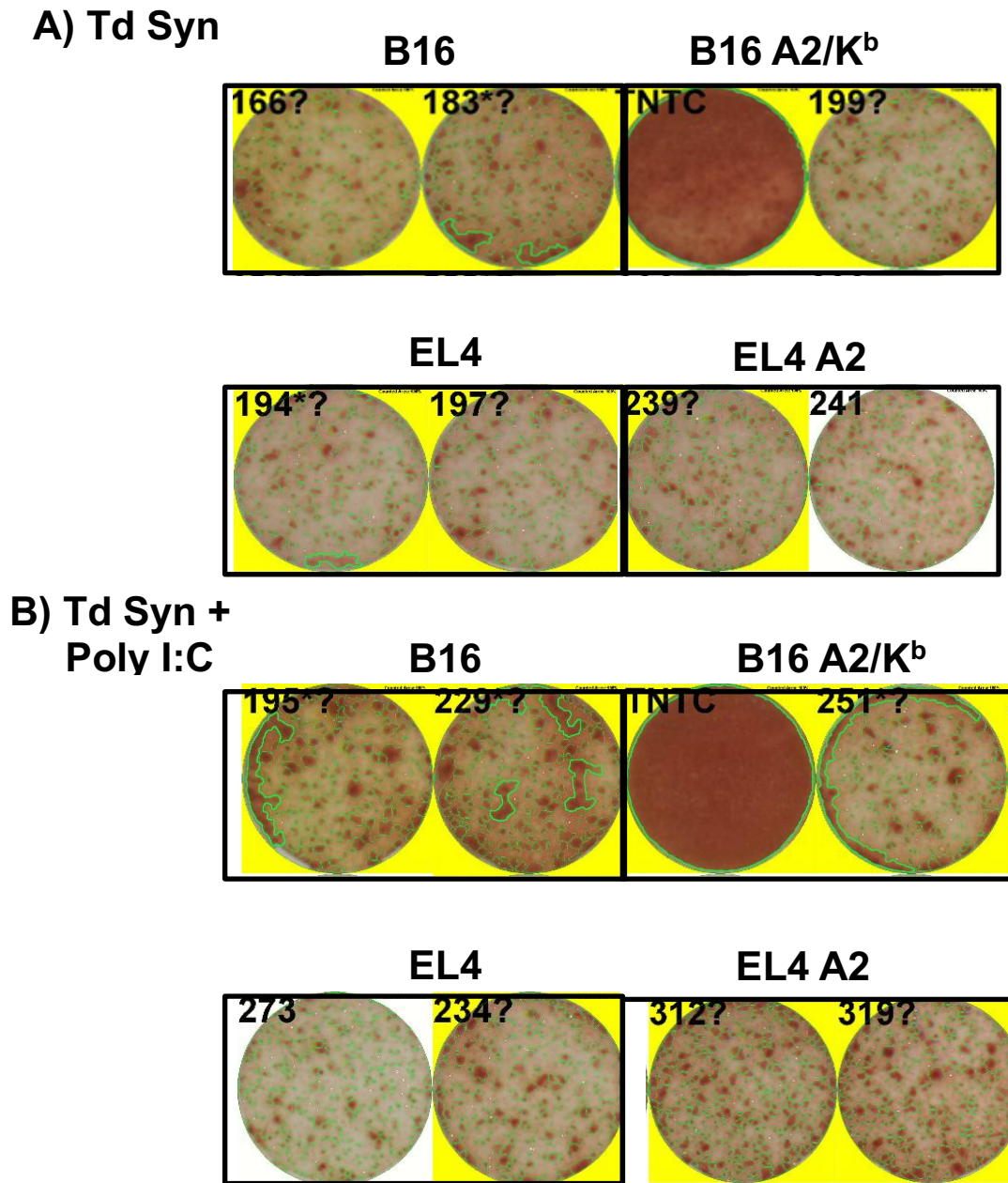
**Figure 100. CD11c<sup>+</sup> MHC II<sup>+</sup> Dendritic Cells in the Tumor Draining Lymph Nodes Three- and Five- Days Post-T Cell Treatment.** Tumor draining lymph nodes from B16 A2/K<sup>b</sup> tumor-bearing mice were isolated A) three and B) five days post-T cell treatment. Expression of CD11c, MHC II, CD80, CD86, and CD205 was assessed by flow cytometry. Frequency (left panel) and total number (right panel) of CD11c<sup>+</sup>MHCII<sup>+</sup> cells. One pilot experiment with 2-3 mice/group. Graph shows mean  $\pm$  SEM; statistical analysis by one-way ANOVA with Tukey's correction [ $*P < 0.05$ ]



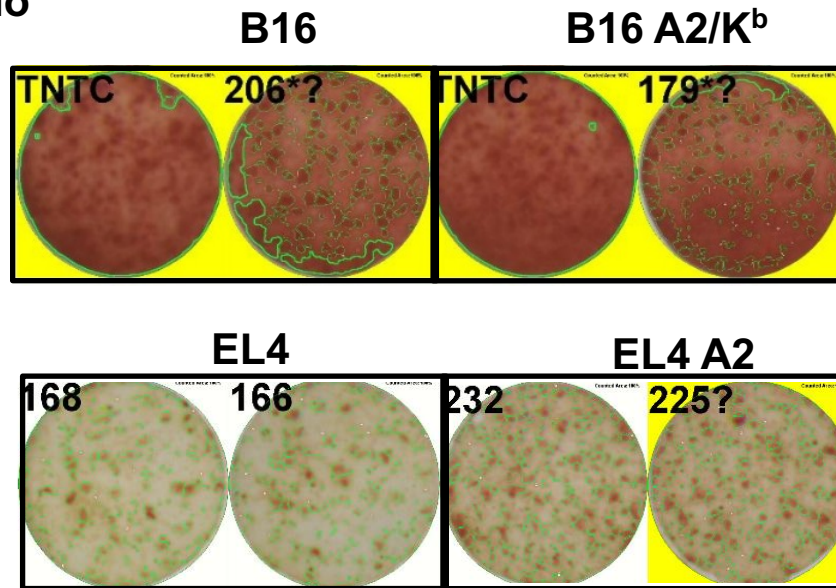
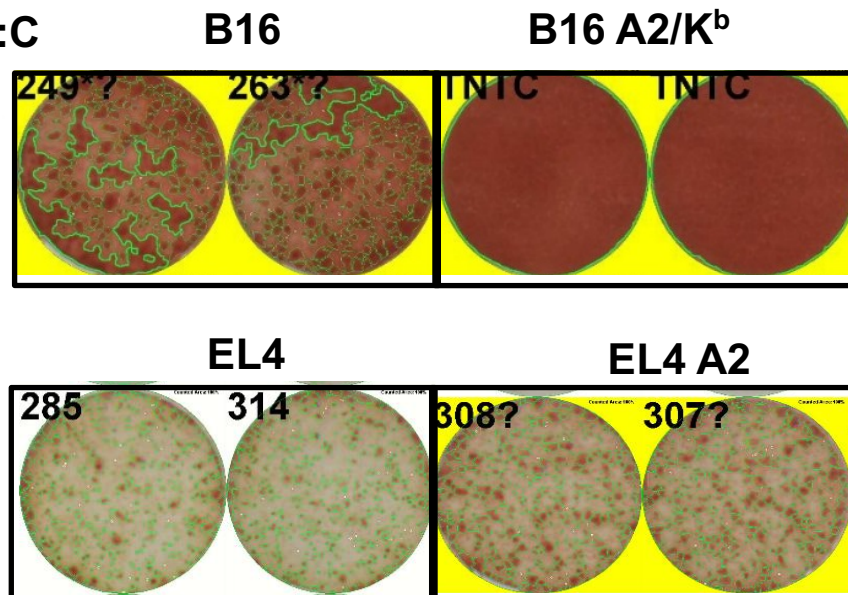
**Figure 101. Expression of Co-Stimulatory Molecules on CD11c<sup>+</sup> MHC II<sup>+</sup> Dendritic Cells in the Tumor Draining Lymph Nodes Three- and Five- Days Post-T Cell Treatment.** Tumor draining lymph nodes from B16 A2/K<sup>b</sup> tumor-bearing mice were isolated A) three and B) five days post-T cell treatment. Expression of CD11c, MHC II, CD80, CD86, and CD205 was assessed by flow cytometry. Frequency (left panel) and total number (right panel) of positive cells gated on CD11c<sup>+</sup>MHCII<sup>+</sup> cells. One pilot experiment with 2-3 mice/group. Graph shows mean  $\pm$  SEM; Statistics performed using one-way ANOVA with Tukey's correction (\*P<0.05)



**Figure 102. CD205<sup>+</sup> DCs in the Tumor Draining Lymph Nodes Three- and Five-Days Post-T Cell Treatment.** Tumor draining lymph nodes from B16 A2/K<sup>b</sup> tumor-bearing mice were isolated A) three and B) five days post-T cell treatment. Expression of CD11c, MHC II, CD80, CD86, and CD205 was assessed by flow cytometry. Frequency (left panel) and total number (right panel) of CD205<sup>+</sup> cells gated on CD11c<sup>+</sup>MHCII<sup>+</sup> cells. One pilot experiment with 2-3 mice/group. Graph shows mean  $\pm$  SEM; No statistical significance was detected by one-way ANOVA with Tukey's correction.



**Figure 103. Tumor Antigen-Specific IFN- $\gamma$ <sup>+</sup> Cells in the Tumor Draining Lymph Nodes of Mice Treated with the Combination of Intratumoral TIL 1383I TCR Transduced Syngeneic T Cells and Poly I:C.** B16 A2/K<sup>b</sup> tumor-bearing mice were intratumorally treated on day 10 post-tumor inoculation with TIL 1383I TCR transduced syngeneic T cells and one day later received an intratumoral injection of A) PBS or B) 40  $\mu$ g poly I:C. Mice were sacrificed 11 days after poly I:C treatment. Cells from the tumor draining lymph nodes were re-stimulated with irradiated B16 A2/K<sup>b</sup> tumor cells for 5 days and then co-cultured with B16, B16 A2/K<sup>b</sup>, EL4, and EL4 A2 tumor targets in an IFN- $\gamma$  ELISPOT assay. Wells are presented in duplicate with 3 mice per group from one pilot experiment. Yellow indicates high background and spots could not be enumerated.

**A) Td Allo****B) Td Allo + Poly I:C**

**Figure 104. Tumor Antigen-Specific IFN- $\gamma$ <sup>+</sup> Cells in the Tumor Draining Lymph Nodes of Mice Treated with the Combination of Intratumoral TIL 1383I TCR Transduced Allogeneic T Cells and Poly I:C.** B16 A2/K<sup>b</sup> tumor-bearing mice were intratumorally treated on day 10 post-tumor inoculation with TIL 1383I TCR transduced allogeneic T cells and one day later received an intratumoral injection of A) ) PBS or B) 40  $\mu$ g poly I:C. Mice were sacrificed 11 days after poly I:C treatment. Cells from the tumor draining lymph nodes were re-stimulated with irradiated B16 A2/K<sup>b</sup> tumor cells for 5 days and then co-cultured with B16, B16 A2/K<sup>b</sup>, EL4, and EL4 A2 tumor targets in an IFN- $\gamma$  ELISPOT assay. Wells are presented in duplicate with 3 mice per group from one pilot experiment. Yellow indicates high background and spots could not be enumerated.

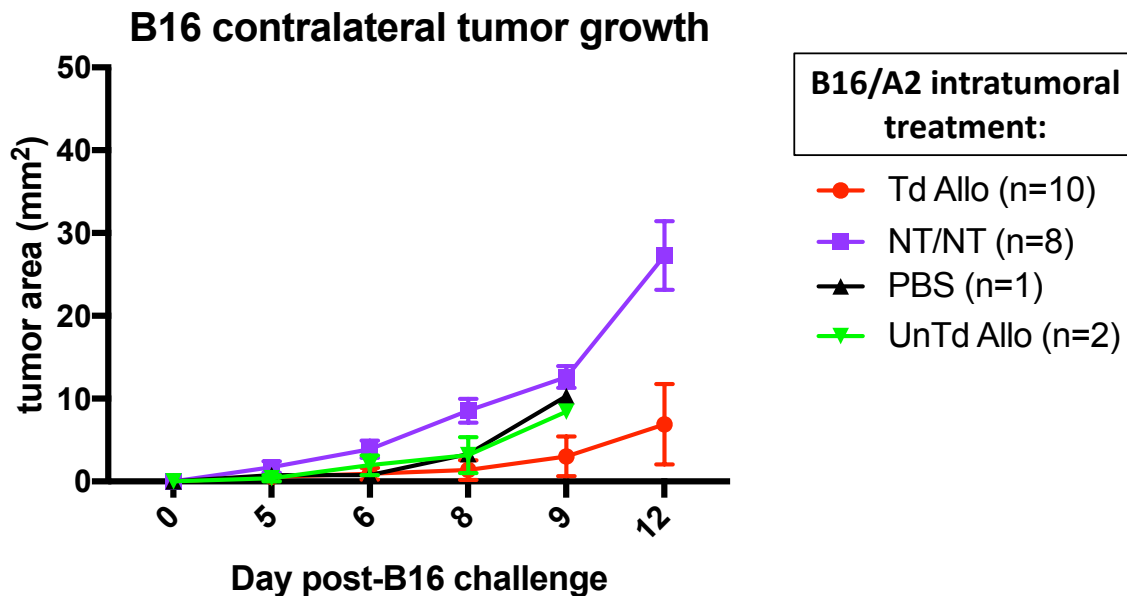


**Figure 105. Average Growth of Contralateral B16 Tumors in Mice with Pre-Existing B16 A2/K<sup>b</sup> Tumors Treated with TIL 1383I TCR Transduced Allogeneic T Cells.** Primary B16 A2/K<sup>b</sup> tumors, implanted on the right flank of mice, were treated with TIL 1383I TCR transduced allogeneic T cells (red), untransduced allogeneic T cells (green), or PBS (black) and seven days later were inoculated with  $1.0 \times 10^5$  B16 tumor cells on the left, contralateral flank. Mice were monitored for survival and development of B16 tumors. NT/NT (Purple): no primary B16 A2/K<sup>b</sup> tumor/No Treatment. Mice were sacrificed when one tumor or the sum of both tumors reached  $>150 \text{ mm}^2$  or  $>10\%$  body weight. Data represent one pilot experiment with 1-10 mice/group.

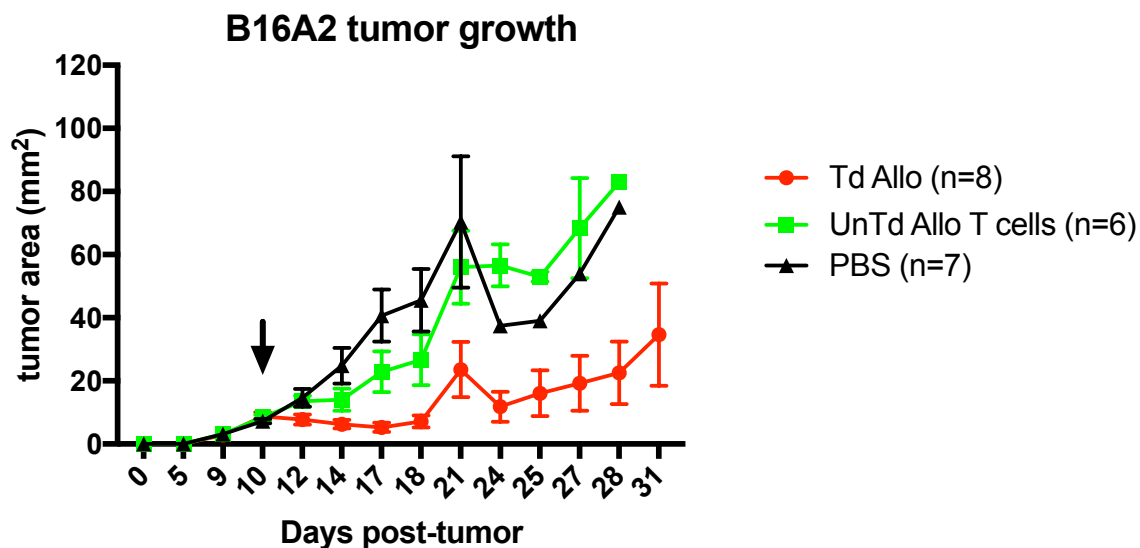


**Figure 106. Average Growth of B16 A2/K<sup>b</sup> Tumors Following Intratumoral Treatment with TIL 1383I TCR Transduced Allogeneic T Cells and B16 Tumor Challenge Seven Days Later.** Primary B16 A2/K<sup>b</sup> tumors, implanted on the right flank of mice, were treated with TIL 1383I TCR transduced allogeneic T cells (red), untransduced allogeneic T cells (green), or PBS (black) and seven days later were inoculated with  $1.0 \times 10^5$  B16 tumor cells on the left, contralateral flank. Mice were monitored for survival and development of B16 tumors. Mice were sacrificed when one tumor or the sum of both tumors reached  $>150 \text{ mm}^2$  or  $>10\%$  body weight. Data represent one pilot experiment with 7-10 mice/group.



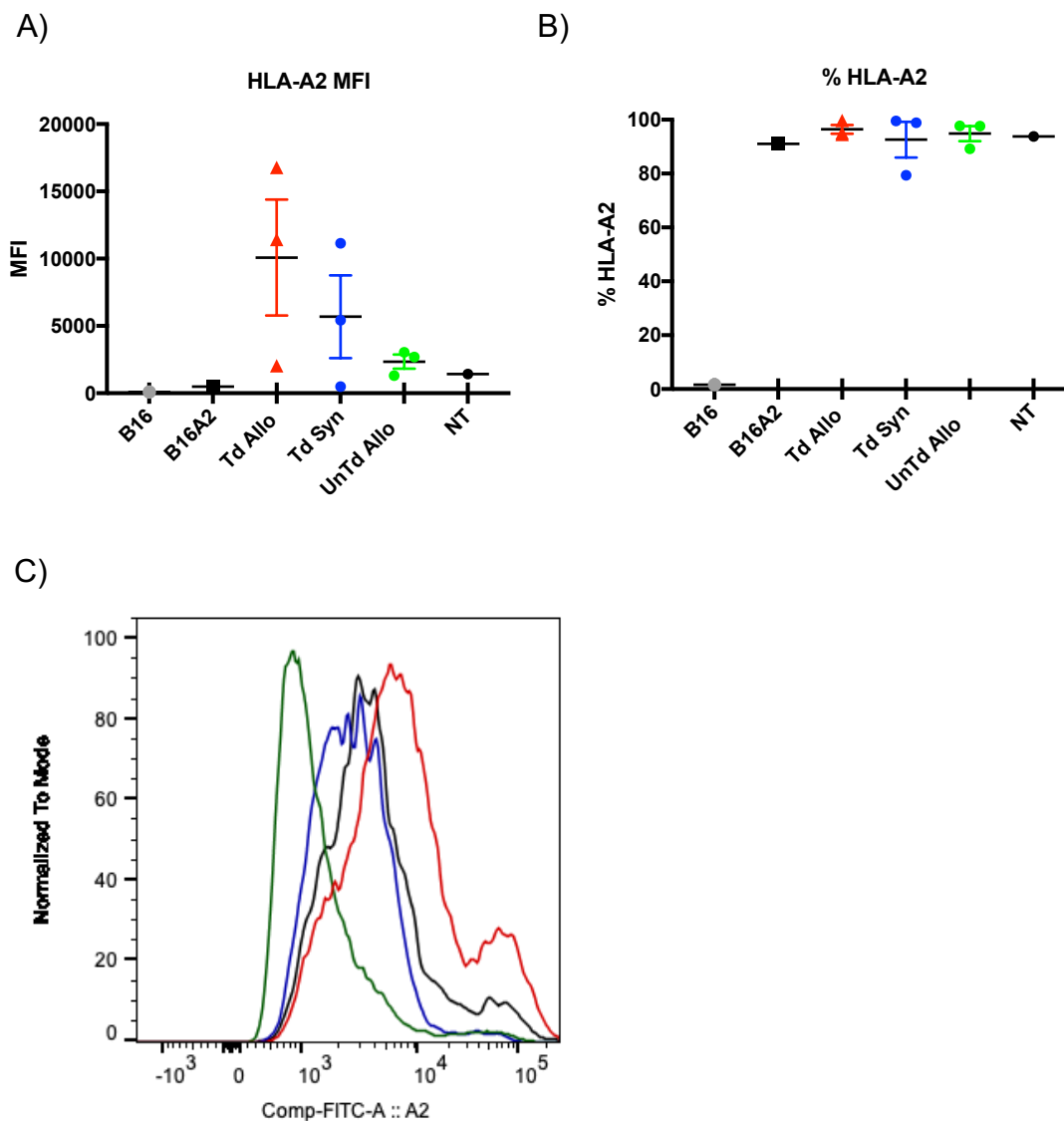


**Figure 107. Expression of HLA-A2 on B16 A2/K<sup>b</sup> Tumor Cells 10 Days Post-Intratumoral Treatment.** B16 A2/K<sup>b</sup> tumor-bearing mice were intratumorally treated with untransduced allogeneic T cells, TIL 1383I TCR transduced syngeneic T cells, or TIL 1383I TCR transduced allogeneic T cells. Ten days later, tumors were harvested and cells were analyzed for expression of HLA-A2 by flow cytometry. One pilot experiment A) MFI B) Frequency C) Representative histograms



## REFERENCE LIST

1. Moore, T. et al. Clinical and immunologic evaluation of three metastatic melanoma patients treated with autologous melanoma-reactive TCR-transduced T cells. *Cancer Immunology, Immunotherapy* 67, 311–325 (2018).
2. Duval, L. et al. Adoptive transfer of allogeneic cytotoxic T lymphocytes equipped with a HLA-A2 restricted MART-1 T-cell receptor: a phase I trial in metastatic melanoma. *Clinical cancer research : an official journal of the American Association for Cancer Research* 12, 1229–36 (2006).
3. Takahama, Y. Journey through the thymus: stromal guides for T-cell development and selection. *Nat Rev Immunol* 6, nri1781 (2006).
4. Love, P. E. & Bhandoola, A. Signal integration and crosstalk during thymocyte migration and emigration. *Nat Rev Immunol* 11, 469 (2011).
5. Serra, P. et al. RAG-dependent peripheral T cell receptor diversification in CD8+ T lymphocytes. *Proc National Acad Sci* 99, 15566–15571 (2002).
6. Bruno, L., Scheffold, A., Radbruch, A. & Owen, M. J. Threshold of pre-T-cell-receptor surface expression is associated with  $\alpha\beta$  T-cell lineage commitment. *Curr Biol* 9, 559–568 (1999).
7. Biro, J. et al. Regulation of T cell receptor (TCR)  $\beta$  gene expression by CD3 complex signaling in immature thymocytes: Implications for TCR $\beta$  allelic exclusion. *Proc National Acad Sci* 96, 3882–3887 (1999).
8. Sieh, P. & Chen, J. Distinct Control of the Frequency and Allelic Exclusion of the V $\beta$  Gene Rearrangement at the TCR $\beta$  Locus. *J Immunol* 167, 2121–2129 (2001).
9. Derbinski, J., Schulte, A., Kyewski, B. & Klein, L. Promiscuous gene expression in medullary thymic epithelial cells mirrors the peripheral self. *Nat Immunol* 2, 1032–1039 (2001).
10. Surh, C. D. & Sprent, J. T-cell apoptosis detected in situ during positive and negative selection in the thymus. *Nature* 372, 100–103 (1994).

11. Ashton-Rickardt, P. G. et al. Evidence for a differential avidity model of T cell selection in the thymus. *Cell* 76, 651–663 (1994).
12. Singer, A., Adoro, S. & Park, J.-H. Lineage fate and intense debate: myths, models and mechanisms of CD4- versus CD8-lineage choice. *Nat Rev Immunol* 8, nri2416 (2008).
13. Germain, R. N. T-cell development and the CD4–CD8 lineage decision. *Nat Rev Immunol* 2, 309–322 (2002).
14. Qi, Q. et al. Diversity and clonal selection in the human T-cell repertoire. *Proc National Acad Sci* 111, 13139–13144 (2014).
15. Davis, M. M. & Bjorkman, P. J. T-cell antigen receptor genes and T-cell recognition. *Nature* 334, 334395a0 (1988).
16. Porcelli, S., Yockey, C., Brenner, M. & Balk, S. Analysis of T cell antigen receptor (TCR) expression by human peripheral blood CD4-8- alpha/beta T cells demonstrates preferential use of several V beta genes and an invariant TCR alpha chain. *J Exp Medicine* 178, 1–16 (1993).
17. Garboczi, D. N. & Biddison, W. E. Shapes of MHC Restriction. *Immunity* 10, 1–7 (1999).
18. Ferreira, C. et al. TCR- $\alpha$  CDR3 Loop Audition Regulates Positive Selection. *J Immunol* 177, 2477–2485 (2006).
19. Miles, J. J., Douek, D. C. & Price, D. A. Bias in the  $\alpha\beta$  T-cell repertoire: implications for disease pathogenesis and vaccination. *Immunology and Cell Biology* 89, 375–387 (2011).
20. Turner, S. J., Doherty, P. C., McCluskey, J. & Rossjohn, J. Structural determinants of T-cell receptor bias in immunity. *Nat Rev Immunol* 6, nri1977 (2006).
21. Lossius, A., Johansen, J. N., Vartdal, F. & Holmøy, T. High-throughput sequencing of immune repertoires in multiple sclerosis. *Ann Clin Transl Neur* 3, 295–306 (2016).
22. Doyle, C. & Strominger, J. L. Interaction between CD4 and class II MHC molecules mediates cell adhesion. *Nature* 330, 330256a0 (1987).
23. Norment, A. M., Littman, D. R., Parham, P., Salter, R. D. & Engelhard, V. H. Cell-cell adhesion mediated by CD8 and MHC class I molecules. *Nature* 336, 79 (1988).

24. Shaw, A. et al. Short related sequences in the cytoplasmic domains of CD4 and CD8 mediate binding to the amino-terminal domain of the p56lck tyrosine protein kinase. *Mol Cell Biol* 10, 1853–1862 (1990).
25. Lin, J. & Weiss, A. Identification of the Minimal Tyrosine Residues Required for Linker for Activation of T Cell Function. *J Biol Chem* 276, 29588–29595 (2001).
26. Imboden, J. & Stobo, J. Transmembrane signalling by the T cell antigen receptor. Perturbation of the T3-antigen receptor complex generates inositol phosphates and releases calcium ions from intracellular stores. *J Exp Medicine* 161, 446–456 (1985).
27. Chen, L. & Flies, D. B. Molecular mechanisms of T cell co-stimulation and co-inhibition. *Nat Rev Immunol* 13, 542 (2013).
28. Viola, A. & Lanzavecchia, A. T Cell Activation Determined by T Cell Receptor Number and Tunable Thresholds. *Science* 273, 104–106 (1996).
29. Krummel, M. & Allison, J. CTLA-4 engagement inhibits IL-2 accumulation and cell cycle progression upon activation of resting T cells. *The Journal of experimental medicine* 183, 2533–40 (1996).
30. Krummel, M. & Allison, J. CD28 and CTLA-4 have opposing effects on the response of T cells to stimulation. *The Journal of experimental medicine* 182, 459–65 (1995).
31. Curtsinger, J. M. & Mescher, M. F. Inflammatory cytokines as a third signal for T cell activation. *Curr Opin Immunol* 22, 333–340 (2010).
32. Zhang, N. & Bevan, M. J. CD8<sup>+</sup> T Cells: Foot Soldiers of the Immune System. *Immunity* 35, 161–168 (2011).
33. Curtsinger, J. M., Lins, D. C. & Mescher, M. F. Signal 3 Determines Tolerance versus Full Activation of Naive CD8 T Cells. *J Exp Medicine* 197, 1141–1151 (2003).
34. Mosmann, T., Cherwinski, H., Bond, M., Giedlin, M. & Coffman, R. Two types of murine helper T cell clone. I. Definition according to profiles of lymphokine activities and secreted proteins. *J Immunol Baltim Md* 1950 136, 2348–57 (1986).
35. Szabo, S. et al. A novel transcription factor, T-bet, directs Th1 lineage commitment. *Cell* 100, 655–69 (2000).
36. Bhat, P., Leggatt, G., Waterhouse, N. & Frazer, I. H. Interferon- $\gamma$  derived from cytotoxic lymphocytes directly enhances their motility and cytotoxicity. *Cell Death Dis* 8, e2836 (2017).

37. Elsas, V. A., Hurwitz, A. & of Experimental, A. J. Combination immunotherapy of B16 melanoma using anti-cytotoxic T lymphocyte-associated antigen 4 (CTLA-4) and granulocyte/macrophage colony .... (1999). doi:10.1084/jem.190.3.355
38. Li, K. et al. Adoptive cell therapy with CD4<sup>+</sup> T helper 1 cells and CD8<sup>+</sup> cytotoxic T cells enhances complete rejection of an established tumour, leading to generation of endogenous memory responses to non-targeted tumour epitopes. *Clin Transl Immunol* 6, e160 (2017).
39. Li, K. et al. Conditions for the generation of cytotoxic CD4<sup>+</sup> Th cells that enhance CD8<sup>+</sup> CTL-mediated tumor regression. *Clin Transl Immunol* 5, e95 (2016).
40. Simmons, W. J. et al. Tim-3<sup>+</sup> T-bet<sup>+</sup> Tumor-Specific Th1 Cells Colocalize with and Inhibit Development and Growth of Murine Neoplasms. *J Immunol* 174, 1405–1415 (2005).
41. Takatsu, K. Cytokines Involved in B-Cell Differentiation and Their Sites of Action. *P Soc Exp Biol Med* 215, 121–133 (1997).
42. Missol, E., Sochanik, A. & Szala, S. Introduction of murine Il-4 gene into B16(F10) melanoma tumors by direct gene transfer with DNA-liposome complexes. *Cancer Lett* 97, 189–193 (1995).
43. Tepper, R., Coffman, R. & Leder, P. An eosinophil-dependent mechanism for the antitumor effect of interleukin-4. *Science* 257, 548–551 (1992).
44. Lorvik, K. et al. Adoptive Transfer of Tumor-Specific Th2 Cells Eradicates Tumors by Triggering an In Situ Inflammatory Immune Response. *Cancer Res* 76, 6864–6876 (2016).
45. Shiao, S. L. et al. TH2-Polarized CD4<sup>+</sup> T Cells and Macrophages Limit Efficacy of Radiotherapy. *Cancer Immunol Res* 3, 518–525 (2015).
46. Veldhoen, M. et al. Transforming growth factor- $\beta$  ‘reprograms’ the differentiation of T helper 2 cells and promotes an interleukin 9-producing subset. *Nat Immunol* 9, ni.1659 (2008).
47. Dardalhon, V. et al. IL-4 inhibits TGF- $\beta$ -induced Foxp3<sup>+</sup> T cells and, together with TGF- $\beta$ , generates IL-9<sup>+</sup> IL-10<sup>+</sup> Foxp3<sup>–</sup> effector T cells. *Nat Immunol* 9, ni.1677 (2008).
48. Purwar, R. et al. Robust tumor immunity to melanoma mediated by interleukin-9-producing T cells. *Nat Med* 18, 1248 (2012).

49. Lu, Y. et al. Th9 cells promote antitumor immune responses in vivo. *Journal of Clinical Investigation* 122, 4160–4171 (2012).
50. Renauld, J. et al. Thymic lymphomas in interleukin 9 transgenic mice. *Oncogene* 9, 1327–32 (1994).
51. Parrot, T. et al. IL-9 promotes the survival and function of human melanoma-infiltrating CD4+CD8+ double-positive T cells. *Eur J Immunol* 46, 1770–1782 (2016).
52. Wang, L. et al. IL-17 can promote tumor growth through an IL-6–Stat3 signaling pathway. *J Exp Medicine* 206, 1457–1464 (2009).
53. Muranski, P. et al. Tumor-specific Th17-polarized cells eradicate large established melanoma. *Blood* 112, 362–373 (2008).
54. Gershon, R. & Kondo, K. Cell interactions in the induction of tolerance: the role of thymic lymphocytes. *Immunology* 18, 723–37 (1970).
55. Sakaguchi, S., Sakaguchi, N., Asano, M., Itoh, M. & Toda, M. Immunologic self-tolerance maintained by activated T cells expressing IL-2 receptor alpha-chains (CD25). Breakdown of a single mechanism of self-tolerance causes various autoimmune diseases. *J Immunol Baltim Md* 1950 155, 1151–64 (1995).
56. Brunkow, M. E. et al. Disruption of a new forkhead/winged-helix protein, scurfy, results in the fatal lymphoproliferative disorder of the scurfy mouse. *Nat Genet* 27, 68 (2001).
57. Hori, S., Nomura, T. & Sakaguchi, S. Control of Regulatory T Cell Development by the Transcription Factor Foxp3. *Science* 299, 1057–1061 (2003).
58. Liu, Y. et al. Hypoxia induced HMGB1 and mitochondrial DNA interactions mediate tumor growth in hepatocellular carcinoma through Toll-like receptor 9. *J Hepatol* 63, 114–21 (2015).
59. Nishikawa, H. & Sakaguchi, S. Regulatory T cells in tumor immunity. *Int J Cancer* 127, 759–767 (2010).
60. Sugiyama, D. et al. Anti-CCR4 mAb selectively depletes effector-type FoxP3+CD4+ regulatory T cells, evoking antitumor immune responses in humans. *Proc National Acad Sci* 110, 17945–17950 (2013).
61. Liu, V. C. et al. Tumor Evasion of the Immune System by Converting CD4+CD25– T Cells into CD4+CD25+ T Regulatory Cells: Role of Tumor-Derived TGF- $\beta$ . *J Immunol* 178, 2883–2892 (2007).

62. Medawar, P. The behaviour and fate of skin autografts and skin homografts in rabbits: A report to the War Wounds Committee of the Medical Research Council. *J Anat* 78, 176–99 (1944).
63. MAIN, R., COCHRUM, K., JONES, M. & KOUNTZ, S. Immunological Potential of the in vitro Mixed Skin Cell-Leukocyte Reaction. *Nat New Biology* 229, 89 (1971).
64. Hirschhorn, K., Bach, F., Kolodny, R. L., Firschein, L. I. & Hashem, N. Immune Response and Mitosis of Human Peripheral Blood Lymphocytes in vitro. *Science* 142, 1185–1187 (1963).
65. B, I., Vas, M. & Lowenstein, L. The Development of Large Immature Mononuclear Cells in Mixed Leukocyte Cultures. *Blood* 23, 108–16 (1964).
66. Korngold, R. & Sprent, J. Lethal graft-versus-host disease after bone marrow transplantation across minor histocompatibility barriers in mice. Prevention by removing mature T cells from marrow. *J Exp Medicine* 148, 1687–1698 (1978).
67. Simonsen, M. Graft Versus Host Reactions. Their Natural History, and Applicability as Tools of Research. *Chem Immunol Allergy* 6, 349–467 (1962).
68. Cerottini, J. & Brunner, K. Cell-mediated cytotoxicity, allograft rejection, and tumor immunity. *Adv Immunol* 18, 67–132 (1974).
69. Benichou, G. & of ..., V. A. Contributions of direct and indirect T cell alloreactivity during allograft rejection in mice. (1999).
70. Benichou, G. Direct and indirect antigen recognition: the pathways to allograft immune rejection. *Frontiers in bioscience : a journal and virtual library* 4, D476-80 (1999).
71. Benichou, G. & Thomson, A. Direct versus indirect allorecognition pathways: on the right track. *American journal of transplantation : official journal of the American Society of Transplantation and the American Society of Transplant Surgeons* 9, 655–6 (2009).
72. Liu, Z. et al. Contribution of direct and indirect recognition pathways to T cell alloreactivity. *The Journal of experimental medicine* 177, 1643–50 (1993).
73. Baker, R. J. et al. Loss of Direct and Maintenance of Indirect Alloresponses in Renal Allograft Recipients: Implications for the Pathogenesis of Chronic Allograft Nephropathy. *J Immunol* 167, 7199–7206 (2001).
74. Liu, Z. et al. Limited usage of T cell receptor V beta genes by allopeptide-specific T cells. *J Immunol Baltim Md 1950* 150, 3180–6 (1993).

75. Dietrich, P. et al. In vivo T-cell clonal amplification at time of acute graft-versus-host disease. *Blood* 84, 2815–20 (1994).
76. Villers, D. et al. Alteration of the T cell repertoire after bone marrow transplantation. *Bone Marrow Transpl* 13, 19–26 (1994).
77. Lakkis, F. G. & Lechler, R. I. Origin and biology of the allogeneic response. *Cold Spring Harbor perspectives in medicine* 3, (2013).
78. Simpson, E. & Roopenian, D. Minor histocompatibility antigens. *Curr Opin Immunol* 9, 655–661 (1997).
79. Spierings, E., Wieles, B. & Goulmy, E. Minor histocompatibility antigens – big in tumour therapy. *Trends Immunol* 25, 56–60 (2004).
80. Perreault, C. et al. Minor histocompatibility antigens. *Blood* 76, 1269–80 (1990).
81. Wilson, D. B. & Nowell, P. C. Quantitative Studies on the Mixed Lymphocyte Interaction in Rats IV. Immunologic Potentiality of the Responding Cells. *J Exp Medicine* 131, 391–407 (1970).
82. Ferrara, J. L., Levine, J. E., Reddy, P. & Holler, E. Graft-versus-host disease. *Lancet* 373, 1550–1561 (2009).
83. Choi, S. & Reddy, P. Current and emerging strategies for the prevention of graft-versus-host disease. *Nat Rev Clin Oncol* 11, 536 (2014).
84. Markey, K. A. et al. Conventional dendritic cells are the critical donor APC presenting alloantigen after experimental bone marrow transplantation. *Blood* 113, 5644–5649 (2009).
85. Lu, Y. & Waller, E. K. Dichotomous Role of Interferon- $\gamma$  in Allogeneic Bone Marrow Transplant. *Biol Blood Marrow Tr* 15, 1347–1353 (2009).
86. Malard, F. et al. Increased Th17/Treg ratio in chronic liver GVHD. *Bone Marrow Transpl* 49, 539 (2014).
87. Chen, X. et al. Absence of regulatory T-cell control of TH1 and TH17 cells is responsible for the autoimmune-mediated pathology in chronic graft-versus-host disease. *Blood* 110, 3804–3813 (2007).
88. Choi, S. W. et al. TNF-Inhibition with Etanercept for Graft-versus-Host Disease Prevention in High-Risk HCT: Lower TNFR1 Levels Correlate with Better Outcomes. *Biol Blood Marrow Tr* 18, 1525–1532 (2012).

89. Yi, T. et al. Reciprocal differentiation and tissue-specific pathogenesis of Th1, Th2, and Th17 cells in graft-versus-host disease. *Blood* 114, 3101–3112 (2009).
90. Weber, M. et al. Donor and host B cell-derived IL-10 contributes to suppression of graft-versus-host disease. *Eur J Immunol* 44, 1857–1865 (2014).
91. Briones, J., Novelli, S. & Sierra, J. T-Cell Co-stimulatory Molecules in Acute-Graft-Versus Host Disease: Therapeutic Implications. *Bone Marrow Res* 2011, 976793 (2011).
92. Blazar, B. et al. Infusion of anti-B7.1 (CD80) and anti-B7.2 (CD86) monoclonal antibodies inhibits murine graft-versus-host disease lethality in part via direct effects on CD4+ and CD8+ T cells. *J Immunol Baltim Md* 157, 3250–9 (1996).
93. Wallace, P. M. et al. CTLA4Ig Treatment Ameliorates the Lethality of Murine Graft-Versus-Host Disease Across Major Histocompatibility Complex Barriers. *Transplantation* 58, 602–610 (1994).
94. Sato, M. et al. Inducible Costimulator (ICOS) Up-Regulation on Activated T Cells in Chronic Graft-Versus-Host Disease After Dog Leukocyte Antigen–Nonidentical Hematopoietic Cell Transplantation. *Transplant J* 96, 34–41 (2013).
95. Beilhack, A. et al. In vivo analyses of early events in acute graft-versus-host disease reveal sequential infiltration of T-cell subsets. *Blood* 106, 1113–1122 (2005).
96. Matas, H. J., Gillingham, K. J., Payne, W. & Najarian, J. S. The Impact of an Acute Rejection Episode on Long-Term Renal Allograft Survival (t1/2)<sup>1,2</sup>. *Transplantation* 57, 857–859 (1994).
97. Talmage, D., Dart, G., Radovich, J. & Lafferty, K. Activation of transplant immunity: effect of donor leukocytes on thyroid allograft rejection. *Science* 191, 385–388 (1976).
98. Schuler, G. & einman, R. Murine epidermal Langerhans cells mature into potent immunostimulatory dendritic cells in vitro. *J Exp Medicine* 161, 526–546 (1985).
99. Auchincloss, H. et al. The role of 'indirect' recognition in initiating rejection of skin grafts from major histocompatibility complex class II-deficient mice. *Proc National Acad Sci* 90, 3373–3377 (1993).
100. Lee, R., Grusby, M., Glimcher, L., Winn, H. & Auchincloss, H. Indirect recognition by helper cells can induce donor-specific cytotoxic T lymphocytes in vivo. *J Exp Medicine* 179, 865–872 (1994).



101. Dalloul, A., Chmouzis, E., Ngo, K. & Fung-Leung, W. Adoptively transferred CD4+ lymphocytes from CD8 -/- mice are sufficient to mediate the rejection of MHC class II or class I disparate skin grafts. *J Immunol Baltim Md* 1950 156, 4114–9 (1996).
102. Graca, L., Cobbold, S. P. & Waldmann, H. Identification of Regulatory T Cells in Tolerated Allografts. *J Exp Medicine* 195, 1641–1646 (2002).
103. Fan, Z. et al. In vivo tracking of ‘color-coded’ effector, natural and induced regulatory T cells in the allograft response. *Nat Med* 16, 718 (2010).
104. Kolb, H. et al. Graft-versus-leukemia effect of donor lymphocyte transfusions in marrow grafted patients. *Blood* 86, 2041–50 (1995).
105. Falkenburg, J., Marijt, W., Heemskerk, M. & Willemze, R. Minor histocompatibility antigens as targets of graft-versus-leukemia reactions. *Curr Opin Hematol* 9, 497–502 (2002).
106. Fontaine, P. et al. Adoptive transfer of minor histocompatibility antigen-specific T lymphocytes eradicates leukemia cells without causing graft-versus-host disease. *Nat Med* 7, 789–794 (2001).
107. Spierings, E. & Goulmy, E. Expanding the immunotherapeutic potential of minor histocompatibility antigens. *J Clin Invest* 115, 3397–3400 (2005).
108. Jones, S. C., Murphy, G. F., Friedman, T. M. & Korngold, R. Importance of minor histocompatibility antigen expression by nonhematopoietic tissues in a CD4+ T cell-mediated graft-versus-host disease model. *J Clin Invest* 112, 1880–1886 (2003).
109. Armistead, P. M. et al. Common Minor Histocompatibility Antigen Discovery Based upon Patient Clinical Outcomes and Genomic Data. *Plos One* 6, e23217 (2011).
110. Marijt, E. et al. Phase I/II feasibility study evaluating the generation of leukemia-reactive cytotoxic T lymphocyte lines for treatment of patients with relapsed leukemia after allogeneic stem cell transplantation. *Haematologica* 92, 72–80 (2007).
111. Laurell, A. et al. Intratumorally injected pro-inflammatory allogeneic dendritic cells as immune enhancers: a first-in-human study in unfavourable risk patients with metastatic renal cell carcinoma. *Journal for immunotherapy of cancer* 5, 52 (2017).
112. Wallgren, A., Andersson, B., Bäcker, A. & Karlsson-Parra, A. Direct Allorecognition Promotes Activation of Bystander Dendritic Cells and Licenses Them for Th1 Priming: A Functional Link Between Direct and Indirect Allosensitization. *Scand J Immunol* 62, 234–242 (2005).

113. Lövgren, T. et al. Enhanced stimulation of human tumor-specific T cells by dendritic cells matured in the presence of interferon- $\gamma$  and multiple toll-like receptor agonists. *Cancer Immunol Immunother* 66, 1333–1344 (2017).
114. Bevan, M. Minor H antigens introduced on H-2 different stimulating cells cross-react at the cytotoxic T cell level during in vivo priming. *Journal of immunology* (Baltimore, Md. : 1950) 117, 2233–8 (1976).
115. of Medicine, B. M. Cross-priming for a secondary cytotoxic response to minor H antigens with H-2 congenic cells which do not cross-react in the cytotoxic assay. (1976). doi:10.1084/jem.143.5.1283
116. Shen, Z., Reznikoff, G., Dranoff, G. & Rock, K. Cloned dendritic cells can present exogenous antigens on both MHC class I and class II molecules. *J Immunol Baltim Md 1950* 158, 2723–30 (1997).
117. Sallusto, F., Cella, M., Danieli, C. & Lanzavecchia, A. Dendritic cells use macropinocytosis and the mannose receptor to concentrate macromolecules in the major histocompatibility complex class II compartment: downregulation by cytokines and bacterial products. *J Exp Medicine* 182, 389–400 (1995).
118. Lanzavecchia, A. Mechanisms of antigen uptake for presentation. *Curr Opin Immunol* 8, 348–354 (1996).
119. Morrison, L., Lukacher, A., Braciale, V., Fan, D. & Braciale, T. Differences in antigen presentation to MHC class I-and class II-restricted influenza virus-specific cytolytic T lymphocyte clones. *J Exp Medicine* 163, 903–921 (1986).
120. Rodriguez, A., Regnault, A., Kleijmeer, M., Ricciardi-Castagnoli, P. & Amigorena, S. Selective transport of internalized antigens to the cytosol for MHC class I presentation in dendritic cells. *Nature cell biology* 1, 362–8 (1999).
121. Delamarre, L., Holcombe, H. & Mellman, I. Presentation of exogenous antigens on major histocompatibility complex (MHC) class I and MHC class II molecules is differentially regulated during dendritic cell maturation. *The Journal of experimental medicine* 198, 111–22 (2003).
122. Shen, L., Sigal, L. J., Boes, M. & Rock, K. L. Important Role of Cathepsin S in Generating Peptides for TAP-Independent MHC Class I Crosspresentation In Vivo. *Immunity* 21, 155–165 (2004).
123. Vyas, J. M., der Veen, A. G. & Ploegh, H. L. The known unknowns of antigen processing and presentation. *Nat Rev Immunol* 8, nri2368 (2008).

124. Brossart, P. & Blood, B. M. Presentation of exogenous protein antigens on major histocompatibility complex class I molecules by dendritic cells: pathway of presentation and regulation by .... (1997).
125. Kovacsics-Bankowski, M. & Science, R. K. A phagosome-to-cytosol pathway for exogenous antigens presented on MHC class I molecules. (1995).  
doi:10.1126/science.7809629
126. Guernonprez, P. & Amigorena, S. Pathways for antigen cross presentation. Springer seminars in immunopathology 26, 257–71 (2005).
127. Burgdorf, S., Schölz, C., Kautz, A., Tampé, R. & Kurts, C. Spatial and mechanistic separation of cross-presentation and endogenous antigen presentation. Nat Immunol 9, 558–566 (2008).
128. Basler, M., Kirk, C. J. & Groettrup, M. The immunoproteasome in antigen processing and other immunological functions. Curr Opin Immunol 25, 74–80 (2013).
129. Delamarre, L., Pack, M., Chang, H., Mellman, I. & Trombetta, S. E. Differential Lysosomal Proteolysis in Antigen-Presenting Cells Determines Antigen Fate. Science 307, 1630–1634 (2005).
130. Trombetta, S. E., Ebersold, M., Garrett, W., Pypaert, M. & Mellman, I. Activation of Lysosomal Function During Dendritic Cell Maturation. Science 299, 1400–1403 (2003).
131. Mantegazza, A. R. et al. NADPH oxidase controls phagosomal pH and antigen cross-presentation in human dendritic cells. Blood 112, 4712–4722 (2008).
132. Savina, A. et al. NOX2 Controls Phagosomal pH to Regulate Antigen Processing during Crosspresentation by Dendritic Cells. Cell 126, 205–218 (2006).
133. van de Ven, R. et al. Characterization of four conventional dendritic cell subsets in human skin-draining lymph nodes in relation to T-cell activation. Blood 118, 2502–10 (2011).
134. Miller, J. C. et al. Deciphering the transcriptional network of the dendritic cell lineage. Nat Immunol 13, 888 (2012).
135. Dorner, B. G. et al. Selective Expression of the Chemokine Receptor XCR1 on Cross-presenting Dendritic Cells Determines Cooperation with CD8+ T Cells. Immunity 31, 823–33 (2009).

136. Poulin, L. et al. Characterization of human DNGR-1+ BDCA3+ leukocytes as putative equivalents of mouse CD8 $\alpha$ + dendritic cells. *J Exp Medicine* 207, 1261–1271 (2010).
137. Edwards, A. D. et al. Relationships Among Murine CD11<sup>high</sup> Dendritic Cell Subsets as Revealed by Baseline Gene Expression Patterns. *J Immunol* 171, 47–60 (2003).
138. Hildner, K. et al. Batf3 Deficiency Reveals a Critical Role for CD8 $\alpha$ + Dendritic Cells in Cytotoxic T Cell Immunity. *Science* 322, 1097–1100 (2008).
139. Bedoui, S. et al. Cross-presentation of viral and self antigens by skin-derived CD103+ dendritic cells. *Nature Immunology* 10, 488–495 (2009).
140. Rio, M., Bernhardt, G., Rodriguez-Barbosa, J. & Förster, R. Development and functional specialization of CD103+ dendritic cells. *Immunol Rev* 234, 268–281 (2010).
141. Apte, S. H. et al. Subcutaneous cholera toxin exposure induces potent CD103+ dermal dendritic cell activation and migration. *Eur J Immunol* 43, 2707–2717 (2013).
142. Desch, N. A. et al. CD103+ pulmonary dendritic cells preferentially acquire and present apoptotic cell-associated antigen. *J Exp Medicine* 208, 1789–1797 (2011).
143. Ramos, M. et al. A8.19 Non-lymphoid CD103+ dendritic cells are required for the initiation of collagen-induced arthritis. *Ann Rheum Dis* 73, A83 (2014).
144. Burgdorf, S., Kautz, A., Böhnert, V., Knolle, P. A. & Kurts, C. Distinct pathways of antigen uptake and intracellular routing in CD4 and CD8 T cell activation. *Science (New York, N.Y.)* 316, 612–6 (2007).
145. den Haan, J. M. & Bevan, M. J. Constitutive versus activation-dependent cross-presentation of immune complexes by CD8(+) and CD8(-) dendritic cells in vivo. *The Journal of experimental medicine* 196, 817–27 (2002).
146. Platzer, B., Stout, M. & Fiebiger, E. Antigen Cross-Presentation of Immune Complexes. *Frontiers in Immunology* 5, 140 (2014).
147. Schnurr, M. et al. Tumor antigen processing and presentation depend critically on dendritic cell type and the mode of antigen delivery. *Blood* 105, 2465–2472 (2005).
148. Bonifaz, L. C. et al. In vivo targeting of antigens to maturing dendritic cells via the DEC-205 receptor improves T cell vaccination. *The Journal of experimental medicine* 199, 815–24 (2004).

149. Jiang, W. et al. The receptor DEC-205 expressed by dendritic cells and thymic epithelial cells is involved in antigen processing. *Nature* 375, 151–5 (1995).
150. Heath, W., Belz, G. & Immunological ..., G. Cross-presentation, dendritic cell subsets, and the generation of immunity to cellular antigens. (2004). doi:10.1111/j.0105-2896.2004.00142.x
151. East, L. & et Subjects, I. C. The mannose receptor family. (2002).
152. McKay, P., Imami, N. & journal of ..., J. M. The gp200-MR6 molecule which is functionally associated with the IL-4 receptor modulates B cell phenotype and is a novel member of the human macrophage .... (1998). doi:10.1002/(SICI)1521-4141(199812)28:12<4071::AID-IMMU4071>3.0.CO;2-O
153. Dudziak, D. et al. Differential Antigen Processing by Dendritic Cell Subsets in Vivo. *Science* 315, 107–111 (2007).
154. Bonifaz, L., Bonnyay, D., Mahnke, K. & of ..., R. M. Efficient targeting of protein antigen to the dendritic cell receptor DEC-205 in the steady state leads to antigen presentation on major histocompatibility complex class I .... (2002). doi:10.1084/jem.20021598
155. Gutiérrez-Martínez, E. et al. Cross-Presentation of Cell-Associated Antigens by MHC Class I in Dendritic Cell Subsets. *Frontiers in immunology* 6, 363 (2015).
156. Ackerman, A. L., Kyritsis, C., Tampé, R. & Cresswell, P. Access of soluble antigens to the endoplasmic reticulum can explain cross-presentation by dendritic cells. *Nature immunology* 6, 107–13 (2005).
157. Tel, J. et al. Targeting Uptake Receptors on Human Plasmacytoid Dendritic Cells Triggers Antigen Cross-Presentation and Robust Type I IFN Secretion. *J Immunol* 191, 5005–5012 (2013).
158. Joffre, O. P., Segura, E., Savina, A. & Amigorena, S. Cross-presentation by dendritic cells. *Nature reviews. Immunology* 12, 557–69 (2012).
159. Lennerz, V. et al. The response of autologous T cells to a human melanoma is dominated by mutated neoantigens. *Proceedings of the National Academy of Sciences of the United States of America* 102, 16013–8 (2005).
160. Wolkers, M. C., Brouwenstijn, N., Bakker, A. H., Toebe, M. & Schumacher, T. N. Antigen Bias in T Cell Cross-Priming. *Science* 304, 1314–1317 (2004).
161. Brusa, D. et al. Post-apoptotic tumors are more palatable to dendritic cells and enhance their antigen cross-presentation activity. *Vaccine* 26, 6422–6432 (2008).

162. Matheoud, D. et al. Cross-presentation by dendritic cells from live cells induces protective immune responses in vivo. *Blood* 115, 4412–4420 (2010).
163. Zeelenberg, I. S. et al. Antigen Localization Controls T Cell-Mediated Tumor Immunity. *J Immunol* 187, 1281–1288 (2011).
164. Kurts, C., Miller, J., Subramaniam, R. M., Carbone, F. R. & Heath, W. R. Major Histocompatibility Complex Class I-restricted Cross-presentation Is Biased towards High Dose Antigens and Those Released during Cellular Destruction. *J Exp Medicine* 188, 409–414 (1998).
165. Norbury, C. C. et al. CD8+ T Cell Cross-Priming via Transfer of Proteasome Substrates. *Science* 304, 1318–1321 (2004).
166. Li, M. et al. Cell-Associated Ovalbumin Is Cross-Presented Much More Efficiently than Soluble Ovalbumin In Vivo. *J Immunol* 166, 6099–6103 (2001).
167. Shen, L. & Rock, K. L. Cellular protein is the source of cross-priming antigen in vivo. *P Natl Acad Sci Usa* 101, 3035–3040 (2004).
168. Unger, W. et al. Glycan-modified liposomes boost CD4+ and CD8+ T-cell responses by targeting DC-SIGN on dendritic cells. *J Control Release* 160, 88–95 (2012).
169. Nierkens, S., Tel, J., Janssen, E. & Adema, G. J. Antigen cross-presentation by dendritic cell subsets: one general or all sergeants? *Trends Immunol* 34, 361–370 (2013).
170. Belz, G. T. et al. Distinct migrating and nonmigrating dendritic cell populations are involved in MHC class I-restricted antigen presentation after lung infection with virus. *P Natl Acad Sci Usa* 101, 8670–8675 (2004).
171. Akira, S., Uematsu, S. & Takeuchi, O. Pathogen Recognition and Innate Immunity. *Cell* 124, 783–801 (2006).
172. Gordon, S. Pattern Recognition Receptors Doubling Up for the Innate Immune Response. *Cell* 111, 927–930 (2002).
173. Suresh, R. & Mosser, D. M. Pattern recognition receptors in innate immunity, host defense, and immunopathology. *Adv Physiol Educ* 37, 284–91 (2013).
174. Zhan, Y. et al. GM-CSF increases cross-presentation and CD103 expression by mouse CD8+ spleen dendritic cells. *Eur J Immunol* 41, 2585–2595 (2011).
175. Dranoff, G. et al. Vaccination with irradiated tumor cells engineered to secrete murine granulocyte-macrophage colony-stimulating factor stimulates potent,

- specific, and long-lasting anti-tumor immunity. *Proc National Acad Sci* 90, 3539–3543 (1993).
176. Spadaro, F. et al. IFN- $\alpha$  enhances cross-presentation in human dendritic cells by modulating antigen survival, endocytic routing, and processing. *Blood* 119, 1407–17 (2012).
  177. Schulz, O. et al. CD40 Triggering of Heterodimeric IL-12 p70 Production by Dendritic Cells In Vivo Requires a Microbial Priming Signal. *Immunity* 13, 453–462 (2000).
  178. Banchereau, J. & Steinman, R. M. Dendritic cells and the control of immunity. *Nature* 392, 245–252 (1998).
  179. Cui, Z. & Qiu, F. CD4 $\alpha$  T Helper Cell Response is Required for Memory in CD8 $\alpha$  T Lymphocytes Induced by a Poly(I:C)-adjuvanted MHC I-restricted Peptide Epitope. *J Immunother* 30, 180–189 (2007).
  180. Reinman, Turley, S. & of Experimental ..., M. I. The induction of tolerance by dendritic cells that have captured apoptotic cells. (2000).
  181. Kurts, C. et al. Constitutive class I-restricted exogenous presentation of self antigens in vivo. *J Exp Medicine* 184, 923–930 (1996).
  182. Hawiger, D., Inaba, K., Dorsett, Y. & of ..., G. M. Dendritic cells induce peripheral T cell unresponsiveness under steady state conditions in vivo. (2001). doi:10.1084/jem.194.6.769
  183. Liu, K. et al. Immune tolerance after delivery of dying cells to dendritic cells in situ. *The Journal of experimental medicine* 196, 1091–7 (2002).
  184. vey, G. et al. Peripheral deletion of autoreactive CD8 T cells by cross presentation of self-antigen occurs by a Bcl-2-inhibitable pathway mediated by Bim. *The Journal of experimental medicine* 196, 947–55 (2002).
  185. Belz, G. T. et al. The CD8 $\alpha$ (+) dendritic cell is responsible for inducing peripheral self-tolerance to tissue-associated antigens. *The Journal of experimental medicine* 196, 1099–104 (2002).
  186. Huang, A. et al. Role of bone marrow-derived cells in presenting MHC class I-restricted tumor antigens. *Science* 264, 961–965 (1994).
  187. Ochsenbein, A. et al. Roles of tumour localization, second signals and cross priming in cytotoxic T-cell induction. *Nature* 411, 1058–64 (2001).

188. Kurts, C., Robinson, B. W. & Knolle, P. A. Cross-priming in health and disease. *Nat Rev Immunol* 10, 403 (2010).
189. Hotblack, A. et al. Tumor-Resident Dendritic Cells and Macrophages Modulate the Accumulation of TCR-Engineered T Cells in Melanoma. *Molecular therapy : the journal of the American Society of Gene Therapy* 26, 1471–1481 (2018).
190. Brown, M. C. et al. Cancer immunotherapy with recombinant poliovirus induces IFN-dominant activation of dendritic cells and tumor antigen-specific CTLs. *Science Translational Medicine* 9, ean4220 (2017).
191. Lee, J. M. et al. Phase I Trial of Intratumoral Injection of CCL21 Gene-Modified Dendritic Cells in Lung Cancer Elicits Tumor-Specific Immune Responses and CD8<sup>+</sup> T-cell Infiltration. *Clinical cancer research : an official journal of the American Association for Cancer Research* 23, 4556–4568 (2017).
192. Spranger, S., Dai, D., Horton, B. & Gajewski, T. F. Tumor-Residing Batf3 Dendritic Cells Are Required for Effector T Cell Trafficking and Adoptive T Cell Therapy. *Cancer cell* 31, 711–723.e4 (2017).
193. Roberts, E. W. et al. Critical Role for CD103<sup>+</sup>/CD141<sup>+</sup> Dendritic Cells Bearing CCR7 for Tumor Antigen Trafficking and Priming of T Cell Immunity in Melanoma. *Cancer Cell* 30, 324–336 (2016).
194. Ladányi, A. et al. Density of DC-LAMP<sup>+</sup> mature dendritic cells in combination with activated T lymphocytes infiltrating primary cutaneous melanoma is a strong independent prognostic factor. *Cancer Immunol Immunother* 56, 1459–1469 (2007).
195. Houde, M. et al. Phagosomes are competent organelles for antigen cross-presentation. *Nature* 425, 402 (2003).
196. Ackerman, A. L., Giodini, A. & Cresswell, P. A Role for the Endoplasmic Reticulum Protein Retrotranslocation Machinery during Crosspresentation by Dendritic Cells. *Immunity* 25, 607–617 (2006).
197. Luke, J. J., Bao, R., Sweis, R. F., Spranger, S. & Gajewski, T. F. WNT/ $\beta$ -catenin pathway activation correlates with immune exclusion across human cancers. *Clinical cancer research : an official journal of the American Association for Cancer Research* (2019). doi:10.1158/1078-0432.CCR-18-1942
198. Spranger, S. & Gajewski, T. F. Impact of oncogenic pathways on evasion of antitumour immune responses. *Nature reviews. Cancer* 18, 139–147 (2018).



199. Gajewski, T. F. et al. Tumor Immune Microenvironment in Cancer Progression and Cancer Therapy. *Advances in experimental medicine and biology* 1036, 19–31 (2017).
200. Harimoto, H. et al. Inactivation of tumor-specific CD8<sup>+</sup> CTLs by tumor-infiltrating tolerogenic dendritic cells. *Immunol Cell Biol* 91, 545–555 (2013).
201. Simon, S. & Labarriere, N. PD-1 expression on tumor-specific T cells: Friend or foe for immunotherapy? *Oncoimmunology* 7, 00–00 (2017).
202. Jantsch, J. et al. Hypoxia and Hypoxia-Inducible Factor-1 $\alpha$  Modulate Lipopolysaccharide-Induced Dendritic Cell Activation and Function. *J Immunol* 180, 4697–4705 (2008).
203. Cham, C. M., Driessens, G., O’Keefe, J. P. & Gajewski, T. F. Glucose deprivation inhibits multiple key gene expression events and effector functions in CD8<sup>+</sup> T cells. *Eur J Immunol* 38, 2438–2450 (2008).
204. Rosenberg, S., Yang, J., White, D. & einberg, S. Durability of complete responses in patients with metastatic cancer treated with high-dose interleukin-2: identification of the antigens mediating response. *Ann Surg* 228, 307–19 (1998).
205. Medrano, R., Hunger, A., Mendonça, S., Barbuto, J. M. & Strauss, B. E. Immunomodulatory and antitumor effects of type I interferons and their application in cancer therapy. *Oncotarget* 5, 71249–71284 (2015).
206. Creagan, E. T. et al. Phase II study of recombinant leukocyte a interferon (rIFN- $\alpha$ A) in disseminated malignant melanoma. *Cancer* 54, 2844–2849 (1984).
207. Creagan, E. et al. Phase II study of low-dose recombinant leukocyte A interferon in disseminated malignant melanoma. *J Clin Oncol* 2, 1002–1005 (1984).
208. Creagan, E. et al. Phase II study of recombinant leukocyte A interferon (IFN-rA) plus cimetidine in disseminated malignant melanoma. *J Clin Oncol* 3, 977–981 (1985).
209. Kirkwood, J. M. et al. High- and Low-Dose Interferon Alfa-2b in High-Risk Melanoma: First Analysis of Intergroup Trial E1690/S9111/C9190. *J Clin Oncol* 18, 2444–2458 (2000).
210. Kirkwood, J. et al. High-dose interferon alfa-2b does not diminish antibody response to GM2 vaccination in patients with resected melanoma: results of the Multicenter Eastern Cooperative Oncology Group Phase II Trial E2696. *J Clin Oncol Official J Am Soc Clin Oncol* 19, 1430–6 (2001).

211. Kirkwood, J. et al. Comparison of Intramuscular and Intravenous Recombinant Alpha-2 Interferon in Melanoma and Other Cancers. *Ann Intern Med* 103, 32 (1985).
212. Golomb, H. et al. Alpha-2 interferon therapy of hairy-cell leukemia: a multicenter study of 64 patients. *J Clin Oncol* 4, 900–905 (1986).
213. Solal-Celigny, P. et al. Recombinant Interferon Alfa-2b Combined with a Regimen Containing Doxorubicin in Patients with Advanced Follicular Lymphoma. *New Engl J Medicine* 329, 1608–1614 (1993).
214. Kirkwood, J. et al. Interferon alfa-2b adjuvant therapy of high-risk resected cutaneous melanoma: the Eastern Cooperative Oncology Group Trial EST 1684. *J Clin Oncol* 14, 7–17 (1996).
215. Groopman, J. et al. Recombinant Alpha-2 Interferon Therapy for Kaposi's Sarcoma Associated with the Acquired Immunodeficiency Syndrome. *Ann Intern Med* 100, 671 (1984).
216. Wang, W. et al. Modulation of Signal Transducers and Activators of Transcription 1 and 3 Signaling in Melanoma by High-Dose IFN $\alpha$ 2b. *Clin Cancer Res* 13, 1523–1531 (2007).
217. Wang, W. et al. Effects of High-Dose IFN $\alpha$ 2b on Regional Lymph Node Metastases of Human Melanoma: Modulation of STAT5, FOXP3, and IL-17. *Clin Cancer Res* 14, 8314–8320 (2008).
218. Moschos, S. J. et al. Neoadjuvant Treatment of Regional Stage IIIB Melanoma With High-Dose Interferon Alfa-2b Induces Objective Tumor Regression in Association With Modulation of Tumor Infiltrating Host Cellular Immune Responses. *J Clin Oncol* 24, 3164–3171 (2006).
219. Duluc, D. et al. Interferon- $\gamma$  reverses the immunosuppressive and protumoral properties and prevents the generation of human tumor-associated macrophages. *Int J Cancer* 125, 367–373 (2009).
220. Fuertes, M. B. et al. Host type I IFN signals are required for antitumor CD8 $^{+}$  T cell responses through CD8 $\alpha^{+}$  dendritic cells. *J Exp Medicine* 208, 2005–2016 (2011).
221. Kalb, M. L., Glaser, A., Stary, G., Koszik, F. & Stingl, G. TRAIL $^{+}$  Human Plasmacytoid Dendritic Cells Kill Tumor Cells In Vitro: Mechanisms of Imiquimod- and IFN- $\alpha$ -Mediated Antitumor Reactivity. *J Immunol* 188, 1583–1591 (2012).
222. Bell, E. Innate immunity: TLR signalling. *Nat Rev Immunol* 3, nri1185 (2003).

223. Akira, S. & Takeda, K. Toll-like receptor signalling. *Nat Rev Immunol* 4, 499–511 (2004).
224. Herr, H. W. & Morales, A. History of Bacillus Calmette-Guerin and Bladder Cancer: An Immunotherapy Success Story. *J Urology* 179, 53–56 (2008).
225. Adams, S. et al. Topical TLR7 Agonist Imiquimod Can Induce Immune-Mediated Rejection of Skin Metastases in Patients with Breast Cancer. *Clin Cancer Res* 18, 6748–6757 (2012).
226. Navabi, H. et al. A clinical grade poly I:C-analogue (Ampligen®) promotes optimal DC maturation and Th1-type T cell responses of healthy donors and cancer patients in vitro. *Vaccine* 27, 107–115 (2009).
227. Nakamura, O., Shitara, N., Matsutani, M., Takakura, K. & Machida, H. Phase I-II trials of poly(ICLC) in malignant brain tumor patients. *J Interferon Res* 2, 1–4 (1982).
228. Rodríguez-Ruiz, M. et al. OUP accepted manuscript. *Ann Oncol* (2018). doi:10.1093/annonc/mdy089
229. Dillon, P. M. et al. A pilot study of the immunogenicity of a 9-peptide breast cancer vaccine plus poly-ICLC in early stage breast cancer. *J Immunother Cancer* 5, 92 (2017).
230. Sabbatini, P. et al. Phase I Trial of Overlapping Long Peptides from a Tumor Self-Antigen and Poly-ICLC Shows Rapid Induction of Integrated Immune Response in Ovarian Cancer Patients. *Clin Cancer Res* 18, 6497–6508 (2012).
231. Sabado, R. et al. Phase I/II study of the TLR3 agonist poly-ICLC as an adjuvant for NY-ESO-1 protein vaccination with or without Montanide ISA-51 vg in patients with melanoma. *J Clin Oncol* 32, TPS9119–TPS9119 (2014).
232. Ayala, M. A. et al. Dual activation of Toll-like receptors 7 and 9 impairs the efficacy of antitumor vaccines in murine models of metastatic breast cancer. *J Cancer Res Clin* 143, 1713–1732 (2017).
233. Shen, Y., Zeng, M., Qiu, F. & Tang, H. [Resiquimod (R848) has more stronger immune adjuvantivity than other tested TLR agonists]. *Xi Bao Yu Fen Zi Mian Yi Xue Za Zhi Chin J Cell Mol Immunol* 33, 591–596 (2017).
234. Manome, Y. et al. The inhibition of malignant melanoma cell invasion of bone by the TLR7 agonist R848 is dependent upon pro-inflammatory cytokines produced by bone marrow macrophages. *Oncotarget* 9, 29934–29943 (2018).

235. Li, T. & Chen, Z. J. The cGAS–cGAMP–STING pathway connects DNA damage to inflammation, senescence, and cancer. *J Exp Med* 215, jem.20180139 (2018).
236. Corrales, L. & Gajewski, T. F. Molecular Pathways: Targeting the Stimulator of Interferon Genes (STING) in the Immunotherapy of Cancer. *Clin Cancer Res* 21, 4774–4779 (2015).
237. Corrales, L., Matson, V., Flood, B., Spranger, S. & Gajewski, T. F. Innate immune signaling and regulation in cancer immunotherapy. *Cell Res* 27, 96 (2017).
238. Sun, L., Wu, J., Du, F., Chen, X. & Chen, Z. J. Cyclic GMP-AMP Synthase Is a Cytosolic DNA Sensor That Activates the Type I Interferon Pathway. *Science* 339, 786–791 (2013).
239. Ran, Y., Shu, H.-B. & Wang, Y.-Y. MITA/STING: A central and multifaceted mediator in innate immune response. *Cytokine Growth F R* 25, 631–639 (2014).
240. Verdeil, G., Marquardt, K., Surh, C. D. & Sherman, L. A. Adjuvants targeting innate and adaptive immunity synergize to enhance tumor immunotherapy. *Proceedings of the National Academy of Sciences of the United States of America* 105, 16683–8 (2008).
241. Simons, J. et al. Bioactivity of autologous irradiated renal cell carcinoma vaccines generated by ex vivo granulocyte-macrophage colony-stimulating factor gene transfer. *Cancer Res* 57, 1537–46 (1997).
242. Thomas, M. C., Greten, T. F., Pardoll, D. M. & Jaffee, E. M. Enhanced Tumor Protection by Granulocyte-Macrophage Colony-Stimulating Factor Expression at the Site of an Allogeneic Vaccine. *Hum Gene Ther* 9, 835–843 (1998).
243. Nemunaitis, J. et al. Phase II Study of Belagenpumatucel-L, a Transforming Growth Factor Beta-2 Antisense Gene-Modified Allogeneic Tumor Cell Vaccine in Non–Small-Cell Lung Cancer. *J Clin Oncol* 24, 4721–4730 (2006).
244. Thomas, A. et al. Mesothelin-specific CD8+ T Cell Responses Provide Evidence of In Vivo Cross-Priming by Antigen-Presenting Cells in Vaccinated Pancreatic Cancer Patients. *J Exp Medicine* 200, 297–306 (2004).
245. Kayaga, J. et al. Anti-tumour activity against B16-F10 melanoma with a GM-CSF secreting allogeneic tumour cell vaccine. *Gene Ther* 6, 3300961 (1999).
246. Powell, K. L., Stephens, A. S. & Ralph, S. J. Development of a potent melanoma vaccine capable of stimulating CD8+ T-cells independently of dendritic cells in a mouse model. *Cancer Immunol Immunother* 64, 861–872 (2015).

247. Eric, L. et al. A Lethally Irradiated Allogeneic Granulocyte-Macrophage Colony Stimulating Factor-Secreting Tumor Vaccine for Pancreatic Adenocarcinoma. *Ann Surg* 253, 328–335 (2011).
248. Thomas, D. A. & Massagué, J. TGF- $\beta$  directly targets cytotoxic T cell functions during tumor evasion of immune surveillance. *Cancer Cell* 8, 369–80 (2005).
249. einman, R. & Witmer. Lymphoid dendritic cells are potent stimulators of the primary mixed leukocyte reaction in mice. *Proc National Acad Sci* 75, 5132–5136 (1978).
250. Romani, N. et al. Presentation of exogenous protein antigens by dendritic cells to T cell clones. Intact protein is presented best by immature, epidermal Langerhans cells. *J Exp Medicine* 169, 1169–1178 (1989).
251. Bhardwaj, N., Young, J., Nisanian, A., Baggers, J. & einman, R. Small amounts of superantigen, when presented on dendritic cells, are sufficient to initiate T cell responses. *J Exp Medicine* 178, 633–642 (1993).
252. Strunk, D. et al. Generation of human dendritic cells/Langerhans cells from circulating CD34+ hematopoietic progenitor cells. *Blood* 87, 1292–302 (1996).
253. Butterfield, L. H. et al. Determinant spreading associated with clinical response in dendritic cell-based immunotherapy for malignant melanoma. *Clin Cancer Res Official J Am Assoc Cancer Res* 9, 998–1008 (2003).
254. Mukherji, B. et al. Induction of antigen-specific cytolytic T cells in situ in human melanoma by immunization with synthetic peptide-pulsed autologous antigen presenting cells. *Proc National Acad Sci* 92, 8078–8082 (1995).
255. Nestle, F. O. et al. Vaccination of melanoma patients with peptide- or tumorlysate-pulsed dendritic cells. *Nat Med* 4, 328–332 (1998).
256. Hsu, F. J. et al. Vaccination of patients with B-cell lymphoma using autologous antigen-pulsed dendritic cells. *Nat Med* 2, 52 (1996).
257. Tendeloo, V. F. et al. Induction of complete and molecular remissions in acute myeloid leukemia by Wilms' tumor 1 antigen-targeted dendritic cell vaccination. *Proc National Acad Sci* 107, 13824–13829 (2010).
258. Rosenblatt, J. et al. Vaccination with Dendritic Cell/Tumor Fusions following Autologous Stem Cell Transplant Induces Immunologic and Clinical Responses in Multiple Myeloma Patients. *Clin Cancer Res* 19, 3640–3648 (2013).
259. Chakraborty, N. G. et al. Immunization with a tumor-cell-lysate-loaded autologous-antigen-presenting-cell-based vaccine in melanoma. *Cancer Immunol Immunother* 47, 58–64 (1998).

260. Takahashi, H., Nakagawa, Y., Yokomuro, K. & Berzofsky, J. A. Induction of CD8+ cytotoxic T lymphocytes by immunization with syngeneic irradiated HIV-1 envelope derived peptide-pulsed dendritic cells. *Int Immunol* 5, 849–857 (1993).
261. Rosalia, R. A. et al. Dendritic cells process synthetic long peptides better than whole protein, improving antigen presentation and T-cell activation. *Eur J Immunol* 43, 2554–2565 (2013).
262. Palucka, A. K. et al. Dendritic Cells Loaded With Killed Allogeneic Melanoma Cells can Induce Objective Clinical Responses and MART-1 Specific CD8&plus; T-cell Immunity. *J Immunother* 29, 545–557 (2006).
263. Banchereau, J. et al. Immune and clinical responses in patients with metastatic melanoma to CD34(+) progenitor-derived dendritic cell vaccine. *Cancer Res* 61, 6451–8 (2001).
264. Banchereau, J. et al. Extended survival and broad immune responses following vaccination of patients with metastatic melanoma with peptide-pulsed CD34+ progenitor derived dendritic cells (DCs). *J Clin Oncol Official J Am Soc Clin Oncol* 23, 2525 (2005).
265. Thurner, B., Haendle, I. & ... Medicine, R. C. Vaccination with mage-3A1 peptide-pulsed mature, monocyte-derived dendritic cells expands specific cytotoxic T cells and induces regression of some metastases in .... (1999).
266. Butterfield, L. H. et al. A Phase I/II Trial Testing Immunization of Hepatocellular Carcinoma Patients with Dendritic Cells Pulsed with Four  $\alpha$ -Fetoprotein Peptides. *Clin Cancer Res* 12, 2817–2825 (2006).
267. Rosenberg, S. et al. Immunologic and therapeutic evaluation of a synthetic peptide vaccine for the treatment of patients with metastatic melanoma. *Nature medicine* 4, 321–7 (1998).
268. Liu, T.-Y., Hussein, W. M., Toth, I. & Skwarczynski, M. Advances in Peptide-based Human Papillomavirus Therapeutic Vaccines. *Curr Top Med Chem* 12, 1581–1592 (2012).
269. Kawakami, Y. et al. Identification of the immunodominant peptides of the MART-1 human melanoma antigen recognized by the majority of HLA-A2-restricted tumor infiltrating lymphocytes. *J Exp Medicine* 180, 347–352 (1994).
270. Purcell, A. W., McCluskey, J. & Rossjohn, J. More than one reason to rethink the use of peptides in vaccine design. *Nat Rev Drug Discov* 6, nrd2224 (2007).

271. Butterfield, L. et al. Generation of melanoma-specific cytotoxic T lymphocytes by dendritic cells transduced with a MART-1 adenovirus. *J Immunol Baltim Md* 1950 161, 5607–13 (1998).
272. Okada, N. et al. Dendritic cells transduced with gp100 gene by RGD fiber-mutant adenovirus vectors are highly efficacious in generating anti-B16BL6 melanoma immunity in mice. *Gene Ther* 10, 1891 (2003).
273. Ribas, A. et al. Characterization of antitumor immunization to a defined melanoma antigen using genetically engineered murine dendritic cells. *Cancer Gene Ther* 6, 523 (1999).
274. Yang, S., Linette, G. P., Longerich, S., Roberts, B. L. & Haluska, F. G. HLA-A2.1/Kb Transgenic Murine Dendritic Cells Transduced with an Adenovirus Encoding Human gp100 Process the Same A2.1-Restricted Peptide Epitopes as Human Antigen-Presenting Cells and Elicit A2.1-Restricted Peptide-Specific CTL. *Cell Immunol* 204, 29–37 (2000).
275. Butterfield, L. H. et al. T Cell Responses to HLA-A\*0201-Restricted Peptides Derived from Human  $\alpha$  Fetoprotein. *J Immunol* 166, 5300–5308 (2001).
276. Mehrotra, S. et al. Antigen presentation by MART-1 adenovirus-transduced interleukin-10-polarized human monocyte-derived dendritic cells. *Immunology* 113, 472–481 (2004).
277. Meng, W. S. & Butterfield, L. H. Activation of antigen-presenting cells by DNA delivery vectors. *Expert Opin Biol Ther* 5, 1019–1028 (2005).
278. Dylla, J., Latouche, J.-B., Schnell, S. & Sadelain, M. Lentivirus-transduced human monocyte-derived dendritic cells efficiently stimulate antigen-specific cytotoxic T lymphocytes. *Blood* 97, 114–121 (2001).
279. Diebold, S. et al. Efficient gene delivery into human dendritic cells by adenovirus polyethylenimine and mannose polyethylenimine transfection. *Hum Gene Ther* 10, 775–86 (1999).
280. Schumacher, L. et al. Human Dendritic Cell Maturation by Adenovirus Transduction Enhances Tumor Antigen-Specific T-Cell Responses. *J Immunother* 27, 191–200 (2004).
281. Vujanovic, L. et al. Regulation of antigen presentation machinery in human dendritic cells by recombinant adenovirus. *Cancer Immunol Immunother* 58, 121–133 (2009).

282. Rouard, H. et al. Adenoviral transduction of human 'clinical grade' immature dendritic cells enhances co-stimulatory molecule expression and T-cell stimulatory capacity. *J Immunol Methods* 241, 69–81 (2000).
283. Liu, Y. et al. Hierarchy of  $\alpha$  Fetoprotein (AFP)-Specific T Cell Responses in Subjects with AFP-Positive Hepatocellular Cancer. *J Immunol* 177, 712–721 (2006).
284. Butterfield, L. H. et al. Adenovirus MART-1–engineered Autologous Dendritic Cell Vaccine for Metastatic Melanoma. *J Immunother* 31, 294–309 (2008).
285. Goldszmid, R., Idoyaga, J. & of ..., B. A. Dendritic cells charged with apoptotic tumor cells induce long-lived protective CD4+ and CD8+ T cell immunity against B16 melanoma. (2003). doi:10.4049/jimmunol.171.11.5940
286. Miyamoto, K. *Neuroimmunological Diseases*. 283–292 (2016). doi:10.1007/978-4-431-55594-0\_18
287. KÖHLER, G. & MILSTEIN, C. Continuous cultures of fused cells secreting antibody of predefined specificity. *Nature* 256, 256495a0 (1975).
288. Taylor, R. P. & Lindorfer, M. A. The role of complement in mAb-based therapies of cancer. *Methods* 65, 18–27 (2014).
289. Bast, R. C. et al. Cell growth regulation in epithelial ovarian cancer. *Cancer* 71, 1597–1601 (1993).
290. Dubé, P. E. et al. Epidermal growth factor receptor inhibits colitis-associated cancer in mice. *J Clin Invest* 122, 2780–2792 (2012).
291. Ingthorsson, S. et al. HER2 induced EMT and tumorigenicity in breast epithelial progenitor cells is inhibited by coexpression of EGFR. *Oncogene* 35, 4244 (2016).
292. Hubert, P. & Amigorena, S. Antibody-dependent cell cytotoxicity in monoclonal antibody-mediated tumor immunotherapy. *Oncoimmunology* 1, 103–105 (2012).
293. Dunkelberger, J. R. & Song, W.-C. Complement and its role in innate and adaptive immune responses. *Cell Res* 20, 34–50 (2009).
294. Leavy, O. Therapeutic antibodies: past, present and future. *Nat Rev Immunol* 10, 297 (2010).
295. Sgro, C. Side-effects of a monoclonal antibody, muromonab CD3/orthoclone OKT3: bibliographic review. *Toxicology* 105, 23–29 (1995).



296. Harding, F. A., ickler, M., Razo, J. & DuBridge, R. The immunogenicity of humanized and fully human antibodies. *Mabs* 2, 256–265 (2010).
297. Leahy, M. F. & Turner, H. J. Radioimmunotherapy of relapsed indolent non-Hodgkin lymphoma with <sup>131</sup>I-rituximab in routine clinical practice: 10-year single-institution experience of 142 consecutive patients. *Blood* 117, 45–52 (2011).
298. Vaklavas, C. & Forero-Torres, A. Safety and efficacy of brentuximab vedotin in patients with Hodgkin lymphoma or systemic anaplastic large cell lymphoma. *Ther Adv Hematology* 3, 209–225 (2012).
299. FDA Approves Kadcyla for Breast Cancer. *Cancer Discov* 3, 366–366 (2013).
300. Younes, A., Yasothan, U. & Kirkpatrick, P. Brentuximab vedotin. *Nat Rev Drug Discov* 11, 19 (2012).
301. Newland, A. M., Li, J. X., Wasco, L. E., Aziz, M. T. & Lowe, D. K. Brentuximab Vedotin: A CD30-Directed Antibody-Cytotoxic Drug Conjugate. *Pharmacother J Hum Pharmacol Drug Ther* 33, 93–104 (2013).
302. Lambert, J. M. & Chari, R. V. Ado-trastuzumab Emtansine (T-DM1): An Antibody–Drug Conjugate (ADC) for HER2-Positive Breast Cancer. *J Med Chem* 57, 6949–6964 (2014).
303. Dahlén, E., Veitonmäki, N. & Norlén, P. Bispecific antibodies in cancer immunotherapy. *Ther Adv Vaccines Immunother* 6, 3–17 (2018).
304. Möller, S. A. & Reisfeld, R. A. Bispecific-monoclonal-antibody-directed lysis of ovarian carcinoma cells by activated human T lymphocytes. *Cancer Immunol Immunother* 33, 210–216 (1991).
305. Weiner, L. M., Alpaugh, K. R. & von Mehren, M. Redirected cellular cytotoxicity employing bispecific antibodies and other multifunctional binding proteins. *Cancer Immunol Immunother* 45, 190–192 (1997).
306. Weiner, G. J. Rituximab: complementary mechanisms of action. *Blood* 101, 788–788 (2003).
307. Weiner, G. J. Rituximab: Mechanism of Action. *Semin Hematol* 47, 115–123 (2010).
308. Alidzanovic, L. et al. The VEGF rise in blood of bevacizumab patients is not based on tumor escape but a host-blockade of VEGF clearance. *Oncotarget* 7, 57197–57212 (2016).

309. Hayashi, K. et al. Panitumumab Provides Better Survival Outcomes Compared to Cetuximab for Metastatic Colorectal Cancer Patients Treated with Prior Bevacizumab within 6 Months. *Oncology* 1–8 (2018). doi:10.1159/000493321
310. Uemura, M. et al. First-line cetuximab-based chemotherapies for patients with advanced or metastatic KRAS wild-type colorectal cancer. *Mol Clin Oncol* 5, 375–379 (2016).
311. Yamazaki, T., Iwaya, A. & Katayanagi, N. [Outcomes of cetuximab combination chemotherapy in clinical practice for patients with metastatic colorectal cancer]. *Gan Kagaku Ryoho Cancer Chemother* 40, 2529–33 (2013).
312. LIN, L. et al. Efficacy of cetuximab-based chemotherapy in metastatic colorectal cancer according to RAS and BRAF mutation subgroups: A meta-analysis. *Mol Clin Oncol* 4, 1017–1024 (2016).
313. van der Velden, V. et al. High CD33-antigen loads in peripheral blood limit the efficacy of gemtuzumab ozogamicin (Mylotarg®) treatment in acute myeloid leukemia patients. *Leukemia* 18, 2403350 (2004).
314. Rajvanshi, P., Shulman, H. M., Sievers, E. L. & nald, G. B. Hepatic sinusoidal obstruction after gemtuzumab ozogamicin (Mylotarg) therapy. *Blood* 99, 2310–2314 (2002).
315. Parigger, J., Zwaan, C., Reinhardt, D. & Kaspers, G. Dose-related efficacy and toxicity of gemtuzumab ozogamicin in pediatric acute myeloid leukemia. *Expert Rev Anticanc* 16, 137–146 (2016).
316. Shaughnessy, A. F. Monoclonal antibodies: magic bullets with a hefty price tag. *Bmj Br Medical J* 345, e8346 (2012).
317. Hurwitz, H. et al. Bevacizumab plus Irinotecan, Fluorouracil, and Leucovorin for Metastatic Colorectal Cancer. *New Engl J Medicine* 350, 2335–2342 (2004).
318. ..., Malenkovich, N., Nishimura, H., Okazaki, T. & Nature ..., H. T. PD-L2 is a second ligand for PD-1 and inhibits T cell activation. (2001).
319. Okazaki, T. & Honjo, T. PD-1 and PD-1 ligands: from discovery to clinical application. *International immunology* 19, 813–24 (2007).
320. Francisco, L. M., Sage, P. T. & Sharpe, A. H. The PD-1 pathway in tolerance and autoimmunity. *Immunol Rev* 236, 219–242 (2010).
321. Okazaki, T. & Honjo, T. The PD-1-PD-L pathway in immunological tolerance. *Trends in immunology* 27, 195–201 (2006).

322. Sharpe, A. H., Wherry, J. E., Ahmed, R. & Freeman, G. J. The function of programmed cell death 1 and its ligands in regulating autoimmunity and infection. *Nat Immunol* 8, ni1443 (2007).
323. Ahmadzadeh, M. et al. Tumor antigen–specific CD8 T cells infiltrating the tumor express high levels of PD-1 and are functionally impaired. *Blood* 114, 1537–1544 (2009).
324. Tumei, P. C. et al. PD-1 blockade induces responses by inhibiting adaptive immune resistance. *Nature* 515, 568 (2014).
325. Blattman, J. N. & Greenberg, P. D. PD-1 blockade: rescue from a near-death experience. *Nat Immunol* 7, 227–228 (2006).
326. Taghiloo, S. et al. Frequency and functional characterization of exhausted CD8+ T cells in chronic lymphocytic leukemia. *Eur J Haematol* 98, 622–631 (2017).
327. Barber, D. L. et al. Restoring function in exhausted CD8 T cells during chronic viral infection. *Nature* 439, 682 (2006).
328. PD-1/PD-L1 pathway inhibition to restore effector functions in exhausted CD8 + T cells: chances, limitations and potential risks. *Transl Cancer Res* 7, S530–S537 (2018).
329. Dong, H. et al. Tumor-associated B7-H1 promotes T-cell apoptosis: A potential mechanism of immune evasion. *Nat Med* 8, 793 (2002).
330. Topalian, S., Hodi, F. & of ..., B. J. Safety, activity, and immune correlates of anti–PD-1 antibody in cancer. (2012). doi:10.1056/nejmoa1200690
331. Brahmer, J. R. et al. Phase I Study of Single-Agent Anti–Programmed Death-1 (MDX-1106) in Refractory Solid Tumors: Safety, Clinical Activity, Pharmacodynamics, and Immunologic Correlates. *J Clin Oncol* 28, 3167–3175 (2010).
332. Patnaik, A. et al. Phase I Study of Pembrolizumab (MK-3475; Anti–PD-1 Monoclonal Antibody) in Patients with Advanced Solid Tumors. *Clin Cancer Res* 21, 4286–4293 (2015).
333. Robert, C. et al. Anti-programmed-death-receptor-1 treatment with pembrolizumab in ipilimumab-refractory advanced melanoma: a randomised dose-comparison cohort of a phase 1 trial. *Lancet* 384, 1109–1117 (2014).
334. Ribas, A. et al. P0116 Updated clinical efficacy of the anti-PD-1 monoclonal antibody pembrolizumab (MK-3475) in 411 patients with melanoma. *Eur J Cancer* 51, e24 (2015).

335. Motzer, R. J. et al. Nivolumab versus Everolimus in Advanced Renal-Cell Carcinoma. *New Engl J Medicine* 373, 1803–1813 (2015).
336. Chen, R. et al. Phase II Study of the Efficacy and Safety of Pembrolizumab for Relapsed/Refractory Classic Hodgkin Lymphoma. *J Clin Oncol* 35, JCO.2016.72.131 (2017).
337. and of Oncology, H. R., str University, 197022 IP & Lepik, K. Immune Checkpoint Inhibitors in the Treatment of Lymphomas. *Clin Oncohematology* 11, 303–312 (2018).
338. Ansell, S. M. Nivolumab in the Treatment of Hodgkin Lymphoma. *Clin Cancer Res* 23, 1623–1626 (2017).
339. Yamaguchi, K. et al. Activation of central/effector memory T cells and T-helper 1 polarization in malignant melanoma patients treated with anti-programmed death-1 antibody. *Cancer science* 109, 3032–3042 (2018).
340. Patsoukis, N. et al. PD-1 alters T-cell metabolic reprogramming by inhibiting glycolysis and promoting lipolysis and fatty acid oxidation. *Nat Commun* 6, 6692 (2015).
341. Bengsch, B. et al. Bioenergetic Insufficiencies Due to Metabolic Alterations Regulated by the Inhibitory Receptor PD-1 Are an Early Driver of CD8+ T Cell Exhaustion. *Immunity* 45, 358–73 (2016).
342. Gupta, S., Roy, A. & Dwarkanath, B. S. Metabolic Cooperation and Competition in the Tumor Microenvironment: Implications for Therapy. *Frontiers Oncol* 7, 68 (2017).
343. Renner, K. et al. Metabolic Hallmarks of Tumor and Immune Cells in the Tumor Microenvironment. *Front Immunol* 8, 248 (2017).
344. Chang, C.-H. et al. Metabolic Competition in the Tumor Microenvironment Is a Driver of Cancer Progression. *Cell* 162, 1229–41 (2015).
345. Fehrenbacher, L. et al. Atezolizumab versus docetaxel for patients with previously treated non-small-cell lung cancer (POPLAR): a multicentre, open-label, phase 2 randomised controlled trial. *Lancet Lond Engl* 387, 1837–46 (2016).
346. Rittmeyer, A. et al. Atezolizumab versus docetaxel in patients with previously treated non-small-cell lung cancer (OAK): a phase 3, open-label, multicentre randomised controlled trial. *Lancet* 389, (2017).

347. Huang, R. et al. CTLA4 Blockade Induces Frequent Tumor Infiltration by Activated Lymphocytes Regardless of Clinical Responses in Humans. *Clin Cancer Res* 17, 4101–4109 (2011).
348. Antonia, S. J. Durvalumab after Chemoradiotherapy in Stage III Non–Small-Cell Lung Cancer. *New Engl J Med* 380, 989–990 (2019).
349. Antonia, S. J. et al. Overall Survival with Durvalumab after Chemoradiotherapy in Stage III NSCLC. *New Engl J Med* (2018). doi:10.1056/nejmoa1809697
350. Chen, S. et al. Combination of 4-1BB Agonist and PD-1 Antagonist Promotes Antitumor Effector/Memory CD8 T Cells in a Poorly Immunogenic Tumor Model. *Cancer Immunol Res* 3, 149–160 (2015).
351. Juneja, V. R. et al. PD-L1 on tumor cells is sufficient for immune evasion in immunogenic tumors and inhibits CD8 T cell cytotoxicity. *Journal of Experimental Medicine* 214, jem.20160801 (2017).
352. Curran, M., Montalvo, W. & of the ..., Y. H. PD-1 and CTLA-4 combination blockade expands infiltrating T cells and reduces regulatory T and myeloid cells within B16 melanoma tumors. (2010). doi:10.1073/pnas.0915174107
353. Masteller, E. L., Chuang, E., Mullen, A. C., Reiner, S. L. & Thompson, C. B. Structural Analysis of CTLA-4 Function In Vivo. *J Immunol* 164, 5319–5327 (2000).
354. Friedline, R. H. et al. CD4+ regulatory T cells require CTLA-4 for the maintenance of systemic tolerance. *J Exp Medicine* 206, 421–434 (2009).
355. Schadendorf, D. et al. Pooled Analysis of Long-Term Survival Data From Phase II and Phase III Trials of Ipilimumab in Unresectable or Metastatic Melanoma. *J Clin Oncol* 33, 1889–1894 (2015).
356. Eggermont, A. et al. Prolonged Survival in Stage III Melanoma with Ipilimumab Adjuvant Therapy. *New Engl J Medicine* 375, 1845–1855 (2016).
357. Du, X. et al. A reappraisal of CTLA-4 checkpoint blockade in cancer immunotherapy. *Cell Res* 28, 416–432 (2018).
358. van Rooij, N. et al. Tumor Exome Analysis Reveals Neoantigen-Specific T-Cell Reactivity in an Ipilimumab-Responsive Melanoma. *J Clin Oncol* 31, e439–e442 (2013).
359. Ménard, C. et al. CTLA-4 Blockade Confers Lymphocyte Resistance to Regulatory T-Cells in Advanced Melanoma: Surrogate Marker of Efficacy of Tremelimumab? *Clinical Cancer Research* 14, 5242–5249 (2008).

360. Auslander, N. et al. Robust prediction of response to immune checkpoint blockade therapy in metastatic melanoma. *Nature medicine* 24, 1545–1549 (2018).
361. Dijkstra, K. K., Voabil, P., Schumacher, T. N. & Voest, E. E. Genomics- and Transcriptomics-Based Patient Selection for Cancer Treatment With Immune Checkpoint Inhibitors: A Review. *Jama Oncol* (2016). doi:10.1001/jamaoncol.2016.2214
362. Leach, D. R., Krummel, M. F. & Allison, J. P. Enhancement of antitumor immunity by CTLA-4 blockade. *Science* 271, 1734–1736 (1996).
363. Spranger, S. et al. Mechanism of tumor rejection with doublets of CTLA-4, PD-1/PD-L1, or IDO blockade involves restored IL-2 production and proliferation of CD8<sup>+</sup> T cells directly within the tumor microenvironment. *J Immunother Cancer* 2, 3 (2014).
364. Weber, J. S. et al. Safety Profile of Nivolumab Monotherapy: A Pooled Analysis of Patients With Advanced Melanoma. *Journal of clinical oncology : official journal of the American Society of Clinical Oncology* 35, 785–792 (2017).
365. Day, D., Khoja, L., Chen, T., Siu, L. L. & Hansen, A. Tumor- and class-specific patterns of immune-related adverse events (irAEs) of immune checkpoint inhibitors (ICIs): A systematic review (SR). *J Clin Oncol* 34, 3065–3065 (2016).
366. Fecher, L. A., Agarwala, S. S., Hodi, S. F. & Weber, J. S. Ipilimumab and Its Toxicities: A Multidisciplinary Approach. *Oncol* 18, 733–743 (2013).
367. Byrne, E. H. & Fisher, D. E. Immune and molecular correlates in melanoma treated with immune checkpoint blockade. *Cancer* 123, 2143–2153 (2017).
368. Muik, A. et al. Re-engineering Vesicular Stomatitis Virus to Abrogate Neurotoxicity, Circumvent Humoral Immunity, and Enhance Oncolytic Potency. *Cancer Res* 74, 3567–3578 (2014).
369. Kaufman, H. L., Kohlhapp, F. J. & Zloza, A. Oncolytic viruses: a new class of immunotherapy drugs. *Nat Rev Drug Discov* 14, 642 (2015).
370. Naik, J. D., Twelves, C. J., Selby, P. J., Vile, R. G. & Chester, J. D. Immune Recruitment and Therapeutic Synergy: Keys to Optimizing Oncolytic Viral Therapy? *Clin Cancer Res* 17, 4214–4224 (2011).
371. Chesney, J. et al. Randomized, Open-Label Phase II Study Evaluating the Efficacy and Safety of Talimogene Laherparepvec in Combination With Ipilimumab Versus Ipilimumab Alone in Patients With Advanced, Unresectable Melanoma. *J Clin Oncol* 36, JCO.2017.73.737 (2017).

372. Ribas, A. et al. Oncolytic Virotherapy Promotes Intratumoral T Cell Infiltration and Improves Anti-PD-1 Immunotherapy. *Cell* 170, 1109-1119.e10 (2017).
373. Ribas, A. et al. Oncolytic Virotherapy Promotes Intratumoral T Cell Infiltration and Improves Anti-PD-1 Immunotherapy. *Cell* 174, 1031–1032 (2018).
374. MITCHISON, N. Studies on the immunological response to foreign tumor transplants in the mouse. I. The role of lymph node cells in conferring immunity by adoptive transfer. *The Journal of experimental medicine* 102, 157–77 (1955).
375. Berendt, M. & North, R. T-cell-mediated suppression of anti-tumor immunity. An explanation for progressive growth of an immunogenic tumor. *The Journal of experimental medicine* 151, 69–80 (1980).
376. Eberlein, T., Rosenstein, M. & Rosenberg, S. Regression of a disseminated syngeneic solid tumor by systemic transfer of lymphoid cells expanded in interleukin 2. *The Journal of experimental medicine* 156, 385–97 (1982).
377. Grimm, E., Mazumder, A., Zhang, H. & Rosenberg, S. Lymphokine-activated killer cell phenomenon. Lysis of natural killer-resistant fresh solid tumor cells by interleukin 2-activated autologous human peripheral blood lymphocytes. *J Exp Medicine* 155, 1823–1841 (1982).
378. Yang, J., Mulé, J. & Rosenberg, S. Murine lymphokine-activated killer (LAK) cells: phenotypic characterization of the precursor and effector cells. *J Immunol Baltim Md* 1950 137, 715–22 (1986).
379. Rosenberg, S. et al. Observations on the systemic administration of autologous lymphokine-activated killer cells and recombinant interleukin-2 to patients with metastatic cancer. *The New England journal of medicine* 313, 1485–92 (1985).
380. Rosenberg, S. Lymphokine-activated killer cells: A new approach to immunotherapy of cancer. *Jnci J National Cancer Inst* 75, 595–603 (1985).
381. Topalian, S. L., Muul, L. M., Solomon, D. & Rosenberg, S. A. Expansion of human tumor infiltrating lymphocytes for use in immunotherapy trials. *J Immunol Methods* 102, 127–141 (1987).
382. Muul, L., Spiess, P., Director, E. & Rosenberg, S. Identification of specific cytolytic immune responses against autologous tumor in humans bearing malignant melanoma. *Journal of immunology (Baltimore, Md. : 1950)* 138, 989–95 (1987).
383. Rosenberg, S., Spiess, P. & Science, L. R. A new approach to the adoptive immunotherapy of cancer with tumor-infiltrating lymphocytes. (1986).  
doi:10.1126/science.3489291

384. Rosenberg, S. A. et al. Use of Tumor-Infiltrating Lymphocytes and Interleukin-2 in the Immunotherapy of Patients with Metastatic Melanoma. *New Engl J Medicine* 319, 1676–1680 (1988).
385. Rosenberg, S. et al. Treatment of patients with metastatic melanoma with autologous tumor-infiltrating lymphocytes and interleukin 2. *Journal of the National Cancer Institute* 86, 1159–66 (1994).
386. Dudley, M. E. et al. Cancer Regression and Autoimmunity in Patients After Clonal Repopulation with Antitumor Lymphocytes. *Science* 298, 850–854 (2002).
387. Fridman, W., Pagès, F., Sautès-Fridman, C. & Galon, J. The immune contexture in human tumours: impact on clinical outcome. *Nat Rev Cancer* 12, 298 (2012).
388. Besser, M. J. et al. Clinical Responses in a Phase II Study Using Adoptive Transfer of Short-term Cultured Tumor Infiltration Lymphocytes in Metastatic Melanoma Patients. *Clin Cancer Res* 16, 2646–2655 (2010).
389. Nguyen, L. T. et al. Phase II clinical trial of adoptive cell therapy for patients with metastatic melanoma with autologous tumor-infiltrating lymphocytes and low-dose interleukin-2. *Cancer Immunol Immunother* 1–13 (2019). doi:10.1007/s00262-019-02307-x
390. Klein, E., Becker, S., Svedmyr, E., Jondal, M. & VEAAnky, F. Tumor Infiltrating Lymphocytes\*. *Ann Ny Acad Sci* 276, 207–216 (1976).
391. Whiteside, T. L., Jost, L. M. & Herberman, R. B. Tumor-infiltrating lymphocytes Potential and limitations to their use for cancer therapy. *Crit Rev Oncol Hemat* 12, 25–47 (1992).
392. Woroniecka, K. et al. T Cell Exhaustion Signatures Vary with Tumor Type and are Severe in Glioblastoma. *Clin Cancer Res* 24, clincanres.1846.2017 (2018).
393. Rosenberg, S. A. et al. Gene Transfer into Humans — Immunotherapy of Patients with Advanced Melanoma, Using Tumor-Infiltrating Lymphocytes Modified by Retroviral Gene Transduction. *New Engl J Medicine* 323, 570–578 (1990).
394. Gross, G., Waks, T. & Eshhar, Z. Expression of immunoglobulin-T-cell receptor chimeric molecules as functional receptors with antibody-type specificity. *Proceedings of the National Academy of Sciences of the United States of America* 86, 10024–8 (1989).
395. Eshhar, Z., Waks, T., Gross, G. & Schindler, D. Specific activation and targeting of cytotoxic lymphocytes through chimeric single chains consisting of antibody-binding domains and the gamma or zeta subunits of the immunoglobulin and T-cell receptors. *Proc National Acad Sci* 90, 720–724 (1993).



396. Gong, M. C. et al. Cancer Patient T Cells Genetically Targeted to Prostate-Specific Membrane Antigen Specifically Lyse Prostate Cancer Cells and Release Cytokines in Response to Prostate-Specific Membrane Antigen. *Neoplasia* 1, 123–127 (1999).
397. Krause, A. et al. Antigen-dependent CD28 Signaling Selectively Enhances Survival and Proliferation in Genetically Modified Activated Human Primary T Lymphocytes. *J Exp Medicine* 188, 619–626 (1998).
398. Frigault, M. J. et al. Identification of Chimeric Antigen Receptors That Mediate Constitutive or Inducible Proliferation of T Cells. *Cancer Immunol Res* 3, 356–367 (2015).
399. Long, A. H. et al. 4-1BB costimulation ameliorates T cell exhaustion induced by tonic signaling of chimeric antigen receptors. *Nat Med* 21, 581–590 (2015).
400. Carpenito, C. et al. Control of large, established tumor xenografts with genetically retargeted human T cells containing CD28 and CD137 domains. *Proc National Acad Sci* 106, 3360–3365 (2009).
401. Maher, J., Brentjens, R. J., Gunset, G., Rivière, I. & Sadelain, M. Human T-lymphocyte cytotoxicity and proliferation directed by a single chimeric TCR $\zeta$ /CD28 receptor. *Nat Biotechnol* 20, 70–75 (2002).
402. Brentjens, R. J. et al. Eradication of systemic B-cell tumors by genetically targeted human T lymphocytes co-stimulated by CD80 and interleukin-15. *Nat Med* 9, nm827 (2003).
403. Davila, M. L., Brentjens, R., Wang, X., Rivière, I. & Sadelain, M. How do CARs work? *Oncoimmunology* 1, 1577–1583 (2014).
404. Brentjens, R. J. et al. CD19-Targeted T Cells Rapidly Induce Molecular Remissions in Adults with Chemotherapy-Refractory Acute Lymphoblastic Leukemia. *Sci Transl Med* 5, 177ra38-177ra38 (2013).
405. Kochenderfer, J. N. et al. B-cell depletion and remissions of malignancy along with cytokine-associated toxicity in a clinical trial of anti-CD19 chimeric-antigen-receptor–transduced T cells. *Blood* 119, 2709–2720 (2012).
406. Pegram, H. J. et al. Tumor-targeted T cells modified to secrete IL-12 eradicate systemic tumors without need for prior conditioning. *Blood* 119, 4133–4141 (2012).
407. Lamers, C. et al. Treatment of Metastatic Renal Cell Carcinoma With Autologous T-Lymphocytes Genetically Retargeted Against Carbonic Anhydrase IX: First Clinical Experience. *J Clin Oncol* 24, e20–e22 (2006).

408. Morgan, R. A. et al. Case Report of a Serious Adverse Event Following the Administration of T Cells Transduced With a Chimeric Antigen Receptor Recognizing ERBB2. *Mol Ther J Am Soc Gene Ther* 18, 843–51 (2010).
409. June, C. H. & Sadelain, M. Chimeric Antigen Receptor Therapy. *New England Journal of Medicine* 379, 64–73 (2018).
410. Frey, N. & Porter, D. Cytokine Release Syndrome with Chimeric Antigen Receptor T cell Therapy. *Biology Blood Marrow Transplant J Am Soc Blood Marrow Transplant* (2018). doi:10.1016/j.bbmt.2018.12.756
411. Fitzgerald, J. C. et al. Cytokine Release Syndrome After Chimeric Antigen Receptor T Cell Therapy for Acute Lymphoblastic Leukemia. *Crit Care Med* 45, e124–e131 (2017).
412. Xu, X.-J. & Tang, Y.-M. Cytokine release syndrome in cancer immunotherapy with chimeric antigen receptor engineered T cells. *Cancer Lett* 343, 172–178 (2014).
413. Brudno, J. N. & Kochenderfer, J. N. Toxicities of chimeric antigen receptor T cells: recognition and management. *Blood* 127, 3321–3330 (2016).
414. Gust, J., Taraseviciute, A. & Turtle, C. J. Neurotoxicity Associated with CD19-Targeted CAR-T Cell Therapies. *Cns Drugs* 32, 1091–1101 (2018).
415. Giavridis, T. et al. CAR T cell–induced cytokine release syndrome is mediated by macrophages and abated by IL-1 blockade. *Nat Med* 24, 731–738 (2018).
416. The Tumor Lysis Syndrome. *New Engl J Med* 379, 1094–1094 (2018).
417. Porter, D. L., Levine, B. L., Kalos, M., Bagg, A. & June, C. H. Chimeric Antigen Receptor–Modified T Cells in Chronic Lymphoid Leukemia. *New Engl J Medicine* 365, 725–733 (2011).
418. Marin, V. et al. Comparison of different suicide-gene strategies for the safety improvement of genetically manipulated T cells. *Hum Gene Ther Method* 23, 376–86 (2012).
419. Jones, B. S., Lamb, L. S., Goldman, F. & Stasi, A. Improving the safety of cell therapy products by suicide gene transfer. *Front Pharmacol* 5, 254 (2014).
420. Hoyos, V. et al. Engineering CD19-specific T lymphocytes with interleukin-15 and a suicide gene to enhance their anti-lymphoma/leukemia effects and safety. *Leukemia* 24, 1160 (2010).

421. Gargett, T. & Brown, M. P. The inducible caspase-9 suicide gene system as a “safety switch” to limit on-target, off-tumor toxicities of chimeric antigen receptor T cells. *Front Pharmacol* 5, 235 (2014).
422. Sotillo, E. et al. Convergence of Acquired Mutations and Alternative Splicing of CD19 Enables Resistance to CART-19 Immunotherapy. *Cancer Discov* 5, 1282–1295 (2015).
423. Shilyansky, J. et al. T-cell receptor usage by melanoma-specific clonal and highly oligoclonal tumor-infiltrating lymphocyte lines. *Proc National Acad Sci* 91, 2829–2833 (1994).
424. Cole, D. et al. Characterization of the functional specificity of a cloned T-cell receptor heterodimer recognizing the MART-1 melanoma antigen. *Cancer Res* 55, 748–52 (1995).
425. Theobald, M., Biggs, J., Dittmer, D., Levine, A. & Sherman, L. Targeting p53 as a general tumor antigen. *Proc National Acad Sci* 92, 11993–11997 (1995).
426. Nishimura, M. et al. MHC class I-restricted recognition of a melanoma antigen by a human CD4+ tumor infiltrating lymphocyte. *Cancer research* 59, 6230–8 (1999).
427. Johnson, L. A. et al. Gene therapy with human and mouse T-cell receptors mediates cancer regression and targets normal tissues expressing cognate antigen. *Blood* 114, 535–546 (2009).
428. Parkhurst, M. R. et al. T Cells Targeting Carcinoembryonic Antigen Can Mediate Regression of Metastatic Colorectal Cancer but Induce Severe Transient Colitis. *Mol Ther J Am Soc Gene Ther* 19, 620–6 (2011).
429. Linette, G. P. et al. Cardiovascular toxicity and titin cross-reactivity of affinity-enhanced T cells in myeloma and melanoma. *Blood* 122, 863–871 (2013).
430. Køllgaard, T. et al. Longitudinal immune monitoring of patients receiving intratumoral injection of a MART-1 T-cell receptor-transduced cell line (C-Cure 709). *Cytotherapy* 11, 631–41 (2009).
431. Angulo, G., Yuen, C., Palla, S. L., Anderson, P. M. & Zweidler-McKay, P. A. Absolute lymphocyte count is a novel prognostic indicator in ALL and AML. *Cancer* 112, 407–415 (2008).
432. Simeone, E. et al. Immunological and biological changes during ipilimumab treatment and their potential correlation with clinical response and survival in patients with advanced melanoma. *Cancer Immunol Immunother* 63, 675–683 (2014).

433. Krieg, C. et al. High-dimensional single-cell analysis predicts response to anti-PD-1 immunotherapy. *Nat Med* 24, 144 (2018).
434. Page, D. B. et al. Deep Sequencing of T-cell Receptor DNA as a Biomarker of Clonally Expanded TILs in Breast Cancer after Immunotherapy. *Cancer Immunol Res* 4, 835–844 (2016).
435. Jang, M. & Yew, P. Immunopharmacogenomics. 3–25 (2015). doi:10.1007/978-4-431-55726-5\_1
436. Disis, M. L. Immunologic biomarkers as correlates of clinical response to cancer immunotherapy. *Cancer Immunol Immunother* 60, 433–442 (2011).
437. Ranieri, E. et al. Dendritic Cell/Peptide Cancer Vaccines: Clinical Responsiveness and Epitope Spreading. *Immunol Invest* 29, 121–125 (2009).
438. Hopkins, A. C. et al. T cell receptor repertoire features associated with survival in immunotherapy-treated pancreatic ductal adenocarcinoma. *Jci Insight* 3, e122092 (2018).
439. Postow, M. A. et al. Peripheral T cell receptor diversity is associated with clinical outcomes following ipilimumab treatment in metastatic melanoma. *J Immunother Cancer* 3, 23 (2015).
440. Cui, J.-H. et al. TCR Repertoire as a Novel Indicator for Immune Monitoring and Prognosis Assessment of Patients With Cervical Cancer. *Front Immunol* 9, 2729 (2018).
441. Hogan, S. A. et al. Peripheral blood TCR repertoire profiling may facilitate patient stratification for immunotherapy against melanoma. *Cancer Immunol Res* 7, canimm.0136.2018 (2018).
442. McNeel, D. G. TCR diversity – a universal cancer immunotherapy biomarker? *J Immunother Cancer* 4, 69 (2016).
443. Bailey, P. et al. Exploiting the neoantigen landscape for immunotherapy of pancreatic ductal adenocarcinoma. *Sci Rep-uk* 6, 35848 (2016).
444. Efremova, M., Finotello, F., Rieder, D. & Trajanoski, Z. Neoantigens Generated by Individual Mutations and Their Role in Cancer Immunity and Immunotherapy. *Front Immunol* 8, 1679 (2017).
445. Rizvi, N. A. et al. Mutational landscape determines sensitivity to PD-1 blockade in non–small cell lung cancer. *Science* 348, 124–128 (2015).

446. McGranahan, N. et al. Clonal neoantigens elicit T cell immunoreactivity and sensitivity to immune checkpoint blockade. *Science* 351, 1463–1469 (2016).
447. Le, D. T. et al. Mismatch repair deficiency predicts response of solid tumors to PD-1 blockade. *Science* 357, 409–413 (2017).
448. Lee, V., Murphy, A., Le, D. T. & Diaz, L. A. Mismatch Repair Deficiency and Response to Immune Checkpoint Blockade. *Oncol* 21, 1200–1211 (2016).
449. Jia, Q. et al. Local mutational diversity drives intratumoral immune heterogeneity in non-small cell lung cancer. *Nat Commun* 9, 5361 (2018).
450. Trujillo, J. A., Sweis, R. F., Bao, R. & Luke, J. J. T Cell-Inflamed versus Non-T Cell-Inflamed Tumors: A Conceptual Framework for Cancer Immunotherapy Drug Development and Combination Therapy Selection. *Cancer immunology research* 6, 990–1000 (2018).
451. Spranger, S. et al. Density of immunogenic antigens does not explain the presence or absence of the T-cell–inflamed tumor microenvironment in melanoma. *Proc National Acad Sci* 113, E7759–E7768 (2016).
452. Pauken, K. E. & Wherry, J. E. Overcoming T cell exhaustion in infection and cancer. *Trends Immunol* 36, 265–276 (2015).
453. Schietinger, A. et al. Tumor-Specific T Cell Dysfunction Is a Dynamic Antigen-Driven Differentiation Program Initiated Early during Tumorigenesis. *Immunity* 45, 389–401 (2016).
454. Turan, T. et al. Immune oncology, immune responsiveness and the theory of everything. *Journal for immunotherapy of cancer* 6, 50 (2018).
455. Thorsson, V. et al. The Immune Landscape of Cancer. *Immunity* 48, 812-830.e14 (2018).
456. Roussel, H. et al. Composite biomarkers defined by multiparametric immunofluorescence analysis identify ALK-positive adenocarcinoma as a potential target for immunotherapy. *Oncoimmunology* 6, 00–00 (2017).
457. Gangaplara, A. et al. Type I interferon signaling attenuates regulatory T cell function in viral infection and in the tumor microenvironment. *PLoS pathogens* 14, e1006985 (2018).
458. Gnjatic, S. et al. Identifying baseline immune-related biomarkers to predict clinical outcome of immunotherapy. *Journal for immunotherapy of cancer* 5, 44 (2017).

459. Tang, H., Wang, Y., Chlewicki, L., Zhang, Y. & cell, G. J. Facilitating T cell infiltration in tumor microenvironment overcomes resistance to PD-L1 blockade. (2016).
460. Balatoni, T. et al. Tumor-infiltrating immune cells as potential biomarkers predicting response to treatment and survival in patients with metastatic melanoma receiving ipilimumab therapy. *Cancer immunology, immunotherapy* : CII 67, 141–151 (2018).
461. Daud, A. I. et al. Tumor immune profiling predicts response to anti-PD-1 therapy in human melanoma. *J Clin Invest* 126, 3447–3452 (2016).
462. Hirsch, F. R. et al. PD-L1 Immunohistochemistry Assays for Lung Cancer: Results from Phase 1 of the Blueprint PD-L1 IHC Assay Comparison Project. *J Thorac Oncol* 12, 208–222 (2017).
463. Fluxá, P. et al. High CD8+ and absence of Foxp3+ T lymphocytes infiltration in gallbladder tumors correlate with prolonged patients survival. *Bmc Cancer* 18, 243 (2018).
464. Salama, P. et al. Tumor-Infiltrating FOXP3+ T Regulatory Cells Show Strong Prognostic Significance in Colorectal Cancer. *J Clin Oncol* 27, 186–192 (2008).
465. Shen, Z. et al. Higher intratumoral infiltrated Foxp3+ Treg numbers and Foxp3+/CD8+ ratio are associated with adverse prognosis in resectable gastric cancer. *J Cancer Res Clin* 136, 1585–1595 (2010).
466. Liu, L. et al. Low intratumoral regulatory T cells and high peritumoral CD8+ T cells relate to long-term survival in patients with pancreatic ductal adenocarcinoma after pancreatectomy. *Cancer Immunol Immunother* 65, 73–82 (2016).
467. Liu, F. et al. CD8+ cytotoxic T cell and FOXP3+ regulatory T cell infiltration in relation to breast cancer survival and molecular subtypes. *Breast Cancer Res Tr* 130, 645–655 (2011).
468. Roszkowski, J. J. et al. Simultaneous generation of CD8+ and CD4+ melanoma-reactive T cells by retroviral-mediated transfer of a single T-cell receptor. *Cancer research* 65, 1570–6 (2005).
469. Koya, R. C. et al. Kinetic phases of distribution and tumor targeting by T cell receptor engineered lymphocytes inducing robust antitumor responses. *Proceedings of the National Academy of Sciences of the United States of America* 107, 14286–91 (2010).
470. Moore, T. et al. Correction to: Clinical and immunologic evaluation of three metastatic melanoma patients treated with autologous melanoma-reactive TCR-transduced T cells. *Cancer immunology, immunotherapy* : CII 67, 327 (2018).

471. Fisher, B. et al. Tumor localization of adoptively transferred indium-111 labeled tumor infiltrating lymphocytes in patients with metastatic melanoma. *J Clin Oncol* 7, 250–261 (1989).
472. Takayama, T. et al. Distribution and therapeutic effect of intraarterially transferred tumor-infiltrating lymphocytes in hepatic malignancies. A preliminary report. *Cancer* 68, 2391–2396 (1991).
473. Griffith, K. et al. In vivo distribution of adoptively transferred indium-111-labeled tumor infiltrating lymphocytes and peripheral blood lymphocytes in patients with metastatic melanoma. *J Natl Cancer I* 81, 1709–17 (1989).
474. Dudley, M. E. et al. Adoptive Transfer of Cloned Melanoma-Reactive T Lymphocytes for the Treatment of Patients with Metastatic Melanoma. *J Immunother* 24, 363–373 (2001).
475. Rosenberg, S. A. et al. Durable complete responses in heavily pretreated patients with metastatic melanoma using T-cell transfer immunotherapy. *Clinical cancer research : an official journal of the American Association for Cancer Research* 17, 4550–7 (2011).
476. Soliman, H. H. Cancer Therapeutic Targets. 277–284 (2017). doi:10.1007/978-1-4419-0717-2\_134
477. Hirschhaeuser, F., Sattler, U. & Mueller-Klieser, W. Lactate: A Metabolic Key Player in Cancer. *Cancer Res* 71, 6921–6925 (2011).
478. Joyce, J. A. & Fearon, D. T. T cell exclusion, immune privilege, and the tumor microenvironment. *Science* 348, 74–80 (2015).
479. Corbet, C. & Feron, O. Tumour acidosis: from the passenger to the driver's seat. *Nat Rev Cancer* 17, nrc.2017.77 (2017).
480. Moses, R., Pierson, R., Winn, H. & Auchincloss, H. Xenogeneic proliferation and lymphokine production are dependent on CD4+ helper T cells and self antigen-presenting cells in the mouse. *J Exp Medicine* 172, 567–575 (1990).
481. Shultz, L. D., Brehm, M. A., Garcia-Martinez, V. J. & Greiner, D. L. Humanized mice for immune system investigation: progress, promise and challenges. *Nat Rev Immunol* 12, 786 (2012).
482. Volk, A. et al. Comparison of three humanized mouse models for adoptive T cell transfer. *J Gene Medicine* 14, 540–548 (2012).

483. Han, T. et al. Evaluation of 3 Clinical Dendritic Cell Maturation Protocols Containing Lipopolysaccharide and Interferon- $\gamma$ . *J Immunother* 32, 399–407 (2009).
484. Trevejo, J. M. et al. TNF- $\alpha$ -dependent maturation of local dendritic cells is critical for activating the adaptive immune response to virus infection. *Proc National Acad Sci* 98, 12162–12167 (2001).
485. Edwards, J. et al. CD103+ tumor-resident CD8+ T cells are associated with improved survival in immunotherapy naive melanoma patients and expand significantly during anti-PD1 treatment. *Clinical Cancer Research* 24, clincanres.2257.2017 (2018).
486. Susek, K., Karvouni, M., Alici, E. & Lundqvist, A. The Role of CXC Chemokine Receptors 1–4 on Immune Cells in the Tumor Microenvironment. *Front Immunol* 9, 2159 (2018).
487. Voort, T. J., Felder, M., Yang, R. K., Sondel, P. M. & Rakhmievich, A. L. Intratumoral Delivery of Low Doses of Anti-CD40 mAb Combined With Monophosphoryl Lipid A Induces Local and Systemic Antitumor Effects in Immunocompetent and T Cell-Deficient Mice. *J Immunother* 36, 29–40 (2013).
488. Schölch, S., Rauber, C., Weitz, J., Koch, M. & Huber, P. E. TLR activation and ionizing radiation induce strong immune responses against multiple tumor entities. *Oncoimmunology* 4, e1042201 (2015).
489. Forte, G. et al. Polyinosinic-Polycytidylic Acid Limits Tumor Outgrowth in a Mouse Model of Metastatic Lung Cancer. *J Immunol* 188, 5357–5364 (2012).
490. Mauri, D. N. et al. LIGHT, a New Member of the TNF Superfamily, and Lymphotoxin  $\alpha$  Are Ligands for Herpesvirus Entry Mediator. *Immunity* 8, 21–30 (1998).
491. Tang, H. et al. Facilitating T Cell Infiltration in Tumor Microenvironment Overcomes Resistance to PD-L1 Blockade. *Cancer Cell* 29, 285–96 (2016).
492. Lee, Y. et al. Recruitment and Activation of Naive T Cells in the Islets by Lymphotoxin  $\beta$  Receptor-Dependent Tertiary Lymphoid Structure. *Immunity* 25, 499–509 (2006).
493. Zou, W. et al. LIGHT Delivery to Tumors by Mesenchymal Stem Cells Mobilizes an Effective Antitumor Immune Response. *Cancer Res* 72, 2980–2989 (2012).
494. Hailemichael, Y. et al. Cancer vaccine formulation dictates synergy with CTLA-4 and PD-L1 checkpoint blockade therapy. *The Journal of clinical investigation* 128, 1338–1354 (2018).



495. Wei, S. C. et al. Distinct Cellular Mechanisms Underlie Anti-CTLA-4 and Anti-PD-1 Checkpoint Blockade. *Cell* 170, 1120–1133.e17 (2017).
496. Fehlings, M. et al. Checkpoint blockade immunotherapy reshapes the high-dimensional phenotypic heterogeneity of murine intratumoural neoantigen-specific CD8<sup>+</sup> T cells. *Nature communications* 8, 562 (2017).
497. Barth, R., Mulé, J., Spiess, P. & Rosenberg, S. Interferon gamma and tumor necrosis factor have a role in tumor regressions mediated by murine CD8<sup>+</sup> tumor-infiltrating lymphocytes. *J Exp Medicine* 173, 647–658 (1991).
498. Kyi, C. et al. Therapeutic Immune Modulation Against Solid Cancers with Intratumoral Poly-ICLC: A Pilot Trial. *Clinical cancer research : an official journal of the American Association for Cancer Research* (2018). doi:10.1158/1078-0432.CCR-17-1866
499. Preynat-Seauve, O. et al. Tumor-Infiltrating Dendritic Cells Are Potent Antigen-Presenting Cells Able to Activate T Cells and Mediate Tumor Rejection. *J Immunol* 176, 61–67 (2006).
500. Regateiro, F. S. et al. Foxp3 Expression Is Required for the Induction of Therapeutic Tissue Tolerance. *J Immunol* 189, 3947–3956 (2012).
501. Hall, B. Mechanisms maintaining enhancement of allografts. I. Demonstration of a specific suppressor cell. *J Exp Medicine* 161, 123–133 (1985).
502. Sánchez-Fueyo, A. et al. Influence of direct and indirect allorecognition pathways on CD4<sup>+</sup>CD25<sup>+</sup> regulatory T-cell function in transplantation. *Transplant Int* 20, 534–541 (2007).
503. Fields, P. et al. B7.1 is a quantitatively stronger costimulus than B7.2 in the activation of naive CD8<sup>+</sup> TCR-transgenic T cells. *J Immunol Baltim Md* 1950 161, 5268–75 (1998).
504. van der Merwe, A. P., Bodian, D. L., Daenke, S., Linsley, P. & Davis, S. J. CD80 (B7-1) Binds Both CD28 and CTLA-4 with a Low Affinity and Very Fast Kinetics. *J Exp Medicine* 185, 393–404 (1997).
505. Larsen, C. et al. Regulation of immunostimulatory function and co-stimulatory molecule (B7-1 and B7-2) expression on murine dendritic cells. *J Immunol Baltim Md* 1950 152, 5208–19 (1994).
506. Zheng, Y. et al. CD86 and CD80 Differentially Modulate the Suppressive Function of Human Regulatory T Cells. *J Immunol* 172, 2778–2784 (2004).

507. Yang, J. et al. Third-party Tolerogenic Dendritic Cells Reduce Allo-reactivity In vitro and Ameliorate the Severity of Acute graft-Versus-host Disease in Allo-bone Marrow Transplantation. *Scand J Immunol* 78, 486–496 (2013).
508. Wu, L., Zhang, H., Jiang, Y., Gallo, R. C. & Cheng, H. Induction of antitumor cytotoxic lymphocytes using engineered human primary blood dendritic cells. *Proceedings of the National Academy of Sciences of the United States of America* 115, E4453–E4462 (2018).
509. Butler, M. et al. Altered expression and endocytic function of CD205 in human dendritic cells, and detection of a CD205–DCL-1 fusion protein upon dendritic cell maturation. *Immunology* 120, 362–371 (2007).
510. Zeh, H., Perry-Lalley, D., Dudley, M., Rosenberg, S. & Yang, J. High avidity CTLs for two self-antigens demonstrate superior in vitro and in vivo antitumor efficacy. *J Immunol Baltim Md* 1950 162, 989–94 (1999).
511. Bloom, M. B. et al. Identification of Tyrosinase-related Protein 2 as a Tumor Rejection Antigen for the B16 Melanoma. *J Exp Medicine* 185, 453–460 (1997).
512. Mendiratta, S. et al. Therapeutic tumor immunity induced by polyimmunization with melanoma antigens gp100 and TRP-2. *Cancer Res* 61, 859–63 (2001).
513. Antin, J. H. T-cell depletion in GVHD: less is more? *Blood* 117, 6061–6062 (2011).
514. Huang, B. et al. Toll-Like Receptors on Tumor Cells Facilitate Evasion of Immune Surveillance. *Cancer Res* 65, 5009–5014 (2005).
515. Bowne, W. B. et al. Coupling and Uncoupling of Tumor Immunity and Autoimmunity. *J Exp Medicine* 190, 1717–1722 (1999).
516. Wang, W. et al. Human H-Y: a male-specific histocompatibility antigen derived from the SMCY protein. *Science* 269, 1588–1590 (1995).
517. Klarquist, J. and Janssen, E. Melanoma-infiltrating dendritic cells: limitations and opportunities of mouse models. *Oncoimmunology* 1(9):154-1593 (2012).
518. Prometheus Laboratories Inc. Proleukin (Aldesleukin) Injection Label-FDA. (2011). Retrieved from [https://www.accessdata.fda.gov/drugsatfda\\_docs/label/2012/103293s5130lbl.pdf](https://www.accessdata.fda.gov/drugsatfda_docs/label/2012/103293s5130lbl.pdf)
519. Denayer, T. et al. Animal models in translational medicine: Validation and prediction. *New Horizons in Translational medicine*. 2(1) 5-11 (2014)
520. Schering Corp. Intron A Summary and Basis of Approval. (2014). Retrieved from [https://www.accessdata.fda.gov/drugsatfda\\_docs/label/2014/103132s5190lbl.pdf](https://www.accessdata.fda.gov/drugsatfda_docs/label/2014/103132s5190lbl.pdf)

- 521. Melief, C.J.M. Cancer Immunotherapy by Dendritic Cells. *Immunity* 29, 372-383 (2008).
- 522. Malchow S. et al Aire-dependent thymic development of tumor-associated regulatory T cells. *Science* 339, 1219-24 (2013).
- 523. Ishida T, Ueda R: CCR4 as a novel molecular target for immunotherapy of cancer. *Cancer Sci.* 2006, 97 (11): 1139-46
- 524. Shevach EM. Mechanisms of foxp3<sup>+</sup> T regulatory cell-mediated suppression. *Immunity* 30, 636-45 (2009).

## VITA

Erica L. Fleming-Trujillo was born in Palos Heights, Illinois on May 2, 1989 to David and Linda Fleming. She attended the University of Iowa in Iowa City where she earned a Bachelor of Science degree in Biology with a focus in Genetics and Biotechnology in 2011. As an undergraduate, she worked in the laboratory of Stanley Perlman, M.D., Ph.D. studying the immune response to coronavirus infections in the lung and central nervous system and continued working full time for a year following graduation.

Erica matriculated into the Integrative Program in Biomedical Sciences at Loyola University of Chicago in 2012 and joined the Department of Microbiology and Immunology. She completed her dissertation work in the lab of Michael I. Nishimura, Ph.D. where she aimed to improve upon the efficacy of T cell-based cancer immunotherapy by targeting the tumor microenvironment. In 2016, Erica was awarded an F31 Predoctoral Ruth L. Kirchstein National Research Service Award from the National Cancer Institute that provided funding for her research.

After completion of her graduate studies, Erica will continue her research training as a Postdoctoral Research Fellow in the laboratory of Dai Horiuchi, Ph.D. at Northwestern University. There, she will investigate resistance mechanisms to immunotherapy in triple negative breast cancer.

